

博士論文

Study on Isolable π -Electron Species Containing an Inverted Si=Si Bond and an Unsupported Si-Si π -Bond

(反転 Si=Si 結合および Si-Si π 単結合を持つ単離可能 π 電子
化学種の研究)

糠澤 拓実

令和 3 年

Study on Isolable π -Electron Species Containing an
Inverted Si=Si Bond and an Unsupported Si-Si π -Bond

Takumi Nukazawa

Department of Chemistry, Graduate School of Science,

Tohoku University

2021

Preface

The studies described in this doctoral dissertation have been carried out under the direction of Professor Takeaki Iwamoto at the Department of Chemistry, Graduate School of Science, Tohoku University during 2016 to 2021.

This doctoral dissertation is concerned with the chemistry of silicon π -electron species having unique structure, electronic properties and reactivity. The author convinces that the present studies have contributes not only to the progress of the field in silicon chemistry but also to more in general of the field in organic chemistry and organometallic chemistry.

The author especially wishes to express great thanks to Professor Takeaki Iwamoto for his continuing guidance and valuable discussions throughout the course of studies. It is a great pleasure to thanks Professor Shintaro Ishida for his helpful discussions and encouragement. The author is grateful to Ms. Masako Sasaki and Ms. Mika Ando for their establishment of the comfortable environment in research. The author should like to express appreciation to Dr. Shigeru Sasaki, Naohiko Akasaka, Tomohiro Iimura, Tomoyuki Kosai, Yuki Yokouchi, Siwat Chinaroj, Ryo Kobayashi, Shunya Honda, Messrs. Yushi Kato, Yuko Suzuki, Tomofumi Tamura, Ryo Yamaguchi, Yasunori Miura, Hitomi Ichikawa, Shohei Sugawara, Makoto Tamura, Takuro Karakida, Kaho Tanaka, Kentaro Fujieda, Yuichiro Matsumoto, Maiko Mori, Shunya Abe, Kaho Ishikawa, Taichi Koike, Takehiro Sato, Hiroshi Nakagawa, Takuya Nomura, Takuro Hatakeyama, Daichi Yanagisawa, Kenya Uchida, Hiroki Kawauchi, Shohei Kawakami, Atsuhiko Sato, Kotone Kubota, Mayu Nozawa, Sei Yokoyama, Kouta Asami, Yuya Ushijima, Kazuma Oshima, Yoshiki Ota, Hayato Sasaki, Kento Masuda, Kazuto Mizoguchi, Raiki Osawa, Kawai Kentaro, Masaki Kuribayashi, Kengo Sakamoto, Ryoya Chino, Takuro Shiojima, Kazutoshi Fujita, Yukihiro Morino, Yusuke Yoshida, Keitaro Watanabe, Shohei Wada, Tomoki Ishikawa, Yasuhiro Katayama, Naoki Sakurada, Ryotaro Hayasaka, Kosuke Machida, Kento Miwa for their valuable discussions to all of the members of Professor Iwamoto's group at Tohoku University for the establishment of the comfortable environment in research.

Finally, the author would also like to express his deep appreciation to his family members, Mr. Shigemi Nukazawa, Ms. Hiroko Nukazawa, Ms. Mami Nukazawa, Ms. Mina Nukazawa for their kind encouragement and support.

Takumi Nukazawa

Department of Chemistry
Graduate School of Science
Tohoku University

December 2021.

Contents

| | | |
|------------|---|-----|
| Chapter 1. | General Introduction | 1 |
| Chapter 2. | Synthesis and Reactivity of a New Tetrasilabicyclo[1.1.0]but-1(3)-ene | 7 |
| Chapter 3. | Synthesis of 1,3-Diodotetrasilabicyclo[1.1.0]butane with π -Type Single-Bonding Character | 51 |
| Chapter 4. | Synthesis and Isomerization of a Planar 1,3-Dichlorotetrasilabicyclo[1.1.0]butane | 89 |
| Chapter 5. | Synthesis of π -Conjugated Species with an Unsupported Si-Si π -Bond via Direct π -Extension | 147 |
| Chapter 6. | Reactions of a Bicyclo[1.1.0]tetrasil-1(3)-ene with Nucleophilic Reagents | 199 |

(Compounds are independently numbered in each chapter.)

List of Abbreviations

Bu: *n*-Butyl

t-Bu: *tert*-Butyl

Cp*: Pentamethylcyclopentadienyl (C₅Me₅)

DME: 1,2-Dimethoxy ethane

Dep: 2,6-Diethylphenyl

DMAP: 4-(Dimethylamino)pyridine

Et: Ethyl

Et₂O: Diethylether

Et₃N·HBr: Triethylamine hydrobromide

eV: Electron volt

Hex: Hexyl

HOMO: Highest occupied molecular orbital

i-Pr: Isopropyl

LUMO: Lowest unoccupied molecular orbital

Me: Methyl

Mes*: 2,4,6-Tri(*tert*-butyl)phenyl

NHC: *N*-Heterocyclic carbene

Ph: Phenyl

THF: Tetrahydrofuran

Tip: 2,4,6-Triisopropylphenyl

TD-DFT: Time-dependent density functional theory

UV: Ultraviolet

VT: Variable-Temperature

vis: Visible

WBI: Wiberg bond indices

XRD: X-ray diffraction

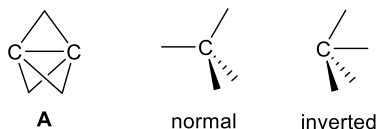
Chapter 1

General Introduction

1-1. Introduction

Molecules that exhibit nonclassical geometries and chemical bonds have fascinated experimental and theoretical chemists,¹ since the exploration of such molecules usually leads to a deeper understanding of their molecular structures and chemical bonds as well as to the discovery of unexpected reactivity. A representative example of such an intriguing organic molecule is [1.1.1]propellane **A** (Chart 1-1).² This compound has a nonclassical single bond between bridgehead carbon atoms that adopt an inverted (or a hemispheroidal) geometry; the direction of the bridgehead single bond is diametrically opposite to that expected for typical C–C bonds in a normal tetrahedral geometry (Chart 1-1).³ The theoretical and experimental investigation for the nature of the inverted single bond in **A** revealed that the single bond exhibits diradical or ionic characters. Currently, the high reactivity of **A** has been utilized for the bond-forming reactions.⁴

Chart 1-1. [1.1.1]Propellane **A** and Schematic Representation of Normal/Inverted Single Bonds



Such nonclassical bonds with an inverted geometry should also be possible for multiple bonds. Bicyclo[1.1.0]but-1(3)-ene **B** represents one extreme example of compounds with an inverted double bond, whereby the direction of the double bond is formally oriented in the diametrically opposite direction to that expected for a normal C=C double bond geometry (Chart 1-2).^{5,6} Theoretical study suggested that compound **B** exhibits the several resonance structures (Chart 1-3),⁵ implying the high reactivity of the inverted double bond. Although **B** and its derivatives have been proposed as reactive intermediates,⁶ they have not yet been isolated and their molecular structures and reactivity have not been investigated experimentally.

Chart 1-2. Bicyclo[1.1.0]but-1(3)-ene **B** and Schematic Representation of Normal/Inverted Double Bonds

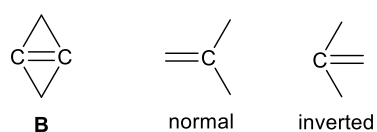
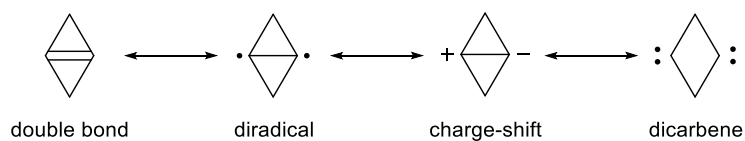
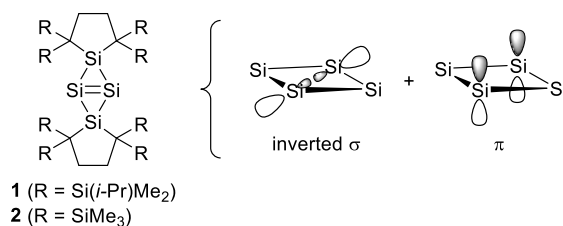


Chart 1-3. Resonance Structures of Bicyclo[1.1.0]but-1(3)-ene **B**



Recently, our group synthesized tetrasilabicyclo[1.1.0]but-1(3)-ene **1**, the first isolable silicon analogue of bicyclo[1.1.0]but-1(3)-ene (Chart 1-4).⁷ Single-crystal X-ray diffraction (XRD) analysis of **1** revealed that the central Si₄ bicyclic skeleton is planar, and DFT calculation suggested that the bridgehead Si=Si bond comprises a π -bond and an inverted σ -bond as found between bridgehead atoms in pentasila[1.1.1]propellane (Chart 1-4).⁸ In spite of the highly-distorted Si=Si bond in **1**, it exhibits very low reactivity toward small molecules such as H₂O, methanol, cyclohexa-1,4-diene, Bu₃SnH, Ph₃P, or BPh₃ probably due to severe steric demand of the Si(*i*-Pr)Me₂ groups. In this thesis, the author synthesized new tetrasilabicyclo[1.1.0]but-1(3)-ene **2** that has less bulky SiMe₃ groups to examine the reactivity of the inverted Si=Si bond (Chart 1-4). Through the investigation of the reactivity of **2** for various reagents, the author found that **2** could be the useful precursor for the synthesis of unconventional π -electron compounds of silicon.

Chart 1-4. Tetrasilabicyclo[1.1.0]but-1(3)-enes **1** and **2**

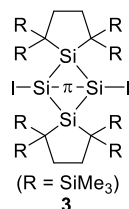


In chapter 2, the author described the synthesis and isolation of tetrasilabicyclo[1.1.0]but-1(3)-ene **2**. Single-crystal XRD analysis and spectroscopic analysis indicated that the structural and electronic characteristics of **2** are virtually identical to those of **1**. The reactions of **2** with carbon tetrachloride and methanol were also described.

In chapter 3, the author described the synthesis and properties of 1,3-diiodotetrasilabicyclo[1.1.0]butane **3** via 1,2-diiodination of **2** (Chart 1-5). Single-crystal

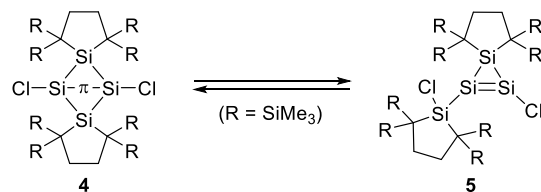
XRD analysis and theoretical study suggested that **3** exhibits the π -type single bond (the unsupported π -bond) between the bridgehead silicon atoms.

Chart 1-5. 1,3-Diiodotetrasilabicyclo[1.1.0]butane **3**



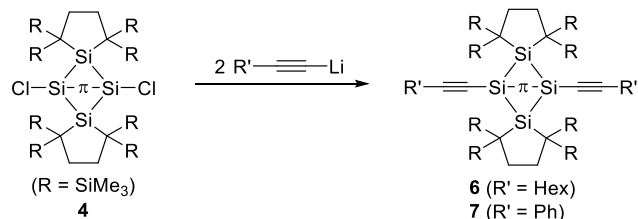
In chapter 4, the author described the synthesis of 1,3-dichlorotetrasilabicyclo[1.1.0]butane **4** with the π -type bridgehead Si–Si bond via 1,2-dichlorination of **2**. The interconversion between **4** and its isomer, 1-chloro-2-(chlorosilyl)cyclotrisilene **5** is also described (Scheme 1-1).

Scheme 1-1. Interconversion between **4** and **5**



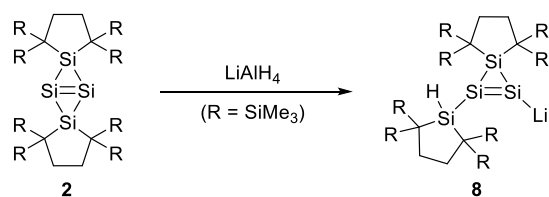
In chapter 5, the author described the reactions of **4** with a lithium acetylide to provide bicyclo[1.1.0]tetrasilanes **6** and **7** with alkynyl groups on the bridgehead silicon atoms (Scheme 1-2). π -Conjugation between the unsupported Si–Si π -bond of the bicyclo[1.1.0]tetrasilane unit and the alkynyl groups were examined in detail.

Scheme 1-2. Reactions of **4** with a lithium acetylide



In chapter 6, the author described the reactions of **2** with nucleophilic reagents. The reaction of **2** with lithium aluminum hydride (LiAlH_4) unexpectedly provided the first isolable cyclotrisilenide **8** (Scheme 1-3).

Scheme 1-3. Reaction of **2** with LiAlH₄



1-2. References

- (1) (a) Hoffmann, R.; Hopf, H. *Angew. Chem., Int. Ed.* **2008**, *47*, 4474–4481. See also: (b) Borden, W. T. *Chem. Rev.* **1989**, *89*, 1095–1109. (c) Mastryukov, V. S.; Boggs, J. E. *Struct. Chem.* **2000**, *11*, 97–103. (d) Vázquez, S.; Camps, P. *Tetrahedron* **2005**, *61*, 5147–5208.
- (2) (a) Wiberg, K. B.; Walker, F. H. *J. Am. Chem. Soc.* **1982**, *104*, 5239–5240. (b) Levin, M. D.; Kaszynski, P.; Michl, J. *Chem. Rev.* **2000**, *100*, 169–234. (c) Nied, D.; Breher, F. *Chem. Soc. Rev.* **2011**, *40*, 3455–3466. (d) Dilmaç, A. M.; Spuling, E.; de Meijere, A.; Bräse, S. *Angew. Chem., Int. Ed.* **2017**, *56*, 5684–5718.
- (3) (a) Wiberg, K. B. *Acc. Chem. Res.* **1984**, *17*, 379–386. (b) Iwamoto, T.; Ishida, S. *Chem. Lett.* **2014**, *43*, 164–170. (c) Heider, Y.; Scheschkewitz, D. *Dalton Trans.* **2018**, *47*, 7104–7112. (d) Heider, Y.; Poitiers, N. E.; Willmes, P.; Leszczyńska, K. I.; Huch, V.; Scheschkewitz, D. *Chem. Sci.* **2019**, *10*, 4523–4530. (e) Heider, Y.; Scheschkewitz, D. *Chem. Rev.* **2021**, *121*, 9674–9718
- (4) (a) Gianatassio, R.; Lopchuk, J. M.; Wang, J.; Pan, C. M.; Malins, L. R.; Prieto, L.; Brandt, T. A.; Collins, M. R.; Gallego, G. M.; Sach, N. W.; Spangler, J. E.; Zhu, H.; Zhu, J.; Baran, P. S. *Science* **2016**, *351*, 241–246. (b) Lopchuk, J. M.; Fjelbye, K.; Kawamata, Y.; Malins, L. R.; Pan, C. M.; Gianatassio, R.; Wang, J.; Prieto, L.; Bradow, J.; Brandt, T. A.; Collins, M. R.; Elleraas, J.; Ewanicki, J.; Farrell, W.; Fadeyi, O. O.; Gallego, G. M.; Mousseau, J. J.; Oliver, R.; Sach, N. W.; Smith, J. K.; Spangler, J. E.; Zhu, H.; Zhu, J.; Baran, P. S. *J. Am. Chem. Soc.* **2017**, *139*, 3209–3226. (c) Kanazawa, J.; Maeda, K.; Uchiyama, M. *J. Am. Chem. Soc.* **2017**, *139*, 17791–17794. (d) Kanazawa, J.; Uchiyama, M. *Synlett* **2019**, *30*, 1–11.

- (5) (a) Hehre, W. J.; Pople, J. A. *J. Am. Chem. Soc.* **1975**, *97*, 6941–6955. (b) Wagner, H. U.; Szeimies, G.; Chandrasekhar, J.; Schleyer, P. v. R.; Pople, J. A.; Binkley, J. S. *J. Am. Chem. Soc.* **1978**, *100*, 1210–1213. (c) Kollmar, H.; Carrion, F.; Dewar, M. J. S.; Bingham, R. C. *J. Am. Chem. Soc.* **1981**, *103*, 5292–5303. (d) Hess, B. A. Jr.; Allen, W. D.; Michalska, D.; Schaad, L. J.; Schaefer H. F. III *J. Am. Chem. Soc.* **1987**, *109*, 1615–1621. (e) Hess, B. A. Jr.; Michalska, D.; Schaad, L. J. *J. Am. Chem. Soc.* **1987**, *109*, 7546–7547. (f) Hrovat, D. A.; Borden, W. T. *J. Am. Chem. Soc.* **1988**, *110*, 4710–4718. (g) Wiberg, K. B.; Artis, D. R.; Bonneville, G. *J. Am. Chem. Soc.* **1991**, *113*, 7969–7979. (h) Prakash, G. K. S.; Rasul, G.; Reddy, V. P.; Casanova, J. *J. Am. Chem. Soc.* **1992**, *114*, 6484–6486. (i) Nguyen, T. L.; Le, T. N.; Mebel, A. M.; Lin, S. H. *Chem. Phys. Lett.* **2000**, *326*, 468–476. (j) Dinadayalane, T. C.; Priyakumar, U. D.; Sastry, G. N. *J. Phys. Chem. A* **2004**, *108*, 11433–11448. (k) Rasul, G.; Olah, G. A.; Prakash, G. K. S. *J. Phys. Chem. A* **2006**, *110*, 7197–7201. (l) Cremer, D.; Kraka, E.; Joo, H.; Stearns, J. A.; Zwier, T. S. *Phys. Chem. Chem. Phys.* **2006**, *8*, 5304–5316. (m) Mebel, A. M.; Kislov, V. V.; Kaiser, R. I. *J. Chem. Phys.* **2006**, *125*, 133113. (n) Fujita, Y.; Abe, M.; Shiota, Y.; Suzuki, T.; Yoshizawa, K. *Bull. Chem. Soc. Jpn.* **2016**, *89*, 770–778.
- (6) (a) Szeimies, G.; Harnisch, J.; Baumgärtel, O. *J. Am. Chem. Soc.* **1977**, *99*, 5183–5184. (b) Szeimies-Seebach, U.; Harnisch, J.; Szeimies, G.; Van Meerssche, M.; Germain, G.; Declercq, J.-P. *Angew. Chem., Int. Ed. Engl.* **1978**, *17*, 848–850. (c) Zoch, H.-G.; Szeimies, G.; Romer, R.; Schmitt, R. *Angew. Chem., Int. Ed. Engl.* **1981**, *20*, 877–878. (d) Schlüter, A.-D.; Harnisch, H.; Harnisch, J.; Szeimies-Seebach, U.; Szeimies, G. *Chem. Ber.* **1985**, *118*, 3513–3528.
- (7) Iwamoto, T.; Abe, T.; Sugimoto, K.; Hashizume, D.; Matsui, H.; Kishi, R.; Nakano, M.; Ishida, S. *Angew. Chem., Int. Ed.* **2019**, *58*, 4371–4375.
- (8) Nied, D.; Köppe, R.; Klopper, W.; Schnöckel, H.; Breher, F. *J. Am. Chem. Soc.* **2010**, *132*, 10264–10265.

Chapter 2

Synthesis and Reactivity of a New Tetrasilabicyclo[1.1.0]but-1(3)-ene

The contents of this chapter are published in part in

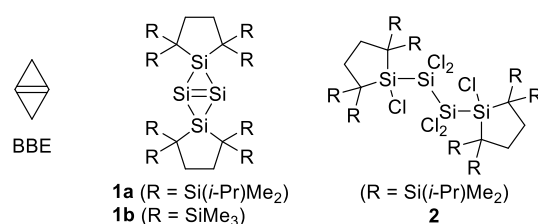
Nukazawa, T.; Kosai, T.; Honda, S.; Ishida, S.; Iwamoto, T. *Dalton Trans.* **2019**, 48,
10874–10880.

DOI: 10.1039/c9dt01627a

2-1. Introduction

Molecules that exhibit a distorted structure have attracted experimental and theoretical chemists.¹ Among such molecules, bicyclo[1.1.0]but-1(3)-ene (BBE) (Chart 2-1) is an intriguing molecule as it has an extremely-strained bridgehead C=C double bond in the bicyclic framework, whereby the orientation of the double bond is diametrically opposite to that of typical double bonds in acyclic alkenes.² Although BBE and its derivatives have been proposed as reactive intermediates³ and theoretically examined,⁴ their molecular structures have not been proved experimentally. Recently, we reported synthesis and X-ray diffraction analysis of tetrasilabicyclo[1.1.0]but-1(3)-ene **1a**, the first isolable silicon analogue of BBE (Chart 2-1).⁵ While the Si=Si distance in **1a** [2.4716(12) Å] is rather long compared to those of typical Si=Si bonds (2.118–2.312 Å),⁶ DFT calculation suggested that the bridgehead bond comprises a σ -bond as found between bridgehead atoms in pentasila[1.1.1]propellane⁷ and a π -bond. In spite of the highly-distorted Si=Si bond in **1a**, it exhibits very low reactivity toward small molecules probably due to severe steric demand of the Si(*i*-Pr)Me₂ groups; **1a** does not react with H₂O, methanol, cyclohexa-1,4-diene, Bu₃SnH, Ph₃P, or BPh₃. **1a** only reacted with CCl₄ to provide hexachlorinated product **2**, although the mechanism for the reaction remains unclear. To examine further reactivity of tetrasilabicyclo[1.1.0]but-1(3)-ene, the author designed a new derivative that contains less bulky SiMe₃ substituents (**1b**). In this chapter, the author reports the synthesis, molecular structure and reactivity of **1b**. While the structural and spectroscopic characteristics of **1b** resemble those of **1a**, **1b** reacts with CCl₄ or methanol and the products of the reaction with CCl₄ substantially depend on the reaction conditions.

Chart 2-1. Structures of Bicyclo[1.1.0]but-1(3)-ene (BBE), Tetrasilabicyclo[1.1.0]but-1(3)-ene **1a** (R = Si(*i*-Pr)Me₂) and **1b** (R = SiMe₃) as well as Hexachlorinated Product **2**

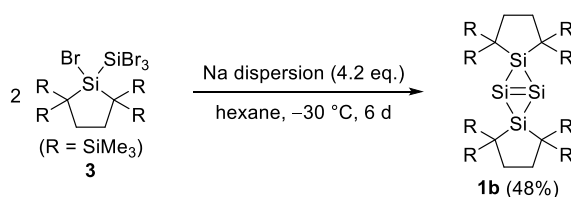


2-2. Results and Discussion

2-2-1. Synthesis of Tetrasilabicyclo[1.1.0]but-1(3)-ene **1b**

Orange crystals of **1b** were obtained in 48% yield by the reductive debromination of tetrabromodisilane **3** with finely dispersed sodium in hexane at $-30\text{ }^{\circ}\text{C}$ (Scheme 2-1)⁸ and characterized by a combination of multinuclear NMR spectroscopy, high-resolution mass spectrometry, elemental analysis, and single-crystal X-ray diffraction (XRD) analysis. Compound **1b** was air- and moisture sensitive but thermally stable.

Scheme 2-1. Synthesis of **1b**



2-2-2. Molecular Structure of **1b**

The molecular structure of **1b** determined by XRD analysis is displayed in Figure 2-1. The molecule has a crystallographic inversion centre between Si1 and Si1* atoms and the central Si₄ bicyclic skeleton is planar with the dihedral angle of Si2–Si1–Si1*–Si2* of 180° , accordingly. The Si1–Si1* distance in **1b** [2.4873(10) Å] is substantially longer than the reported range of Si=Si double bonds with three-coordinate unsaturated silicon atoms (2.118–2.312 Å)⁶ and very similar to that of **1a** [2.4716(12) Å].⁵ The distances of the peripheral Si–Si bond forming the four-membered ring of **1b** [Si1–Si2: 2.2928(7) Å, and Si1–Si2*: 2.3004(7) Å] are also comparable to those of **1a** [2.2959(8) Å and 2.3098(8) Å].

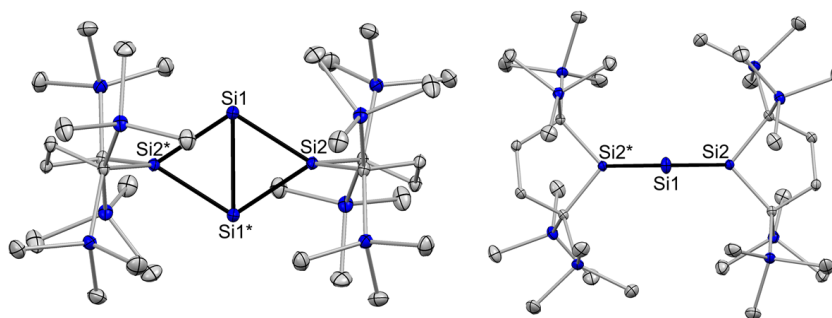


Figure 2-1. ORTEPs of **1b** (left: top view, right: side view; atomic displacement parameters set at 50% probability; hydrogen atoms omitted for clarity). Selected bond lengths (Å) and angles ($^{\circ}$): Si1–Si1* 2.4873(10), Si1–Si2 2.2928(7), Si1–Si2* 2.3004(7), Si2–Si1–Si2* 114.43(2), Si1–Si2–Si1* 65.57(2), Si2–Si1–Si1*–Si2* 180.

2-2-3. NMR Spectra and UV-vis Absorption Spectrum of **1b**

The ^1H NMR spectrum of **1b** in a C_6D_6 solution shows one singlet signal (0.32 ppm) due to eight equivalent SiMe_3 groups and one singlet signal (2.21 ppm) due to eight methylene protons in the five-membered rings, suggesting a facile ring flipping of the terminal silacyclopentane rings on the NMR time scale. In the ^{29}Si NMR spectrum, Si1 (Si1^*) and Si2 (Si2^*) nuclei resonate at 216.6 and 94.6 ppm (Figure 2-2a), respectively. These values are virtually the same as those of **1a** (217.0 and 94.5 ppm).⁵ The UV-vis absorption spectrum of **1b** in hexane (Figure 2-2b) exhibits a weak and broad band around 400 nm (ϵ 1800) and two broad and intense bands at 342 and 326 nm (ϵ 14000 and 12000), which resembles that of **1a**. These results indicate that the structural and electronic characteristics of **1b** are virtually identical to those of **1a**.

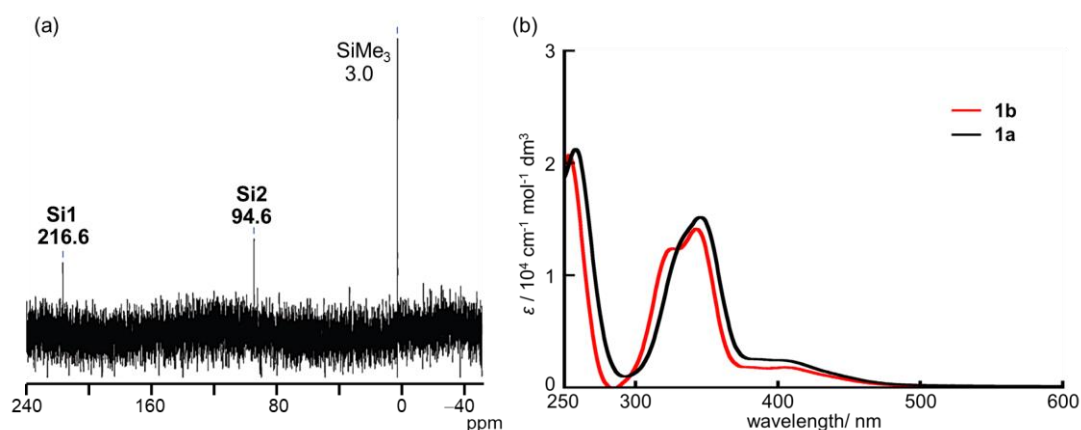


Figure 2-2. (a) ^{29}Si NMR spectrum of **1b** in C_6D_6 at room temperature. (b) UV-vis absorption spectra of **1b** (red) and **1a** (black) in hexane at room temperature.

2-2-4. Reaction of **1b** with Carbon Tetrachloride

The reaction of **1b** with an excess amount of carbon tetrachloride as a solvent proceeded at room temperature to provide 1,1,3,3-tetrachlorocyclotetrasilane **4** in 79% yield (Scheme 2-2, Figure 2-3a). Interestingly, the reaction of **1b** with six equivalents of carbon tetrachloride in toluene afforded hexachlorotetrasilane **5** (35%) together with **4** (17%) (Scheme 2-2). Formation of an acyclic hexachlorotetrasilane (**2**) was also found in the reaction of **1a** with carbon tetrachloride as shown in Chart 2-1. The formation of hexachloroethane ($\text{CCl}_3\text{-CCl}_3$) was confirmed by ^{13}C NMR spectrum measured during the reaction of **1b** with excess carbon

tetrachloride in C_6D_6 (Figure 2-27), which suggests chlorine abstraction from carbon tetrachloride to form trichloromethyl radical during the reaction similar to the reaction of tetrasilyldisilene with carbon tetrachloride providing a 1,2-dichlorinated product.⁹ As **4** does not react with two equivalents of carbon tetrachloride in toluene, **4** is not an intermediate for the formation of **5**.

Scheme 2-2. Reaction of **1b** with CCl_4

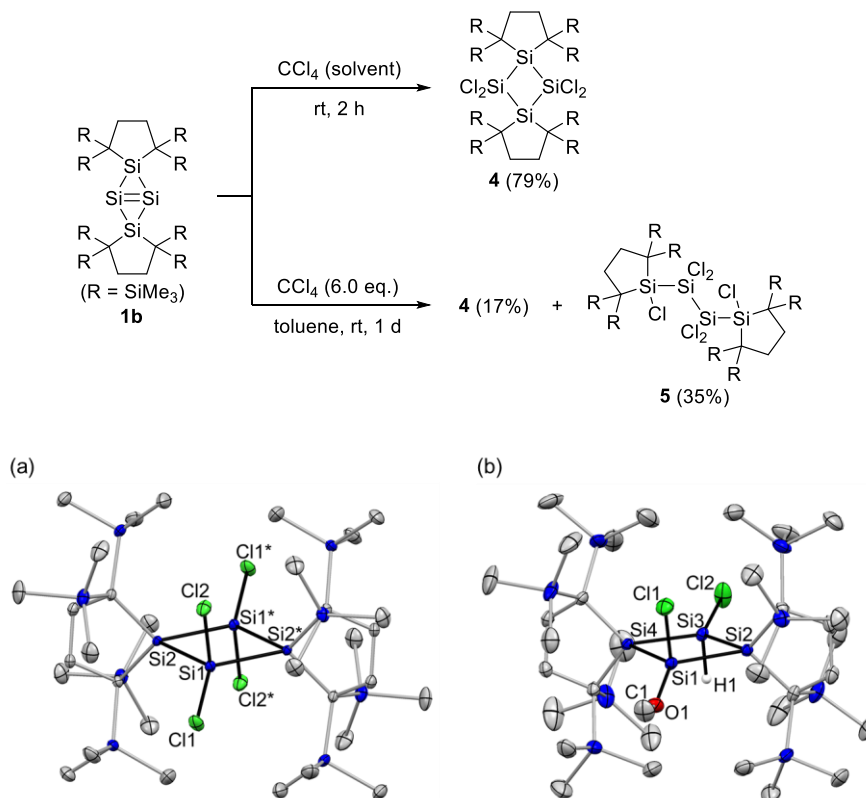


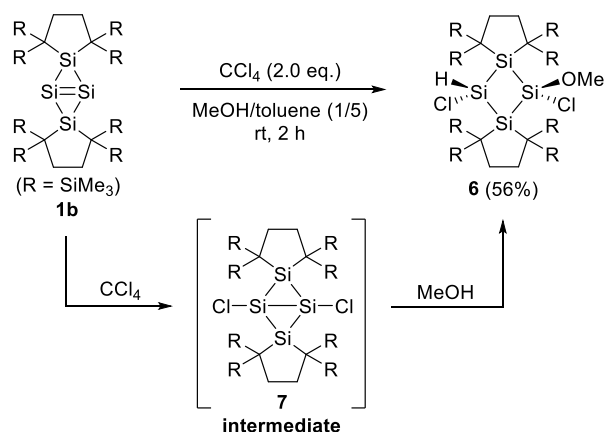
Figure 2-3. ORTEPs of (a) **4** and (b) **6** with thermal ellipsoids at 50% probability; hydrogen atoms have been omitted for clarity.

2-2-5. Trapping Reaction of the Intermediate in Reaction of 1b with CCl_4

Although the reaction of **1b** with two equivalents of carbon tetrachloride in toluene at room temperature afforded a complex mixture that does not exhibit NMR signals of **4** and **5**,¹⁰ a similar reaction of **1b** in the presence of methanol (toluene/methanol=5/1) afforded *cis*-1,3-dichloro-1-methoxycyclotetrasilane **6** in 56% yield (Scheme 2-3, Figure 2-3). As **1b** does not react with methanol in toluene in the absence of carbon tetrachloride at room temperature, these results indicate that **6** is a product resulting from the reaction of an

intermediate with methanol after the reaction with carbon tetrachloride. As *syn*-addition of H₂O toward the bridgehead Si–Si bond of bicyclo[1.1.0]tetrasilane was reported by Masamune et al.,¹¹ the intermediate is likely to be 1,3-dichlorobicyclo[1.1.0]tetrasilane **7** (Scheme 2-3) resulting from the 1,2-addition of chlorine atoms across the Si=Si double bond of **1b**.

Scheme 2-3. Reaction of **1b** with CCl₄ in the presence of MeOH



2-2-6. Monitoring Reaction of **1b** with CCl₄ by ¹H NMR Spectroscopy

The reaction of **1b** with excess carbon tetrachloride in toluene-*d*₈ monitored by ¹H NMR spectroscopy at lower temperatures provided further insight into the reaction with carbon tetrachloride. The ¹H NMR spectrum just after the addition of excess carbon tetrachloride to a toluene-*d*₈ solution of **1b** at –30 °C (Figure 2-4) exhibited mainly two singlet signals at 0.36 and 1.78 ppm with the ratio of 9 : 1 together with signals of a trace amount of **4** and no signals due to **1b** were observed. At –30 °C, the observed signals of the intermediate gradually decreased, while signals of **4** gradually increased but signals assignable to **5** were not observed (Figure 2-4).¹² This result indicates that **1b** reacted immediately with carbon tetrachloride at –30 °C to provide an intermediate. Although the intermediate has not been able to be fully identified on account of its low solubility, the ¹H NMR signals are consistent with the structure of **7** which contains thirty-six protons of SiMe₃ moiety and four protons of CH₂ moiety in the silacyclopentane rings. After the mixture was warmed up above 10 °C, the ¹H signals of **5** appeared and increased (Figure 2-4). These results suggest that the activation barrier of the rate controlling step to afford **5** from the intermediate is higher than those to provide **4**.

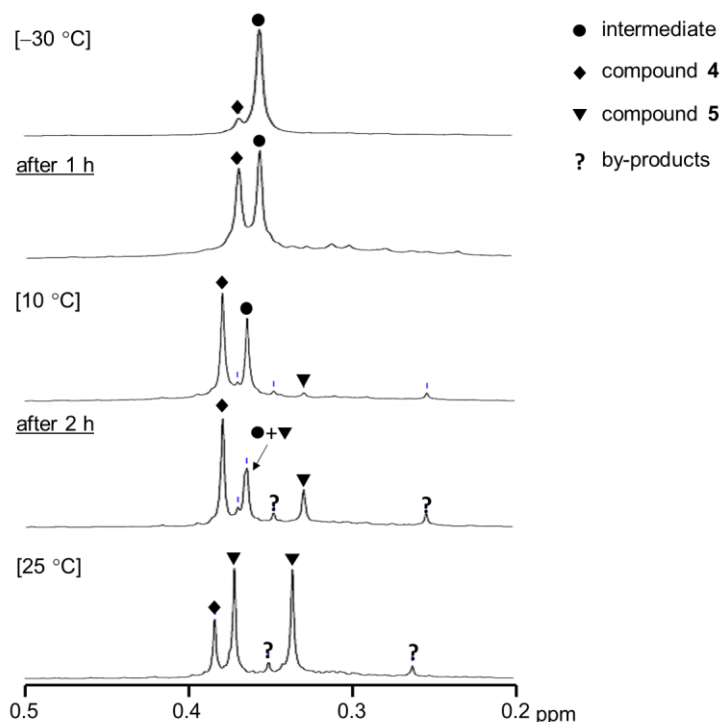
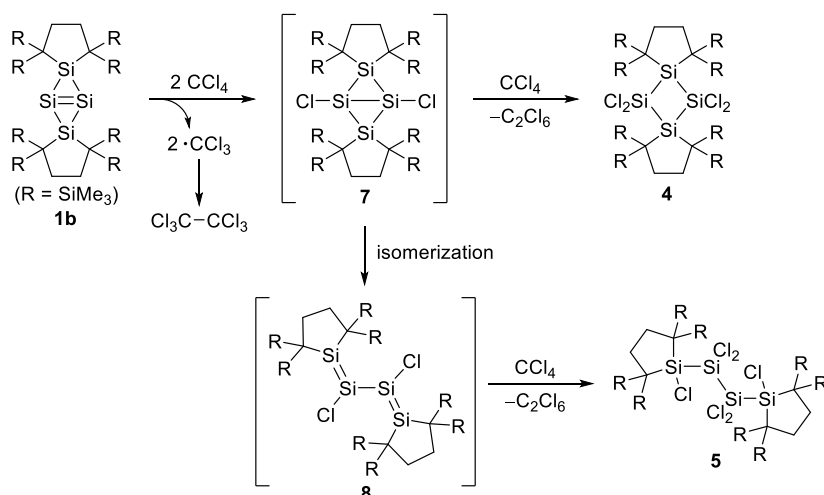


Figure 2-4. ^1H NMR spectra (SiMe_3 region) of the reaction mixture of the reaction of **1b** with excess carbon tetrachloride in toluene- d_8 at $-30\text{ }^\circ\text{C}$, $10\text{ }^\circ\text{C}$, and $25\text{ }^\circ\text{C}$.

2-2-7. Possible Mechanism for Reaction of **1b** with CCl_4

Scheme 2-4 exhibits a possible mechanism for the reaction of **1b** with carbon tetrachloride. Compound **1b** reacts with carbon tetrachloride to afford 1,3-dichlorobicyclo[1.1.0]tetrasilane **7**. In the presence of a large excess amount ($>\text{ca. } 500\text{ eq.}$) of carbon tetrachloride, **7** reacts with an extra amount of carbon tetrachloride to provide **4**. When six equivalents of carbon tetrachloride are used, isomerisation of **7** to a tetrasiladiene **8** may compete with the chlorination of **7**, and **8** should undergo further chlorination reactions at the $\text{Si}=\text{Si}$ double bonds to furnish **5**.¹³ These processes are consistent with the mechanism proposed previously for the reaction of **1a** with carbon tetrachloride⁵ and the results of the ^1H NMR spectra observed during the reaction in toluene- d_8 at low temperatures. In the case of the reaction of **1b** with two equivalents of carbon tetrachloride, the isomerisation of **7** to **8** and the subsequent decomposition of **8** may occur. The generation of **7** even in this condition is supported by the formation of **6** that should result from *syn*-addition of methanol to the bridgehead $\text{Si}-\text{Si}$ bond of **7**.¹⁴

Scheme 2-4. Possible Mechanism for Reaction of **1b** and CCl₄



2-2-8. Reaction of **1b** with Methanol

The existence of an intermediate similar to **8** was suggested in the reaction of **1b** with methanol. The reaction of **1b** with methanol in THF proceeded at 70 °C to provide 1,3,3-trimethoxytetrasilane **9** as a sole product, which was isolated in 54% yield (Scheme 2-5), while this reaction did not proceed at room temperature. Compound **9** was characterised by a combination of multinuclear NMR spectroscopy, high-resolution mass spectrometry, elemental analysis, and single-crystal XRD analysis (Figure 2-5). Although the mechanism for the regioselective addition of methanol to **1b** providing **9** remains unclear, one possible mechanism can involve the addition of methanol to the Si=Si double bond in **1b** affording 1-methoxybicyclo[1.1.0]tetrasilane **10** followed by valence isomerisation to a 2-methoxytetrasiladiene **11** similar to isomerisation of **7** to **8**,¹⁴ and the subsequent addition of methanol to the Si=Si double bond in the 2-methoxytetrasiladiene to furnish **9** (Scheme 2-5). The selective formation of **9** suggests that the Si=Si double bonds in intermediate **11** are significantly polarised as found in the unsymmetrically-substituted disilenes,^{15a} or suggested for possible intermediates in the double alcohol addition to an Si-Si triple bond in a disilyne^{15b} or cumulative Si=Si double bonds in a trisilaallene.^{15c}

Scheme 2-5. Reaction of **1b** with Methanol and the Possible Mechanism

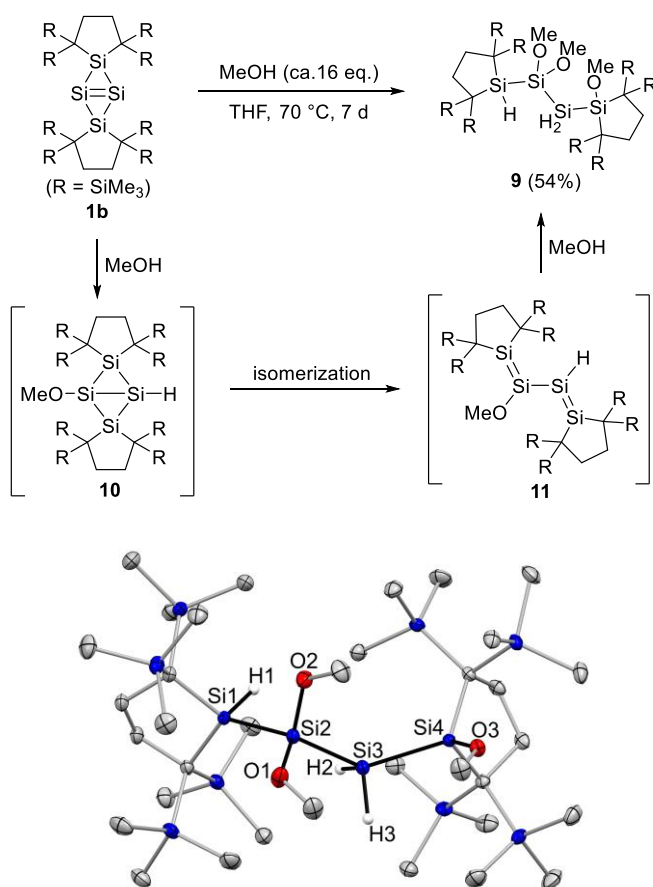


Figure 2-5. ORTEP of **9** with thermal ellipsoids at 50% probability; hydrogen atoms omitted for clarity.

2-3. Summary

Tetrasilabicyclo[1.1.0]but-1(3)-ene **1b** was newly synthesized as orange crystals by the reductive debromination of the corresponding tetrabromodisilane **3** with finely dispersed sodium in hexane. The structural and spectroscopic characteristics of **1b** closely resemble those of **1a**. The reaction of **1b** with carbon tetrachloride providing tetrachlorocyclotetrasilane **4** and hexachlorotetrasilane **5** suggests the generation of 1,3-dichlorobicyclo[1.1.0]tetrasilane **7** and tetrasiladiene **8**, the latter of which was supported by the reaction of **1b** with methanol.

2-4. Experimental Section

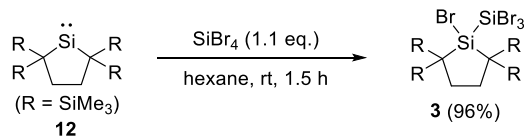
General Procedures

All reactions involving air-sensitive compounds were performed under argon or nitrogen atmosphere using a high vacuum line and standard Schlenk techniques, or a glove box, as well as dry and oxygen-free solvents. Reactions at lower temperatures were performed using an EYELA PSL-1400 cryobath. NMR spectra were recorded on a Bruker Avance III 500 FT NMR spectrometer. The ^1H and ^{13}C NMR chemical shifts were referenced to residual ^1H and ^{13}C shifts of the solvents: C_6D_6 (^1H : δ 7.16 and ^{13}C : δ 128.0).¹⁶ The ^{29}Si NMR chemical shifts were relative to Me_4Si in ppm (δ 0.00). The sampling of air-sensitive compounds was carried out using a VAC NEXUS 100027 type glove box. Mass spectra were recorded on a Bruker Daltonics SolariX 9.4 T spectrometer. UV-vis spectra were recorded on a JASCO V-770 spectrometer. X-ray analysis was carried out using a Bruker AXS APEXII CCD diffractometer. Recycling preparative gel permeation chromatography (GPC) using dry toluene as an eluent was performed at 5.0 mL min^{-1} rate using a Japan Analytical Industry Co., LC-9201 equipped with a JAIGEL-H column (Japan Analytical Industry Co., ϕ 20 mm \times 600 nm) which was connected to the glove box.

Materials

Dry and degassed hexane, THF and toluene were prepared using a VAC 103991 solvent purifier. C_6D_6 was dried by molecular sieves 4\AA after degassing through five freeze–pump–thaw cycles. Carbon tetrachloride was dried by calcium hydride after degassing through three freeze–pump–thaw cycles. Methanol was dried by molecular sieves 3\AA after degassing through three freeze–pump–thaw cycles. 2,2,5,5-Tetrakis(trimethylsilyl)-1-silacyclopentane-1,1-diyl **12**¹⁷ was prepared according to published procedure. Silicon tetrabromide and finely dispersed sodium (Strem) were commercially available and used without further purification.

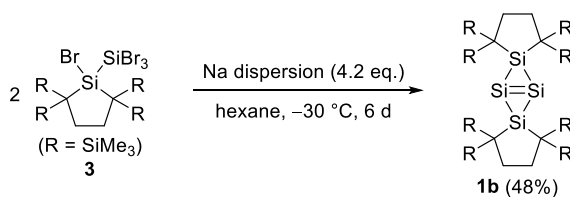
Synthesis of Tetrabromodisilane **3**



To a Schlenk tube (100 mL) equipped with a magnetic stir bar, a solution of **12** (2.01 g, 5.39 mmol) in hexane (18.0 mL) was placed. To the solution, silicon tetrabromide (0.74 mL, 5.96 mmol) was added and the mixture was stirred for 1.5 hours at room temperature. The colour of the solution turned immediately from orange to colourless. After the volatiles were removed in vacuo at room temperature, **3** was obtained as a white powder (3.74 g, 5.19 mmol) in 96% yield.

3: A white powder; mp 151-152 °C; δ_{H} (500 MHz, C_6D_6 , 298 K) 0.339 (18H, s, SiCH_3), 0.341 (18H, s, SiCH_3), 1.86-1.96 (4H, m, CH_2); δ_{C} (125 MHz, C_6D_6 , 297 K) 4.8 (SiCH_3), 5.2 (SiCH_3), 17.3 (C), 34.0 (CH_2); δ_{Si} (99 MHz, C_6D_6 , 296 K) -20.6 (Si-SiBr_3), 4.1 (SiMe_3), 7.8 (SiMe_3), 30.4 (Si-SiBr_3); HRMS (APCI) found, 700.82391. Calcd for $\text{C}_{15}\text{H}_{37}\text{Br}_4\text{Si}_6$ [(M-Me) $^+$], 700.82389; Found: C, 27.02; H, 5.78. Calcd for $\text{C}_{16}\text{H}_{40}\text{Br}_4\text{Si}_6$: C, 26.67; H, 5.60%.

Synthesis of Tetrasilabicyclo[1.1.0]but-1(3)-ene **1b**⁸



To a Schlenk tube (30 mL) equipped with a magnetic stir bar and four nichrome wires (φ = 1.0 mm, l = 2.0 cm, Figure 2-6), **3** (500 mg, 0.695 mmol) and finely dispersed sodium (66.7 mg, 2.90 mmol) were placed. To the Schlenk tube, hexane (5.0 mL) was added and then the mixture was stirred for 6 days at -30 °C. After the solvent was distilled off at room temperature, the crude materials were extracted with hot toluene (ca. 150 mL). The filtrate was concentrated in vacuo, and the residue was washed with hexane to provide an orange powder of **1b** (134 mg, 167 μmol) in 48% yield.

1b: An orange powder; mp 275-276 °C; δ_{H} (500 MHz, C_6D_6 , 300 K) 0.32 (72H, s, SiCH_3), 2.21 (8H, s, CH_2); δ_{C} (125 MHz, C_6D_6 , 333 K) 4.4 (SiCH_3), 19.5 (C), 34.6 (CH_2); δ_{Si} (99 MHz, C_6D_6 , 333 K) 3.0 (SiMe_3), 94.5 (Si), 216.6 ($\text{Si}=\text{Si}$); λ_{max} (hexane)/nm 405sh ($\epsilon/\text{dm}^3 \text{ mol}^{-1} \text{ cm}^{-1}$ 1.8×10^3), 342 (1.4×10^4), 326sh (1.2×10^4); HRMS (APCI) found, 800.34856. Calcd for $\text{C}_{32}\text{H}_{80}\text{Si}_{12}$ [M^+], 800.34857; Found: C, 47.68; H, 10.10. Calcd for $\text{C}_{32}\text{H}_{80}\text{Si}_{12}$: C, 47.92; H, 10.05%.

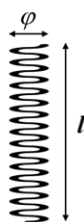
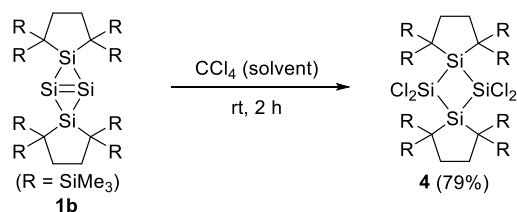


Figure 2-6. Nichrome wire (φ : diameter, l : length).

Reaction of **1b** with Carbon Tetrachloride

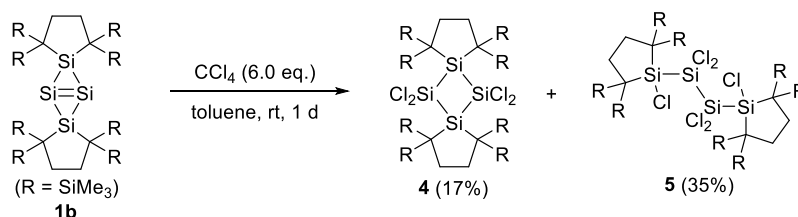


To a Schlenk tube (10 mL) equipped with a magnetic stir bar, **1b** (49.8 mg, 62.1 μmol) was placed. To the Schlenk tube, dry and degassed carbon tetrachloride (2 mL) was transferred and then the mixture was stirred at room temperature for 2 hours. The colour of the resulting suspension turned gradually from orange to yellow. After the volatiles were removed in vacuo, the crude material was washed with hexane to furnish a pale yellow powder of **4** (46.4 mg, 49.2 μmol) in 79% yield.

4: A pale yellow powder; mp 170-173 °C (decomp.); δ_{H} (500 MHz, C_6D_6 , 333 K) 0.43 (72H, s, SiCH_3), 2.09 (8H, s, CH_2); δ_{C} (CP MAS, 294 K) 5.7 (SiCH_3), 7.3 (SiCH_3), 18.8 (C), 37.5 (CH_2); δ_{Si} (CP MAS, 294 K) 6.4 (SiMe_3), 8.8 (SiMe_3), 28.1 (ring Si), 31.6 (ring Si); HRMS (APCI) found, 940.22440. Calcd for $\text{C}_{32}\text{H}_{80}\text{Cl}_4\text{Si}_{12}$ [M^+], 940.22398; Found: C, 40.76; H, 8.36. Calcd for $\text{C}_{32}\text{H}_{80}\text{Cl}_4\text{Si}_{12}$: C, 40.72; H, 8.54%.

We tried to measure the ^{13}C and ^{29}Si NMR spectra of **4**, but **4** is less soluble in organic solvent and measurement of these spectra was unsuccessful.

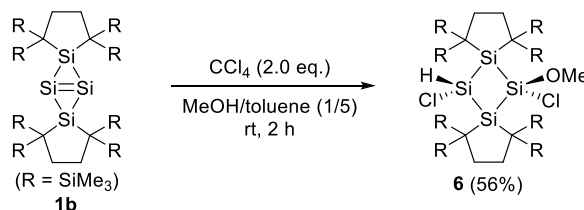
Reaction of **1b** with Carbon Tetrachloride in Toluene



To a Schlenk tube (100 mL) equipped with a magnetic stir bar, **1b** (50.3 mg, 62.7 μmol) and toluene (4.0 mL) were placed. To the Schlenk tube, a toluene solution of carbon tetrachloride (381 μmol , (1.0 mL, 0.381 M)) was added and then the mixture was stirred at room temperature for 1 day. The colour of the resulting suspension turned gradually from orange to pale yellow. After the volatiles were removed in vacuo, the crude material was washed with hexane to give a pale yellow powder of **4** (10.0 mg, 10.6 μmol) in 17% yield. The filtrate was purified by recrystallisation from hot DME to give colourless crystals of **5** (22.1 mg, 21.8 μmol) in 35% yield.

5: Colourless crystals; mp. 234-236 $^{\circ}\text{C}$ (from hexane, decomp.); δ_{H} (500 MHz, C_6D_6 , 298 K) 0.38 (36H, s, SiCH_3), 0.41 (36H, s, SiCH_3), 1.90-2.08 (8H, m, CH_2); δ_{C} (125 MHz, C_6D_6 , 298 K) 4.9 (SiCH_3), 5.3 (SiCH_3), 19.6 (C), 34.6 (CH_2); δ_{Si} (99 MHz, C_6D_6 , 297 K) 3.2 (SiCl_2), 3.5 (SiMe_3), 6.8 (SiMe_3), 39.7 (SiCl); HRMS (APCI) found, 995.13872. Calcd for $\text{C}_{31}\text{H}_{77}\text{Cl}_6\text{Si}_{12}$ [(M-Me) $^+$], 995.13821; Found: C, 38.20; H, 8.07. Calcd for $\text{C}_{32}\text{H}_{80}\text{Cl}_6\text{Si}_{12}$: C, 37.88; H, 7.95%.

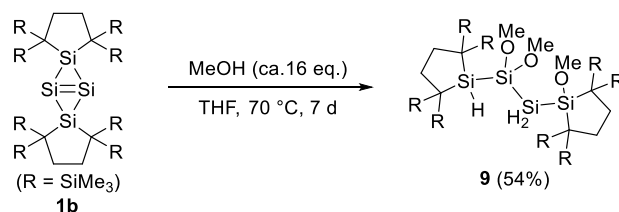
Reaction of **1b** with Carbon Tetrachloride in the presence of Methanol



To a Schlenk tube (20 mL) equipped with a magnetic stir bar, **1b** (30.1 mg, 37.5 μmol), toluene (2.8 mL) and methanol (0.6 mL) were placed. To the Schlenk tube, a toluene solution of carbon tetrachloride (76.2 μmol , (0.2 mL, 0.381 M)) was added and then the mixture was stirred at room temperature for 2 hours. The colour of the resulting suspension turned gradually from orange to pale yellow. After the volatiles were removed in vacuo, the crude material was purified by recrystallisation from hot hexane to provide yellow crystals of **6** (18.9 mg, 20.9 μmol) in 56% yield.

6: Yellow crystals; mp 163-165 $^{\circ}\text{C}$ (from hexane, decomp.); δ_{H} (500 MHz, C_6D_6 , 295 K) 0.33 (18H, s, SiCH_3), 0.42 (18H, s, SiCH_3), 0.44 (18H, s, SiCH_3), 0.46 (18H, s, SiCH_3), 1.75-1.90 (4H, m, CH_2), 2.03-2.20 (4H, m, CH_2), 3.55 (3H, s, OCH_3), 5.73 (1H, s, SiH); δ_{C} (125 MHz, C_6D_6 , 297 K) 4.6 (SiCH_3), 5.0 (SiCH_3), 5.5 (SiCH_3), 6.0 (SiCH_3), 15.4 (C), 16.2 (C), 36.5 (CH_2), 36.6 (CH_2), 53.8 (OCH_3); δ_{Si} (99 MHz, C_6D_6 , 296 K) -16.5 (SiHCl), 4.9 (SiMe_3), 5.2 (SiMe_3), 5.8 (SiMe_3), 6.0 (SiMe_3), 11.8 ($\text{Si}(\text{OMe})\text{Cl}$), 22.9 (Si); HRMS (APCI) found, 901.30481. Calcd for $\text{C}_{33}\text{H}_{83}\text{Cl}_2\text{OSi}_{12}$ [(M-H) $^+$], 901.30467; Found: C, 43.70; H, 9.35. Calcd for $\text{C}_{33}\text{H}_{84}\text{Cl}_2\text{OSi}_{12}$: C, 43.80; H, 9.36%.

Reaction of **1b** with Methanol



To a stock bottle (10 mL) equipped with a magnetic stir bar, **1b** (50.3 mg, 62.7 μmol) was placed. To the bottle, dry and degassed THF (5.0 ml) and methanol (ca.32 mg, 1.0 mmol) were added, and then the mixture was stirred at 70 $^{\circ}\text{C}$ for 7 days. The colour of the resulting suspension turned to pale yellow from orange. After the volatiles were removed in vacuo, the crude was purified by GPC (eluent: toluene) to provide a white solid of **9** (30.1 mg, 33.5 μmol) in 54% yield.

9: A white solid; mp 150-152 °C (decomp.); δ_{H} (500 MHz, C_6D_6 , 298 K) 0.31 (18H, s, SiCH_3), 0.32 (18H, s, SiCH_3), 0.35 (36H, s, SiCH_3), 1.86-2.16 (8H, m, CH_2), 3.56 (3H, s, OCH_3), 3.59 (6H, s, OCH_3), 3.62 (2H, s, SiH), 4.46 (1H, s, SiH); δ_{C} (125 MHz, C_6D_6 , 298 K) 2.9 (SiCH_3), 3.7 (SiCH_3), 4.1 (SiCH_3), 4.8 (SiCH_3), 7.7 (C), 18.8 (C), 34.3 (CH_2), 34.9 (CH_2), 53.4 (OCH_3), 54.0 (OCH_3); δ_{Si} (99 MHz, C_6D_6 , 298 K) -110.6 (SiH_2), -18.7 (SiH), 1.5 (SiMe_3), 3.3 (SiMe_3), 3.7 (SiMe_3), 4.9 (SiMe_3), 9.0 ($\text{Si}(\text{OMe})_2$), 41.7 (SiOMe); HRMS (APCI) found, 895.41979. Calcd for $\text{C}_{35}\text{H}_{91}\text{O}_3\text{Si}_{12}$ [(M-H)⁺], 895.41939; Found: C, 46.97; H, 10.31. Calcd for $\text{C}_{35}\text{H}_{92}\text{O}_3\text{Si}_{12}$: C, 46.81; H, 10.33%.

NMR Spectra

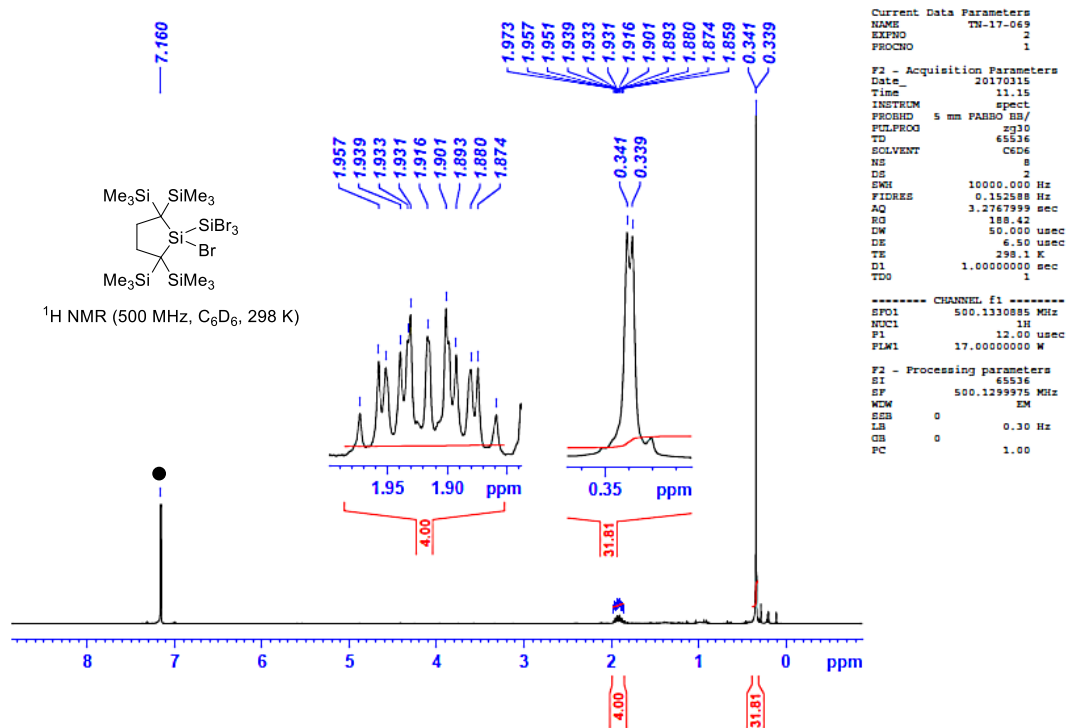


Figure 2-7. ¹H NMR spectrum of **3** in C_6D_6 at 298 K (● = C_6HD_5).

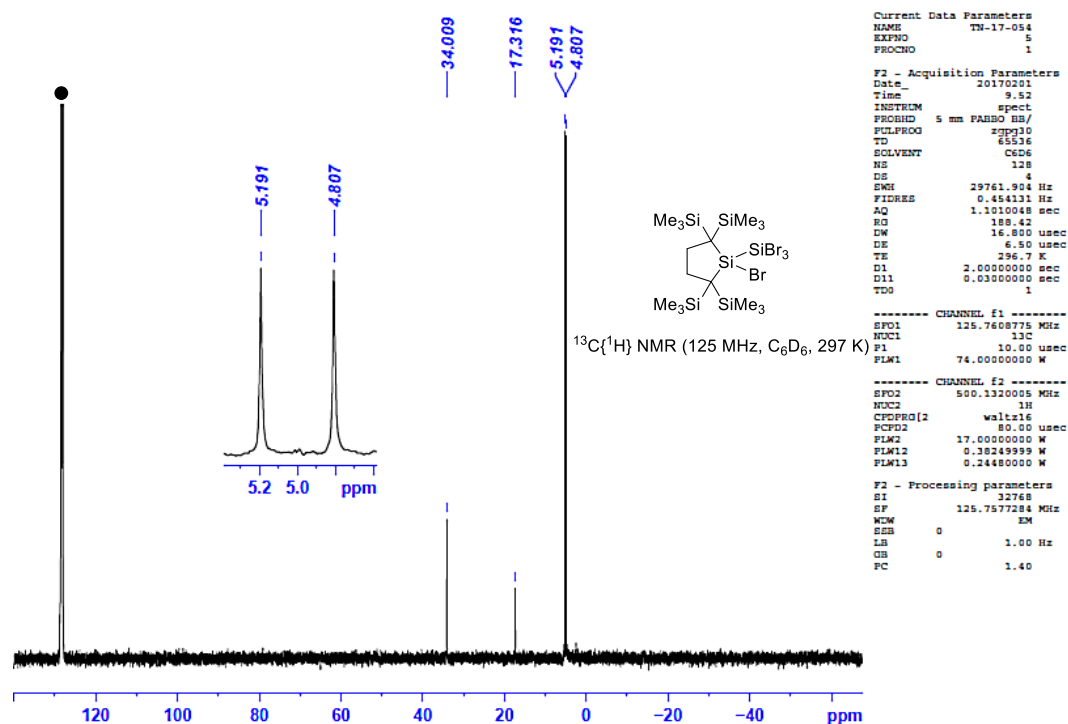


Figure 2-8. ¹³C{¹H} NMR spectrum of **3** in C₆D₆ in 297 K (● = C₆D₆).

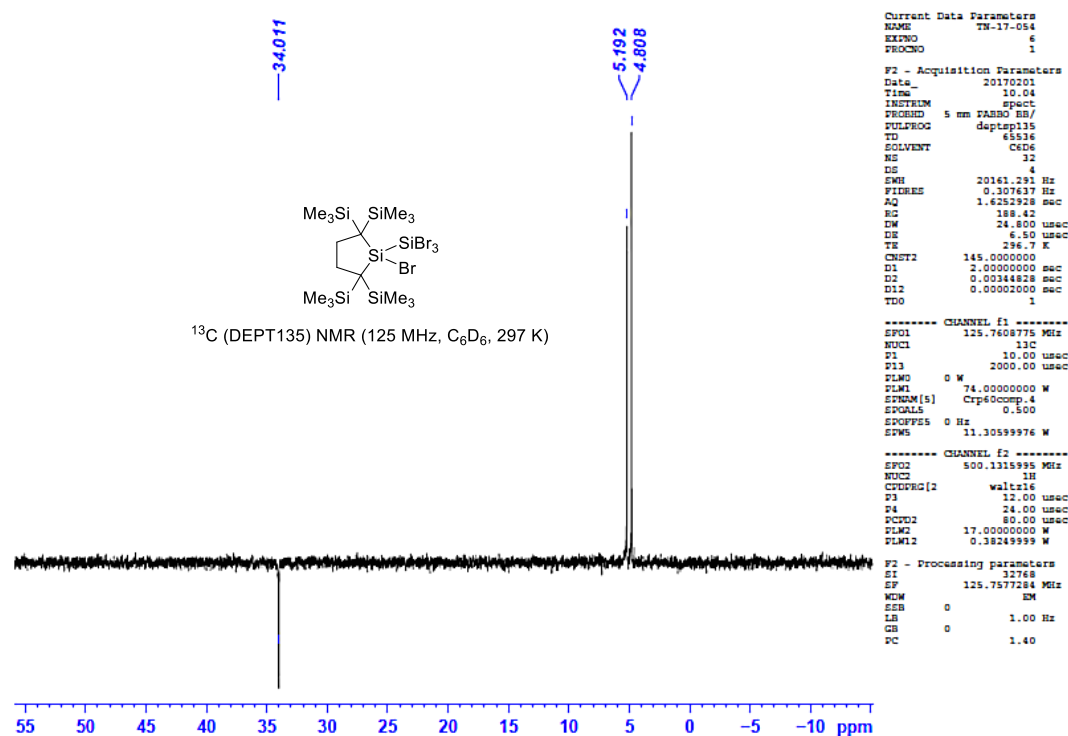


Figure 2-9. ¹³C (DEPT135) NMR spectrum of **3** in C₆D₆ at 297 K.

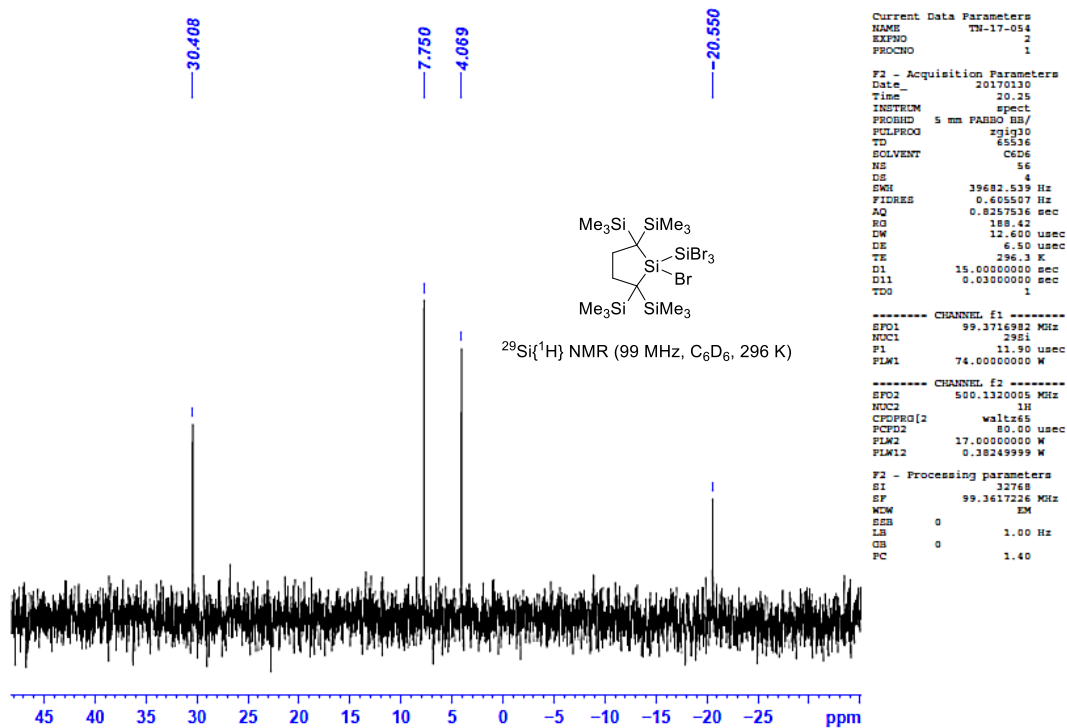


Figure 2-10. $^{29}\text{Si}\{^1\text{H}\}$ NMR spectrum of **3** in C_6D_6 at 296 K.

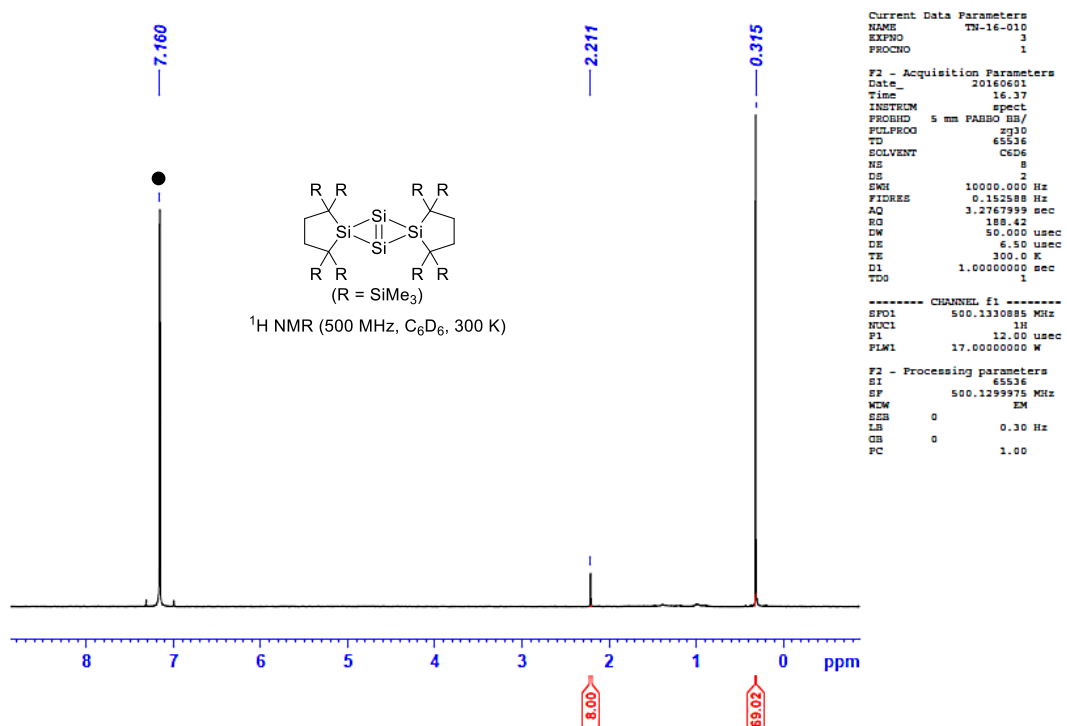


Figure 2-11. ^1H NMR spectrum of **1b** in C_6D_6 at 300 K (● = C_6HD_5).

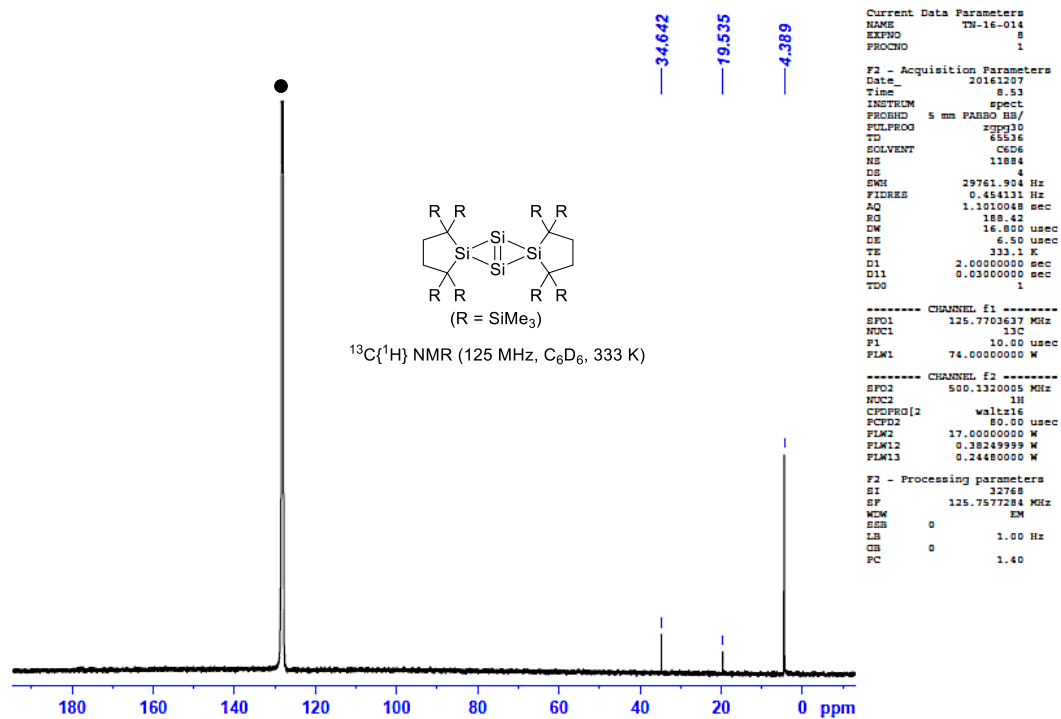


Figure 2-12. ¹³C{¹H} NMR spectrum of **1b** in C₆D₆ at 333 K (● = C₆D₆).

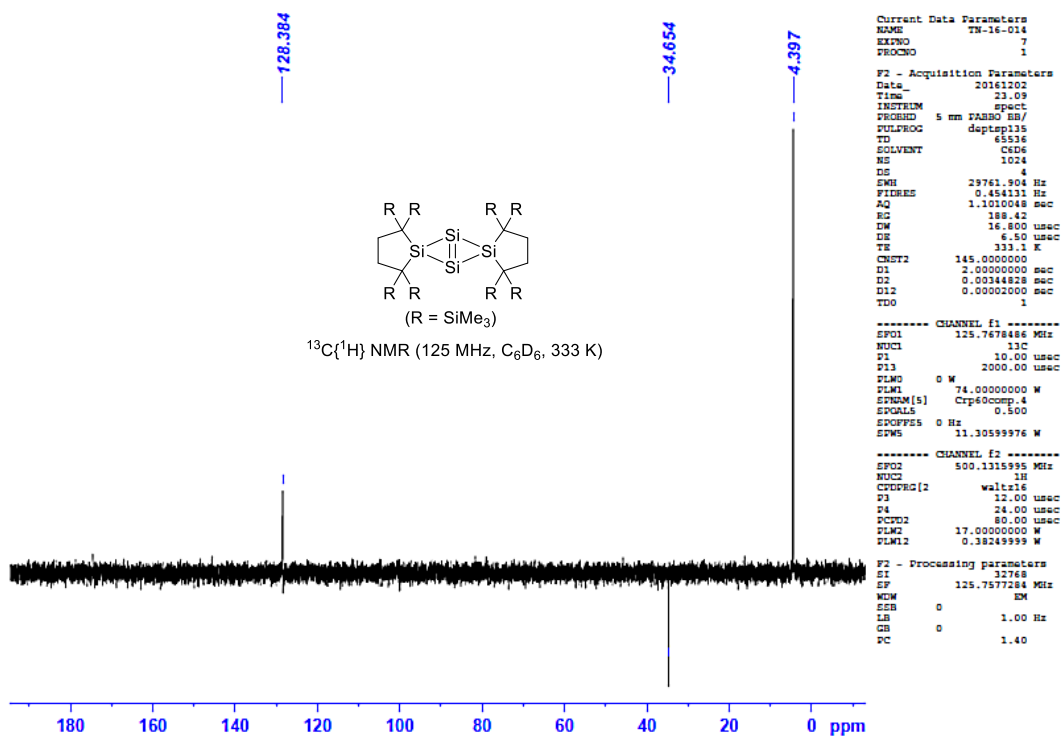


Figure 2-13. ¹³C (DEPT135) NMR spectrum of **1b** in C₆D₆ at 333 K.

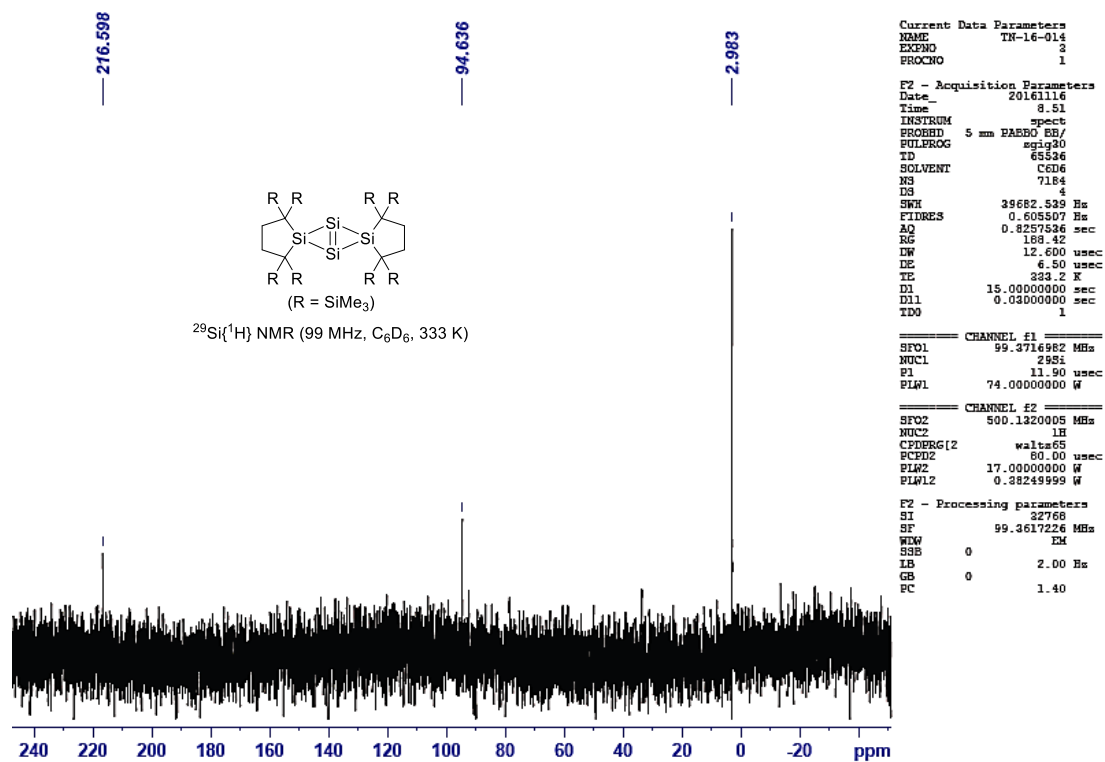


Figure 2-14. ²⁹Si{¹H} NMR spectrum of **1b** in C₆D₆ at 333 K.

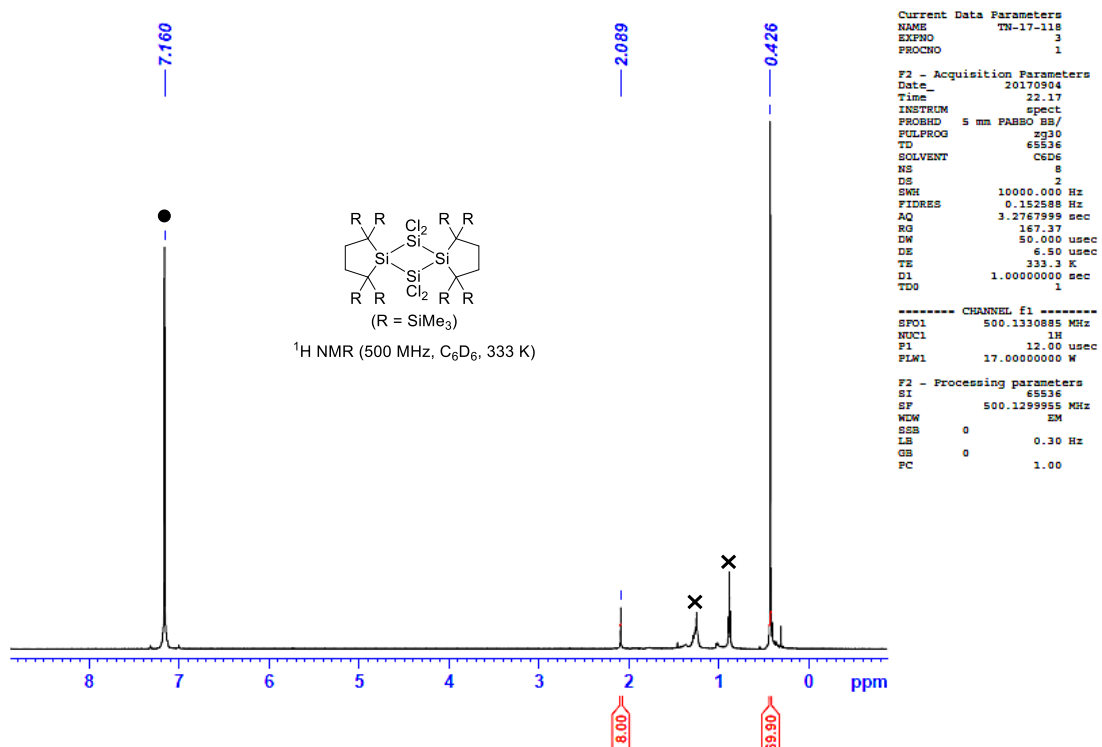


Figure 2-15. ¹H NMR spectrum of **4** in C₆D₆ at 333 K (● = C₆HD₅, × = hexane).

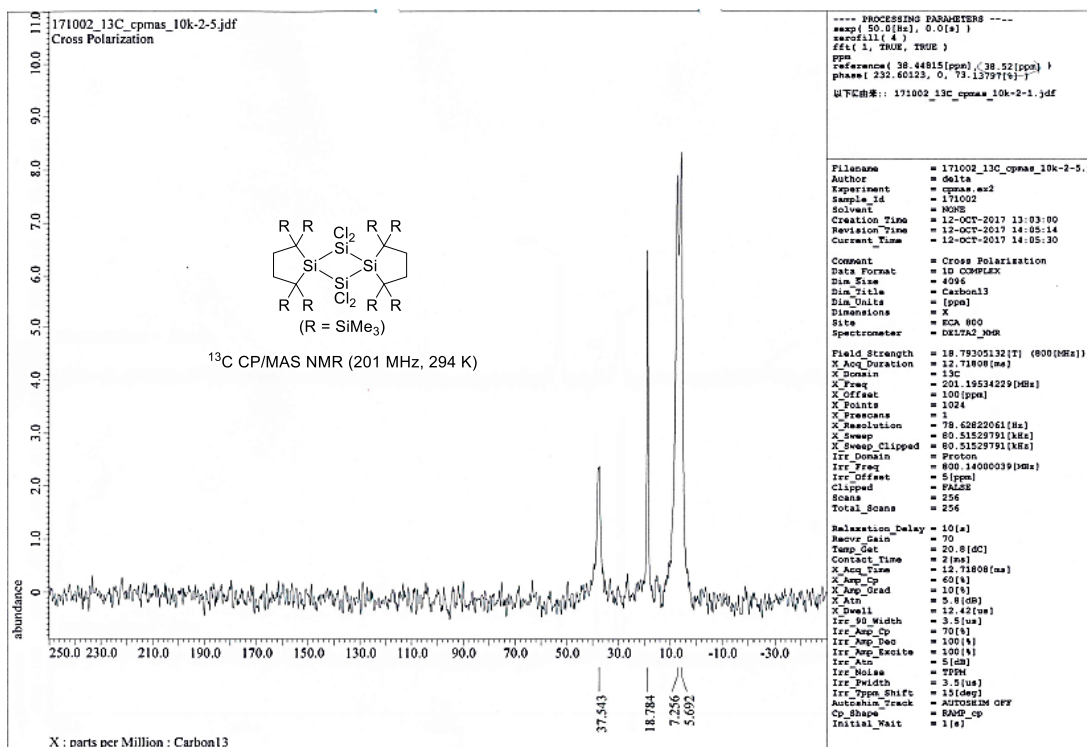


Figure 2-16. ¹³C{¹H} CP/MAS spectrum of **4** at 294 K.

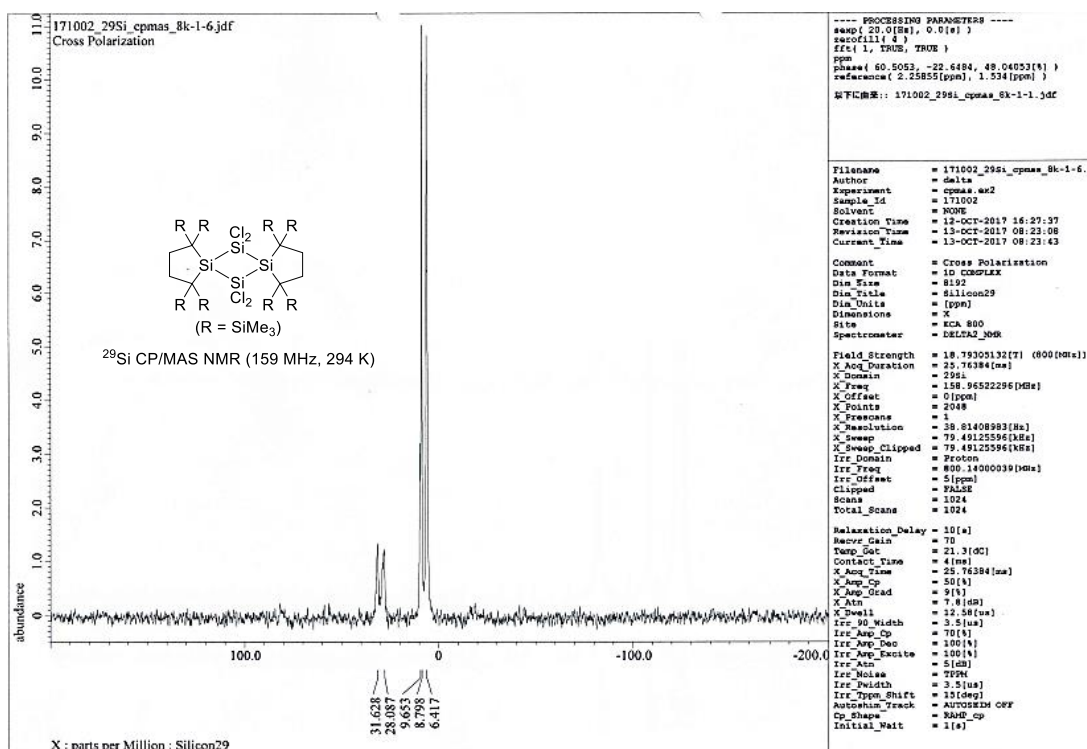


Figure 2-17. ²⁹Si{¹H} CP/MAS spectrum of **4** at 294 K.

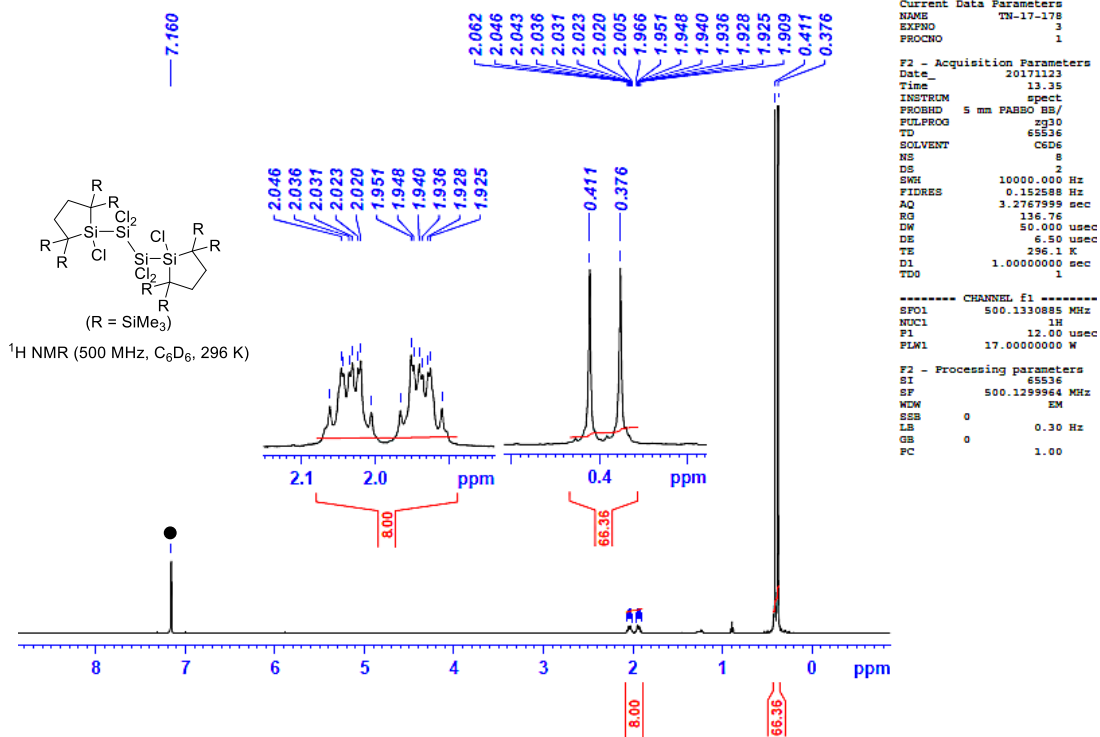


Figure 2-18. ^1H NMR spectrum of **5** in C_6D_6 at 296 K (● = C_6HD_5).

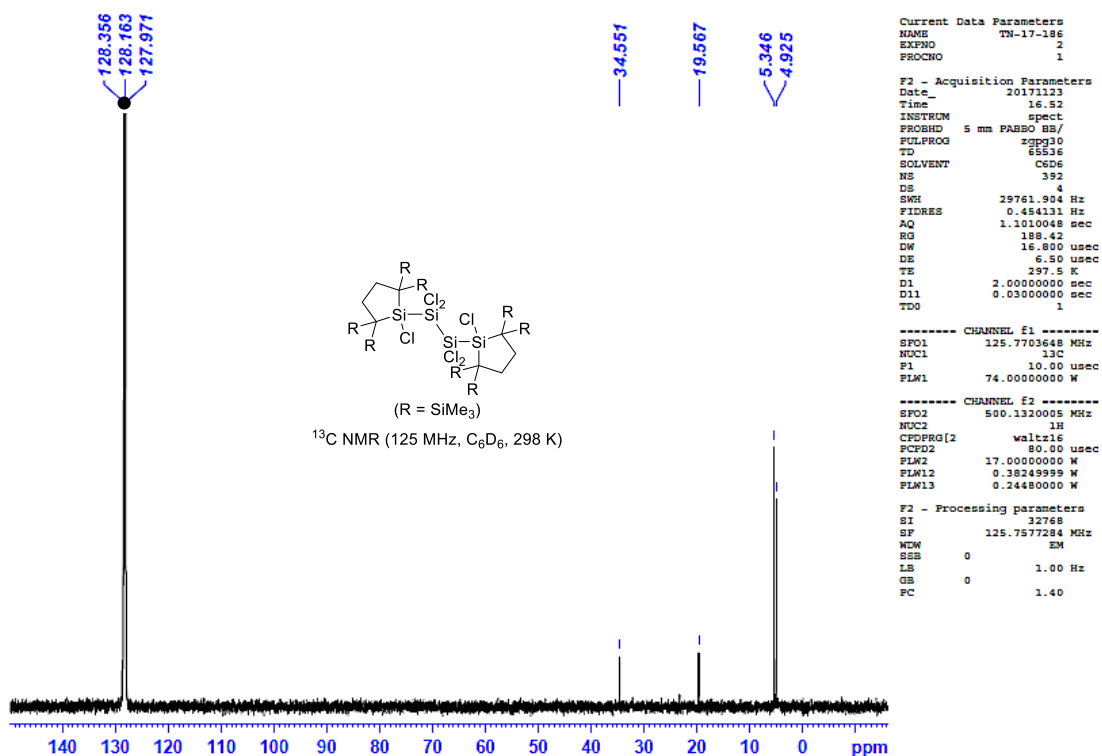


Figure 2-19. $^{13}\text{C}\{^1\text{H}\}$ NMR spectrum of **5** in C_6D_6 at 298 K (● = C_6D_6).

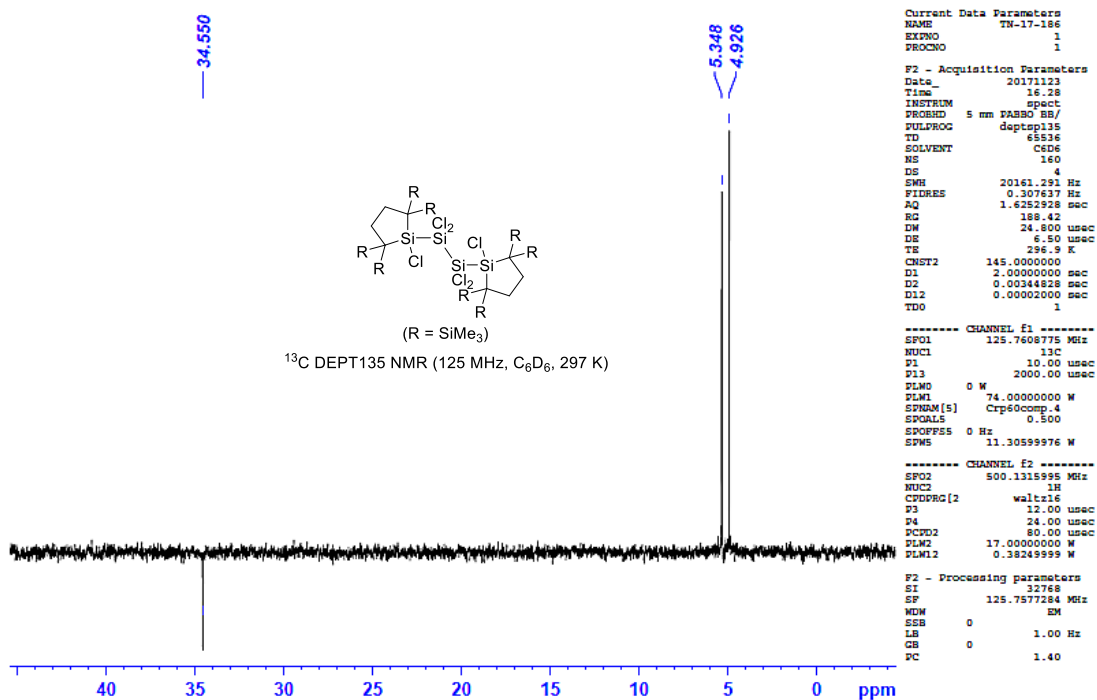


Figure 2-20. ¹³C (DEPT135) NMR spectrum of **5** in C₆D₆ at 297 K.

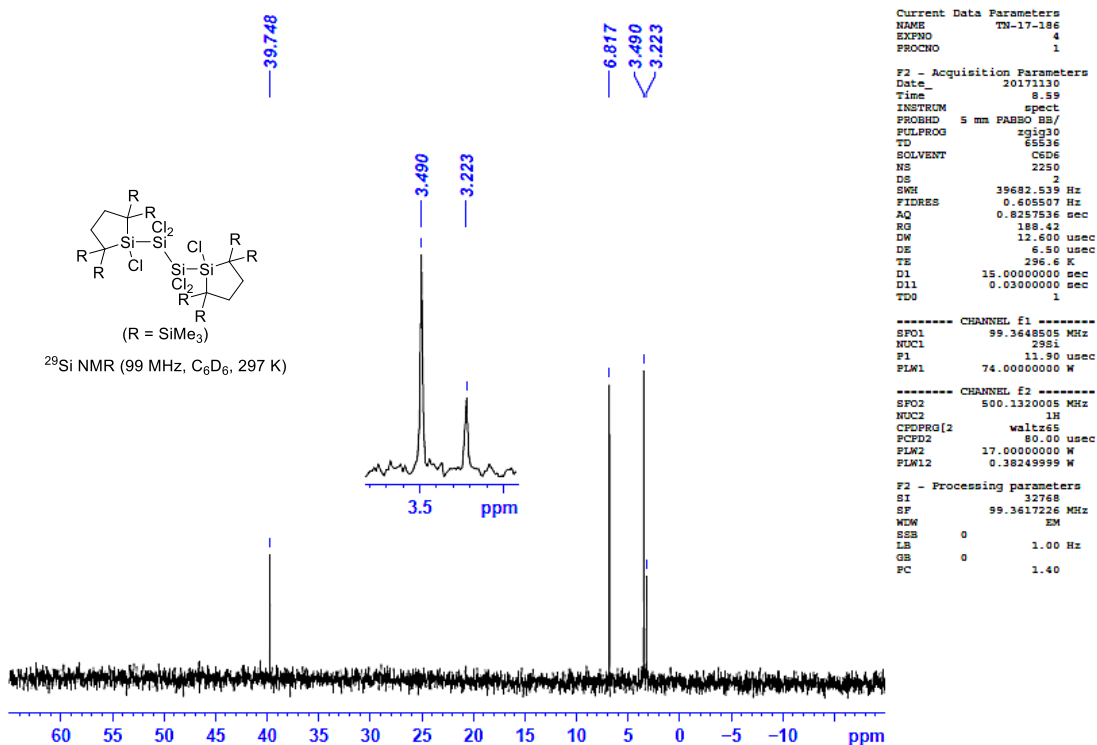


Figure 2-21. ²⁹Si{¹H} NMR spectrum of **5** in C₆D₆ at 297 K.

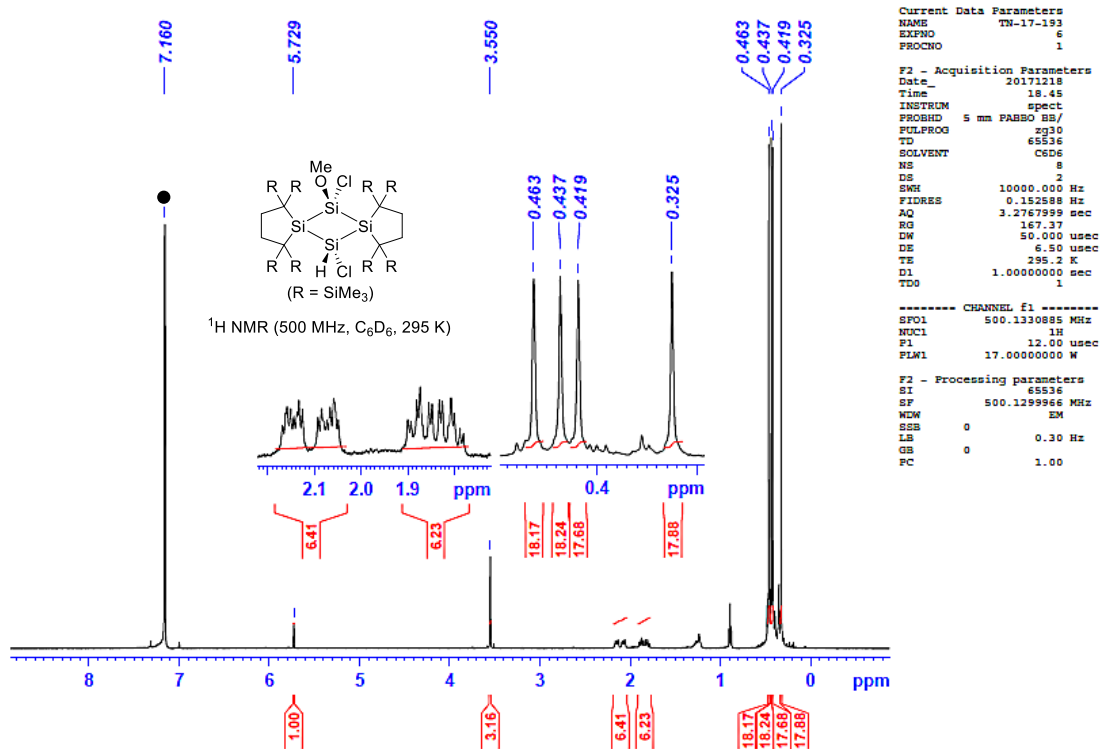


Figure 2-22. ¹H NMR spectrum of **6** in C₆D₆ at 295 K (● = C₆HD₅).

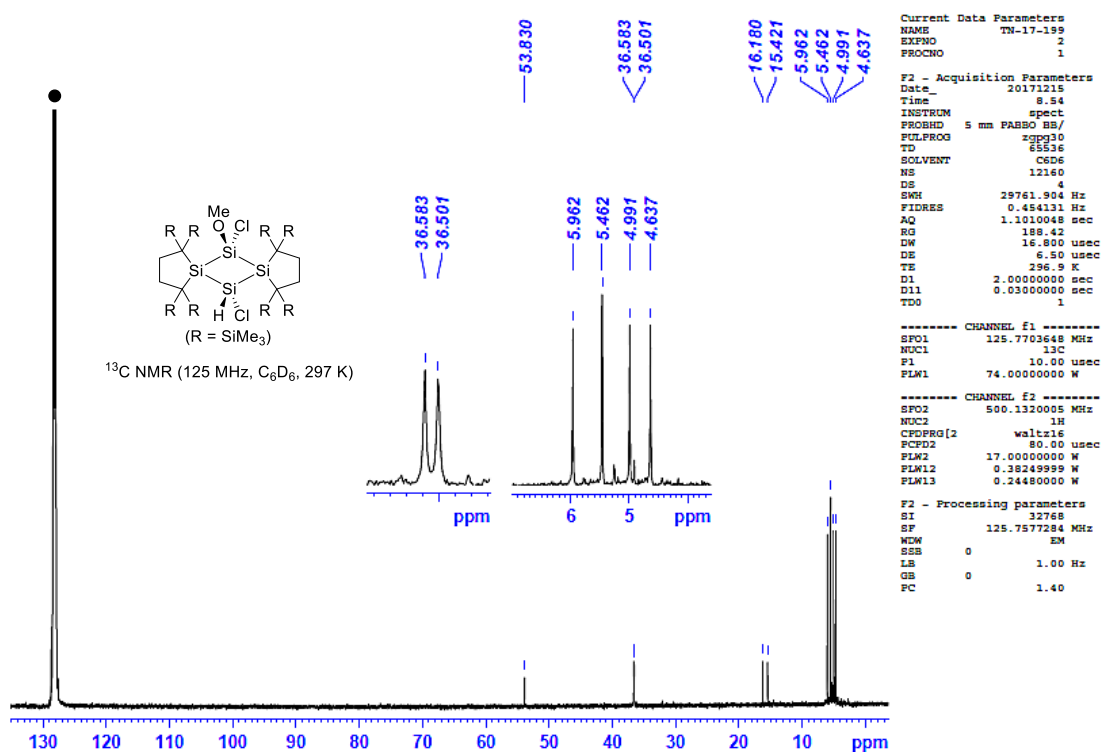


Figure 2-23. ¹³C{¹H} NMR spectrum of **6** in C₆D₆ at 297 K (● = C₆D₆).

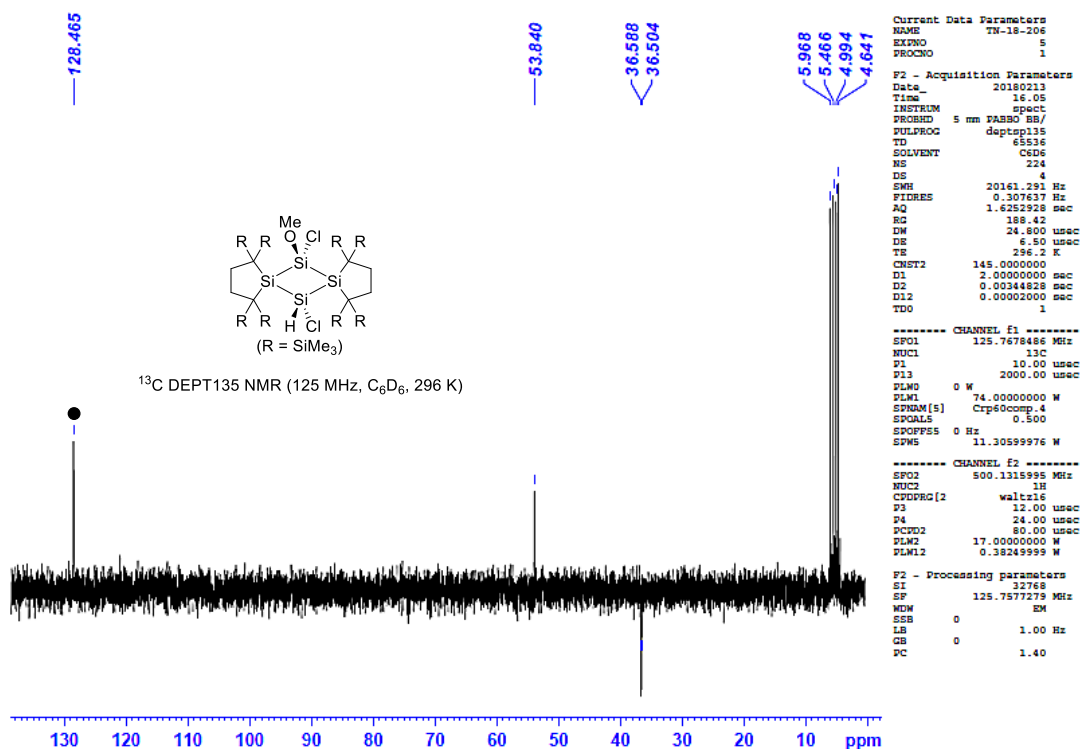


Figure 2-24. ^{13}C (DEPT135) NMR spectrum of **6** in C_6D_6 at 296 K (● = C_6D_6).

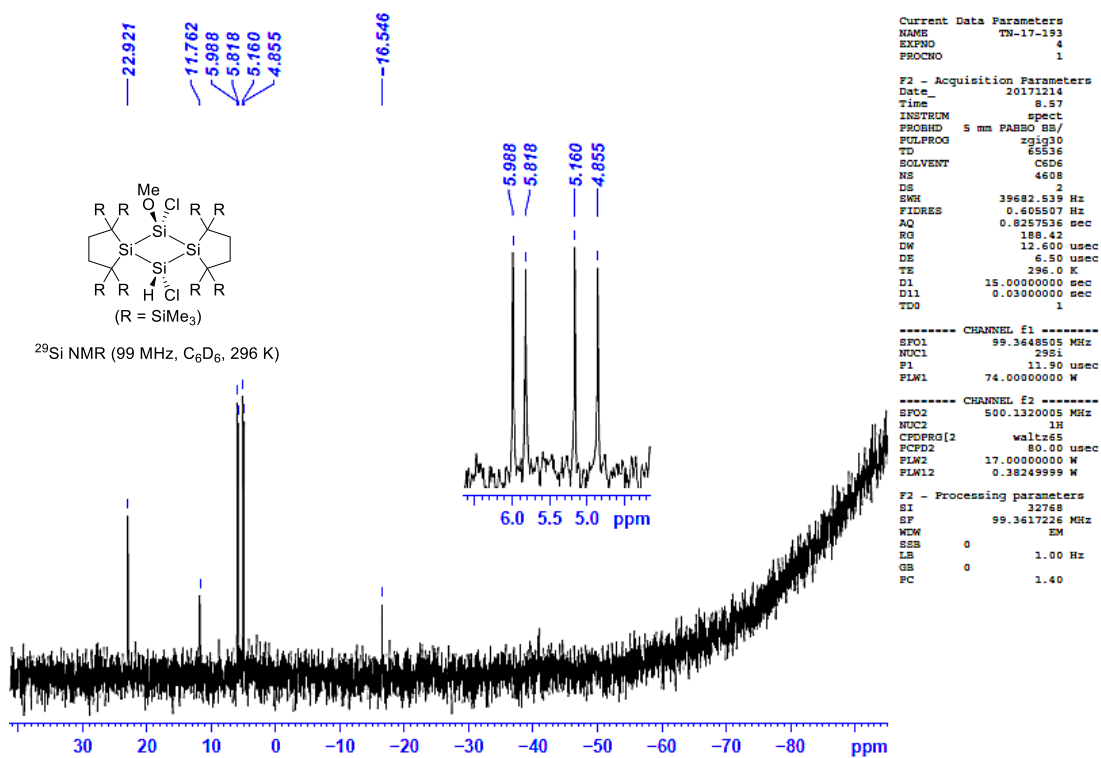


Figure 2-25. $^{29}\text{Si}\{^1\text{H}\}$ NMR spectrum of **6** in C_6D_6 at 296 K.

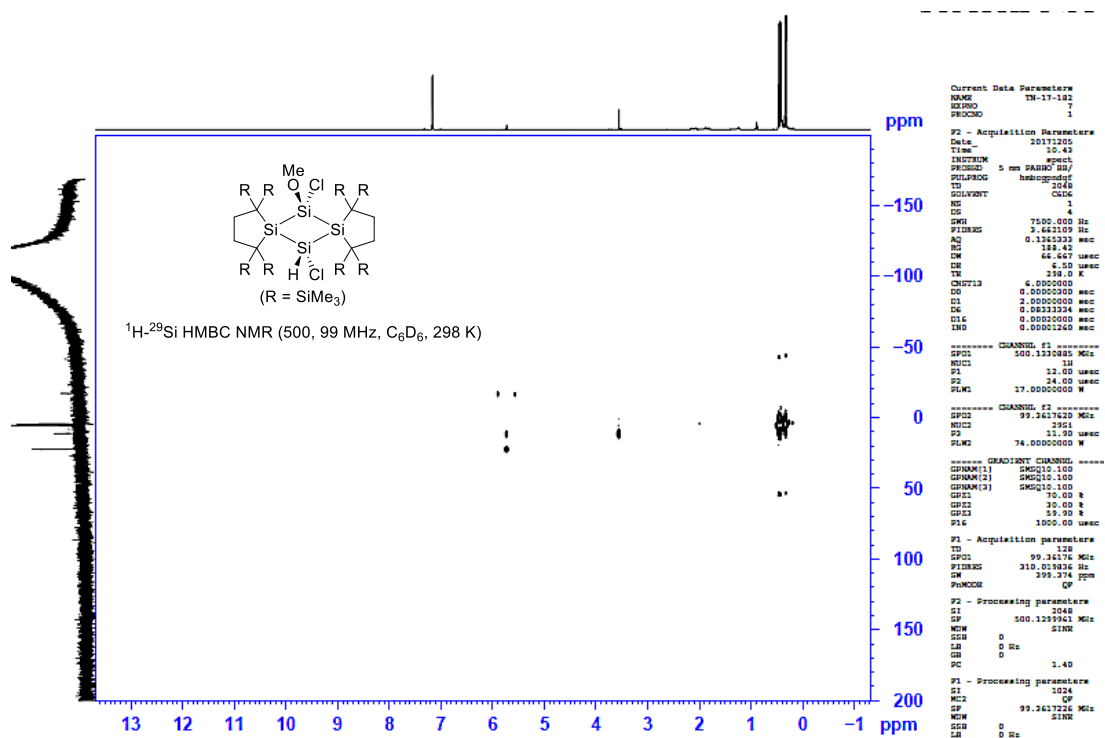


Figure 2-26. ^1H - ^{29}Si HMBC NMR spectrum of **6** in C_6D_6 at 298 K.

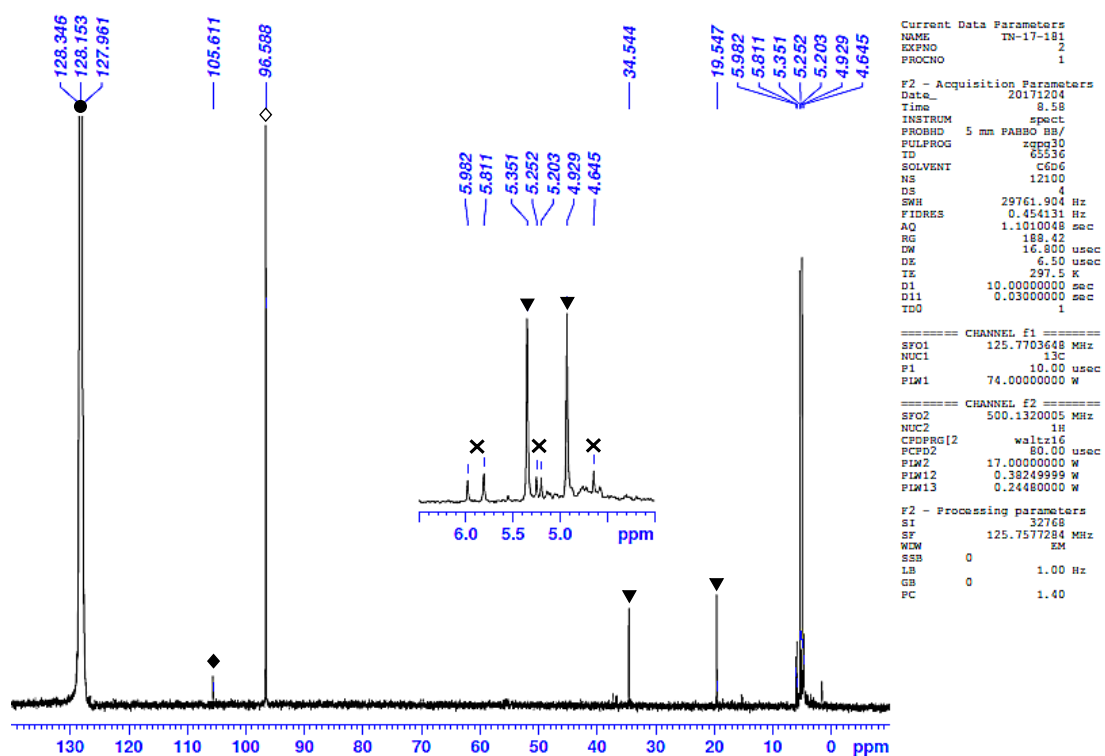


Figure 2-27. ^{13}C NMR spectrum of the reaction mixture of **1b** with CCl_4 in C_6D_6 at 298 K (\bullet = C_6D_6 , \blacktriangledown = **5**, \diamond = Carbon Tetrachloride, \blacklozenge = Hexachloroethane, \times = by products).

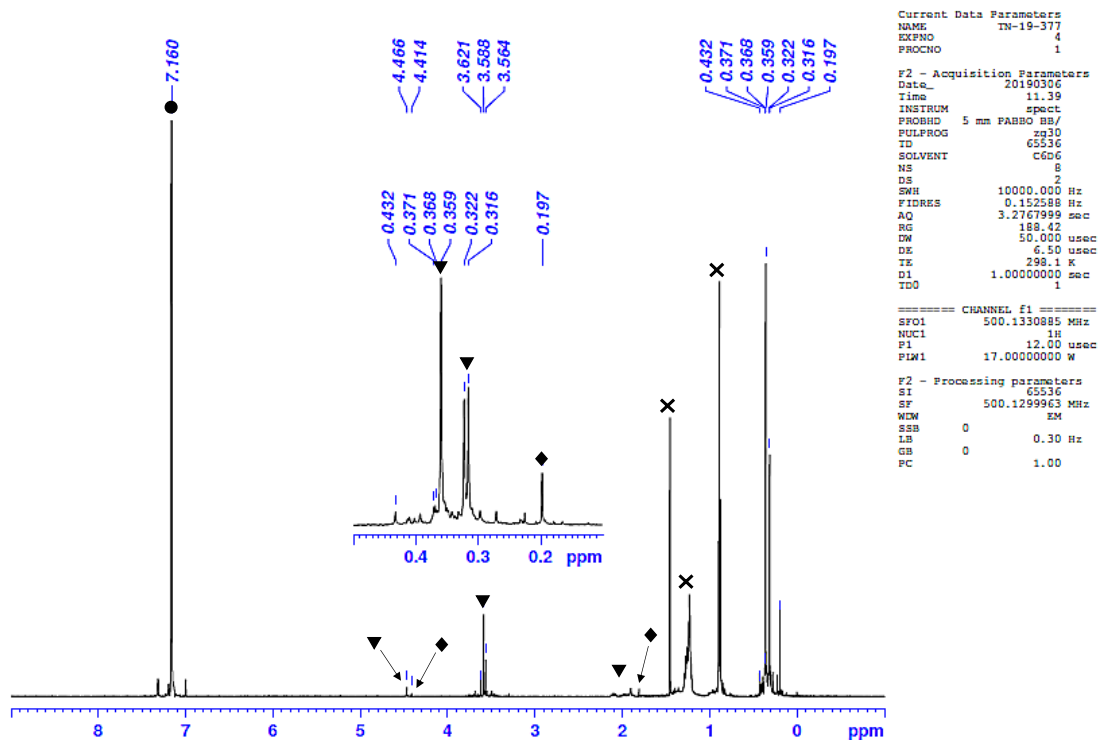


Figure 2-28. ^1H NMR spectrum of the reaction mixture of **1b** with MeOH in C_6D_6 at 298 K ($\bullet = \text{C}_6\text{HD}_5$, $\blacktriangledown = \mathbf{9}$, $\blacklozenge = \text{Dihydrosilane}^{18}$, $\times = \text{impurity}$).

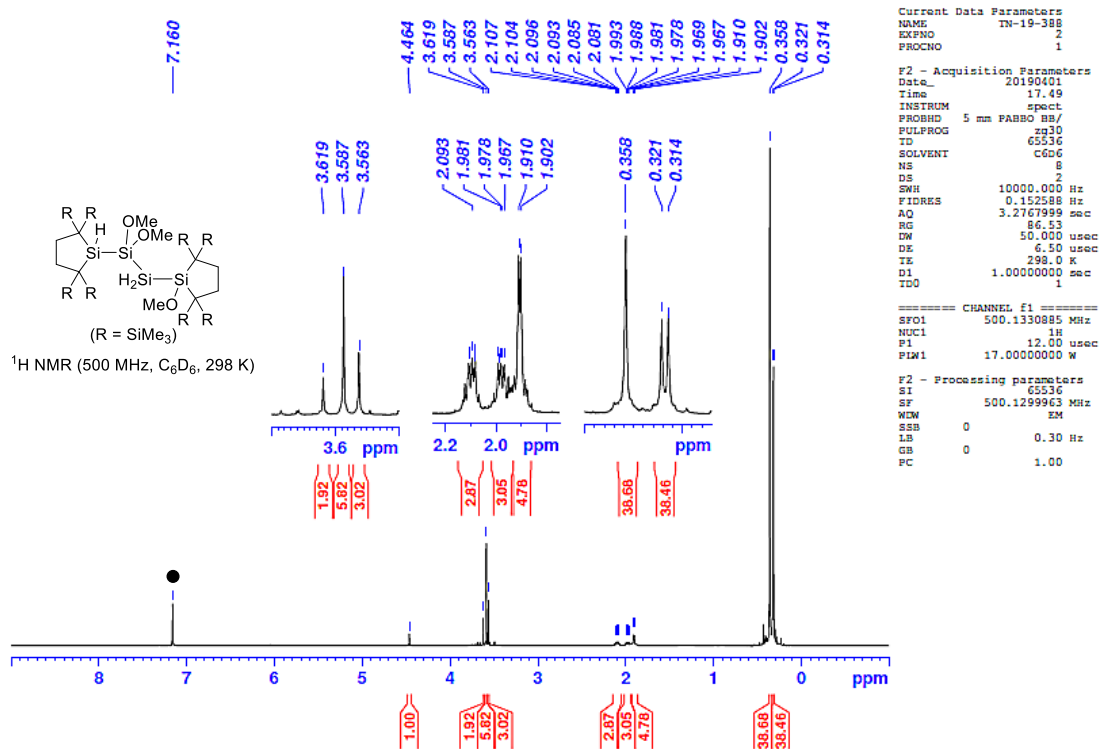


Figure 2-29. ^1H NMR spectrum of **9** in C_6D_6 at 298 K ($\bullet = \text{C}_6\text{HD}_5$).

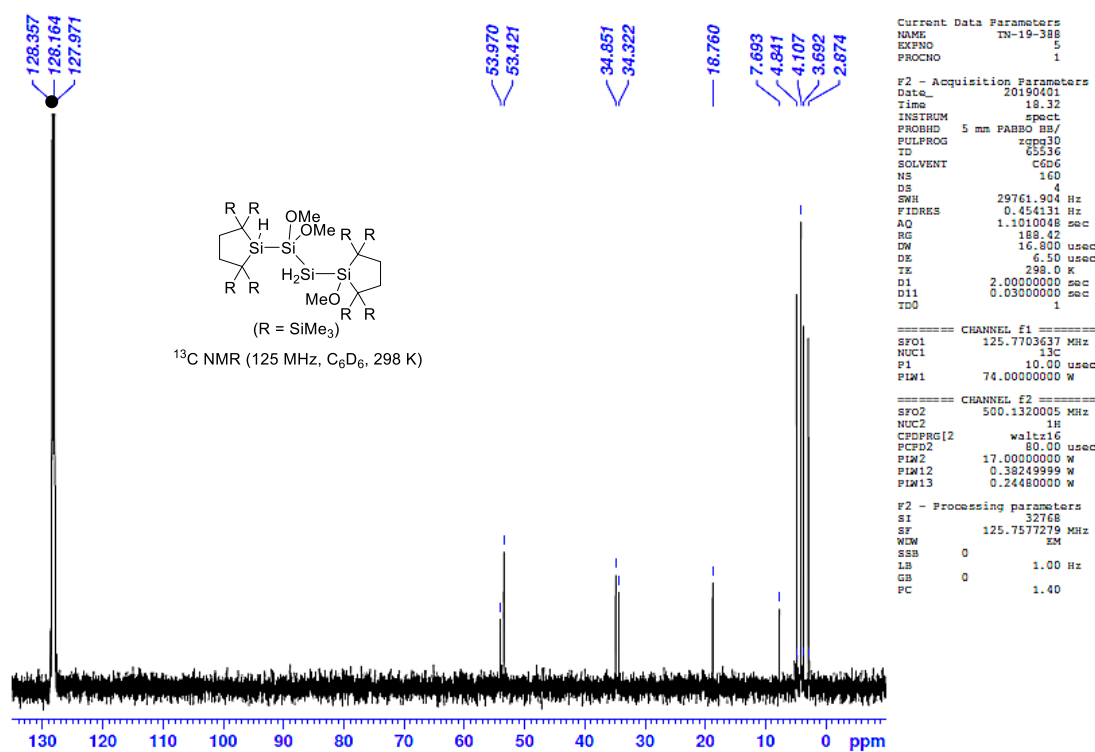


Figure 2-30. $^{13}\text{C}\{^1\text{H}\}$ spectrum of **9** in C_6D_6 at 298 K (● = C_6D_6).

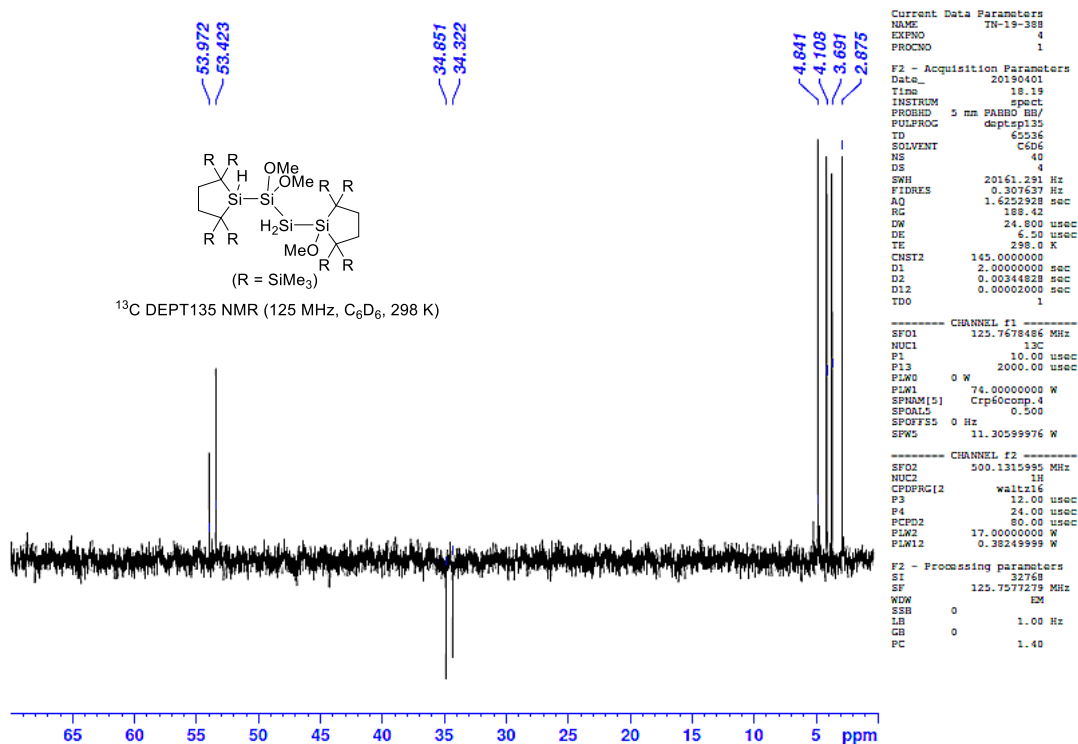


Figure 2-31. ^{13}C (DEPT135) NMR spectrum of **9** in C_6D_6 at 298 K.

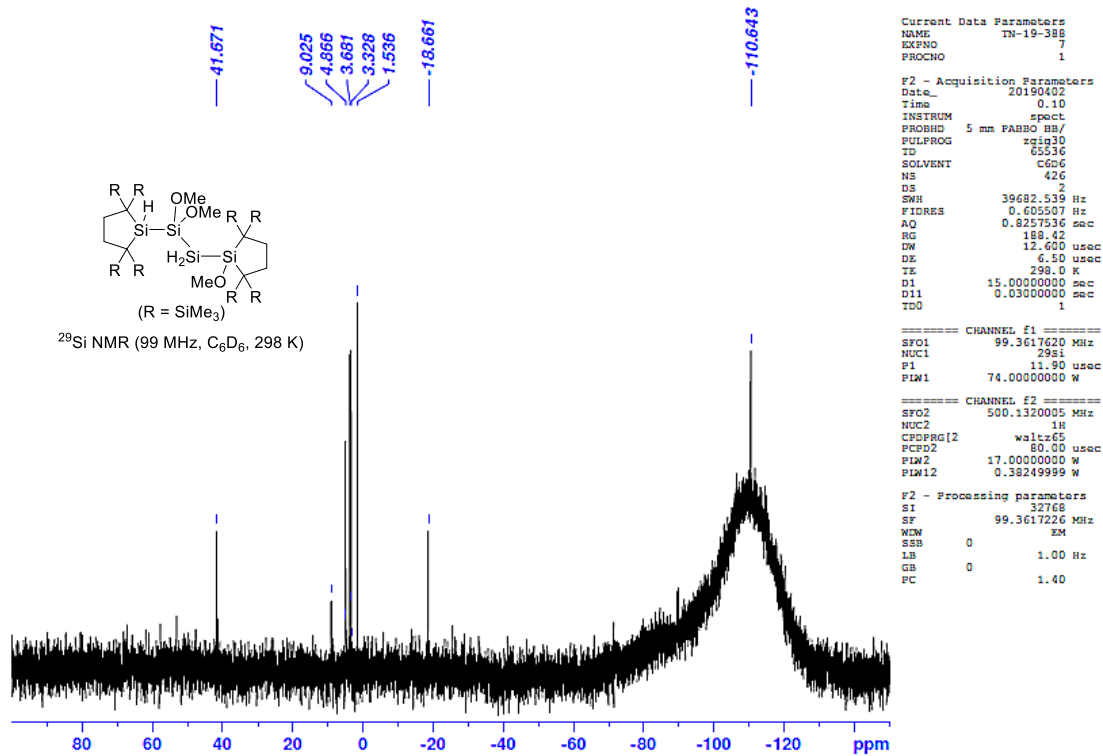


Figure 2-32. ²⁹Si{¹H} spectrum of **9** in C₆D₆ at 298 K.

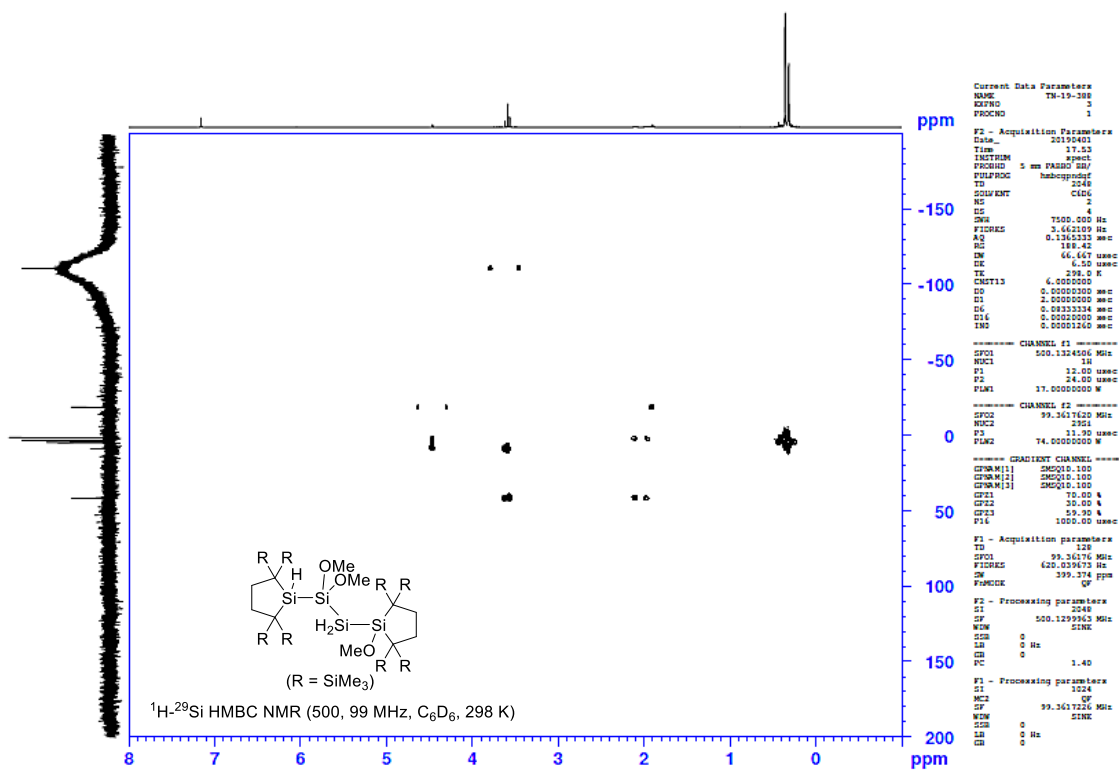


Figure 2-33. ¹H-²⁹Si HMBC NMR spectrum of **9** in C₆D₆ at 298 K.

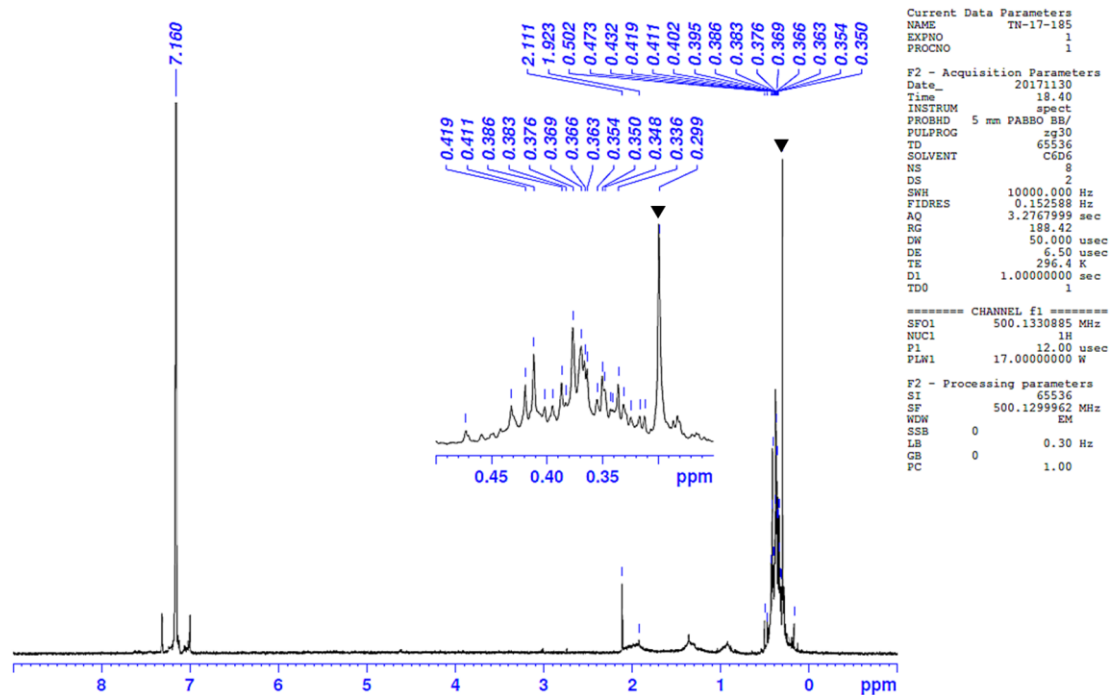


Figure 2-34. ^1H NMR spectrum for the reaction mixture of **1b** with 2 equivalents of CCl_4 recorded in C_6D_6 at 296 K (\blacktriangledown = silicon grease).

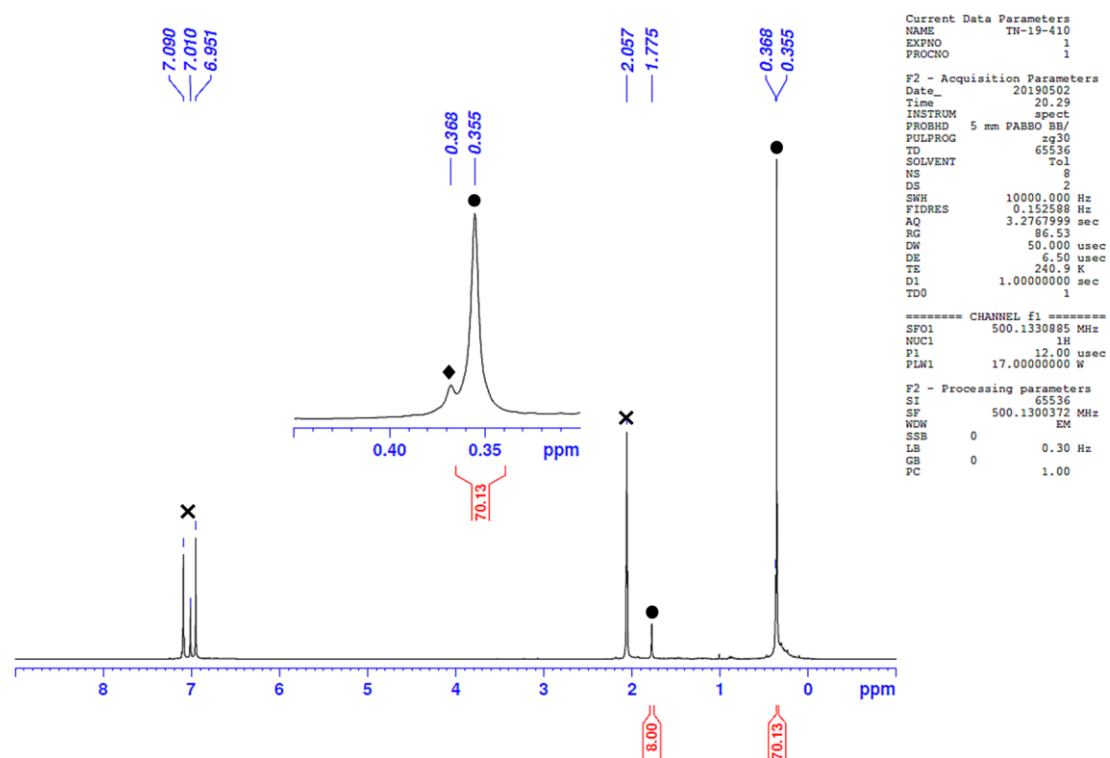


Figure 2-35. ^1H NMR spectrum of the mixture after addition of excess carbon tetrachloride to a toluene- d_8 solution of **1b** at 241 K (\bullet = intermediate, \blacklozenge = **4**, \times = $\text{C}_7\text{D}_7\text{H}$).

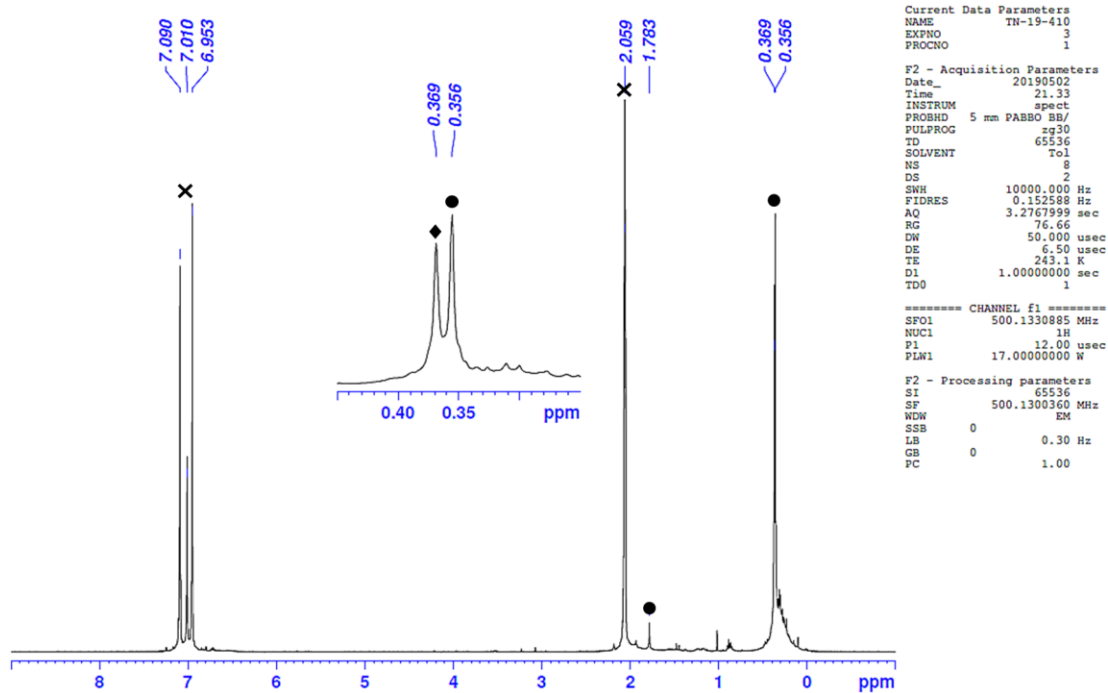


Figure 2-36. ^1H NMR spectrum of the reaction mixture after the reaction of **1b** with excess carbon tetrachloride for 1 hour in toluene- d_8 at 243 K (● = intermediate, ◆ = **4**, × = $\text{C}_7\text{D}_7\text{H}$).

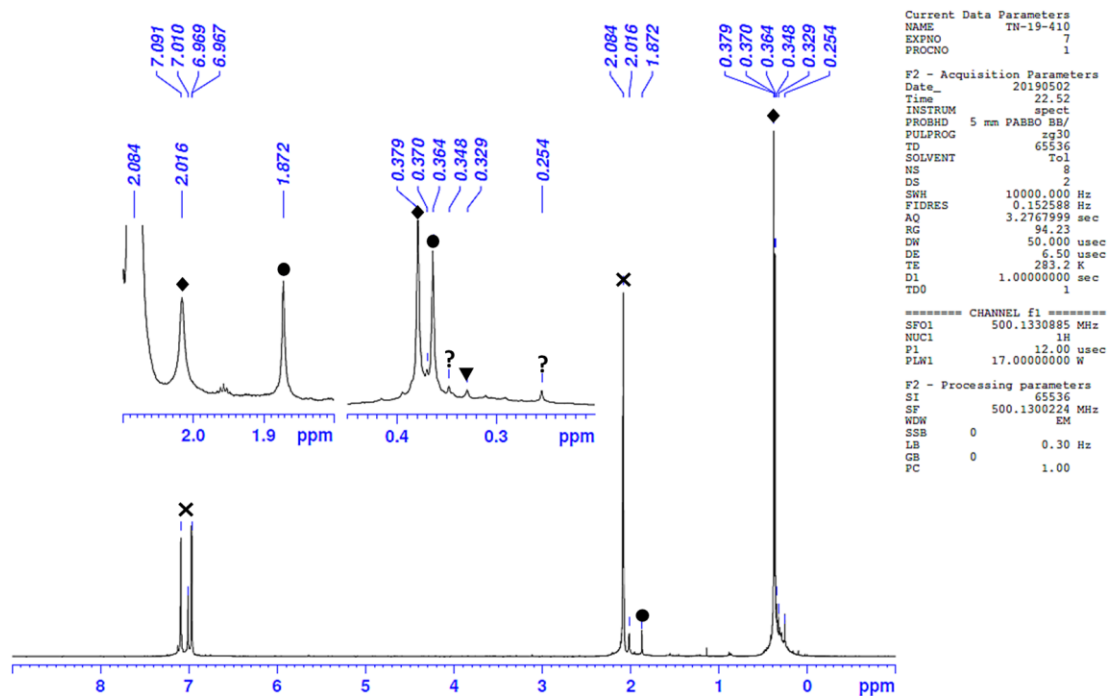


Figure 2-37. ^1H NMR spectrum of the reaction mixture of the reaction of **1b** with excess carbon tetrachloride in toluene- d_8 at 283 K (● = intermediate, ◆ = **4**, ▼ = **5**, × = $\text{C}_7\text{D}_7\text{H}$).

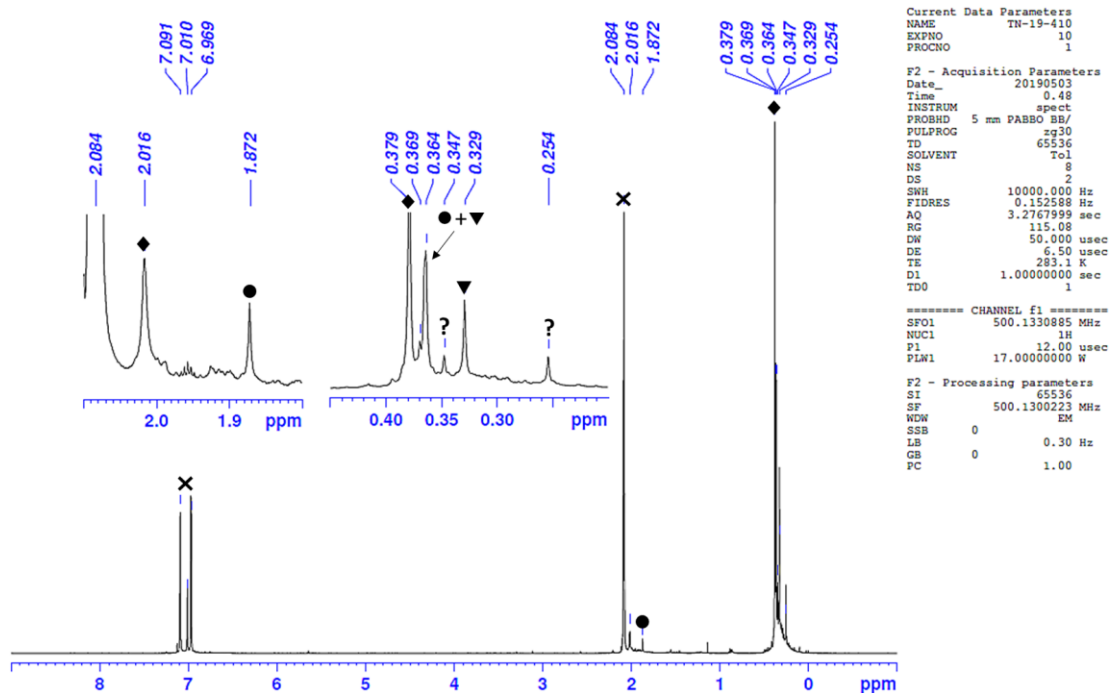


Figure 2-38. ^1H NMR spectrum of the reaction mixture of the reaction of **1b** with excess carbon tetrachloride in toluene- d_8 for additional 2 hours at 283 K (\bullet = intermediate, \blacklozenge = **4**, \blacktriangledown = **5**, \times = $\text{C}_7\text{D}_7\text{H}$).

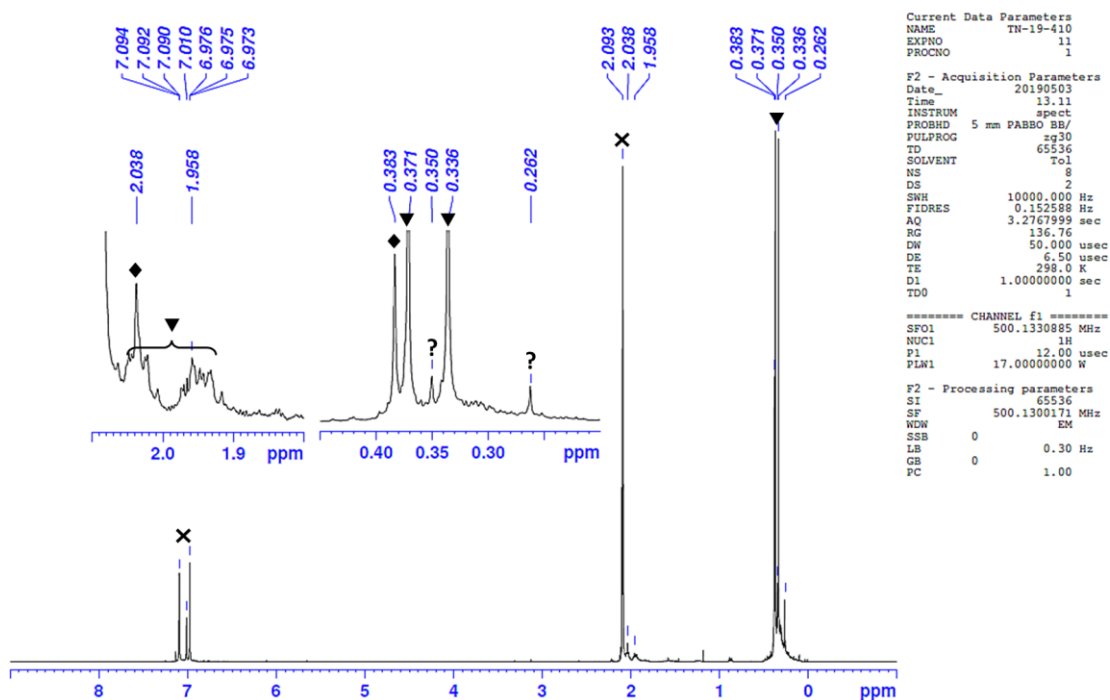


Figure 2-39. ^1H NMR spectrum of the reaction mixture of the reaction of **1b** with excess carbon tetrachloride in toluene- d_8 for additional several hours at 298 K (\blacklozenge = **4**, \blacktriangledown = **5**, \times = $\text{C}_7\text{D}_7\text{H}$).

X-ray Diffraction Analysis

Single crystals suitable for X-ray diffraction study were obtained by recrystallisation in an inert atmosphere using the following conditions; from toluene at room temperature for **1b**, from toluene at room temperature for **4**, from hexane at $-35\text{ }^{\circ}\text{C}$ for **5**, from hexane at room temperature for **6**, and from hexane at $-35\text{ }^{\circ}\text{C}$ for **9**. For data collection, the single crystals coated by Apiezon grease were mounted on the glass fibre and then transferred to the cold nitrogen gas stream of the diffractometer. X-ray diffraction data were collected on a Bruker AXS APEX II CCD diffractometer using a graphite monochromated Mo-K α radiation. An empirical absorption correction based on the multiple measurements of equivalent reflections was applied using the program SADABS¹⁹ and the structures were solved by direct methods and refined by full-matrix least squares against F^2 using all data (SHELXL-2014).²⁰ Molecular structure was analysed by Yadokari-XG software.²¹

Crystal data of **1b** (100 K) [CCDC-1908502]: $\text{C}_{32}\text{H}_{80}\text{Si}_{12}$; Fw 802.04; triclinic; $P-1$, $a = 9.2308(5)\text{ \AA}$, $b = 11.5172(6)\text{ \AA}$, $c = 13.2387(6)\text{ \AA}$, $\alpha = 64.9580(10)^{\circ}$, $\beta = 75.3080(10)^{\circ}$, $\gamma = 66.7880(10)^{\circ}$, $V = 1165.54(10)\text{ \AA}^3$, $Z = 1$, $D_{\text{calc}} = 1.143\text{ Mg/m}^3$, $R1 = 0.0333$ ($I > 2\sigma(I)$), $wR2 = 0.0841$ (all data), GOF = 0.997.

Crystal data of **4** (100 K) [CCDC-1908503]: $\text{C}_{32}\text{H}_{80}\text{Cl}_4\text{Si}_{12}$; Fw 943.84; triclinic; $P-1$, $a = 10.6683(5)\text{ \AA}$, $b = 10.7582(5)\text{ \AA}$, $c = 12.9529(6)\text{ \AA}$, $\alpha = 69.0200(10)^{\circ}$, $\beta = 84.5210(10)^{\circ}$, $\gamma = 65.6520(10)^{\circ}$, $V = 1262.24(10)\text{ \AA}^3$, $Z = 1$, $D_{\text{calc}} = 1.242\text{ Mg/m}^3$, $R1 = 0.0318$ ($I > 2\sigma(I)$), $wR2 = 0.0816$ (all data), GOF = 1.049.

Crystal data of **5** (100 K) [CCDC-1908504]: $\text{C}_{32}\text{H}_{80}\text{Cl}_6\text{Si}_{12}$; Fw 1014.74; triclinic, $P-1$, $a = 11.7581(5)\text{ \AA}$, $b = 20.4191(9)\text{ \AA}$, $c = 23.6336(10)\text{ \AA}$, $\alpha = 99.4190(10)^{\circ}$, $\beta = 104.2580(10)^{\circ}$, $\gamma = 94.1290(10)^{\circ}$, $V = 5387.7(4)\text{ \AA}^3$, $Z = 4$, $D_{\text{calc}} = 1.251\text{ Mg/m}^3$, $R1 = 0.0330$ ($I > 2\sigma(I)$), $wR2 = 0.0913$, GOF = 1.023.

Crystal data of **6** (100 K) [CCDC-1908505]: $C_{36}H_{91}Cl_2OSi_{12}$; Fw 948.06; monoclinic; $P2_1/c$, $a = 18.4326(8) \text{ \AA}$, $b = 12.7398(6) \text{ \AA}$, $c = 23.2524(10) \text{ \AA}$, $\beta = 93.1569(12)^\circ$, $V = 5452.0(4) \text{ \AA}^3$, $Z = 4$, $D_{\text{calc}} = 1.155 \text{ Mg/m}^3$, $R1 = 0.0428$ ($I > 2\sigma(I)$), $wR2 = 0.1130$ (all data), $GOF = 1.060$.

Crystal data of **9** (100 K) [CCDC-1908569]: $C_{35}H_{92}O_3Si_{12}$; Fw 898.14; triclinic, $P-1$, $a = 11.3627(5) \text{ \AA}$, $b = 16.4034(8) \text{ \AA}$, $c = 17.0141(8) \text{ \AA}$, $\alpha = 112.0530(10)^\circ$, $\beta = 94.2250(10)^\circ$, $\gamma = 109.5290(10)^\circ$, $V = 2697.1(2) \text{ \AA}^3$, $Z = 2$, $D_{\text{calc}} = 1.106 \text{ Mg/m}^3$, $R1 = 0.0270$ ($I > 2\sigma(I)$), $wR2 = 0.0769$, $GOF = 1.033$.

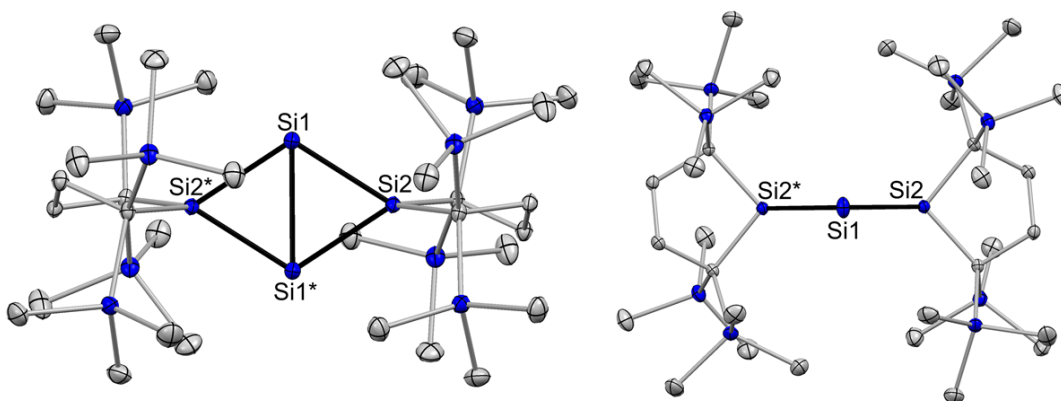


Figure 2-40. ORTEPs of **1b**. Thermal ellipsoids are shown at the 50% probability level. Hydrogen atoms were omitted for clarity.

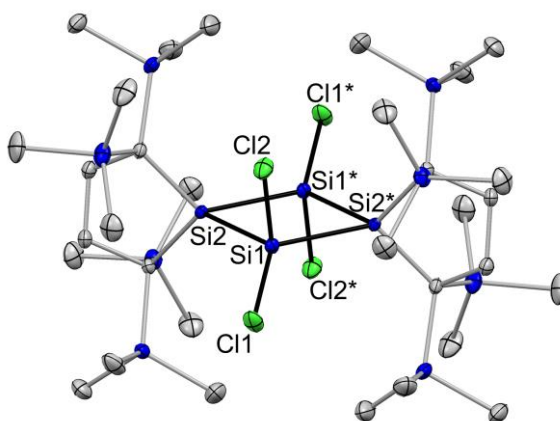


Figure 2-41. ORTEP of **4**. Thermal ellipsoids are shown at the 50% probability level. Hydrogen atoms were omitted for clarity.

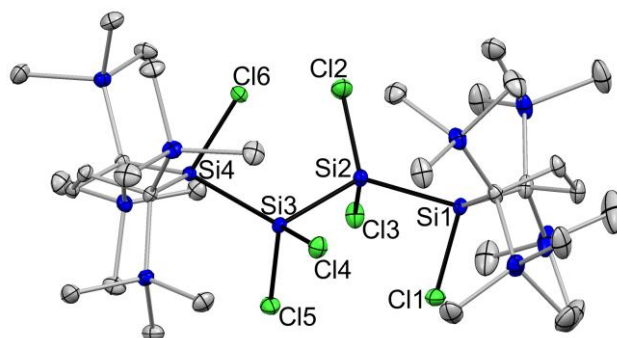


Figure 2-42. ORTEP of **5**. Thermal ellipsoids are shown at the 50% probability level. Hydrogen atoms were omitted for clarity.

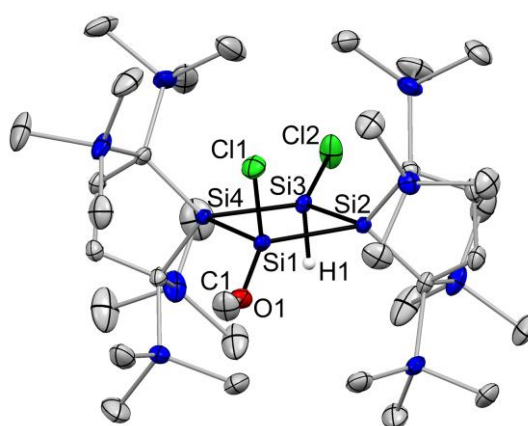


Figure 2-43. ORTEP of **6**. Thermal ellipsoids are shown at the 50% probability level. Hydrogen atoms were omitted for clarity.

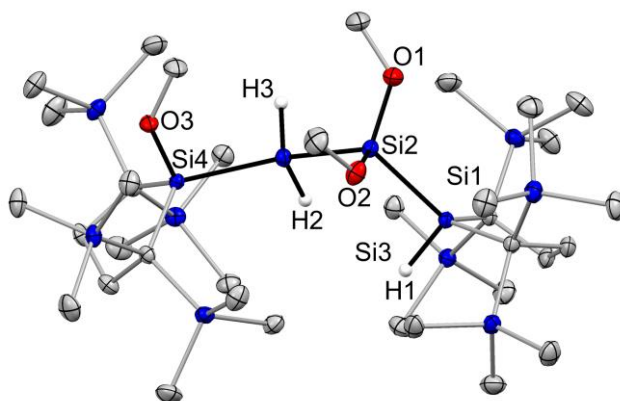


Figure 2-44. ORTEP of **9**. Thermal ellipsoids are shown at the 50% probability level. Hydrogen atoms were omitted for clarity.

UV-vis Absorption Spectrum

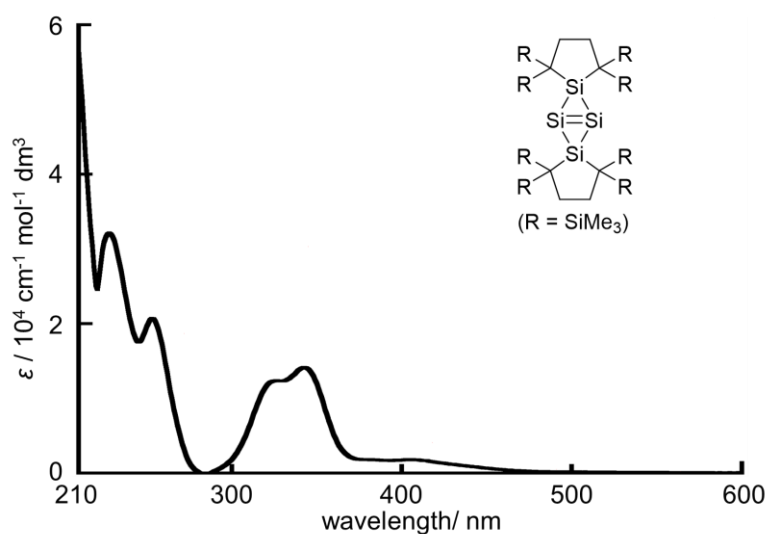


Figure 2-45. UV-vis absorption spectrum of **1b** in hexane at room temperature.

Computational Study

All theoretical calculations were performed using a Gaussian 09²² program. Geometry optimization was carried out at the B3LYP-D3/6-31G(d) level of theory. For bicyclo[1.1.0]tetrasilanes **7** and **10**, two conformers, which differ primarily in the geometry around the bridgehead silicon atoms, were located. Although the free energy differences between the two conformers are rather small (13.2 and 27.7 kJ mol⁻¹ for **7** and **10**, respectively), the energies of more stable conformers were used to estimate the free energy differences for the isomerization of bicyclo[1.1.0]tetrasilanes to the corresponding tetrasilane-1,3-dienes. The atomic coordinates and energies of the optimized structures are summarized in Tables 2-1 to 2-6.

Table 2-1. Atomic Coordinates of **7** (SB) at the B3LYP-D3/6-31G(d) Level of Theory

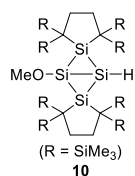
| Atom | X | Y | Z |
|------|---------------|---------------|---------------|
| Si | 0.0442091195 | 1.2271276015 | 0.0491167086 |
| Si | 0.0508583763 | -1.2270579803 | 0.04370215 |
| Si | -1.6088816335 | -0.0195568032 | 1.1266099575 |
| Si | 1.0537451361 | 0.0192361516 | -1.6559799213 |
| C | 3.0093720023 | -0.0158627755 | -1.7611526686 |
| C | 3.1770519156 | -0.3140229673 | -3.2935595434 |
| C | 2.087705982 | 0.3947752555 | -4.1174459936 |
| C | 0.6514623208 | 0.069634806 | -3.549474391 |
| C | -3.5182222973 | -0.0713226813 | 0.8081068778 |
| C | -4.0222051534 | -0.3959518137 | 2.2681514496 |
| C | -3.151618612 | 0.3139990045 | 3.3197662425 |
| C | -1.6278830788 | 0.0166945932 | 3.0849561954 |
| Cl | 0.5859271666 | 3.196743634 | 0.5682382301 |
| Cl | 0.5945458605 | -3.1960146584 | 0.5632946537 |
| Si | 3.913697695 | 1.6375149344 | -1.3180368718 |
| C | 5.6318197073 | 1.7172909625 | -2.131898094 |
| C | 4.1215500069 | 1.8338629123 | 0.5536553805 |
| C | 3.1245867017 | 3.2262954218 | -1.9701145259 |
| Si | 3.837136969 | -1.4566534962 | -0.7749530485 |
| C | 3.3307561733 | -3.1261063119 | -1.5199045281 |
| C | 3.4961076467 | -1.4091405361 | 1.093925997 |
| C | 5.7301260718 | -1.4763714189 | -0.9397243442 |
| Si | -0.4655442576 | 1.5318362141 | -4.1157644513 |
| Si | -2.2895675619 | 1.3623803617 | -3.654478951 |
| C | -0.2458196289 | 1.7455934495 | -5.9922644197 |
| C | 0.0044825313 | 3.224505106 | -3.4091609333 |
| Si | 0.0031076582 | -1.6215907633 | -4.2848194192 |
| C | -0.3519067827 | -3.0039920529 | -3.0374347967 |
| C | 1.2562201728 | -2.3177261125 | -5.532483813 |
| C | -1.6255578594 | -1.5387609508 | -5.2666321513 |
| Si | -0.6071560408 | 1.4586256454 | 3.8676622191 |
| C | 1.2449071753 | 1.412111703 | 3.4446490288 |
| C | -0.6884193697 | 1.4793630945 | 5.7660592438 |
| C | -1.3748158531 | 3.1272907861 | 3.3936462611 |

| | | | | | | | |
|---|--------------|--------------|---------------|--|--------------|--------------|---------------|
| H | 5.3266333108 | 4.7264052893 | -2.9374287274 | H | 3.4144685282 | 3.2680197205 | -4.5448595891 |
| H | 5.8043046705 | 4.2889091287 | -1.2917784049 | H | 4.2780850639 | 1.7359674764 | -4.3833096152 |
| H | 1.5166818335 | 3.3291747905 | -1.4945117192 | H | 2.5427762939 | 1.8260756274 | -4.0218610105 |
| H | 2.2456113495 | 4.7059605111 | -2.3261588922 | E+ZPVE = -5661.372998 au, Free E (298.15 K) = -5661.479784 au. | | | |
| H | 2.5967369397 | 4.4111158652 | -0.6160944951 | Job name: TN_Cl_diene | | | |

Table 2-4. Atomic Coordinates of **10** (LB) at the B3LYP-D3/6-31G(d) Level of Theory

| | | | | | | | |
|--|--|--|--|---|---------------|---------------|---------------|
| | | | | H | -1.9208603819 | 2.6099346064 | 4.1234132303 |
| | | | | H | -3.4422889781 | -1.8780470364 | 4.1005272604 |
| | | | | H | -1.7487922194 | -1.6098437351 | 3.6542318301 |
| | | | | H | -2.3778429085 | -0.9608050617 | 5.1708008437 |
| | | | | H | -2.4714106651 | 3.7738468505 | 1.7874293582 |
| | | | | H | -4.027453425 | 4.5389843952 | 1.4993294665 |
| | | | | H | -3.76453898 | 3.6129947679 | 2.9781949227 |
| | | | | H | -6.6832441898 | 1.5139208006 | 0.6640895771 |
| | | | | H | -6.4916037279 | 3.201035873 | 1.1478082336 |
| | | | | H | -6.3563242286 | 1.9160818115 | 2.3555352054 |
| | | | | H | -3.157382828 | 2.3847667142 | -1.3366926 |
| | | | | H | -4.9075148137 | 2.182801531 | -1.4831710714 |
| | | | | H | -4.2385670403 | 3.7274177478 | -0.9482678162 |
| | | | | H | 0.1812810907 | -3.3593965278 | -0.3782885166 |
| | | | | H | -0.2341111185 | -5.0778851561 | -0.4875300193 |
| | | | | H | -0.7045292837 | -3.9716758558 | -1.782647474 |
| | | | | H | -4.2937932776 | -5.166244336 | 0.4058457403 |
| | | | | H | -2.8474315664 | -6.1612443428 | 0.2041244102 |
| | | | | H | -3.5495378383 | -5.3427522522 | -1.1939779744 |
| | | | | H | -1.1741754791 | -3.2116171609 | 2.5253381675 |
| | | | | H | -2.6291037301 | -4.19230982 | 2.7298985498 |
| | | | | H | -1.1242082376 | -4.9441370714 | 2.191128175 |
| | | | | H | -3.5995933601 | 0.3011210639 | -2.5507876082 |
| | | | | H | -4.8542040548 | -0.5826443825 | -3.4293588874 |
| | | | | H | -5.1912403108 | 0.0561481861 | -1.819282867 |
| | | | | H | -5.4712253488 | -4.0743766891 | -1.3248079542 |
| | | | | H | -5.9079132456 | -3.1299218169 | -2.7544010997 |
| | | | | H | -6.299271572 | -2.5194860254 | -1.1468186292 |
| | | | | H | -3.2611335757 | -2.6888934255 | -4.0632126572 |
| | | | | H | -1.7985592788 | -2.3763452101 | -3.1180000992 |
| | | | | H | -2.6354710387 | -3.9324367497 | -2.9733853904 |
| | | | | H | 1.165581975 | -3.7231760014 | 1.8934773842 |
| | | | | H | 2.5256269739 | -2.6015438334 | 2.1534037669 |
| | | | | H | 1.0031459497 | -2.3805849749 | 3.0497064976 |
| | | | | H | 1.1796309258 | -2.2353276984 | -1.8355629027 |
| | | | | H | 0.8159326974 | -2.2158612123 | -3.5596654512 |
| | | | | H | 2.3077754275 | -2.9713307471 | -2.9760116483 |
| | | | | H | 4.7621797981 | 0.1407304523 | -4.0009436114 |
| | | | | H | 3.9737058022 | -1.1594375676 | -4.9020682223 |
| | | | | H | 4.7990232304 | -1.5197409172 | -3.3824784169 |
| | | | | H | 0.5093974843 | 0.781740625 | -3.9535933212 |
| | | | | H | 2.0185357444 | 1.5172110392 | -4.522997047 |
| | | | | H | 1.4694364557 | -0.0185815779 | -5.1990233631 |
| | | | | H | 3.0407091469 | -0.2713972047 | 2.0160447429 |
| | | | | H | 4.6791089435 | -0.9368180992 | 2.0823204142 |
| | | | | H | 4.4376765389 | 0.7842901388 | 1.7735193389 |
| | | | | H | 6.0418968795 | -0.2431789317 | -1.8634663251 |
| | | | | H | 6.5311135322 | -0.8381529946 | -0.2714282827 |
| | | | | H | 6.1240467838 | 0.8665161324 | -0.4855598276 |
| | | | | H | 4.5324451385 | -2.9462703189 | 0.2452368031 |
| | | | | H | 2.8564999598 | -2.7886515575 | -0.3111213153 |
| | | | | H | 4.185946999 | -2.8063046153 | -1.4806485142 |
| | | | | H | 0.5296680951 | 2.930453849 | -3.2406834271 |
| | | | | H | 0.3265362506 | 4.6748999287 | -3.4184762134 |
| | | | | H | 1.9511483081 | 3.9871032944 | -3.3596369483 |
| | | | | H | 1.536443752 | 6.3366251997 | 0.1383134349 |
| | | | | H | 1.1340570253 | 6.5996906924 | -1.5612492579 |
| | | | | H | 2.7055503517 | 5.9272826588 | -1.125145799 |
| | | | | H | -1.5770635527 | 4.3271391152 | -1.5159324143 |
| | | | | H | -1.2904841042 | 3.3922304723 | -0.0582854477 |
| | | | | H | -1.1922983822 | 5.153616991 | 0.0012846279 |
| | | | | H | 3.0909141175 | 1.7851952151 | 3.1854103834 |
| | | | | H | 1.9577218875 | 2.7450436926 | 4.1407395946 |
| | | | | H | 1.3599758639 | 1.4217672749 | 3.130597481 |
| | | | | H | 0.5144865884 | 4.8010060267 | 3.4126994454 |
| | | | | H | -0.5650192535 | 4.0219444163 | 2.2624172195 |
| | | | | H | 0.2843882132 | 5.5017969129 | 1.8079801832 |
| | | | | H | 4.3328049617 | 4.1294258271 | 1.9334281352 |
| | | | | H | 3.4103392394 | 5.4838364631 | 1.2674517573 |
| | | | | H | 3.350616805 | 5.1365644882 | 3.0006374069 |

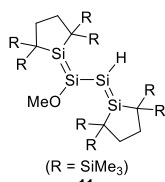
Table 2-5. Atomic Coordinates of **10** (metastable conformer, SB) at the B3LYP-D3/6-31G(d) Level of Theory



| Atom | X | Y | Z |
|------|---------------|----------------|---------------|
| C | -4.4974264645 | 0.956148829 | -0.0021058323 |
| C | -4.5185020754 | -0.4938352232 | 0.5130263562 |
| C | -3.3129963058 | -1.3110665428 | -0.0702062652 |
| Si | -1.9194650357 | 0.0598929971 | -0.0440889026 |
| C | -3.0743295986 | 1.6142995364 | 0.1688101012 |
| Si | -0.0822693689 | -0.2958755307 | -1.3779633249 |
| Si | -0.0002847047 | -0.3528456311 | 1.1956032341 |
| Si | 1.8671246108 | -0.0214263062 | -0.1585846 |
| C | 3.0529309113 | 1.5288179923 | -0.1926414457 |
| C | 4.4675995955 | 0.8390669208 | -0.147107913 |
| C | 4.4457698755 | -0.5261692228 | -0.8544703268 |
| C | 3.2464802356 | -1.40155589 | -0.3427555495 |
| Si | -2.9000644256 | 2.3490461234 | 1.9459138642 |
| Si | -2.9535853393 | 3.0638790412 | -1.1093452192 |
| C | -4.220764755 | 3.685461767 | 2.2414815712 |
| C | -1.1806245986 | 3.0913972335 | 2.250569107 |
| C | -3.139570597 | 1.1060712533 | 3.3554492462 |
| C | -1.9271969 | 4.5627329231 | -0.5568422656 |
| C | -4.6996885281 | 3.7560135196 | -1.4074510124 |
| C | -2.2788222634 | 2.6123396916 | -2.8241475099 |
| C | -1.4350887331 | -3.7942332736 | 0.7833604623 |
| C | -4.4507103498 | -4.1411084065 | 0.7796509891 |
| C | -3.1781883831 | -2.4504745513 | 2.8880675744 |
| C | -3.5279306213 | -0.5762126009 | -3.2269214358 |
| C | -5.5652645118 | -2.3605872483 | -2.0087500364 |
| Si | -3.0647992313 | -2.8649751739 | 1.0430757332 |
| Si | 3.7445708558 | -2.2060060258 | 1.3367358863 |
| C | -2.6706258177 | -3.3448792324 | -2.4512072282 |
| O | -1.800913455 | -0.9715107606 | 2.7312220142 |
| Si | -3.703988549 | -1.8829746708 | -1.8708640685 |
| Si | 2.9376864237 | -2.7746119594 | -1.6617509079 |
| C | 0.2512315707 | -2.0472539647 | 3.5476916437 |
| C | 1.371947109 | -3.8123282882 | -1.4367929568 |
| C | 4.4055771907 | -3.9834580884 | -1.7260798711 |
| C | 2.824777247 | -2.08681199567 | -3.4263237379 |
| Si | 2.825605471 | 2.506388118 | -1.8496261756 |
| C | 3.6148183921 | -1.0552301898 | 2.838851526 |
| C | 5.5762883204 | -2.7092921803 | 1.3437983288 |
| Si | 2.9750555918 | 2.8058994297 | 1.2648900119 |
| C | 2.7221130392 | -3.7583304036 | 1.7200073733 |
| C | 3.1478511257 | 1.4684020269 | -3.4131158306 |
| C | 4.2220353277 | 3.8519518196 | -1.9722729612 |
| C | 1.1745002467 | 3.3048441279 | -2.051314147 |
| C | 2.3288929383 | 2.1704327468 | 2.935103953 |
| C | 1.9669153035 | 4.3742680765 | 0.9132717481 |
| C | 4.7416211031 | 3.4124864166 | 1.6206042081 |
| H | -4.7880434023 | 0.9420447988 | -1.0596427748 |
| H | -5.2748849232 | 1.5413900069 | 0.5057107868 |
| H | -5.4830015751 | -0.957090675 | 0.2698794986 |
| H | -4.465009328 | -0.4712613351 | 1.6046837654 |
| H | -0.1397049436 | -0.878668617 | -2.7528095647 |
| H | 4.785424366 | 0.6815861983 | 0.890385401 |
| H | 5.2430602316 | 1.4759415779 | -0.5918915378 |
| H | 4.3565548051 | -0.356658094 | -1.9305252067 |
| H | 5.4083276348 | -1.0323025481 | -0.7116013376 |
| H | -5.2362611856 | 3.2908442335 | 2.1182731766 |
| H | -4.1348413366 | 4.0411910028 | 3.2761164865 |
| H | -4.118733787 | 4.5542371032 | 1.5845580539 |
| H | -0.435266603 | 2.6774527686 | 1.5667246174 |
| H | -0.8506050979 | 2.8541627448 | 3.2684095315 |
| H | -1.1652696175 | 4.1790307853 | 2.1399943851 |

E+ZPVE = -4856.612432 au, Free E (298.15 K) = -4856.712362 au.
Job name: TN22

Table 2-6. Atomic Coordinates of 11 at the B3LYP-D3/6-31G(d) Level of Theory



| Atom | X | Y | Z |
|------|---------------|---------------|---------------|
| C | -3.4227080783 | 1.6427884371 | 3.0712952186 |
| C | -4.1144936155 | 0.3057517859 | 2.7193195517 |
| C | -3.9469225979 | -0.0414318128 | 1.1942619971 |
| Si | -2.1644229123 | 0.5934871686 | 0.9165041642 |
| C | -1.9952939047 | 1.7868495182 | 2.4007163984 |
| Si | -1.0898307922 | 0.7453948305 | -1.0287500043 |

| | | | |
|----|---------------|---------------|---------------|
| Si | 1.2216707637 | 0.9643954697 | -0.9089158184 |
| Si | 2.613854173 | -0.6042995492 | -1.6112271278 |
| C | 4.4008306542 | -0.2828197032 | -2.1846182941 |
| C | 5.0736793333 | -1.6736629704 | -1.8849576 |
| C | 4.0608524817 | -2.8366282095 | -2.0156538491 |
| C | 2.6749973714 | -2.4851559319 | -1.3503796442 |
| O | -1.6480580504 | -0.4837312146 | -2.0688321441 |
| Si | -1.7257600586 | 3.6294808939 | 1.8800507603 |
| Si | -0.6568286446 | 1.2377296724 | 3.6759082026 |
| C | -1.7400238733 | -0.2508025178 | -3.4690722386 |
| C | 0.0983455575 | 4.1191107961 | 1.7438833195 |
| C | -2.5524593454 | 4.7585341688 | 3.1655514717 |
| C | -2.4786552878 | 4.0987579254 | 0.2028834253 |
| C | -0.6894327791 | 2.3893167131 | 5.1873087991 |
| C | 1.1205141323 | 1.2250423376 | 3.0275271461 |
| C | -1.0134505045 | -0.5089227633 | 4.31835801 |
| C | -5.5110878764 | -2.6740291044 | 1.9030619152 |
| Si | -4.0209381244 | -1.9565051846 | 0.9665905343 |
| C | -2.5271414396 | -2.8196625342 | 1.7525446898 |

| | | | | | | | |
|----|---------------|---------------|---------------|---|---------------|---------------|---------------|
| C | -4.0722981536 | -2.4612533159 | -0.8538483311 | H | -1.5735016672 | -2.5063954328 | 1.3212261864 |
| C | -4.7476007721 | 1.1296406205 | -1.6473000793 | H | -2.6275049644 | -3.8995568577 | 1.5825809906 |
| C | -5.9066014106 | 2.4569508895 | 0.8998535951 | H | -2.4838402801 | -2.6626447484 | 2.8352440402 |
| C | -6.9160762664 | -0.1846514221 | 0.046561431 | H | -4.9892429314 | -2.1433226432 | -1.3606532981 |
| Si | -5.3063179053 | 0.8245707026 | 0.1319518195 | H | -3.2206962949 | -2.0366507977 | -1.3941875114 |
| C | 0.8675093534 | -2.6200355325 | -3.9728920422 | H | -4.0130656629 | -3.5543705735 | -0.9272369071 |
| C | -0.3615539392 | -3.4404709634 | -1.3079455984 | H | -4.3132325674 | 0.2248094515 | -2.0831720634 |
| Si | 1.2531302072 | -3.4022276828 | -2.2849795039 | H | -5.6082500361 | 1.4268998165 | -2.2591541076 |
| Si | 5.2998210324 | 1.0916361147 | -1.1650028558 | H | -3.9937741449 | 1.9207101053 | -1.7108341307 |
| C | 1.7926253269 | -5.1755872754 | -2.697116757 | H | -6.3187904392 | 2.2907041017 | 1.9022316358 |
| C | 2.4387335673 | -4.8902300369 | 0.6917891313 | H | -6.7235118746 | 2.8413855269 | 0.2755982746 |
| Si | 2.6547819976 | -3.0118523124 | 0.5040560092 | H | -5.1532317332 | 3.2440699255 | 0.9718850657 |
| C | 1.2910216673 | -2.1313170811 | 1.4765059022 | H | -7.6585113387 | 0.4174820427 | -0.4927928617 |
| C | 4.3042445708 | -2.6584354496 | 1.3632028458 | H | -6.8176224091 | -1.1363182829 | -0.4831355647 |
| C | 7.1793828009 | 0.8706642099 | -1.3242451725 | H | -7.3240462799 | -0.3916017062 | 1.0421191197 |
| C | 4.9348745393 | 0.9846637776 | 0.700949083 | H | 1.5665308135 | -2.9598234475 | -4.7441078552 |
| C | 4.8204376044 | 2.8424861539 | -1.7015467968 | H | -0.1351311391 | -2.9395239688 | -4.2829838635 |
| Si | 4.4472473593 | 0.1480123251 | -0.4680677483 | H | 0.8722132982 | -1.5257647554 | -3.9608274983 |
| C | 6.1216542246 | 0.8617484092 | -4.6113270688 | H | -0.2694847645 | -3.8829380991 | -0.3123878727 |
| C | 3.084981084 | 1.369832559 | -4.5492717912 | H | -1.0935326583 | -4.0367169753 | -1.8678381948 |
| C | 4.251125705 | -1.3957153144 | -5.1498409813 | H | -0.7812020268 | -2.4359090685 | -1.2079231604 |
| H | -3.3605155636 | 1.7439756236 | 4.1624934751 | H | 1.0531282567 | -5.6151109819 | -3.378875386 |
| H | -4.0725185966 | 2.4573487284 | 2.7435543192 | H | 2.7597408885 | -5.1927961553 | -3.2129703565 |
| H | -5.1731674069 | 0.3550643743 | 3.0080942978 | H | 1.8661568443 | -5.8283037715 | -1.8238724123 |
| H | -3.677228643 | -0.4899606096 | 3.3355708009 | H | 3.1862933222 | -5.4504718061 | 0.1187263194 |
| H | 1.6498570138 | 2.2010754768 | -1.6385613358 | H | 2.5837322752 | -5.14104302 | 1.7505066031 |
| H | 5.9322315755 | -1.8580030537 | -2.5450241287 | H | 1.4480139579 | -5.2518520997 | 0.4015668635 |
| H | 5.4755780935 | -1.6774938694 | -0.8651968063 | H | 1.7235472565 | -1.3377353258 | 2.0913414336 |
| H | 4.4899648653 | -3.750092375 | -1.5821695678 | H | 0.7758086695 | -2.8308042421 | 2.145213117 |
| H | 3.9202043415 | -3.0541827402 | -3.079924778 | H | 0.5370761208 | -1.6645213618 | 0.8364056365 |
| H | -1.9490251462 | -1.2091459012 | -3.9541988588 | H | 5.1495151992 | -3.1596511934 | 0.878220243 |
| H | -2.551748945 | 0.4512308382 | -3.7046858027 | H | 4.5223416198 | -1.5902842637 | 1.4227841599 |
| H | -0.8015858978 | 0.1485359283 | -3.878817028 | H | 4.2442999881 | -3.0399795206 | 2.3906637145 |
| H | 0.667395637 | 3.4223674655 | 1.1177955292 | H | 7.5738213874 | 1.1324412714 | -2.3087430191 |
| H | 0.1511193513 | 5.107610764 | 1.2704519601 | H | 7.6738547382 | 1.5134928274 | -0.5849072661 |
| H | 0.5997337627 | 4.1903647915 | 2.7142942687 | H | 7.4763044425 | -0.162051322 | -1.1064145651 |
| H | -3.6456119138 | 4.7204898361 | 3.0948796768 | H | 3.9175961676 | 0.8806573547 | 0.9635793214 |
| H | -2.2504579791 | 5.7962892341 | 2.9762692259 | H | 5.3398605607 | 1.9123843339 | 1.1605996175 |
| H | -2.2762271009 | 4.511873444 | 4.1948237165 | H | 5.533184849 | 0.1614442503 | 1.158671911 |
| H | -1.8133811855 | 3.8168191937 | -0.6186830942 | H | 5.0290692808 | 3.0500696174 | -2.7551989507 |
| H | -3.4489325526 | 3.6398109456 | 0.0001853125 | H | 3.7582803185 | 3.0378086411 | -1.5227284105 |
| H | -2.6113885266 | 5.1886533247 | 0.1777118265 | H | 5.3943502617 | 3.5610470949 | -1.1030006071 |
| H | -1.6870109069 | 2.4872539765 | 5.6303091044 | H | 6.9467896221 | 0.1816063371 | -4.3713334084 |
| H | -0.0267995995 | 1.9781648333 | 5.9594443196 | H | 6.1020892852 | 0.9779403529 | -5.7026253832 |
| H | -0.3274139156 | 3.3952951571 | 4.9483950218 | H | 6.3534539718 | 1.8401638014 | -4.1809068474 |
| H | 1.1903223184 | 0.9180220647 | 1.9793255965 | H | 2.0993079058 | 0.8924278872 | -4.5351835855 |
| H | 1.7034970927 | 0.5126536045 | 3.6247362516 | H | 3.267226315 | 1.7381140161 | -5.5668033893 |
| H | 1.6042354154 | 2.2013783027 | 3.1177881459 | H | 3.0338200116 | 2.2332689229 | -3.8794715665 |
| H | -0.2863442796 | -0.7548846339 | 5.1026113279 | H | 4.3498674021 | -1.0967433031 | -6.201161383 |
| H | -2.0136784014 | -0.6083235178 | 4.7533459704 | H | 5.0275911625 | -2.1428018035 | -4.9493716762 |
| H | -0.9066430268 | -1.2552977262 | 3.5254848918 | H | 3.2765950101 | -1.8743800498 | -5.0354561133 |
| H | -6.4697048488 | -2.5112346714 | 1.4044694549 | | | | |
| H | -5.3722303097 | -3.7573586276 | 2.0098688505 | | | | |
| H | -5.5820718688 | -2.25577788 | 2.9143348895 | | | | |

E+ZPVE = -4856.598911 au, Free E (298.15 K) = -4856.705569 au.
 Job name: TN14_diene_OMe

2-5. Reference

- (1) (a) R. Hoffmann, H. Hopf, *Angew. Chem., Int. Ed.* **2008**, *47*, 4474–4481. See also: (b) W. T. Borden, *Chem. Rev.* **1989**, *89*, 1095–1109; (c) V. S. Mastryukov, J. E. Boggs, *Struct. Chem.* **2000**, *11*, 97–103; (d) S. Vázquez, P. Camps, *Tetrahedron* **2005**, *61*, 5147–5208.
- (2) (a) K. B. Wiberg, *Acc. Chem. Res.* **1984**, *17*, 379–386; (b) T. Iwamoto, S. Ishida, *Chem. Lett.* **2014**, *43*, 164–170; (c) Y. Heider, D. Scheschkewitz, *Dalton Trans.* **2018**, *47*, 7104–7112.
- (3) (a) G. Szeimies, J. Harnisch, O. Baumgärtel, *J. Am. Chem. Soc.* **1977**, *99*, 5183–5184; (b) U. Szeimies-Seebach, J. Harnisch, G. Szeimies, M. Van Meerssche, G. Germain, J.-P. Declercq, *Angew. Chem., Int. Ed. Engl.* **1978**, *17*, 848–850; (c) H.-G. Zoch, G. Szeimies, R. Romer, R. Schmitt, *Angew. Chem., Int. Ed. Engl.* **1981**, *20*, 877–878; (d)

- A.-D. Schlüter, H. Harnisch, J. Harnisch, U. Szeimies-Seebach, G. Szeimies, *Chem. Ber.* **1985**, *118*, 3513–3528.
- (4) (a) W. J. Hehre, J. A. Pople, *J. Am. Chem. Soc.* **1975**, *97*, 6941–6955; (b) H. U. Wagner, G. Szeimies, J. Chandrasekhar, P. v. R. Schleyer, J. A. Pople, J. S. Binkley, *J. Am. Chem. Soc.* **1978**, *100*, 1210–1213; (c) H. Kollmar, F. Carrion, M. J. S. Dewar, R. C. Bingham, *J. Am. Chem. Soc.* **1981**, *103*, 5292–5303; (d) B. A. Hess, Jr., W. D. Allen, D. Michalska, L. J. Schaad, H. F. Schaefer III, *J. Am. Chem. Soc.* **1987**, *109*, 1615–1621; (e) B. A. Hess, Jr., D. Michalska, L. J. Schaad, *J. Am. Chem. Soc.* **1987**, *109*, 7546–7547; (f) D. A. Hrovat, W. T. Borden, *J. Am. Chem. Soc.* **1988**, *110*, 4710–4718; (g) K. B. Wiberg, D. R. Artis, G. Bonneville, *J. Am. Chem. Soc.* **1991**, *113*, 7969–7979; (h) G. K. S. Prakash, G. Rasul, V. P. Reddy, J. Casanova, *J. Am. Chem. Soc.* **1992**, *114*, 6484–6486; (i) T. L. Nguyen, T. N. Le, A. M. Mebel, S. H. Lin, *Chem. Phys. Lett.* **2000**, *326*, 468–476; (j) T. C. Dinadayalane, U. D. Priyakumar, G. N. Sastry, *J. Phys. Chem. A* **2004**, *108*, 11433–11448; (k) G. Rasul, G. A. Olah, G. K. S. Prakash, *J. Phys. Chem. A* **2006**, *110*, 7197–7201; (l) D. Cremer, E. Kraka, H. Joo, J. A. Stearns, T. S. Zwier, *Phys. Chem. Chem. Phys.* **2006**, *8*, 5304–5316; (m) A. M. Mebel, V. V. Kislov, R. I. Kaiser, *J. Chem. Phys.* **2006**, *125*, 133113; (n) Y. Fujita, M. Abe, Y. Shiota, T. Suzuki, K. Yoshizawa, *Bull. Chem. Soc. Jpn.* **2016**, *89*, 770–778. For silicon analogues of BBE, see: (o) B. F. Yates, H. F. Schaefer III, *Chem. Phys. Lett.* **1989**, *155*, 563–571.
- (5) T. Iwamoto, T. Abe, K. Sugimoto, D. Hashizume, H. Matsui, R. Kishi, M. Nakano, S. Ishida, *Angew. Chem., Int. Ed.* **2019**, *58*, 4371–4375.
- (6) (a) K. Leszczynska, K. Abersfelder, A. Mix, B. Neumann, H. G. Stammler, M. J. Cowley, P. Jutzi, D. Scheschkewitz, *Angew. Chem., Int. Ed.* **2012**, *51*, 6785–6788; (b) D. Wendel, T. Szilvasi, C. Jandl, S. Inoue, B. Rieger, *J. Am. Chem. Soc.* **2017**, *139*, 9156–9159. For recent comprehensive reviews, see: (c) T. Iwamoto, M. Kira, *Adv. Organomet. Chem.* **2006**, *54*, 73–148; (d) R. C. Fischer, P. P. Power, *Chem. Rev.* **2010**, *110*, 3877–3927; (e) T. Iwamoto, S. Ishida, in *Structure and Bonding*, Springer, Berlin,

- 2014**, vol. 156, pp. 125–202; (f) C. Präsang, D. Scheschkewitz, *Chem. Soc. Rev.* **2016**, *45*, 900–921.
- (7) D. Nied, R. Köppe, W. Klopfer, H. Schnöckel, F. Breher, *J. Am. Chem. Soc.* **2010**, *132*, 10264–10265.
- (8) (a) In this reaction condition, we did not observe the formation of a trisilaallene, which is obtained by the reduction of the corresponding tetrachlorodisilane with potassium graphite in THF. See: S. Ishida, T. Iwamoto, C. Kabuto, M. Kira, *Nature* **2003**, *421*, 725–727; (b) For a study on the machine learning concerning the optimization of the reaction conditions, see: M. Fujinami, J. Seino, T. Nukazawa, S. Ishida, T. Iwamoto, H. Nakai, *Chem. Lett.* **2019**, *48*, 961–964.
- (9) T. Iwamoto, H. Sakurai, M. Kira, *Bull. Chem. Soc. Jpn.* **1998**, *71*, 2741–2747.
- (10) The ¹H NMR spectrum of the reaction mixture (Figure 2-34) was very complicated in the SiMe₃ region and it was difficult to identify signals of **4** and **5** clearly.
- (11) S. Masamune, Y. Kabe, S. Collins, D. J. Williams, R. Jones, *J. Am. Chem. Soc.* **1985**, *107*, 5552–5553.
- (12) As an orange precipitate which might be due to the intermediate was observed at low temperatures, it was difficult to discuss the formation of the products quantitatively.
- (13) S. Boomgaarden, W. Saak, M. Weidenbruch, *Z. Anorg. Allg. Chem.* **2001**, *627*, 349–352.
- (14) The isomerisation of bicyclo[1.1.0]tetrasilane **7** (or **10**) to tetrasiladiene **8** (or **11**) is predicted to be endergonic [49.7 kJ mol⁻¹ (or 45.6 kJ mol⁻¹)] (298.15 K) at the B3LYP-D3/6-31G(d) level of theory. The activation barriers for the isomerisation as well as the relative reactivity of the bridgehead Si–Si bonds in **7** and **10** and the Si=Si bond in **8** and **11** toward carbon tetrachloride and methanol should be responsible for the formation of **4** and **5** as well as **9**.
- (15) (a) M. Ichinohe, Y. Arai, A. Sekiguchi, N. Takagi, S. Nagase, *Organometallics* **2001**, *20*, 4141–4143; (b) A. Sekiguchi, M. Ichinohe, R. Kinjo, *Bull. Chem. Soc. Jpn.* **2006**, *79*,

- 825–832; (c) T. Iwamoto, T. Abe, S. Ishida, C. Kabuto, M. Kira, *J. Organomet. Chem.* **2007**, *692*, 263–270.
- (16) G. R. Fulmer, A. J. M. Miller, N. H. Sherden, H. E. Gottlieb, A. Nudelman, B. M. Stoltz, J. E. Bercaw, K. I. Goldberg, *Organometallics* **2010**, *29*, 2176–2179.
- (17) M. Kira, S. Ishida, T. Iwamoto, C. Kabuto, *J. Am. Chem. Soc.* **1999**, *121*, 9722–9723.
- (18) M. Kira, T. Hino, Y. Kubota, N. Matsuyama, H. Sakurai, *Tetrahedron Lett.* **1988**, *29*, 6939–6942.
- (19) G. M. Sheldrick, *SADABS, Empirical Absorption Correction Program*, Göttingen, Germany, 1996.
- (20) G. M. Sheldrick, *SHELXL-2014, Program for the Refinement of Crystal Structures*, University of Göttingen, Germany, 2014.
- (21) K. Wakita, *Yadokari-XG, Software for Crystal Structure Analyses*, 2001; Release of Software (Yadokari-XG 2009) for Crystal Structure Analyses; C. Kabuto, S. Akine, T. Nemoto, E. Kwon, *J. Crystallogr. Soc. Jpn.* **2009**, *51*, 218–224.
- (22) Gaussian 09, Revision D.01, M. J. Frisch, G. W. Trucks, H. B. Schlegel, G. E. Scuseria, M. A. Robb, J. R. Cheeseman, G. Scalmani, V. Barone, B. Mennucci, G. A. Petersson, H. Nakatsuji, M. Caricato, X. Li, H. P. Hratchian, A. F. Izmaylov, J. Bloino, G. Zheng, J. L. Sonnenberg, M. Hada, M. Ehara, K. Toyota, R. Fukuda, J. Hasegawa, M. Ishida, T. Nakajima, Y. Honda, O. Kitao, H. Nakai, T. Vreven, J. A. Montgomery, Jr., J. E. Peralta, F. Ogliaro, M. Bearpark, J. J. Heyd, E. Brothers, K. N. Kudin, V. N. Staroverov, R. Kobayashi, J. Normand, K. Raghavachari, A. Rendell, J. C. Burant, S. S. Iyengar, J. Tomasi, M. Cossi, N. Rega, J. M. Millam, M. Klene, J. E. Knox, J. B. Cross, V. Bakken, C. Adamo, J. Jaramillo, R. Gomperts, R. E. Stratmann, O. Yazyev, A. J. Austin, R. Cammi, C. Pomelli, J. W. Ochterski, R. L. Martin, K. Morokuma, V. G. Zakrzewski, G. A. Voth, P. Salvador, J. J. Dannenberg, S. Dapprich, A. D. Daniels, Ö. Farkas, J. B. Foresman, J. V. Ortiz, J. Cioslowski, D. J. Fox, Gaussian, Inc., Wallingford CT, 2009.

Chapter 3

Synthesis of 1,3-Diiodotetrasilabicyclo[1.1.0]butane with π -Type Single-Bonding Character

The contents of this chapter are published in part in

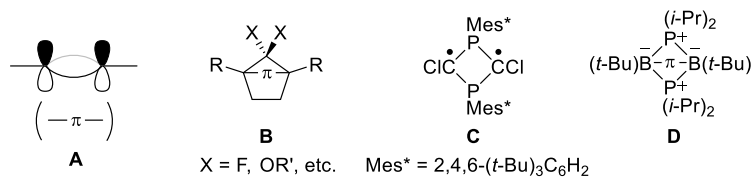
Nukazawa, T.; Iwamoto, T. *J. Am. Chem. Soc.* **2020**, *142*, 9920–9924.

DOI: 10.1021/jacs.0c03874

3-1. Introduction

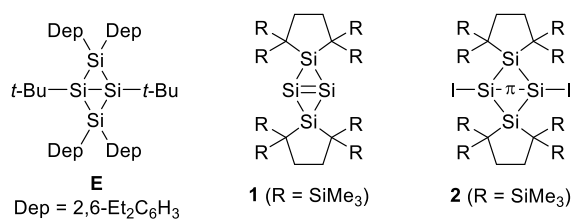
π -Bonding interactions are crucial for controlling the structure, reactivity, and electronic properties of organic/inorganic π -electron systems. In organic compounds and compounds of main-group elements, these interactions are typically found in multiple bonds with an underlying σ -bond framework. Although compounds that contain a π -bond without a σ -bond framework (π -single bonding; Chart 3-1, **A**)¹ are generally unstable and tend to isomerize into the singly σ -bonded structures, meticulous molecular design can increase the lifetime of such compounds. For instance, singlet cycloalkane-1,3-diyl derivatives such as **B** (Chart 3-1), which exhibit π -type single bonding between the bridgehead carbon atoms, have been generated as persistent compounds.^{1,2} Abe et al. found that such structures can be thermodynamically stabilized by the introduction of electronegative substituents X at the bridge positions^{1,2b,c} and electron-donating groups as the bridgehead substituents R.^{2d} Abe et al. also found that the lifetime of such species can be increased up to ~ 20 μ s at room temperature by kinetic stabilization with substituents that lengthen the bridgehead bond distance^{3a,b} or increase the planarity.^{3c,d} Noticeably, these species have small π - π^* gaps,² which is reflected in their bathochromically shifted $\pi \rightarrow \pi^*$ absorption bands ($\lambda \approx 600$ nm) compared with those of typical monoalkenes ($\lambda < 300$ nm). Moreover, various isolable diradicaloids have been reported since the first isolation of **C** (Chart 3-1),^{4,5} reported by Niecke and co-workers.^{4a} While these diradicaloids have planar ring structures, most of these species do not exhibit bonding character between the bridgehead atoms. Among these, an important example is the isolable 1,3-dibora-2,4-diphosphacyclobutane-1,3-diyl **D**, reported by Bertrand and co-workers, which contains a planar four-membered P_2B_2 ring with through-space π -type single-bond character between the bridgehead boron atoms (Chart 3-1).⁵ The planar structure of **D** was attributed to the presence of the bulky groups on the ring.^{5d,e} Compound **D** exhibits ionic and radical reactivity in various reactions.⁶ Although compounds that contain π -type single bonding exhibit intriguing photophysical properties and reactivity, isolable examples of these compounds remain scarce.^{7,8}

Chart 3-1. Schematic Illustration of π -Bonding without a σ -Bond Framework (**A**) and Structures of Compounds **B–D**



We recently reported tetrasilabicyclo[1.1.0]but-1(3)-ene **1** (Chart 3-2), which contains a highly strained bridgehead Si=Si bond. We found that the reaction of **1** with carbon tetrachloride and methanol resulted in the addition of multiple Cl atoms or methanol moieties to the silicon framework.⁹ In this chapter, the author reports that the 1,2-diiodination of **1** provides 1,3-diiodotetrasilabicyclo[1.1.0]butane **2** (Chart 3-2), which exhibits a planar structure with π -type single bonding between the bridgehead silicon atoms. Such a planar structure has been proposed as a possible intermediate or transition state for the ring inversion of bent tetrasilabicyclo[1.1.0]butanes such as **E**, the first tetrasilabicyclo[1.1.0]butane reported by Masamune et al.,^{10a} which have been examined theoretically.¹¹ DFT calculations indicated that the high planarity of **2** should most likely be attributed to the bulky substituents at the bridge positions.

Chart 3-2. Structures of Compounds **E**, **1**, and **2**

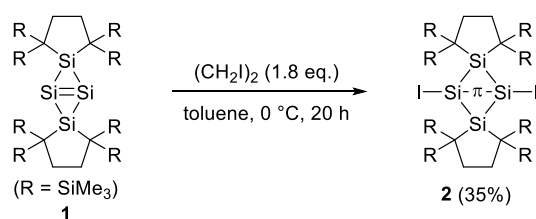


3-2. Results and Discussion

3-2-1. Synthesis of 1,3-Diiodotetrasilabicyclo[1.1.0]butane **2**

The reaction of **1** with 1,2-diiodoethane (1.8 equiv) at 0 °C delivered air-sensitive reddish-orange crystals of **2** in 35% yield after recrystallization from toluene (Scheme 3-1). The molecular structure of **2** was determined using a combination of multinuclear NMR spectroscopy, mass spectrometry, elemental analysis, and single crystal X-ray diffraction (XRD) analysis.¹²

Scheme 3-1. Synthesis of **2**



3-2-2. Molecular Structures of **2**

Compound **2** provided two different types of single crystals (Figure 3-1). The red crystalline blocks that were obtained from recrystallization from benzene at room temperature, **2_p**, contain a planar Si₄ ring (dihedral angle of the bicyclic ring, φ , equal to 180°) on a crystallographic inversion center (Figure 3-1a and Table 3-1). The geometry around the bridgehead atoms is planar [sum of the angles of the bridgehead Si1 atom excluding the central bridgehead bond, ΣSi , equal to 360.00(3)°], and the Si-I moieties are very slightly bent in a *trans* configuration [Si1*-Si1-I1 angle, θ , equal to 178.49(4)°] with respect to the Si₄ ring plane. Noticeably, the distance between the bridgehead silicon atoms [$d = 2.5822(11)$ Å] is much longer than those in previously reported tetrasilabicyclo[1.1.0]butanes (2.35–2.47 Å)¹⁰ and **1** [2.4873(10) Å]^{9b} but still shorter than the longest hitherto-reported Si-Si single bond [2.697 Å for (*t*-Bu)₃Si-Si(*t*-Bu)₃]¹³ and the corresponding transannular Si⋯Si distance in a 1,1,3,3-tetrachlorocyclotetrasilane without a bridgehead bond, obtained from the tetrachlorination of **1** [2.9182(9) Å].^{9b} The two silacyclopentane moieties at the bridge positions adopt a half-chair conformation and exhibit an eclipsed conformation as viewed along the Si2-Si2* axis (Figure 3-1a). On the other hand, the orange plates that were obtained upon recrystallization from hexane at -35 °C, **2_c**, adopt a slightly *cis*-bent Si₄ framework [$\varphi = 161.57(4)^\circ$, $\theta = 168.55^\circ$] (Figure 3-1b and Table 3-1). The bridgehead Si atoms adopt an almost planar geometry ($\Sigma\text{Si} = 359.9^\circ$). The distance between the bridgehead Si atoms [$d = 2.5251(10)$ Å] is slightly shorter than that in **2_p** [2.5822(11) Å]. The two silacyclopentane moieties exhibit a staggered conformation as viewed along the Si3-Si4 axis (Figure 3-1b). As mentioned above, both **2_p** and **2_c** exhibit highly planar silicon rings ($\varphi > 160^\circ$) and a planar geometry around the bridgehead silicon atoms ($\Sigma\text{Si} > 359.9^\circ$, $\theta > 169^\circ$) as well as

substantially elongated bridgehead distances ($d = 2.53\text{--}2.58 \text{ \AA}$). These properties contrast sharply with the structural characteristics reported for highly bent tetrasilabicyclo[1.1.0]butanes, which exhibit short bridgehead Si–Si distances ($\varphi = 121.0\text{--}129.3^\circ$, $\theta = 146.3\text{--}151.7^\circ$, $d = 2.35\text{--}2.47 \text{ \AA}$).

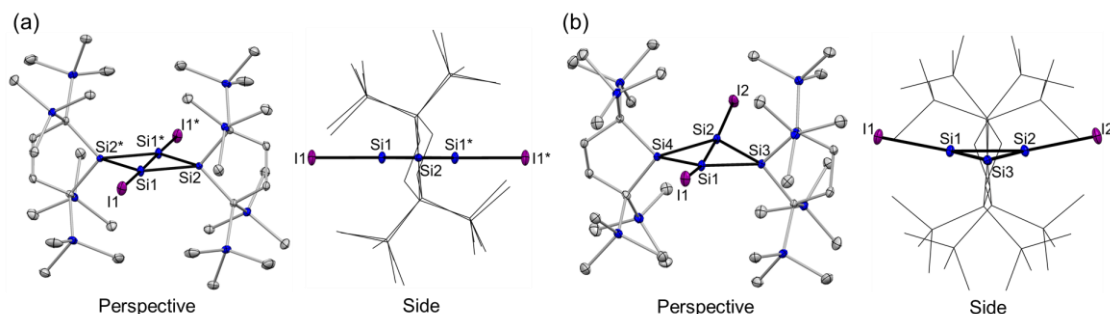
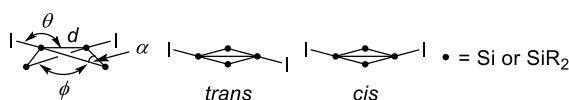


Figure 3-1. (a) ORTEPs of (a) **2_p** and (b) **2_c** with thermal ellipsoids at 50% probability; hydrogen atoms have been omitted for clarity.

Table 3-1. Selected Structural Parameters of **2** and **2'**



| compound | $d/\text{\AA}$ | θ/deg | φ/deg | α/deg | $\Delta G^{\text{a,b}}$ |
|-----------------------|----------------|----------------------------|----------------------|---------------------|-------------------------|
| XRD | | | | | |
| 2_p | 2.5822(11) | 178.49(4) (<i>trans</i>) | 180.00 | 66.98(3) | - |
| 2_c | 2.5251(10) | 168.55(4) | 161.57(4) | 65.34(3) | - |
| | | 168.56(4) (<i>cis</i>) | | 65.28(3) | |
| DFT ^a | | | | | |
| 2'_c | 2.501 | 168.77 (<i>cis</i>) | 159.59 | 64.48 | 0.0 |
| 2'_p | 2.609 | 178.54 (<i>trans</i>) | 180.00 | 67.80 | 15.7 |
| 2'_i | 2.847 | 121.54 | 176.55 | 71.85 | 28.1 |
| | | 129.16 (<i>cis</i>) | | 71.87 | |

^aCalculated at the B3LYP-D3/6-311G(d) [H,C,Si], SDD [I] level of theory. ^bAt 298.15 K, in kJ mol⁻¹.

3-2-3. NMR Spectra of **2**

The NMR spectra of **2** indicate that **2** adopts a highly symmetric structure in solution. The ¹H NMR spectrum of **2** in benzene-*d*₆ at room temperature shows one singlet at 0.47 ppm for the eight equivalent SiMe₃ groups and another singlet for the eight methylene protons of the five-membered rings at 1.98 ppm. In the ²⁹Si NMR spectrum of **2**, signals were observed at 4.0 (bridge Si), 5.0 (SiMe₃), and 103.8 ppm (bridgehead Si) (Figure 3-2). These results suggest that **2** adopts an almost planar structure similar to **2_p** or a slightly *cis*-bent structure similar to that of **2_c** in which

the Si₄ ring undergoes facile ring flipping on the NMR time scale. Notably, the ²⁹Si NMR resonance of the bridgehead Si nuclei appears much further downfield (103.8 ppm) than those of reported tetrasilabicyclo[1.1.0]butanes (-145.1 to 14.8 ppm)¹⁰ and close to that of a structurally similar trisilacyclopropene (142.9 ppm).¹⁴

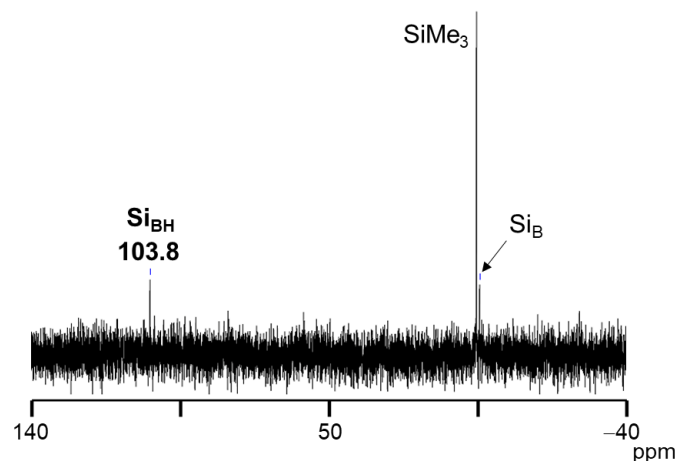


Figure 3-2. ²⁹Si NMR spectrum of **2** in benzene-*d*₆ at room temperature (Si_{BH}: bridgehead Si, Si_B: bridge Si).

3-2-4. Theoretical Study

The molecular structure of **2** was further examined using theoretical calculations. The two structures of **2** observed in the solid state (**2_p** and **2_c**) were located as local minima (**2'_p** and **2'_c**) at the B3LYP-D3/6-311G(d) [H,C,Si], SDD [I] level of theory, and the structural characteristics of **2'_p** and **2'_c** are in good agreement with those obtained from the XRD analysis (Table 3-1). Our calculations suggest that at 298.15 K, **2'_c** is more stable than **2'_p** in terms of free energy by 15.7 kJ mol⁻¹. The chemical shift of the ²⁹Si NMR resonance of the bridgehead silicon nuclei of **2'_c**, calculated at the M06L/6-311+G(2df,p) [H,C,Si], SDD [I] level of theory (99.8 ppm), is closer to the observed value (103.8 ppm) than that calculated for **2'_p** (152.3 ppm).¹⁵ These results imply that **2** predominantly adopts a structure similar to **2'_c** in solution, which is consistent with the features of the UV-vis spectrum (*vide infra*).

The frontier Kohn–Sham orbitals of **2'_p** and **2'_c** provide further insight into the characteristics of the bridgehead Si–Si bond. The HOMO and LUMO orbitals of **2'_p** represent an in-phase and out-of-phase combination of the bridgehead Si 3p orbitals (π- and π*-orbitals) (Figure 3-3a). Conversely, **2'_c** exhibits similar but slightly *cis*-oriented π- and π*-type orbitals,¹⁶

which could be considered as extremely distorted σ - and σ^* - (banana-type) orbitals (Figure 3-3b). Natural bond orbital analysis¹⁷ indicated that the bridgehead bond is formed by interactions between almost pure p orbitals of Si ($2'_p$, 99.9%; $2'_c$, 95.2%). The angles of deviation between the axis through the two bridgehead silicon atoms and the direction of the natural hybrid orbital that forms the bridgehead natural bond ($2'_p$, 82.1°; $2'_c$, 61.9°) are substantially higher than those of the peripheral banana-type σ (Si–Si) bond (13.6–18.6°), suggesting that both $2'_p$ and $2'_c$ involve formally π -type bonding interactions between the bridgehead silicon atoms with very slight *trans* or *cis* deformation.¹⁸ The Wiberg bond indices between the bridgehead silicon atoms of $2'_c$ (0.77) and $2'_p$ (0.70) are not substantially lower than those of the peripheral Si–Si bonds (0.95–0.98). The significantly larger singlet–triplet gap ($2'_p$, 107.2 kJ mol⁻¹; $2'_c$, 149.8 kJ mol⁻¹) also provides evidence for the presence of considerable bonding interactions between the bridgehead silicon atoms in $2'_p$ and $2'_c$.

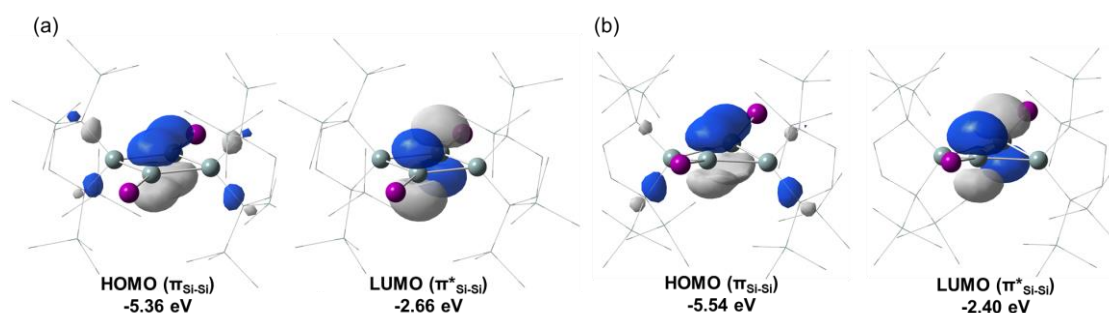


Figure 3-3. Frontier orbitals of (a) $2'_p$ and (b) $2'_c$ calculated at the B3LYP-D3/6-311G(d) [H,C,Si], SDD [I] level of theory (isosurface level: 0.05 e·au⁻³); hydrogen atoms have been omitted for clarity.

3-2-5. UV-vis Absorption Spectrum of **2**

The UV-vis absorption spectrum of **2** provided further insight into its structure in solution. In hexane, **2** exhibits an intense absorption band at 435 nm ($\epsilon = 2400 \text{ M}^{-1} \text{ cm}^{-1}$) with a tail extending up to 600 nm (Figure 3-4). The observed absorption spectrum of **2** was in better agreement with the band positions and corresponding oscillator strengths of $2'_c$ (Figure 3-4, red bars) than those of $2'_p$ (Figure 3-15) calculated at the TD-B3LYP-D3/6-311G(d) [H,C,Si], SDD [I] level of theory. The absorption band at 435 nm was assigned to the HOMO(π)→LUMO(π^*) transition ($\lambda_{\text{calcd}} = 446 \text{ nm}$). Thus, it is reasonable to conclude that $2'_c$ is the dominant structure in

solution, which is consistent with the calculated relative stabilities of **2'**_p and **2'**_c.¹⁹ It is noteworthy that the band of **2** is bathochromically shifted compared to the $\pi \rightarrow \pi^*$ transition of a structurally similar trisilacyclopentene that exhibits a planar Si=Si double bond in the three-membered ring (391 nm).¹⁴

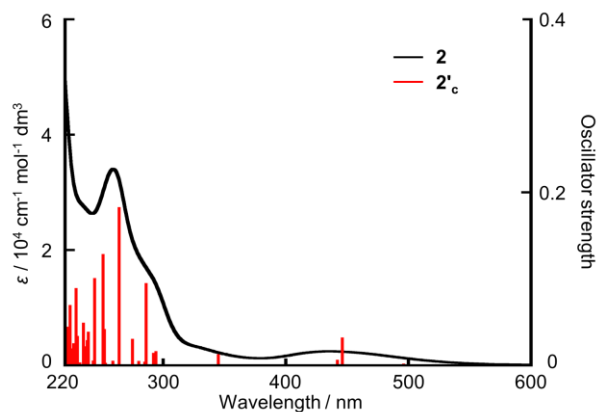


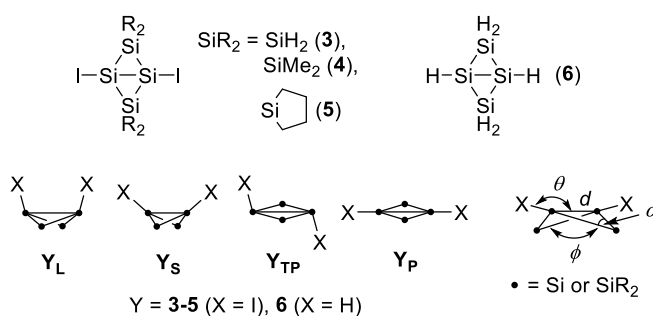
Figure 3-4. UV-vis spectrum of **2** in hexane at room temperature (black) and calculated band positions (red bars).

3-2-6. The Effects of the Substituents for the Planar Structure of **2**

The reason that **2** adopts a planar structure merits further discussion. Similar to previously reported theoretical studies,¹¹ three different structures of 1,3-diiodotetrasilabicyclo[1.1.0]butane (**3_L**, **3_S**, and **3_{TP}**) were located as local minima at the B3LYP-D3/6-311G(d) [H,C,Si], SDD [I] level of theory (Table 3-2). These correspond to (i) a bent structure ($\varphi = 152.4^\circ$) with an acute Si–Si–I bond angle ($\theta = 103.2^\circ$) and an extremely long Si–Si bridgehead distance ($d = 3.063 \text{ \AA}$) (**3_L**); (ii) a highly bent structure ($\varphi = 124.5^\circ$) with a wide Si–Si–I bond angle ($\theta = 150.8^\circ$) and a typical Si–Si single bond distance ($d = 2.357 \text{ \AA}$) (**3_S**); and (iii) a planar structure ($\varphi = 180.0^\circ$) with an acute Si–Si–I bond angle ($\theta = 100.9^\circ$) in a *trans* arrangement and a long Si–Si distance ($d = 3.073 \text{ \AA}$) (**3_{TP}**). A planar structure (**3_P**) similar to **2_p** and **2_c** was located as a saddle point with two imaginary vibrational frequencies. **3_L** is the most stable isomer and is more than 90 kJ mol⁻¹ lower in energy than **3_P**, which in turn is similar to the parent system (**6**, Table 3-2),¹¹ implying that the electronic effects of the iodine atoms are not crucial for the observed planar structure of **2**. The relative energies of the isomers remain essentially unchanged with increasing steric demand at the bridge SiR₂ moieties (SiH₂ (**3**) < SiMe₂ (**4**) < Si(CH₂)₄ (**5**); Table 3-2).²⁰ However, in the case of **2'**, which contains very bulky SiR₂ groups, the planar and almost planar structures **2'**_p and **2'**_c

were located as local minima,²¹ while structures corresponding to **3_S** and **3_{TB}** were not located, which is probably due to the severe steric demand. Structure **2'₁**, which corresponds to **3_L** (Table 3-1), was located as another local minimum, but its free energy was 28.1 kJ mol⁻¹ higher than that of **2'_c**. These results indicate that the presence of sterically highly demanding substituents at the bridge positions is most likely responsible for the observed planar structures. The prediction of such steric effects is unprecedented for tetrasilabicyclo[1.1.0]butanes.²²

Table 3-2. Selected Structural Parameters and the Relative Energies of Isomers of **3-6**



| Compound ^{a,b} | distance/Å | | angle/deg | | ΔG^d |
|--|-------------|--------------------|-------------------------------|---------------------|--------------|
| | d (Si-Si) | θ (X-Si-Si) | ϕ (Si ₄ ring) | α (Si-Si-Si) | |
| 3_L (<i>C</i> _{2v}) | 3.0625 | 103.24 | 152.42 | 80.82 | 0.0 |
| 3_S (<i>C</i> _{2v}) | 2.3569 | 150.79 | 124.53 | 61.17 | 43.3 |
| 3_{TP} (<i>C</i> _{2h}) | 3.0734 | 100.93 | 180.00 | 80.34 | 25.0 |
| 3_P (<i>D</i> _{2h}) ^c | 2.6691 | 180.00 | 180.00 | 71.26 | 91.1 |
| 4_L (<i>C</i> _{2v}) | 2.9944 | 104.11 | 157.85 | 78.58 | 0.0 |
| 4_{TP} (<i>C</i> _{2h}) | 3.0428 | 102.98 | 180.00 | 78.84 | 27.6 |
| 4_P (<i>D</i> _{2h}) ^c | 2.6449 | 180.00 | 180.00 | 70.14 | 96.0 |
| 5_L (<i>C</i> _s) | 3.0057 | 104.27 | 160.56 | 79.04 | 0.0 |
| 5_{TP} (<i>C</i> _{2h}) | 3.0131 | 99.48 | 180.00 | 78.33 | 16.0 |
| 5_P (<i>C</i> _i) ^c | 2.6583 | 179.91 | 180.00 | 70.71 | 84.8 |
| 6_L (<i>C</i> _{2v}) | 2.8796 | 92.34 | 141.99 | 76.02 | 0.0 |
| 6_{TP} (<i>C</i> _{2h}) | 2.9474 | 89.78 | 180.00 | 77.48 | 45.1 |
| 6_P (<i>D</i> _{2h}) ^c | 2.8160 | 180.00 | 180.00 | 75.47 | 102.8 |

^aCalculated at the B3LYP-D3/6-311G(d) [H,C,Si], SDD [I] level of theory. ^b**4_S**, **5_S**, and **6_S** were not found. ^cSaddle point with two imaginary vibrational frequencies. ^dAt 298.15 K, in kJ mol⁻¹.

3-3. Conclusion

In conclusion, the author has synthesized a planar silicon analogue of bicyclo[1.1.0]butane that exhibits π -type single bonding between the bridgehead Si atoms.²³ 1,3-Diiodotetrasilabicyclo[1.1.0]butane **2** was obtained by 1,2-diiodination of the corresponding

bridgehead disilene **1**. The formal formation of a π -bonding species after a 1,2-addition is interesting, as 1,2-additions of double bonds usually afford singly σ -bonded compounds. While planar silicon rings with slight *trans* or *cis* deformation (**2_p** and **2_c**) were observed in the XRD analysis, the NMR analysis and DFT calculations suggest that **2_c** is the dominant structure in solution. The distinct absorption band of **2** in the visible region indicates that this silicon species with π -single bonding should represent an intriguing silicon-based chromophore.

3-4. Experimental Section

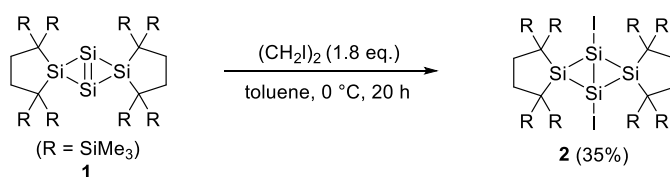
General Procedures

All reactions involving air-sensitive compounds were performed under argon or nitrogen atmosphere using a high-vacuum line and a standard Schlenk techniques, or a glove box, as well as dry and oxygen-free solvents. The reactions at lower temperatures were performed using an EYELA PSL-1400 cryobath. NMR spectra were recorded on a Bruker Avance III 500 FT NMR spectrometer. The ^1H and ^{13}C NMR chemical shifts were referenced to residual ^1H and ^{13}C shifts of the solvents: C_6D_6 (^1H : δ 7.16 and ^{13}C : δ 128.0).²⁴ The ^{29}Si NMR chemical shifts were relative to Me_4Si in ppm (δ 0.00). The sampling of air-sensitive compounds was carried out using a VAC NEXUS 100027 type glove box. Mass spectra was recorded on a Bruker Daltonics SolariX 9.4T spectrometer. UV-vis spectra were recorded on a JASCO V-770 and V-660 spectrometer. X-ray analysis was carried out using a Bruker AXS APEXII CCD diffractometer.

Materials

Dry and degassed hexane, benzene, and toluene were prepared using a VAC 103991 solvent purifier. Benzene-*d*₆ was degassed through five freeze-pump-thaw cycles and then dried over molecular sieves 4Å. 3-Methylpentane was dried in a tube covered with potassium mirror and then distilled under reduced pressure prior to use. 1,2-Diiodoethane was purified by recrystallization from hexane. Tetrasilabicyclo[1.1.0]but-1(3)-ene **1** was prepared according to published procedure.^{9b}

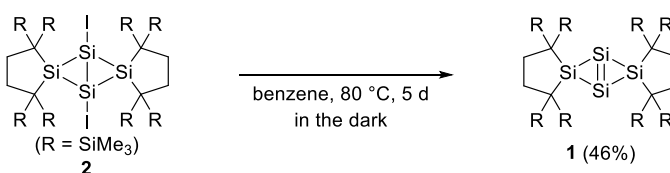
Synthesis of 1,3-Diiodobicyclo[1.1.0]tetrasilane **2** [TN470,504]



To a Schlenk tube (30 mL) equipped with a magnetic stir bar, **1** (30.3 mg, 37.8 μmol) and 1,2-diiodoethane (19.6 mg, 69.5 μmol) were placed. To the mixture, dry and degassed toluene (3.0 mL, cooled to $-35\text{ }^\circ\text{C}$) was added, and then the mixture was stirred at $0\text{ }^\circ\text{C}$ for 20 hours. The original orange suspension turned to a red solution. After the volatiles were removed in vacuo at room temperature, recrystallization from hot toluene provided red crystals of **2** (13.9 mg, 13.2 μmol) in 35% yield.

2: red crystals; mp $125\text{-}127\text{ }^\circ\text{C}$ (decomp.); ^1H NMR (500 MHz, C_6D_6 , 300 K) 0.47 (s, 72H, SiCH₃), 1.98 (s, 8H, CH₂); ^{13}C NMR (126 MHz, C_6D_6 , 302 K) 6.0 (SiCH₃), 16.0 (C), 34.4 (CH₂); ^{29}Si NMR (99 MHz, C_6D_6 , 301 K) 4.0 (Si), 5.0 (SiMe₃), 103.8 (Si-I); UV-vis (hexane, 293 K) $\lambda_{\text{max}}/\text{nm}$ (ϵ) 435 (2.4×10^3), 292 (sh, 1.5×10^4), 259 (3.4×10^4); HRMS (APCI₊) Calcd for $\text{C}_{32}\text{H}_{81}\text{I}_2\text{Si}_{12}$ [(M+H)⁺], 1055.16520; Found, 1055.16533; Anal. Calcd for $\text{C}_{32}\text{H}_{80}\text{I}_2\text{Si}_{12}$: C, 36.40; H, 7.64%. Found: C, 36.62; H, 7.74%.

Thermolysis of **2** [TN581]



To a stock bottle (10 mL) equipped with a magnetic stir bar, **2** (30.5 mg, 28.9 μmol) and then dry and degassed benzene (3.0 mL) were added. The mixture was stirred at $80\text{ }^\circ\text{C}$ for 5 days in the dark. The resulting solution turned from red to orange. After the volatiles were removed in vacuo at room temperature, the crude was washed with hexane to provide an orange solid of **1** (10.7 mg, 13.3 μmol) in 46% yield.

NMR spectra

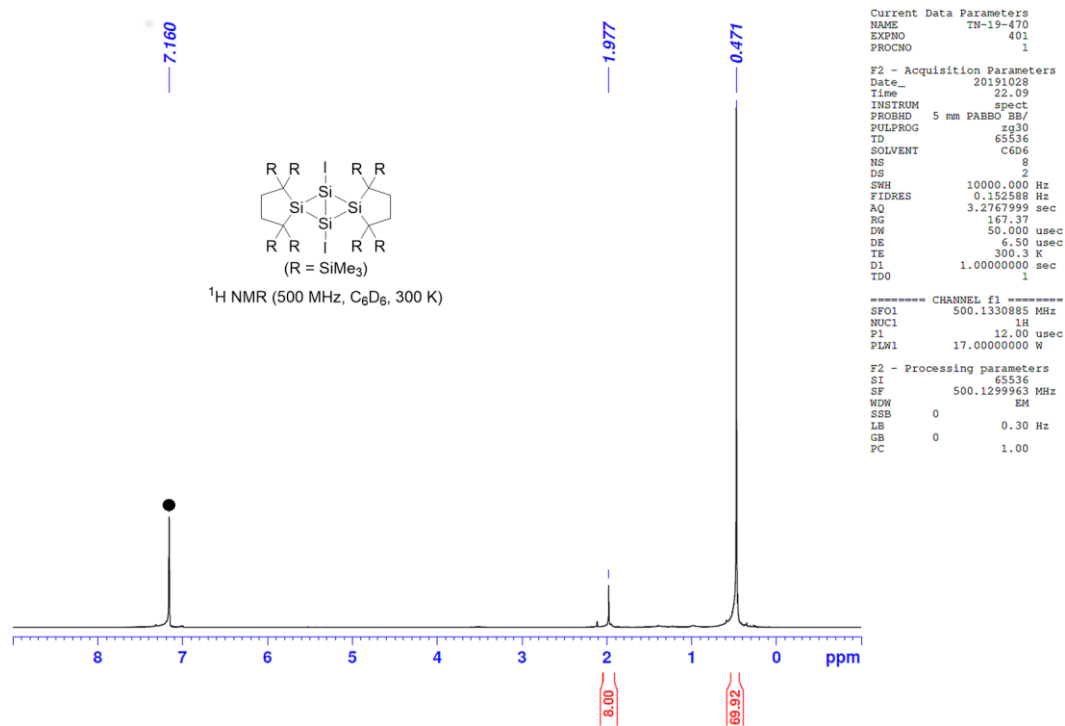


Figure 3-5. ^1H NMR spectrum of **2** in C_6D_6 at 300 K (● = C_6HD_5).

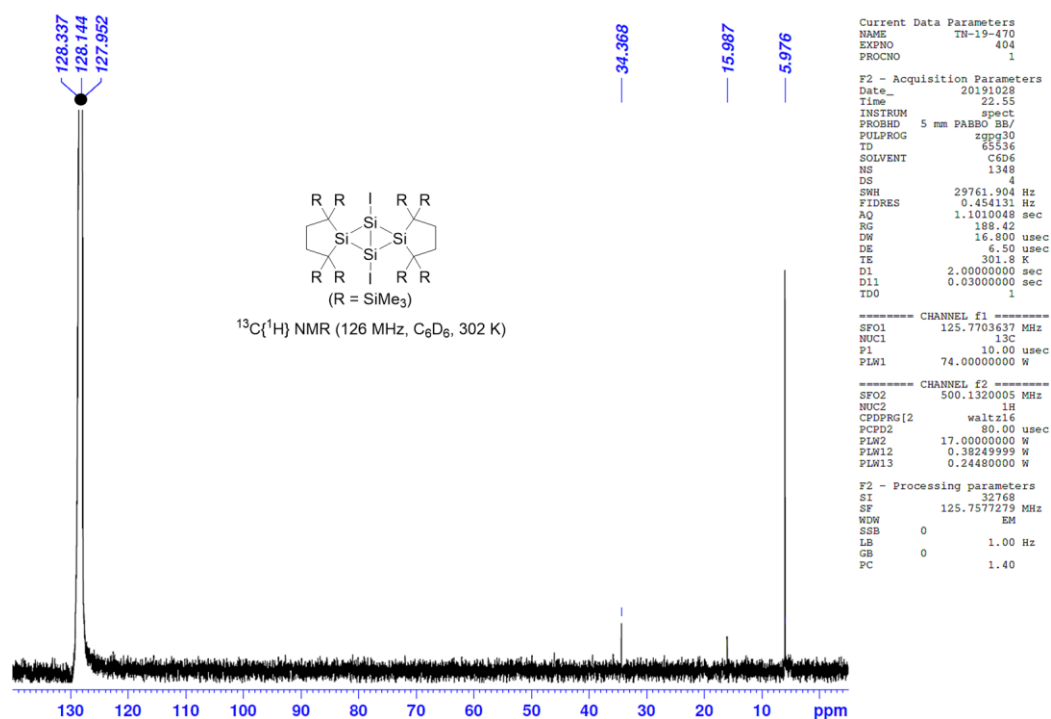


Figure 3-6. $^{13}\text{C}\{^1\text{H}\}$ NMR spectrum of **2** in C_6D_6 in 302 K (● = C_6D_6).

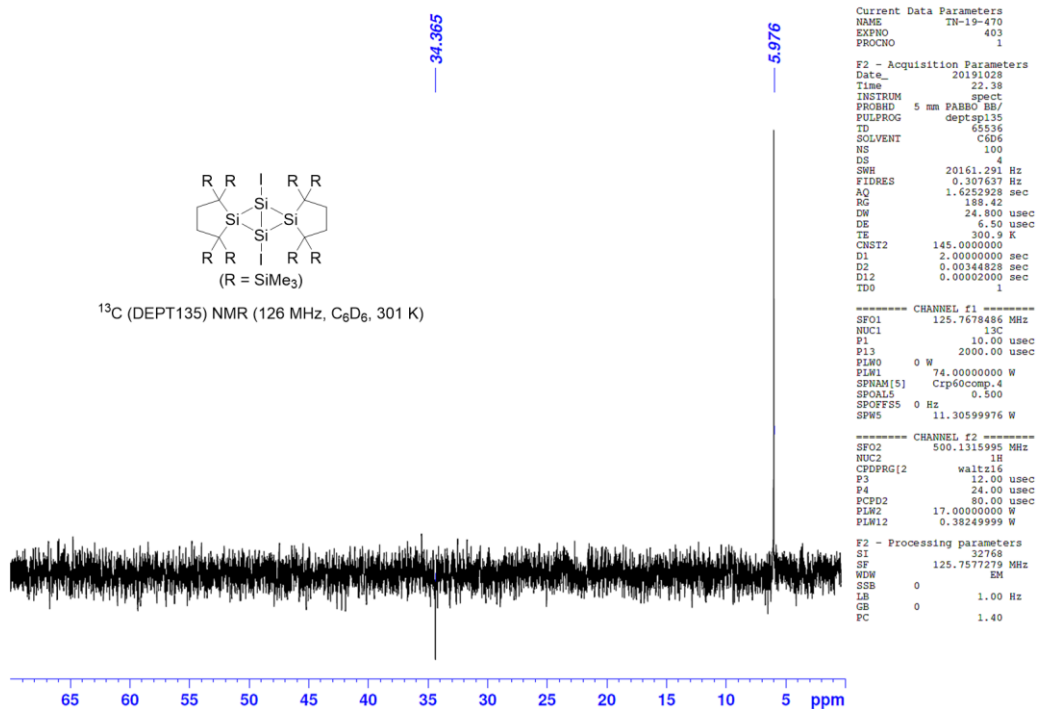


Figure 3-7. ^{13}C (DEPT135) NMR spectrum of **2** in C_6D_6 at 301 K.

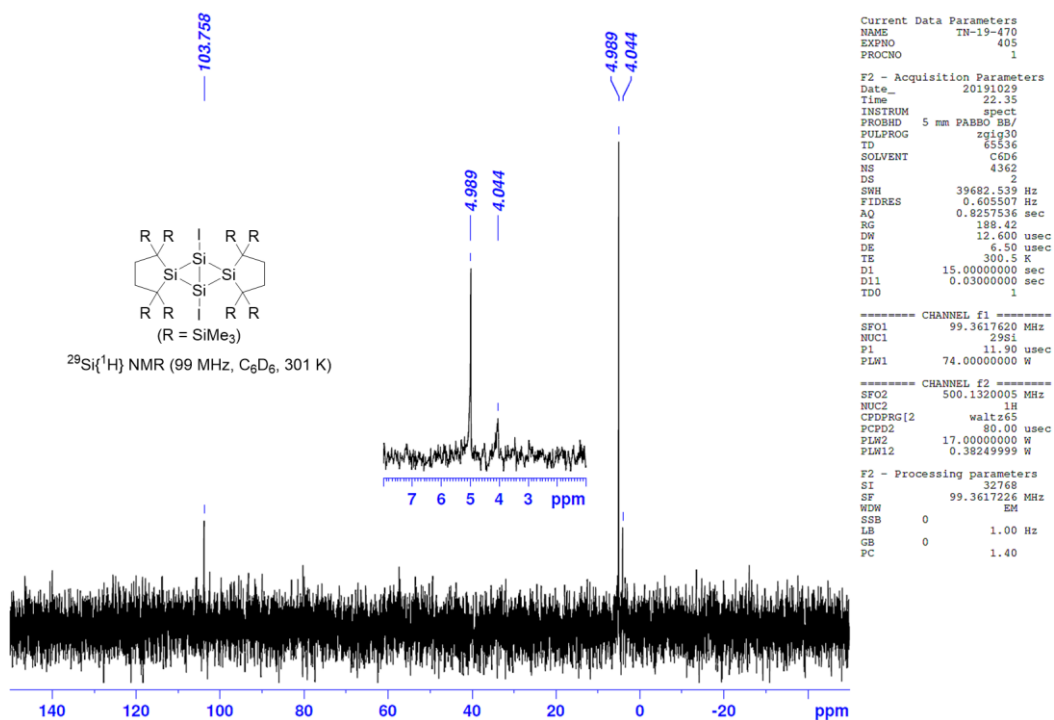


Figure 3-8. $^{29}\text{Si}\{^1\text{H}\}$ NMR spectrum of **2** in C_6D_6 at 301 K.

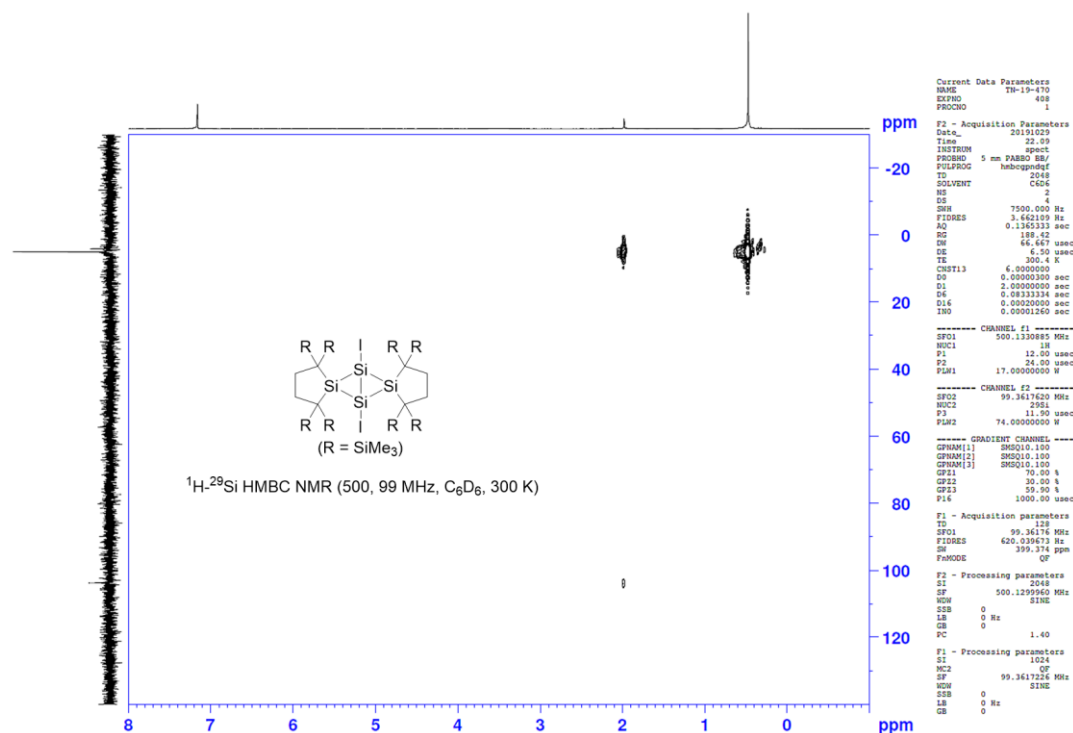


Figure 3-9. ¹H-²⁹Si HMBC NMR spectrum of **2** in C₆D₆ at 300 K.

X-ray Diffraction Analysis

Single crystals suitable for X-ray diffraction study were obtained by recrystallization in an inert atmosphere using the following conditions; from benzene at room temperature for **2_p**, from hexane at $-35\text{ }^{\circ}\text{C}$ for **2_c**. For data collection, the single crystals coated by Apiezon grease were mounted on the glass fiber and then transferred to the cold nitrogen gas stream of the diffractometer. X-ray diffraction data were collected on a Bruker AXS APEX II CCD diffractometer using a graphite monochromated Mo-K α radiation. An empirical absorption correction based on the multiple measurements of equivalent reflections was applied using the program SADABS²⁵ and the structures were solved by direct methods and refined by full-matrix least squares against F^2 using all data (SHELXL-2014/7).²⁶ Molecular structure was analysed by Yadokari-XG software.²⁷

Crystal data of **2_p** (100 K) [CCDC-1992431]: C₃₂H₈₀Si₁₂I₂; Fw 1055.82; monoclinic; *P*2₁/*n*, *a* = 11.0227(3) Å, *b* = 18.3233(5) Å, *c* = 12.8616(3) Å, β = 107.8710(10)°, *V* = 2472.35(11) Å³, *Z* = 2, *D*_{calc} = 1.418 Mg/m³, *R*1 = 0.0235 (*I* > 2σ(*I*)), *wR*2 = 0.0523 (all data), GOF = 1.026.

Crystal data of **2_c** (100 K) [CCDC-1992432]: C₃₂H₈₀Si₁₂I₂; Fw 1055.82; triclinic; *P*-1, *a* = 11.6852(3) Å, *b* = 14.2348(4) Å, *c* = 17.0541(5) Å, α = 68.0820(10)°, β = 78.1770(10)°, γ = 76.5200(10)°, *V* = 2537.24(12) Å³, *Z* = 2, *D*_{calc} = 1.382 Mg/m³, *R*1 = 0.0313 (*I* > 2σ(*I*)), *wR*2 = 0.0687 (all data), GOF = 1.013.

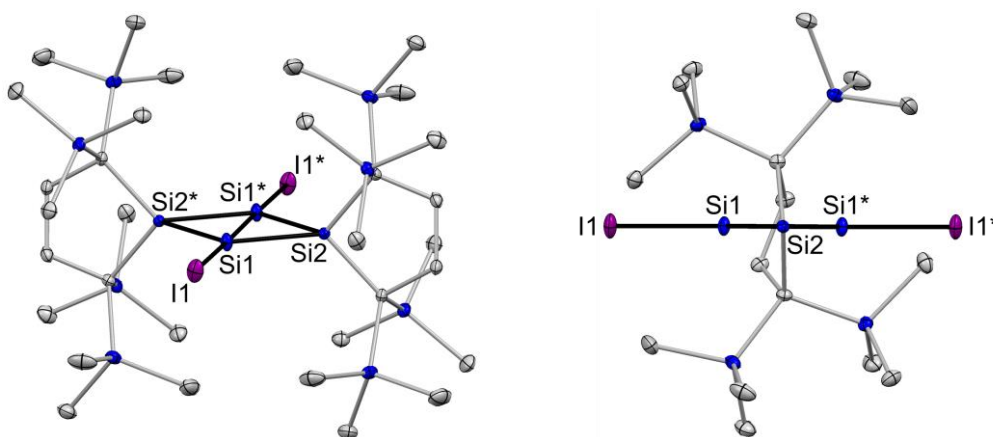


Figure 3-10. ORTEPs of **2_p**. Thermal ellipsoids are shown at the 50% probability level. Hydrogen atoms are omitted for clarity.

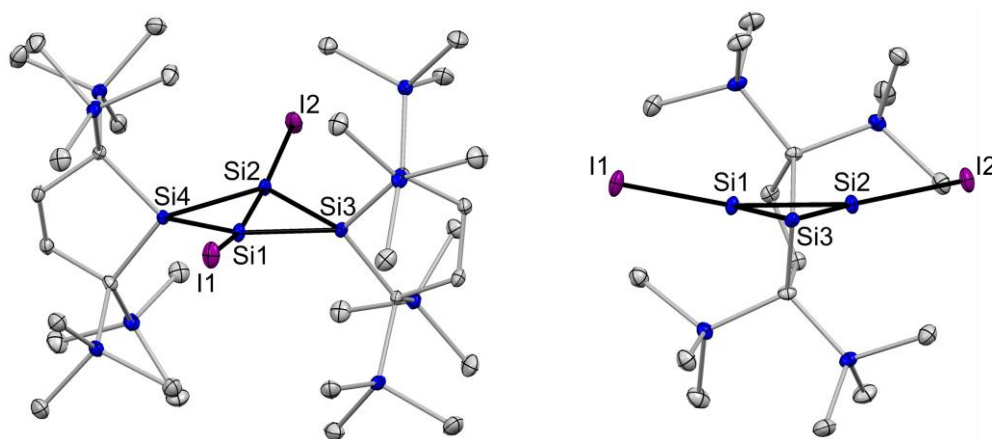


Figure 3-11. ORTEPs of **2_c**. Thermal ellipsoids are shown at the 50% probability level. Hydrogen atoms are omitted for clarity.

UV-vis Absorption Spectra

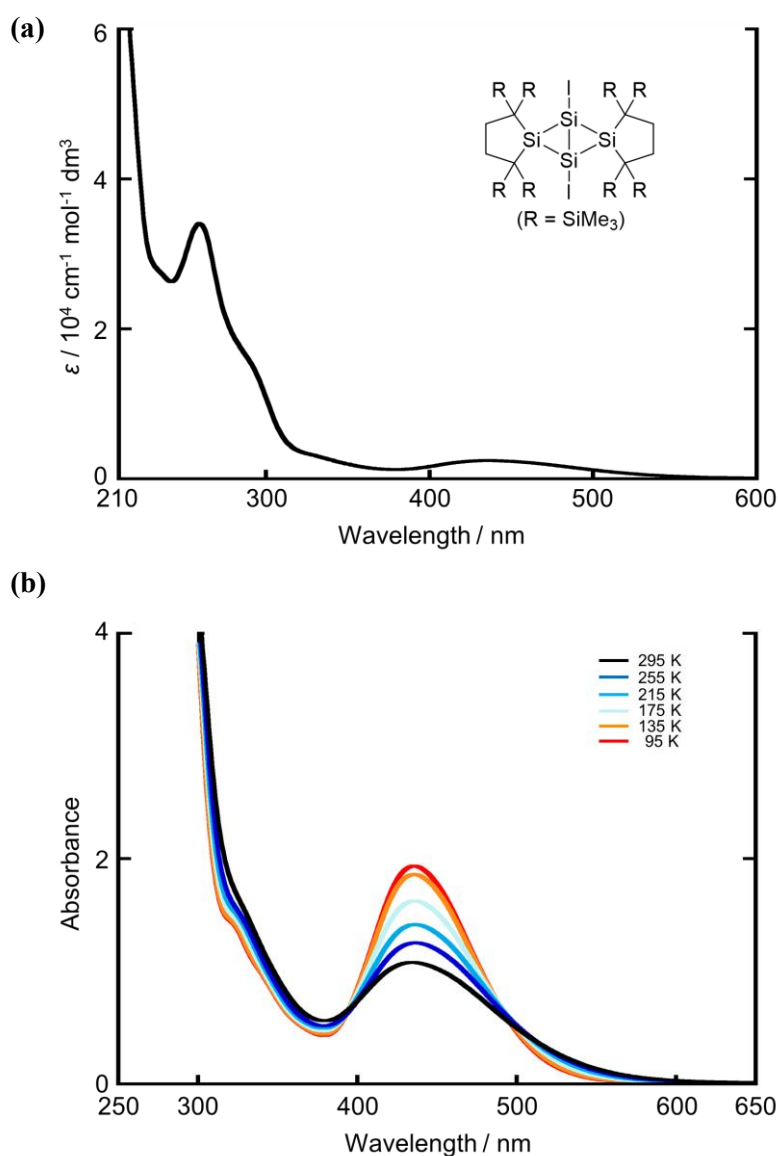


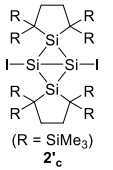
Figure 3-12. (a) UV-vis absorption spectrum of **2** in hexane at room temperature and (b) Temperature-dependent UV-vis absorption spectra of **2** in 3-methylpentane at 295 K to 95 K.

Computational Study

All theoretical calculations were performed using a Gaussian 09²⁸ program or GRRM14 program.²⁹ Geometry optimization was carried out at the B3LYP-D3/B1 (B1: SDD[I], 6-311G(d) [others]) level of theory. The atomic coordinates and energies of optimized structures are summarized in Tables 3-3 to 3-18. Isotropic chemical shielding tensors were calculated at the GIAO/M06L/B2 and B3 (B2: 6-311G(d) [I], 6-311+G(2df,p) [others]; B3: SDD [I], 6-

311+G(2df,p) [others]) level of theory (Table 3-19). Absolute isotropic shielding tensors of ^{29}Si nucleus in tetramethylsilane were calculated to be 361.4 (GIAO/M06L/B2 and B3). Natural bond orbital (NBO)³⁰ calculations of $2'_c$ and $2'_p$ were performed at the B3LYP-D3/B1 level of theory (Tables 3-20 and 3-21). Excitation energies and oscillator strengths of $2'_c$, $2'_p$, and $2'_i$ were calculated at the B3LYP/B1 level of theory (Tables 3-22 to 3-24).

Table 3-3. Atomic Coordinates of $2'_c$ at the B3LYP-D3/6-311G(d) [H,C,Si], SDD [I] Level of Theory

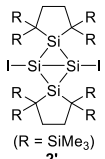


(R = SiMe₃)
 $2'_c$

| Atom | X | Y | Z |
|------|-----------------|-----------------|------------------|
| Si | 11.844852084991 | 9.553027254733 | 12.512055885122 |
| Si | 11.981065972061 | 5.949830017868 | 11.016803044828 |
| Si | 12.253694645279 | 7.278997011780 | 12.925642274061 |
| Si | 12.274417055003 | 8.244249683971 | 10.618051212204 |
| Si | 8.846203940731 | 10.838304654481 | 11.748065610370 |
| Si | 9.672403319674 | 5.617980648655 | 8.814244195547 |
| Si | 14.031153179728 | 3.661534410087 | 12.048288352971 |
| Si | 14.948728643098 | 5.386039042447 | 9.581136489834 |
| Si | 13.800467182515 | 11.957635449648 | 11.565195120368 |
| Si | 9.032446899775 | 4.491863290848 | 11.655151238797 |
| Si | 9.429945942391 | 9.747719525092 | 14.614824529841 |
| Si | 14.711590479723 | 10.286230209920 | 14.070980108441 |
| I | 12.716627808241 | 6.409784154853 | 15.259318479346 |
| I | 12.784220269777 | 9.141707646518 | 8.304925054210 |
| C | 15.615394845704 | 8.803249881240 | 13.342481132148 |
| H | 16.407780716486 | 8.499607387954 | 14.043325429414 |
| H | 16.084912638623 | 9.034500503923 | 12.386106397905 |
| H | 14.974260898154 | 7.937196245534 | 13.183735850232 |
| H | 14.263991298899 | 9.924432146766 | 15.870720119206 |
| C | 13.457995098014 | 9.211254649472 | 16.014966079238 |
| H | 14.007584139399 | 10.839035630381 | 16.412540928970 |
| H | 15.150037858293 | 9.502442647901 | 16.356627427553 |
| C | 16.032789832577 | 11.634180818185 | 14.270090158548 |
| H | 16.809367957248 | 11.222043093975 | 14.923934035734 |
| H | 15.644232583400 | 12.527256212134 | 14.766269536341 |
| H | 16.524774770838 | 11.945397709739 | 13.347787535267 |
| C | 14.336899360232 | 13.679669039734 | 12.150340235512 |
| H | 14.775798595734 | 14.202036081010 | 11.292954673160 |
| H | 15.070357272360 | 13.701772237455 | 12.953718810961 |
| H | 13.474454851044 | 14.273624501073 | 12.467296970273 |
| C | 15.242589058284 | 11.133714134500 | 10.664585165610 |
| H | 15.052589515340 | 10.085948425289 | 10.430794072752 |
| H | 16.176343710486 | 11.182365666552 | 11.228458418634 |
| H | 15.409036243467 | 11.644463571790 | 9.711430170863 |
| C | 12.481614040266 | 12.380755969008 | 10.284594729252 |
| H | 12.974029862403 | 12.856391155508 | 9.429908304270 |
| H | 11.755490355039 | 13.097862864796 | 10.675359550328 |
| H | 11.938781855410 | 11.527669104219 | 9.893621462905 |
| C | 13.176297715616 | 10.876391283150 | 13.047942207538 |
| H | 12.293217859753 | 11.773142613995 | 13.985814857086 |
| H | 12.238802150347 | 11.332031870631 | 14.980329464919 |
| H | 12.736847810412 | 12.763995681662 | 14.125149463682 |
| C | 10.863910981939 | 11.919644843500 | 13.438985519329 |
| H | 10.890060383666 | 12.585059703258 | 12.572923544855 |
| H | 10.238483114466 | 12.432743069777 | 14.177515584543 |
| C | 10.252594036959 | 10.523120878604 | 13.044391648710 |
| C | 8.905799889946 | 7.954133078617 | 14.314781593663 |
| H | 7.820739348743 | 7.832741669456 | 14.353116824365 |
| H | 9.337158077124 | 7.297958629381 | 15.074022222837 |
| H | 9.236644896076 | 7.580893766557 | 13.346050762331 |
| C | 10.533120801398 | 9.768199746993 | 16.145710467820 |
| H | 9.983992885225 | 9.275273926204 | 16.955523829351 |
| H | 10.768731015527 | 10.778856469173 | 16.4888011719857 |
| H | 11.465619991198 | 9.222090106678 | 16.022196191450 |
| C | 7.925303500016 | 10.759081942156 | 15.174087087430 |
| H | 7.091011097038 | 10.778646713053 | 14.472616593919 |
| H | 8.192717273369 | 11.794769283352 | 15.402428350670 |
| H | 7.555348328035 | 10.316953667119 | 16.105645078696 |
| C | 9.357824535125 | 10.925405301666 | 9.932544870616 |

E+ZPVE = -4764.385798 au, Free E (298.15 K) = -4764.492166 au.
Job name: TN87a_bent

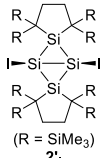
Table 3-4. Atomic Coordinates of $2'_p$ at the B3LYP-D3/6-311G(d) [H,C,Si], SDD [I] Level of Theory



| Atom | X | Y | Z |
|------|-----------------|------------------|-----------------|
| I | 0.458661316324 | 6.885349461895 | 5.921936860855 |
| Si | 2.496481950878 | 8.377627113979 | 6.071742644396 |
| Si | 4.093683750162 | 8.516905463403 | 4.375803439341 |
| C | 5.407673637631 | 7.190003065321 | 3.828141509524 |
| C | 5.178541772882 | 7.189535874321 | 2.265157642694 |
| H | 6.083931584610 | 6.887957776892 | 1.730308249910 |
| H | 4.425531855358 | 6.452638078844 | 1.986401016451 |
| C | 4.718263254290 | 8.569888056704 | 1.759880863219 |
| H | 4.460920795081 | 8.503666212315 | 0.698537117856 |
| H | 5.554696206387 | 9.266546195012 | 1.815586054789 |
| C | 3.516102907052 | 9.091563640065 | 2.617740298804 |
| Si | 3.332814553743 | 10.993738648434 | 2.398388548012 |
| C | 4.984878832885 | 11.888306918751 | 2.584779877052 |
| H | 4.811201166170 | 12.955061422583 | 2.407191511588 |
| H | 5.731828296535 | 11.562482290934 | 1.857060641014 |
| H | 5.426136050615 | 11.804510741741 | 3.576786512274 |
| C | 2.745606720318 | 11.456141549012 | 0.657939117018 |
| H | 1.705849602294 | 11.185792758252 | 0.462498856644 |
| H | 3.363492845759 | 11.010545151982 | -0.126461089756 |
| H | 2.820480411114 | 12.5432822020473 | 0.548395331445 |
| C | 2.117116767352 | 11.777553627915 | 3.611247681895 |
| H | 2.228025133421 | 11.383194653754 | 4.620886900883 |
| H | 1.077605335792 | 11.633246787177 | 3.314704292064 |
| H | 2.297006833635 | 12.855601902342 | 3.659241292590 |
| Si | 1.912980653624 | 8.197888933657 | 1.994186550325 |
| C | 1.854125341588 | 8.154857898532 | 0.099976416772 |
| H | 0.899646772661 | 7.703221499964 | -0.193200972233 |
| H | 2.640295723232 | 7.518200148060 | -0.315676068228 |
| H | 1.918078060160 | 9.125874666403 | -0.388892014731 |
| C | 0.334346001222 | 9.042788088291 | 2.593639490898 |
| H | -0.514056150739 | 8.373630241049 | 2.421188587181 |
| H | 0.133823569247 | 9.967354273940 | 2.046802457662 |
| H | 0.341298998782 | 9.279255580198 | 3.657300142579 |
| C | 1.829441834347 | 6.363500107391 | 2.453078542124 |
| H | 2.229342481485 | 6.133113309895 | 3.435187293180 |
| H | 2.364723159245 | 5.751853043471 | 1.721820711339 |
| H | 0.787080332667 | 6.032332539001 | 2.454268205984 |
| Si | 7.248216761293 | 7.733086002336 | 4.092841622641 |
| C | 8.410575619179 | 6.506474081549 | 3.222484362074 |
| H | 8.341816701092 | 6.591777432213 | 2.134433238330 |
| H | 8.264483785918 | 5.457256602251 | 3.478912525405 |
| H | 9.440642403430 | 6.764961693002 | 3.492031061970 |
| C | 7.684513093247 | 9.366266095682 | 3.245760949104 |
| H | 7.027383380124 | 10.198444568117 | 3.485407981142 |
| H | 7.715578944449 | 9.257201443627 | 2.158339319133 |
| H | 8.690604238573 | 9.656337085320 | 3.567042517270 |
| C | 7.732402729399 | 7.843121311916 | 5.920180310805 |
| H | 8.317055316670 | 8.745936978746 | 6.103464132527 |
| H | 8.338817372607 | 6.987790395341 | 6.222571197622 |
| H | 6.870369727690 | 7.877482512119 | 6.587824182712 |
| Si | 5.250347412497 | 5.370657920370 | 4.516519112098 |
| C | 6.570257103903 | 4.847049698711 | 5.774659329069 |
| H | 6.522754341778 | 5.416921887460 | 6.702051757565 |
| H | 7.598648238885 | 4.870278010371 | 5.416550044156 |
| H | 6.346425505919 | 3.805708367026 | 6.031084929215 |
| C | 5.410822410436 | 4.177271367033 | 3.054411142206 |
| H | 5.523762934698 | 3.158065344779 | 3.437497669998 |
| H | 6.278891655865 | 4.389736759454 | 2.425858692856 |
| H | 4.527105839530 | 4.182427575616 | 2.411128607187 |

E+ZPVE = -4764.381407 au, Free E (298.15 K) = -4764.486143 au.
Job name: TN87a_planar

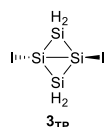
Table 3-5. Atomic Coordinates of $2'_l$ at the B3LYP-D3/6-311G(d) [H,C,Si], SDD [I] Level of Theory



| Atom | X | Y | Z |
|------|-----------------|-----------------|-----------------|
| I | -0.149133220871 | -0.998135872420 | 3.398857620056 |
| Si | -0.04884482464 | 0.549274853588 | 1.365383931219 |
| Si | -1.963994614462 | 0.298603081309 | -0.123469691083 |
| C | -3.474876888607 | -0.952061032929 | -0.131205415092 |
| C | -4.648245355727 | 0.077873904832 | 0.058153924245 |
| H | -5.614849716152 | -0.362101794853 | -0.191570398218 |
| H | -4.727948999512 | 0.383135111186 | 1.105573614158 |

| | | | |
|----|-----------------|----------------|-----------------|
| C | -4.375537074323 | 1.319557440338 | -0.792388499091 |
| H | -5.188758708784 | 2.041025480357 | -0.699854190543 |
| H | -4.358378636393 | 1.028595990286 | -1.847670882923 |
| Si | -2.995730038939 | 1.937884997732 | -0.362352977909 |
| C | -2.454507059207 | 3.142894102089 | -1.754224562604 |
| C | -2.333089070802 | 2.338078043404 | -3.457233608700 |
| H | -2.032986164167 | 3.117479395846 | -4.166055938352 |
| H | -3.278702286163 | 1.928641212040 | -3.815282463033 |
| H | -1.582691992597 | 1.548839655169 | -3.512558696231 |
| C | -3.751686240486 | 4.508752596817 | -1.957239695617 |
| H | -3.837249732677 | 5.169250682964 | -1.092462402729 |
| H | -4.745158798332 | 4.098823084187 | -2.160778194693 |
| H | -3.480846228485 | 5.133008013703 | -2.815140461962 |
| C | -0.780379438101 | 3.934992755440 | -1.427564827334 |
| H | -0.084014222298 | 3.218597201572 | -0.990570362915 |
| H | -0.833639301279 | 4.791222869064 | -0.757512760092 |
| H | -0.339523885261 | 4.278279411612 | -2.366057770747 |
| H | -3.319039390796 | 2.955574752840 | 1.281305969688 |
| Si | -5.111707122329 | 3.575452810310 | 1.284141318492 |

Table 3-8. Atomic Coordinates of **3_{TP}** at the B3LYP-D3/6-311G(d) [H,Si], SDD [I] Level of Theory

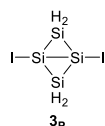


| Atom | X | Y | Z |
|------|-----------------|----------------|----------------|
| Si | -1.180735705629 | 0.983516528972 | 0.000000000000 |
| Si | 0.000000000000 | 0.000000000000 | 1.820290726303 |

| | | | |
|----|-----------------|-----------------|-----------------|
| I | 0.074366626853 | 3.261015647536 | 0.000000000000 |
| Si | 1.180735705629 | -0.983516528972 | 0.000000000000 |
| Si | 0.000000000000 | 0.000000000000 | -1.820290726303 |
| I | -0.074366626853 | -3.261015647536 | 0.000000000000 |
| H | -0.666586418481 | -1.023395540652 | 2.656297120409 |
| H | 0.666586418481 | 1.023395540652 | 2.656297120409 |
| H | -0.666586418481 | -1.023395540652 | -2.656297120409 |
| H | 0.666586418481 | 1.023395540652 | -2.656297120409 |

E+ZPVE = -1183.310452 au, Free E (298.15 K) = -1183.350584 au.
Job name: ti554MIN24G1TP

Table 3-9. Atomic Coordinates of **3_P** at the B3LYP-D3/6-311G(d) [H,Si], SDD [I] Level of Theory

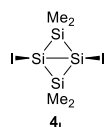


| Atom | X | Y | Z |
|------|-----------------|-----------------|-----------------|
| Si | 0.285411920708 | -0.969712882368 | -0.871351342250 |
| Si | -0.431831060038 | 1.138598150242 | -1.408572935572 |

| | | | |
|----|-----------------|-----------------|-----------------|
| I | 0.818201044808 | -2.779837371744 | -2.497869892263 |
| Si | -0.285435800525 | 0.969713793529 | 0.871353915456 |
| Si | 0.431807180221 | -1.138597239082 | 1.408575508779 |
| I | -0.818224924625 | 2.779838282905 | 2.497872465469 |
| H | -1.777069866868 | 1.291547520878 | -2.019439628122 |
| H | 0.510977675031 | 2.046754994248 | -2.110414733423 |
| H | -0.511001554848 | -2.046754083087 | 2.110417306629 |
| H | 1.777045987051 | -1.291546609717 | 2.019442201329 |

E+ZPVE = -1183.288909 au, Free E (298.15 K) = -1183.325406 au.
Job name: ti554MIN24G1SAD

Table 3-10. Atomic Coordinates of **4_L** at the B3LYP-D3/6-311G(d) [H,C,Si], SDD [I] Level of Theory

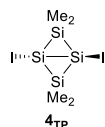


| Atom | X | Y | Z |
|------|-----------------|-----------------|-----------------|
| Si | -1.497210957574 | 0.000000000000 | 0.373990115235 |
| Si | 0.000000000000 | 1.795867712087 | 0.725521802508 |
| I | -2.119761092547 | 0.000000000000 | -2.102196679705 |
| Si | 1.497210957575 | 0.000000000000 | 0.373990115235 |
| Si | 0.000000000000 | -1.795867712087 | 0.725521802508 |
| I | 2.119761092546 | 0.000000000000 | -2.102196679705 |
| C | 0.000000000000 | 2.414284981742 | 2.508447377151 |
| H | 0.884511593288 | 3.028315874908 | 2.700566147136 |

| | | | |
|---|-----------------|-----------------|-----------------|
| H | -0.884511593288 | 3.028315874908 | 2.700566147136 |
| H | 0.000000000000 | 1.591994366244 | 3.227847242182 |
| C | 0.000000000000 | 3.194623702429 | -0.526849862742 |
| H | -0.884395576188 | 3.825853928626 | -0.402003917461 |
| H | 0.884395576188 | 3.825853928626 | -0.402003917461 |
| H | 0.000000000000 | 2.802770766062 | -1.545091066952 |
| C | 0.000000000000 | -2.414284981742 | 2.508447377151 |
| H | -0.884511593288 | -3.028315874908 | 2.700566147136 |
| H | 0.884511593288 | -3.028315874908 | 2.700566147136 |
| H | 0.000000000000 | -1.591994366244 | 3.227847242182 |
| C | 0.000000000000 | -3.194623702429 | -0.526849862742 |
| H | 0.884395576188 | -3.825853928626 | -0.402003917461 |
| H | -0.884395576188 | -3.825853928626 | -0.402003917461 |
| H | 0.000000000000 | -2.802770766062 | -1.545091066952 |

E+ZPVE = -1340.568198 au, Free E (298.15 K) = -1340.617029 au.
Job name: ti554MIN24G2LB

Table 3-11. Atomic Coordinates of **4_{TP}** at the B3LYP-D3/6-311G(d) [H,C,Si], SDD [I] Level of Theory

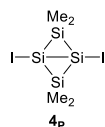


| Atom | X | Y | Z |
|------|-----------------|-----------------|-----------------|
| Si | 1.520636320627 | -0.047970553497 | -0.000000001127 |
| Si | -0.000004207451 | -0.000002582559 | 1.850840575881 |
| I | 2.028134011796 | -2.617872149388 | -0.000000000679 |
| Si | -1.520644736367 | 0.047965389008 | 0.000000000578 |
| Si | -0.000004208290 | -0.000002581930 | -1.850840575430 |
| I | -2.028142427537 | 2.617866984898 | 0.000000001130 |
| C | -0.001492690317 | 1.538779128230 | 2.932990252203 |
| H | -0.980002458259 | 1.678729861534 | 3.400680189241 |

| | | | |
|---|-----------------|-----------------|-----------------|
| H | 0.739369247801 | 1.421061859079 | 3.729765308604 |
| H | 0.228130742052 | 2.443538654177 | 2.371138281265 |
| C | 0.001484275906 | -1.538784293716 | 2.932990251679 |
| H | 0.979994044060 | -1.678735027179 | 3.400680188226 |
| H | -0.739377661851 | -1.421067024836 | 3.729765308456 |
| H | -0.228139156718 | -2.443543819472 | 2.371138280538 |
| C | -0.001492691647 | 1.538779129227 | -2.932990251228 |
| H | 0.739369246110 | 1.421061860347 | -3.729765308005 |
| H | -0.980002459800 | 1.678729862690 | -3.400680187775 |
| H | 0.228130740977 | 2.443538654983 | -2.371138280087 |
| C | 0.001484274576 | -1.538784292719 | -2.932990251752 |
| H | -0.739377663542 | -1.421067023569 | -3.729765308153 |
| H | 0.979994042518 | -1.678735026023 | -3.400680188790 |
| H | -0.228139157793 | -2.443543818666 | -2.371138280814 |

E+ZPVE = -1340.557669 au, Free E (298.15 K) = -1340.606512 au.
Job name: ti554MIN24G2TP

Table 3-12. Atomic Coordinates of **4_P** at the B3LYP-D3/6-311G(d) [H,C,Si], SDD [I] Level of Theory

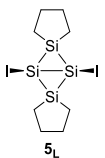


| Atom | X | Y | Z |
|------|-----------------|-----------------|----------------|
| Si | 1.322469409544 | 0.000000000000 | 0.000000000000 |
| Si | 0.000000000000 | 1.883643754939 | 0.000000000000 |
| I | 3.835635746357 | 0.000000000000 | 0.000000000000 |
| Si | -1.322469409544 | 0.000000000000 | 0.000000000000 |
| Si | 0.000000000000 | -1.883643754939 | 0.000000000000 |
| I | -3.835635746357 | 0.000000000000 | 0.000000000000 |

| | | | | | | | |
|---|-----------------|-----------------|-----------------|---|-----------------|-----------------|-----------------|
| C | 0.000000000000 | 2.988241125774 | -1.530843037140 | H | -0.882238272526 | -3.636395555049 | -1.535369487410 |
| H | -0.882238272526 | 3.636395555049 | -1.535369487410 | H | 0.000000000000 | -2.403215294490 | -2.451487466808 |
| H | 0.882238272526 | 3.636395555049 | -1.535369487410 | C | 0.000000000000 | -2.988241125774 | 1.530843037140 |
| H | 0.000000000000 | 2.403215294490 | -2.451487466808 | H | -0.882238272526 | -3.636395555049 | 1.535369487410 |
| C | 0.000000000000 | 2.988241125774 | 1.530843037140 | H | 0.882238272526 | -3.636395555049 | 1.535369487410 |
| H | 0.882238272526 | 3.636395555049 | 1.535369487410 | H | 0.000000000000 | -2.403215294490 | 2.451487466808 |
| H | -0.882238272526 | 3.636395555049 | 1.535369487410 | C | 0.000000000000 | -2.988241125774 | -1.530843037140 |
| H | 0.000000000000 | 2.403215294490 | 2.451487466808 | H | 0.882238272526 | -3.636395555049 | -1.535369487410 |
| C | 0.000000000000 | -2.988241125774 | -1.530843037140 | | | | |
| H | 0.882238272526 | -3.636395555049 | -1.535369487410 | | | | |

E+ZPVE = -1340.533937 au, Free E (298.15 K) = -1340.580461 au.
Job name: ti554MIN24G2SAD

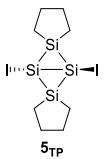
Table 3-13. Atomic Coordinates of 5_L at the B3LYP-D3/6-311G(d) [H,C,Si], SDD [I] Level of Theory



| | | | | | | | |
|----|-----------------|-----------------|-----------------|----|-----------------|-----------------|-----------------|
| Si | -1.117391707324 | -0.519305291345 | -1.795551985524 | Si | -1.117391707324 | -0.519305291345 | -1.795551985524 |
| I | 0.559502020743 | 2.564691150563 | 0.000000000000 | I | 0.559502020743 | 2.564691150563 | 0.000000000000 |
| C | -2.627663132550 | -1.175133783332 | 2.752421062230 | C | -2.627663132550 | -1.175133783332 | 2.752421062230 |
| C | -2.396455264703 | -0.593793751630 | 4.169732345273 | H | -2.732692319873 | 0.449738175924 | 4.195853595935 |
| H | -2.732692319873 | 0.449738175924 | 4.195853595935 | H | -2.982720184640 | -1.131709321675 | 4.921277034889 |
| C | -2.982720184640 | -1.131709321675 | 4.921277034889 | H | -0.88935449834 | -0.647401609529 | 4.492684623584 |
| H | -0.88935449834 | -0.647401609529 | 4.492684623584 | H | -0.589522614210 | -1.693498044139 | 4.627379030128 |
| H | -0.589522614210 | -1.693498044139 | 4.627379030128 | H | -0.670318247685 | -0.134613660981 | 5.434209603864 |
| H | -0.670318247685 | -0.134613660981 | 5.434209603864 | C | -0.095113166862 | -0.031598907144 | 3.315361808768 |
| C | -0.095113166862 | -0.031598907144 | 3.315361808768 | Si | -0.225623569776 | -1.769162616646 | 0.000000000000 |
| Si | -0.225623569776 | -1.769162616646 | 0.000000000000 | | | | |

E+ZPVE = -1495.350671 au, Free E (298.15 K) = -1495.402237 au.
Job name: ti554MIN24G3LB

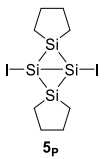
Table 3-14. Atomic Coordinates of 5_{TP} at the B3LYP-D3/6-311G(d) [H,C,Si], SDD [I] Level of Theory



| | | | | | | | |
|----|-----------------|-----------------|----------------|----|-----------------|-----------------|----------------|
| Si | 0.000000000000 | 0.000000000000 | 1.849455843720 | Si | 0.000000000000 | 0.000000000000 | 1.849455843720 |
| I | 2.717963099908 | 1.763345214185 | 0.000000000000 | I | 2.717963099908 | 1.763345214185 | 0.000000000000 |
| C | -0.622233652522 | -1.268547620036 | 3.115564646693 | C | -0.622233652522 | -1.268547620036 | 3.115564646693 |
| C | -0.000425513781 | -0.771118199234 | 4.441843641021 | C | -0.000425513781 | -0.771118199234 | 4.441843641021 |
| H | 1.032638284601 | -1.130060246929 | 4.522568462243 | H | 1.032638284601 | -1.130060246929 | 4.522568462243 |
| H | -0.539550288814 | -1.167737091175 | 5.307517771334 | H | -0.539550288814 | -1.167737091175 | 5.307517771334 |
| C | 0.000425513781 | 0.771118199234 | 4.441843641021 | C | 0.000425513781 | 0.771118199234 | 4.441843641021 |
| H | -1.032638284601 | 1.130060246929 | 4.522568462243 | H | -1.032638284601 | 1.130060246929 | 4.522568462243 |
| H | 0.539550288814 | 1.167737091175 | 5.307517771334 | H | 0.539550288814 | 1.167737091175 | 5.307517771334 |
| C | -0.000425513781 | -0.771118199234 | 4.441843641021 | C | -0.000425513781 | -0.771118199234 | 4.441843641021 |
| H | 1.032638284601 | -1.130060246929 | 4.522568462243 | H | 1.032638284601 | -1.130060246929 | 4.522568462243 |
| H | -0.539550288814 | -1.167737091175 | 5.307517771334 | H | -0.539550288814 | -1.167737091175 | 5.307517771334 |
| C | -0.622233652522 | -1.268547620036 | 3.115564646693 | C | -0.622233652522 | -1.268547620036 | 3.115564646693 |
| Si | 1.413420437365 | -0.521412835850 | 0.000000000000 | Si | 1.413420437365 | -0.521412835850 | 0.000000000000 |

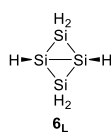
E+ZPVE = -1495.345616 au, Free E (298.15 K) = -1495.396126 au.
Job name: ti554MIN24G3TP

Table 3-15. Atomic Coordinates of 5_P at the B3LYP-D3/6-311G(d) [H,C,Si], SDD [I] Level of Theory



| | | | | | | | |
|----|-----------------|-----------------|-----------------|----|-----------------|-----------------|-----------------|
| Si | -0.179454959277 | -0.951614457666 | -0.910435447533 | Si | -0.179454959277 | -0.951614457666 | -0.910435447533 |
| Si | -0.432564054140 | 1.216804171297 | -1.357248808526 | I | -0.514892582832 | 2.750810680476 | 2.629267493655 |
| I | -0.514892582832 | 2.750810680476 | 2.629267493655 | C | 2.091043581166 | -1.698270014383 | 2.164006529821 |
| C | 2.091043581166 | -1.698270014383 | 2.164006529821 | C | 1.664487208374 | -2.499207508662 | 3.414553638574 |
| C | 1.664487208374 | -2.499207508662 | 3.414553638574 | H | 1.426151171008 | -1.805215384575 | 4.229735264008 |
| H | 1.426151171008 | -1.805215384575 | 4.229735264008 | H | 2.470571470380 | -3.144193117650 | 3.777512655911 |
| H | 2.470571470380 | -3.144193117650 | 3.777512655911 | C | 0.404344493231 | -3.325349150629 | 3.073860933504 |
| C | 0.404344493231 | -3.325349150629 | 3.073860933504 | H | 0.681179770140 | -4.127651746428 | 2.379149383949 |
| H | 0.681179770140 | -4.127651746428 | 2.379149383949 | H | -0.000744815317 | -3.810186699109 | 3.967365100239 |
| H | -0.000744815317 | -3.810186699109 | 3.967365100239 | C | -0.635052000195 | -2.399137000802 | 2.403756717830 |
| C | -0.635052000195 | -2.399137000802 | 2.403756717830 | H | -2.723985209900 | 0.839870475743 | -2.397308829904 |
| H | -2.723985209900 | 0.839870475743 | -2.397308829904 | H | -2.655968319155 | 2.333340448672 | -1.472110203817 |
| H | -2.655968319155 | 2.333340448672 | -1.472110203817 | H | 1.179304883722 | 1.819247066465 | -3.157874103984 |
| H | 1.179304883722 | 1.819247066465 | -3.157874103984 | H | 1.381114824448 | 2.940479131558 | -1.818737824138 |
| H | 1.381114824448 | 2.940479131558 | -1.818737824138 | H | 2.723985209900 | -0.839870475743 | 2.397308829904 |
| H | 2.723985209900 | -0.839870475743 | 2.397308829904 | H | 2.655968319155 | -2.333340448672 | 1.472110203817 |
| H | 2.655968319155 | -2.333340448672 | 1.472110203817 | H | -1.179304883722 | -1.819247066465 | 3.157874103984 |
| H | -1.179304883722 | -1.819247066465 | 3.157874103984 | H | -1.381114824448 | -2.940479131558 | 1.818737824138 |
| H | -1.381114824448 | -2.940479131558 | 1.818737824138 | | | | |

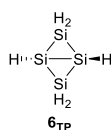
E+ZPVE = -1495.320608 au, Free E (298.15 K) = -1495.369943 au.
Job name: ti554MIN24G3SAD

Table 3-16. Atomic Coordinates of **6_L** at the B3LYP-D3/6-311G(d) Level of Theory

| Atom | X | Y | Z |
|------|-----------------|-----------------|-----------------|
| Si | -1.439767966756 | 0.435207437142 | 0.000225108213 |
| Si | 0.000228096595 | 1.034701389212 | 1.742127972419 |
| H | -1.501123470425 | -1.063035755931 | -0.000140653645 |

| | | | |
|----|-----------------|-----------------|-----------------|
| Si | 1.439837033175 | 0.435136883286 | -0.000070570317 |
| Si | -0.000129599978 | 1.035566528514 | -1.741675458315 |
| H | 1.501119042772 | -1.063109314556 | -0.000448924625 |
| H | 0.000335645888 | 0.222258629545 | 2.983410017394 |
| H | 0.000296586173 | 2.481055606350 | 2.064021706503 |
| H | -0.000276987269 | 0.223740368711 | -2.983360856883 |
| H | -0.000127136975 | 2.482080440179 | -2.062850808430 |

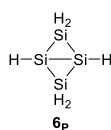
E+ZPVE = -1161.579368 au, Free E (298.15 K) = -1161.609617 au.
Job name: ti554MIN23G5L

Table 3-17. Atomic Coordinates of **6_{TP}** at the B3LYP-D3/6-311G(d) Level of Theory

| Atom | X | Y | Z |
|------|-----------------|----------------|----------------|
| Si | -1.128758438050 | 0.947499098181 | 0.000000000000 |
| Si | 0.000000000000 | 0.000000000000 | 1.836836798354 |
| H | -0.147343070151 | 2.107492947122 | 0.000000000000 |

| | | | |
|----|-----------------|-----------------|-----------------|
| Si | 1.128758438050 | -0.947499098181 | 0.000000000000 |
| Si | 0.000000000000 | 0.000000000000 | -1.836836798354 |
| H | 0.147343070151 | -2.107492947122 | 0.000000000000 |
| H | -0.605980736278 | -1.051219592740 | 2.688324629783 |
| H | 0.605980736278 | 1.051219592740 | 2.688324629783 |
| H | -0.605980736278 | -1.051219592740 | -2.688324629783 |
| H | 0.605980736278 | 1.051219592740 | -2.688324629783 |

E+ZPVE = -1161.561993 au, Free E (298.15 K) = -1161.592445 au.
Job name: ti554MIN23G5PT

Table 3-18. Atomic Coordinates of **6_P** at the B3LYP-D3/6-311G(d) Level of Theory

| Atom | X | Y | Z |
|------|----------------|----------------|----------------|
| Si | 1.407981345557 | 0.000000000000 | 0.000000000000 |
| Si | 0.000000000000 | 1.819499831760 | 0.000000000000 |
| H | 2.901895517455 | 0.000000000000 | 0.000000000000 |

| | | | |
|----|-----------------|-----------------|-----------------|
| Si | -1.407981345557 | 0.000000000000 | 0.000000000000 |
| Si | 0.000000000000 | -1.819499831760 | 0.000000000000 |
| H | -2.901895517455 | 0.000000000000 | 0.000000000000 |
| H | 0.000000000000 | 2.710612256493 | -1.193741394528 |
| H | 0.000000000000 | 2.710612256493 | 1.193741394528 |
| H | 0.000000000000 | -2.710612256493 | -1.193741394528 |
| H | 0.000000000000 | -2.710612256493 | 1.193741394528 |

E+ZPVE = -1161.541984 au, Free E (298.15 K) = -1161.570454 au.
Job name: ti554MIN23G5SAD

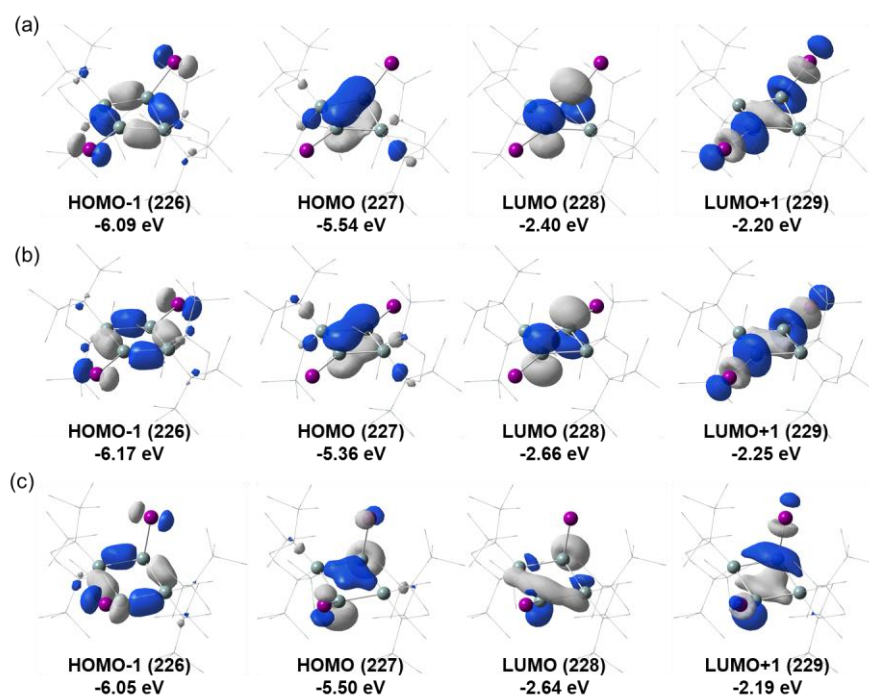


Figure 3-13. Frontier Kohn-Sham orbitals of (a) $2'_c$, (b) $2'_p$ and (c) $2'_1$ at the TD-B3LYP-D3/6-311G(d) [H,C,Si], SDD [I]/B3LYP-D3/6-311G(d) [H,C,Si], SDD [I] level of theory. [td_b_TN81b_bent, td_a_TN81b_planar, td_a_TN85a]

Table 3-19. Experimental and Theoretical Isotropic ^{29}Si Chemical Shifts of Iodosilanes

| Compound | ^{29}Si chemical shift | | | Note |
|---|---------------------------------|---------------------------|---------------------------|----------------|
| | observed | calculated ^{a,c} | calculated ^{b,c} | |
| H ₃ SiI | -83.3 ^d | -43.2 (404.6) | -35.2 (396.6) | TN86a_H |
| Me ₃ SiI | 8.9 ^d | 39.0 (322.4) | 46.3 (315.1) | TN86a_Me |
| (Me ₃ Si) ₃ SiI | -54.1 ^e | -35.9 (397.3) | -19.7 (381.1) | TN86a_TMS_GRRM |
| Tip ₂ Si=SiTipI ^f | 51.7 ^g | 80.3 (281.1) | 94.1 (267.3) | TN83a |
| 2 (bridge) | 4.0 | - | - | |
| 2 (bridgehead) | 103.8 | - | - | |
| 2' _c (bridge) | - | -2.8 (364.2) | -2.9 (364.3) | TN81b_bent |
| 2' _c (bridgehead) | - | 129.3 (232.1) | 139.1 (222.3) | TN81b_bent |
| 2' _p (bridge) | - | 5.7 (355.7) | 5.2 (356.2) | TN81b_planar |
| 2' _p (bridgehead) | - | 182.6 (178.7) | 191.0 (170.4) | TN81b_planar |
| 2' ₁ (bridge) | - | 119.9 (241.5) | 119.8 (241.6) | TN85a |
| | | 118.6 (242.8) | 118.3 (243.1) | |
| 2' ₁ (bridgehead) | - | 12.1 (349.3) | 23.6 (337.8) | TN85a |
| | | -6.3 (367.7) | 6.4 (355.0) | |

^aGIAO/M06L/6-311G(d) [I], 6-311+G(2df,p) [others] level of theory. Absolute chemical shift for tetramethylsilane = 361.4. ^bGIAO/M06L/SDD [I], 6-311+G(2df,p) [others] level of theory. ^cThe absolute chemical shift is shown in the parentheses. ^dReference 31. ^eReference 32. ^fTip = 2,4,6-triisopropylphenyl. ^gReference 33.

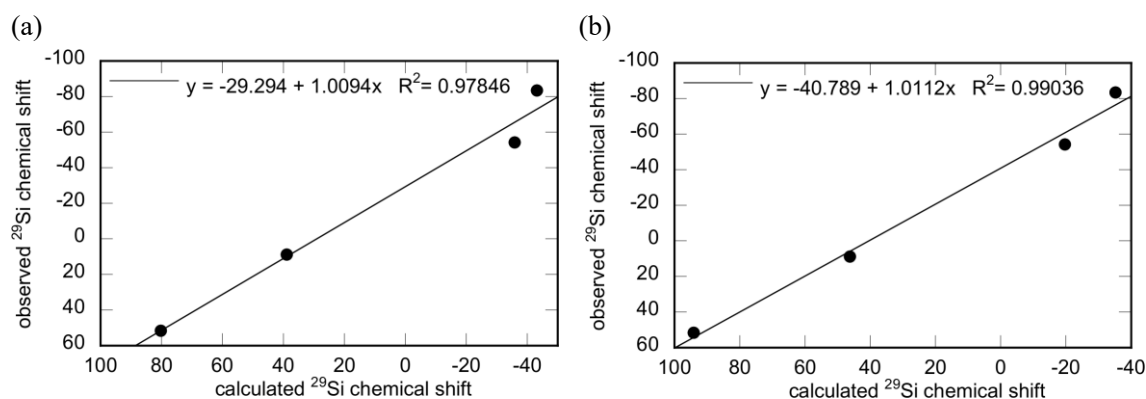
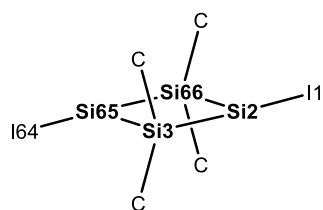


Figure 3-14. A plot of observed ^{29}Si chemical shift (δ_{obs}) vs calculated ^{29}Si chemical shift (δ_{calc}) at (a) the M06L/6-311G(d) [I], 6-311+G(2df,p) [others] level of theory ($\delta_{\text{obs}} = 1.009\delta_{\text{calc}} - 29.3$, $R^2 = 0.978$) and (b) the M06L/SDD [I], 6-311+G(2df,p) [others] level of theory ($\delta_{\text{obs}} = 1.011\delta_{\text{calc}} - 40.8$, $R^2 = 0.990$).

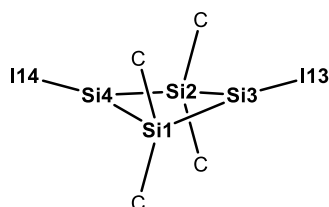
Table 3-20. Natural Bond Orbital (NBO) Analysis for $2'_p$



| NBO | NBO ^a analysis | | | | |
|----------|---------------------------|---------------|--|-------------------------------|------------------|
| | occ., ^a | population | hybrids | NHO ^a bond bending | WBI ^a |
| Si2-Si65 | 1.633 | 50.00% (Si2) | s 0.72%, p 98.96%, d 0.32% ($\text{sp}^{99.99}\text{d}^{0.45}$) (Si2) | 82.1 (Si2) | 0.6990 |
| | | 50.00% (Si65) | s 0.72%, p 98.96%, d 0.32% ($\text{sp}^{99.99}\text{d}^{0.45}$) (Si65) | 82.1 (Si65) | |
| Si2-Si3 | 1.883 | 55.48% (Si2) | s 41.20%, p 58.52%, d 0.28% ($\text{sp}^{1.42}\text{d}^{0.01}$) (Si2) | 13.9 (Si2) | 0.9777 |
| | | 44.52% (Si3) | s 21.14%, p 78.22%, d 0.64% ($\text{sp}^{3.70}\text{d}^{0.03}$) (Si3) | 13.6 (Si3) | |
| Si2-Si66 | 1.884 | 56.18% (Si2) | s 42.23%, p 57.51%, d 0.26% ($\text{sp}^{1.36}\text{d}^{0.01}$) (Si2) | 14.4 (Si2) | 0.9707 |
| | | 43.82% (Si66) | s 20.11%, p 79.25%, d 0.63% ($\text{sp}^{3.94}\text{d}^{0.03}$) (Si66) | 14.2 (Si66) | |
| Si2-I1 | 1.966 | 34.27% (Si1) | s 15.69%, p 83.56%, d 0.74% ($\text{sp}^{5.32}\text{d}^{0.05}$) (Si2) | 2.7 (Si2) | 0.9181 |
| | | 65.73% (I1) | s 17.38%, p 82.62% ($\text{sp}^{4.72}$) (I1) | | |

^aNBO: natural bond orbital. NHO: natural hybrid orbital. NPA: natural atomic orbital. occ.: occupancy. WBI: Wiberg bond index. JOB number: TN87a_planarNBO

Table 3-21. Natural Bond Orbital (NBO) Analysis for $2'_c$



| NBO | NBO ^a analysis | | | | |
|---------|---------------------------|--------------|---|-------------------------------|------------------|
| | occ., ^a | population | hybrids | NHO ^a bond bending | WBI ^a |
| Si3-Si4 | 1.689 | 50.00% (Si3) | s 4.38%, p 95.25%, d 0.37% ($\text{sp}^{21.73}\text{d}^{0.08}$) (Si3) | 62.0 (Si3) | 0.7693 |
| | | 50.00% (Si4) | s 4.38%, p 95.25%, d 0.37% ($\text{sp}^{21.73}\text{d}^{0.08}$) (Si4) | 62.0 (Si4) | |

| | | | | | |
|---------|-------|--------------|---|------------|--------|
| Si3-Si1 | 1.874 | 56.39% (Si3) | s 39.92%, p 59.80%, d 0.29% (sp ^{1.50} d ^{0.01}) (Si3) | 16.9 (Si3) | 0.9467 |
| | | 43.61% (Si1) | s 20.17%, p 79.22%, d 0.61% (sp ^{3.93} d ^{0.03}) (Si1) | 15.3 (Si1) | |
| Si3-Si2 | 1.885 | 56.06% (Si3) | s 39.70%, p 60.02%, d 0.28% (sp ^{1.51} d ^{0.01}) (Si3) | 18.8 (Si3) | 0.9595 |
| | | 43.94% (Si2) | s 20.63%, p 78.79%, d 0.59% (sp ^{3.82} d ^{0.03}) (Si2) | 16.6 (Si2) | |
| Si3-I13 | 1.969 | 34.83% (Si3) | s 15.86%, p 83.47%, d 0.68% (sp ^{5.26} d ^{0.04}) (Si3) | 2.0 (Si3) | 0.9044 |
| | | 65.17% (I13) | s 16.95%, p 83.05% (sp ^{4.90}) (I13) | 1.2 (I13) | |

^aNBO: natural bond orbital. NHO: natural hybrid orbital. NPA: natural atomic orbital. occ.: occupancy. WBI: Wiberg bond index. JOB number: TN87a_bentNBO

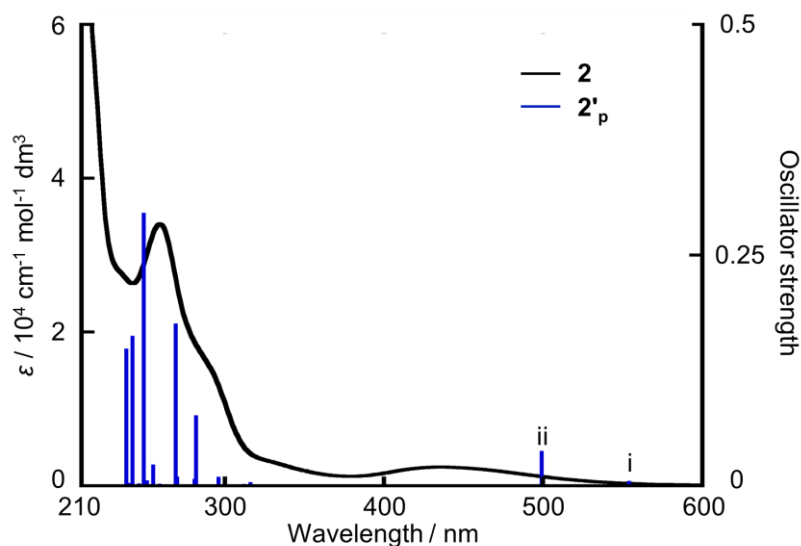


Figure 3-15. Experimental UV-vis absorption spectrum of **2** in hexane (black) and calculated band positions of **2'**_p at the TD-B3LYP-D3/6-311G(d) [H,C,Si], SDD [I]/B3LYP-D3/6-311G(d) [H,C,Si], SDD [I] level of theory (blue). i: $\pi(\text{Si-Si}) \rightarrow \sigma^*(\text{I-Si})$, ii: a mixture of $\pi(\text{Si-Si}) \rightarrow \pi^*(\text{Si-Si})$ and $\pi(\text{Si-Si}) \rightarrow \sigma^*(\text{I-Si})$ transitions. [td_a_TN81b_planar]

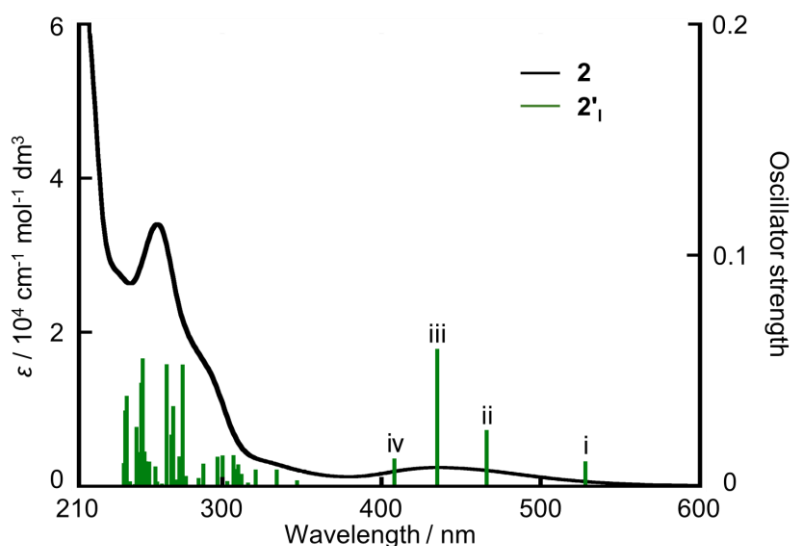


Figure 3-16. Experimental UV-vis absorption spectrum of **2** in hexane (black) and calculated band positions of **2'**₁ at the TD-B3LYP-D3/6-311G(d) [H,C,Si], SDD [I]/B3LYP-D3/6-311G(d) [H,C,Si], SDD [I] level of theory (green). i: $\sigma(\text{Si-Si}) \rightarrow \sigma^*(\text{Si-Si})$, ii: $\sigma(\text{peripheral Si}_4 \text{ ring}) \rightarrow$

$\sigma^*(\text{Si-Si})$, iii: a mixture of $\sigma(\text{Si-Si}) \rightarrow \sigma^*(\text{Si-Si})$ and $\sigma(\text{Si-Si}) \rightarrow \sigma^*(\text{I-Si})$, iv: $\sigma(\text{peripheral Si}_4 \text{ ring}) \rightarrow \sigma^*(\text{I-Si})$ transitions. [td_a_TN85a]

Table 3-22. Transition Energy, Wavelength, and Oscillator Strengths of the Electronic Transition of $2'_c$ (The 227th orbital is highest occupied orbital shown in Figure 3-13) [td_b_TN81b_bent]

| | | | |
|---|---|---|---|
| Excited State 1: Singlet-A 227 -> 229 0.70371 | 2.4989 eV 496.15 nm f=0.0021 <S**2>=0.000 | Excited State 16: Singlet-B 219 -> 228 0.59193 222 -> 229 0.17330 224 -> 229 0.24108 226 -> 230 0.19093 | 4.3535 eV 284.79 nm f=0.0043 <S**2>=0.000 |
| Excited State 2: Singlet-B 225 -> 229 -0.11590 226 -> 228 -0.22127 227 -> 228 0.65426 | 2.7813 eV 445.78 nm f=0.0324 <S**2>=0.000 | Excited State 17: Singlet-A 216 -> 229 0.10740 218 -> 228 -0.28424 221 -> 229 0.57863 223 -> 229 0.24297 | 4.3782 eV 283.19 nm f=0.0010 <S**2>=0.000 |
| Excited State 3: Singlet-B 226 -> 228 0.66903 227 -> 228 0.21504 | 2.8057 eV 441.90 nm f=0.0064 <S**2>=0.000 | Excited State 18: Singlet-B 218 -> 229 -0.19894 221 -> 228 -0.14189 222 -> 229 0.54043 224 -> 229 -0.28976 225 -> 229 0.20926 | 4.4357 eV 279.52 nm f=0.0051 <S**2>=0.000 |
| Excited State 4: Singlet-A 226 -> 229 0.70427 | 3.0712 eV 403.70 nm f=0.0001 <S**2>=0.000 | Excited State 19: Singlet-A 218 -> 228 0.12571 219 -> 229 -0.13470 221 -> 229 -0.20441 223 -> 229 0.64659 | 4.4457 eV 278.88 nm f=0.0000 <S**2>=0.000 |
| Excited State 5: Singlet-B 227 -> 230 0.70132 | 3.5864 eV 345.71 nm f=0.0014 <S**2>=0.000 | Excited State 20: Singlet-A 218 -> 228 0.60815 221 -> 229 0.31397 | 4.4940 eV 275.89 nm f=0.0008 <S**2>=0.000 |
| Excited State 6: Singlet-A 225 -> 228 0.18836 227 -> 231 0.67441 | 3.5907 eV 345.29 nm f=0.0129 <S**2>=0.000 | Excited State 21: Singlet-B 218 -> 229 -0.22600 220 -> 229 0.54368 224 -> 229 -0.18555 225 -> 229 -0.30052 | 4.5130 eV 274.73 nm f=0.0307 <S**2>=0.000 |
| Excited State 7: Singlet-A 222 -> 228 -0.11422 224 -> 228 -0.10557 225 -> 228 0.65860 227 -> 231 -0.17828 | 3.9556 eV 313.44 nm f=0.0003 <S**2>=0.000 | Excited State 22: Singlet-B 218 -> 229 0.61143 220 -> 229 0.16757 222 -> 229 0.20756 224 -> 229 -0.16157 | 4.5351 eV 273.39 nm f=0.0005 <S**2>=0.000 |
| Excited State 8: Singlet-A 222 -> 228 0.37953 224 -> 228 0.56522 225 -> 228 0.13496 | 4.0595 eV 305.42 nm f=0.0002 <S**2>=0.000 | Excited State 23: Singlet-A 218 -> 228 0.10376 219 -> 229 0.66349 223 -> 229 0.13151 | 4.5576 eV 272.04 nm f=0.0008 <S**2>=0.000 |
| Excited State 9: Singlet-B 219 -> 228 -0.10544 221 -> 228 0.40139 223 -> 228 0.53068 225 -> 229 0.17240 | 4.1888 eV 295.99 nm f=0.0015 <S**2>=0.000 | Excited State 24: Singlet-A 217 -> 228 0.68395 | 4.6544 eV 266.38 nm f=0.0000 <S**2>=0.000 |
| Excited State 10: Singlet-B 219 -> 228 0.12845 221 -> 228 0.42234 222 -> 229 -0.14515 223 -> 228 -0.35395 224 -> 229 -0.21799 225 -> 229 0.28659 226 -> 230 0.12822 | 4.2145 eV 294.18 nm f=0.0164 <S**2>=0.000 | Excited State 25: Singlet-B 215 -> 229 -0.18709 216 -> 228 0.11051 217 -> 229 -0.11552 220 -> 229 0.38947 221 -> 228 -0.19121 224 -> 229 0.18845 225 -> 229 0.39397 | 4.6892 eV 264.40 nm f=0.1829 <S**2>=0.000 |
| Excited State 11: Singlet-A 220 -> 228 0.10947 222 -> 228 0.52162 224 -> 228 -0.39001 226 -> 231 0.23724 | 4.2276 eV 293.27 nm f=0.0011 <S**2>=0.000 | Excited State 26: Singlet-A 215 -> 228 0.67988 | 4.7726 eV 259.79 nm f=0.0004 <S**2>=0.000 |
| Excited State 12: Singlet-A 220 -> 228 0.29099 222 -> 228 -0.25529 226 -> 231 0.57583 | 4.2353 eV 292.74 nm f=0.0001 <S**2>=0.000 | Excited State 27: Singlet-B 212 -> 228 0.15993 216 -> 228 0.65747 | 4.7864 eV 259.04 nm f=0.0053 <S**2>=0.000 |
| Excited State 13: Singlet-B 219 -> 228 -0.12059 221 -> 228 0.26258 222 -> 229 0.30175 223 -> 228 -0.28274 224 -> 229 0.40823 226 -> 230 -0.23257 | 4.2357 eV 292.71 nm f=0.0146 <S**2>=0.000 | Excited State 28: Singlet-A 213 -> 228 0.13790 214 -> 228 -0.24234 216 -> 229 0.61720 | 4.8959 eV 253.24 nm f=0.0029 <S**2>=0.000 |
| Excited State 14: Singlet-A 220 -> 228 0.61492 226 -> 231 -0.30836 | 4.3097 eV 287.69 nm f=0.0002 <S**2>=0.000 | Excited State 29: Singlet-B 212 -> 228 0.64887 216 -> 228 -0.15351 | 4.9053 eV 252.76 nm f=0.0009 <S**2>=0.000 |
| Excited State 15: Singlet-B 219 -> 228 -0.28092 224 -> 229 0.17377 226 -> 230 0.57994 227 -> 232 0.17340 | 4.3400 eV 285.68 nm f=0.0951 <S**2>=0.000 | Excited State 30: Singlet-A 213 -> 228 -0.28539 214 -> 228 0.56694 | 4.9121 eV 252.41 nm f=0.0009 <S**2>=0.000 |

216 -> 229 0.27277

Excited State 31: Singlet-B 4.9198 eV 252.01 nm f=0.0420 <S**2>=0.000
215 -> 229 -0.20011
217 -> 229 0.56529
227 -> 232 -0.32413

Excited State 32: Singlet-B 4.9451 eV 250.72 nm f=0.1287 <S**2>=0.000
215 -> 229 -0.19129
217 -> 229 0.29893
226 -> 230 -0.14087
227 -> 232 0.53831
227 -> 237 -0.10899

Excited State 33: Singlet-A 5.0063 eV 247.65 nm f=0.0000 <S**2>=0.000
213 -> 228 0.61995
214 -> 228 0.31654

Excited State 34: Singlet-B 5.0657 eV 244.75 nm f=0.0010 <S**2>=0.000
209 -> 228 0.34965
211 -> 228 0.57881
212 -> 228 -0.14569

Excited State 35: Singlet-B 5.0913 eV 243.52 nm f=0.1010 <S**2>=0.000
213 -> 229 0.19354
214 -> 229 -0.27101
215 -> 229 0.52678
217 -> 229 0.19255
225 -> 229 0.11342
226 -> 232 0.11913

Excited State 36: Singlet-B 5.1005 eV 243.08 nm f=0.0056 <S**2>=0.000
205 -> 228 -0.12129
206 -> 228 -0.12400
209 -> 228 0.58235
211 -> 228 -0.33573
215 -> 229 0.10387

Excited State 37: Singlet-A 5.1123 eV 242.52 nm f=0.0015 <S**2>=0.000
210 -> 228 0.67575
212 -> 229 -0.14476

Excited State 38: Singlet-A 5.1184 eV 242.23 nm f=0.0008 <S**2>=0.000
210 -> 228 0.14838
211 -> 229 0.11968
212 -> 229 0.64243
219 -> 229 -0.11470

Excited State 39: Singlet-B 5.1837 eV 239.18 nm f=0.0390 <S**2>=0.000
204 -> 228 0.17257
205 -> 228 0.35458
206 -> 228 0.38446
209 -> 228 0.11133
211 -> 228 -0.17731
214 -> 229 -0.32450
215 -> 229 -0.15283

Excited State 40: Singlet-A 5.1903 eV 238.87 nm f=0.0001 <S**2>=0.000
208 -> 228 0.68489

Excited State 41: Singlet-B 5.1937 eV 238.72 nm f=0.0292 <S**2>=0.000
205 -> 228 0.26196
206 -> 228 0.12403
207 -> 228 0.43898
214 -> 229 0.38334
215 -> 229 0.10662
225 -> 231 0.14720
226 -> 232 0.11921

Excited State 42: Singlet-B 5.2141 eV 237.79 nm f=0.0136 <S**2>=0.000
204 -> 228 -0.11542
206 -> 228 -0.24578
207 -> 228 0.50180
214 -> 229 -0.37561

Excited State 43: Singlet-B 5.2486 eV 236.23 nm f=0.0221 <S**2>=0.000
207 -> 228 0.13309
213 -> 229 0.58166
214 -> 229 0.12294
225 -> 231 -0.26984
226 -> 232 -0.12330

Excited State 44: Singlet-B 5.2621 eV 235.62 nm f=0.0494 <S**2>=0.000
206 -> 228 -0.11178
213 -> 229 0.25963
225 -> 231 0.59179
226 -> 232 -0.15267

Excited State 45: Singlet-B 5.2782 eV 234.90 nm f=0.0010 <S**2>=0.000
204 -> 228 -0.19314
205 -> 228 -0.44017
206 -> 228 0.48341
207 -> 228 0.14072

Excited State 46: Singlet-A 5.2938 eV 234.21 nm f=0.0003 <S**2>=0.000
209 -> 229 -0.14873
211 -> 229 -0.35482
212 -> 229 0.13191
224 -> 230 -0.10317
225 -> 230 0.53410

Excited State 47: Singlet-B 5.3053 eV 233.70 nm f=0.0001 <S**2>=0.000
204 -> 228 0.60536
205 -> 228 -0.24966
210 -> 229 -0.10542
226 -> 232 -0.17418

Excited State 48: Singlet-A 5.3053 eV 233.70 nm f=0.0000 <S**2>=0.000
209 -> 229 0.32103
211 -> 229 0.45137
212 -> 229 -0.11359
225 -> 230 0.40055

Excited State 49: Singlet-A 5.3276 eV 232.72 nm f=0.0002 <S**2>=0.000
203 -> 228 0.17271
209 -> 229 0.57448
211 -> 229 -0.33426

Excited State 50: Singlet-B 5.3425 eV 232.07 nm f=0.0035 <S**2>=0.000
204 -> 228 0.10035
210 -> 229 0.67721

Excited State 51: Singlet-A 5.3477 eV 231.85 nm f=0.0008 <S**2>=0.000
202 -> 228 -0.19208
203 -> 228 0.63951
209 -> 229 -0.14927
211 -> 229 0.10859

Excited State 52: Singlet-B 5.3816 eV 230.38 nm f=0.0340 <S**2>=0.000
222 -> 231 0.11222
224 -> 231 0.23462
227 -> 234 -0.24394
227 -> 235 0.44316
227 -> 237 0.36369

Excited State 53: Singlet-A 5.4130 eV 229.05 nm f=0.0004 <S**2>=0.000
205 -> 229 0.20227
206 -> 229 0.12494
207 -> 229 0.25566
223 -> 231 0.31968
224 -> 230 0.39441
227 -> 233 -0.18938
227 -> 236 -0.22230

Excited State 54: Singlet-B 5.4154 eV 228.95 nm f=0.0893 <S**2>=0.000
204 -> 228 0.11220
213 -> 229 0.10665
221 -> 230 -0.22761
222 -> 231 -0.28480
224 -> 231 0.28361
226 -> 232 0.39066
227 -> 234 0.12038

Excited State 55: Singlet-A 5.4212 eV 228.70 nm f=0.0034 <S**2>=0.000
202 -> 228 0.38708
203 -> 228 0.15538
205 -> 229 0.26327
206 -> 229 0.15591
207 -> 229 0.26258
227 -> 233 0.29728
227 -> 236 0.21658

Excited State 56: Singlet-B 5.4285 eV 228.39 nm f=0.0022 <S**2>=0.000
208 -> 229 0.67415
223 -> 230 -0.13781

Excited State 57: Singlet-A 5.4289 eV 228.38 nm f=0.0016 <S**2>=0.000
202 -> 228 0.15363
205 -> 229 -0.18590
206 -> 229 -0.10025
207 -> 229 -0.26089
223 -> 231 0.56260
227 -> 233 0.13389

| | | | | | | |
|-----------------------------|-----------|-----------|----------|--------------|-----------------------------|-----------|
| Excited State 58: Singlet-A | 5.4324 eV | 228.23 nm | f=0.0019 | <S**2>=0.000 | 206 -> 229 | 0.48312 |
| 202 -> 228 | 0.50748 | | | | 207 -> 229 | 0.17069 |
| 203 -> 228 | 0.14112 | | | | | |
| 205 -> 229 | -0.17260 | | | | Excited State 66: Singlet-B | 5.5085 eV |
| 206 -> 229 | -0.19452 | | | | 201 -> 228 | 0.18802 |
| 223 -> 231 | -0.13457 | | | | 219 -> 230 | -0.20414 |
| 227 -> 233 | -0.26848 | | | | 221 -> 230 | 0.13491 |
| 227 -> 236 | -0.20004 | | | | 222 -> 231 | 0.50854 |
| | | | | | 224 -> 231 | 0.19113 |
| Excited State 59: Singlet-A | 5.4471 eV | 227.61 nm | f=0.0003 | <S**2>=0.000 | 226 -> 232 | 0.13092 |
| 202 -> 228 | -0.11991 | | | | 227 -> 234 | 0.17758 |
| 204 -> 229 | -0.10649 | | | | | |
| 205 -> 229 | -0.19837 | | | | Excited State 67: Singlet-A | 5.5211 eV |
| 206 -> 229 | -0.37547 | | | | 220 -> 230 | 0.25518 |
| 207 -> 229 | 0.49726 | | | | 227 -> 233 | -0.34970 |
| 224 -> 230 | -0.12789 | | | | 227 -> 236 | 0.48021 |
| | | | | | 227 -> 238 | 0.11257 |
| | | | | | 227 -> 239 | 0.15310 |
| Excited State 60: Singlet-B | 5.4487 eV | 227.55 nm | f=0.0189 | <S**2>=0.000 | | |
| 222 -> 231 | -0.16085 | | | | Excited State 68: Singlet-B | 5.5385 eV |
| 223 -> 230 | 0.35276 | | | | 218 -> 231 | -0.15922 |
| 224 -> 231 | 0.46467 | | | | 219 -> 230 | 0.10454 |
| 226 -> 232 | -0.24795 | | | | 221 -> 230 | 0.57624 |
| 227 -> 235 | -0.15879 | | | | 222 -> 231 | -0.19598 |
| | | | | | 226 -> 232 | 0.14887 |
| | | | | | 227 -> 234 | 0.13201 |
| Excited State 61: Singlet-A | 5.4549 eV | 227.29 nm | f=0.0255 | <S**2>=0.000 | | |
| 205 -> 229 | -0.16109 | | | | Excited State 69: Singlet-A | 5.5458 eV |
| 206 -> 229 | -0.12934 | | | | 204 -> 229 | 0.67934 |
| 221 -> 231 | 0.13759 | | | | | |
| 222 -> 230 | 0.10616 | | | | Excited State 70: Singlet-A | 5.5492 eV |
| 223 -> 231 | -0.17194 | | | | 200 -> 228 | 0.10619 |
| 224 -> 230 | 0.48749 | | | | 220 -> 230 | 0.57385 |
| 225 -> 230 | 0.13768 | | | | 221 -> 231 | -0.17259 |
| 227 -> 233 | 0.30786 | | | | 222 -> 230 | -0.12942 |
| 227 -> 236 | 0.13609 | | | | 227 -> 233 | 0.20225 |
| | | | | | 227 -> 236 | -0.18756 |
| Excited State 62: Singlet-B | 5.4581 eV | 227.15 nm | f=0.0196 | <S**2>=0.000 | | |
| 220 -> 231 | 0.11318 | | | | Excited State 71: Singlet-A | 5.5661 eV |
| 221 -> 230 | -0.17133 | | | | 218 -> 230 | -0.23019 |
| 223 -> 230 | 0.55938 | | | | 220 -> 230 | 0.14755 |
| 224 -> 231 | -0.24697 | | | | 221 -> 231 | 0.61398 |
| 226 -> 232 | 0.18767 | | | | 224 -> 230 | -0.11628 |
| | | | | | 227 -> 236 | -0.12279 |
| Excited State 63: Singlet-A | 5.4809 eV | 226.21 nm | f=0.0164 | <S**2>=0.000 | | |
| 220 -> 230 | 0.12128 | | | | | |
| 222 -> 230 | 0.65221 | | | | Excited State 72: Singlet-B | 5.5669 eV |
| 224 -> 230 | -0.16213 | | | | 202 -> 229 | -0.11346 |
| | | | | | 203 -> 229 | 0.22884 |
| Excited State 64: Singlet-B | 5.4964 eV | 225.57 nm | f=0.0001 | <S**2>=0.000 | 226 -> 232 | -0.18684 |
| 201 -> 228 | 0.66115 | | | | 227 -> 234 | 0.53843 |
| 222 -> 231 | -0.14595 | | | | 227 -> 235 | 0.28881 |
| | | | | | | |
| Excited State 65: Singlet-A | 5.5040 eV | 225.26 nm | f=0.0001 | <S**2>=0.000 | | |
| 205 -> 229 | -0.47384 | | | | | |

Table 3-23. Transition Energy, Wavelength, and Oscillator Strengths of the Electronic Transition of 2'p (The 227th orbital is highest occupied orbital shown in Figure 3-13) [td_a_TN81b_planar]

| | | | | | | | | | |
|-----------------------------|-----------|-----------|----------|--------------|------------------------------|-----------|-----------|----------|--------------|
| Excited State 1: Singlet-AU | 2.2364 eV | 554.39 nm | f=0.0054 | <S**2>=0.000 | Excited State 8: Singlet-AU | 3.8492 eV | 322.10 nm | f=0.0011 | <S**2>=0.000 |
| 227 -> 228 | -0.39735 | | | | 221 -> 228 | 0.10491 | | | |
| 227 -> 229 | 0.58096 | | | | 223 -> 228 | 0.25899 | | | |
| | | | | | 225 -> 228 | 0.57842 | | | |
| | | | | | 227 -> 231 | -0.26791 | | | |
| Excited State 2: Singlet-AU | 2.4845 eV | 499.02 nm | f=0.0378 | <S**2>=0.000 | Excited State 9: Singlet-AG | 3.9080 eV | 317.26 nm | f=0.0000 | <S**2>=0.000 |
| 227 -> 228 | 0.57396 | | | | 224 -> 228 | 0.70129 | | | |
| 227 -> 229 | 0.39673 | | | | | | | | |
| | | | | | Excited State 10: Singlet-AU | 3.9194 eV | 316.33 nm | f=0.0039 | <S**2>=0.000 |
| Excited State 3: Singlet-AG | 2.6239 eV | 472.52 nm | f=0.0000 | <S**2>=0.000 | 221 -> 228 | 0.14793 | | | |
| 226 -> 228 | 0.70477 | | | | 222 -> 228 | 0.61511 | | | |
| | | | | | 223 -> 228 | -0.23853 | | | |
| Excited State 4: Singlet-AG | 3.1095 eV | 398.72 nm | f=0.0000 | <S**2>=0.000 | 225 -> 228 | 0.13270 | | | |
| 226 -> 229 | 0.70449 | | | | 225 -> 229 | -0.13134 | | | |
| | | | | | Excited State 11: Singlet-AU | 3.9684 eV | 312.43 nm | f=0.0020 | <S**2>=0.000 |
| Excited State 5: Singlet-AG | 3.3945 eV | 365.25 nm | f=0.0000 | <S**2>=0.000 | 221 -> 228 | 0.64422 | | | |
| 227 -> 230 | 0.70446 | | | | 222 -> 228 | -0.22306 | | | |
| | | | | | 223 -> 228 | -0.14812 | | | |
| Excited State 6: Singlet-AU | 3.5280 eV | 351.43 nm | f=0.0114 | <S**2>=0.000 | Excited State 12: Singlet-AG | 4.0267 eV | 307.90 nm | f=0.0000 | <S**2>=0.000 |
| 225 -> 228 | 0.24676 | | | | 218 -> 228 | 0.19663 | | | |
| 227 -> 231 | 0.64635 | | | | 219 -> 228 | 0.58839 | | | |
| | | | | | 220 -> 228 | -0.32020 | | | |
| Excited State 7: Singlet-AU | 3.7611 eV | 329.65 nm | f=0.0002 | <S**2>=0.000 | Excited State 13: Singlet-AG | 4.0617 eV | 305.25 nm | f=0.0000 | <S**2>=0.000 |
| 221 -> 228 | 0.19326 | | | | | | | | |
| 222 -> 228 | 0.23735 | | | | | | | | |
| 223 -> 228 | 0.57315 | | | | | | | | |
| 225 -> 228 | -0.26948 | | | | | | | | |

| | | | | | | | |
|-------------------|------------|-----------|-----------|----------|--------------|-------------------|--------------|
| 219 -> 228 | 0.31438 | | | | | 222 -> 229 | -0.13081 |
| 220 -> 228 | 0.62178 | | | | | 223 -> 229 | 0.19256 |
| Excited State 14: | Singlet-AU | 4.1869 eV | 296.12 nm | f=0.0098 | <S**2>=0.000 | 225 -> 229 | 0.52790 |
| 221 -> 229 | 0.14680 | | | | | Excited State 28: | Singlet-AG |
| 222 -> 229 | 0.18189 | | | | | 4.6097 eV | 268.96 nm |
| 223 -> 229 | 0.61034 | | | | | f=0.0000 | <S**2>=0.000 |
| 225 -> 229 | -0.21669 | | | | | 210 -> 228 | 0.12771 |
| 226 -> 230 | -0.11624 | | | | | 212 -> 228 | 0.18620 |
| | | | | | | 214 -> 228 | 0.64410 |
| | | | | | | 226 -> 231 | -0.10323 |
| Excited State 15: | Singlet-AG | 4.2184 eV | 293.91 nm | f=0.0000 | <S**2>=0.000 | Excited State 29: | Singlet-AU |
| 218 -> 228 | 0.64939 | | | | | 4.7146 eV | 262.98 nm |
| 219 -> 228 | -0.20829 | | | | | f=0.0004 | <S**2>=0.000 |
| 224 -> 229 | -0.11749 | | | | | 206 -> 228 | 0.11616 |
| | | | | | | 213 -> 228 | 0.68377 |
| Excited State 16: | Singlet-AU | 4.2927 eV | 288.82 nm | f=0.0016 | <S**2>=0.000 | Excited State 30: | Singlet-AG |
| 216 -> 228 | -0.13617 | | | | | 4.7559 eV | 260.69 nm |
| 217 -> 228 | 0.26833 | | | | | f=0.0000 | <S**2>=0.000 |
| 221 -> 229 | 0.38159 | | | | | 207 -> 228 | 0.11137 |
| 222 -> 229 | 0.44513 | | | | | 209 -> 228 | -0.13347 |
| 223 -> 229 | -0.20332 | | | | | 210 -> 228 | 0.45626 |
| | | | | | | 212 -> 228 | 0.43112 |
| | | | | | | 214 -> 228 | -0.24120 |
| Excited State 17: | Singlet-AU | 4.2946 eV | 288.70 nm | f=0.0007 | <S**2>=0.000 | Excited State 31: | Singlet-AU |
| 216 -> 228 | -0.14547 | | | | | 4.7886 eV | 258.91 nm |
| 217 -> 228 | 0.60811 | | | | | f=0.0022 | <S**2>=0.000 |
| 221 -> 229 | -0.16538 | | | | | 217 -> 229 | 0.69205 |
| 222 -> 229 | -0.21534 | | | | | Excited State 32: | Singlet-AU |
| 223 -> 229 | 0.10088 | | | | | 4.8281 eV | 256.80 nm |
| | | | | | | f=0.0004 | <S**2>=0.000 |
| Excited State 18: | Singlet-AG | 4.3068 eV | 287.88 nm | f=0.0000 | <S**2>=0.000 | 206 -> 228 | 0.17609 |
| 218 -> 228 | 0.12800 | | | | | 211 -> 228 | 0.67968 |
| 218 -> 229 | 0.16555 | | | | | Excited State 33: | Singlet-AG |
| 219 -> 229 | -0.19356 | | | | | 4.8290 eV | 256.75 nm |
| 224 -> 229 | 0.63828 | | | | | f=0.0000 | <S**2>=0.000 |
| | | | | | | 209 -> 228 | 0.57650 |
| | | | | | | 210 -> 228 | -0.16168 |
| | | | | | | 212 -> 228 | 0.35232 |
| Excited State 19: | Singlet-AU | 4.3895 eV | 282.46 nm | f=0.0763 | <S**2>=0.000 | Excited State 34: | Singlet-AU |
| 222 -> 229 | 0.18396 | | | | | 4.8689 eV | 254.65 nm |
| 223 -> 229 | 0.10712 | | | | | f=0.0232 | <S**2>=0.000 |
| 226 -> 230 | 0.61958 | | | | | 215 -> 229 | -0.37209 |
| 227 -> 232 | -0.23451 | | | | | 216 -> 229 | 0.55527 |
| | | | | | | Excited State 35: | Singlet-AG |
| Excited State 20: | Singlet-AU | 4.4123 eV | 280.99 nm | f=0.0076 | <S**2>=0.000 | 4.8756 eV | 254.30 nm |
| 221 -> 229 | 0.50902 | | | | | f=0.0000 | <S**2>=0.000 |
| 222 -> 229 | -0.40141 | | | | | 207 -> 228 | 0.11844 |
| 225 -> 229 | -0.22346 | | | | | 209 -> 228 | 0.36455 |
| 226 -> 230 | 0.14350 | | | | | 210 -> 228 | 0.45222 |
| | | | | | | 212 -> 228 | -0.36846 |
| Excited State 21: | Singlet-AG | 4.4379 eV | 279.38 nm | f=0.0000 | <S**2>=0.000 | Excited State 36: | Singlet-AU |
| 218 -> 229 | 0.14655 | | | | | 4.9322 eV | 251.38 nm |
| 219 -> 229 | 0.48022 | | | | | f=0.0059 | <S**2>=0.000 |
| 220 -> 229 | -0.18411 | | | | | 206 -> 228 | 0.23044 |
| 224 -> 229 | 0.14420 | | | | | 208 -> 228 | 0.65415 |
| 226 -> 231 | -0.41795 | | | | | 213 -> 228 | -0.11370 |
| | | | | | | Excited State 37: | Singlet-AG |
| Excited State 22: | Singlet-AU | 4.4525 eV | 278.46 nm | f=0.0016 | <S**2>=0.000 | 4.9333 eV | 251.32 nm |
| 215 -> 228 | 0.24865 | | | | | f=0.0000 | <S**2>=0.000 |
| 216 -> 228 | 0.61184 | | | | | 205 -> 228 | -0.20390 |
| 217 -> 228 | 0.17407 | | | | | 207 -> 228 | 0.64962 |
| | | | | | | 210 -> 228 | -0.15093 |
| Excited State 23: | Singlet-AG | 4.4829 eV | 276.57 nm | f=0.0000 | <S**2>=0.000 | Excited State 38: | Singlet-AG |
| 218 -> 229 | -0.20931 | | | | | 4.9363 eV | 251.17 nm |
| 219 -> 229 | 0.36995 | | | | | f=0.0000 | <S**2>=0.000 |
| 220 -> 229 | -0.20973 | | | | | 227 -> 233 | 0.68874 |
| 224 -> 229 | 0.15359 | | | | | 227 -> 236 | 0.12077 |
| 226 -> 231 | 0.48712 | | | | | Excited State 39: | Singlet-AU |
| | | | | | | 4.9625 eV | 249.84 nm |
| Excited State 24: | Singlet-AG | 4.5083 eV | 275.01 nm | f=0.0000 | <S**2>=0.000 | f=0.0031 | <S**2>=0.000 |
| 218 -> 229 | 0.57506 | | | | | 206 -> 228 | 0.61936 |
| 220 -> 229 | -0.27780 | | | | | 208 -> 228 | -0.24343 |
| 224 -> 229 | -0.17779 | | | | | 211 -> 228 | -0.17504 |
| 226 -> 231 | 0.21028 | | | | | Excited State 40: | Singlet-AU |
| | | | | | | 4.9650 eV | 249.72 nm |
| Excited State 25: | Singlet-AG | 4.5325 eV | 273.54 nm | f=0.0000 | <S**2>=0.000 | f=0.2959 | <S**2>=0.000 |
| 218 -> 229 | 0.23926 | | | | | 217 -> 231 | -0.12287 |
| 219 -> 229 | 0.27547 | | | | | 226 -> 230 | 0.22709 |
| 220 -> 229 | 0.58004 | | | | | 227 -> 232 | 0.61794 |
| 226 -> 231 | 0.13319 | | | | | Excited State 41: | Singlet-AG |
| | | | | | | 4.9758 eV | 249.17 nm |
| Excited State 26: | Singlet-AU | 4.5994 eV | 269.56 nm | f=0.0100 | <S**2>=0.000 | f=0.0000 | <S**2>=0.000 |
| 215 -> 228 | 0.63893 | | | | | 204 -> 228 | 0.26000 |
| 216 -> 228 | -0.22074 | | | | | 205 -> 228 | 0.61314 |
| | | | | | | 207 -> 228 | 0.18264 |
| Excited State 27: | Singlet-AU | 4.6094 eV | 268.98 nm | f=0.1759 | <S**2>=0.000 | Excited State 42: | Singlet-AG |
| 215 -> 229 | 0.15035 | | | | | 5.0384 eV | 246.08 nm |
| 216 -> 228 | 0.13014 | | | | | f=0.0000 | <S**2>=0.000 |
| 216 -> 229 | 0.22308 | | | | | 204 -> 228 | 0.64550 |
| 221 -> 229 | 0.15581 | | | | | 205 -> 228 | -0.24513 |
| | | | | | | Excited State 43: | Singlet-AU |
| | | | | | | 5.0408 eV | 245.96 nm |
| | | | | | | f=0.0024 | <S**2>=0.000 |
| | | | | | | 203 -> 228 | 0.69427 |
| | | | | | | Excited State 44: | Singlet-AG |
| | | | | | | 5.0582 eV | 245.12 nm |
| | | | | | | f=0.0000 | <S**2>=0.000 |
| | | | | | | 210 -> 229 | 0.15717 |
| | | | | | | 212 -> 229 | 0.20832 |
| | | | | | | 214 -> 229 | 0.62858 |
| | | | | | | Excited State 45: | Singlet-AU |
| | | | | | | 5.1219 eV | 242.07 nm |
| | | | | | | f=0.1624 | <S**2>=0.000 |
| | | | | | | 202 -> 228 | 0.27920 |
| | | | | | | 213 -> 229 | -0.19054 |

| | | | | | |
|------------------------------|---|--|--|------------------------------|---|
| 215 -> 229 | 0.49957 | | | 210 -> 229 | 0.10164 |
| 216 -> 229 | 0.26890 | | | | |
| 225 -> 229 | -0.11453 | | | Excited State 48: Singlet-AU | 5.2189 eV 237.57 nm f=0.1486 <S**2>=0.000 |
| 226 -> 233 | 0.11057 | | | 202 -> 228 | 0.41692 |
| Excited State 46: Singlet-AU | 5.1750 eV 239.58 nm f=0.0031 <S**2>=0.000 | | | 211 -> 229 | 0.16149 |
| 202 -> 228 | 0.47325 | | | 213 -> 229 | -0.40573 |
| 213 -> 229 | 0.50423 | | | 215 -> 229 | -0.18775 |
| Excited State 47: Singlet-AG | 5.1917 eV 238.81 nm f=0.0000 <S**2>=0.000 | | | 216 -> 229 | -0.18753 |
| 201 -> 228 | 0.67578 | | | 225 -> 229 | 0.10330 |
| | | | | 226 -> 233 | -0.11684 |

Table 3-24. Transition Energy, Wavelength, and Oscillator Strengths of the Electronic Transition of 2¹₁ (The 227th orbital is highest occupied orbital shown in Figure 3-13) [td_a_TN85a]

| | | | | | |
|---|---|--|--|-----------------------------|---|
| Excited State 1: Singlet-A | 2.3474 eV 528.18 nm f=0.0108 <S**2>=0.000 | | | 218 -> 228 | 0.60343 |
| 227 -> 228 | 0.58145 | | | 219 -> 228 | -0.12500 |
| 227 -> 229 | -0.39803 | | | 220 -> 228 | -0.21981 |
| This state for optimization and/or second-order correction. | | | | | |
| Total Energy, E(TD-HF/TD-KS) = -4765.34702507 | | | | | |
| Copying the excited state density for this state as the 1-particle RhoCI density. | | | | | |
| Excited State 2: Singlet-A | 2.6587 eV 466.33 nm f=0.0243 <S**2>=0.000 | | | Excited State 16: Singlet-A | 4.3036 eV 288.09 nm f=0.0098 <S**2>=0.000 |
| 226 -> 228 | 0.69611 | | | 216 -> 228 | -0.17359 |
| Excited State 3: Singlet-A | 2.8477 eV 435.38 nm f=0.0595 <S**2>=0.000 | | | 217 -> 228 | -0.20814 |
| 227 -> 228 | 0.38512 | | | 226 -> 230 | 0.62682 |
| 227 -> 229 | 0.57388 | | | Excited State 17: Singlet-A | 4.3138 eV 287.41 nm f=0.0008 <S**2>=0.000 |
| Excited State 4: Singlet-A | 3.0372 eV 408.21 nm f=0.0120 <S**2>=0.000 | | | 217 -> 228 | 0.14729 |
| 226 -> 229 | 0.69583 | | | 218 -> 228 | 0.14375 |
| Excited State 5: Singlet-A | 3.5703 eV 347.27 nm f=0.0026 <S**2>=0.000 | | | 224 -> 229 | 0.63623 |
| 225 -> 228 | 0.70346 | | | Excited State 18: Singlet-A | 4.3428 eV 285.49 nm f=0.0036 <S**2>=0.000 |
| Excited State 6: Singlet-A | 3.7151 eV 333.73 nm f=0.0072 <S**2>=0.000 | | | 216 -> 228 | 0.39538 |
| 227 -> 230 | 0.69686 | | | 217 -> 228 | 0.48763 |
| Excited State 7: Singlet-A | 3.8635 eV 320.91 nm f=0.0073 <S**2>=0.000 | | | 226 -> 230 | 0.27350 |
| 224 -> 228 | 0.40348 | | | Excited State 19: Singlet-A | 4.4046 eV 281.49 nm f=0.0031 <S**2>=0.000 |
| 227 -> 231 | 0.56338 | | | 219 -> 229 | -0.18365 |
| Excited State 8: Singlet-A | 3.9288 eV 315.58 nm f=0.0016 <S**2>=0.000 | | | 221 -> 229 | 0.35096 |
| 222 -> 228 | -0.14040 | | | 222 -> 229 | 0.18471 |
| 223 -> 228 | -0.11314 | | | 223 -> 229 | 0.51491 |
| 224 -> 228 | 0.53966 | | | Excited State 20: Singlet-A | 4.4245 eV 280.22 nm f=0.0032 <S**2>=0.000 |
| 227 -> 231 | -0.38933 | | | 219 -> 229 | 0.13286 |
| Excited State 9: Singlet-A | 3.9777 eV 311.70 nm f=0.0054 <S**2>=0.000 | | | 220 -> 229 | -0.26661 |
| 219 -> 228 | -0.12429 | | | 221 -> 229 | 0.19589 |
| 221 -> 228 | 0.31773 | | | 222 -> 229 | 0.52471 |
| 222 -> 228 | 0.21357 | | | 223 -> 229 | -0.25572 |
| 223 -> 228 | 0.54711 | | | Excited State 21: Singlet-A | 4.4689 eV 277.44 nm f=0.0044 <S**2>=0.000 |
| Excited State 10: Singlet-A | 3.9945 eV 310.39 nm f=0.0095 <S**2>=0.000 | | | 216 -> 228 | 0.52140 |
| 219 -> 228 | 0.17061 | | | 217 -> 228 | -0.40457 |
| 220 -> 228 | -0.14987 | | | 221 -> 229 | -0.12833 |
| 221 -> 228 | 0.18871 | | | 224 -> 229 | 0.11914 |
| 222 -> 228 | 0.55514 | | | Excited State 22: Singlet-A | 4.4927 eV 275.97 nm f=0.0031 <S**2>=0.000 |
| 223 -> 228 | -0.29132 | | | 219 -> 229 | -0.23013 |
| Excited State 11: Singlet-A | 4.0139 eV 308.89 nm f=0.0075 <S**2>=0.000 | | | 220 -> 229 | 0.11336 |
| 225 -> 229 | 0.69591 | | | 221 -> 229 | 0.45750 |
| Excited State 12: Singlet-A | 4.0399 eV 306.90 nm f=0.0135 <S**2>=0.000 | | | 222 -> 229 | -0.24294 |
| 220 -> 228 | 0.10877 | | | 223 -> 229 | -0.36099 |
| 221 -> 228 | 0.57306 | | | Excited State 23: Singlet-A | 4.5157 eV 274.56 nm f=0.0527 <S**2>=0.000 |
| 222 -> 228 | -0.27389 | | | 215 -> 228 | 0.14087 |
| 223 -> 228 | -0.23692 | | | 219 -> 229 | -0.14629 |
| 224 -> 228 | -0.10570 | | | 220 -> 229 | 0.13300 |
| Excited State 13: Singlet-A | 4.0869 eV 303.37 nm f=0.0022 <S**2>=0.000 | | | 221 -> 229 | -0.16551 |
| 218 -> 228 | 0.12355 | | | 222 -> 229 | 0.18780 |
| 219 -> 228 | -0.38470 | | | 223 -> 229 | -0.10987 |
| 220 -> 228 | 0.49442 | | | 226 -> 231 | 0.56667 |
| 222 -> 228 | 0.20208 | | | Excited State 24: Singlet-A | 4.5351 eV 273.39 nm f=0.0129 <S**2>=0.000 |
| 223 -> 228 | -0.18131 | | | 215 -> 228 | -0.19618 |
| Excited State 14: Singlet-A | 4.1300 eV 300.21 nm f=0.0134 <S**2>=0.000 | | | 219 -> 229 | -0.21401 |
| 218 -> 228 | 0.26589 | | | 220 -> 229 | 0.47643 |
| 219 -> 228 | 0.51357 | | | 221 -> 229 | -0.13171 |
| 220 -> 228 | 0.36871 | | | 222 -> 229 | 0.28356 |
| Excited State 15: Singlet-A | 4.1719 eV 297.19 nm f=0.0128 <S**2>=0.000 | | | 223 -> 229 | -0.10603 |
| | | | | 226 -> 231 | -0.23395 |
| | | | | Excited State 25: Singlet-A | 4.5765 eV 270.92 nm f=0.0029 <S**2>=0.000 |
| | | | | 215 -> 228 | 0.62973 |
| | | | | 220 -> 229 | 0.18407 |
| | | | | 226 -> 231 | -0.18035 |

| | | | | | | | | | |
|-----------------------------|-----------|-----------|----------|--------------|-----------------------------|-----------|-----------|----------|--------------|
| Excited State 26: Singlet-A | 4.6047 eV | 269.26 nm | f=0.0347 | <S**2>=0.000 | 204 -> 228 | 0.13220 | | | |
| 214 -> 228 | -0.30133 | | | | 205 -> 228 | 0.26577 | | | |
| 219 -> 229 | 0.49134 | | | | 206 -> 228 | 0.24546 | | | |
| 220 -> 229 | 0.26916 | | | | 207 -> 228 | 0.37344 | | | |
| 221 -> 229 | 0.10586 | | | | 209 -> 228 | 0.10059 | | | |
| 226 -> 231 | 0.16818 | | | | 215 -> 229 | -0.17426 | | | |
| 227 -> 232 | -0.10478 | | | | 227 -> 232 | -0.33670 | | | |
| Excited State 27: Singlet-A | 4.6326 eV | 267.64 nm | f=0.0224 | <S**2>=0.000 | Excited State 39: Singlet-A | 4.9717 eV | 249.38 nm | f=0.0448 | <S**2>=0.000 |
| 214 -> 228 | 0.52895 | | | | 206 -> 228 | 0.14626 | | | |
| 218 -> 229 | 0.35243 | | | | 207 -> 228 | 0.35341 | | | |
| 219 -> 229 | 0.19980 | | | | 208 -> 228 | 0.13745 | | | |
| 220 -> 229 | 0.16092 | | | | 209 -> 228 | 0.16185 | | | |
| Excited State 28: Singlet-A | 4.6804 eV | 264.90 nm | f=0.0528 | <S**2>=0.000 | 215 -> 229 | 0.21257 | | | |
| 214 -> 228 | -0.26096 | | | | 227 -> 232 | 0.39562 | | | |
| 218 -> 229 | 0.53280 | | | | 227 -> 233 | -0.17693 | | | |
| 219 -> 229 | -0.10579 | | | | Excited State 40: Singlet-A | 4.9871 eV | 248.61 nm | f=0.0123 | <S**2>=0.000 |
| 221 -> 229 | -0.12509 | | | | 204 -> 228 | 0.12132 | | | |
| 227 -> 233 | 0.21263 | | | | 206 -> 228 | 0.58022 | | | |
| Excited State 29: Singlet-A | 4.7268 eV | 262.30 nm | f=0.0012 | <S**2>=0.000 | 207 -> 228 | -0.28904 | | | |
| 210 -> 228 | -0.10403 | | | | 227 -> 233 | 0.14057 | | | |
| 213 -> 228 | 0.67255 | | | | Excited State 41: Singlet-A | 5.0290 eV | 246.54 nm | f=0.0148 | <S**2>=0.000 |
| Excited State 30: Singlet-A | 4.7898 eV | 258.85 nm | f=0.0020 | <S**2>=0.000 | 205 -> 228 | 0.36354 | | | |
| 211 -> 228 | -0.10851 | | | | 207 -> 228 | -0.17710 | | | |
| 212 -> 228 | 0.66493 | | | | 214 -> 229 | 0.25236 | | | |
| Excited State 31: Singlet-A | 4.8019 eV | 258.20 nm | f=0.0004 | <S**2>=0.000 | 215 -> 229 | 0.45969 | | | |
| 211 -> 228 | 0.66125 | | | | 227 -> 232 | -0.10540 | | | |
| 212 -> 228 | 0.13108 | | | | Excited State 42: Singlet-A | 5.0331 eV | 246.34 nm | f=0.0257 | <S**2>=0.000 |
| Excited State 32: Singlet-A | 4.8114 eV | 257.69 nm | f=0.0086 | <S**2>=0.000 | 204 -> 228 | 0.19232 | | | |
| 216 -> 229 | 0.33268 | | | | 205 -> 228 | 0.45445 | | | |
| 217 -> 229 | 0.59110 | | | | 207 -> 228 | -0.24830 | | | |
| Excited State 33: Singlet-A | 4.8781 eV | 254.17 nm | f=0.0005 | <S**2>=0.000 | 214 -> 229 | -0.12690 | | | |
| 209 -> 228 | -0.27450 | | | | 215 -> 229 | -0.28701 | | | |
| 210 -> 228 | -0.27224 | | | | 227 -> 232 | 0.17458 | | | |
| 216 -> 229 | 0.47626 | | | | 227 -> 233 | -0.13422 | | | |
| 217 -> 229 | -0.28281 | | | | Excited State 43: Singlet-A | 5.0578 eV | 245.14 nm | f=0.0009 | <S**2>=0.000 |
| 227 -> 233 | -0.11484 | | | | 204 -> 228 | 0.62592 | | | |
| Excited State 34: Singlet-A | 4.8847 eV | 253.82 nm | f=0.0011 | <S**2>=0.000 | 205 -> 228 | -0.21443 | | | |
| 209 -> 228 | 0.37042 | | | | 206 -> 228 | -0.14517 | | | |
| 210 -> 228 | 0.38280 | | | | 214 -> 229 | 0.14557 | | | |
| 216 -> 229 | 0.35869 | | | | Excited State 44: Singlet-A | 5.0838 eV | 243.88 nm | f=0.0004 | <S**2>=0.000 |
| 217 -> 229 | -0.19454 | | | | 227 -> 232 | 0.12307 | | | |
| Excited State 35: Singlet-A | 4.8915 eV | 253.47 nm | f=0.0107 | <S**2>=0.000 | 227 -> 234 | 0.63973 | | | |
| 207 -> 228 | -0.17714 | | | | 227 -> 235 | 0.13976 | | | |
| 208 -> 228 | 0.17490 | | | | 227 -> 236 | 0.17969 | | | |
| 209 -> 228 | 0.46601 | | | | Excited State 45: Singlet-A | 5.1275 eV | 241.80 nm | f=0.0021 | <S**2>=0.000 |
| 210 -> 228 | -0.42499 | | | | 203 -> 228 | 0.67480 | | | |
| Excited State 36: Singlet-A | 4.9265 eV | 251.67 nm | f=0.0108 | <S**2>=0.000 | Excited State 46: Singlet-A | 5.1634 eV | 240.12 nm | f=0.0391 | <S**2>=0.000 |
| 207 -> 228 | 0.12278 | | | | 201 -> 228 | 0.11393 | | | |
| 208 -> 228 | -0.34435 | | | | 203 -> 228 | -0.13327 | | | |
| 210 -> 228 | -0.26318 | | | | 211 -> 229 | -0.10656 | | | |
| 214 -> 229 | 0.13049 | | | | 212 -> 229 | 0.14850 | | | |
| 215 -> 229 | -0.11207 | | | | 213 -> 229 | 0.39739 | | | |
| 227 -> 232 | 0.19504 | | | | 214 -> 229 | -0.37528 | | | |
| 227 -> 233 | 0.42616 | | | | 215 -> 229 | 0.24102 | | | |
| Excited State 37: Singlet-A | 4.9399 eV | 250.99 nm | f=0.0150 | <S**2>=0.000 | 227 -> 233 | 0.12527 | | | |
| 206 -> 228 | -0.17705 | | | | Excited State 47: Singlet-A | 5.1840 eV | 239.17 nm | f=0.0328 | <S**2>=0.000 |
| 208 -> 228 | 0.54614 | | | | 201 -> 228 | -0.14655 | | | |
| 214 -> 229 | 0.12904 | | | | 210 -> 229 | -0.10022 | | | |
| 215 -> 229 | -0.13103 | | | | 213 -> 229 | 0.52232 | | | |
| 227 -> 233 | 0.30193 | | | | 214 -> 229 | 0.37146 | | | |
| Excited State 38: Singlet-A | 4.9686 eV | 249.54 nm | f=0.0554 | <S**2>=0.000 | 227 -> 233 | -0.11323 | | | |
| | | | | | Excited State 48: Singlet-A | 5.2160 eV | 237.70 nm | f=0.0101 | <S**2>=0.000 |
| | | | | | 202 -> 228 | 0.66930 | | | |
| | | | | | 225 -> 230 | -0.10610 | | | |

3-5. Reference and Notes

- (1) For recent reviews of π single bonding compounds, see: (a) Abe, M. *Chem. Rev.* **2013**, *113*, 7011–7088. (b) Abe, M.; Akisaka, R. *Chem. Lett.* **2017**, *46*, 1586–1592. For a study

- on compounds that contain multiple π bonds unsupported by an underlying σ -bond framework, see: (c) Jemmis, E. D.; Pathak, B.; King, R. B.; Schaefer, H. F., III. *Chem. Commun.* **2006**, 2164–2166.
- (2) (a) Adam, W.; Borden, W. T.; Burda, C.; Foster, H.; Heidenfelder, T.; Heubes, M.; Hrovat, D. A.; Kita, F.; Lewis, S. B.; Scheutzow, D.; Wirz, J. *J. Am. Chem. Soc.* **1998**, *120*, 593–594. (b) Abe, M.; Adam, W.; Nau, W. M. *J. Am. Chem. Soc.* **1998**, *120*, 11304–11310. (c) Abe, M.; Adam, W.; Heidenfelder, T.; Nau, W. M.; Zhang, X. *J. Am. Chem. Soc.* **2000**, *122*, 2019–2026. (d) Abe, M.; Adam, W.; Hara, M.; Hattori, M.; Majima, T.; Nojima, M.; Tachibana, K.; Tojo, S. *J. Am. Chem. Soc.* **2002**, *124*, 6540–6541.
- (3) (a) Abe, M.; Furunaga, H.; Ma, D.; Gagliardi, L.; Bodwell, G. J. *J. Org. Chem.* **2012**, *77*, 7612–7619. (b) Harada, Y.; Wang, Z.; Kumashiro, S.; Hatano, S.; Abe, M. *Chem. Eur. J.* **2018**, *24*, 14808–14815. (c) Ye, J.; Fujiwara, Y.; Abe, M. *Beilstein J. Org. Chem.* **2013**, *9*, 925–933. (d) Akisaka, R.; Abe, M. *Chem. Asian J.* **2019**, *14*, 4223–4228.
- (4) (a) Niecke, E.; Fuchs, A.; Baumeister, F.; Nieger, M.; Schoeller, W. W. *Angew. Chem., Int. Ed. Engl.* **1995**, *34*, 555–557. (b) Sugiyama, H.; Ito, S.; Yoshifuji, M. *Angew. Chem., Int. Ed.* **2003**, *42*, 3802–3804. (c) Cox, H.; Hitchcock, P. B.; Lappert, M. F.; Pierssens, L. J. *Angew. Chem., Int. Ed.* **2004**, *43*, 4500–4504. (d) Cui, C.; Brynda, M.; Olmstead, M. M.; Power, P. P. *J. Am. Chem. Soc.* **2004**, *126*, 6510–6511. (e) Henke, P.; Pankewitz, T.; Klopper, W.; Breher, F.; Schnöckel, H. *Angew. Chem., Int. Ed.* **2009**, *48*, 8141–8145. (f) Wang, X.; Peng, Y.; Olmstead, M. M.; Fettinger, J. C.; Power, P. P. *J. Am. Chem. Soc.* **2009**, *131*, 14164–14165. (g) Takeuchi, K.; Ichinohe, M.; Sekiguchi, A. *J. Am. Chem. Soc.* **2011**, *133*, 12478–12481. (h) Beweries, T.; Kuzora, R.; Rosenthal, U.; Schulz, A.; Villinger, A. *Angew. Chem., Int. Ed.* **2011**, *50*, 8974–8978. (i) Zhang, S.-H.; Xi, H.-W.; Lim, K. H.; Meng, Q.; Huang, M.-B.; So, C.-W. *Chem. Eur. J.* **2012**, *18*, 4258–4263. (j) Demeshko, S.; Godemann, C.; Kuzora, R.; Schulz, A.; Villinger, A. *Angew. Chem., Int.*

- Ed.* **2013**, *52*, 2105–2108. (k) Hinz, A.; Schulz, A.; Villinger, A. *Angew. Chem., Int. Ed.* **2015**, *54*, 668–672.
- (5) (a) Scheschkewitz, D.; Amii, H.; Gornitzka, H.; Schoeller, W. W.; Bourissou, D.; Bertrand, G. *Science* **2002**, *295*, 1880–1881. (b) Seierstad, M.; Kinsinger, C. R.; Cramer, C. J. *Angew. Chem., Int. Ed.* **2002**, *41*, 3894–3896. (c) Schoeller, W. W.; Rozhenko, A.; Bourissou, D.; Bertrand, G. *Chem. Eur. J.* **2003**, *9*, 3611–3617. (d) Cheng, M.-J.; Hu, C.-H. *Mol. Phys.* **2003**, *101*, 1319–1323. (e) Scheschkewitz, D.; Amii, H.; Gornitzka, H.; Schoeller, W. W.; Bourissou, D.; Bertrand, G. *Angew. Chem., Int. Ed.* **2004**, *43*, 585–587. (f) Rodriguez, A.; Olsen, R. A.; Ghaderi, N.; Scheschkewitz, D.; Tham, F. S.; Mueller, L. J.; Bertrand, G. *Angew. Chem., Int. Ed.* **2004**, *43*, 4880–4883.
- (6) (a) Amii, H.; Vranicar, L.; Gornitzka, H.; Bourissou, D.; Bertrand, G. *J. Am. Chem. Soc.* **2004**, *126*, 1344–1345. (b) Fuks, G.; Saffon, N.; Maron, L.; Bertrand, G.; Bourissou, D. *J. Am. Chem. Soc.* **2009**, *131*, 13681–13689.
- (7) In a symposium, Kyushin et al. presented the synthesis of hexakis(tert-butyl)tetrasilabicyclo[1.1.0]butane with a planar structure. Kyushin, S.; Kurosaki, Y.; Matsumoto, N.; Matsumoto, H.; Kyomen, T.; Hanaya, M.; Kudo, T. Silicon–Silicon π Single Bond. In Abstract of the 53rd Symposium on Organometallic Chemistry, Osaka, Japan, September 8–9, 2006; Kinka Chemical Society Japan: Osaka, 2006, A102. (See also, Kyushin, S.; Kurosaki, Y.; Otsuka, K.; Imai, H.; Ishida, S.; Kyomen, T.; Hanaya, M.; Matsumoto, H. *Nat. Commun.* **2020**, *11*, 4009.)
- (8) Fisher, Frenking, and co-workers reported an N-heterocyclic gallylene-bridged Ge₂ species whose [Ge₂Ga₂] framework is topologically similar to that of **1**. A theoretical investigation suggested that the central Ge–Ge bond is a π -bond with a weak σ -type interaction. See: Doddi, A.; Gemel, C.; Winter, M.; Fischer, R. A.; Goedecke, C.; Rzepa, H. S.; Frenking, G. *Angew. Chem., Int. Ed.* **2013**, *52*, 450–454.

- (9) (a) Iwamoto, T.; Abe, T.; Sugimoto, K.; Hashizume, D.; Matsui, H.; Kishi, R.; Nakano, M.; Ishida, S. *Angew. Chem., Int. Ed.* **2019**, *58*, 4371–4375. (b) Nukazawa, T.; Kosai, T.; Honda, S.; Ishida, S.; Iwamoto, T. *Dalton Trans.* **2019**, *48*, 10874–10880. (c) Fujinami, M.; Seino, J.; Nukazawa, T.; Ishida, S.; Iwamoto, T.; Nakai, H. *Chem. Lett.* **2019**, *48*, 961–964.
- (10) (a) Masamune, S.; Kabe, Y.; Collins, S.; Williams, D. J.; Jones, R. *J. Am. Chem. Soc.* **1985**, *107*, 5552–5553. (b) Jones, R.; Williams, D. J.; Kabe, Y.; Masamune, S. *Angew. Chem., Int. Ed. Engl.* **1986**, *25*, 173–174. (c) Takanashi, K.; Lee, V. Ya.; Ichinohe, M.; Sekiguchi, A. *Chem. Lett.* **2007**, *36*, 1158–1159. (d) Ueba-Ohshima, K.; Iwamoto, T.; Kira, M. *Organometallics* **2008**, *27*, 320–323. (e) Iwamoto, T.; Akasaka, N.; Ishida, S. *Nat. Commun.* **2014**, *5*, 5353.
- (11) (a) Dabish, T.; Schoeller, *J. Chem. Soc., Chem. Commun.* **1986**, 896–898. (b) Schoeller, W. W.; Dabish, T.; Busch, T. *Inorg. Chem.* **1987**, *26*, 4383–4389. (c) Schleyer, P. v. R.; Sax, A. F.; Kalcher, J.; Janoschek, R. *Angew. Chem., Int. Ed. Engl.* **1987**, *26*, 364–366. (d) Collins, S.; Dutler, R.; Rauk, A. *J. Am. Chem. Soc.* **1987**, *109*, 2564–2569. (e) Nagase, S.; Kudo, T. *J. Chem. Soc., Chem. Commun.* **1988**, 54–56. (f) Boatz, J. A.; Gordon, M. *S. J. Phys. Chem.* **1988**, *92*, 3037–3042. (g) Boatz, J. A.; Gordon, M. *S. J. Phys. Chem.* **1989**, *93*, 2888–2891. (h) Müller, T. *In Organosilicon Chemistry IV*; Auner, N., Weis, J., Eds.; Wiley-VCH: Weinheim, Germany, 2000; pp 110–116. (i) Koch, R.; Bruhn, T.; Weidenbruch, M. *J. Mol. Struct.: THEOCHEM* **2004**, *680*, 91–97. (j) Konno, Y.; Kudo, T.; Sakai, S. *Theor. Chem. Acc.* **2011**, *130*, 371–383. (k) Kira, M. *Organometallics* **2014**, *33*, 644–652.
- (12) Compound **2** is stable at room temperature but decomposes after 5 days at 80 °C in the dark to unexpectedly form **1** (46%) and other unidentified products.

- (13) Wiberg, N.; Schuster, H.; Simon, A.; Peters, K. *Angew. Chem., Int. Ed. Engl.* **1986**, *25*, 79–80.
- (14) Uchiyama, K.; Nagendran, S.; Ishida, S.; Iwamoto, T.; Kira, M. *J. Am. Chem. Soc.* **2007**, *129*, 10638–10639.
- (15) A linear relationship was observed between the experimentally observed isotropic chemical shift (δ_{obs}) for several mono-iodinated silicon compounds and the corresponding calculated chemical shift (δ_{calc}) obtained at the M06L/6-311+G(2df,p) [H,C,Si], SDD [I] level of theory ($\delta_{\text{obs}} = 1.011\delta_{\text{calc}} - 40.8$, $R^2 = 0.990$) (Figure 3-14 and Table 3-19). The ^{29}Si NMR chemical shifts predicted for $2'_c$ and $2'_p$ in the main text were corrected using this equation with raw δ_{calc} values of 139.1 ($2'_c$) and 191.0 ($2'_p$).
- (16) According to the IUPAC definition, a π -bond contains a nodal plane that includes the internuclear bond axis. See: IUPAC. σ , π (Sigma, Pi). In *Compendium of Chemical Terminology (the "Gold Book")*, 2nd ed. [Online]; McNaught, A. D., Wilkinson, A., Eds.; Blackwell, 1997. DOI: 10.1351/goldbook
- (17) Glendening, E. D.; Badenhop, J. K.; Reed, A. E.; Carpenter, J. E.; Bohmann, J. A.; Morales, C. M.; Karafiloglou, P.; Landis, C. R.; Weinhold, F. *NBO 7.0*; Theoretical Chemistry Institute, University of Wisconsin: Madison, WI, 2018.
- (18) The deformation of the bicyclic ring relative to the planar structure in the parent tetrasilabicyclo[1.1.0]butane has been qualitatively explained by a second-order Jahn–Teller distortion. For details, see ref 11k.
- (19) We did not observe a significant change in the UV-vis spectrum at lower temperatures (Figure 3-12).
- (20) A structure similar to 3_s was not located for 4 or 5 as a local minimum.¹¹
- (21) Although the origin of the difference between the relative stabilities of $2'_p$ and $2'_c$ remains unclear at this point, it may originate from a balance among the bonding interactions between the bridgehead Si atoms [$d = 2.501 \text{ \AA}$ ($2'_c$), 2.609 \AA ($2'_p$)], the strain originating from the Si(bridgehead)–Si(bridge)–Si(bridgehead) angle [$\alpha = 64.5^\circ$

- (2'c), 68.0° (2'p)], and the arrangement of the bulky silacyclopentane rings at the bridge positions.
- (22) In previously reported theoretical studies, the introduction of bulky substituents at the bridgehead position resulted in destabilization of structures similar to **3_L** and **3_{TP}** with acute bond angles ($\theta \approx 100^\circ$) and the stabilization of structures similar to **3_S**;^{11f,g,i} these predictions are consistent with the reported structures of such species with bulky bridgehead groups.¹⁰
- (23) During checking the galley proof of the final published version, we were informed that Scheschkewitz et al. obtained a tetrasilicon analogue of a cyclobutane-1,3-diyl. Yildiz, C. B.; Leszczynska, K. I.; Gonzalez-Gallardo, S.; Zimmer, M.; Azizoglu, A.; Biskup, T.; Kay, C. W. M.; Huch, V.; Rzepa, H. S.; Scheschkewitz, D. *Angew. Chem., Int. Ed.* **2020**, *59*, 15087–15092.
- (24) Fulmer, G. R.; Miller, A. J. M.; Sherden, N. H.; Gottlieb, H. E.; Nudelman, A.; Stoltz, B. M.; Bercaw, J. E.; Goldberg, K. I. *Organometallics* **2010**, *29*, 2176–2179.
- (25) Sheldrick, G. M. *SADABS, Empirical Absorption Correction Program*; Göttingen, Germany, 1996.
- (26) Sheldrick, G. M. *Acta Crystallogr., Sect. C: Struct. Chem.*, **2015**, *71*, 3–8.
- (27) Wakita, K. Yadokari-XG: Software for Crystal Structure Analyses, 2001; Release of Software (Yadokari-XG 2009) for Crystal Structure Analyses, Kabuto, C.; Akine, S.; Nemoto, T.; Kwon, E. *J. Crystallogr. Soc. Jpn.*, **2009**, *51*, 218–224.
- (28) Gaussian 09, Revision D.01, Frisch, M. J.; Trucks, G. W.; Schlegel, H. B.; Scuseria, G. E.; Robb, M. A.; Cheeseman, J. R.; Scalmani, G.; Barone, V.; Mennucci, B.; Petersson, G. A.; Nakatsuji, H.; Caricato, M.; Li, X.; Hratchian, H. P.; Izmaylov, A. F.; Bloino, J.; Zheng, G.; Sonnenberg, J. L.; Hada, M.; Ehara, M.; Toyota, K.; Fukuda, R.; Hasegawa, J.; Ishida, M.; Nakajima, T.; Honda, Y.; Kitao, O.; Nakai, H.; Vreven, T.; Montgomery, J. A., Jr.; Peralta, J. E.; Ogliaro, F.; Bearpark, M.; Heyd, J. J.; Brothers, E.; Kudin, K. N.; Staroverov, V. N.; Kobayashi, R.; Normand, J.; Raghavachari, K.; Rendell, A.; Burant, J.

C.; Iyengar, S. S.; Tomasi, J.; Cossi, M.; Rega, N.; Millam, J. M.; Klene, M.; Knox, J. E.; Cross, J. B.; Bakken, V.; Adamo, C.; Jaramillo, J.; Gomperts, R.; Stratmann, R. E.; Yazyev, O.; Austin, A. J.; Cammi, R.; Pomelli, C.; Ochterski, J. W.; Martin, R. L.; Morokuma, K.; Zakrzewski, V. G.; Voth, G. A.; Salvador, P.; Dannenberg, J. J.; Dapprich, S.; Daniels, A. D.; Farkas, Ö.; Foresman, J. B.; Ortiz, J. V.; Cioslowski, J.; Fox, D. J. Gaussian, Inc., Wallingford CT, 2009.

- (29) **GRRM14**, Maeda, S.; Harabuchi, Y.; Osada, Y.; Taketsugu, T.; Morokuma, K.; Ohno, K. see <https://iqce.jp/GRRM/> (accessed date March 21, 2020); Maeda, S.; Ohno, K.; Morokuma, K. *Phys. Chem. Chem. Phys.* **2013**, *15*, 3683–3701.
- (30) **NBO 7.0**, Glendening, E. D.; Badenhoop, J. K.; Reed, A. E.; Carpenter, J. E.; Bohmann, J. A.; Morales, C. M.; Karafiloglou, P.; Landis, C. R.; Weinhold, F. Theoretical Chemistry Institute, University of Wisconsin, Madison (2018).
- (31) Olah, G. A.; Field, L. D. *Organometallics* **1982**, *1*, 1485–1487.
- (32) $(\text{Me}_3\text{Si})_3\text{SiI}$ was prepared according to the published procedure and the ^{29}Si NMR spectrum was recorded measured in C_6D_6 . Bürger, H.; Kilian, W.; Burczyk, K. *J. Organomet. Chem.* **1970**, *21*, 291–301.
- (33) Hartmann, M.; Haji-Abdi, A.; Abersfelder, K.; Haycock, P. R.; White, A. J. P.; Scheschkewitz, D. *Dalton Trans.* **2010**, *39*, 9288–9295.

Chapter 4

Synthesis and Isomerization of a Planar 1,3-Dichlorotetrasilabicyclo[1.1.0]butane

The contents of this chapter are published in part in

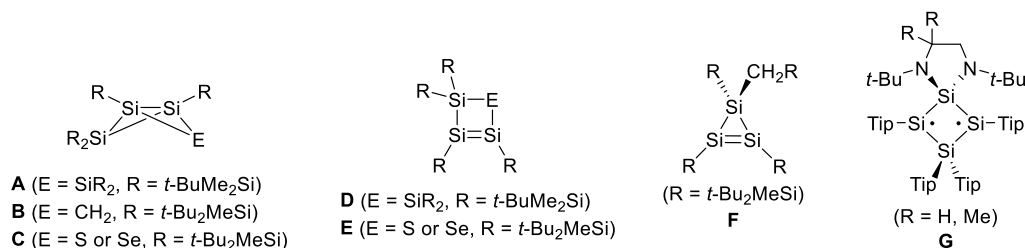
Nukazawa, T.; Iwamoto, T. *Dalton Trans.* **2020**, *49*, 16728–16735.

DOI: 10.1039/d0dt03408h

4-1. Introduction

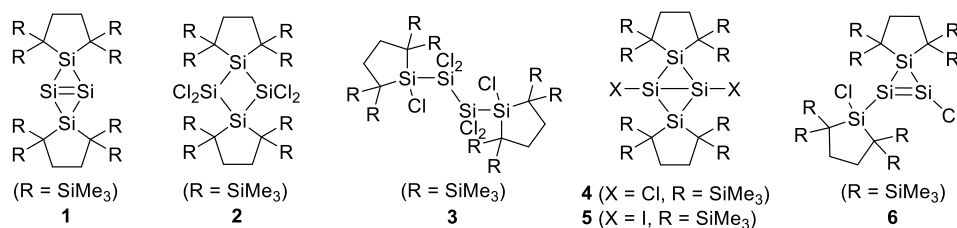
Bicyclo[1.1.0]butane is a highly strained compound and the interconversion between it and its C_4R_6 skeletal isomers such as cyclobutene and 1,3-butadiene, etc. has attracted experimental and theoretical chemists.^{1,2} Its heavy element analogues, in which the carbon atoms in the bicyclo[1.1.0]butane framework are partially or fully replaced with heavy element atoms, have also been extensively studied, as they often exhibit structures and properties that are not found in all-carbon bicyclo[1.1.0]butanes.^{3,4} Silabicyclo[1.1.0]butanes are among such heavy element analogues of bicyclo[1.1.0]butane. After the pioneering works on 2,4-disilabicyclo[1.1.0]butane by Fritz^{5l} and tetrasilabicyclo[1.1.0]butane by Masamune,^{5a} various silabicyclo[1.1.0]butane derivatives have been synthesized and some of these compounds exhibited the conversion to skeletal isomers.^{5,6} For example, bicyclo[1.1.0]tetrasilane **A** thermally isomerises to the corresponding cyclotetrasilene **D**, which reverts to **A** upon irradiation (Chart 4-1).^{5d,e,6b} 1,2,3-Trisilabicyclo[1.1.0]butane **B** undergoes thermal isomerization to 3-alkylcyclotrisilene **F**, while trisilabicyclo[1.1.0]butane **C** containing a chalcogen atom (S, Se) was photochemically transformed into the corresponding cyclobutene **E** (Chart 4-1).^{5j,k} Very recently, Scheschkewitz reported cyclotetrasilane-1,3-diyl **G** converts into the corresponding cyclotetrasilene.⁷ As aforementioned, silabicyclobutanes often exhibit interconversion modes which are not observed in all-carbon bicyclo[1.1.0]butanes. Theoretical studies on silabicyclo[1.1.0]butanes have revealed that the relative stabilities among the skeletal isomers and bond stretch isomers are substantially different from those of all-carbon C_4R_6 isomers and are remarkably dependent on the steric demand of the substituents on the bicyclobutane framework,⁸ which should be responsible for the interconversion modes of silabicyclo[1.1.0]butane.

Chart 4-1. Structures of Compounds **A–G** (Tip = 2,4,6-triisopropylphenyl)



Previously, we reported the reaction of bicyclo[1.1.0]tetrasil-1(3)-ene **1** with carbon tetrachloride providing tetra- and hexa-chlorinated tetrasilanes **2** and **3**, suggesting the existence of 1,3-dichlorobicyclo[1.1.0]tetrasilane **4** and its isomer as intermediates in this reaction (Chart 4-2).⁹ The formation of **4** was also supported by the formation of a methanol adduct of **4** in the reaction of **1** with carbon tetrachloride in the presence of methanol and the observation of ¹H NMR signals that are consistent with the structure of **4** at low temperature. Our recent results on the 1,2-iodination of **1** providing 1,3-diiodobicyclo[1.1.0]tetrasilane **5**¹⁰ encouraged us to isolate **4** by carefully conducting the reaction of **1** with carbon tetrachloride at lower temperatures. In this chapter, the author reports the synthesis and isolation of 1,3-dichlorobicyclo[1.1.0]tetrasilane **4** by the 1,2-dichlorination of **1** and the interconversion between **4** and its isomer, 1-chloro-2-(chlorosilyl)cyclotrisilene **6** (Chart 4-2).

Chart 4-2. Structures of Compounds **1–6**



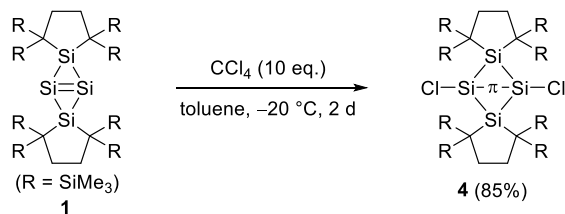
4-2. Results and Discussion

4-2-1. Synthesis of 1,3-Dichlorotetrasilabicyclo[1.1.0]butane **4**

A mixture of **1** and carbon tetrachloride was stirred at –20 °C for two days (Scheme 4-1). After the volatiles were removed under reduced pressure at 0 °C, pure **4** was obtained as an orange solid in 85% yield. The molecular structure of **4** was determined using a combination of

multinuclear NMR spectroscopy, mass spectrometry, elemental analysis, and single-crystal X-ray diffraction (XRD) analysis.¹¹

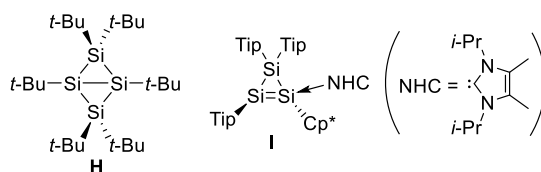
Scheme 4-1. Synthesis of **4**



4-2-2. Molecular Structure of **4**

Recrystallization from toluene at $-35\text{ }^\circ\text{C}$ provided single crystals of **4** suitable for XRD analysis (Figure 4-1). While 1,3-diiodo derivative **5** provides two types of single crystals that exhibit different structures, *cis*-bent (**5_c**) and planar structures (**5_p**) in the solid state, **4** forms only single crystals, the structural characteristics of which are very similar to those of **5_p**. The molecule has a crystallographic inversion centre between the Si1 and Si1* atoms and the central Si₄ bicyclic skeleton is planar [dihedral angle Si2–Si1–Si1*–Si2*, 180°]. The geometry around the bridgehead silicon atoms is almost planar [the angle sum of the bridgehead Si1 atom excluding the central bridgehead bond is 359.97°] and the Si–Cl moieties are very slightly bent in a *trans* configuration [the Si1*–Si1–Cl1 angle is $178.27(11)^\circ$] with respect to the Si₄ ring plane. The Si1–Si1* distance in **4** [$2.581(2)\text{ \AA}$] is very similar to that in **5_p** [$2.5822(11)\text{ \AA}$]¹⁰ but much longer than those of the previously reported bicyclo[1.1.0]tetrasilanes with bent structures ($2.35\text{--}2.47\text{ \AA}$)⁵ and much shorter than those of cyclotetrasilane-1,3-diyls **G** [$2.871(1)\text{ \AA}$] (Chart 4-1) and bicyclo[1.1.0]tetrasilane **H** [$2.853(1)\text{ \AA}$] (Chart 4-3) containing a planar Si₄ ring reported very recently by Scheschkewitz and Kyushin, respectively.^{7,12}

Chart 4-3. Related Compounds **H** and **I** (Tip = 2,4,6-triisopropylphenyl and Cp* = C₅Me₅)



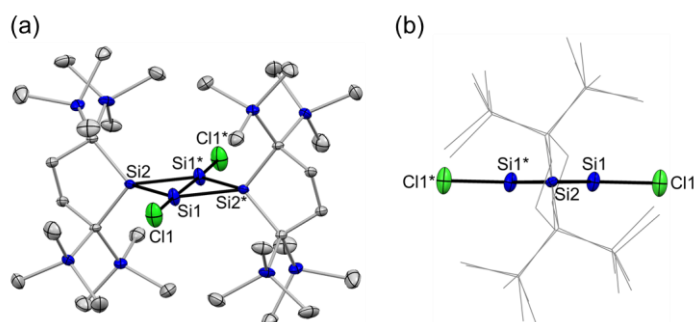


Figure 4-1. ORTEPs of **4** (a: perspective view; b: side view) with thermal ellipsoids at 50% probability; hydrogen atoms are omitted for clarity. Selected bond lengths (Å) and angles (deg): Si1–Si1* 2.581(2), Si1–Cl1 2.0690(18), Si1–Si2 2.3249(17), Si1–Si2* 2.3361(17), Si2–Si1–Si2* 112.74(6), Si1–Si2–Si1* 67.26(6), Si1*–Si1–Cl1 178.27(11), Si2–Si1–Si1*–Si2* 180.0.

4-2-3. NMR Spectra of **4**

The NMR spectra of **4** indicate that **4** adopts a highly symmetrical structure in solution. The ^1H NMR spectrum of **4** in C_6D_6 solution at room temperature shows two singlet signals at 0.42 and 1.93 ppm due to the eight equivalent SiMe_3 groups and the eight methylene protons of the five-membered rings, respectively. Compound **4** exhibits three ^{29}Si resonances at -7.9 (bridge Si), 4.6 (SiMe_3), and 126.4 ppm (bridgehead Si).¹³ The chemical shift of the bridgehead Si nuclei (126.4 ppm) is similar to that of **5** (103.8 ppm)¹⁰ but far downfield shifted compared with those of the reported bent bicyclo[1.1.0]tetrasilanes (-145.1 to 14.8 ppm) (Figure 4-2).⁵ Similar downfield-shifted ^{29}Si resonances were observed for the bridgehead silicon nuclei of **G** (198.24 ppm)⁷ and **H** (117.4 ppm)¹² that have planar ring structures (Figure 4-2).

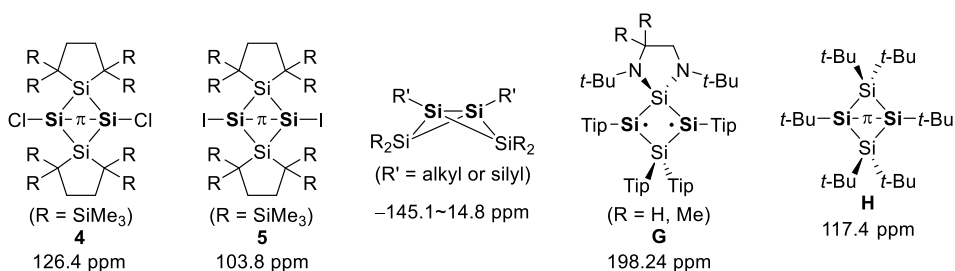


Figure 4-2. ^{29}Si NMR Chemical shifts of the bridgehead silicon atoms in **4** and the related compounds.

4-2-4. Theoretical Study

The structure of **4** was further examined by DFT calculations. The planar structure of **4** observed in the solid state is in good agreement with the optimized structure of **4** (**4_{opt}**)

calculated at the B3LYP-D3/6-311G(d) level of theory (Table 4-1). The frontier orbitals of **4**_{opt} (Figure 4-3a), which are π and π^* -type orbitals on the bridgehead silicon atoms, are similar to those of **5** (**5**_p) indicating that compound **4** is another example of a molecule with a π -type single bonding.^{7,10,12} It should be noted that two slightly-bent 1,3-dichlorobicyclotetrasilanes with highly pyramidalized bridgehead silicon atoms (**4'**_{opt}) and almost planar bridgehead silicon atoms (**4''**_{opt}) were located as local minima and higher in free energy (298.15 K) by 1.6 and 5.3 kJ mol⁻¹ than **4**_{opt} (Figure 4-3b, Table 4-1). Although the small relative energies suggest that these two structures could also exist in solution, the observed ²⁹Si resonances of bridge and bridgehead Si nuclei (-7.9 and 126.4) are close to those of **4**_{opt} (-17.1 and 150.2) calculated at the GIAO/M06L/6-311+G(2df,p) level of theory but substantially far from those of **4'**_{opt} (138.3, -43.5) and **4''**_{opt} (-25.1, 86.5) implying that **4** predominantly adopts a planar structure similar to that of **4**_{opt} in solution.

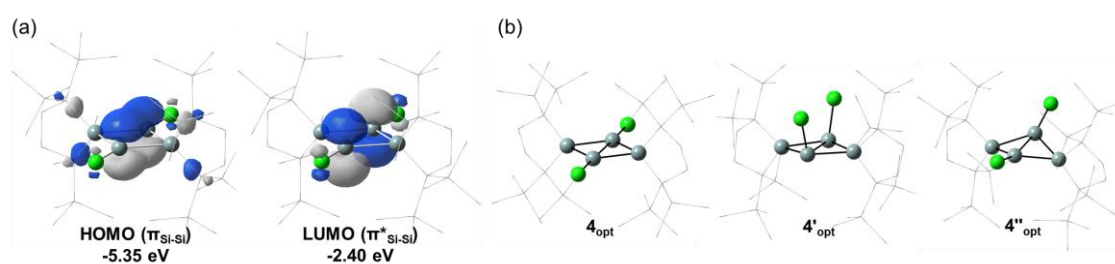


Figure 4-3. (a) Frontier orbitals of **4**_{opt} calculated at the B3LYP-D3/6-311G(d) level of theory (isosurface level: 0.05 e·a.u.⁻³); hydrogen atoms are omitted for clarity. (b) Structures of **4**_{opt}, **4'**_{opt}, and **4''**_{opt} optimized at the B3LYP-D3/6-311G(d) level of theory.

Table 4-1. Selected Structural Parameters of **4**, **4**_{opt}, **4'**_{opt} and **4''**_{opt}

| compound | $d/\text{\AA}$ | θ/deg | φ/deg | α/deg | $\Delta G^{\text{a,b}}$ |
|---------------------------|----------------|----------------------------------|----------------------|---------------------|-------------------------|
| XRD | | | | | |
| 4 | 2.581(2) | 178.27(11) (<i>trans</i>) | 180.00 | 67.26(6) | - |
| DFT ^a | | | | | |
| 4 _{opt} | 2.583 | 178.57 (<i>trans</i>) | 180.00 | 67.49 | 0.0 |
| 4' _{opt} | 2.893 | 109.187 118.79 (<i>cis</i>) | -174.45 | 73.12 73.23 | 1.6 |
| 4'' _{opt} | 2.443 | 160.68 (<i>cis</i>) | -149.60 | 63.15 | 5.3 |

^aCalculated at the B3LYP-D3/6-311G(d) level of theory. ^bAt 298.15 K, in kJ mol⁻¹.

4-2-5. Interconversion between Tetrasilabicyclo[1.1.0]butane **4** and Cyclotrisilene **6**

The author found an unexpected spectral change in the ^1H NMR spectrum of **4**. Immediately after the crystals of **4** were dissolved in C_6D_6 solution at room temperature, the ^1H NMR spectrum of the resulting solution showed only two singlet signals at 0.42 and 1.93 ppm (Figure 4-4a). After a few minutes, a set of new signals appeared at 0.37, 0.43, and 0.50 ppm in the ratio of 1:2:1 in the region for SiMe_3 protons with a decrease in the intensity of the signals of **4** (Figure 4-4b). After one day, no further decrease of the intensity of the original signals of **4** and an increase in the intensity of new signals were observed at room temperature. This observed behavior suggests that **4** equilibrates with a new species in solution at room temperature. The new species can be identified as chloro(chlorosilyl)-substituted cyclotrisilene **6** (Scheme 4-2) by NMR spectroscopy and the product analysis of the reaction with 4-(dimethylamino)pyridine (DMAP) (*vide infra*).

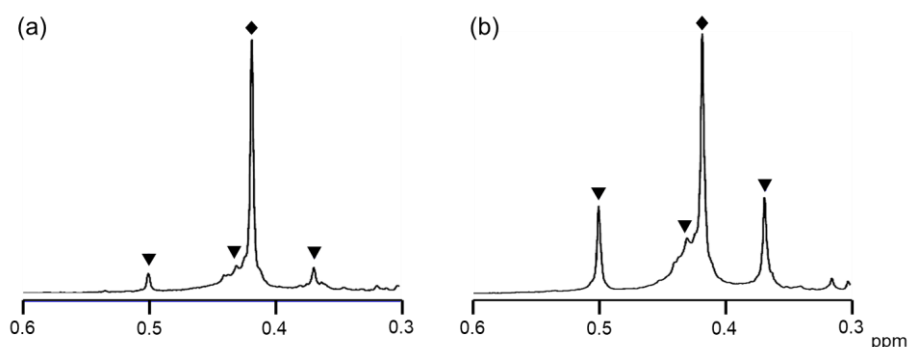
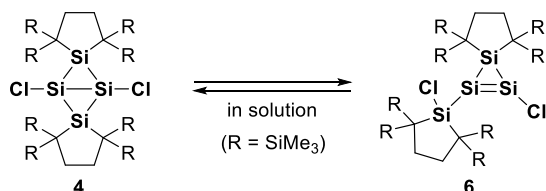


Figure 4-4. ^1H NMR spectra (SiMe_3 region, a: 5 min, b: 1 day) of **4** in C_6D_6 at room temperature ($\blacklozenge = \mathbf{4}$, $\blacktriangledown = \mathbf{6}$).

Scheme 4-2. Interconversion between **4** and **6**



4-2-6. Trapping Cyclotrisilene **6** with 4-(Dimethylamino)pyridine (DMAP)

As soon as DMAP was added to the equilibrium mixture of **4** and **6** in C_6D_6 solution, the ^1H NMR spectrum showed that the signals of **6** disappeared and new signals assignable to

cyclotrisilene-DMAP adduct **7** appeared, while the signals of **4** remained unchanged (Figure 4-5), suggesting that **7** was a product resulting from the reaction of **6** with DMAP. DMAP-adduct **7** could be alternatively obtained as dark red crystals in 64% yield by the reaction of **4** with DMAP in toluene at room temperature for one day (Scheme 4-3). Compound **7** was characterized by a combination of multinuclear NMR spectroscopy, mass spectrometry, elemental analysis, and XRD analysis. As Scheschkewitz reported that an *N*-heterocyclic carbene (NHC) can coordinate a double-bond silicon atom of a cyclotrisilene providing complex **I** (Chart 4-3) similar to **7**,¹⁴ it is reasonable to consider that cyclotrisilene **6** was generated from **4** in solution (Scheme 4-2).

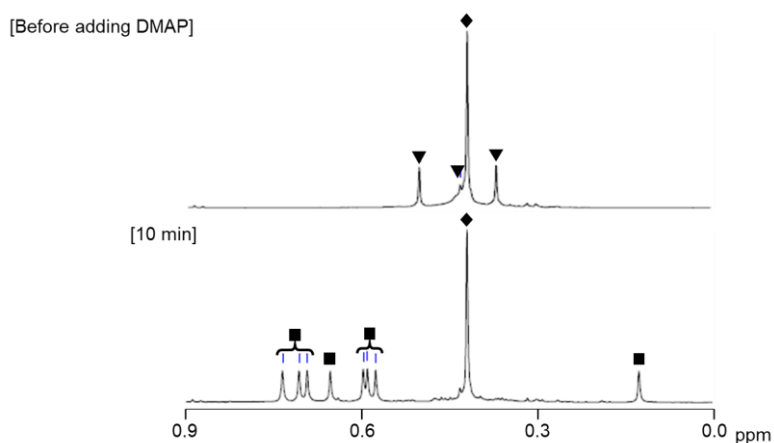
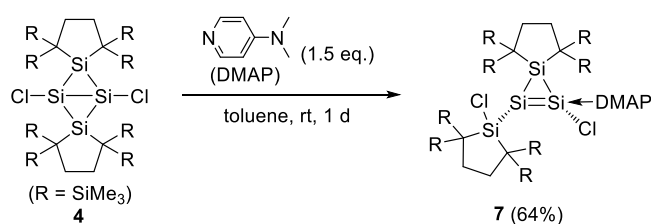


Figure 4-5. ¹H NMR spectra (SiMe₃ region) of the reaction mixture of **4+6** with DMAP in C₆D₆ at room temperature (◆ = **4**, ▼ = **6**, ■ = **7**).

Scheme 4-3. Synthesis of **7**



4-2-7. Molecular Structure of **7**

The molecular structure of **7** determined by XRD analysis reveals that DMAP coordinates to the chlorinated double bond silicon atom (Si1) (Figure 4-6). The DMAP and the chlorosilyl groups are arranged in a *trans* fashion with respect to the cyclotrisilene ring plane.

The Si1–Si2 distance [2.2145(7) Å] is significantly longer than those of the reported base-free cyclotrisilenes (2.118–2.186 Å).¹⁵ The elongation of the Si=Si bond upon the coordination of a Lewis base was found in cyclotrisilene-NHC adduct **I** [2.2700(5) Å]^{14a} and related base-coordinated disilenes.¹⁶ The geometry around the Si2 atom is highly pyramidalized [the angle sum: 333.19°]. In the ²⁹Si NMR spectrum of **7**, the Si1 and Si2 nuclei resonate at 6.1 and –114.2 ppm, respectively, indicating the highly polarized Si=Si double bond similar to the reported base-coordinated disilenes.¹⁶

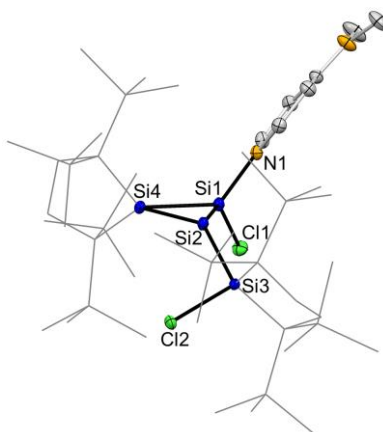


Figure 4-6. ORTEP of **7** with thermal ellipsoids at 50% probability; hydrogen atoms are omitted for clarity. Selected bond lengths (Å) and angles (deg): Si1–Si2 2.2145(7), Si1–N1 1.8789(15), Si1–Si4 2.2986(7), Si1–Cl1 2.1107 (6), Si2–Si3 2.3791(7), Si2–Si4 2.3893(7), Si3–Cl2 2.1317(6), Si2–Si1–Si4 63.90(2), Si1–Si2–Si4 59.76(2), Si1–Si4–Si2 56.34(2).

4-2-8. Elimination Reaction of DMAP from **7**

The elimination of DMAP from **7** provided further information on the equilibrium between **4** and **6**. When **7** was treated with BPh₃ in toluene-*d*₈ solution at –30 °C, the ¹H NMR spectrum of the reaction mixture showed four singlet signals at 0.35, 0.38, 0.45, and 0.48 ppm in the region for SiMe₃ protons, which correspond with those of **6** in the equilibrium mixture of **4** and **6** (Scheme 4-4 and Figure 4-7a,b). The seven ²⁹Si NMR resonances observed at 2.9, 3.3, 6.1, 32.9, 48.7, 78.2, and 104.1 ppm¹³ are comparable to the theoretical ²⁹Si chemical shifts of **6**_{opt} calculated at the M06L/6-311+G(2df,p) level of theory (Table 4-20). Upon warming to room temperature, the signals of **4** gradually appeared and the ratio of **4** : **6** reached 7 : 8 after one day (Scheme 4-4 and Figure 4-7c). These results are consistent with the notion that cyclotrisilene **6** equilibrates with bicyclo[1.1.0]tetrasilane **4** in solution.

Scheme 4-4. Reaction of **7** with BPh₃

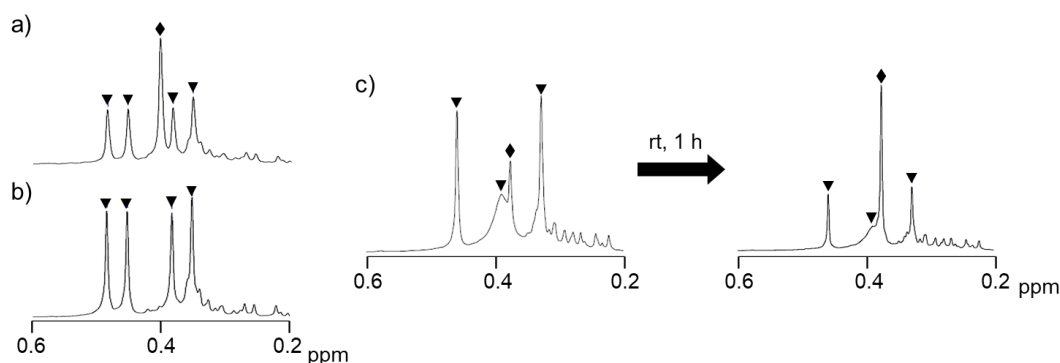
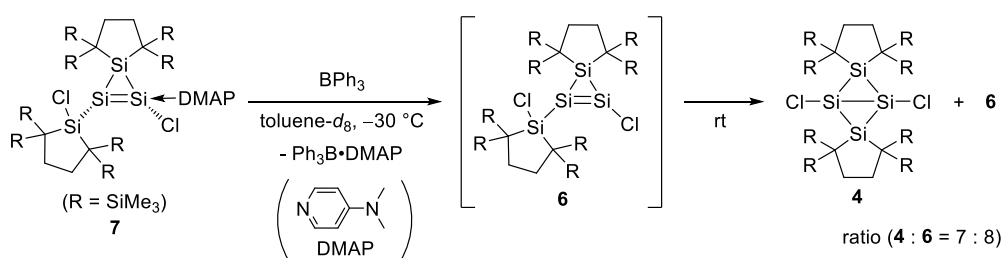
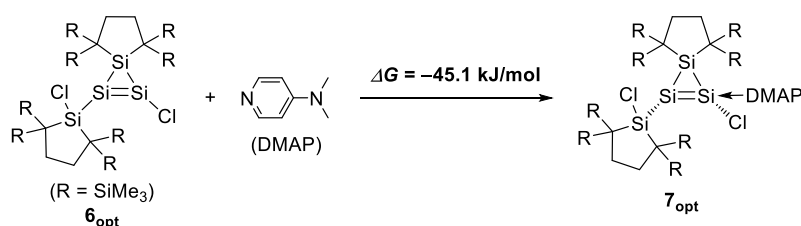


Figure 4-7. ¹H NMR spectra (SiMe₃ region) of a) the equilibrium mixture of **4**+**6** and b) the reaction mixture of **7** with BPh₃ in toluene-*d*₈ at -30 °C. c) ¹H NMR spectra (SiMe₃ region) of the reaction mixture of **7** with BPh₃ (left: just after warming up, right: after 1 hour) in toluene-*d*₈ at room temperature (♦ = **4**, ▼ = **6**).

4-2-9. Theoretical Calculations for **6** and **7**

The theoretical calculations provided further insight into the behavior of **4** in solution. In addition to **4**, **6** and **7** were located as local minima (**6**_{opt} and **7**_{opt}) at the B3LYP-D3/6-311G(d) level of theory, and the structural parameters of **7**_{opt} are in good agreement with those obtained from the XRD analysis. Cyclotrisilene **6**_{opt} is lower only by 6.9 kJ mol⁻¹ in free energy (298.15 K) than **4**_{opt}, which is consistent with the fact that **6** is a dominant species in the equilibrium mixture.¹⁷ The formation of DMAP-adduct **7**_{opt} from **6**_{opt} and DMAP was found to be exergonic (-45.1 kJ mol⁻¹), which is also consistent with the observed facile formation of **7** (Scheme 4-5). These experimental and theoretical results corroborate that the compound which equilibrates with **4** in solution is cyclotrisilene **6**.

Scheme 4-5. Formation of DMAP-adduct **7_{opt}**



4-2-10. Possible Isomerization Mechanism

A possible isomerisation route between **4** and **6** examined by the DFT calculation at the B3LYP-D3/B1 level of theory (B1: 6-311G(d) [Si₄Cl₂ core], 6-31G(d) [C atoms in silacyclopentane rings], 3-21G* [other atoms]) is shown in Figure 4-8. After the isomerization of **4_{opt}** to *cis*-bent bicyclic tetrasilane **4'_{opt}** that has a long bridgehead Si–Si distance [2.888 Å] and highly-pyramidalized bridgehead silicon atoms, which should be regarded as a long bond isomer of bicyclo[1.1.0]tetrasilane,^{8,18,19} the ring-opening reaction of **4'_{opt}** provides tetrasila-1,3-diene **8_{opt}**.^{20,21} Finally, the 1,2-chlorine migration accompanied by the ring closure, which can be rationalized by a simultaneous disilene–silylsilylene isomerisation via 1,2-chlorine migration and disilene–silylsilylene–cyclotrisilene isomerisation,^{14,22} afforded **6_{opt}**. The calculated activation barrier of the rate-controlling step (isomerisation of **8_{opt}** to **6_{opt}**) [61.5 kJ mol⁻¹] is consistent with the fact that the isomerisation occurs at room temperature.²³

The observed isomerisation mode between **4** and **6** is different from the isomerisation of **G** containing a similar planar silicon ring to the corresponding cyclotetrasilene derivative.⁷ As for **4**, the bulky dialkylsilylene [2,2,5,5-tetrakis(trimethylsilyl)silacyclopentane-1,1-diyl] moiety located at the bridge positions, which cannot dimerize due to its steric demand,²⁴ should prohibit such isomerisation to the corresponding cyclotetrasilene derivative in which two silylene moieties need to connect.

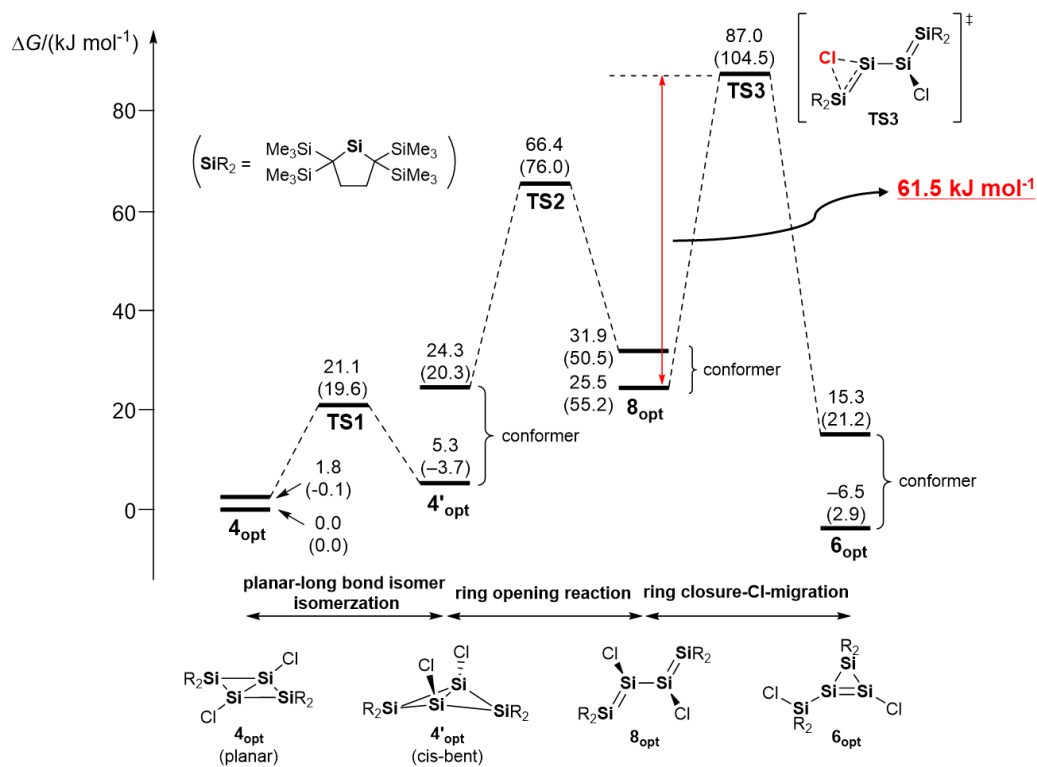
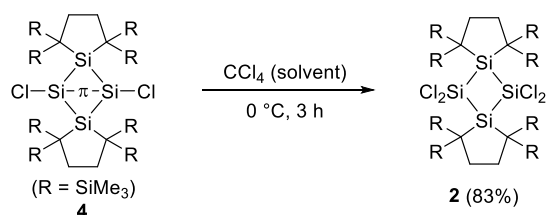


Figure 4-8. A possible isomerization route between **4_{opt}** and **6_{opt}** calculated at the B3LYP-D3/6-311G(d) [Si_4Cl_2 core], 6-31G(d) [C atoms in silacyclopentane rings], 3-21G* [other atoms] level of theory. The values in brackets and parentheses are relative Gibbs free energies (298.15 K) and relative energies including zero-point vibrational energy correction in kJ mol^{-1} , respectively.

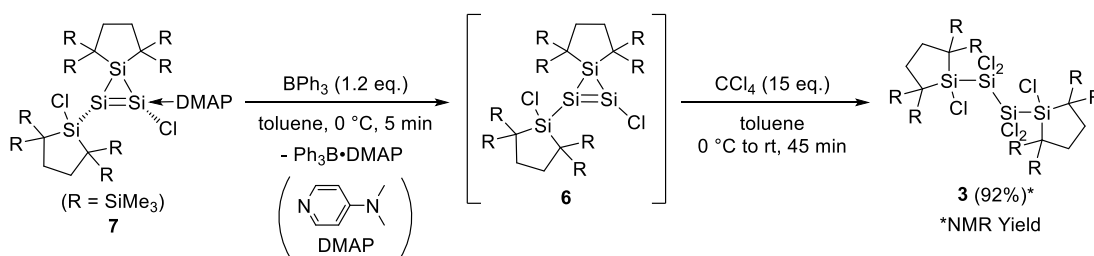
4-2-11. Reaction of **4** and **6** with CCl_4

Finally, we examined the reaction of **4** and **6** with carbon tetrachloride. As expected, **4** was treated with carbon tetrachloride at 0°C to provide **2** as a major product in 83% yield (Scheme 4-6). Conversely, when carbon tetrachloride was added to **6**, which was generated in situ from **7** and BPh_3 in toluene at 0°C , acyclic tetrasilane **3** was obtained as a major product (NMR yield: 92%) and cyclic tetrasilane **2** was not observed (Scheme 4-7). These results indicated that **6** was a key intermediate for the generation of **3**.²⁵

Scheme 4-6. Reaction of **4** with CCl_4



Scheme 4-7. Reaction of **6** with CCl₄



4-3. Conclusion

In conclusion, 1,3-dichlorobicyclo[1.1.0]tetrasilane **4** was synthesized by 1,2-dichlorination of the corresponding bridgehead disilene **1** at low temperature. The molecular structure and ²⁹Si NMR suggest that **4** exhibits a π -type single bonding between the bridgehead silicon atoms. Compound **4** equilibrates with cyclotrisilene **6** in solution at room temperature, which is an unprecedented interconversion mode among Si₄R₆ isomers.

4-4. Experimental Section

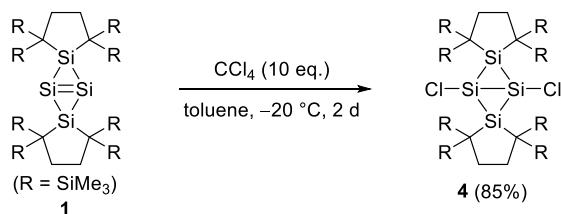
General Procedures

All reactions involving air-sensitive compounds were performed under an argon or nitrogen atmosphere using a high-vacuum line and standard Schlenk techniques, or a glove box, as well as dry and oxygen-free solvents. The reactions at lower temperatures were performed using an EYELA PSL-1400 cryobath. The NMR spectra were recorded on a Bruker Avance III 500 FT NMR spectrometer. The ¹H and ¹³C NMR chemical shifts were referenced to residual ¹H and ¹³C shifts of the solvents: C₆D₆ (¹H: δ 7.16 and ¹³C: δ 128.0), THF-*d*₈ (¹H: δ 3.58 and ¹³C: δ 67.2), and toluene-*d*₈ (¹H: δ 2.08).²⁶ The ²⁹Si NMR chemical shifts were relative to Me₄Si in ppm (δ 0.00). The sampling of air-sensitive compounds was carried out using a VAC NEXUS 100027 type glove box. Mass spectra were recorded on a Bruker Daltonics SolariX 9.4 T spectrometer. UV-vis spectra were recorded on a JASCO V-770 spectrometer. X-ray analysis was carried out using a Bruker AXS APEXII CCD diffractometer.

Materials

Dry and degassed hexane, benzene, and toluene were prepared using a VAC 103991 solvent purifier. C_6D_6 was degassed through five freeze–pump–thaw cycles and then dried over molecular sieves 4Å. THF- d_8 and toluene- d_8 were dried in a tube covered with a potassium mirror and then distilled under reduced pressure prior to use. Carbon tetrachloride was dried over calcium hydride and degassed through three freeze–pump–thaw cycles. 4-(Dimethylamino)pyridine (DMAP), triphenylborane, and ferrocene were commercially available and used without further purification. Bicyclo[1.1.0]tetrasil-1(3)-ene **1** was prepared according to the published procedure.^{9b}

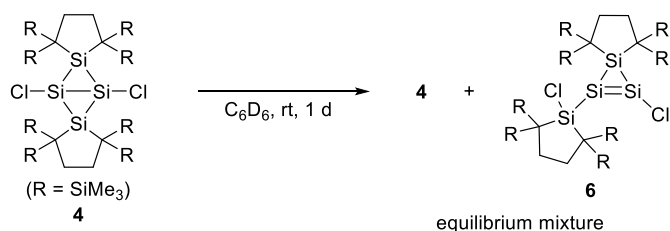
Synthesis of 1,3-Dichlorobicyclo[1.1.0]tetrasilane **4** [TN420,438]



To a Schlenk tube (10 mL) equipped with a magnetic stir bar, **1** (30.4 mg, 37.9 μ mol) and toluene (3.0 mL) were added. After the mixture was cooled to -20 °C, carbon tetrachloride (59 mg, 384 μ mol) was added to the Schlenk tube. Then the mixture was stirred at -20 °C for 2 days. The resulting suspension turned from orange to deep orange. After the volatiles were removed in vacuo at 0 °C, the crude was washed with hexane to provide an orange solid of **4** (28.2 mg, 32.3 μ mol) in 85% yield.

4: an orange solid; mp 161–162 °C (decomp.); δ_H (500 MHz, C_6D_6 , 298 K) 0.42 (72H, s, $SiCH_3$), 1.93 (8H, s, CH_2); δ_C (126 MHz, C_6D_6 , 333 K) 5.0 ($SiCH_3$), 15.9 (C), 34.5 (CH_2); δ_{Si} (99 MHz, C_6D_6 , 333 K) -7.9 (Si), 4.6 ($SiMe_3$), 126.4 ($Si-Cl$); HRMS (APCI_positive) found, 870.28636. Calcd for $C_{32}H_{80}Cl_2Si_{12}$ [M^+], 870.28628; found: C, 44.10; H, 9.13. Calcd for $C_{32}H_{80}Cl_2Si_{12}$: C, 44.03; H, 9.24%.

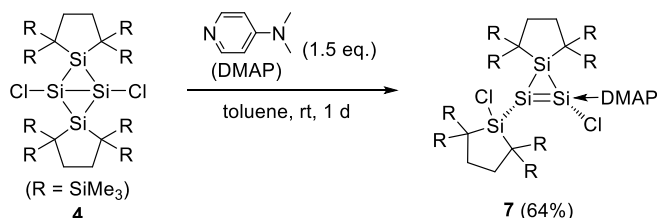
Thermal Isomerisation of **4** to (Chloro)(chlorosilyl)cyclotrisilene **6** [TN631]



To a J. Young NMR tube, **4** was added. To the NMR tube, C_6D_6 was added and immediately the ^1H NMR spectrum of the mixture was recorded at room temperature. Then, the mixture was left for one day at room temperature and the NMR spectra of the mixture were recorded again. See Figures 4-9 and 4-10 for details. The NMR data of **6** were obtained by subtracting the signals of **4** from the spectrum of the equilibrium mixture.

6: δ_{H} (500 MHz, C_6D_6 , 302 K) 0.37 (18H, s, SiCH_3), 0.43 (36H, brs, SiCH_3), 0.50 (18H, s, SiCH_3), 1.86–2.05 (8H, m, CH_2); δ_{C} (126 MHz, C_6D_6 , 333 K) 4.1 (SiCH_3), 5.0 (SiCH_3), 5.5 (SiCH_3), 20.7 (C), 21.4 (C), 33.9 (CH_2), 34.4 (CH_2); δ_{Si} (99 MHz, C_6D_6 , 333 K) 2.9 (SiMe_3), 3.3 (SiMe_3), 6.1 (SiMe_3), 32.9 (Si), 48.7 ($\text{Si}=\text{Si}-\text{Cl}$), 78.2 (Si), 104.1 ($\text{Si}=\text{Si}-\text{Cl}$).

Reaction of **4** with 4-(Dimethylamino)pyridine (DMAP) [TN590,680]

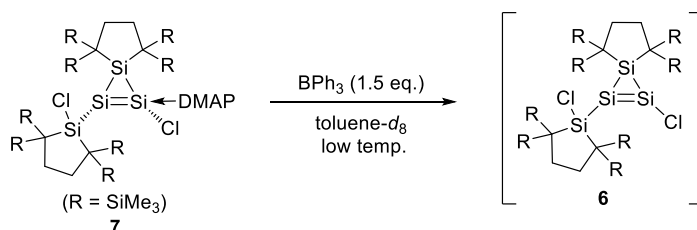


To a Schlenk tube (30 mL) equipped with a magnetic stir bar, **4** (60.6 mg, 69.4 μmol) and DMAP (12.3 mg, 101 μmol) were added. To the mixture, toluene (5.0 mL) was added and then the mixture was stirred at room temperature for one day. The resulting suspension turned from orange to dark red. After the volatiles were removed in vacuo at room temperature, recrystallization from hot benzene provided dark red crystals of **7**·(benzene)₂ (51.3 mg, 44.6 μmol) in 64% yield.

7·(benzene)₂: red crystals; mp 80–81 °C (decomp.); δ_{H} (500 MHz, $\text{THF}-d_8$, 296 K) –0.11 (9H, s, SiCH_3), 0.278 (9H, s, SiCH_3), 0.284 (9H, s, SiCH_3), 0.29 (9H, s, SiCH_3), 0.31 (9H, s, SiCH_3),

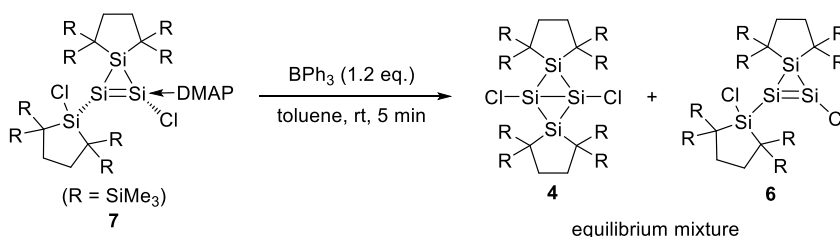
0.32 (9H, s, SiCH₃), 0.35 (9H, s, SiCH₃), 0.42 (9H, s, SiCH₃), 1.61–1.70 (1H, m, CH₂), 1.85–2.20 (7H, m, CH₂), 3.21 (6H, s, N(CH₃)₂ of DMAP), 6.91 (2H, d, *J* = 7.6 Hz, *m*-CH of DMAP), 7.30 (12H, s, benzene), 8.79 (2H, d, *J* = 7.6 Hz, *o*-CH of DMAP); δ_C (126 MHz, THF-*d*₈, 301 K) 4.1 (SiCH₃), 4.6 (SiCH₃), 5.4 (SiCH₃), 5.48 (SiCH₃), 5.52 (SiCH₃), 5.54 (SiCH₃), 5.55 (SiCH₃), 5.7 (SiCH₃), 16.1 (C), 18.5 (C), 20.2 (C), 21.0 (C), 34.5 (CH₂), 35.3 (CH₂), 35.5 (CH₂), 35.9 (CH₂), 39.6 (NCH₃), 107.1 (*m*-CH, DMAP), 128.9 (benzene), 146.7 (*o*-CH, DMAP), 157.2 (*p*-C, DMAP); δ_{Si} (99 MHz, THF-*d*₈, 301 K) -114.2 (Si=Si←DMAP), 1.3 (SiMe₃), 1.7 (SiMe₃), 1.9 (SiMe₃), 3.1 (SiMe₃), 3.3 (SiMe₃), 3.8 (SiMe₃), 4.5 (SiMe₃), 5.0 (SiMe₃), 6.0 (Si), 6.1 (Si=Si←DMAP), 42.4 (Si); λ_{max} (hexane)/nm 519 ($\epsilon/dm^3 \text{ mol}^{-1} \text{ cm}^{-1}$, 1.1×10^3), 362 (5.4×10^3), 315sh (7.6×10^3); HRMS (APCI_solid) found, 993.37924. Calcd for C₃₉H₉₀Cl₂N₂Si₁₂ [M⁺], 993.37850; found: C, 52.98; H, 8.91; N, 2.50. Calcd for C₃₉H₉₀Cl₂N₂Si₁₂ + 2C₆H₆: C, 53.21; H, 8.93; N, 2.43%.

Reaction of **7** and BPh₃ at Low Temperature [TN675,721]



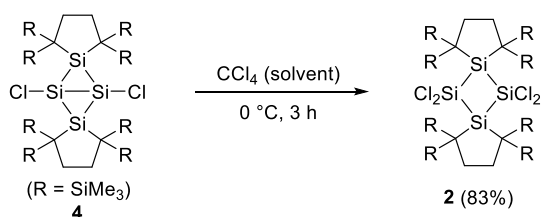
In a sealed NMR tube, **7** (10.3 mg, 9.0 μmol), triphenylborane (3.3 mg, 13.6 μmol) and toluene-*d*₈ (ca. 0.5 mL) were mixed at -30 °C and then the ¹H NMR spectrum of the mixture was recorded at the same temperature. Then, the ¹H NMR spectra of the mixture were recorded at -20, -10, 0 °C, and finally room temperature. See Figure 4-25 for details.

Reaction of **7** and BPh₃ at Room Temperature [TN699]



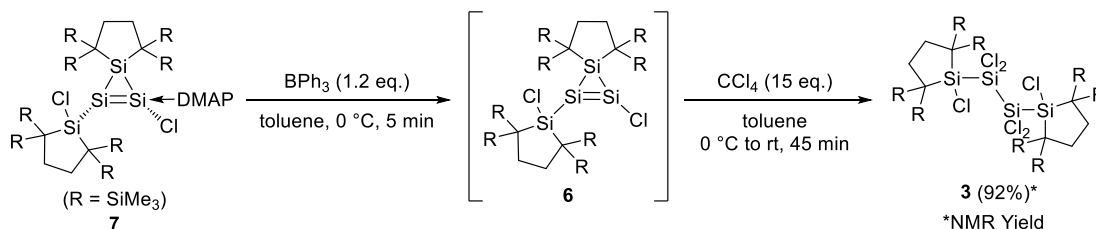
To a Schlenk tube (30 mL) equipped with a magnetic stir bar, compound **7** (24.9 mg, 21.6 μmol) and toluene (10.0 mL) were added. To the mixture triphenylborane (6.2 mg, 25.6 μmol) was added at room temperature and then the mixture was stirred for 5 min. The resulting solution turned to orange from dark red and the equilibrium mixture of **4** and **6** was obtained in 86% yield. The yield was determined by ^1H HMR integral using ferrocene as an internal standard. See Figure 4-26.

Reaction of **4** with CCl_4 [TN704]



To a Schlenk tube (10 mL) equipped with a magnetic stir bar, **4** (30.0 mg, 34.4 μmol) was added. To the Schlenk tube, carbon tetrachloride (2.0 mL, cooled to $0\text{ }^\circ\text{C}$) was added and then the mixture was stirred for 3 hours at $0\text{ }^\circ\text{C}$. The resulting suspension turned from orange to yellow. After the volatiles were removed in vacuo at $0\text{ }^\circ\text{C}$, the residue was washed with hexane to provide a pale yellow solid of **2** (26.8 mg, 28.4 μmol) in 83% yield. The formation of **2** (ref. 9b) was confirmed by comparison with the ^1H NMR spectrum of the authentic sample reported in the literature.

Reaction of **7** with CCl_4 in the Presence of BPh_3 (Reaction of **6** with CCl_4) [TN667]



To a Schlenk tube (30 mL) equipped with a magnetic stir bar, **7** (30.4 mg, 26.4 μmol) and toluene (5.0 mL) were added. To the mixture, a toluene solution of triphenylborane (0.20 mL, 7.8 mg, 32.2 μmol) was added at $0\text{ }^\circ\text{C}$, and then the mixture was stirred for 5 min. The

resulting solution turned from dark red to deep orange. Then, carbon tetrachloride (ca. 61 mg, 397 μmol) was added at 0 $^{\circ}\text{C}$, and the mixture was further stirred at room temperature for 45 min. The volatiles were removed in vacuo at room temperature to provide **3** in 92% yield. The yield was determined by ^1H HMR integral using ferrocene as an internal standard. See Figure 4-23. The formation of **3** (ref. 9b) was confirmed by comparison with the ^1H NMR spectrum of the authentic sample reported in the literature.

NMR spectra

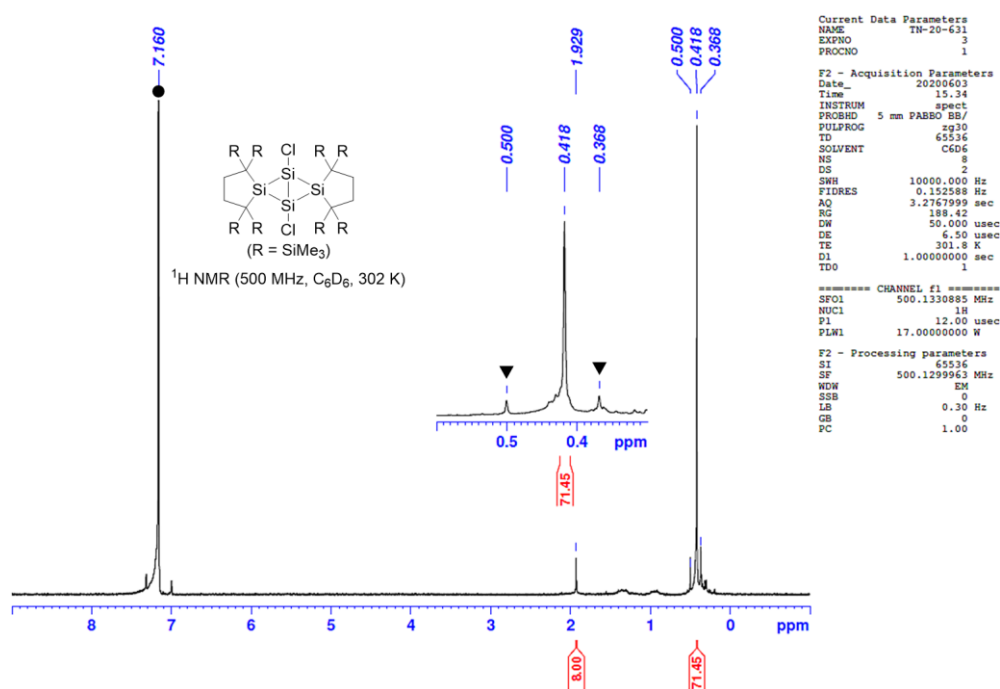


Figure 4-9. ^1H NMR spectrum of **4** in C_6D_6 at 302 K (\bullet = C_6HD_5 , \blacktriangledown = **6**).

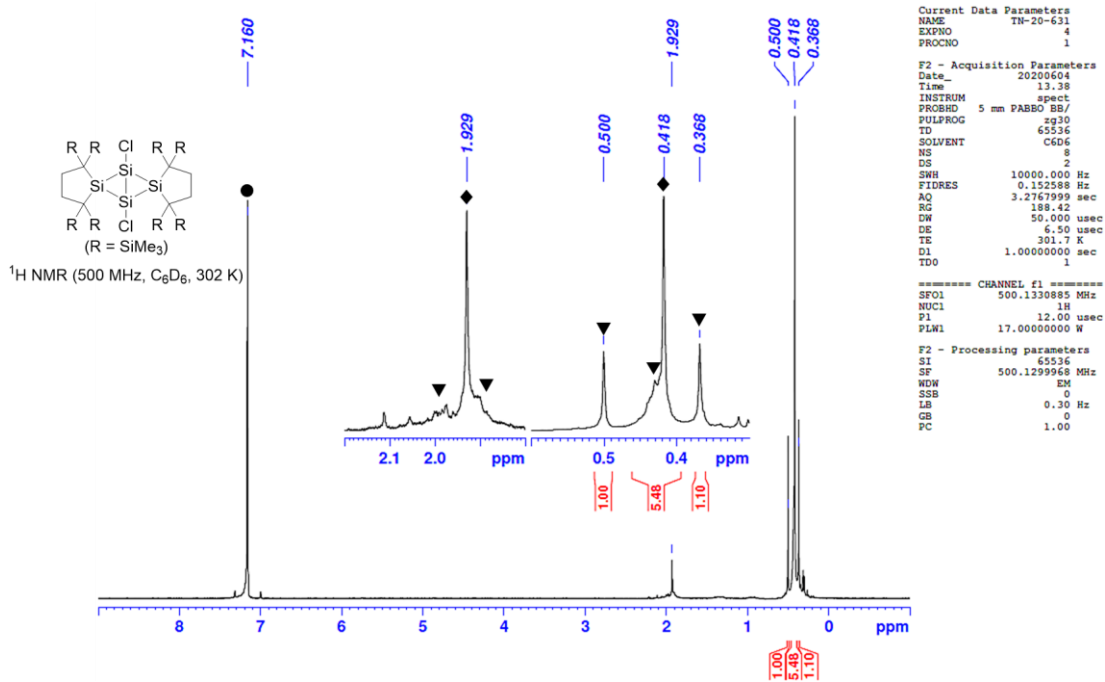


Figure 4-10. ¹H NMR spectrum of **4** in C₆D₆ at 302 K after 1 day (● = C₆HD₅, ◆ = **4**, ▼ = **6**).

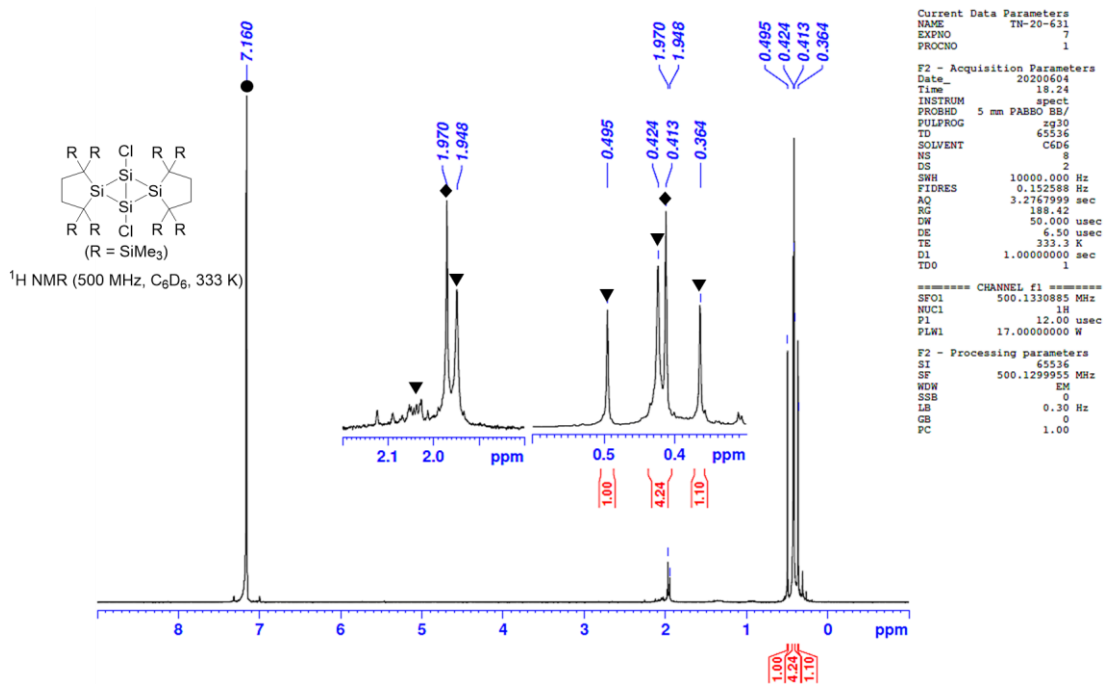


Figure 4-11. ¹H NMR spectrum of **4** in C₆D₆ at 333 K (● = C₆HD₅, ◆ = **4**, ▼ = **6**).

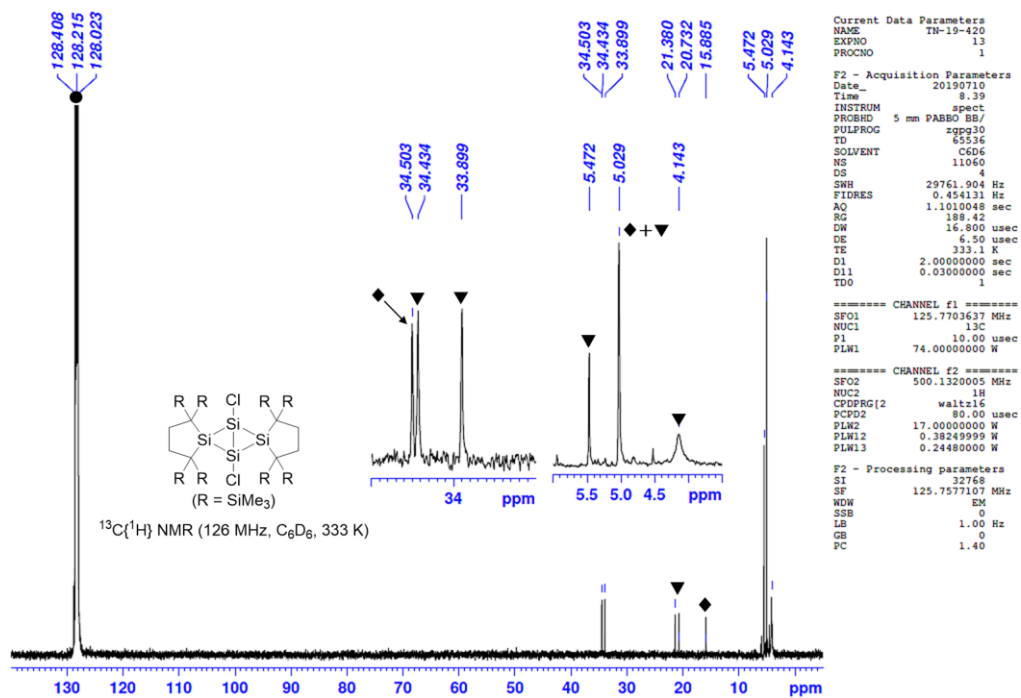


Figure 4-12. $^{13}\text{C}\{^1\text{H}\}$ NMR spectrum of **4** in C_6D_6 in 333 K (● = C_6D_6 , ◆ = **4**, ▼ = **6**).

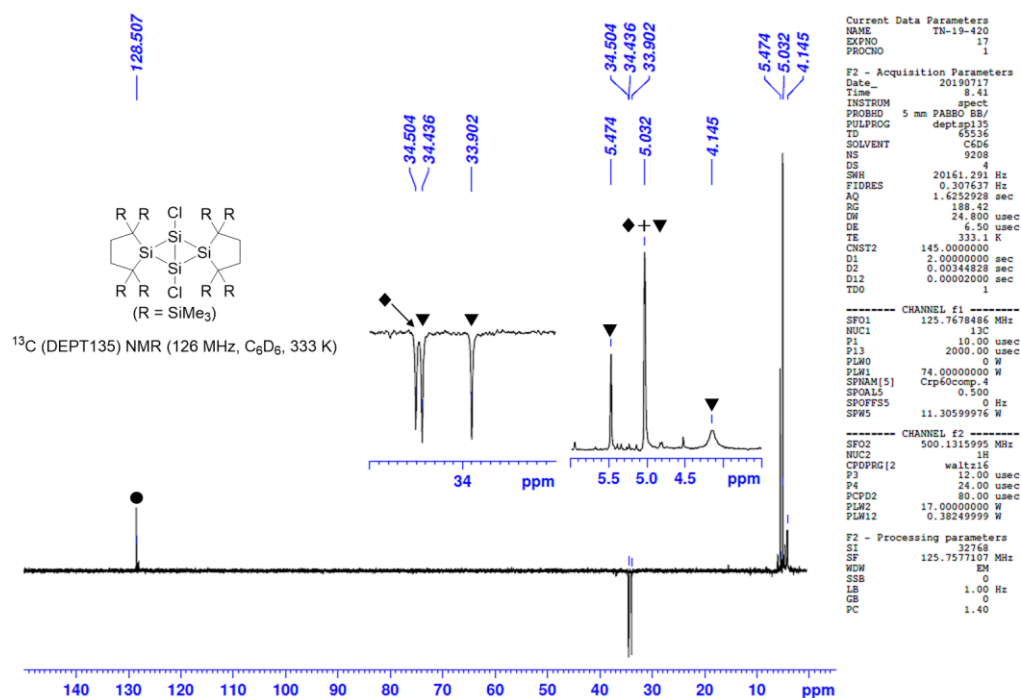


Figure 4-13. ^{13}C (DEPT135) NMR spectrum of **4** in C_6D_6 at 333 K (● = C_6D_6 , ◆ = **4**, ▼ = **6**).

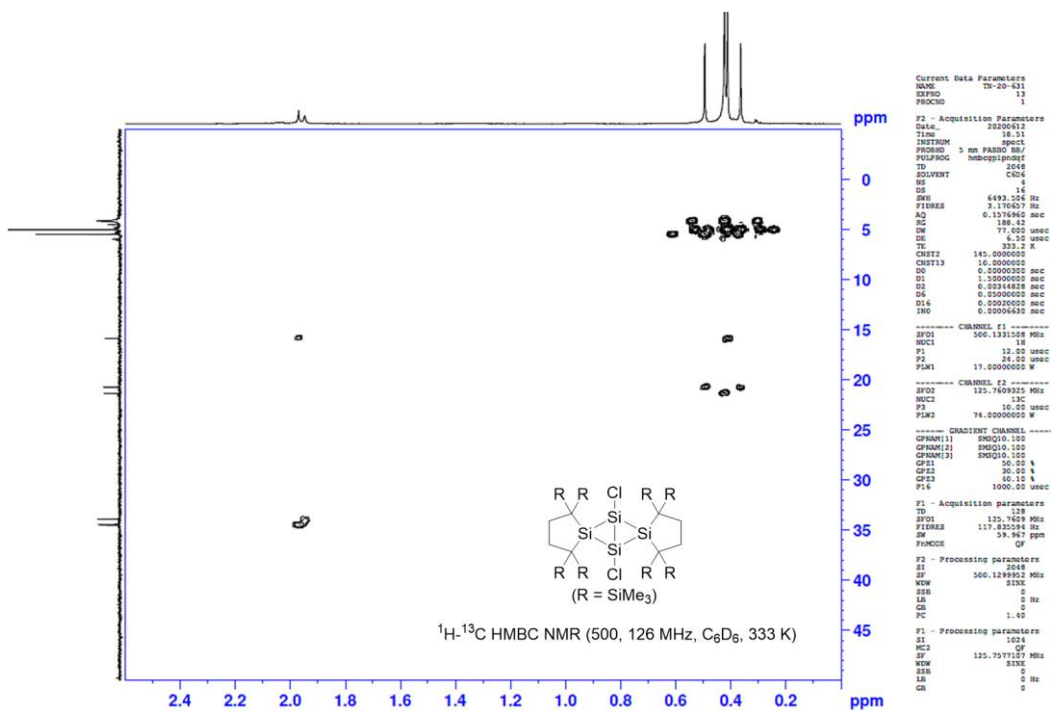


Figure 4-14. ^1H - ^{13}C HMBC NMR spectrum of **4** in C_6D_6 at 333 K.

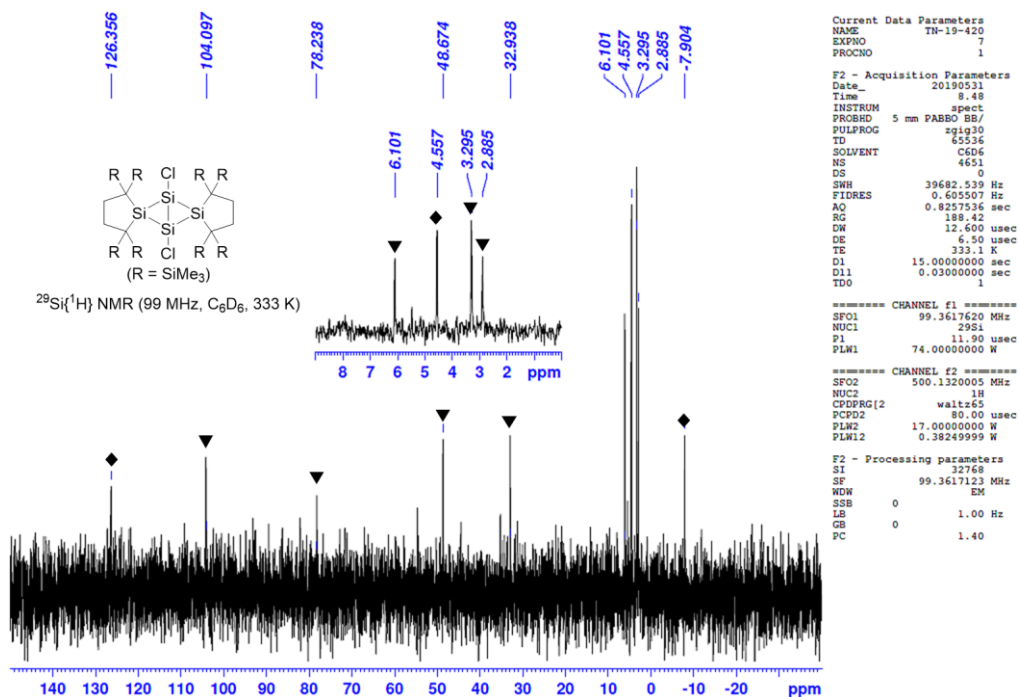


Figure 4-15. $^{29}\text{Si}\{^1\text{H}\}$ NMR spectrum of **4** in C_6D_6 at 333 K. (\blacklozenge = **4**, \blacktriangledown = **6**).

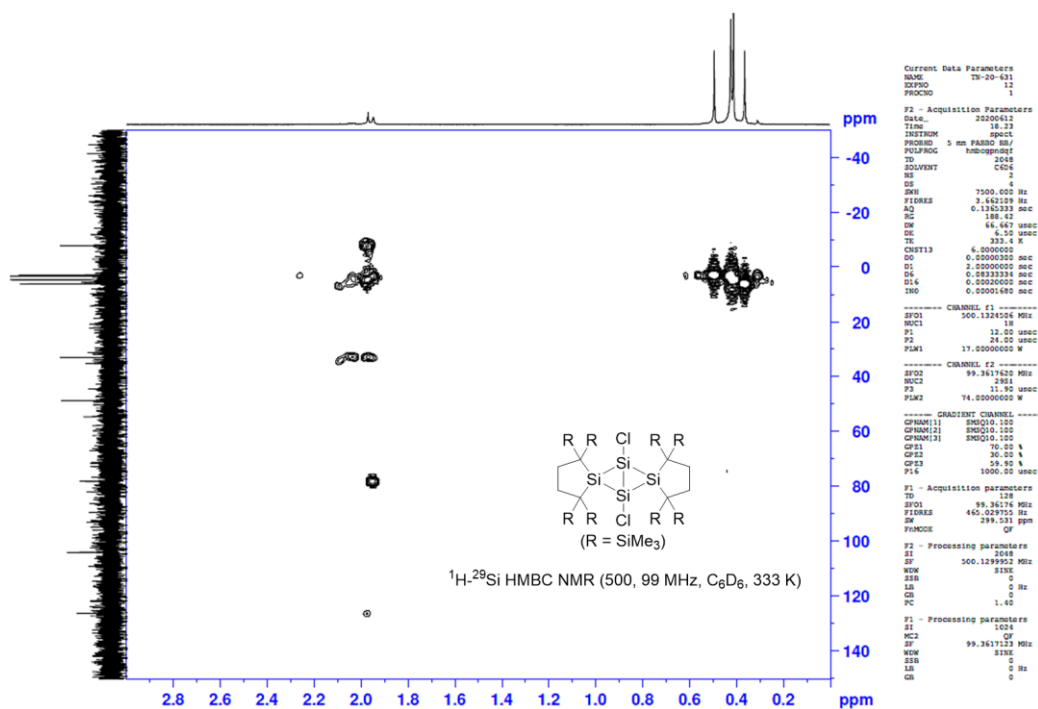


Figure 4-16. ^1H - ^{29}Si HMBC NMR spectrum of **4** in C_6D_6 at 333 K.

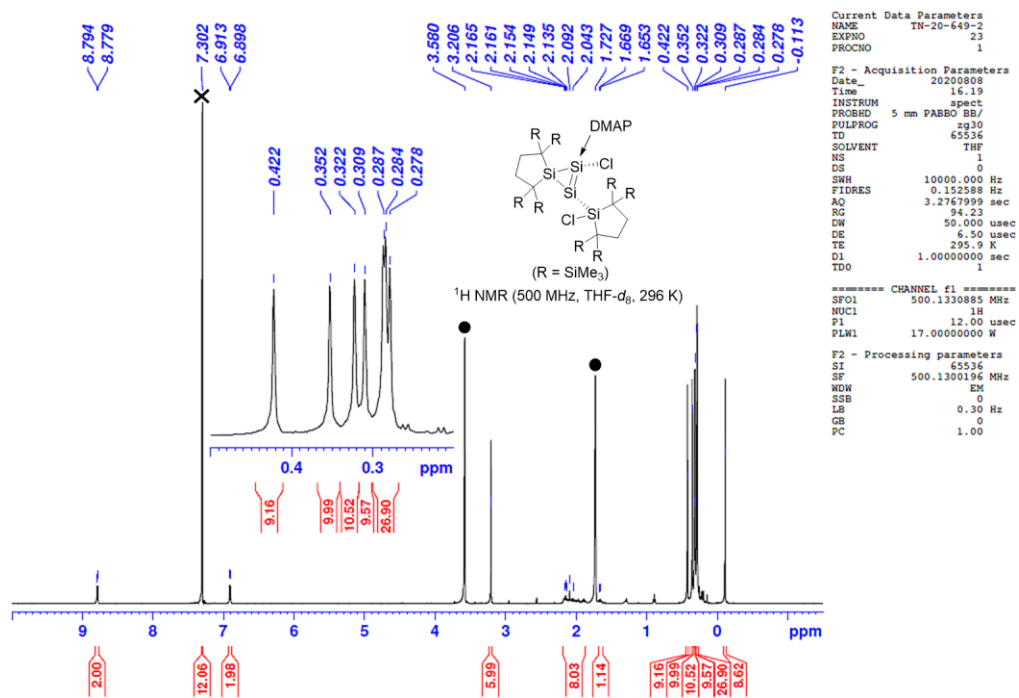


Figure 4-17. ^1H NMR spectrum of **7**·(benzene) $_2$ in THF-d_8 at 296 K (● = THF-d_8 , × = benzene).

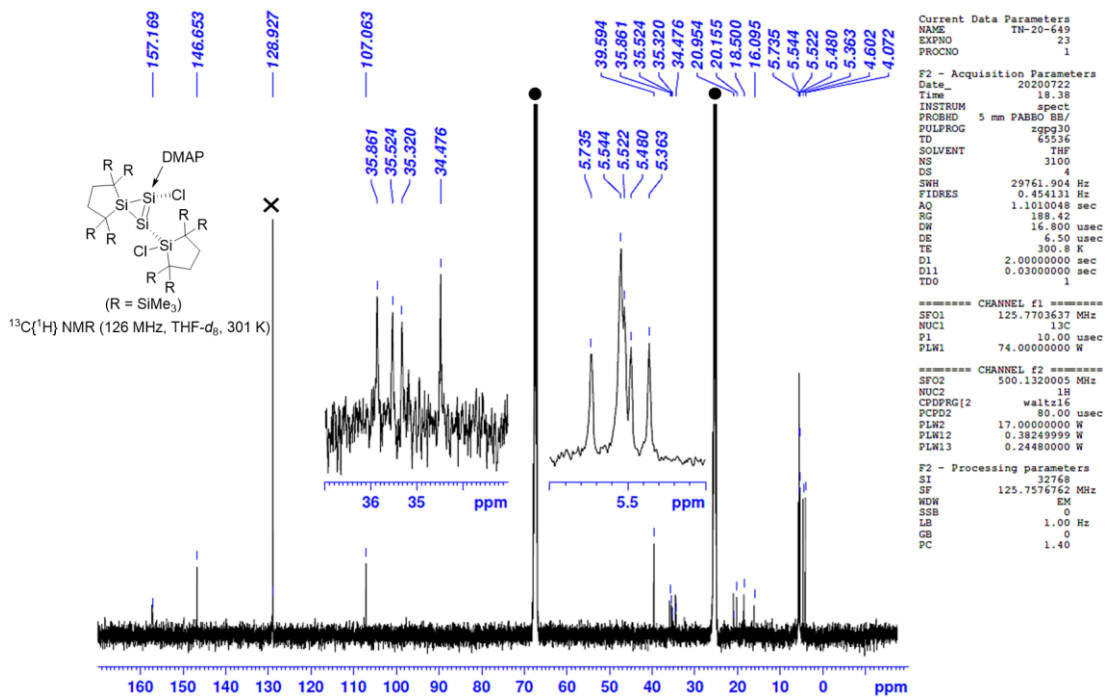


Figure 4-18. $^{13}\text{C}\{^1\text{H}\}$ NMR spectrum of $7 \cdot (\text{benzene})_2$ in $\text{THF-}d_8$ in 301 K ($\bullet = \text{THF-}d_8$, $\times = \text{benzene}$).

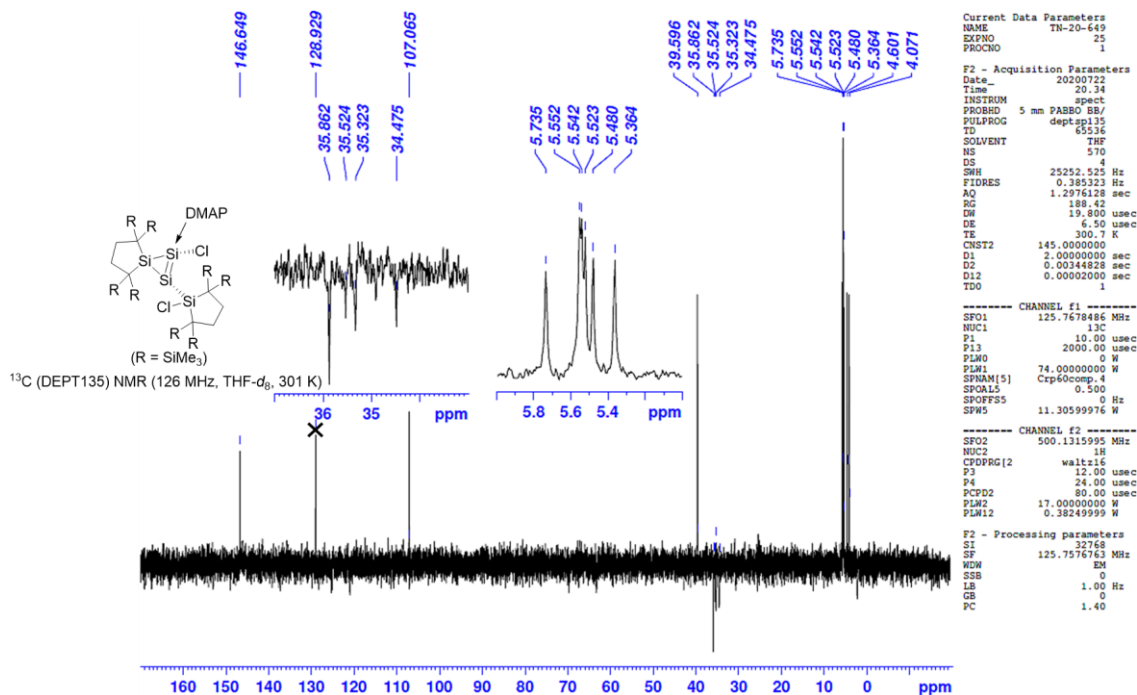


Figure 4-19. ^{13}C (DEPT135) NMR spectrum of $7 \cdot (\text{benzene})_2$ in $\text{THF-}d_8$ at 301 K ($\times = \text{benzene}$).

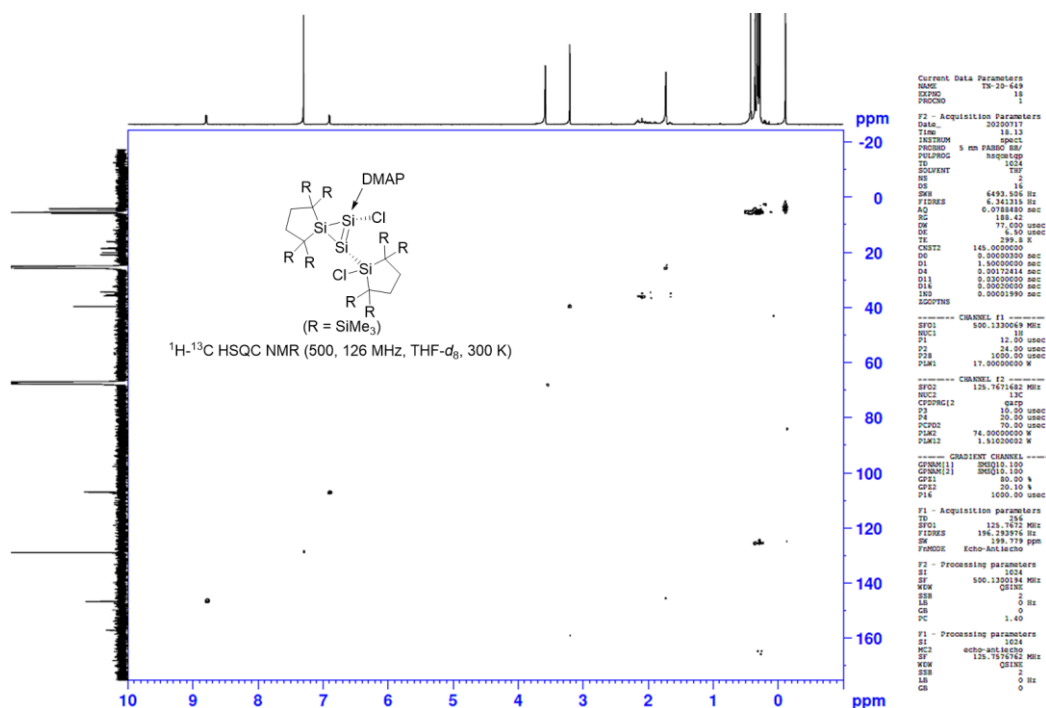


Figure 4-20. ^1H - ^{13}C HSQC NMR spectrum of $7 \cdot (\text{benzene})_2$ in THF-d_8 at 300 K.

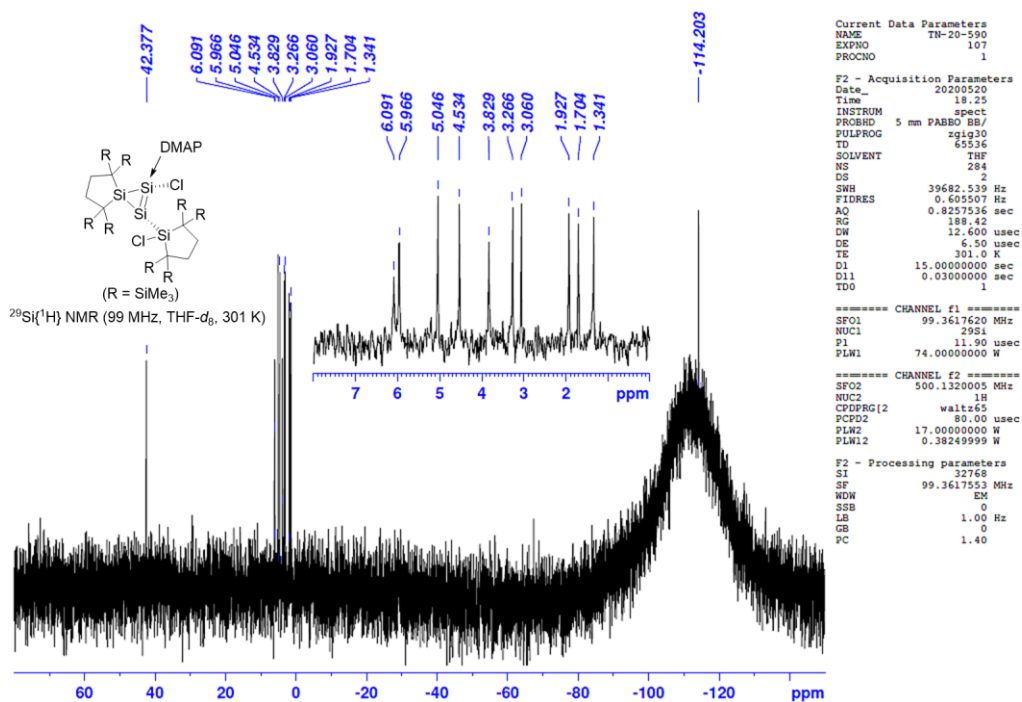


Figure 4-21. $^{29}\text{Si}\{^1\text{H}\}$ NMR spectrum of $7 \cdot (\text{benzene})_2$ in THF-d_8 at 301 K.

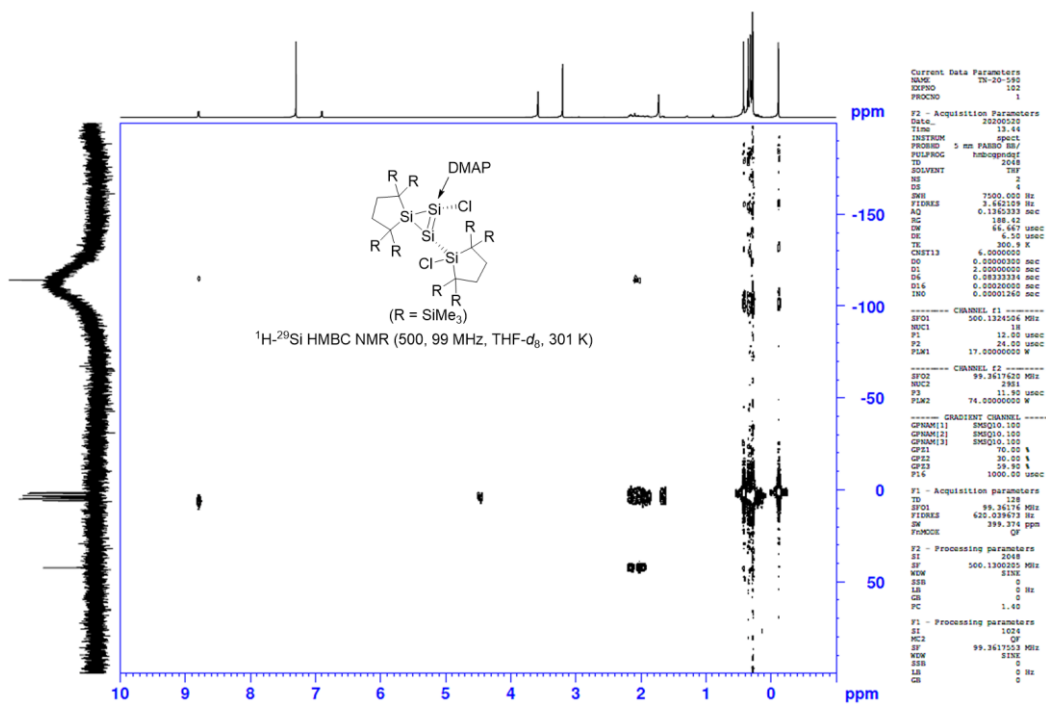


Figure 4-22. ^1H - ^{29}Si HMBC NMR spectrum of **7**·(benzene)₂ in THF- d_8 at 301 K.

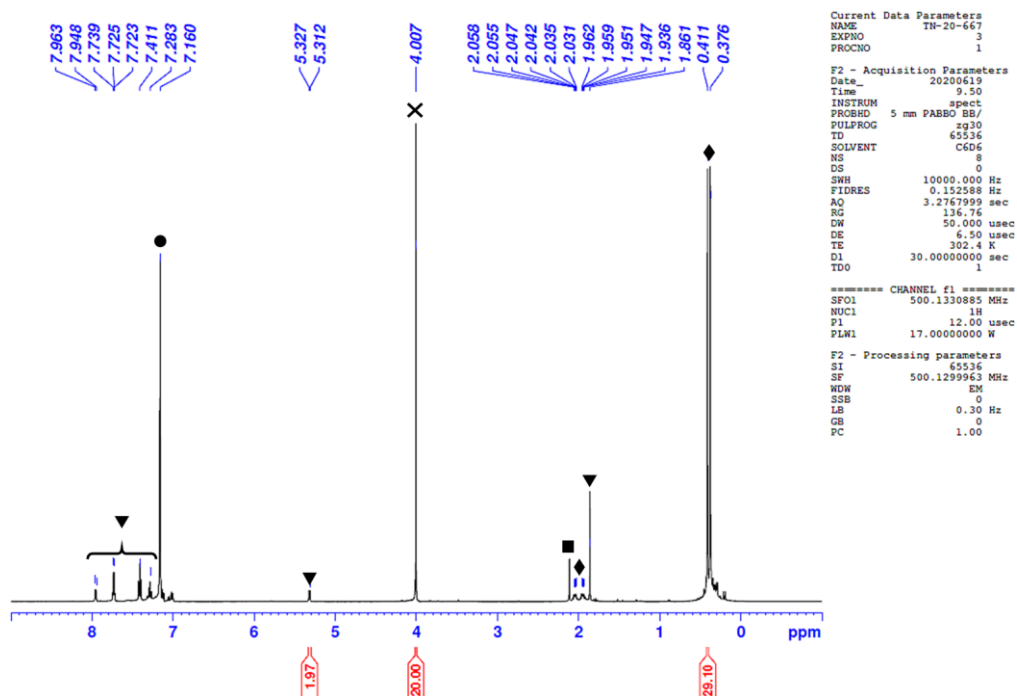


Figure 4-23. ^1H NMR spectrum of the reaction mixture of **7** with CCl_4 in the presence of BPh_3 in C_6D_6 at 302 K (\bullet = C_6HD_5 , \blacktriangledown = $\text{BPh}_3\cdot\text{DMAP}$, \blacklozenge = **3**, \times = ferrocene, \blacksquare = toluene).

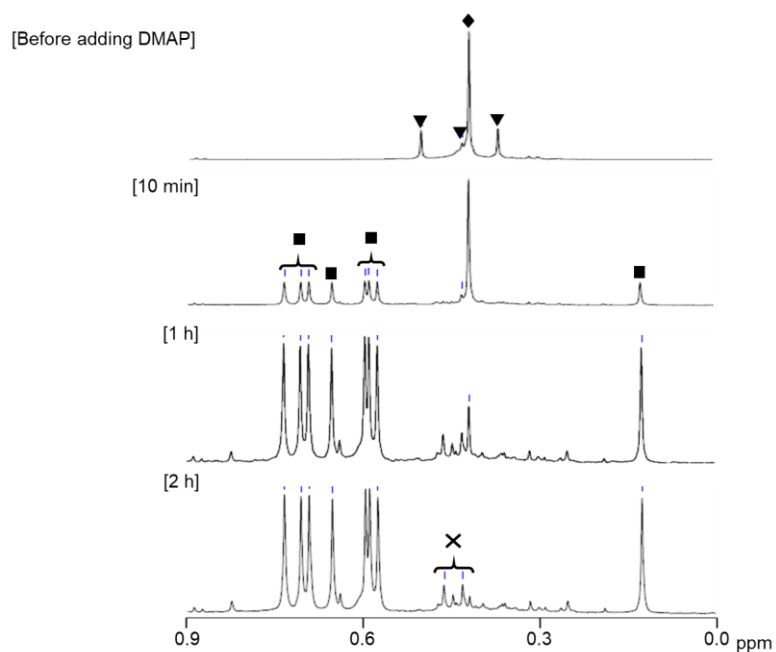


Figure 4-24. ^1H NMR spectra (SiMe_3 region) of the reaction mixture of **4+6** with DMAP in C_6D_6 at room temperature ($\blacklozenge = \mathbf{4}$, $\blacktriangledown = \mathbf{6}$, $\blacksquare = \mathbf{7}$, $\times =$ by products). [TN579]

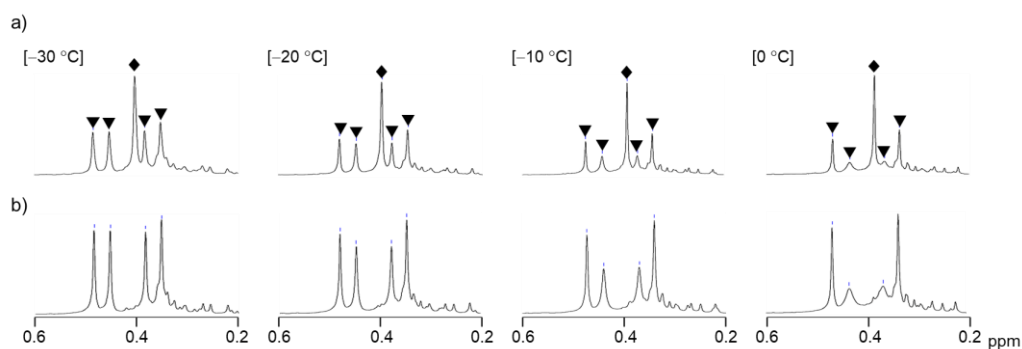


Figure 4-25. ^1H NMR spectra (SiMe_3 region) of a) the equilibrium mixture of **4+6** and b) the reaction mixture of **7** with BPh_3 in $\text{toluene-}d_8$ at variable temperature ($\blacklozenge = \mathbf{4}$, $\blacktriangledown = \mathbf{6}$).

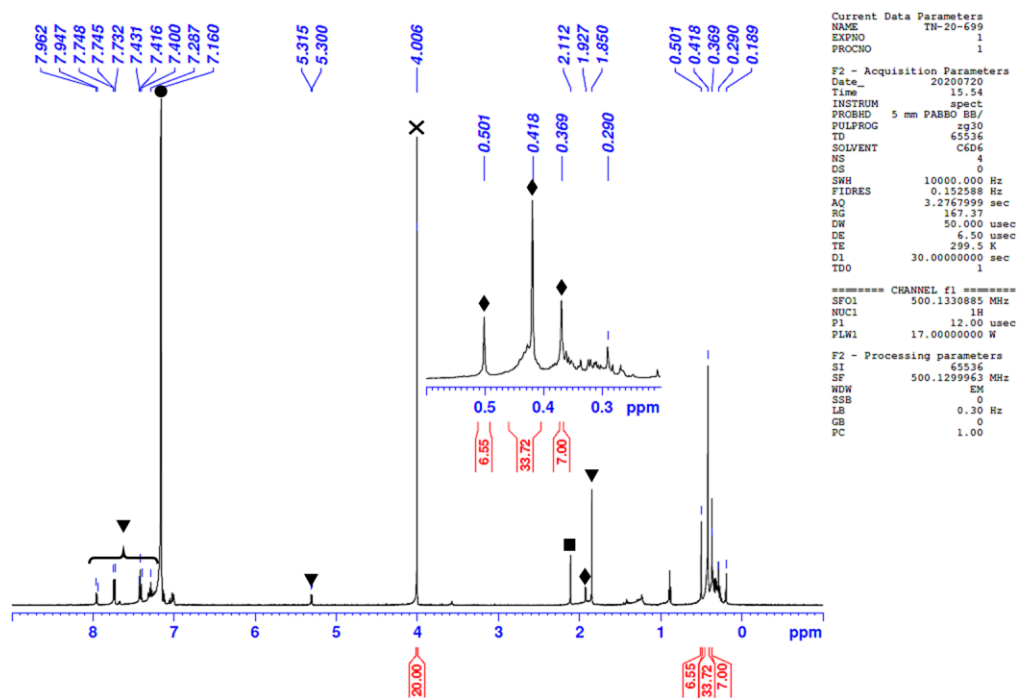


Figure 4-26. ^1H NMR spectrum of the reaction mixture of **7** with BPh_3 in C_6D_6 at 300 K (● = C_6HD_5 , ▼ = $\text{BPh}_3 \cdot \text{DMAP}$, ◆ = **4**+**6**, × = ferrocene, ■ = toluene).

X-ray Diffraction Analysis

Single crystals suitable for the X-ray diffraction study were obtained by recrystallization in an inert atmosphere under the following conditions; from toluene at $-35\text{ }^\circ\text{C}$ for **4** and from benzene at room temperature for **7**. For data collection, the single crystals coated with Apiezon grease were mounted on the glass fibre and then transferred to the cold nitrogen gas stream of the diffractometer. X-ray diffraction data were collected using a Bruker AXS APEX II CCD diffractometer using a graphite monochromated $\text{Mo-K}\alpha$ radiation. An empirical absorption correction based on the multiple measurements of equivalent reflections was applied using the program SADABS²⁷ and the structures were solved by direct methods and refined by full-matrix least squares against F^2 using all data (SHELXL-2014/7).²⁸ The molecular structure was analysed by using the Yadokari-XG software.²⁹

Crystal data of **4** (100 K) [CCDC-2032837]: $\text{C}_{32}\text{H}_{80}\text{Si}_{12}\text{Cl}_2$; Fw 872.91; monoclinic; space group $P2_1/n$, $a = 11.4596(9)\text{ \AA}$, $b = 17.1621(13)\text{ \AA}$, $c = 13.4942(10)\text{ \AA}$, $\beta = 112.624(2)^\circ$, $V = 2449.7(3)\text{ \AA}^3$, $Z = 2$, $D_{\text{calc}} = 1.183\text{ Mg m}^{-3}$, $R1 = 0.0661$ ($I > 2\sigma(I)$), $wR_2 = 0.1657$ (all data), GOF = 1.079.

Crystal data of **7** (100 K) [CCDC-2032838]: $C_{39}H_{90}Si_{12}Cl_2N_2$; Fw 995.08; triclinic; space group $P-1$, $a = 13.5086(3)$ Å, $b = 15.0599(4)$ Å, $c = 16.6833(4)$ Å, $\alpha = 89.3640(10)^\circ$, $\beta = 85.2090(10)^\circ$, $\gamma = 76.7430(10)^\circ$, $V = 3291.92(14)$ Å³, $Z = 2$, $D_{\text{calc}} = 1.162$ Mg m⁻³, $R1 = 0.0356$ ($I > 2\sigma(I)$), $wR2 = 0.0887$ (all data), GOF = 1.015.

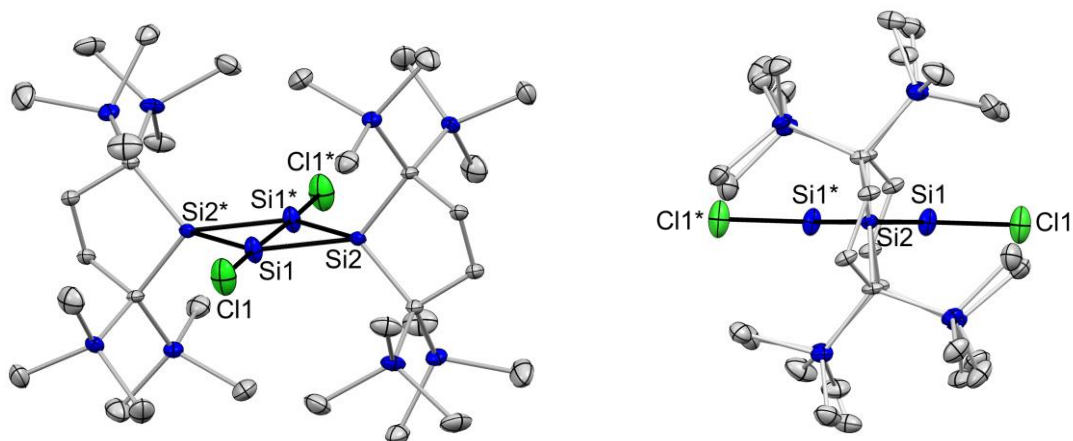


Figure 4-27. ORTEPs of **4**. Thermal ellipsoids are shown at the 50% probability level. Hydrogen atoms were omitted for clarity.

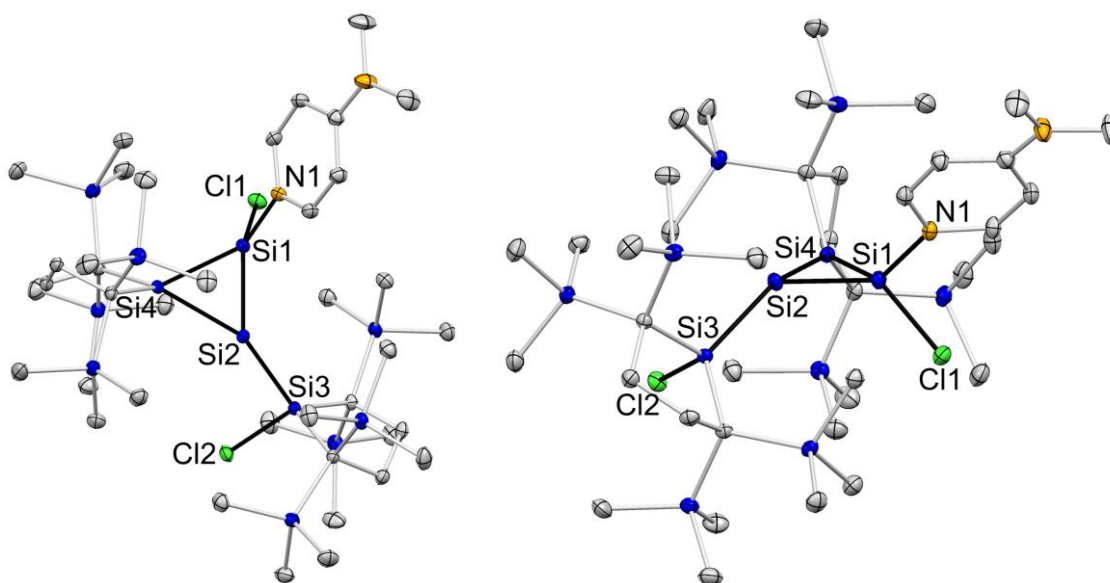


Figure 4-28. ORTEPs of **7**. Thermal ellipsoids are shown at the 50% probability level. Hydrogen atoms were omitted for clarity.

UV-vis Absorption Spectrum

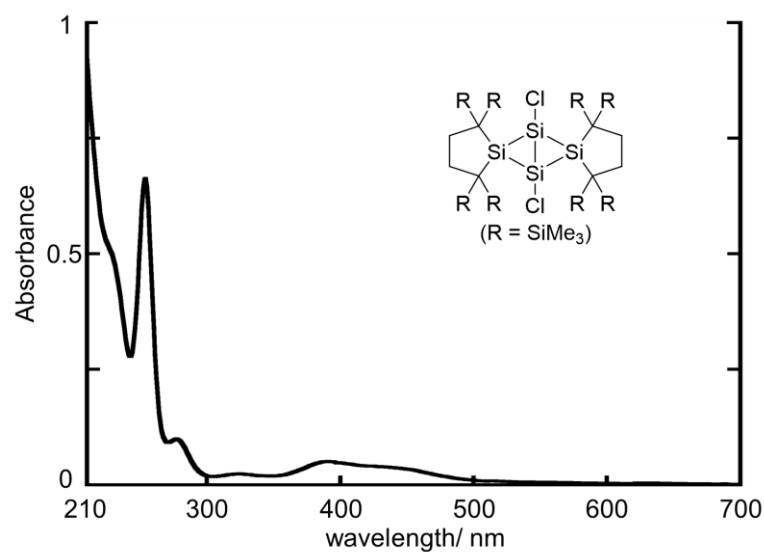


Figure 4-29. UV-vis absorption spectrum of the equilibrium mixture of **4** and **6** in hexane at room temperature.

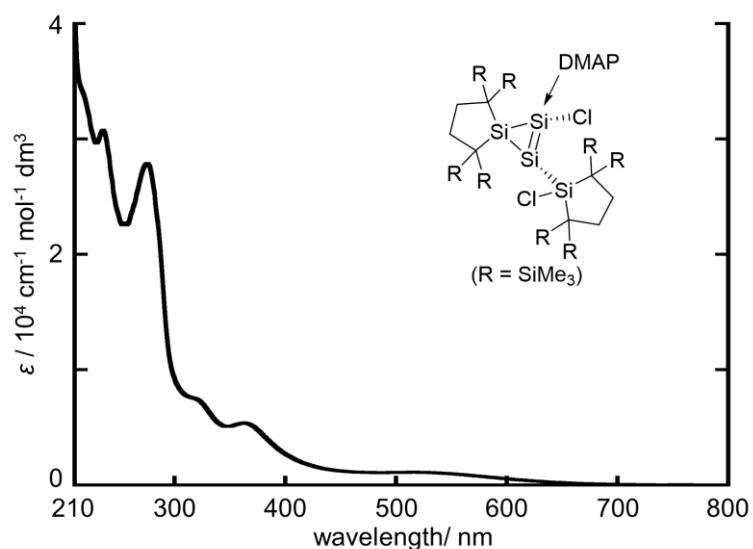


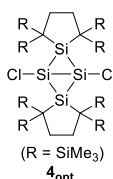
Figure 4-30. UV-vis absorption spectrum of **7**·(benzene)₂ dissolved in hexane at room temperature.

Computational Study

All theoretical calculations were performed using the Gaussian 09³⁰ program or GRRM14³¹ program. Geometry optimization and frequency analyses were carried out at the B3LYP-D3/6-311G(d) level of theory. The atomic coordinates and energies of all equilibrium

and transition structures are summarized in Tables 4-2 to 4-18. Frontier Kohn-Sham orbitals and their energy levels of $\mathbf{4}_{\text{opt}}$ were shown in Figure 4-31. Isotropic chemical shielding tensors were calculated at the GIAO/M06L/6-311+G(2df,p) level of theory (Tables 4-19 and 4-20). Absolute isotropic shielding tensors of the ^{29}Si nucleus in tetramethylsilane were calculated to be 361.4. Excitation energies and oscillator strengths of $\mathbf{4}_{\text{opt}}$ and $\mathbf{6}_{\text{opt}}$ were calculated at the B3LYP-D3/6-311G(d) level of theory (Tables 4-21 and 4-22). A possible reaction route between $\mathbf{4}_{\text{opt}}$ and $\mathbf{6}_{\text{opt}}$ calculated at the B3LYP-D3/B1 (basis B1: 6-311G(d) [core Si_4Cl_2], 6-31G(d) [carbon atoms in silacyclopentane rings], 3-21G* [others]) were shown in Figure 4-33. As for the isomerisation of $\mathbf{4}$ to $\mathbf{6}$, the molecular geometries for the transition states were initially estimated by using the Reaction Plus software package,³² based on the nudged elastic band (NEB) method³³ and subsequently optimized and confirmed by IRC calculations³⁴ at the B3LYP-D3/B1 level of theory (B1: 6-311G(d) [Si_4Cl_2 core], 6-31G(d) [C atoms in silacyclopentane rings], and 3-21G* [other atoms]) using the GRRM14 software package. The natural atomic orbital charges of $\mathbf{8}_{\text{opt}}$ were calculated using the NBO 7.0 program.³⁵

Table 4-2. Atomic Coordinates of $\mathbf{4}_{\text{opt}}$ at the B3LYP-D3/6-311G(d) Level of Theory



| | | | |
|----|----------------|-----------------|-----------------|
| C | 1.426807887036 | 11.201865509537 | 2.818608149815 |
| H | 1.568782253017 | 10.634781909698 | 1.897894621052 |
| H | 0.663718426835 | 11.947924493552 | 2.576525227454 |
| C | 2.751076658847 | 11.909397679427 | 3.157541714619 |
| H | 2.561477392233 | 12.667205464900 | 3.918248842096 |
| H | 3.110679189379 | 12.454635159167 | 2.280220364728 |
| C | 3.808663177770 | 10.875397517517 | 3.675341736931 |
| C | 4.470173436127 | 13.022507291603 | 5.903479515832 |
| H | 3.931804794265 | 12.541327054486 | 6.720071071040 |
| H | 3.809988754445 | 13.773659095460 | 5.464386559865 |
| H | 5.309394816154 | 13.562265542047 | 6.355439252356 |
| C | 6.225486720326 | 12.892903111339 | 3.478090923984 |
| H | 5.615112261950 | 13.593062959674 | 2.900700520259 |
| H | 6.832305145779 | 12.318462962687 | 2.774856300091 |
| H | 6.914195799795 | 13.491020536630 | 4.084111674584 |
| C | 4.834935593968 | 11.200836094816 | 0.733485615226 |
| H | 5.329039978555 | 12.127551819783 | 1.024322716649 |
| H | 3.888103986504 | 11.465114526687 | 0.252974824265 |
| H | 5.455155328293 | 10.724786875721 | -0.033504845141 |
| C | 6.364854010166 | 10.683849637464 | 5.572704948949 |
| H | 6.931748960697 | 11.275215886608 | 6.297989388132 |
| H | 7.084081297213 | 10.180772368588 | 4.926340074083 |
| H | 5.827841449947 | 9.915350393413 | 6.128123240450 |
| C | 6.208726387906 | 9.112607056678 | 2.529110189106 |
| H | 6.145862171524 | 8.446154353266 | 3.391533477857 |
| H | 7.029049028631 | 9.811954069800 | 2.702885376935 |
| H | 6.486891779970 | 8.494491235146 | 1.669365789719 |
| C | 3.495665447539 | 8.620858822133 | 1.352587309837 |
| H | 3.971885088756 | 8.350406969511 | 0.403446504072 |
| H | 2.478613764875 | 8.936340348336 | 1.116587195387 |
| H | 3.444546485351 | 7.710414287994 | 1.945778628216 |
| Si | 2.842048860624 | 9.512868299981 | 7.072936458170 |
| Si | 3.597727425359 | 7.411719720588 | 7.696092344986 |
| H | 6.441575762617 | 8.320438198319 | 9.160905967666 |
| Si | 6.389181694877 | 5.809973658349 | 7.284996313214 |
| Si | 1.701497906603 | 7.199403452519 | 10.311925983138 |
| Si | 1.085182310855 | 5.346582287856 | 7.820081340423 |
| Cl | 2.322493225973 | 11.046854694980 | 8.424200027657 |
| Cl | 6.988430605761 | 6.753570497690 | 5.755231891643 |
| H | 6.475685509483 | 7.706132908197 | 5.617534741944 |
| H | 8.056635538306 | 6.972329240143 | 5.814308937147 |
| H | 6.816321039996 | 6.161736366626 | 4.853956867892 |
| C | 5.524390458292 | 4.235279247996 | 6.696668298306 |
| H | 5.359091492045 | 3.527457249373 | 7.513013874187 |

| Atom | X | Y | Z |
|------|-----------------|-----------------|----------------|
| Si | 3.426576512558 | 7.649231326746 | 5.382876149481 |
| Si | 2.670897947823 | 9.750379906139 | 4.759720262665 |
| Si | -0.172950389434 | 8.841661428408 | 3.294906639985 |
| Si | -0.120556321694 | 11.352125968377 | 5.170816294436 |
| Si | 4.567127466580 | 9.962696174208 | 2.143886624513 |
| Si | 5.183443062327 | 11.815517338871 | 4.635731267228 |
| Cl | 3.946132147209 | 6.115244931738 | 4.031612579994 |
| C | -0.719805232579 | 10.408529129037 | 6.700580716008 |
| H | -0.207060136301 | 9.455966718530 | 6.838277865706 |
| H | -1.788010165124 | 10.189770386584 | 6.641503670504 |
| H | -0.547695666813 | 11.000363260100 | 7.601855739759 |
| C | 0.744234914891 | 12.926820378730 | 5.759144309345 |
| H | 0.909533881137 | 13.634642377354 | 4.942798733464 |
| H | 1.692221527672 | 12.760106475183 | 6.265780597930 |
| H | 0.083264275169 | 13.420640089275 | 6.479983088906 |
| C | -1.616801156252 | 12.031484250657 | 4.217106844344 |
| H | -2.288617300308 | 12.521832752917 | 4.930107565397 |
| H | -2.204578539896 | 11.287808443309 | 3.678750197084 |
| H | -1.314530916336 | 12.795804761161 | 3.495531016284 |
| C | -0.779016765515 | 9.361594487883 | 1.576063433248 |
| H | 0.003088947335 | 9.313134682954 | 0.813871485995 |
| H | -1.187894598291 | 10.375059406404 | 1.563965953397 |
| H | -1.576789097529 | 8.682136875659 | 1.259549679371 |
| C | -1.737282562733 | 8.463369411378 | 4.297350795623 |
| H | -2.251223349263 | 7.651800298489 | 3.770266564035 |
| H | -2.445124558606 | 9.288364015823 | 4.376720067564 |
| H | -1.528690711248 | 8.103049735190 | 5.303274023648 |
| C | 0.628998502667 | 7.143254062206 | 3.110714355304 |
| H | 0.845417416562 | 6.673511962364 | 4.071765393004 |
| H | 1.540345362062 | 7.128984012606 | 2.518246847896 |
| H | -0.094930751026 | 6.495849201852 | 2.603805845655 |
| C | 0.958461060517 | 10.260288422906 | 3.995061032128 |

Table with 4 columns: element symbol, x, y, z coordinates for atoms H, C, and Si.

Table with 4 columns: element symbol, x, y, z coordinates for atoms H, C, and Si.

E+ZPVE = -5644.583830 au, Free E (298.15 K) = -5644.682819 au.
Job name: ti554MIN23G7TS5FE

Table 4-12. Atomic Coordinates of 4'opt at the B3LYP-D3/B1 Level of Theory

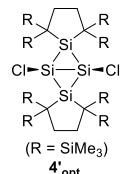


Table with 4 columns: Atom, X, Y, Z coordinates for atoms Si, C, and H.

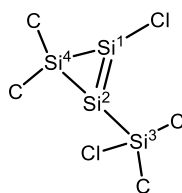
Table with 4 columns: Atom, X, Y, Z coordinates for atoms C, H, and Si.

E+ZPVE = -5644.575026 au, Free E (298.15 K) = -5644.675560 au.
Job name: ti554MIN23G7TS4FE

Table 4-19. Experimental and Theoretical Isotropic ^{29}Si Chemical Shifts of **4**, **4_{opt}**, **4'_{opt}** and **4''_{opt}**

| Compound | SiMe ₃ | Si (bridge) | Si (bridgehead) | note |
|--|--------------------------|---------------|-----------------|--------------|
| 4^a | 4.6 | -7.9 | 126.4 | TN420_7 |
| 4_{opt}^{b,c} | 5.0 (356.4) ^d | -17.1 (378.5) | 150.2 (211.2) | nmr2_TN74a |
| 4'_{opt}^{b,c} | 5.3 (356.1) ^d | 139.5 (221.9) | -37.1 (398.3) | nmr2_TN77_12 |
| | | 137.1 (224.3) | -49.9 (411.3) | 0 |
| 4''_{opt}^{b,c} | 4.8 (356.6) ^d | -25.1 (386.5) | 86.5 (274.8) | nmr_TN84a |

^aExperimental ^{29}Si Chemical Shifts of **4** in benzene-*d*₆ at 333 K. ^bGIAO/M06L/6-311+G(2df,p) level of theory. Absolute chemical shift for tetramethylsilane = 361.4. ^cThe absolute chemical shift is shown in the parentheses. ^dAverage values.

Table 4-20. Experimental and Theoretical Isotropic ^{29}Si Chemical Shifts of **6_{opt}**

| | SiMe ₃ | Si ² =Si ¹ -Cl | Si ² =Si ¹ -Cl | Si ⁴ (Si ₃ ring) | Si ³ (chlorosilyl) | Note |
|----------------------------|--------------------------|--------------------------------------|--------------------------------------|--|-------------------------------|------------|
| Experimental ^a | 2.9, 3.3, 6.1 | 104.1 | 48.7 | 78.2 | 32.9 | TN420_7 |
| Theoretical ^{b,c} | 4.2 (357.2) ^d | 97.0 (264.4) | 49.4 (311.9) | 75.4 (286.0) | 38.1 (323.3) | nmr2_TN82a |

^aExperimental ^{29}Si Chemical Shifts of **6** in benzene-*d*₆ at 333 K. ^bGIAO/M06L/6-311+G(2df,p) level of theory. Absolute chemical shift for tetramethylsilane = 361.4. ^cThe absolute chemical shift is shown in the parentheses. ^dAverage values.

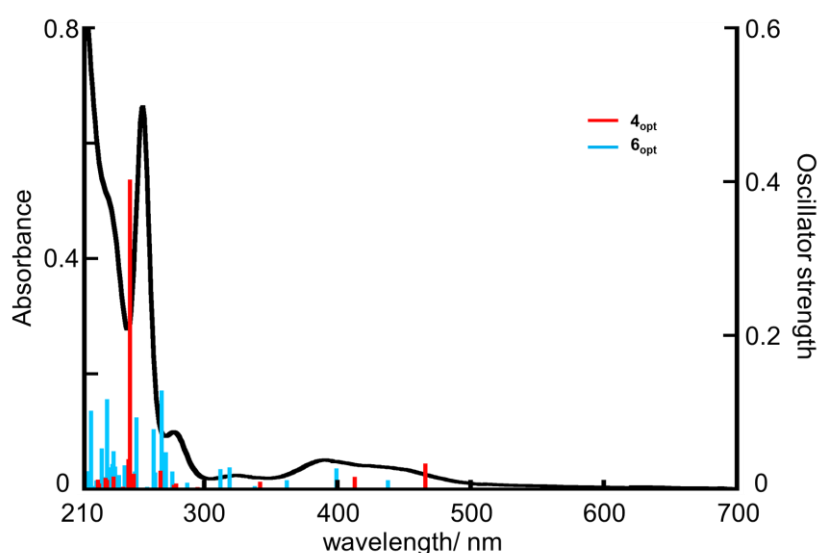
**Figure 4-32.** Experimental UV-vis absorption spectrum of the equilibrium mixture of **4** and **6** in hexane (black) and calculated band positions of **4_{opt}** and **6_{opt}** at the TD-B3LYP-D3/6-311G(d) level of theory (red and light blue).

Table 4-21. Transition Energy, Wavelength, and Oscillator Strengths of the Electronic Transition of 4_{opt} (The 237th orbital is highest occupied orbital shown in Figure 4-31)

| | | | | | | |
|---|--|-----------|-----------|----------|--------------------------|---------------------|
| Excited State 1: <S**2>=0.000 | Singlet-AU | 2.6596 eV | 466.17 nm | f=0.0332 | 226 -> 238 227 -> 238 | -0.10228 0.68694 |
| 237 -> 238 237 -> 239 | 0.67896 -0.17174 | | | | | |
| This state for optimization and/or second-order correction. | | | | | | |
| Total Energy, E(TD-HF/TD-KS) = -5662.97431013 | | | | | | |
| Copying the excited state density for this state as the 1-particle RhoCI density. | | | | | | |
| Excited State 2: <S**2>=0.000 | Singlet-AG | 2.8801 eV | 430.48 nm | f=0.0000 | | |
| 236 -> 238 | 0.70504 | | | | | |
| Excited State 3: <S**2>=0.000 | Singlet-AU | 3.0056 eV | 412.51 nm | f=0.0162 | | |
| 237 -> 238 237 -> 239 | 0.16949 0.67597 | | | | | |
| Excited State 4: <S**2>=0.000 | Singlet-AU | 3.6254 eV | 341.99 nm | f=0.0096 | | |
| 237 -> 240 | 0.68769 | | | | | |
| Excited State 5: <S**2>=0.000 | Singlet-AG | 3.7152 eV | 333.72 nm | f=0.0000 | | |
| 237 -> 241 | 0.70481 | | | | | |
| Excited State 6: <S**2>=0.000 | Singlet-AG | 3.8746 eV | 319.99 nm | f=0.0000 | | |
| 236 -> 239 | 0.69880 | | | | | |
| Excited State 7: <S**2>=0.000 | Singlet-AG | 4.1861 eV | 296.18 nm | f=0.0000 | | |
| 233 -> 238 235 -> 238 | -0.11200 0.69584 | | | | | |
| Excited State 8: <S**2>=0.000 | Singlet-AU | 4.1991 eV | 295.26 nm | f=0.0026 | | |
| 234 -> 238 | 0.70535 | | | | | |
| Excited State 9: <S**2>=0.000 | Singlet-AG | 4.2735 eV | 290.12 nm | f=0.0000 | | |
| 233 -> 238 235 -> 238 236 -> 240 | 0.68739 0.11840 -0.10203 | | | | | |
| Excited State 10: <S**2>=0.000 | Singlet-AU | 4.3196 eV | 287.03 nm | f=0.0013 | | |
| 230 -> 238 231 -> 238 232 -> 238 | -0.35899 0.19538 0.56102 | | | | | |
| Excited State 11: <S**2>=0.000 | Singlet-AU | 4.4516 eV | 278.52 nm | f=0.0074 | | |
| 230 -> 238 231 -> 238 232 -> 238 | -0.30886 0.49899 -0.37371 | | | | | |
| Excited State 12: <S**2>=0.000 | Singlet-AU | 4.4717 eV | 277.27 nm | f=0.0059 | | |
| 230 -> 238 231 -> 238 232 -> 238 | 0.50949 0.44481 0.17234 | | | | | |
| Excited State 13: <S**2>=0.000 | Singlet-AG | 4.5559 eV | 272.14 nm | f=0.0000 | | |
| 229 -> 238 233 -> 238 236 -> 240 | 0.10870 0.10925 0.67874 | | | | | |
| Excited State 14: <S**2>=0.000 | Singlet-AU | 4.6516 eV | 266.54 nm | f=0.0240 | | |
| 236 -> 241 237 -> 242 | 0.55902 -0.42495 | | | | | |
| Excited State 15: <S**2>=0.000 | Singlet-AG | 4.6548 eV | 266.36 nm | f=0.0000 | | |
| 229 -> 238 236 -> 240 | 0.69462 -0.11101 | | | | | |
| Excited State 16: <S**2>=0.000 | Singlet-AU | 4.9319 eV | 251.39 nm | f=0.0005 | | |
| 228 -> 238 | 0.68938 | | | | | |
| Excited State 17: <S**2>=0.000 | Singlet-AG | 4.9464 eV | 250.65 nm | f=0.0000 | | |
| | | | | | | |
| Excited State 18: <S**2>=0.000 | Singlet-AU | 5.0255 eV | 246.71 nm | f=0.0202 | | |
| 223 -> 238 225 -> 238 237 -> 242 | 0.40022 0.52671 0.11984 | | | | | |
| Excited State 19: <S**2>=0.000 | Singlet-AG | 5.0351 eV | 246.24 nm | f=0.0000 | | |
| 224 -> 238 226 -> 238 | -0.18600 0.66703 | | | | | |
| Excited State 20: <S**2>=0.000 | Singlet-AU | 5.0715 eV | 244.47 nm | f=0.4028 | | |
| 225 -> 238 230 -> 240 236 -> 241 237 -> 242 | -0.25689 -0.16019 0.36213 0.48343 | | | | | |
| Excited State 21: <S**2>=0.000 | Singlet-AU | 5.0853 eV | 243.81 nm | f=0.0392 | | |
| 219 -> 238 223 -> 238 225 -> 238 236 -> 241 237 -> 242 | 0.15226 0.50704 -0.37875 -0.11926 -0.16915 | | | | | |
| Excited State 22: <S**2>=0.000 | Singlet-AG | 5.1078 eV | 242.74 nm | f=0.0000 | | |
| 218 -> 238 221 -> 238 224 -> 238 226 -> 238 | -0.10510 -0.11859 0.66031 0.16395 | | | | | |
| Excited State 23: <S**2>=0.000 | Singlet-AG | 5.1488 eV | 240.80 nm | f=0.0000 | | |
| 235 -> 239 | 0.69109 | | | | | |
| Excited State 24: <S**2>=0.000 | Singlet-AU | 5.1605 eV | 240.26 nm | f=0.0005 | | |
| 219 -> 238 234 -> 239 | -0.10107 0.69475 | | | | | |
| Excited State 25: <S**2>=0.000 | Singlet-AG | 5.1750 eV | 239.58 nm | f=0.0000 | | |
| 218 -> 238 220 -> 238 221 -> 238 226 -> 238 | -0.19745 -0.16010 0.64258 0.12372 | | | | | |
| Excited State 26: <S**2>=0.000 | Singlet-AU | 5.1898 eV | 238.90 nm | f=0.0031 | | |
| 219 -> 238 222 -> 238 | 0.56210 -0.37669 | | | | | |
| Excited State 27: <S**2>=0.000 | Singlet-AU | 5.1938 eV | 238.72 nm | f=0.0022 | | |
| 219 -> 238 222 -> 238 223 -> 238 | 0.33384 0.56757 -0.20751 | | | | | |
| Excited State 28: <S**2>=0.000 | Singlet-AG | 5.2111 eV | 237.93 nm | f=0.0000 | | |
| 218 -> 238 220 -> 238 221 -> 238 233 -> 239 | 0.35523 0.52265 0.23219 0.10324 | | | | | |
| Excited State 29: <S**2>=0.000 | Singlet-AG | 5.2177 eV | 237.62 nm | f=0.0000 | | |
| 220 -> 238 233 -> 239 235 -> 239 237 -> 244 237 -> 245 237 -> 246 | -0.12864 0.42332 0.13669 -0.39387 -0.29668 -0.16483 | | | | | |
| Excited State 30: <S**2>=0.000 | Singlet-AU | 5.2547 eV | 235.95 nm | f=0.0003 | | |
| 216 -> 238 217 -> 238 | 0.50300 -0.45883 | | | | | |

| | | | | | | |
|-----------------------------------|------------|-----------|-----------|----------|-----------------------------------|----------------------|
| Excited State 31: <S**2>=0.000 | Singlet-AG | 5.2555 eV | 235.91 nm | f=0.0000 | 219 -> 238 237 -> 247 | -0.10541 -0.22362 |
| 218 -> 238 | 0.48456 | | | | | |
| 220 -> 238 | -0.35848 | | | | Excited State 40: <S**2>=0.000 | Singlet-AG |
| 233 -> 239 | 0.26227 | | | | 5.5714 eV | 222.54 nm |
| 237 -> 244 | 0.17618 | | | | f=0.0000 | |
| 237 -> 245 | 0.12631 | | | | 237 -> 244 | -0.44605 |
| | | | | | 237 -> 245 | 0.46699 |
| | | | | | 237 -> 246 | 0.22863 |
| Excited State 32: <S**2>=0.000 | Singlet-AG | 5.2592 eV | 235.75 nm | f=0.0000 | 237 -> 251 | -0.11452 |
| 218 -> 238 | -0.27171 | | | | Excited State 41: <S**2>=0.000 | Singlet-AG |
| 220 -> 238 | 0.20680 | | | | 5.5938 eV | 221.65 nm |
| 233 -> 239 | 0.47753 | | | | f=0.0000 | |
| 237 -> 244 | 0.29746 | | | | 229 -> 239 | -0.20244 |
| 237 -> 245 | 0.20868 | | | | 235 -> 240 | 0.40339 |
| 237 -> 246 | 0.11740 | | | | 236 -> 242 | 0.52537 |
| | | | | | Excited State 42: <S**2>=0.000 | Singlet-AU |
| Excited State 33: <S**2>=0.000 | Singlet-AU | 5.3132 eV | 233.35 nm | f=0.0009 | 214 -> 238 | 0.20388 |
| 216 -> 238 | 0.45422 | | | | 234 -> 240 | 0.39718 |
| 217 -> 238 | 0.51970 | | | | 237 -> 247 | 0.49449 |
| | | | | | 237 -> 250 | 0.12358 |
| Excited State 34: <S**2>=0.000 | Singlet-AU | 5.3368 eV | 232.32 nm | f=0.0165 | Excited State 43: <S**2>=0.000 | Singlet-AG |
| 230 -> 239 | -0.28837 | | | | 5.6117 eV | 220.94 nm |
| 232 -> 239 | 0.62008 | | | | f=0.0000 | |
| | | | | | 229 -> 239 | 0.66507 |
| Excited State 35: <S**2>=0.000 | Singlet-AU | 5.3509 eV | 231.71 nm | f=0.0007 | 235 -> 240 | 0.16996 |
| 230 -> 239 | -0.13789 | | | | 236 -> 242 | 0.12094 |
| 231 -> 239 | 0.67966 | | | | Excited State 44: <S**2>=0.000 | Singlet-AU |
| | | | | | 5.6269 eV | 220.34 nm |
| Excited State 36: <S**2>=0.000 | Singlet-AU | 5.4520 eV | 227.41 nm | f=0.0120 | 214 -> 238 | -0.11933 |
| 230 -> 239 | 0.30533 | | | | 234 -> 240 | 0.57325 |
| 232 -> 239 | 0.13337 | | | | 237 -> 247 | -0.36564 |
| 237 -> 243 | 0.60911 | | | | Excited State 45: <S**2>=0.000 | Singlet-AG |
| | | | | | 5.6392 eV | 219.86 nm |
| Excited State 37: <S**2>=0.000 | Singlet-AG | 5.4572 eV | 227.19 nm | f=0.0000 | 235 -> 240 | 0.54533 |
| 215 -> 238 | 0.69902 | | | | 236 -> 242 | -0.43265 |
| | | | | | Excited State 46: <S**2>=0.000 | Singlet-AG |
| Excited State 38: <S**2>=0.000 | Singlet-AU | 5.4674 eV | 226.77 nm | f=0.0147 | 213 -> 238 | 0.69754 |
| 230 -> 239 | 0.53689 | | | | Excited State 47: <S**2>=0.000 | Singlet-AU |
| 231 -> 239 | 0.15871 | | | | 5.7024 eV | 217.43 nm |
| 232 -> 239 | 0.24274 | | | | f=0.0012 | |
| 237 -> 243 | -0.32682 | | | | 212 -> 238 | 0.69660 |
| | | | | | Excited State 48: <S**2>=0.000 | Singlet-AG |
| Excited State 39: <S**2>=0.000 | Singlet-AU | 5.5349 eV | 224.00 nm | f=0.0018 | 233 -> 240 | 5.7406 eV |
| 214 -> 238 | 0.63465 | | | | 234 -> 241 | 215.98 nm |
| | | | | | | f=0.0000 |
| | | | | | | -0.45825 |
| | | | | | | 0.52326 |

Table 4-22. Transition Energy, Wavelength, and Oscillator Strengths of the Electronic Transition of $\mathbf{6}_{opt}$ (The 237th orbital is highest occupied orbital)

| | | | | | | | | | |
|---|-----------|-----------|-----------|----------|----------------------------------|-----------|-----------|-----------|----------|
| Excited State 1: <S**2>=0.000 | Singlet-A | 2.8294 eV | 438.21 nm | f=0.0119 | Excited State 5: <S**2>=0.000 | Singlet-A | 3.8813 eV | 319.44 nm | f=0.0282 |
| 235 -> 238 | -0.10313 | | | | 235 -> 238 | -0.47416 | | | |
| 237 -> 238 | 0.55576 | | | | 236 -> 238 | -0.10104 | | | |
| 237 -> 239 | 0.41018 | | | | 236 -> 239 | 0.49811 | | | |
| This state for optimization and/or second-order correction. | | | | | | | | | |
| Total Energy, E(TD-HF/TD-KS) = -5662.96653789 | | | | | | | | | |
| Copying the excited state density for this state as the 1-particle RhoCI density. | | | | | | | | | |
| Excited State 2: <S**2>=0.000 | Singlet-A | 3.1085 eV | 398.86 nm | f=0.0270 | Excited State 6: <S**2>=0.000 | Singlet-A | 3.9716 eV | 312.17 nm | f=0.0262 |
| 235 -> 239 | 0.10704 | | | | 235 -> 238 | 0.44981 | | | |
| 236 -> 238 | -0.11310 | | | | 235 -> 239 | -0.25459 | | | |
| 237 -> 238 | -0.37316 | | | | 236 -> 239 | 0.39936 | | | |
| 237 -> 239 | 0.55405 | | | | 237 -> 238 | 0.11617 | | | |
| | | | | | 237 -> 240 | 0.17884 | | | |
| Excited State 3: <S**2>=0.000 | Singlet-A | 3.4281 eV | 361.67 nm | f=0.0118 | Excited State 7: <S**2>=0.000 | Singlet-A | 4.3211 eV | 286.92 nm | f=0.0086 |
| 235 -> 238 | -0.12710 | | | | 235 -> 239 | 0.13699 | | | |
| 236 -> 238 | 0.66975 | | | | 237 -> 241 | 0.68537 | | | |
| 237 -> 240 | 0.11911 | | | | Excited State 8: <S**2>=0.000 | Singlet-A | 4.4902 eV | 276.12 nm | f=0.0230 |
| | | | | | 232 -> 238 | -0.11710 | | | |
| Excited State 4: <S**2>=0.000 | Singlet-A | 3.6728 eV | 337.57 nm | f=0.0041 | 235 -> 239 | -0.43612 | | | |
| 236 -> 238 | -0.11450 | | | | 236 -> 240 | 0.48258 | | | |
| 236 -> 239 | -0.21754 | | | | 237 -> 241 | 0.10130 | | | |
| 237 -> 240 | 0.64817 | | | | Excited State 9: <S**2>=0.000 | Singlet-A | 4.5790 eV | 270.77 nm | f=0.0479 |
| | | | | | | | | | |

| | | | | | | | | | |
|-------------------|-----------|-----------|-----------|----------|-------------------|-----------|-----------|-----------|----------|
| 232 -> 238 | 0.12873 | | | | 224 -> 238 | 0.11823 | | | |
| 234 -> 238 | 0.59681 | | | | 226 -> 238 | -0.19520 | | | |
| 235 -> 239 | 0.13107 | | | | 227 -> 238 | 0.20345 | | | |
| 236 -> 240 | 0.28444 | | | | 228 -> 238 | 0.54467 | | | |
| | | | | | 236 -> 241 | -0.25899 | | | |
| Excited State 10: | Singlet-A | 4.6190 eV | 268.42 nm | f=0.1284 | Excited State 23: | Singlet-A | 5.3579 eV | 231.40 nm | f=0.0493 |
| <S**2>=0.000 | | | | | <S**2>=0.000 | | | | |
| 231 -> 238 | -0.15323 | | | | 222 -> 238 | -0.13098 | | | |
| 232 -> 238 | -0.29016 | | | | 226 -> 238 | 0.17550 | | | |
| 234 -> 238 | 0.36315 | | | | 227 -> 238 | -0.33953 | | | |
| 235 -> 239 | -0.27410 | | | | 228 -> 238 | 0.39113 | | | |
| 235 -> 240 | 0.15939 | | | | 230 -> 239 | 0.16730 | | | |
| 236 -> 240 | -0.32784 | | | | 236 -> 241 | 0.30798 | | | |
| 236 -> 241 | -0.11324 | | | | | | | | |
| Excited State 11: | Singlet-A | 4.7169 eV | 262.85 nm | f=0.0219 | Excited State 24: | Singlet-A | 5.3723 eV | 230.78 nm | f=0.0327 |
| <S**2>=0.000 | | | | | <S**2>=0.000 | | | | |
| 232 -> 238 | 0.16718 | | | | 225 -> 238 | 0.24705 | | | |
| 233 -> 238 | 0.65947 | | | | 227 -> 238 | 0.43905 | | | |
| 235 -> 239 | -0.10812 | | | | 230 -> 239 | 0.34197 | | | |
| | | | | | 236 -> 241 | 0.20959 | | | |
| Excited State 12: | Singlet-A | 4.7404 eV | 261.55 nm | f=0.0779 | 237 -> 242 | 0.15964 | | | |
| <S**2>=0.000 | | | | | Excited State 25: | Singlet-A | 5.3798 eV | 230.46 nm | f=0.0175 |
| 232 -> 238 | 0.58426 | | | | <S**2>=0.000 | | | | |
| 233 -> 238 | -0.22881 | | | | 225 -> 238 | -0.24750 | | | |
| 235 -> 239 | -0.20115 | | | | 226 -> 238 | -0.10062 | | | |
| 236 -> 240 | -0.11054 | | | | 227 -> 238 | -0.18094 | | | |
| 236 -> 241 | -0.13784 | | | | 229 -> 239 | -0.11187 | | | |
| Excited State 13: | Singlet-A | 4.8290 eV | 256.75 nm | f=0.0029 | 230 -> 239 | 0.52751 | | | |
| <S**2>=0.000 | | | | | 236 -> 241 | -0.21771 | | | |
| 231 -> 238 | 0.66840 | | | | Excited State 26: | Singlet-A | 5.4182 eV | 228.83 nm | f=0.0225 |
| 235 -> 239 | -0.11868 | | | | <S**2>=0.000 | | | | |
| 236 -> 241 | -0.12109 | | | | 225 -> 238 | 0.44183 | | | |
| Excited State 14: | Singlet-A | 4.9788 eV | 249.02 nm | f=0.0933 | 226 -> 238 | 0.15461 | | | |
| <S**2>=0.000 | | | | | 227 -> 238 | -0.10278 | | | |
| 229 -> 238 | 0.11948 | | | | 230 -> 239 | 0.17462 | | | |
| 230 -> 238 | -0.31436 | | | | 236 -> 241 | -0.15071 | | | |
| 234 -> 239 | -0.14263 | | | | 237 -> 242 | -0.29685 | | | |
| 235 -> 240 | 0.55196 | | | | 237 -> 243 | 0.20069 | | | |
| 236 -> 240 | 0.11793 | | | | 237 -> 245 | -0.13121 | | | |
| 237 -> 243 | 0.10112 | | | | Excited State 27: | Singlet-A | 5.4355 eV | 228.10 nm | f=0.0282 |
| Excited State 15: | Singlet-A | 4.9925 eV | 248.34 nm | f=0.0029 | <S**2>=0.000 | | | | |
| <S**2>=0.000 | | | | | 225 -> 238 | -0.33763 | | | |
| 230 -> 238 | 0.58306 | | | | 226 -> 238 | 0.43156 | | | |
| 234 -> 239 | 0.14760 | | | | 227 -> 238 | 0.28293 | | | |
| 235 -> 240 | 0.31559 | | | | 230 -> 239 | 0.10945 | | | |
| Excited State 16: | Singlet-A | 4.9980 eV | 248.07 nm | f=0.0014 | 237 -> 242 | -0.15740 | | | |
| <S**2>=0.000 | | | | | 237 -> 243 | 0.18101 | | | |
| 230 -> 238 | -0.19593 | | | | 237 -> 244 | -0.10193 | | | |
| 234 -> 239 | 0.67251 | | | | Excited State 28: | Singlet-A | 5.4482 eV | 227.57 nm | f=0.1172 |
| Excited State 17: | Singlet-A | 5.0894 eV | 243.61 nm | f=0.0030 | <S**2>=0.000 | | | | |
| <S**2>=0.000 | | | | | 225 -> 238 | 0.12299 | | | |
| 229 -> 238 | 0.11075 | | | | 226 -> 238 | 0.40380 | | | |
| 233 -> 239 | 0.68518 | | | | 229 -> 239 | -0.21172 | | | |
| Excited State 18: | Singlet-A | 5.1050 eV | 242.87 nm | f=0.0006 | 236 -> 241 | -0.17410 | | | |
| <S**2>=0.000 | | | | | 237 -> 242 | 0.20221 | | | |
| 229 -> 238 | 0.59390 | | | | 237 -> 243 | -0.30213 | | | |
| 230 -> 238 | 0.11099 | | | | 237 -> 244 | 0.19641 | | | |
| 232 -> 239 | -0.32523 | | | | Excited State 29: | Singlet-A | 5.4948 eV | 225.64 nm | f=0.0120 |
| Excited State 19: | Singlet-A | 5.1132 eV | 242.48 nm | f=0.0027 | <S**2>=0.000 | | | | |
| <S**2>=0.000 | | | | | 223 -> 238 | 0.26757 | | | |
| 229 -> 238 | 0.31238 | | | | 229 -> 239 | 0.57807 | | | |
| 232 -> 239 | 0.61292 | | | | 234 -> 240 | 0.18565 | | | |
| Excited State 20: | Singlet-A | 5.1707 eV | 239.78 nm | f=0.0312 | 237 -> 243 | -0.10711 | | | |
| <S**2>=0.000 | | | | | Excited State 30: | Singlet-A | 5.5149 eV | 224.82 nm | f=0.0159 |
| 231 -> 239 | 0.67103 | | | | <S**2>=0.000 | | | | |
| 236 -> 241 | 0.15682 | | | | 222 -> 238 | -0.18300 | | | |
| Excited State 21: | Singlet-A | 5.2568 eV | 235.85 nm | f=0.0182 | 223 -> 238 | 0.44787 | | | |
| <S**2>=0.000 | | | | | 224 -> 238 | 0.38222 | | | |
| 236 -> 241 | -0.17062 | | | | 226 -> 238 | -0.11551 | | | |
| 237 -> 242 | 0.42620 | | | | 228 -> 238 | -0.11574 | | | |
| 237 -> 243 | 0.40154 | | | | 229 -> 239 | -0.15239 | | | |
| 237 -> 244 | -0.14640 | | | | 234 -> 240 | -0.17387 | | | |
| 237 -> 245 | 0.18943 | | | | Excited State 31: | Singlet-A | 5.5304 eV | 224.19 nm | f=0.0152 |
| 237 -> 246 | -0.16629 | | | | <S**2>=0.000 | | | | |
| Excited State 22: | Singlet-A | 5.3215 eV | 232.99 nm | f=0.0294 | 222 -> 238 | -0.10745 | | | |
| <S**2>=0.000 | | | | | 223 -> 238 | -0.36817 | | | |
| | | | | | 224 -> 238 | 0.51736 | | | |
| | | | | | 225 -> 238 | -0.10285 | | | |
| | | | | | 229 -> 239 | 0.10611 | | | |

| | | | | | | | | | | | | | |
|---------------|----------|-----------|-----------|-----------|----------|---------------|----------|-----------|-----------|-----------|----------|--|--|
| 234 -> 240 | 0.13521 | | | | | 219 -> 238 | -0.12278 | | | | | | |
| Excited State | 32: | Singlet-A | 5.5370 eV | 223.92 nm | f=0.0529 | 220 -> 238 | 0.23051 | | | | | | |
| <S**2>=0.000 | | | | | | 233 -> 240 | -0.12144 | | | | | | |
| 223 -> 238 | 0.13264 | | | | | 237 -> 244 | 0.10391 | | | | | | |
| 229 -> 239 | -0.21542 | | | | | 237 -> 246 | -0.12245 | | | | | | |
| 234 -> 240 | 0.62294 | | | | | Excited State | 41: | Singlet-A | 5.7232 eV | 216.63 nm | f=0.0030 | | |
| Excited State | 33: | Singlet-A | 5.5728 eV | 222.48 nm | f=0.0008 | <S**2>=0.000 | | | | | | | |
| <S**2>=0.000 | | | | | | 217 -> 238 | 0.13852 | | | | | | |
| 220 -> 238 | -0.24675 | | | | | 232 -> 240 | -0.19315 | | | | | | |
| 221 -> 238 | 0.50277 | | | | | 233 -> 240 | 0.61481 | | | | | | |
| 222 -> 238 | -0.34434 | | | | | 237 -> 246 | -0.10804 | | | | | | |
| 224 -> 238 | -0.13720 | | | | | Excited State | 42: | Singlet-A | 5.7277 eV | 216.46 nm | f=0.0025 | | |
| Excited State | 34: | Singlet-A | 5.5845 eV | 222.02 nm | f=0.0096 | <S**2>=0.000 | | | | | | | |
| <S**2>=0.000 | | | | | | 217 -> 238 | -0.28535 | | | | | | |
| 232 -> 240 | -0.12341 | | | | | 218 -> 238 | 0.20137 | | | | | | |
| 235 -> 241 | -0.11700 | | | | | 220 -> 238 | 0.14849 | | | | | | |
| 237 -> 243 | 0.31238 | | | | | 233 -> 240 | 0.22360 | | | | | | |
| 237 -> 244 | 0.44435 | | | | | 237 -> 244 | -0.26014 | | | | | | |
| 237 -> 246 | 0.29082 | | | | | 237 -> 245 | 0.26557 | | | | | | |
| 237 -> 248 | 0.17765 | | | | | 237 -> 246 | 0.32409 | | | | | | |
| Excited State | 35: | Singlet-A | 5.5998 eV | 221.41 nm | f=0.0016 | Excited State | 43: | Singlet-A | 5.7377 eV | 216.09 nm | f=0.0006 | | |
| <S**2>=0.000 | | | | | | <S**2>=0.000 | | | | | | | |
| 220 -> 238 | -0.19042 | | | | | 215 -> 238 | 0.22025 | | | | | | |
| 221 -> 238 | 0.29492 | | | | | 217 -> 238 | 0.53744 | | | | | | |
| 222 -> 238 | 0.53253 | | | | | 237 -> 244 | -0.11694 | | | | | | |
| 223 -> 238 | 0.15381 | | | | | 237 -> 245 | 0.22823 | | | | | | |
| 224 -> 238 | 0.16191 | | | | | 237 -> 246 | 0.21316 | | | | | | |
| Excited State | 36: | Singlet-A | 5.6259 eV | 220.38 nm | f=0.0035 | Excited State | 44: | Singlet-A | 5.7490 eV | 215.66 nm | f=0.1020 | | |
| <S**2>=0.000 | | | | | | <S**2>=0.000 | | | | | | | |
| 219 -> 238 | 0.22338 | | | | | 225 -> 239 | -0.13323 | | | | | | |
| 220 -> 238 | 0.25045 | | | | | 226 -> 239 | -0.13273 | | | | | | |
| 231 -> 240 | 0.15327 | | | | | 228 -> 239 | 0.19045 | | | | | | |
| 232 -> 240 | 0.50023 | | | | | 235 -> 241 | 0.47476 | | | | | | |
| 233 -> 240 | 0.12924 | | | | | 237 -> 244 | 0.18679 | | | | | | |
| 237 -> 244 | 0.13905 | | | | | 237 -> 245 | 0.25687 | | | | | | |
| Excited State | 37: | Singlet-A | 5.6441 eV | 219.67 nm | f=0.0082 | 237 -> 248 | -0.13173 | | | | | | |
| <S**2>=0.000 | | | | | | Excited State | 45: | Singlet-A | 5.7659 eV | 215.03 nm | f=0.0003 | | |
| 219 -> 238 | 0.61858 | | | | | <S**2>=0.000 | | | | | | | |
| 232 -> 240 | -0.24289 | | | | | 215 -> 238 | 0.10807 | | | | | | |
| Excited State | 38: | Singlet-A | 5.6499 eV | 219.45 nm | f=0.0113 | 216 -> 238 | 0.56521 | | | | | | |
| <S**2>=0.000 | | | | | | 217 -> 238 | -0.15022 | | | | | | |
| 218 -> 238 | -0.31698 | | | | | 218 -> 238 | -0.18423 | | | | | | |
| 219 -> 238 | -0.13618 | | | | | 220 -> 238 | -0.10008 | | | | | | |
| 220 -> 238 | 0.46518 | | | | | 221 -> 238 | -0.17573 | | | | | | |
| 221 -> 238 | 0.27141 | | | | | 228 -> 239 | 0.21036 | | | | | | |
| 232 -> 240 | -0.21428 | | | | | Excited State | 46: | Singlet-A | 5.7766 eV | 214.63 nm | f=0.0126 | | |
| Excited State | 39: | Singlet-A | 5.6580 eV | 219.13 nm | f=0.0023 | <S**2>=0.000 | | | | | | | |
| <S**2>=0.000 | | | | | | 216 -> 238 | -0.14718 | | | | | | |
| 219 -> 238 | -0.12110 | | | | | 218 -> 238 | 0.10519 | | | | | | |
| 235 -> 241 | -0.21434 | | | | | 228 -> 239 | 0.61731 | | | | | | |
| 237 -> 242 | -0.27924 | | | | | 231 -> 240 | -0.11223 | | | | | | |
| 237 -> 244 | 0.11091 | | | | | 235 -> 241 | -0.11925 | | | | | | |
| 237 -> 245 | 0.38376 | | | | | Excited State | 47: | Singlet-A | 5.7791 eV | 214.54 nm | f=0.0131 | | |
| 237 -> 246 | -0.33587 | | | | | <S**2>=0.000 | | | | | | | |
| 237 -> 247 | 0.11529 | | | | | 226 -> 239 | -0.21446 | | | | | | |
| 237 -> 248 | 0.11496 | | | | | 227 -> 239 | 0.63865 | | | | | | |
| 237 -> 250 | 0.11578 | | | | | 235 -> 241 | -0.11092 | | | | | | |
| Excited State | 40: | Singlet-A | 5.7148 eV | 216.95 nm | f=0.0042 | Excited State | 48: | Singlet-A | 5.8101 eV | 213.39 nm | f=0.0236 | | |
| <S**2>=0.000 | | | | | | <S**2>=0.000 | | | | | | | |
| 215 -> 238 | 0.14424 | | | | | 215 -> 238 | -0.13203 | | | | | | |
| 216 -> 238 | 0.23376 | | | | | 231 -> 240 | 0.61093 | | | | | | |
| 218 -> 238 | 0.52346 | | | | | 232 -> 240 | -0.19066 | | | | | | |
| | | | | | | 237 -> 245 | -0.10795 | | | | | | |

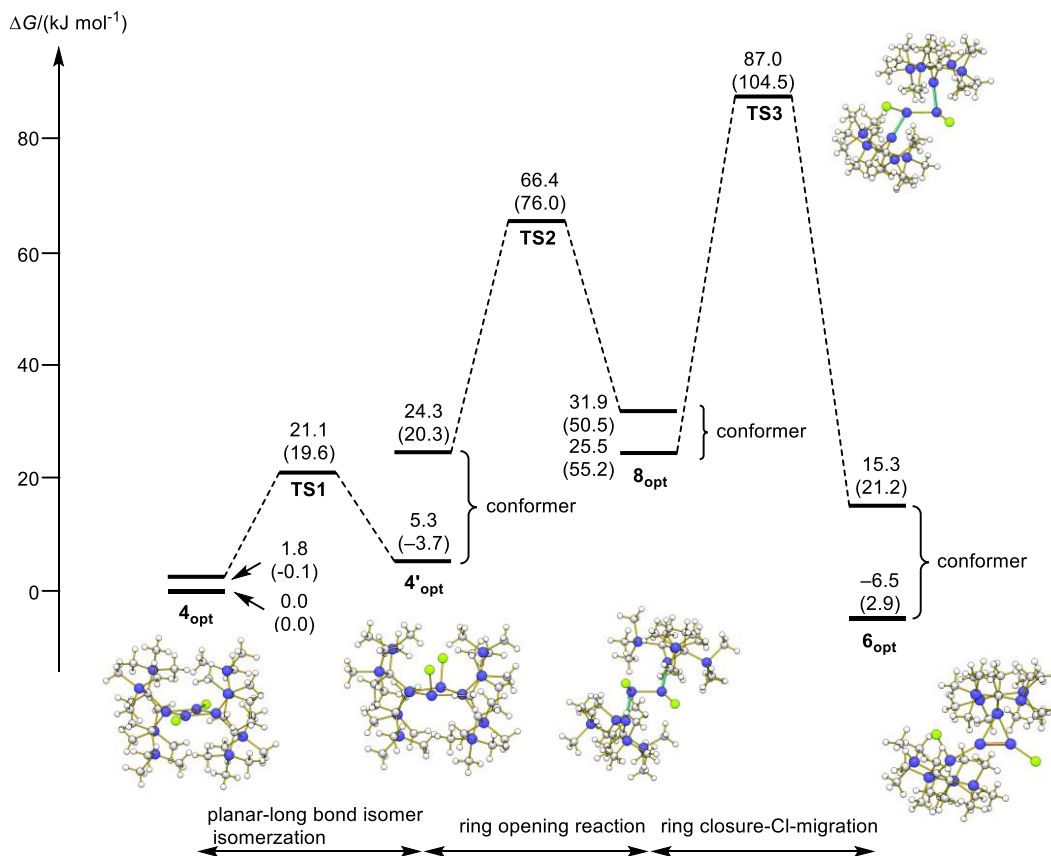


Figure 4-33. A possible reaction route between **4_{opt}** and **6_{opt}** calculated at the B3LYP-D3/B1 level of theory (basis B1: 6-311G(d) [core Si₄Cl₂], 6-31G(d) [carbon atoms in silacyclopentane rings], 3-21G* [others]).

Preliminary estimation of the thermodynamic parameters for the equilibrium between **4** and **6**

In the ¹H NMR spectrum of a mixture of bicyclo[1.1.0]tetrasilane **4** and cyclotrisilene **6**, the signals due to four SiMe₃ groups (36 H) of **6** were substantially broadened and overlapped with that due to eight SiMe₃ groups (72H) of **4** (Figure 4-34). Assuming that only signals of **4** and **6** were overlapped in this region, the equilibrium constants K_{eq} (= [6]:[4]) were determined by using the integral ratio of the SiMe₃ signals of ¹H NMR spectra in C₆D₆ (Table 4-23). A plot of $\ln K_{eq}$ at various reciprocal temperatures are shown in Figure 4-35. The thermodynamic parameters for the isomerisation of **4** to **6** are calculated to be $\Delta H = +14.6 \pm 2.9$ kJ mol⁻¹ and $\Delta S = +49 \pm 9$ J K⁻¹ mol⁻¹.

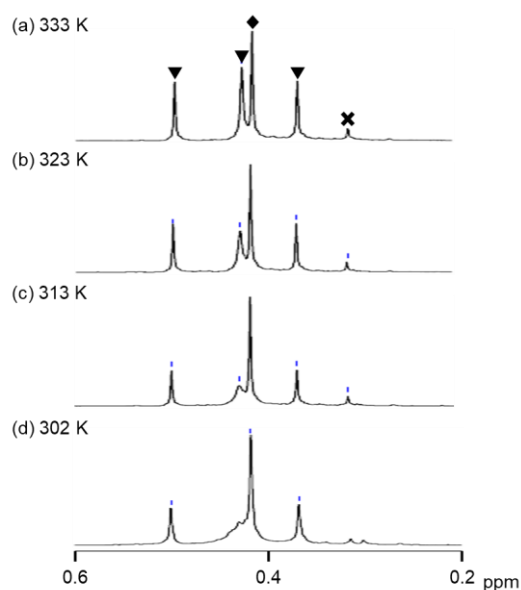


Figure 4-34. ^1H NMR spectra (SiMe₃ region) of a mixture of **4** and **6** in benzene-*d*₆ at (a) 333 K, (b) 323 K, (c) 313 K, and (d) 302 K (♦ = **4**, ▼ = **6**, × = **1**).

Table 4-23. The Equilibrium Constants K_{eq} (= [**6**]:[**4**]) in Benzene-*d*₆ at Various Temperatures

| Temperature/K | Integral ratio (SiMe ₃) | | K_{eq} (= [6]:[4]) ^a |
|---------------|-------------------------------------|-------------------------|--|
| | bicyclotetrasilane 4 | cyclotrisilene 6 | |
| 333 | 2.11 | 4.00 | 1.90 |
| 323 | 2.36 | 4.00 | 1.69 |
| 313 | 3.24 | 4.00 | 1.23 |
| 302 | 3.48 | 4.00 | 1.15 |

^aEquilibrium constants (K_{eq}) were calculated using the integral ratio of SiMe₃ proton signals in the ^1H NMR spectrum.

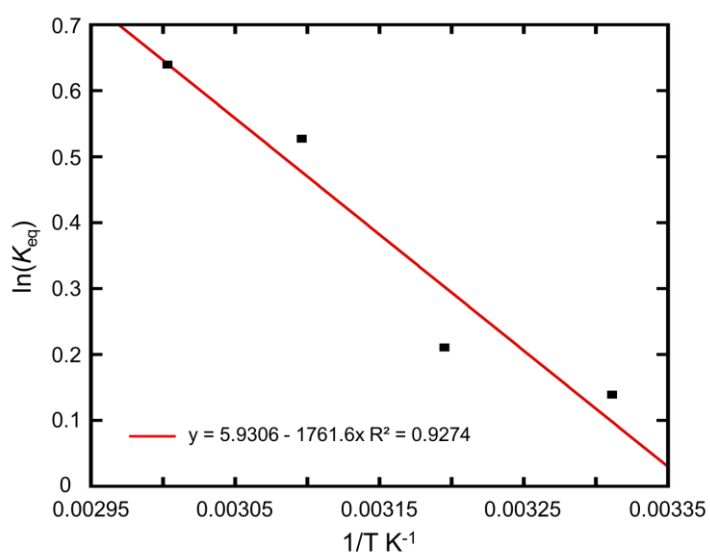


Figure 4-35. A plot of $\ln(K_{\text{eq}})$ vs $1/T$.

4-5. Reference

- (1) For reviews of interconversion among C₄R₆ isomers, see: (a) W. Leigh, *Chem. Rev.* **1993**, *93*, 487–505; (b) W. R. Dolbier Jr., H. Koroniak, K. N. Houk, C. Sheu, *Acc. Chem. Res.* **1996**, *29*, 471–477.
- (2) (a) W. Mahler, *J. Am. Chem. Soc.* **1962**, *84*, 4600–4601; (b) H. M. Frey, I. D. R. Stevens, *Trans. Faraday Soc.* **1965**, *61*, 90–94; (c) W. v. E. Doering, J. F. Coburn Jr., *Tetrahedron Lett.* **1965**, 991–995; (d) E. P. Blanchard Jr., A. Cairncross, *J. Am. Chem. Soc.* **1966**, *88*, 487–495; (e) K. B. Wiberg, J. M. Lavanish, *J. Am. Chem. Soc.* **1966**, *88*, 5272–5273; (f) G. L. Closs, P. E. Pfeffer, *J. Am. Chem. Soc.* **1968**, *90*, 2452–2453; (g) K. A. Nguyen, M. S. Gordon, *J. Am. Chem. Soc.* **1995**, *117*, 3835–3847; (h) A. Kinal, P. Piecuch, *J. Phys. Chem. A* **2007**, *111*, 734–742; (i) R. Berner, A. Lüchow, *J. Phys. Chem. A* **2010**, *114*, 13222–13227.
- (3) For reviews on heavy element analogues of bicyclo[1.1.0]butane, see: (a) H. Grützmacher, F. Breher, *Angew. Chem., Int. Ed.* **2002**, *41*, 4006–4011; (b) F. Breher, *Coord. Chem. Rev.* **2007**, *251*, 1007–1043.
- (4) For reviews on bicyclo[1.1.0]butanes, see: (a) K. B. Wiberg, *Adv. Alicyclic Chem.* **1968**, *2*, 185–254; (b) H. K. Hall Jr., A. B. Padia, *J. Polym. Sci., Part A: Polym. Chem.* **2003**, *41*, 625–635.
- (5) A number of silabicyclo[1.1.0]butanes have been reported. For tetrasilabicyclo[1.1.0]butanes, see: (a) S. Masamune, Y. Kabe, S. Collins, D. J. Williams, R. Jones, *J. Am. Chem. Soc.* **1985**, *107*, 5552–5553; (b) R. Jones, D. J. Williams, Y. Kabe, S. Masamune, *Angew. Chem., Int. Ed. Engl.* **1986**, *25*, 173–174; (c) S. Collins, J. A. Duncan, Y. Kabe, S. Murakami, S. Masamune, *Tetrahedron Lett.* **1985**, *26*, 2837–2840; (d) M. Kira, T. Iwamoto, C. Kabuto, *J. Am. Chem. Soc.* **1996**, *118*, 10303–10304; (e) T. Iwamoto, M. Kira, *Chem. Lett.* **1998**, 277–278; (f) K. Takanashi, V. Ya. Lee, M. Ichinohe, A. Sekiguchi, *Chem. Lett.* **2007**, *36*, 1158–1159; (g) K. Ueba-Ohshima, T. Iwamoto, M. Kira, *Organometallics* **2008**, *27*, 320–323; (h) K. Takanashi, V. Ya. Lee, T. Yokoyama, A. Sekiguchi, *J. Am. Chem. Soc.* **2009**, *131*,

- 916–917; (i) T. Iwamoto, N. Akasaka, S. Ishida, *Nat. Commun.* **2014**, *5*, 5353. For 1,2,3-trisilabicyclo[1.1.0]butanes, see: (j) V. Ya. Lee, H. Yasuda, A. Sekiguchi, *J. Am. Chem. Soc.* **2007**, *129*, 2436–2437; (k) V. Ya. Lee, S. Miyazaki, H. Yasuda, A. Sekiguchi, *J. Am. Chem. Soc.* **2008**, *130*, 2758–2759. For 2,4-disilabicyclo[1.1.0]butanes, see: (l) G. Fritz, S. Wartanessian, E. Matern, W. Höhle, H. G. v. Schnering, *Z. Anorg. Allg. Chem.* **1981**, *475*, 87–108; (m) G. Fritz, J. Thomas, *J. Organomet. Chem.* **1984**, *271*, 107–127; (n) W. Ando, T. Shiba, T. Hidaka, K. Morihashi, O. Kikuchi, *J. Am. Chem. Soc.* **1997**, *119*, 3629–3630. For 1,3-disilabicyclo[1.1.0]butane, see: (o) T. Iwamoto, D. Yin, C. Kabuto, M. Kira, *J. Am. Chem. Soc.* **2001**, *123*, 12730–12731. For 1,3-diphospha-2,4-disilabicyclo[1.1.0]butanes, see: (p) M. Driess, A. D. Fanta, D. R. Powell, R. West, *Angew. Chem., Int. Ed. Engl.* **1989**, *28*, 1038–1040; (q) M. Driess, H. Pritzkow, M. Reising, *Chem. Ber.* **1991**, *124*, 1923–1929; (r) A. D. Fanta, M. Driess, D. R. Powell, R. West, *J. Am. Chem. Soc.* **1991**, *113*, 7806–7808; (s) M. Driess, H. Pritzkow, S. Rell, R. Janoschek, *Inorg. Chem.* **1997**, *36*, 5212–5217. For 1,3-diarsa-2,4-disilabicyclo[1.1.0]butane, see: (t) M. Driess, R. Janoschek, H. Pritzkow, *Angew. Chem., Int. Ed. Engl.* **1992**, *31*, 460–462. For 1,2,3-triphospha-4-silabicyclo[1.1.0]butane, see: (u) M. Driess, *Angew. Chem., Int. Ed. Engl.* **1991**, *30*, 1022–1024. For 2-phospha-4-silabicyclo[1.1.0]butane, see: (v) J. C. Slootweg, F. J. J. de Kanter, M. Schakel, A. W. Ehlers, B. Gehrhus, M. Lutz, A. M. Mills, A. L. Spek, K. Lammertsma, *Angew. Chem., Int. Ed.* **2004**, *43*, 3474–3477.
- (6) Theoretical studies of isomerisation of silabicyclo[1.1.0]butanes: (a) T. Müller, in *Organosilicon Chemistry IV*, ed. N. Auner and J. Weis, Wiley-VCH, Weinheim, 2000, pp. 110–116; (b) J. C. Slootweg, A. W. Ehlers, K. Lammertsma, *J. Mol. Model.* **2006**, *12*, 531–536; (c) Y. Konno, T. Kudo, S. Sakai, *Theor. Chem. Acc.* **2011**, *130*, 371–382.
- (7) C. B. Yildiz, K. I. Leszczyńska, S. González-Gallardo, M. Zimmer, A. Azizoglu, T. Biskup, C. W. M. Kay, V. Huch, H. S. Rzepa, D. Scheschkewitz, *Angew. Chem., Int. Ed.* **2020**, *59*, 15087–15092.

- (8) (a) W. W. Schoeller, T. Dabisch, T. Busch, *Inorg. Chem.* **1987**, *26*, 4383–4389; (b) P. v. R. Schleyer, A. F. Sax, J. Kalcher, R. Janoschek, *Angew. Chem., Int. Ed. Engl.* **1987**, *26*, 364–366; (c) J. A. Boatz, M. S. Gordon, *J. Phys. Chem.* **1988**, *92*, 3037–3042; (d) J. A. Boatz, M. S. Gordon, *J. Phys. Chem.* **1989**, *93*, 2888–2891; (e) R. Koch, T. Bruhn, M. Weidenbruch, *J. Mol. Struct.: THEOCHEM* **2004**, *680*, 91–97; (f) M. Kira, *Organometallics* **2014**, *33*, 644–652. See also ref. 6a and c.
- (9) (a) T. Iwamoto, T. Abe, K. Sugimoto, D. Hashizume, H. Matsui, R. Kishi, M. Nakano, S. Ishida, *Angew. Chem., Int. Ed.* **2019**, *58*, 4371–4375; (b) T. Nukazawa, T. Kosai, S. Honda, S. Ishida, T. Iwamoto, *Dalton Trans.* **2019**, *48*, 10874–10880.
- (10) T. Nukazawa, T. Iwamoto, *J. Am. Chem. Soc.* **2020**, *142*, 9920–9924.
- (11) Unfortunately, we have failed to obtain the corresponding 1,3-dibromo derivative from the reaction of **1** with bromoalkanes such as CHBr_3 , CBr_4 , $(\text{CH}_2\text{Br})_2$, and $(\text{CHBr}_2)_2$.
- (12) S. Kyushin, Y. Kurosaki, K. Otsuka, H. Imai, S. Ishida, T. Kyomen, M. Hanaya, H. Matsumoto, *Nat. Commun.* **2020**, *11*, 4009.
- (13) As **4** undergoes facile isomerisation to cyclotrisilene **6** in solution, the ^{29}Si NMR spectral data of **4** and **6** were taken from the ^{29}Si NMR spectrum of the equilibrium mixture of **4** and **6** recorded at 60 °C and assigned according to the ^1H - ^{29}Si HMBC spectrum.
- (14) (a) K. Leszczyńska, K. Abersfelder, A. Mix, B. Neumann, H.-G. Stammer, M. J. Cowley, P. Jutzi, D. Scheschkewitz, *Angew. Chem., Int. Ed.* **2012**, *51*, 6785–6788; (b) M. J. Cowley, V. Huch, H. S. Rzepa, D. Scheschkewitz, *Nat. Chem.* **2013**, *5*, 876–879.
- (15) For studies on cyclotrisilenes, see: (a) T. Iwamoto, C. Kabuto, M. Kira, *J. Am. Chem. Soc.* **1999**, *121*, 886–887; (b) M. Ichinohe, T. Matsuno, A. Sekiguchi, *Angew. Chem., Int. Ed.* **1999**, *38*, 2194–2196; (c) T. Iwamoto, M. Tamura, C. Kabuto, M. Kira, *Science* **2000**, *290*, 504–506; (d) T. Iwamoto, M. Tamura, C. Kabuto, M. Kira, *Organometallics* **2003**, *22*, 2342–2344; (e) T. Kosai, S. Nishimura, N. Hayakawa, T. Matsuo, T. Iwamoto, *Chem. Lett.* **2019**, *48*, 1168–1170; (f) T. Koike, S. Honda, S. Ishida, T. Iwamoto, *Organometallics* **2020**, *39*, 4149–4152, see also ref. 14a.

- (16) (a) M. Zirngast, M. Flock, J. Baumgartner, C. Marschner, *J. Am. Chem. Soc.* **2008**, *130*, 17460–17470; (b) J. I. Schweizer, M. G. Scheibel, M. Diefenbach, F. Neumeier, C. Würtele, N. Kulminkaya, R. Linser, N. Auner, S. Schneider, M. C. Holthausen, *Angew. Chem., Int. Ed.* **2016**, *55*, 1782–1786; (c) M. W. Stanford, J. I. Schweizer, M. Menche, G. S. Nichol, M. C. Holthausen, M. J. Cowley, *Angew. Chem., Int. Ed.* **2019**, *58*, 1329–1333; (d) I. Balatoni, J. Hlina, R. Zitz, A. Pocheim, J. Baumgartner, C. Marschner, *Inorg. Chem.* **2019**, *58*, 14185–14192. See also ref. 5i.
- (17) In the ^1H NMR spectrum of a mixture of **4** and **6**, the signals due to four SiMe_3 groups (36 H) of **6** were substantially broadened and overlapped with that due to eight SiMe_3 groups (72H) of **4** (Figure 4-34). Assuming that only the signals of **4** and **6** were overlapped in this region, the equilibrium constants $K_{\text{eq}} (= [\mathbf{6}]/[\mathbf{4}])$ at 302–333 K were roughly estimated using the integral ratios (Table 4-23). From the K_{eq} , the thermodynamic parameters for the isomerization of **4** to **6** are calculated to be $\Delta H = +14.6 \pm 2.9 \text{ kJ mol}^{-1}$ and $\Delta S = +49 \pm 9 \text{ J K}^{-1} \text{ mol}^{-1}$ (Figure 4-35) which are consistent with the calculated relative energy and free energy.
- (18) For reviews on bond stretch isomerisation, see: G. Parkin, *Chem. Rev.* **1993**, *93*, 887–911. See also ref. 3.
- (19) For concepts of bond stretch isomerism, see: (a) W.-D. Stohrer, R. Hoffmann, *J. Am. Chem. Soc.* **1972**, *94*, 779–786; (b) W.-D. Stohrer, R. Hoffmann, *J. Am. Chem. Soc.* **1972**, *94*, 1661–1668.
- (20) The isomerisation of a 2,3-disilabutadiene to a long bond isomer of 1,3-disilabicyclobutane was reported. See, D. Motomatsu, S. Ishida, K. Ohno, T. Iwamoto, *Chem. Eur. J.* **2014**, *20*, 9424–9430.
- (21) The HOMO and HOMO–1 of **8_{opt}** are mainly localized on the central chlorinated Si atoms, while LUMO and LUMO+1 are localized on the terminal Si atoms. The orbital feature suggests the presence of two polarized $\text{R}_2\text{Si}^{\delta+}-\text{Si}^{\delta-}\text{Cl}$ bonds, which is

consistent with the natural atomic orbital (NPA) charges of the silicon atoms [+1.4 and 0.0 for terminal and central Si atoms].

- (22) For studies on disilene–silylsilylene interconversion, see: (a) W. D. Wulff, W. F. Goure, T. J. Barton, *J. Am. Chem. Soc.* **1978**, *100*, 6236–6238; (b) H. Sakurai, Y. Nakadira, H. Sakaba, *Organometallics* **1983**, *2*, 1484–1486; (c) G. Maier, H. P. Reisenauer, J. Glatthaar, *Chem. Eur. J.* **2002**, *8*, 4383–4391; (d) M. Ichinohe, R. Kinjo, A. Sekiguchi, *Organometallics* **2003**, *22*, 4621–4623; (e) K. Abersfelder, D. Scheschkewitz, *J. Am. Chem. Soc.* **2008**, *130*, 4114–4121; (f) T. Sasamori, K. Hironaka, Y. Sugiyama, N. Takagi, S. Nagase, Y. Hosoi, Y. Furukawa, N. Tokitoh, *J. Am. Chem. Soc.* **2008**, *130*, 13856–13857; (g) T. Agou, Y. Sugiyama, T. Sasamori, H. Sakai, Y. Furukawa, N. Takagi, J.-D. Guo, S. Nagase, D. Hashizume, N. Tokitoh, *J. Am. Chem. Soc.* **2012**, *134*, 4120–4123; (h) X.-Q. Xiao, H. Zhao, Z. Xu, G. Lai, X.-L. He, Z. Li, *Chem. Commun.* **2013**, *49*, 2706–2708; (i) T. Kosai, T. Iwamoto, *J. Am. Chem. Soc.* **2017**, *139*, 18146–18149; (j) T. Kosai, T. Iwamoto, *Chem. Eur. J.* **2018**, *24*, 7774–7780; (k) D. Reiter, R. Holzner, A. Porzelt, P. J. Altmann, P. Frisch, S. Inoue, *J. Am. Chem. Soc.* **2019**, *141*, 13536–13546. See also ref. 16b.
- (23) In contrast to **4**, **5** does not exhibit similar interconversion. As **5** slowly decomposes to bicyclo[1.1.0]tetrasil-1(3)-ene **1** and unidentified products at room temperature, the activation barrier for the decomposition may be lower in energy than those of the rate-controlling step of the similar interconversion.
- (24) M. Kira, S. Ishida, T. Iwamoto, C. Kabuto, *J. Am. Chem. Soc.* **1999**, *121*, 9722–9723.
- (25) In the reaction of **1** with CCl₄, intermediate **8** should be involved in the formation of acyclic tetrasilane **3**.
- (26) G. R. Fulmer, A. J. M. Miller, N. H. Sherden, H. E. Gottlieb, A. Nudelman, B. M. Stoltz, J. E. Bercaw, K. I. Goldberg, *Organometallics* **2010**, *29*, 2176–2179.
- (27) G. M. Sheldrick, *SADABS, Empirical Absorption Correction Program*; Göttingen, Germany, 1996.
- (28) G. M. Sheldrick, *Acta Crystallogr., Sect. C: Struct. Chem.*, **2015**, *71*, 3–8.

- (29) K. Wakita, Yadokari-XG: Software for Crystal Structure Analyses, 2001; Release of Software (Yadokari-XG 2009) for Crystal Structure Analyses; C. Kabuto, S. Akine, T. Nemoto, E. Kwon, *J. Crystallogr. Soc. Jpn.*, **2009**, *51*, 218–224.
- (30) M. J. Frisch, G. W. Trucks, H. B. Schlegel, G. E. Scuseria, M. A. Robb, J. R. Cheeseman, G. Scalmani, V. Barone, B. Mennucci, G. A. Petersson, H. Nakatsuji, M. Caricato, X. Li, H. P. Hratchian, A. F. Izmaylov, J. Bloino, G. Zheng, J. L. Sonnenberg, M. Hada, M. Ehara, K. Toyota, R. Fukuda, J. Hasegawa, M. Ishida, T. Nakajima, Y. Honda, O. Kitao, H. Nakai, T. Vreven, J. A. Montgomery Jr., J. E. Peralta, F. Ogliaro, M. Bearpark, J. J. Heyd, E. Brothers, K. N. Kudin, V. N. Staroverov, R. Kobayashi, J. Normand, K. Raghavachari, A. Rendell, J. C. Burant, S. S. Iyengar, J. Tomasi, M. Cossi, N. Rega, J. M. Millam, M. Klene, J. E. Knox, J. B. Cross, V. Bakken, C. Adamo, J. Jaramillo, R. Gomperts, R. E. Stratmann, O. Yazyev, A. J. Austin, R. Cammi, C. Pomelli, J. W. Ochterski, R. L. Martin, K. Morokuma, V. G. Zakrzewski, G. A. Voth, P. Salvador, J. J. Dannenberg, S. Dapprich, A. D. Daniels, Ö. Farkas, J. B. Foresman, J. V. Ortiz, J. Cioslowski, D. J. Fox, Gaussian 09, Revision D.01, Gaussian, Inc., Wallingford CT, 2009.
- (31) **GRRM14**; (a) S. Maeda, Y. Harabuchi, Y. Osada, T. Taketsugu, K. Morokuma, K. Ohno, see <https://iqce.jp/GRRM/>, accessed date March 21, 2020; (b) S. Maeda, K. Ohno, K. Morokuma, *Phys. Chem. Chem. Phys.* **2013**, *15*, 3683–3701.
- (32) *Software to optimize reaction paths along the user's expected ones*, HPC Systems Inc., <http://www.hpc.co.jp/chem/react1.html>.
- (33) (a) H. Jónsson, G. Mills, K. W. Jacobsen, in *Classical and Quantum Dynamics in Condensed Phase Simulations*, ed. B. J. Berne, G. Ciccotti, D. F. Coker, World Scientific, **1998**, p. 385; (b) G. Henkelman, H. Jónsson, *J. Chem. Phys.* **2000**, *113*, 9978.
- (34) (a) K. Fukui, *Acc. Chem. Res.* **1981**, *14*, 363–368; (b) K. Ishida, K. Morokuma, A. Komornicki, *J. Chem. Phys.* **1977**, *66*, 2153; (c) M. Page, J. W. McIver, *J. Chem. Phys.* **1988**, *88*, 922; (d) C. Gonzalez, H. B. Schlegel, *J. Chem. Phys.* **1989**, *90*, 2154.

- (35) E. D. Glendening, J. K. Badenhoop, A. E. Reed, J. E. Carpenter, J. A. Bohmann, C. M. Morales, P. Karafiloglou, C. R. Landis, F. Weinhold, *NBO 7.0*, Theoretical Chemistry Institute, University of Wisconsin, Madison, 2018.

Chapter 5

Synthesis of π -Conjugated Species with an Unsupported Si-Si π -Bond via Direct π -Extension

The contents of this chapter are published in part in

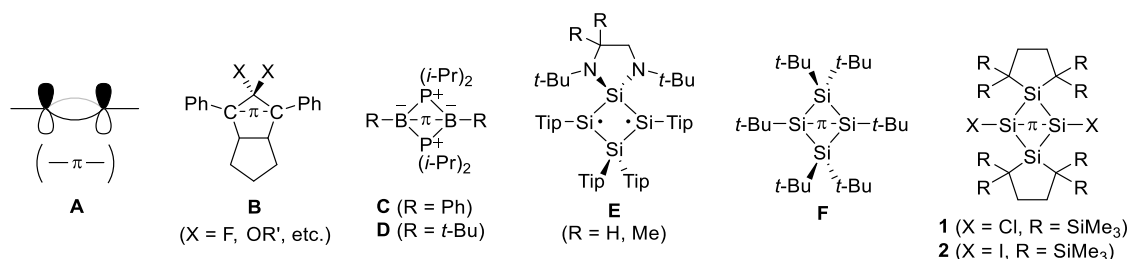
Nukazawa, T.; Iwamoto, T. *Chem. Commun.* **2021**, 57, 9692–9695.

DOI: 10.1039/d1cc04332c

5-1. Introduction

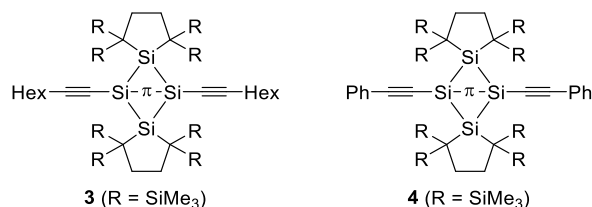
Interactions between π -orbitals, in particular π -conjugation, play a crucial role in the tuning of the structural, electronic, and photochemical properties of organic and inorganic compounds. Generally, π -bonds are found in multiple bonds that have an underlying σ -bond framework in π -electron systems such as aromatic compounds and polyenes. However, compounds that contain π -bonding modes without an underlying strong σ -bond framework (“unsupported” π -bonds; Chart 5-1A)¹ have been synthesized using meticulous molecular-design processes as unconventional π -electron systems (Chart 5-1B–F and 1–2).^{2–6} For example, Abe and co-workers have reported representative examples of persistent singlet cycloalkane-1,3-diyl derivatives that contain an unsupported π -bond (**B**),² which exhibit a substantially red-shifted absorption band arising from a HOMO(π) - LUMO(π^*) transition (~600 nm) compared to those of the corresponding monoalkenes such as 1,2-diphenylethene (~300 nm). Bertrand and co-workers have reported that isolable 1,3-diphenyl-1,3-dibora-2,4-diphosphacyclobutane-1,3-diyl **C** has a π -type B–B bonding interaction (Chart 5-1);³ the longest-wavelength absorption band of **C**, which appears in the visible region, is bathochromically shifted relative to that of 1,3-dialkyl derivative **D**. These results indicate that a compound with an unsupported π -bond may act as a nonclassical π -unit with a substantially narrow π - π^* gap. However, such compounds remain quite rare. They require designed bulky substituents to stabilize unsupported π -bonds and the reactive unsupported π -bond was formed at the last stage in the preparation process, which prevents the facile extension of π -units.

Chart 5-1. Schematic Illustration of Unsupported π -Bond (**A**) and the Structures of Related Compounds **B–F** and **1–2**



Recently, we have synthesized 1,3-dihalobicyclo[1.1.0]tetrasilanes **1** and **2** (Chart 5-1),⁴ which have a planar Si₄ framework with a longer bridgehead Si–Si distance (2.58 Å) compared to a typical Si–Si single bond distance (2.36 Å)⁷ and bridgehead Si–Si distances in highly bent bicyclo[1.1.0]tetrasilanes (2.35–2.47 Å).⁸ Compounds **1** and **2** contain an unsupported π -bond between the bridgehead silicon atoms. Compound **2** shows a distinct absorption band that arises from a $\pi(\text{Si-Si}) \rightarrow \pi^*(\text{Si-Si})$ transition at $\lambda_{\text{max}} = 435$ nm, which is substantially red-shifted compared to that of a structurally similar trisilacyclopentene that exhibits a planar Si=Si double bond in the three-membered ring ($\lambda_{\text{max}} = 391$ nm).⁹ Similar structural characteristics with a planar Si₄ framework were found in related compounds **E**⁵ and **F**,⁶ which were reported independently by Scheschkewitz et al. and Kyushin et al (Chart 5-1). These findings suggest that a compound with an unsupported Si–Si π -bond can serve as a nonclassical π -unit with a narrow π - π^* gap similar to **B–D**. However, electronic communication between an unsupported Si–Si π -bond and other π -electron systems has yet to be reported. In this context, **1** and **2** that contain good leaving groups on the bridgehead silicon atoms are expected to be useful precursors for the synthesis of π -conjugated systems with unsupported Si–Si π -bonds.¹⁰ In this chapter, the author reports the reactions of **1** with a lithium acetylide to provide **3** and **4**, *i.e.*, bicyclo[1.1.0]tetrasilanes with alkynyl groups on the bridgehead silicon atoms (Chart 5-2). Single-crystal X-ray diffraction (XRD) analyses, UV-vis absorption spectra, and theoretical calculations indicated that π -conjugation occurs in these compounds between the unsupported Si–Si π -bond of the bicyclo[1.1.0]tetrasilane unit and the alkynyl (and aryl) groups.

Chart 5-2. Structures of Compounds **3** and **4**

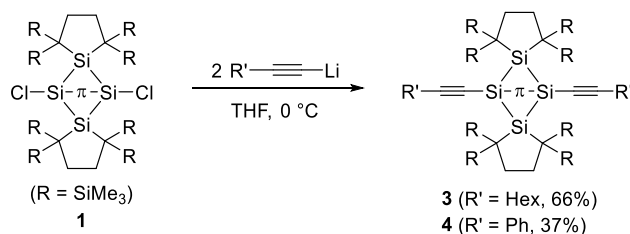


5-2. Results and Discussion

5-2-1. Synthesis of 1,3-Dialkynyltetrasilabicyclo[1.1.0]butanes **3** and **4**

Reddish purple crystals of **3** were obtained in 66% yield following the reaction of **1** with 1-octynyllithium in THF at 0 °C (Scheme 5-1). Similarly, the treatment of **1** with lithium phenylacetylide afforded **4** as a blue solid in 37% yield (Scheme 5-1). The molecular structures of **3** and **4** were determined using a combination of multinuclear NMR spectroscopy, mass spectrometry, elemental analysis, and single-crystal XRD analysis. While **3** was stable at room temperature, **4** slowly decomposed to a complex product mixture in solution at room temperature.

Scheme 5-1. Synthesis of **3** and **4**



5-2-2. Molecular Structures of **3** and **4**

The molecular structures of **3** and **4**, as determined by single-crystal XRD analysis, are shown in Figure 5-1.¹¹ Molecules of **3** and **4** reside on a crystallographic inversion centre and the central Si₄ skeleton is planar (Si2–Si1–Si1*–Si2* angle: 180°). The geometry around the bridgehead silicon atoms is almost planar [sums of the angles at the Si1 atom excluding the bridgehead bond: 360.00° (**3**) and 359.94° (**4**)]. The ethynyl moieties are very slightly bent in a *trans* configuration relative to the plane of the Si₄ ring [Si1*–Si1–C1 angles: 178.59(5)° (**3**) and 177.59(9)° (**4**)]. Noticeably, the distances between the bridgehead silicon atoms [Si1–Si1*: 2.7112(7) Å (**3**) and 2.6992(11) Å (**4**)] are longer than those of **1** [2.581(2) Å] and **2** [2.5822(11) Å],⁴ even though they are still shorter than those of **E** [2.871(1) Å] and **F** [2.853(1) Å].^{5,6} Nevertheless, the length of the C1–C2 bonds [1.200(2) Å (**3**) and 1.208(3) Å (**4**)] are comparable to that of the C≡C bond in bis(trimethylsilyl)acetylene [1.208(3) Å].¹² The Si1–C1

distances [1.8207(15) Å (**3**) and 1.816(2) Å (**4**)] are almost identical to those of the 1,2-dialkynyldisilenes [1.811(4) and 1.8029(19) Å] reported by Tokitoh.¹³ The dihedral angle between the plane of the Si₄ ring and the plane of the phenyl ring in **4** (23.0°) is suitable for effective interactions between the bridgehead Si–Si π -bond in the Si₄ skeleton and the π -system on the phenyl rings via the acetylene moieties.

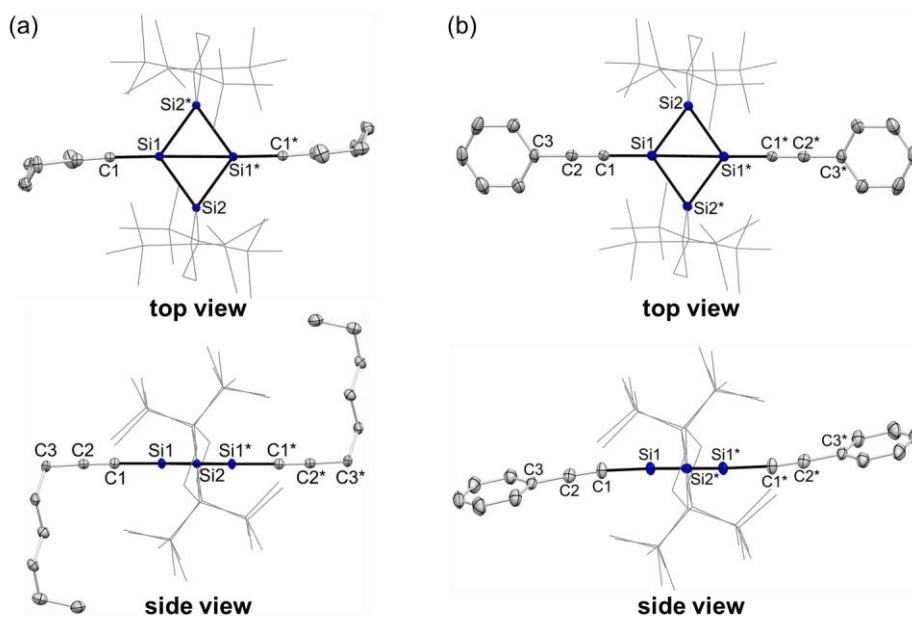


Figure 5-1. ORTEP diagrams of (a) **3** and (b) **4** with thermal ellipsoids at 50% probability; all hydrogen atoms are omitted for clarity.

5-2-3. UV-vis Absorption Spectra of **3** and **4** in the Solid State

The UV-vis spectra of **3** and **4** in the crystalline state demonstrate that substantial interactions occur between the Si₄ framework with an unsupported Si–Si π -bond and the alkynyl groups at the bridgehead silicon atoms. Both **3** and **4** exhibit a distinct absorption band in the visible region (Figure 5-2). The longest-wavelength absorption band maxima of **3** ($\lambda_{\text{max}} = 552$ nm) and **4** ($\lambda_{\text{max}} = 602$ nm) (Figure 5-2), which arise from the $\pi \rightarrow \pi^*$ transition of the bridgehead Si–Si π -bond (*vide infra*), are red-shifted by more than 100 nm compared to that of **2** (435 nm).^{4b} Notably, the maximum of **4** (602 nm) is by 50 nm red-shifted compared to that of **3** (552 nm), even though **3** and **4** exhibit similar bridgehead Si–Si distances. This indicates that the phenyl moieties in **4** interact with the π -orbital of the bridgehead Si–Si bond. A similar

red-shift of the $\pi \rightarrow \pi^*$ transition band upon π -extension has been observed for 1,2-dialkynyldisilenes [$\lambda_{\max} = 437$ (trimethylsilylethynyl), 469 nm (phenylethynyl)].¹³

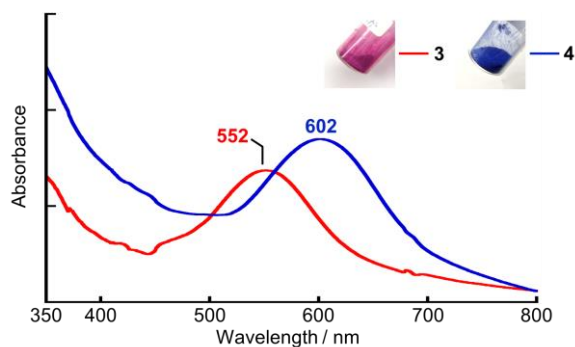


Figure 5-2. UV-vis absorption spectra of **3** (red) and **4** (blue) in a KBr matrix at room temperature.

5-2-4. Theoretical Study

Theoretical calculations for the structures of **3** and **4** in the crystalline state (**3_{cry}** and **4_{cry}**) provided further insight into their electronic properties.¹⁴ The frontier Kohn–Sham orbitals of **3_{cry}** and **4_{cry}** show HOMOs and LUMOs that arise from an in-phase and out-of-phase combination of the bridgehead Si 3p orbitals (π - and π^* -orbitals) (Figure 5-3). Importantly, they include the π -(π^* -) orbitals of the C \equiv C bonds from the ethynyl moieties, which corroborates the presence of conjugation between the bridgehead Si–Si π -bond and the C \equiv C bonds of the ethynyl moieties. Notably, the LUMO of **4_{cry}** involves a contribution from the π^* -orbitals of the phenyl moieties and its energy level (–2.11 eV) is significantly lower than that of **3_{cry}** (–1.88 eV). However, the HOMO energy levels are almost identical (**3_{cry}**: –5.80 eV; **4_{cry}**: –5.82 eV), which is consistent with the fact that the absorption band of **4** is red-shifted relative to that of **3**. The Wiberg bond indices (WBI)¹⁴ between the bridgehead silicon atoms of **3_{cry}** (0.63) and **4_{cry}** (0.63) are slightly smaller than that of **2** (0.70), which supports the presence of a bonding interaction between the bridgehead silicon atoms. Time-dependent density functional theory (TD-DFT) calculations indicated that the observed absorption spectra of **3** and **4** in the solid state are in good agreement with the band positions and oscillator strengths of **3_{cry}** and **4_{cry}** (Figures 5-34 and 5-35).

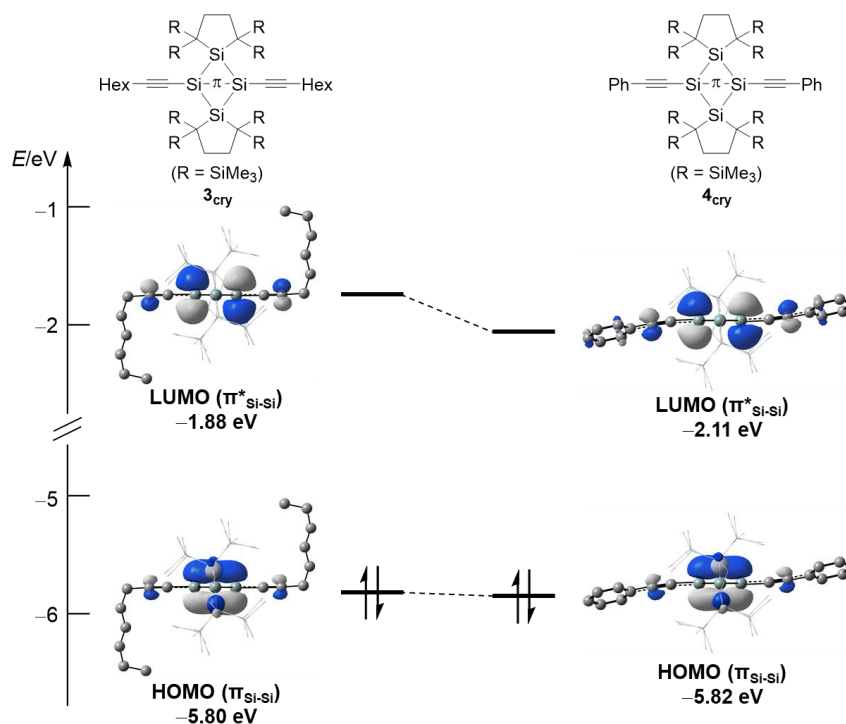


Figure 5-3. Frontier Kohn–Sham orbitals and their energy levels for **3**_{cry} and **4**_{cry} calculated at the M06-2X/6-311G(d) level of theory (isosurface level: 0.04 e·au⁻³); all hydrogen atoms are omitted for clarity.

5-2-5. UV-vis Absorption Spectra of **3** and **4** in Solution

Interestingly, the colors of **3** and **4** observed in solution differ from those observed in the solid state. In organic solvents, the reddish-purple crystals of **3** provide a red solution at room temperature. In hexane, the UV-vis absorption spectrum of **3** shows a longest-wavelength absorption band ($\lambda_{\text{max}} = 518 \text{ nm}$) that is by 34 nm blue-shifted compared to that of **3** in the solid state (Figure 5-4). Similarly, a hexane solution of **4** is purple ($\lambda_{\text{max}} = 560 \text{ nm}$), which is blue-shifted relative to that of the blue solid (Figure 5-4). These results suggest that the structures and electronic properties of **3** and **4** in solution are different from those in the solid state.

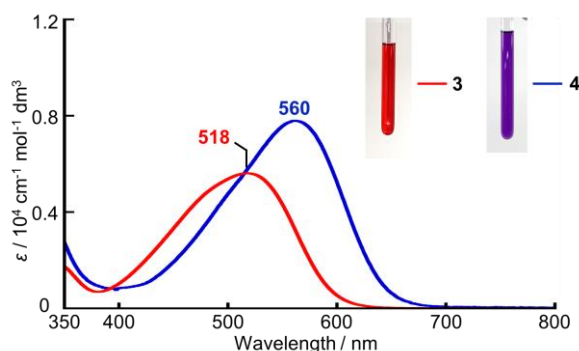


Figure 5-4. UV-vis absorption spectra of **3** (red) and **4** (blue) in hexane at room temperature.

5-2-6. NMR Spectra of **3** and **4**

The NMR spectra of **3** and **4** provided information on their structures in solution. The ^1H NMR spectra of **3** and **4** in C_6D_6 at room temperature show a singlet signal due to the eight magnetically equivalent SiMe_3 groups [**3**: 0.53 ppm; **4**: 0.54 ppm] and another singlet signal due to the eight methylene protons of the five-membered rings [**3**: 2.05 ppm; **4**: 2.05 ppm]. In the ^{29}Si NMR spectra, only three signals [**3**: -8.0 ppm (bridge Si), 4.7 ppm (SiMe_3), and 83.3 ppm (bridgehead Si); **4**: -6.1 ppm (bridge Si), 4.9 ppm (SiMe_3), and 91.5 ppm (bridgehead Si)] were observed (Figure 5-5). These results indicate that **3** and **4** adopt highly symmetric structures in solution. Notably, the chemical shifts for the bridgehead ^{29}Si nuclei of **3** (83.3 ppm) and **4** (91.5 ppm) are close to those of **1** (126.4 ppm) and **2** (103.8 ppm), *i.e.*, molecules that also possess planar Si_4 rings,⁴ but downfield-shifted compared with those of the reported bicyclo[1.1.0]tetrasilanes with highly bent Si_4 rings (-145.1 to 14.8 ppm).⁸ This implies that the Si_4 skeletons of **3** and **4** are highly planar in solution.

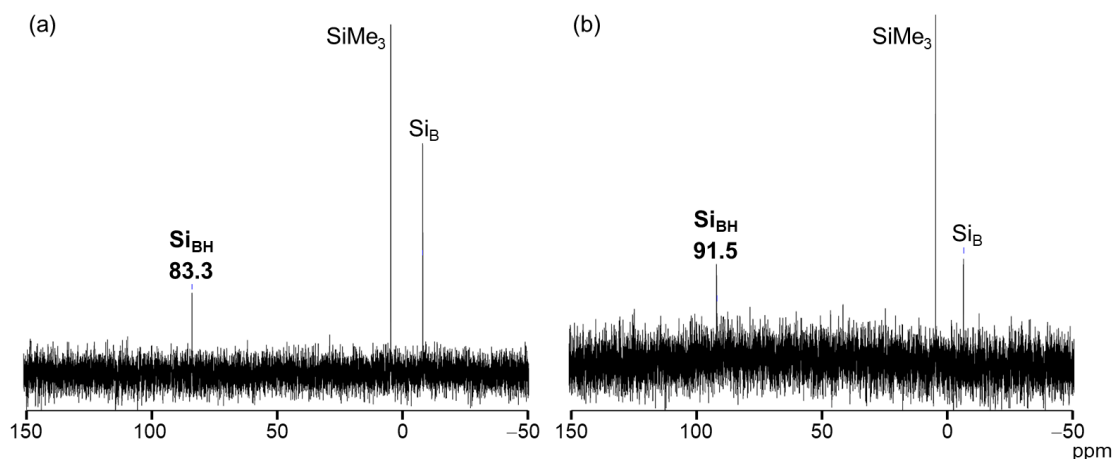


Figure 5-5. ^{29}Si NMR spectra of (a) **3** and (b) **4** in benzene- d_6 at room temperature (Si_{BH} : bridgehead Si, Si_{B} : bridge Si).

5-2-7. Variable-Temperature (VT) UV-vis Absorption and NMR Spectra of **3** and **4**

The variable-temperature (VT) UV-vis absorption and NMR spectra of **3** and **4** provided further insight into their behavior in solution. With decreasing temperature, the absorption band of **3** at 518 nm (293 K) decreased and an absorption band at ~ 480 nm increased with an isosbestic point at 512 nm (Figure 5-6). At 93 K, an absorption band at 478 nm and a shoulder peak at 561 nm were observed. These spectral changes were observed to be reversible. A similar temperature-dependent effect was observed in the UV-vis spectrum of **4** (Figure 5-31). Additionally, while the features of the ^1H NMR spectrum of **3** did not change substantially at lower temperatures (Figure 5-22), the ^{29}Si resonance attributed to the bridgehead silicon nuclei of **3** exhibited a significant upfield-shift upon decreasing the temperature (60 °C: 87.6 ppm; -40 °C: 73.2 ppm) (Figure 5-7 and Table 5-2).¹⁵ These results clearly indicate that the two different structures of **3** and **4** are in equilibrium in solution.

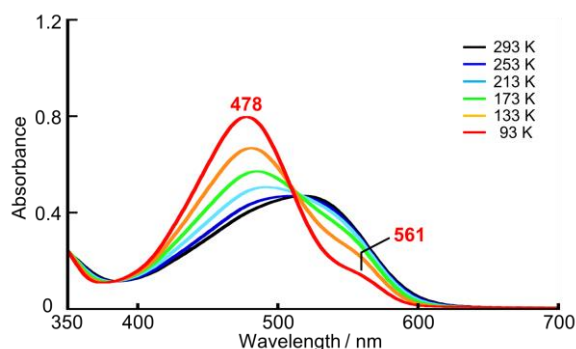


Figure 5-6. VT UV-vis absorption spectra of **3** in 3-methylpentane recorded at 40 K intervals (93–293 K).

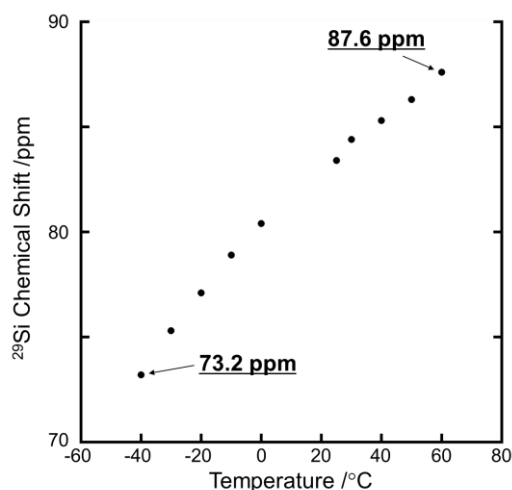
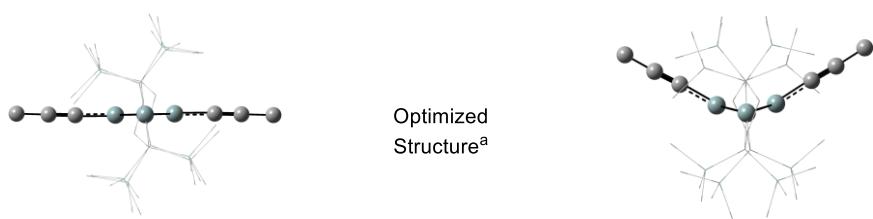


Figure 5-7. A plot of observed ^{29}Si chemical shift of the bridgehead silicon atoms in **3** vs measurement temperature.

5-2-8. Theoretical Calculations for the Behavior of **3** and **4** in Solution

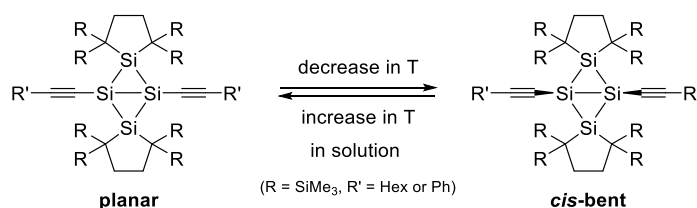
To understand the behavior of **3** and **4** in solution, DFT calculations were conducted using a simplified model (**5**) in which the Hex or Ph groups were replaced by methyl groups. A planar structure (**5_p**) similar to those observed in the crystalline states of **3** and **4** was located as a local minimum at the $\omega\text{B97XD}/6\text{-311G(d)}/\text{SCRF}(\text{solvent} = \text{heptane})$ level of theory (Table 5-1). We also found another local minimum of **5** that contains a *cis*-bent Si_4 framework (**5_c**) similar to that found in **2** (Table 5-1).^{4b} Calculating the Gibbs energy values revealed that **5_c** is slightly more stable than **5_p** (3.5 kJ mol^{-1} at 298.15 K). The bent angle of the silicon framework of **5_c** is 158.6° and the distance between the bridgehead silicon atoms of **5_c** (2.545 \AA) is shorter than that of **5_p** (2.680 \AA). The longest-wavelength absorption band position of **5_c** (430 nm) was blue-shifted compared with that of **5_p** (562 nm). The ^{29}Si NMR resonance due to the bridgehead silicon nuclei of **5_c** (-25.7 ppm) calculated at the $\text{M06L}/6\text{-311+G(2df,p)}$ level of theory was upfield-shifted compared to that of **5_p** (133.7 ppm). These calculations, in conjunction with the observed hypsochromic shift of the absorption band and the upfield-shift of ^{29}Si resonance at lower temperatures, imply that the dominant structures of **3** and **4** in solution are the *cis*-bent structures similar to **5_c** at lower temperature, while at higher temperature they are planar structures similar to **5_p** (Scheme 5-2).¹⁶ A similar equilibrium between a planar and *cis*-bent structures in solution was also observed for compound **C**.^{3g}

Table 5-1. Selected Structural Parameters and Properties of Compounds **5_p** and **5_c**

Optimized Structure^a

| 5_p | | 5_c |
|----------------------|--|----------------------|
| 2.680 | Bridgehead Si-Si /Å | 2.545 |
| 178.37 | Si-Si-C /deg | 148.87 |
| 180.00 | dihedral angle (Si ₄ ring) /deg | 158.58 |
| 0.0 | ΔG /kJ mol ⁻¹ | -3.5 |
| 562 | $\lambda_{\max}(\text{calcd})^b$ /nm | 430 |
| 133.7 | Si _{bridgehead} (calcd) ^c /ppm | -25.7 |

^aoptimized at the ω B97XD/6-311G(d)/SCRF(solvent = heptane) level of theory. ^bcalculated at the TD-M06-2X/6-311G(d) level of theory. ^ccalculated at the GIAO/M06L/6-311+G(2df,p) level of theory.

Scheme 5-2. Possible Behavior of **3** and **4** in Solution

5-3. Conclusion

In conclusion, two bicyclo[1.1.0]tetrasilanes that contain different ethynyl groups (**3** and **4**) were synthesized via direct π -extension of **1**. In the crystalline state, they both possess planar Si₄ bicyclic structures. UV-vis absorption spectra and DFT calculations indicated the presence of effective π -conjugation between an unsupported bridgehead Si-Si π -bond and the two alkynyl units. In solution, a potential equilibrium between a planar structure and a *cis*-bent structure was observed, which may represent the flexible nature of the unsupported π -bond. A compound with an unsupported Si-Si π -bond should be able to serve as a nonclassical π -unit.

5-4. Experimental Section

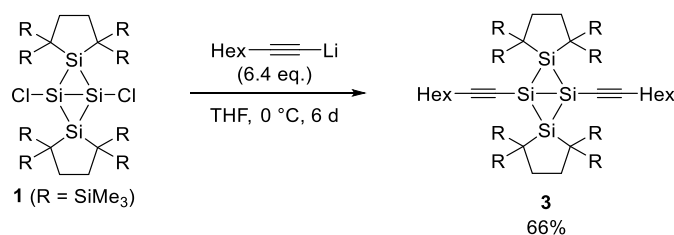
General Procedures

All reactions involving air-sensitive compounds were performed under an argon or nitrogen atmosphere using a high-vacuum line and a standard Schlenk techniques, or a glove box, as well as dry and oxygen-free solvents. Reactions at lower temperatures were performed using an EYELA PSL-1400 cryobath. NMR spectra were recorded on a Bruker Avance III 500 FT NMR spectrometer. The ^1H and ^{13}C NMR chemical shifts were referenced to residual ^1H and ^{13}C shifts of the solvents: C_6D_6 (^1H : δ 7.16 and ^{13}C : δ 128.0), toluene- d_8 (^1H : δ 2.08).¹⁷ The ^{29}Si NMR chemical shifts were relative to Me_4Si in ppm (δ 0.00). The sampling of air-sensitive compounds was carried out using a VAC NEXUS 100027 type glove box. Mass spectra were recorded on a Bruker Daltonics SolariX 9.4T spectrometer and JEOL JMS-T100GCV spectrometer. UV-vis spectra were recorded on JASCO V-770 and V-660 spectrometers. X-ray analysis was carried out using a Bruker AXS APEXII CCD diffractometer.

Materials

Dry and degassed hexane, and THF were prepared using a VAC 103991 solvent purifier. Benzene- d_6 was dried by molecular sieves 4Å after degassing through three freeze-pump-thaw cycles. Toluene- d_8 and 3-methylpentane were dried in a tube covered with potassium mirror and then distilled under reduced pressure prior to use. Hexamethyldisiloxane was dried by lithium aluminum hydride after degassing through three freeze-pump-thaw cycles. 1,3-Dichlorobicyclo[1.1.0]tetrasilane **1** was prepared according to the published procedure.^{4c} 1-Octynyllithium and lithium phenylacetylide were prepared by the reactions of the corresponding alkyne with butyl lithium in THF. 1-Octyne, phenylacetylene and butyl lithium were commercially available and used without further purification.

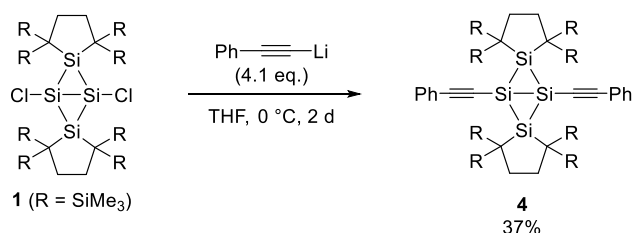
Synthesis of 1,3-Dioctynylbicyclo[1.1.0]tetrasilane **3** [TN864,865]



To a Schlenk tube (30 mL) equipped with a magnetic stir bar, 1,3-dichlorobicyclotetrasilane **1** (30.1 mg, 34.5 μmol) and 1-octynyllithium (25.5 mg, 220 μmol) were charged. To the Schlenk tube, dry and degassed THF (3.0 mL, cooled down to -27 $^{\circ}\text{C}$) was added and the mixture was stirred at 0 $^{\circ}\text{C}$ for 6 days. The color of the resulting solution turned from orange to dark red. After the volatiles were removed in vacuo at 0 $^{\circ}\text{C}$, the crude was extracted with hexane and the filtrate was concentrated in vacuo. Recrystallization from hexamethyldisiloxane provided reddish purple crystals of **3** (23.4 mg, 22.9 μmol) in 66% yield.

3: reddish purple crystals; mp 174 - 176 $^{\circ}\text{C}$ (decomp.); ^1H NMR (500 MHz, C_6D_6 , 296 K) 0.53 (s, 72H, SiCH_3), 0.91 (t, $J = 7.0$ Hz, 6H, CH_3 (octynyl)), 1.16-1.24 (m, 4H, CH_2 (octynyl)), 1.26-1.38 (m, 8H, CH_2 (octynyl)), 1.50 (tt, $J = 7.5$ Hz, $J = 7.0$ Hz, 4H, CH_2 (octynyl)), 2.05 (s, 8H, CH_2 (silacyclopentane ring)), 2.30 (t, $J = 7.0$ Hz, 4H, CH_2 (octynyl)); ^{13}C NMR (126 MHz, C_6D_6 , 297 K) 5.3 (SiCH_3), 13.8 (C), 14.5 (CH_3 (octynyl)), 21.6 (CH_2 (octynyl)), 23.2 (CH_2 (octynyl)), 28.6 (CH_2 (octynyl)), 29.2 (CH_2 (octynyl)), 31.9 (CH_2 (octynyl)), 34.9 (CH_2 (silacyclopentane ring)), 88.5 ($\text{SiC}\equiv$), 130.3 ($\text{HexC}\equiv$); ^{29}Si NMR (99 MHz, C_6D_6 , 296 K) -8.0 (Si), 4.7 (SiMe_3), 83.3 ($\text{SiC}\equiv$); UV-vis (hexane, 293 K) $\lambda_{\text{max}}/\text{nm}$ (ϵ) 518 (5.6×10^3), 475 (sh, 4.6×10^3), 340 (1.9×10^3), 248 (4.1×10^4), 212 (4.3×10^4); UV-vis (KBr matrix, 293 K) $\lambda_{\text{max}}/\text{nm}$ 552, 340, 249; HRMS (FD) Calcd for $\text{C}_{48}\text{H}_{106}\text{Si}_{12}$ [M^+], 1018.55257; Found, 1018.55232; Anal. Calcd for $\text{C}_{48}\text{H}_{106}\text{Si}_{12}$: C, 56.50; H, 10.47%. Found: C, 56.22; H, 10.78%.

Synthesis of 1,3-Diphenylethynylbicyclo[1.1.0]tetrasilane **4** [TN575,577]



To a Schlenk tube (30 mL) equipped with a magnetic stir bar, 1,3-dichlorobicyclotetrasilane **1** (30.0 mg, 34.4 μmol) and lithium phenylacetylide (17.9 mg, 142 μmol) were charged. To the Schlenk tube, dry and degassed THF (5.0 mL, cooled down to -27°C) was added and the mixture was stirred at 0°C for 2 days. The color of the resulting suspension turned from orange to purple. After the volatiles were removed in vacuo at 0°C , the crude was extracted with hexane and the filtrate was concentrated in vacuo. The residue was washed with hexane to provide a blue solid of **4** (12.9 mg, 12.8 μmol) in 37% yield.

4: a blue solid; mp $63\text{--}65^\circ\text{C}$ (decomp.); $^1\text{H NMR}$ (500 MHz, C_6D_6 , 295 K) 0.54 (s, 72H, SiCH_3), 2.05 (s, 8H, CH_2), 6.94–6.99 (m, 2H, aryl), 7.01–7.05 (m, 4H, aryl), 7.64–7.68 (m, 4H, aryl); $^{13}\text{C NMR}$ (126 MHz, C_6D_6 , 296 K) 5.2 (SiCH_3), 14.1 (C), 34.9 (CH_2), 98.6 ($\text{SiC}\equiv$), 123.8 (aryl), 127.2 ($\text{PhC}\equiv$), 128.9 (aryl), 129.5 (aryl), 131.7 (aryl); $^{29}\text{Si NMR}$ (99 MHz, C_6D_6 , 294 K) -6.1 (Si), 4.9 (SiMe_3), 91.5 ($\text{SiC}\equiv$); UV-vis (hexane, 293 K) $\lambda_{\text{max}}/\text{nm}$ (ϵ) 560 (7.8×10^3), 503 (sh, 4.9×10^3), 312 (2.4×10^4), 298 (sh, 2.2×10^4), 277 (2.2×10^4), 247 (3.8×10^4); UV-vis (KBr matrix, 293 K) $\lambda_{\text{max}}/\text{nm}$ 602, 317, 247, 214; HRMS (APCI_{positive}) Calcd for $\text{C}_{48}\text{H}_{90}\text{Si}_{12}$ [M^+], 1002.42682; Found, 1002.42718; Anal. Calcd for $\text{C}_{48}\text{H}_{90}\text{Si}_{12}$: C, 57.41; H, 9.03%. Found: C, 57.60; H, 9.22%.

NMR Spectra

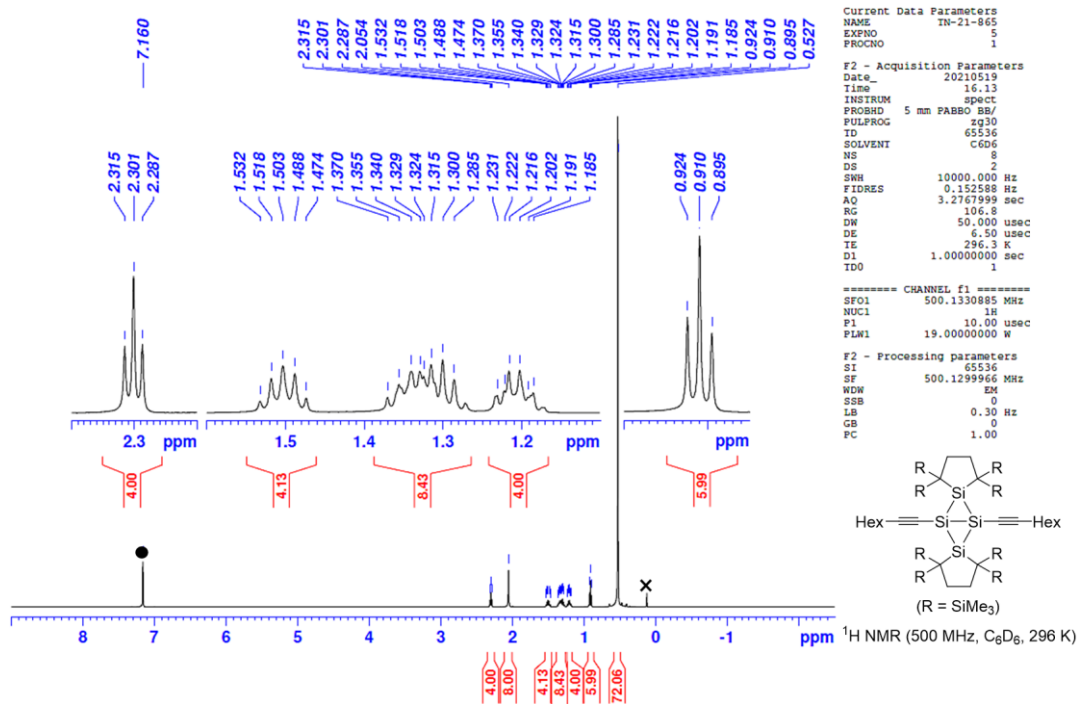


Figure 5-8. ¹H NMR spectrum of **3** in C₆D₆ at 296 K (● = C₆HD₅, x = hexamethyldisiloxane).

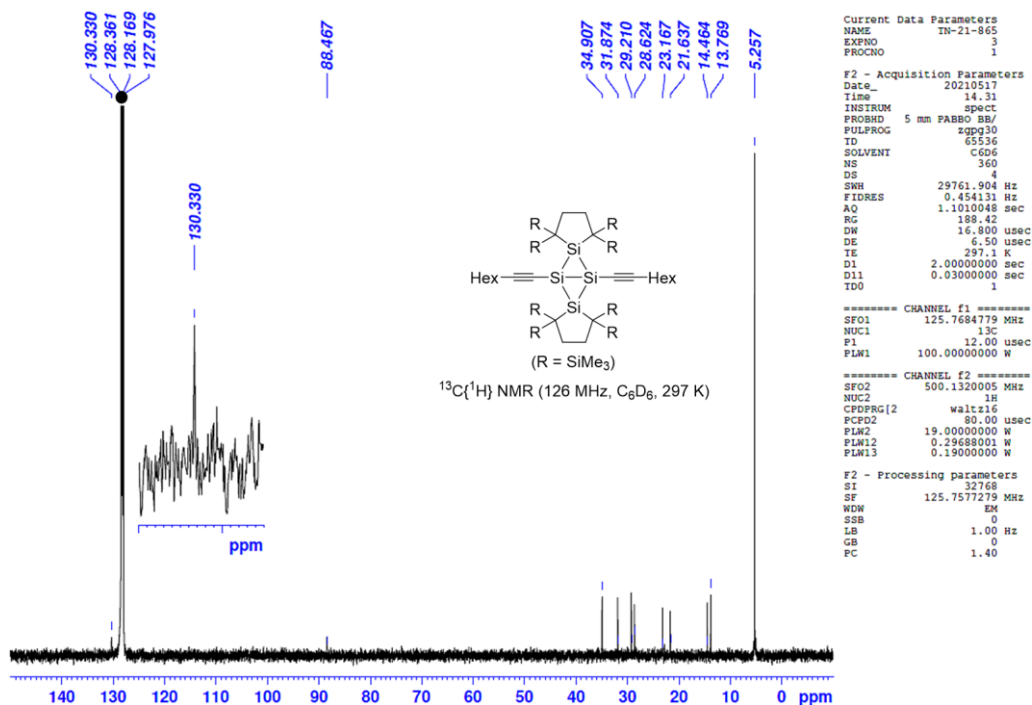


Figure 5-9. ¹³C{¹H} NMR spectrum of **3** in C₆D₆ in 297 K (● = C₆D₆).

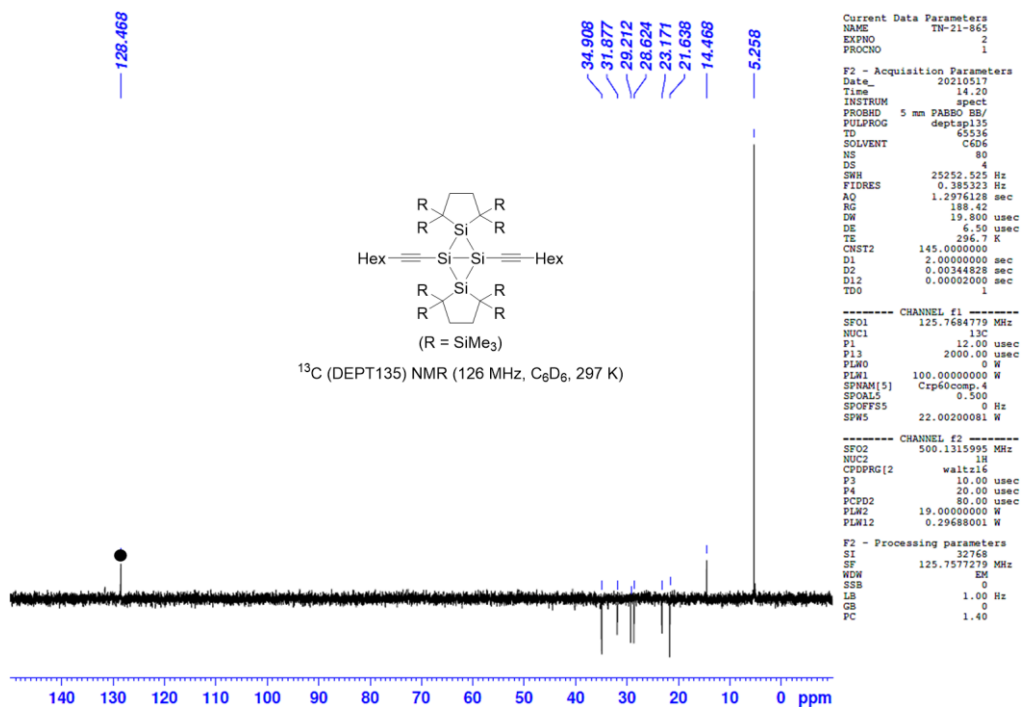


Figure 5-10. ¹³C (DEPT135) NMR spectrum of **3** in C₆D₆ at 297 K (● = C₆D₆).

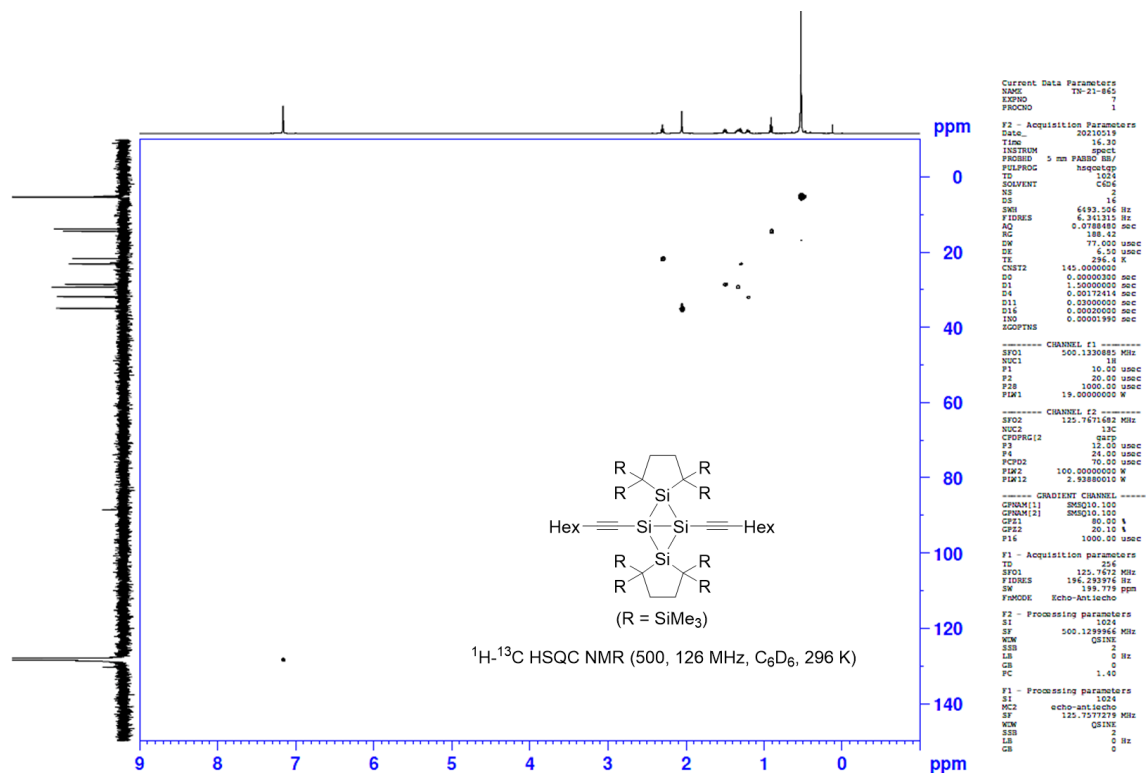


Figure 5-11. ¹H-¹³C HSQC NMR spectrum of **3** in C₆D₆ at 296 K.

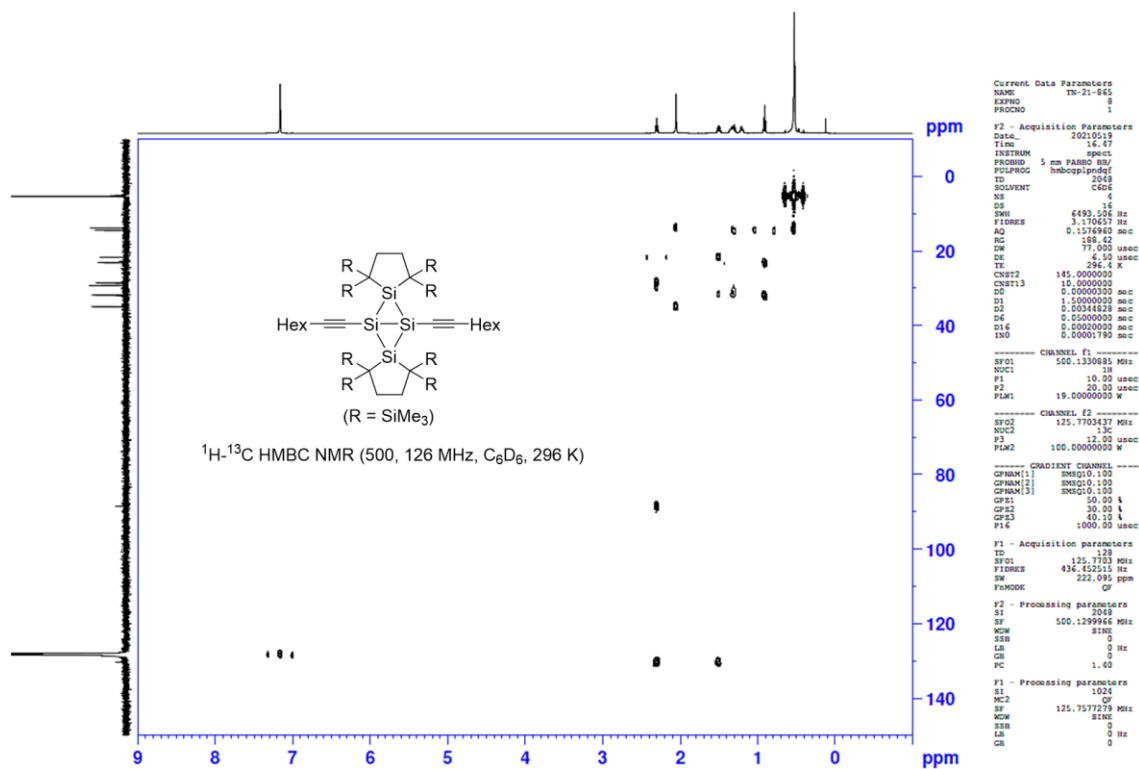


Figure 5-12. ^1H - ^{13}C HMBC NMR spectrum of **3** in C_6D_6 at 296 K.

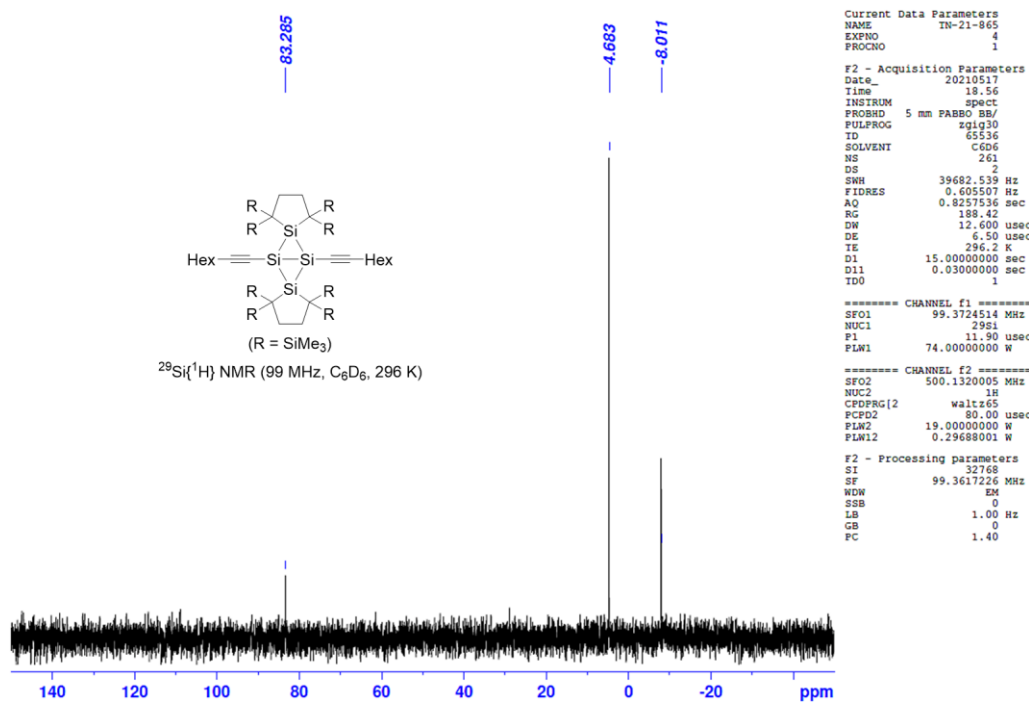


Figure 5-13. $^{29}\text{Si}\{^1\text{H}\}$ NMR spectrum of **3** in C_6D_6 at 296 K.

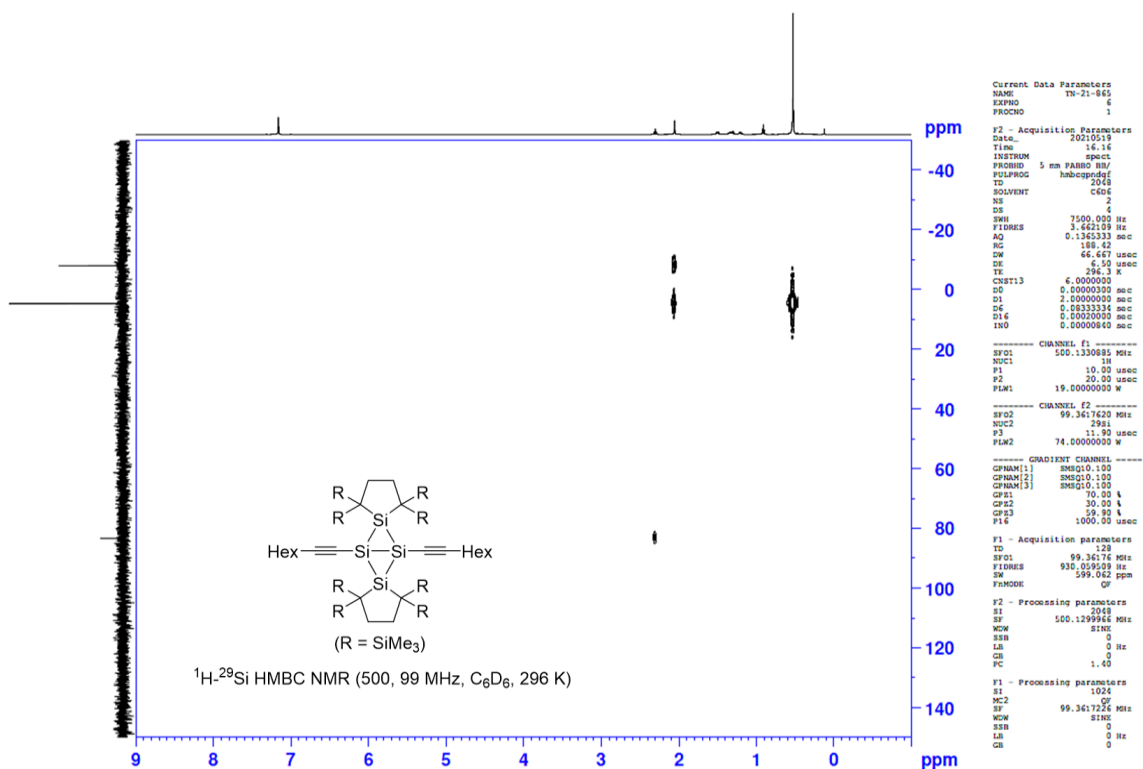


Figure 5-14. ¹H-²⁹Si HMBC NMR spectrum of **3** in C₆D₆ at 296 K.

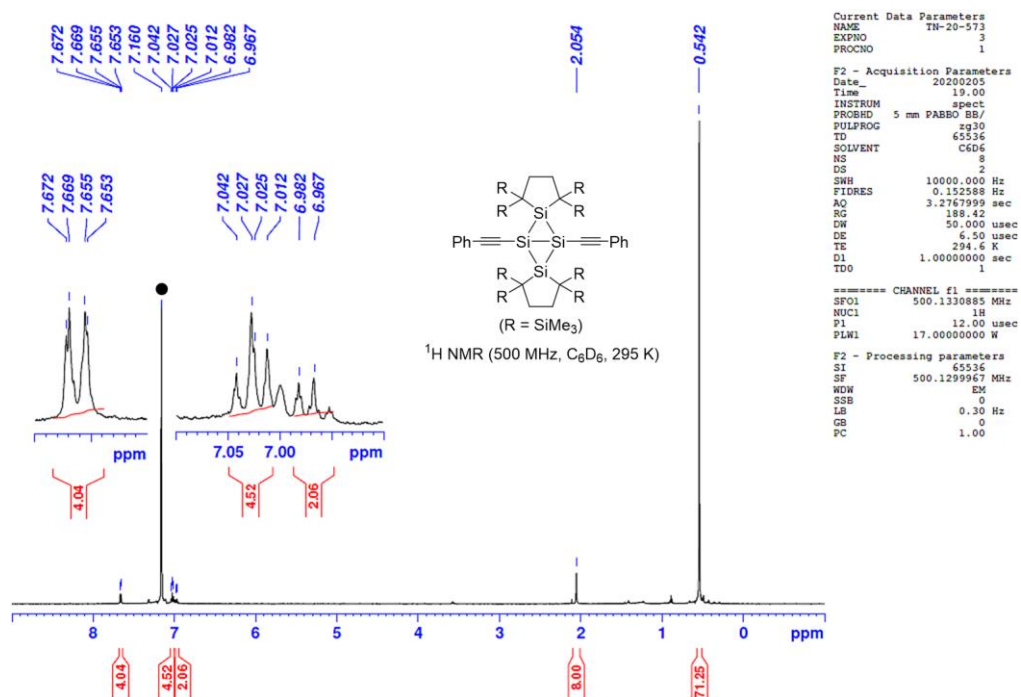


Figure 5-15. ¹H NMR spectrum of **4** in C₆D₆ at 295 K (● = C₆HD₅).

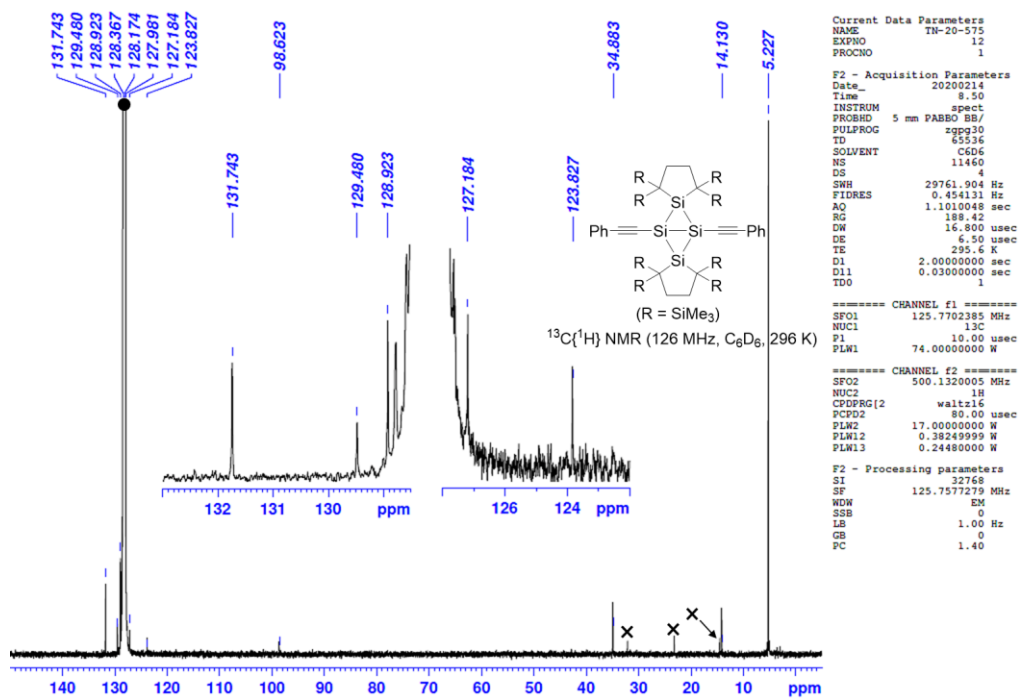


Figure 5-16. $^{13}\text{C}\{^1\text{H}\}$ NMR spectrum of **4** in C_6D_6 in 296 K (● = C_6D_6 , x = hexane).

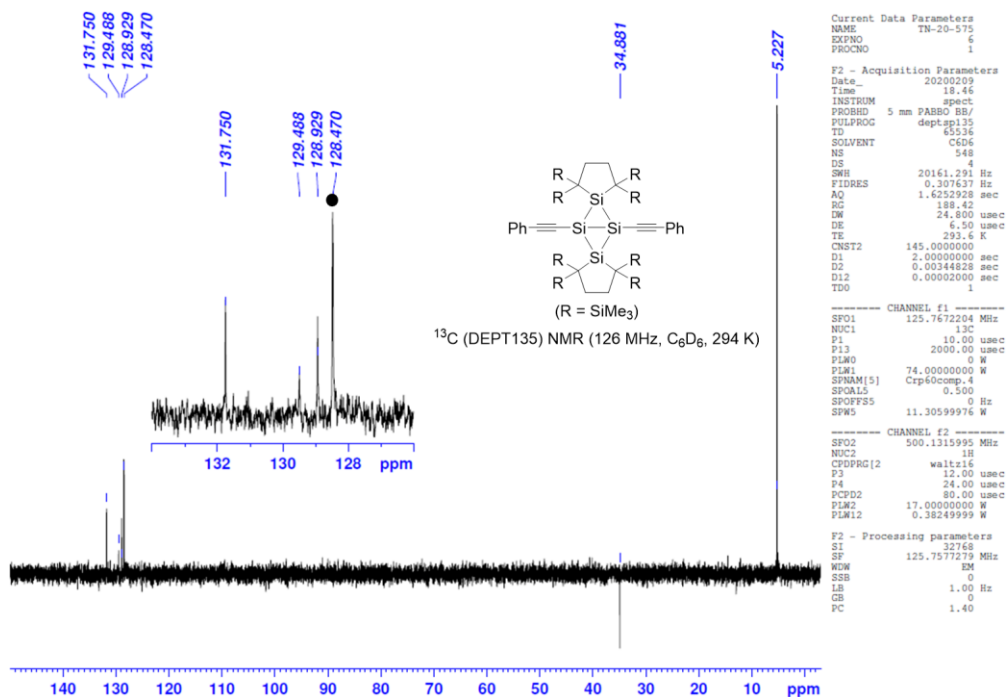


Figure 5-17. ^{13}C (DEPT135) NMR spectrum of **4** in C_6D_6 at 294 K (● = C_6D_6).

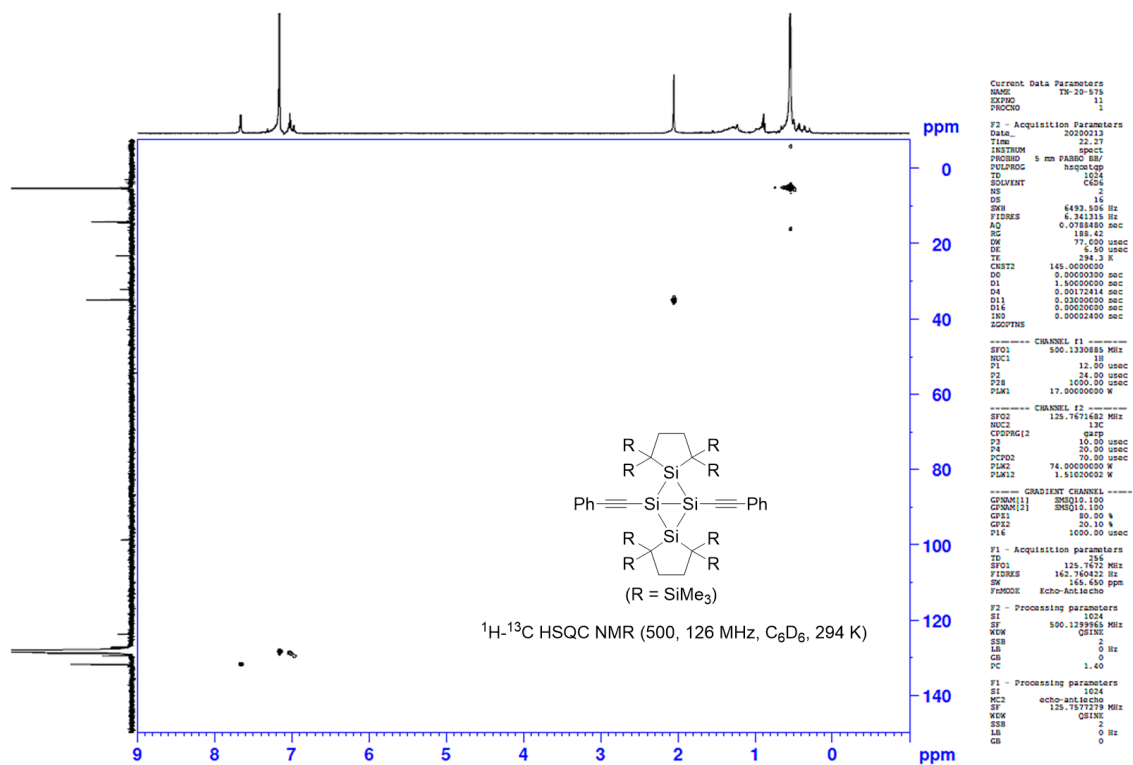


Figure 5-18. ¹H-¹³C HSQC NMR spectrum of **4** in C₆D₆ at 294 K.

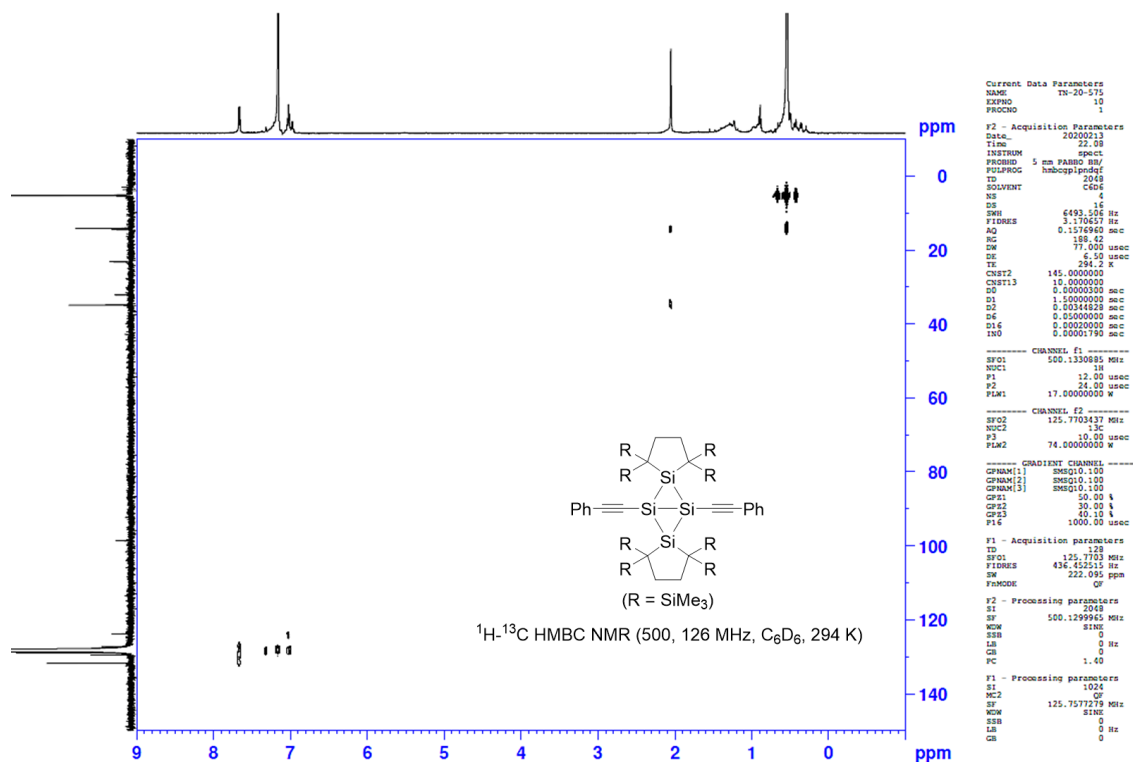


Figure 5-19. ¹H-¹³C HMBC NMR spectrum of **4** in C₆D₆ at 294 K.

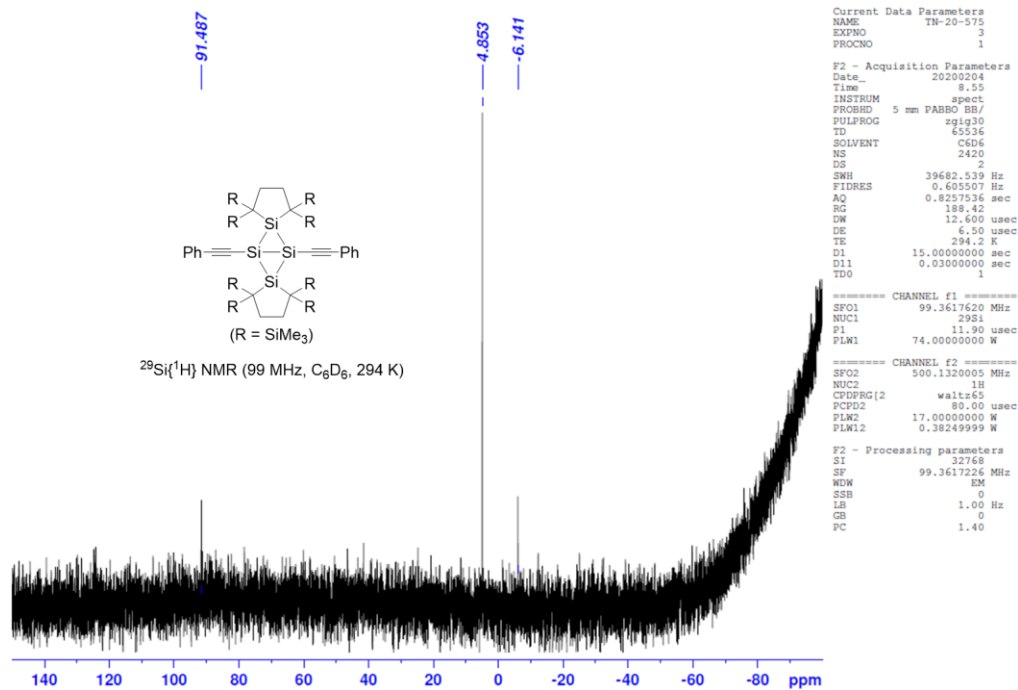


Figure 5-20. ²⁹Si{¹H} NMR spectrum of **4** in C₆D₆ at 294 K.

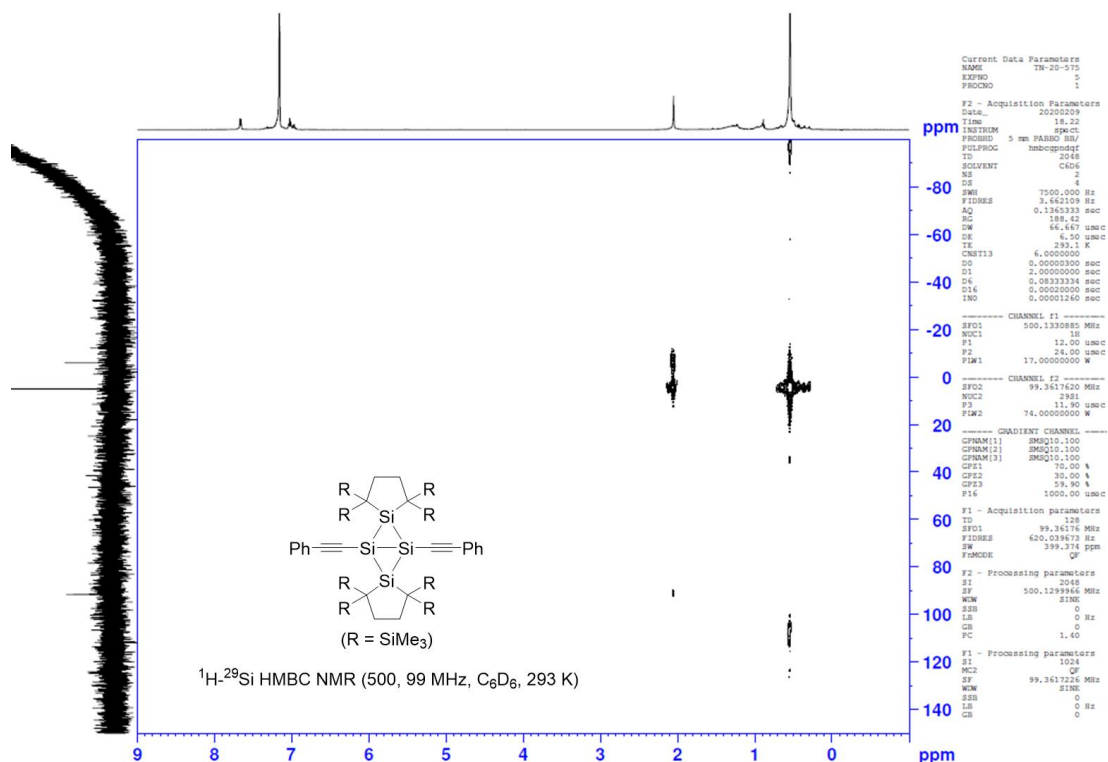


Figure 5-21. ¹H-²⁹Si HMBC NMR spectrum of **4** in C₆D₆ at 293 K.

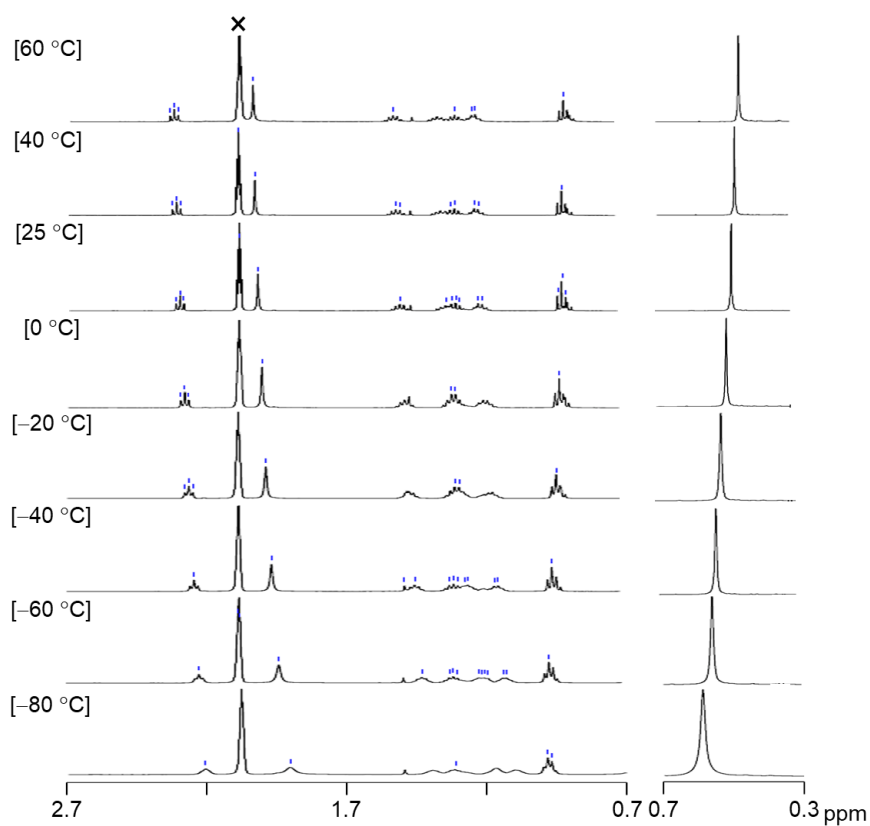


Figure 5-22. ^1H NMR spectra of **3** in toluene- d_8 at variable temperatures ($\times = \text{C}_7\text{D}_7\text{H}$).

Table 5-2. ^{29}Si Chemical Shifts of **3** at Variable Temperatures.

| Temperature/ $^{\circ}\text{C}$ | ^{29}Si chemical shift/ppm ^{a,b} | | | note |
|---------------------------------|--|-----------|-------------------|-------------|
| | Bridgehead Si | Bridge Si | SiMe ₃ | |
| 60 | 87.6 | -7.3 | 4.8 | TN880_NMR27 |
| 50 | 86.3 | -7.5 | 4.6 | TN880_NMR25 |
| 40 | 85.3 | -7.7 | 4.6 | TN880_NMR23 |
| 30 | 84.4 | -8.0 | 4.6 | TN880_NMR21 |
| 25 | 83.4 | -8.1 | 4.5 | TN880_NMR2 |
| 0 | 80.4 | -8.6 | 4.6 | TN880_NMR18 |
| -10 | 78.9 | -8.8 | 4.6 | TN880_NMR17 |
| -20 | 77.1 | -9.2 | 4.6 | TN880_NMR9 |
| -30 | 75.3 | -9.4 | 4.5 | TN880_NMR15 |
| -40 | 73.2 | -9.6 | 4.4 | TN880_NMR5 |

^aThese values were obtained by measurement of the ^1H - ^{29}Si HMBC 2D NMR spectra in toluene- d_8 . ^bSpectral resolution is 0.39 ppm.

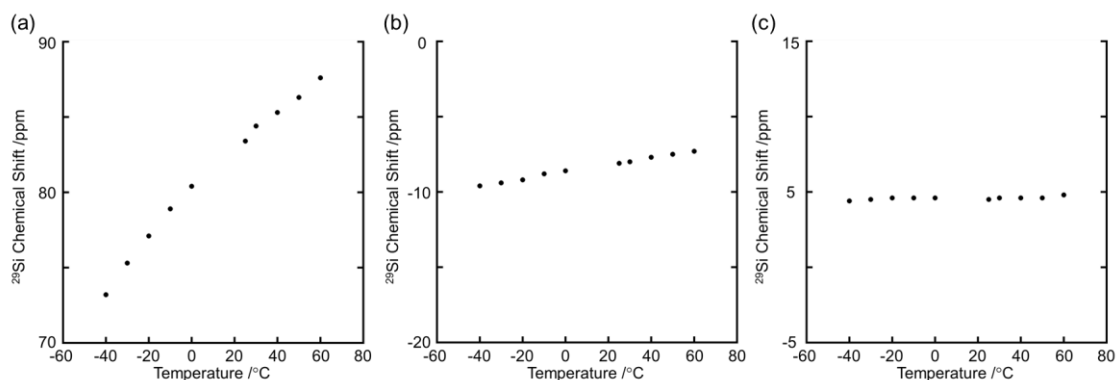


Figure 5-23. A plot of observed ^{29}Si chemical shift of **3** vs measurement temperature (a: bridgehead Si, b: bridge Si, c: SiMe_3).

X-ray Diffraction Analysis

Single crystals suitable for X-ray diffraction study were obtained by recrystallization in an inert atmosphere using the following conditions; from hexamethyldisiloxane at room temperature for **3**, from toluene at $-27\text{ }^\circ\text{C}$ for **4**. For data collection, the single crystals coated by Apiezon grease were mounted on the glass fibre and then transferred to the cold nitrogen gas stream of the diffractometer. X-ray diffraction data were collected on a Bruker AXS APEX II CCD diffractometer using a graphite monochromated $\text{Mo-K}\alpha$ radiation. An empirical absorption correction based on the multiple measurements of equivalent reflections was applied using the program SADABS¹⁸ and the structures were solved by direct methods and refined by full-matrix least squares against F^2 using all data (SHELXL-2018/3).¹⁹ Molecular structure was analysed by Yadokari-XG software.²⁰

Crystal data of **3** [tn87a] (100 K) [CCDC-2095782]: $\text{C}_{48}\text{H}_{106}\text{Si}_{12}$; Fw 1020.40; triclinic; $P-1$, $a = 11.9028(5)\text{ \AA}$, $b = 12.0034(5)\text{ \AA}$, $c = 12.1944(5)\text{ \AA}$, $\alpha = 79.1540(10)^\circ$, $\beta = 81.4440(10)^\circ$, $\gamma = 62.7870(10)^\circ$, $V = 1517.81(11)\text{ \AA}^3$, $Z = 1$, $D_{\text{calc}} = 1.116\text{ Mg/m}^3$, $R1 = 0.0304$ ($I > 2\sigma(I)$), $wR2 = 0.0786$ (all data), GOF = 1.045.

Crystal data of **4** [tn53b] (100 K) [CCDC-2095783]: $\text{C}_{48}\text{H}_{90}\text{Si}_{12}$; Fw 1004.27; monoclinic; $P2_1/c$, $a = 10.9137(5)\text{ \AA}$, $b = 23.4184(12)\text{ \AA}$, $c = 11.4842(6)\text{ \AA}$, $\beta = 90.4870(10)^\circ$, $V = 2935.0(3)\text{ \AA}^3$, $Z = 2$, $D_{\text{calc}} = 1.136\text{ Mg/m}^3$, $R1 = 0.0400$ ($I > 2\sigma(I)$), $wR2 = 0.1013$ (all data), GOF = 1.076.

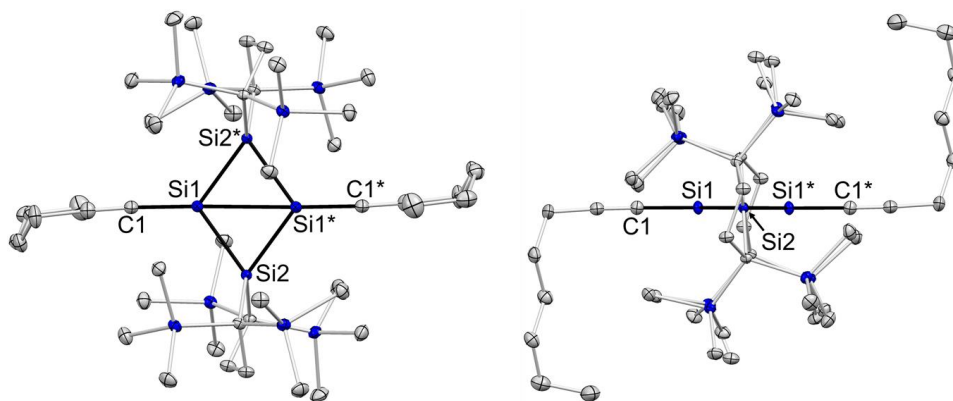


Figure 5-24. ORTEPs of **3**. Thermal ellipsoids are shown at the 50% probability level. Hydrogen atoms were omitted for clarity.

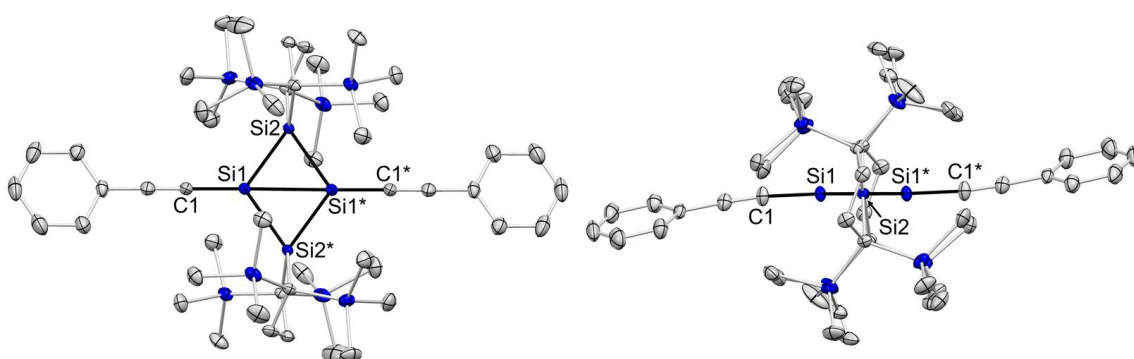


Figure 5-25. ORTEPs of **4**. Thermal ellipsoids are shown at the 50% probability level. Hydrogen atoms were omitted for clarity.

UV-vis Absorption Spectrum [TN575,840,865,867]

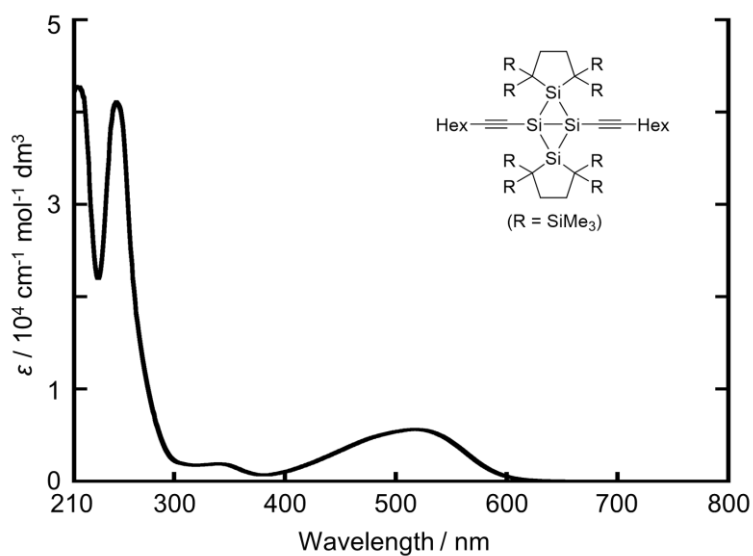


Figure 5-26. UV-vis absorption spectrum of **3** in hexane at room temperature. [TN865]

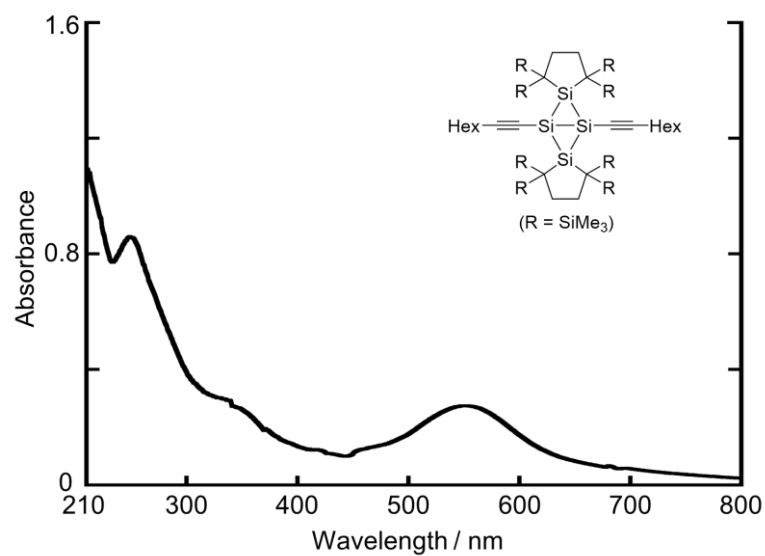


Figure 5-27. UV-vis absorption spectrum of **3** in a KBr matrix at room temperature. [TN867]

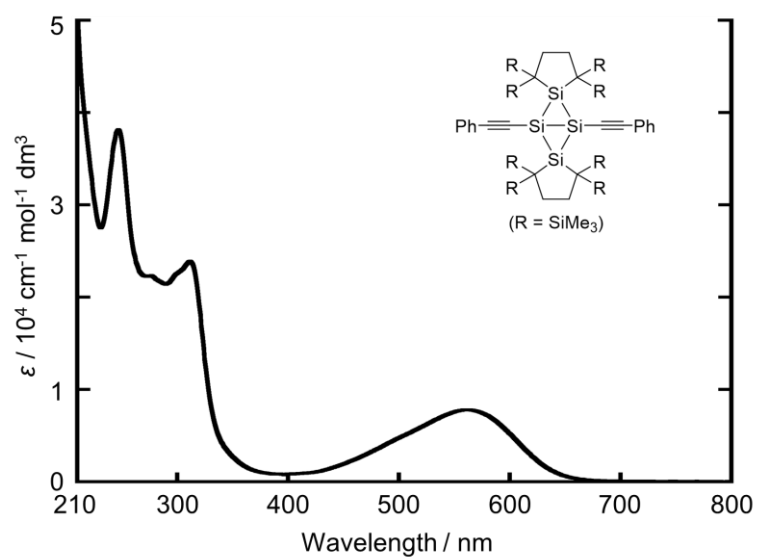


Figure 5-28. UV-vis absorption spectrum of **4** in hexane at room temperature. [TN575]

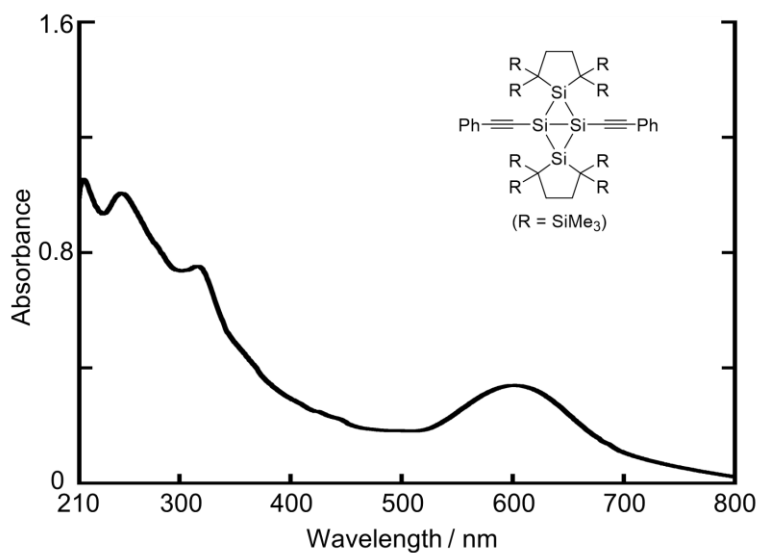


Figure 5-29. UV-vis absorption spectrum of **4** in a KBr matrix at room temperature. [TN840]

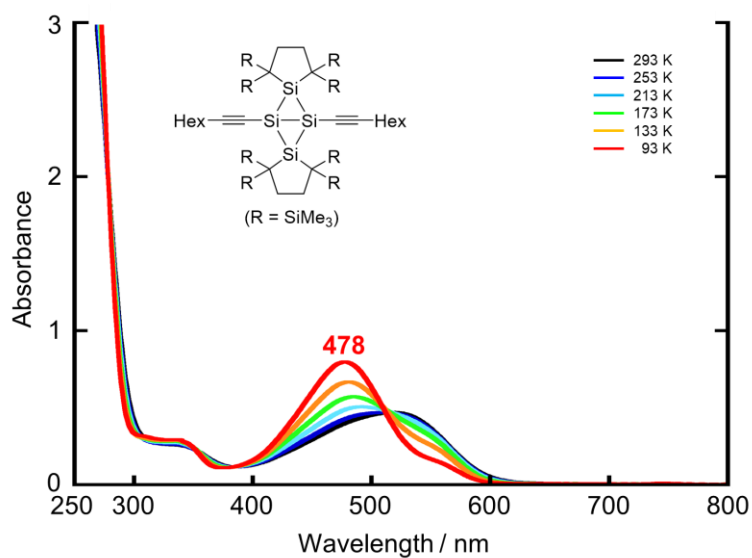


Figure 5-30. Variable-temperature UV-vis absorption spectra of **3** in 3-methylpentane at 40 K intervals from 293 K to 93 K. [TN868]

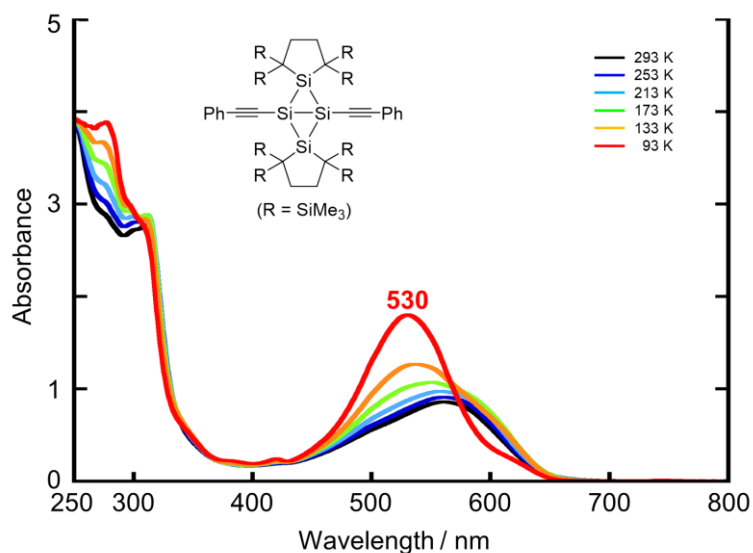
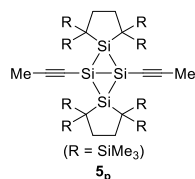


Figure 5-31. Variable-temperature UV-vis absorption spectra of **4** in 3-methylpentane at 40 K intervals from 293 K to 93 K. [TN600]

Computational Study

All theoretical calculations were performed using a Gaussian 09²¹ program or GRRM14 program.²² Geometry optimization was carried out at the ω B97XD/6-311G(d) (**3**_{opt}) and ω B97XD/6-311G(d)/SCRF(solvent = heptane) (**5**_p, **5**_c, **5'**_c, and **5''**_c) level of theory. Frontier Kohn-Sham orbitals and their energy levels of **3**_{cry}, **4**_{cry}, **5**_p, and **5**_c were shown in Figure 5-33. The atomic coordinates and energies of the optimized structures are summarized in Tables 5-3 to 5-7. Isotropic chemical shielding tensors were calculated at the GIAO/M06L/6-311+G(2df,p) level of theory (Table 5-8). Absolute isotropic shielding tensors of ²⁹Si nucleus in tetramethylsilane were calculated to be 361.4 (GIAO/M06L/6-311+G(2df,p)). Natural bond orbital (NBO)²³ calculations of **3**_{cry} and **4**_{cry} were performed at the ω B97XD/6-311G(d) level of theory. Excitation energies and oscillator strengths of **3**_{cry}, **4**_{cry}, **5**_p, and **5**_c were calculated at the M06-2X/6-311G(d) level of theory (Tables 5-9 to 5-12).

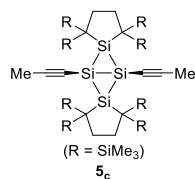
Table 5-4. Atomic Coordinates of $\mathbf{5_p}$ at the ω B97XD/6-311G(d)/SCRF(solvent = heptane) Level of Theory



| Atom | X | Y | Z |
|------|-----------------|-----------------|-----------------|
| Si | -1.331054133558 | -0.036204068321 | -0.148426239565 |
| Si | 0.032654071593 | -1.869939988902 | 0.095367941890 |
| C | -3.137542722239 | -0.043985554198 | -0.318778608211 |
| C | -4.345389218970 | -0.001098395951 | -0.400745606235 |
| C | -0.240126534784 | -3.032633113961 | 1.601726422263 |
| C | 0.501936638482 | -4.314767668018 | 1.114069022172 |
| H | 1.578514215595 | -4.201529801145 | -1.114069022172 |
| H | 0.218072057126 | -5.199359777203 | 1.692602189846 |
| C | 0.216742415279 | -4.553479049967 | -0.373211908213 |
| H | -0.811539864032 | -4.907988561337 | -0.471016608958 |
| C | 0.836039484671 | -5.378895317537 | -0.740973339337 |
| C | 0.446029284377 | -3.241099809564 | -1.206434728667 |
| Si | 2.294165866112 | -3.257800585076 | -1.714854932714 |
| C | 3.489770773757 | -3.434021522610 | -0.267920971955 |
| H | 4.506380479625 | -3.329386840958 | -0.665069091127 |
| H | 3.340204618579 | -4.419485569805 | 0.202038032272 |
| H | 3.368511149962 | -2.673678031943 | 0.502416656606 |
| C | 2.655241752951 | -4.809588838604 | -2.739996200235 |
| H | 1.920725810827 | -5.036728683020 | -3.514086259305 |
| H | 2.734712823682 | -5.691504838129 | -2.097385953563 |
| H | 3.625085988468 | -4.691914553301 | -3.235842117391 |
| C | 2.805277801650 | -1.718571137573 | -2.682184728618 |
| H | 3.723205202009 | -1.297999957686 | -2.264237844717 |
| H | 2.049973363183 | -0.931613164757 | -2.648250867652 |
| H | 2.985292263598 | -1.945119215790 | -3.735876819108 |
| Si | -0.608521176060 | -3.285620495945 | -2.819178287412 |
| C | -1.188328542731 | -5.060713650643 | -3.102480551793 |
| H | -1.970056904356 | -5.371332844406 | -2.403496898821 |
| H | -0.372261185998 | -5.784613474899 | -3.024365388099 |
| H | -1.607683704039 | -5.143981391237 | -4.110423201091 |
| C | -2.144805924174 | -2.199260041247 | -2.858881989016 |
| H | -2.675952237473 | -2.424239874578 | -3.791207312700 |
| H | -1.908755677243 | -1.133019126266 | -2.881992039448 |
| C | -2.842399142965 | -2.367530263562 | -2.040738469167 |
| C | 0.292018272395 | -2.786221595544 | -4.404427522323 |
| H | -0.432716732350 | -2.893475824262 | -5.219585079850 |
| H | 1.154766590337 | -3.401957511784 | -4.661714829626 |
| H | 0.613038810974 | -1.744615338980 | -4.402118194548 |
| Si | 0.559436407463 | -2.446252713799 | 3.228081360207 |
| C | -0.037955261033 | -0.764406414428 | 3.814972458423 |
| H | 0.655838475201 | -0.374229301530 | 4.566476753538 |
| H | -1.031045470422 | -0.789421022224 | 4.265867585610 |
| H | -0.066742192311 | -0.046726730809 | 2.993627424775 |
| C | 0.244560006217 | -3.680846096718 | 4.620034455114 |
| H | 0.573266501819 | -4.690502814250 | 4.355354802254 |
| H | -0.806008151028 | -3.737851829574 | 4.916298364441 |
| H | 0.814137295797 | -3.37518820378 | 5.504262690372 |
| C | 2.434899310686 | -2.326925651834 | 3.093574033371 |
| H | 2.774396399585 | -1.568505716555 | 2.385183419307 |
| H | 2.909573477690 | -3.274196370943 | 2.825187870319 |
| H | 2.823533808898 | -2.040527275900 | 4.077179343940 |
| Si | -2.084440133196 | -3.475984498904 | 1.883413858342 |
| C | -2.974086581781 | -2.264889289366 | 3.016666717864 |
| H | -2.871840085176 | -1.230839910089 | 2.677246674082 |
| H | -2.643274445583 | -2.314484620026 | 4.056599525856 |
| H | -4.043116586903 | -2.503064574320 | 3.004475397351 |
| C | -2.214847281676 | -5.208417969332 | 2.622857013655 |
| H | -1.553952428547 | -5.387194028826 | 3.472423941019 |
| H | -2.005310336124 | -5.975766018227 | 1.870882582301 |
| C | -3.242974816438 | -5.370534359203 | 2.964132963394 |
| H | -3.168913454514 | -3.555043770196 | 0.345282795722 |
| H | -4.116370066141 | -4.020595975234 | 0.640860910189 |
| H | -2.761350766215 | -4.154321732407 | -0.470451935813 |
| H | -3.408975360609 | -2.564154248724 | -0.039953526932 |

E+ZPVE = -4972.787402 au, Free E (298.15 K) = -4972.896005 au.
Job name: TN116db

Table 5-5. Atomic Coordinates of $\mathbf{5_c}$ at the ω B97XD/6-311G(d)/SCRF(solvent = heptane) Level of Theory



| Atom | X | Y | Z |
|------|-----------------|----------------|-----------------|
| Si | -1.270443952028 | 0.073947483656 | -0.260878495385 |
| Si | 0.103133829755 | 1.887382596035 | 0.096545600198 |
| C | -2.815720540426 | 0.191502341269 | -1.196469486215 |
| C | -3.874773589161 | 0.287632270266 | -1.774704689073 |
| C | 0.179284621581 | 3.267891998925 | -1.256860817385 |
| C | 0.797535540580 | 4.431837825224 | -0.416693216917 |
| H | 1.878328647798 | 4.302896225070 | -0.341380926931 |

| | | | | | | | |
|---|-----------------|-----------------|-----------------|---|-----------------|-----------------|-----------------|
| H | 5.423424996063 | -1.212854707601 | -3.492306029561 | H | -3.087442243816 | 4.105524159398 | 2.126964987605 |
| H | 4.396563817141 | -0.214767762449 | -4.531492727959 | H | -3.602762182884 | 3.347003347741 | 0.629370004891 |
| H | 4.316505607347 | -1.969110131368 | -4.632152815028 | H | -1.912936422429 | 3.255851156923 | 1.129931766096 |
| C | -3.280571637238 | 3.040435698348 | -2.026853941400 | C | -2.449412228028 | 1.946900726614 | 4.134581792400 |
| H | -2.574068465730 | 3.333688272559 | -1.254082486446 | H | -1.366552172642 | 1.899673144095 | 4.018459405476 |
| H | -4.296899835237 | 3.221404086224 | -1.664588475792 | H | -2.734641043669 | 1.2444982174833 | 4.920401582117 |
| H | -3.123586093402 | 3.710074197788 | -2.880297586336 | H | -2.690262196596 | 2.951822298227 | 4.498314109888 |
| C | -1.428343543923 | 1.161671226634 | -3.589457205442 | C | -5.208917912550 | 1.943910051643 | 2.925368951684 |
| H | -1.181709865742 | 2.140482198969 | -4.012091128983 | H | -5.317041452318 | 2.863096344382 | 3.510962805633 |
| H | -1.477628704664 | 0.446021238742 | -4.411967236340 | H | -5.633174235744 | 1.128930068722 | 3.516688942792 |
| H | -0.595003056651 | 0.874034165571 | -2.951066056484 | H | -5.824573088584 | 2.062259072114 | 2.028661623386 |
| C | -4.427134834235 | 1.129518448606 | -3.936562595928 | C | -4.271695243003 | -1.297660521785 | 4.238538576332 |
| H | -5.423424996063 | 1.212854707601 | -3.492306029561 | H | -4.158779887801 | -2.121482988826 | 4.951018767709 |
| H | -4.396563817141 | 0.214767762449 | -4.531492727959 | H | -5.235364191445 | -1.434394061051 | 3.737758428567 |
| H | -4.316505607347 | 1.969110131368 | -4.632152815028 | C | -4.329624848653 | -0.374000139384 | 4.818449574892 |
| C | -5.353859550829 | -1.874603247410 | -2.631372143749 | C | -2.830427191563 | -3.104330614421 | 2.348356135326 |
| H | -5.448862602506 | -2.778213567985 | -3.244228504222 | H | -1.981640426279 | -3.306667371568 | 1.691074504193 |
| H | -5.731423626301 | -1.039646975668 | -3.220677386340 | H | -3.741738674440 | -3.401106876652 | 1.828374650781 |
| H | -6.020446660749 | -2.006949330467 | -1.773524071461 | H | -2.725859804179 | -3.765180252586 | 3.216177666044 |
| C | -2.459644901310 | -2.019073857123 | -3.586723960527 | C | -1.213112191048 | -1.194258505176 | 3.915002277423 |
| H | -2.535253137680 | -3.075015417165 | -3.867900291375 | H | -1.043863533826 | -2.111953472388 | 4.487825830925 |
| H | -1.406837803797 | -1.808932878227 | -3.394996290070 | H | -1.143482723929 | -0.354765803940 | 4.604061364944 |
| H | -2.771656950921 | -1.432465627095 | -4.453551122127 | H | -0.396892536806 | -1.102697245633 | 3.19539981173 |
| C | -3.382279544207 | -3.261149944195 | -0.988990691208 | C | 0.099486007009 | 4.919819410484 | -2.621040666250 |
| H | -4.241599492030 | -3.376940263961 | -0.324831152265 | H | -0.852789674440 | 5.456074045214 | -2.604346748894 |
| H | -2.475193016818 | -3.309270548349 | -0.394207999337 | H | 0.887634266805 | 5.609912414268 | -2.309095512825 |
| C | -3.375553094908 | -4.133947910473 | -1.652124409375 | C | 0.303030031727 | 4.616078732431 | -3.651938140622 |
| C | -4.518975534219 | 0.338288986324 | -0.415959085841 | C | -0.099486007009 | -4.919819410484 | -2.621040666250 |
| H | -4.570902849191 | 1.417338294442 | -0.231507926749 | H | 0.852789674440 | -5.456074045214 | -2.604346748894 |
| H | -5.438098376580 | 0.083967240255 | -0.951547611134 | H | -0.887634266805 | -5.609912414268 | -2.309095512825 |
| C | -4.463511690828 | -0.377911098698 | 0.933177470954 | H | -0.303030031727 | -4.616078732431 | -3.651938140622 |
| H | -4.517643448594 | -1.457163688414 | 0.756671605737 | | | | |
| H | -5.340344351431 | -0.132554460561 | 1.535905075942 | | | | |
| C | -2.943603421796 | 3.226063819247 | 1.489377973526 | | | | |

E+ZPVE = -4972.783104 au, Free E (298.15 K) = -4972.888189 au.
Job name: TN124bb

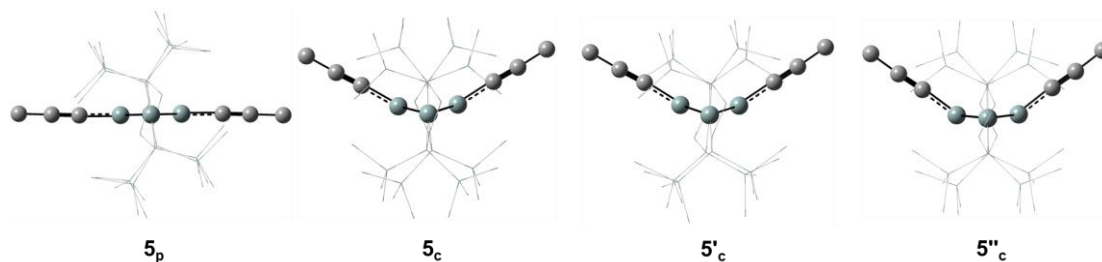


Figure 5-32. Molecular structures (side view) of 5_p , 5_c , $5'_c$, and $5''_c$ optimized at the ω B97XD/6-311G(d)/SCRF(solvent = heptane) level of theory.

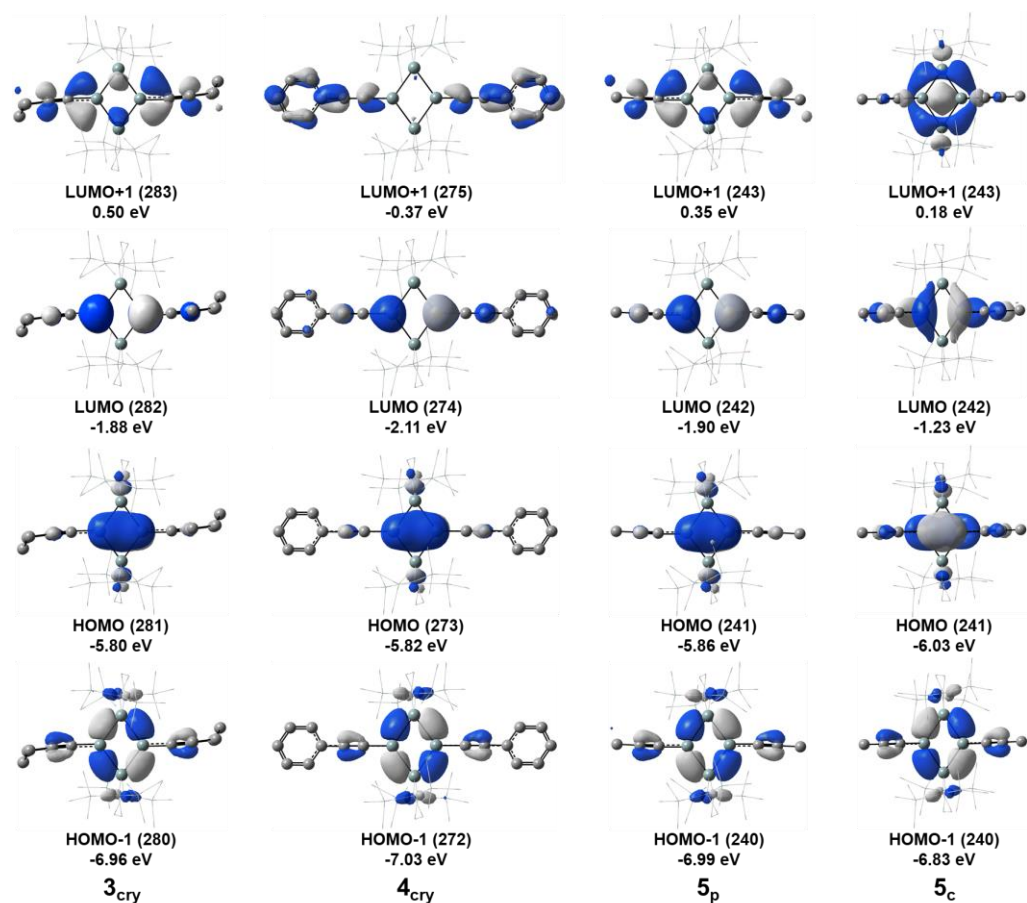


Figure 5-33. Frontier Kohn-Sham orbitals of **3_{cry}**, **4_{cry}**, **5_p**, and **5_c** at the M06-2X/6-311G(d) level of theory (isosurface level: 0.04 e·a.u.⁻³).

Table 5-8. Theoretical Isotropic ²⁹Si Chemical Shifts of **3_{cry}**, **4_{cry}**, **5_p**, **5_c**, **5'_c**, and **5''_c**

| Compound | SiMe ₃ | Bridge Si | Bridgehead Si | note |
|---------------------------------------|--------------------------|---------------|---------------|-------------------|
| 3_{cry} ^{a,b} | 7.5 (353.9) ^c | -17.1 (378.5) | 137.2 (224.2) | nmrTN120_tn87a2 |
| 4_{cry} ^{a,b} | 8.0 (353.4) ^c | -15.9 (377.3) | 129.9 (231.5) | nmr_TN100_tn53b_a |
| 5_p ^{a,b} | 3.6 (357.8) ^c | -21.3 (382.7) | 133.7 (227.7) | nmrTN116db1 |
| 5_c ^{a,b} | 2.7 (358.7) ^c | -15.3 (376.7) | -25.7 (387.1) | nmrTN117bb1 |
| 5'_c ^{a,b} | 3.6 (357.8) ^c | -16.8 (378.2) | -29.4 (390.8) | nmrTN121bb1 |
| 5''_c ^{a,b} | 3.7 (357.7) ^c | -17.5 (378.9) | -44.9 (406.3) | nmrTN124bb1 |
| | | 18.2 (343.2) | -27.4 (388.8) | |

^aGIAO/M06L/6-311+G(2df,p) level of theory. Absolute chemical shift for tetramethylsilane = 361.4. ^bThe absolute chemical shift is shown in the parentheses. ^cAverage values.

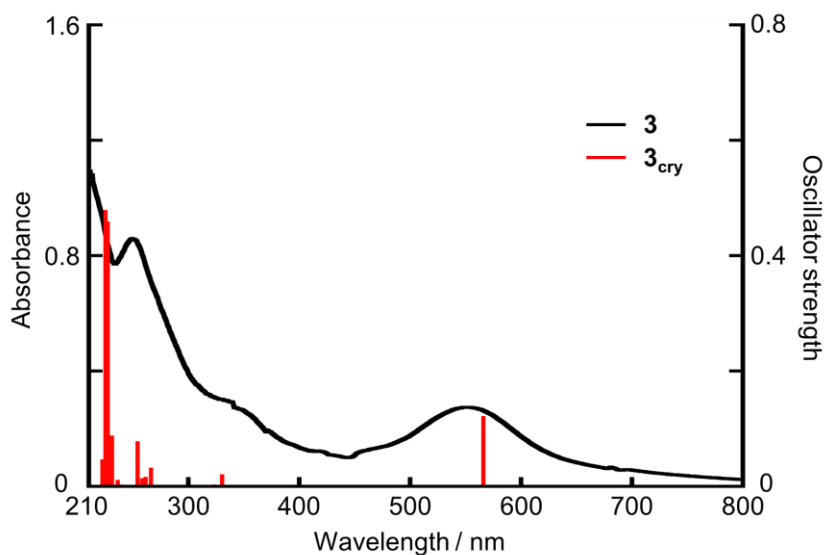


Figure 5-34. Experimental UV-vis absorption spectrum of **3** in a KBr matrix at room temperature (black) and theoretical band positions of 3_{cry} calculated at the TD-M06-2X/6-311G(d) level of theory (red bar). [tdTN120_tn87a2]

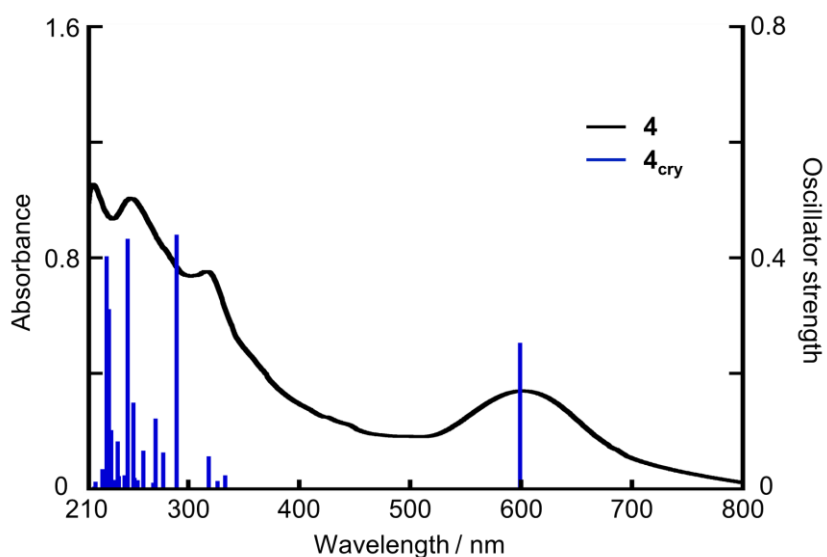


Figure 5-35. Experimental UV-vis absorption spectrum of **4** in a KBr matrix at room temperature (black) and theoretical band positions of 4_{cry} calculated at the TD-M06-2X/6-311G(d) level of theory (blue bar). [td_TN100_tn53b_d]

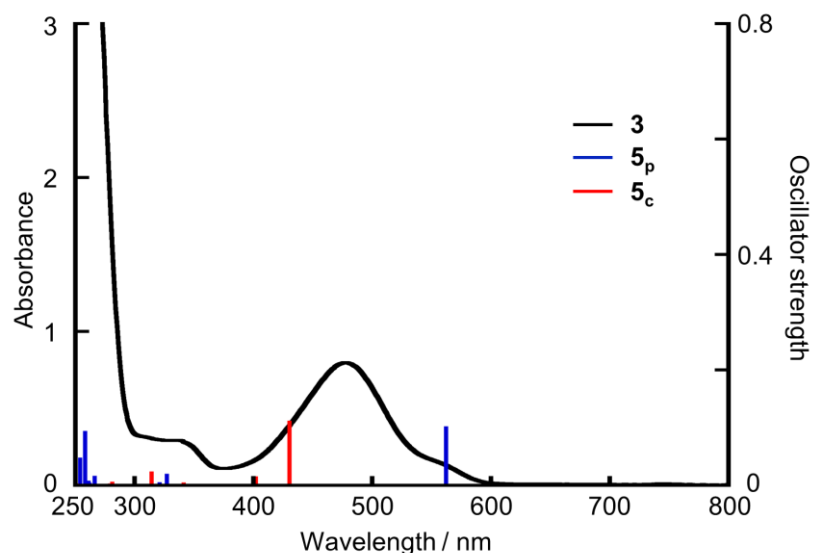


Figure 5-36. Experimental UV-vis absorption spectrum of **3** in 3-methylpentane at 93 K (black) and theoretical band positions of 5_p (blue bar) and 5_c (red bar) calculated at the TD-M06-2X/6-311G(d) level of theory. [tdTN116db1, tdTN117bb1]

Table 5-9. Transition Energy, Wavelength, and Oscillator Strengths of the Electronic Transition of 3_{cry} (The 281th orbital is highest occupied orbital shown in Figure 5-33) [tdTN120_tn87a2]

| | | | | | | | | | |
|---|-----------|-----------|-----------|----------|-------------------|-----------|-----------|-----------|----------|
| Excited State 1: | Singlet-A | 2.1894 eV | 566.29 nm | f=0.1218 | 274 -> 282 | 0.22164 | | | |
| <S**2>=0.000 | | | | | 276 -> 282 | -0.21454 | | | |
| 281 -> 282 | 0.70400 | | | | 277 -> 282 | 0.59868 | | | |
| | | | | | 280 -> 283 | -0.12008 | | | |
| This state for optimization and/or second-order correction. | | | | | | | | | |
| Total Energy, E(TD-HF/TD-KS) = -5365.40034799 | | | | | | | | | |
| Copying the excited state density for this state as the 1-particle RhoCI density. | | | | | | | | | |
| Excited State 2: | Singlet-A | 2.4748 eV | 500.98 nm | f=0.0000 | Excited State 10: | Singlet-A | 4.7524 eV | 260.89 nm | f=0.0164 |
| <S**2>=0.000 | | | | | <S**2>=0.000 | | | | |
| 280 -> 282 | 0.69830 | | | | 255 -> 282 | 0.14380 | | | |
| | | | | | 269 -> 282 | 0.31318 | | | |
| Excited State 3: | Singlet-A | 3.7583 eV | 329.90 nm | f=0.0211 | 270 -> 282 | 0.14869 | | | |
| <S**2>=0.000 | | | | | 279 -> 282 | 0.17967 | | | |
| 272 -> 282 | -0.11190 | | | | 281 -> 286 | 0.46183 | | | |
| 276 -> 282 | -0.14545 | | | | 281 -> 289 | 0.15284 | | | |
| 279 -> 282 | 0.34366 | | | | | | | | |
| 281 -> 284 | 0.56640 | | | | Excited State 11: | Singlet-A | 4.7605 eV | 260.44 nm | f=0.0000 |
| | | | | | <S**2>=0.000 | | | | |
| Excited State 4: | Singlet-A | 3.8429 eV | 322.63 nm | f=0.0034 | 256 -> 282 | -0.16463 | | | |
| <S**2>=0.000 | | | | | 257 -> 282 | 0.34415 | | | |
| 272 -> 282 | -0.10406 | | | | 269 -> 288 | 0.11172 | | | |
| 279 -> 282 | 0.51078 | | | | 273 -> 282 | 0.43028 | | | |
| 281 -> 284 | -0.38319 | | | | 275 -> 282 | -0.30276 | | | |
| 281 -> 286 | -0.18874 | | | | | | | | |
| Excited State 5: | Singlet-A | 3.8683 eV | 320.51 nm | f=0.0000 | Excited State 12: | Singlet-A | 4.7677 eV | 260.05 nm | f=0.0000 |
| <S**2>=0.000 | | | | | <S**2>=0.000 | | | | |
| 281 -> 283 | 0.69629 | | | | 257 -> 282 | 0.13972 | | | |
| | | | | | 273 -> 282 | 0.23849 | | | |
| Excited State 6: | Singlet-A | 3.9886 eV | 310.85 nm | f=0.0005 | 275 -> 282 | 0.62722 | | | |
| <S**2>=0.000 | | | | | | | | | |
| 269 -> 282 | -0.11870 | | | | Excited State 13: | Singlet-A | 4.7722 eV | 259.80 nm | f=0.0142 |
| 272 -> 282 | 0.15346 | | | | <S**2>=0.000 | | | | |
| 274 -> 282 | 0.16207 | | | | 255 -> 282 | -0.12009 | | | |
| 276 -> 282 | 0.56065 | | | | 269 -> 282 | -0.26273 | | | |
| 277 -> 282 | 0.13700 | | | | 270 -> 282 | -0.11321 | | | |
| 279 -> 282 | 0.19980 | | | | 274 -> 282 | 0.31873 | | | |
| 281 -> 286 | 0.14294 | | | | 276 -> 282 | -0.21253 | | | |
| | | | | | 277 -> 282 | -0.28704 | | | |
| Excited State 7: | Singlet-A | 4.0500 eV | 306.13 nm | f=0.0000 | 281 -> 286 | 0.31550 | | | |
| <S**2>=0.000 | | | | | 281 -> 287 | 0.12555 | | | |
| 281 -> 285 | 0.70060 | | | | | | | | |
| Excited State 8: | Singlet-A | 4.5832 eV | 270.52 nm | f=0.0000 | Excited State 14: | Singlet-A | 4.8005 eV | 258.27 nm | f=0.0142 |
| <S**2>=0.000 | | | | | <S**2>=0.000 | | | | |
| 278 -> 282 | 0.69377 | | | | 255 -> 282 | 0.11407 | | | |
| | | | | | 269 -> 282 | 0.23811 | | | |
| Excited State 9: | Singlet-A | 4.6547 eV | 266.36 nm | f=0.0325 | 270 -> 282 | 0.10089 | | | |
| <S**2>=0.000 | | | | | 274 -> 282 | 0.52493 | | | |
| | | | | | 277 -> 282 | -0.14357 | | | |
| | | | | | 281 -> 286 | -0.19927 | | | |
| | | | | | 281 -> 287 | -0.13629 | | | |

| | | | | | | | | | | | |
|-------------------------------|-----|-----------|-----------|-----------|----------|-------------------------------|-----|-----------|-----------|-----------|----------|
| Excited State <S**2>=0.000 | 15: | Singlet-A | 4.8771 eV | 254.21 nm | f=0.0782 | Excited State <S**2>=0.000 | 25: | Singlet-A | 5.4490 eV | 227.53 nm | f=0.4592 |
| 269 -> 282 | | 0.14900 | | | | 265 -> 282 | | -0.12161 | | | |
| 280 -> 285 | | 0.20220 | | | | 267 -> 282 | | 0.12269 | | | |
| 281 -> 286 | | -0.10455 | | | | 270 -> 282 | | -0.11577 | | | |
| 281 -> 287 | | 0.61429 | | | | 280 -> 285 | | 0.56332 | | | |
| | | | | | | 281 -> 287 | | -0.17080 | | | |
| Excited State <S**2>=0.000 | 16: | Singlet-A | 5.1165 eV | 242.32 nm | f=0.0000 | 281 -> 289 | | -0.11404 | | | |
| 280 -> 284 | | 0.66376 | | | | 281 -> 291 | | 0.18586 | | | |
| 281 -> 288 | | 0.11058 | | | | | | | | | |
| Excited State <S**2>=0.000 | 17: | Singlet-A | 5.2006 eV | 238.41 nm | f=0.0000 | Excited State <S**2>=0.000 | 26: | Singlet-A | 5.4997 eV | 225.44 nm | f=0.0000 |
| 259 -> 282 | | -0.22107 | | | | 280 -> 286 | | 0.62932 | | | |
| 264 -> 282 | | 0.21226 | | | | 280 -> 289 | | 0.19356 | | | |
| 268 -> 282 | | -0.29507 | | | | | | | | | |
| 271 -> 282 | | -0.23482 | | | | Excited State <S**2>=0.000 | 27: | Singlet-A | 5.5168 eV | 224.74 nm | f=0.4792 |
| 273 -> 282 | | -0.17298 | | | | 258 -> 282 | | 0.26110 | | | |
| 280 -> 284 | | -0.11026 | | | | 265 -> 282 | | 0.29279 | | | |
| 281 -> 288 | | 0.35385 | | | | 267 -> 282 | | -0.19871 | | | |
| | | | | | | 280 -> 283 | | 0.48146 | | | |
| | | | | | | 280 -> 285 | | 0.13678 | | | |
| Excited State <S**2>=0.000 | 18: | Singlet-A | 5.2046 eV | 238.22 nm | f=0.0033 | Excited State <S**2>=0.000 | 28: | Singlet-A | 5.5678 eV | 222.68 nm | f=0.0000 |
| 270 -> 282 | | 0.17445 | | | | 259 -> 282 | | -0.19050 | | | |
| 272 -> 282 | | 0.58762 | | | | 261 -> 282 | | 0.18507 | | | |
| 276 -> 282 | | -0.21049 | | | | 263 -> 282 | | 0.14678 | | | |
| 279 -> 282 | | 0.11894 | | | | 264 -> 282 | | 0.37656 | | | |
| 280 -> 283 | | 0.11051 | | | | 266 -> 282 | | -0.10314 | | | |
| | | | | | | 268 -> 282 | | 0.48430 | | | |
| Excited State <S**2>=0.000 | 19: | Singlet-A | 5.2604 eV | 235.69 nm | f=0.0115 | Excited State <S**2>=0.000 | 29: | Singlet-A | 5.5727 eV | 222.48 nm | f=0.0465 |
| 280 -> 285 | | -0.23388 | | | | 258 -> 282 | | -0.35256 | | | |
| 281 -> 289 | | -0.26698 | | | | 265 -> 282 | | 0.56120 | | | |
| 281 -> 291 | | 0.55664 | | | | 267 -> 282 | | 0.12014 | | | |
| | | | | | | 270 -> 282 | | -0.14496 | | | |
| Excited State <S**2>=0.000 | 20: | Singlet-A | 5.2709 eV | 235.23 nm | f=0.0000 | Excited State <S**2>=0.000 | 30: | Singlet-A | 5.7273 eV | 216.48 nm | f=0.0000 |
| 256 -> 282 | | 0.12117 | | | | 261 -> 282 | | 0.11943 | | | |
| 257 -> 282 | | -0.14016 | | | | 263 -> 282 | | 0.47840 | | | |
| 268 -> 282 | | 0.15479 | | | | 264 -> 282 | | -0.29406 | | | |
| 271 -> 282 | | 0.28056 | | | | 266 -> 282 | | 0.33956 | | | |
| 273 -> 282 | | 0.27884 | | | | 271 -> 282 | | -0.12746 | | | |
| 281 -> 288 | | 0.48373 | | | | | | | | | |
| Excited State <S**2>=0.000 | 21: | Singlet-A | 5.3194 eV | 233.08 nm | f=0.0000 | Excited State <S**2>=0.000 | 31: | Singlet-A | 5.7308 eV | 216.35 nm | f=0.0000 |
| 256 -> 282 | | 0.15550 | | | | 256 -> 282 | | 0.11080 | | | |
| 257 -> 282 | | -0.21130 | | | | 259 -> 282 | | 0.20557 | | | |
| 259 -> 282 | | -0.16737 | | | | 261 -> 282 | | 0.52110 | | | |
| 264 -> 282 | | 0.29810 | | | | 263 -> 282 | | 0.12175 | | | |
| 266 -> 282 | | 0.17928 | | | | 266 -> 282 | | -0.26795 | | | |
| 268 -> 282 | | -0.23600 | | | | 268 -> 282 | | -0.23503 | | | |
| 271 -> 282 | | 0.17912 | | | | | | | | | |
| 273 -> 282 | | 0.28890 | | | | | | | | | |
| 281 -> 288 | | -0.26773 | | | | | | | | | |
| Excited State <S**2>=0.000 | 22: | Singlet-A | 5.3742 eV | 230.70 nm | f=0.0880 | Excited State <S**2>=0.000 | 32: | Singlet-A | 5.7361 eV | 216.15 nm | f=0.0014 |
| 258 -> 282 | | -0.32587 | | | | 258 -> 282 | | 0.33816 | | | |
| 260 -> 282 | | -0.10605 | | | | 262 -> 282 | | 0.19579 | | | |
| 265 -> 282 | | -0.17302 | | | | 265 -> 282 | | 0.16902 | | | |
| 267 -> 282 | | 0.20476 | | | | 267 -> 282 | | 0.48797 | | | |
| 270 -> 282 | | 0.10968 | | | | 270 -> 282 | | 0.20504 | | | |
| 272 -> 282 | | -0.16309 | | | | | | | | | |
| 274 -> 282 | | 0.13197 | | | | Excited State <S**2>=0.000 | 33: | Singlet-A | 5.8225 eV | 212.94 nm | f=0.0000 |
| 280 -> 283 | | 0.42104 | | | | 257 -> 282 | | 0.12520 | | | |
| | | | | | | 259 -> 282 | | 0.12420 | | | |
| Excited State <S**2>=0.000 | 23: | Singlet-A | 5.4201 eV | 228.75 nm | f=0.0000 | 261 -> 282 | | 0.22432 | | | |
| 256 -> 282 | | -0.17279 | | | | 263 -> 282 | | -0.31923 | | | |
| 257 -> 282 | | 0.23432 | | | | 264 -> 282 | | 0.10886 | | | |
| 263 -> 282 | | 0.24785 | | | | 266 -> 282 | | 0.43929 | | | |
| 271 -> 282 | | 0.52129 | | | | 280 -> 287 | | -0.25035 | | | |
| 273 -> 282 | | -0.21217 | | | | | | | | | |
| Excited State <S**2>=0.000 | 24: | Singlet-A | 5.4285 eV | 228.39 nm | f=0.0781 | Excited State <S**2>=0.000 | 34: | Singlet-A | 5.8448 eV | 212.13 nm | f=0.0027 |
| 260 -> 282 | | -0.13783 | | | | 254 -> 282 | | 0.10154 | | | |
| 262 -> 282 | | -0.13464 | | | | 260 -> 282 | | 0.20497 | | | |
| 267 -> 282 | | -0.20803 | | | | 262 -> 282 | | 0.60464 | | | |
| 269 -> 282 | | -0.19029 | | | | 267 -> 282 | | -0.23013 | | | |
| 270 -> 282 | | 0.52955 | | | | 269 -> 282 | | -0.12183 | | | |
| 272 -> 282 | | -0.14596 | | | | | | | | | |
| 280 -> 283 | | -0.12165 | | | | Excited State <S**2>=0.000 | 35: | Singlet-A | 5.8712 eV | 211.17 nm | f=0.0000 |
| 280 -> 285 | | 0.17297 | | | | 261 -> 282 | | 0.19107 | | | |
| | | | | | | 266 -> 282 | | 0.20316 | | | |
| | | | | | | 280 -> 287 | | 0.57925 | | | |

| | | | | | | | | | | | |
|---|-----------|-----------|-----------|----------|--|-------------------|-----------|-----------|-----------|----------|--|
| 276 -> 284 | -0.16703 | | | | | 274 -> 284 | -0.12304 | | | | |
| 277 -> 284 | -0.10127 | | | | | 276 -> 284 | -0.11128 | | | | |
| 279 -> 284 | -0.10664 | | | | | 277 -> 284 | 0.24624 | | | | |
| 281 -> 294 | 0.45652 | | | | | 278 -> 285 | 0.31532 | | | | |
| 281 -> 295 | 0.38594 | | | | | 281 -> 295 | -0.28166 | | | | |
| 281 -> 297 | 0.12275 | | | | | 281 -> 297 | 0.31211 | | | | |
| 281 -> 312 | -0.10000 | | | | | 281 -> 306 | 0.12596 | | | | |
| Excited State 57: | Singlet-A | 6.5251 eV | 190.01 nm | f=0.0000 | | Excited State 62: | Singlet-A | 6.6603 eV | 186.15 nm | f=0.0001 | |
| <S**2>=0.000 | | | | | | <S**2>=0.000 | | | | | |
| 251 -> 282 | -0.18996 | | | | | 275 -> 284 | 0.14674 | | | | |
| 276 -> 283 | 0.20785 | | | | | 276 -> 283 | 0.15403 | | | | |
| 276 -> 285 | -0.33431 | | | | | 276 -> 285 | 0.28218 | | | | |
| 280 -> 289 | -0.18940 | | | | | 278 -> 284 | 0.17577 | | | | |
| 280 -> 291 | 0.40090 | | | | | 279 -> 283 | 0.15394 | | | | |
| Excited State 58: | Singlet-A | 6.5429 eV | 189.50 nm | f=0.0000 | | 281 -> 300 | 0.28868 | | | | |
| <S**2>=0.000 | | | | | | 281 -> 301 | 0.20141 | | | | |
| 241 -> 282 | -0.12968 | | | | | 281 -> 302 | 0.20002 | | | | |
| 249 -> 282 | 0.11904 | | | | | 281 -> 304 | 0.16239 | | | | |
| 251 -> 282 | 0.62977 | | | | | 281 -> 311 | 0.10881 | | | | |
| 280 -> 291 | 0.10763 | | | | | Excited State 63: | Singlet-A | 6.6607 eV | 186.14 nm | f=0.0311 | |
| Excited State 59: | Singlet-A | 6.5593 eV | 189.02 nm | f=0.0012 | | <S**2>=0.000 | | | | | |
| <S**2>=0.000 | | | | | | 274 -> 284 | -0.11544 | | | | |
| 278 -> 285 | 0.11749 | | | | | 277 -> 284 | 0.37873 | | | | |
| 281 -> 294 | -0.29651 | | | | | 278 -> 285 | 0.10598 | | | | |
| 281 -> 295 | 0.31558 | | | | | 281 -> 295 | 0.21505 | | | | |
| 281 -> 296 | 0.41927 | | | | | 281 -> 296 | -0.22102 | | | | |
| 281 -> 305 | 0.13950 | | | | | 281 -> 297 | -0.37123 | | | | |
| Excited State 60: | Singlet-A | 6.6176 eV | 187.36 nm | f=0.0000 | | 281 -> 305 | -0.10152 | | | | |
| <S**2>=0.000 | | | | | | 281 -> 308 | 0.12553 | | | | |
| 275 -> 284 | 0.11561 | | | | | Excited State 64: | Singlet-A | 6.6885 eV | 185.37 nm | f=0.0073 | |
| 276 -> 283 | -0.12246 | | | | | <S**2>=0.000 | | | | | |
| 276 -> 285 | -0.14926 | | | | | 276 -> 284 | -0.11548 | | | | |
| 278 -> 284 | 0.56146 | | | | | 277 -> 284 | 0.36359 | | | | |
| 281 -> 298 | 0.18486 | | | | | 278 -> 283 | 0.16130 | | | | |
| Excited State 61: | Singlet-A | 6.6351 eV | 186.86 nm | f=0.0162 | | 278 -> 285 | -0.34302 | | | | |
| <S**2>=0.000 | | | | | | 281 -> 296 | 0.12392 | | | | |
| 273 -> 274 | 0.70253 | | | | | 281 -> 297 | 0.23002 | | | | |
| This state for optimization and/or second-order correction. | | | | | | | | | | | |
| Total Energy, E(TD-HF/TD-KS) = -5355.85581669 | | | | | | | | | | | |
| Copying the excited state density for this state as the 1-particle RhoCl density. | | | | | | | | | | | |
| Excited State 1: | Singlet-A | 2.0683 eV | 599.46 nm | f=0.2531 | | 267 -> 274 | -0.30580 | | | | |
| <S**2>=0.000 | | | | | | 271 -> 274 | -0.34001 | | | | |
| 273 -> 274 | 0.70253 | | | | | 272 -> 275 | -0.10428 | | | | |
| Excited State 7: | | | | | | | | | | | |
| Singlet-A | | | | | | | | | | | |
| 4.0407 eV | | | | | | | | | | | |
| 306.84 nm | | | | | | | | | | | |
| f=0.0000 | | | | | | | | | | | |
| Excited State 2: | Singlet-A | 2.4338 eV | 509.42 nm | f=0.0000 | | <S**2>=0.000 | | | | | |
| <S**2>=0.000 | | | | | | 273 -> 275 | -0.16230 | | | | |
| 272 -> 274 | 0.69128 | | | | | 273 -> 277 | 0.29352 | | | | |
| Excited State 3: | Singlet-A | 3.5927 eV | 345.10 nm | f=0.0000 | | 273 -> 280 | -0.16112 | | | | |
| <S**2>=0.000 | | | | | | 273 -> 281 | 0.59153 | | | | |
| 273 -> 275 | 0.54687 | | | | | Excited State 8: | Singlet-A | 4.2487 eV | 291.81 nm | f=0.0000 | |
| 273 -> 277 | 0.39382 | | | | | <S**2>=0.000 | | | | | |
| 273 -> 280 | -0.14822 | | | | | 273 -> 275 | -0.38431 | | | | |
| Excited State 4: | Singlet-A | 3.7244 eV | 332.90 nm | f=0.0235 | | 273 -> 277 | 0.41740 | | | | |
| <S**2>=0.000 | | | | | | 273 -> 280 | -0.12836 | | | | |
| 260 -> 274 | 0.10504 | | | | | 273 -> 281 | -0.35826 | | | | |
| 265 -> 274 | -0.11439 | | | | | Excited State 9: | Singlet-A | 4.2873 eV | 289.19 nm | f=0.4400 | |
| 269 -> 274 | -0.37159 | | | | | <S**2>=0.000 | | | | | |
| 273 -> 276 | 0.15090 | | | | | 265 -> 274 | 0.24723 | | | | |
| 273 -> 278 | 0.52565 | | | | | 267 -> 274 | -0.24980 | | | | |
| Excited State 5: | Singlet-A | 3.8058 eV | 325.78 nm | f=0.0139 | | 269 -> 274 | -0.20276 | | | | |
| <S**2>=0.000 | | | | | | 271 -> 274 | 0.53926 | | | | |
| 269 -> 274 | 0.46444 | | | | | Excited State 10: | Singlet-A | 4.3311 eV | 286.26 nm | f=0.0000 | |
| 271 -> 274 | 0.17930 | | | | | <S**2>=0.000 | | | | | |
| 273 -> 278 | 0.39781 | | | | | 240 -> 274 | 0.10632 | | | | |
| 273 -> 282 | -0.16517 | | | | | 270 -> 274 | 0.64426 | | | | |
| Excited State 6: | Singlet-A | 3.8962 eV | 318.22 nm | f=0.0566 | | Excited State 11: | Singlet-A | 4.4757 eV | 277.02 nm | f=0.0634 | |
| <S**2>=0.000 | | | | | | <S**2>=0.000 | | | | | |
| 254 -> 274 | -0.11254 | | | | | 244 -> 274 | 0.10564 | | | | |
| 260 -> 274 | -0.12464 | | | | | 264 -> 274 | -0.14064 | | | | |
| 265 -> 274 | 0.40284 | | | | | 265 -> 274 | 0.13539 | | | | |

| | | | | | | | | | | |
|-------------------|----------|-----------|-----------|-----------|-------------------|-------------------|-----------|-----------|-----------|----------|
| 272 -> 275 | 0.11886 | | | | 273 -> 280 | 0.40836 | | | | |
| 273 -> 276 | 0.55163 | | | | | | | | | |
| 273 -> 278 | -0.11255 | | | | Excited State 21: | Singlet-A | 4.9528 eV | 250.33 nm | f=0.1494 | |
| 273 -> 283 | 0.13621 | | | | <S**2>=0.000 | | | | | |
| 273 -> 284 | -0.14103 | | | | 253 -> 274 | -0.10538 | | | | |
| | | | | | 262 -> 274 | -0.17485 | | | | |
| Excited State 12: | | Singlet-A | 4.4769 eV | 276.94 nm | f=0.0000 | 272 -> 275 | 0.14065 | | | |
| <S**2>=0.000 | | | | | | 272 -> 281 | -0.22063 | | | |
| 268 -> 274 | 0.68956 | | | | | 273 -> 279 | -0.15687 | | | |
| | | | | | | 273 -> 283 | 0.51844 | | | |
| Excited State 13: | | Singlet-A | 4.5948 eV | 269.83 nm | f=0.1220 | 273 -> 284 | 0.11692 | | | |
| <S**2>=0.000 | | | | | | | | | | |
| 244 -> 274 | 0.14681 | | | | Excited State 22: | Singlet-A | 5.0674 eV | 244.67 nm | f=0.4331 | |
| 253 -> 274 | 0.15208 | | | | <S**2>=0.000 | | | | | |
| 254 -> 274 | 0.12377 | | | | 244 -> 274 | -0.12720 | | | | |
| 264 -> 274 | -0.26872 | | | | 253 -> 274 | -0.22746 | | | | |
| 265 -> 274 | 0.24810 | | | | 254 -> 274 | -0.14857 | | | | |
| 267 -> 274 | 0.30395 | | | | 260 -> 274 | -0.19832 | | | | |
| 269 -> 274 | -0.12778 | | | | 272 -> 275 | 0.43787 | | | | |
| 272 -> 275 | 0.25537 | | | | 272 -> 277 | 0.19371 | | | | |
| 273 -> 276 | -0.23240 | | | | 273 -> 276 | 0.13478 | | | | |
| 273 -> 282 | -0.12188 | | | | 273 -> 283 | -0.22155 | | | | |
| Excited State 14: | | Singlet-A | 4.6313 eV | 267.71 nm | f=0.0106 | Excited State 23: | Singlet-A | 5.0972 eV | 243.24 nm | f=0.0000 |
| <S**2>=0.000 | | | | | <S**2>=0.000 | | | | | |
| 244 -> 274 | -0.10742 | | | | 272 -> 276 | 0.19025 | | | | |
| 253 -> 274 | -0.11278 | | | | 272 -> 278 | 0.64463 | | | | |
| 254 -> 274 | -0.12052 | | | | | | | | | |
| 264 -> 274 | 0.16503 | | | | Excited State 24: | Singlet-A | 5.1128 eV | 242.50 nm | f=0.0000 | |
| 265 -> 274 | 0.33405 | | | | <S**2>=0.000 | | | | | |
| 267 -> 274 | 0.46356 | | | | 243 -> 274 | -0.11701 | | | | |
| 272 -> 275 | -0.19983 | | | | 246 -> 274 | 0.21341 | | | | |
| 273 -> 276 | 0.15259 | | | | 247 -> 274 | 0.10981 | | | | |
| Excited State 15: | | Singlet-A | 4.6386 eV | 267.29 nm | f=0.0000 | 257 -> 274 | 0.13996 | | | |
| <S**2>=0.000 | | | | | 259 -> 274 | 0.23793 | | | | |
| 261 -> 274 | 0.16217 | | | | 261 -> 274 | 0.51016 | | | | |
| 266 -> 274 | 0.65404 | | | | 272 -> 276 | 0.18470 | | | | |
| Excited State 16: | | Singlet-A | 4.7365 eV | 261.76 nm | f=0.0000 | Excited State 25: | Singlet-A | 5.1273 eV | 241.81 nm | f=0.0237 |
| <S**2>=0.000 | | | | | <S**2>=0.000 | | | | | |
| 244 -> 275 | -0.10417 | | | | 245 -> 274 | -0.15853 | | | | |
| 246 -> 274 | -0.23948 | | | | 258 -> 274 | 0.28933 | | | | |
| 247 -> 274 | -0.25549 | | | | 260 -> 274 | 0.51652 | | | | |
| 253 -> 275 | -0.12415 | | | | 265 -> 274 | 0.12933 | | | | |
| 261 -> 274 | 0.39774 | | | | 269 -> 274 | 0.14885 | | | | |
| 266 -> 274 | -0.24187 | | | | 272 -> 275 | 0.15755 | | | | |
| 270 -> 274 | 0.14825 | | | | 273 -> 282 | -0.13633 | | | | |
| 272 -> 276 | -0.14520 | | | | Excited State 26: | Singlet-A | 5.2284 eV | 237.13 nm | f=0.0000 | |
| Excited State 17: | | Singlet-A | 4.7933 eV | 258.66 nm | f=0.0664 | <S**2>=0.000 | | | | |
| <S**2>=0.000 | | | | | 259 -> 274 | -0.13017 | | | | |
| 264 -> 274 | -0.22088 | | | | 262 -> 275 | -0.11177 | | | | |
| 265 -> 274 | 0.10323 | | | | 263 -> 274 | -0.43140 | | | | |
| 269 -> 274 | 0.18215 | | | | 273 -> 277 | 0.18603 | | | | |
| 273 -> 278 | 0.11476 | | | | 273 -> 280 | 0.48043 | | | | |
| 273 -> 282 | 0.56737 | | | | Excited State 27: | Singlet-A | 5.2293 eV | 237.09 nm | f=0.0222 | |
| 273 -> 285 | -0.10833 | | | | <S**2>=0.000 | | | | | |
| Excited State 18: | | Singlet-A | 4.8816 eV | 253.98 nm | f=0.0153 | 262 -> 274 | -0.43459 | | | |
| <S**2>=0.000 | | | | | 263 -> 275 | -0.11707 | | | | |
| 244 -> 274 | 0.12292 | | | | 273 -> 279 | 0.52004 | | | | |
| 253 -> 274 | 0.14658 | | | | Excited State 28: | Singlet-A | 5.2635 eV | 235.55 nm | f=0.0821 | |
| 254 -> 274 | 0.10206 | | | | <S**2>=0.000 | | | | | |
| 264 -> 274 | 0.53631 | | | | 253 -> 274 | 0.11331 | | | | |
| 265 -> 274 | 0.13823 | | | | 270 -> 277 | 0.12019 | | | | |
| 272 -> 275 | 0.22937 | | | | 273 -> 276 | 0.17137 | | | | |
| 273 -> 282 | 0.17956 | | | | 273 -> 283 | -0.11467 | | | | |
| Excited State 19: | | Singlet-A | 4.9323 eV | 251.37 nm | f=0.0192 | 273 -> 284 | 0.58527 | | | |
| <S**2>=0.000 | | | | | Excited State 29: | Singlet-A | 5.2682 eV | 235.35 nm | f=0.0000 | |
| 262 -> 274 | 0.36958 | | | | <S**2>=0.000 | | | | | |
| 262 -> 276 | 0.13036 | | | | 246 -> 274 | -0.12746 | | | | |
| 263 -> 275 | 0.19007 | | | | 249 -> 274 | 0.12082 | | | | |
| 270 -> 280 | -0.14392 | | | | 250 -> 274 | 0.12985 | | | | |
| 271 -> 279 | -0.13658 | | | | 259 -> 274 | 0.58375 | | | | |
| 273 -> 279 | 0.40983 | | | | 261 -> 274 | -0.12718 | | | | |
| 273 -> 283 | 0.23572 | | | | 272 -> 276 | -0.11797 | | | | |
| Excited State 20: | | Singlet-A | 4.9356 eV | 251.20 nm | f=0.0000 | 273 -> 280 | 0.10418 | | | |
| <S**2>=0.000 | | | | | Excited State 30: | Singlet-A | 5.3128 eV | 233.37 nm | f=0.0157 | |
| 262 -> 275 | 0.21034 | | | | <S**2>=0.000 | | | | | |
| 263 -> 274 | 0.40911 | | | | 248 -> 274 | 0.12693 | | | | |
| 263 -> 276 | 0.14436 | | | | 251 -> 274 | 0.12770 | | | | |
| 270 -> 279 | -0.17070 | | | | 254 -> 274 | 0.26577 | | | | |
| 271 -> 280 | -0.14071 | | | | 256 -> 274 | 0.12034 | | | | |
| 273 -> 277 | 0.15536 | | | | 258 -> 274 | 0.51968 | | | | |

| | | | | | | |
|-------------------|-----------|-----------|-----------|----------|------------|----------|
| 273 -> 280 | 0.11795 | | | | 269 -> 275 | -0.20496 |
| Excited State 48: | Singlet-A | 5.9102 eV | 209.78 nm | f=0.0000 | 272 -> 276 | -0.10083 |
| <S**2>=0.000 | | | | | 272 -> 283 | 0.55473 |
| | | | | | 272 -> 284 | 0.12467: |

Table 5-11. Transition Energy, Wavelength, and Oscillator Strengths of the Electronic Transition of 5_p (The 241th orbital is highest occupied orbital shown in Figure 5-33) [tdTN116db1]

| | | | | | | | | | |
|---|------------|-----------|-----------|----------|-------------------|------------|-----------|-----------|----------|
| Excited State 1: | Singlet-AU | 2.2067 eV | 561.84 nm | f=0.1023 | 223 -> 242 | 0.11513 | | | |
| <S**2>=0.000 | | | | | 230 -> 242 | -0.11841 | | | |
| 241 -> 242 | 0.70320 | | | | 231 -> 248 | 0.10068 | | | |
| This state for optimization and/or second-order correction. | | | | | 233 -> 242 | 0.35785 | | | |
| Total Energy, E(TD-HF/TD-KS) = -4973.38334234 | | | | | 236 -> 242 | 0.45293 | | | |
| Copying the excited state density for this state as the 1-particle RhoCI density. | | | | | 238 -> 242 | -0.12637 | | | |
| Excited State 2: | Singlet-AG | 2.4947 eV | 496.98 nm | f=0.0000 | Excited State 13: | Singlet-AU | 4.7500 eV | 261.02 nm | f=0.0082 |
| <S**2>=0.000 | | | | | <S**2>=0.000 | | | | |
| 240 -> 242 | 0.69761 | | | | 234 -> 242 | 0.53368 | | | |
| Excited State 3: | Singlet-AU | 3.7962 eV | 326.60 nm | f=0.0203 | 235 -> 242 | 0.10919 | | | |
| <S**2>=0.000 | | | | | 237 -> 242 | 0.39784 | | | |
| 232 -> 242 | -0.11554 | | | | 240 -> 243 | 0.11637 | | | |
| 239 -> 242 | 0.40747 | | | | Excited State 14: | Singlet-AU | 4.8080 eV | 257.87 nm | f=0.0943 |
| 241 -> 244 | 0.53048 | | | | <S**2>=0.000 | | | | |
| Excited State 4: | Singlet-AG | 3.8037 eV | 325.96 nm | f=0.0000 | 231 -> 242 | 0.17320 | | | |
| <S**2>=0.000 | | | | | 234 -> 242 | -0.11134 | | | |
| 241 -> 243 | 0.69593 | | | | 240 -> 245 | -0.13426 | | | |
| Excited State 5: | Singlet-AU | 3.8590 eV | 321.29 nm | f=0.0053 | 241 -> 246 | 0.35087 | | | |
| <S**2>=0.000 | | | | | 241 -> 247 | 0.48987 | | | |
| 239 -> 242 | 0.47933 | | | | 241 -> 250 | -0.15387 | | | |
| 241 -> 244 | -0.44044 | | | | Excited State 15: | Singlet-AU | 4.8747 eV | 254.34 nm | f=0.0481 |
| 241 -> 246 | -0.13289 | | | | <S**2>=0.000 | | | | |
| 241 -> 250 | 0.10706 | | | | 231 -> 242 | -0.13400 | | | |
| Excited State 6: | Singlet-AU | 4.0402 eV | 306.88 nm | f=0.0013 | 235 -> 242 | 0.14767 | | | |
| <S**2>=0.000 | | | | | 239 -> 242 | 0.13217 | | | |
| 231 -> 242 | 0.11222 | | | | 241 -> 246 | 0.44400 | | | |
| 232 -> 242 | -0.16820 | | | | 241 -> 247 | -0.37809 | | | |
| 234 -> 242 | -0.20897 | | | | 241 -> 250 | -0.19876 | | | |
| 235 -> 242 | 0.56404 | | | | Excited State 16: | Singlet-AG | 5.1141 eV | 242.43 nm | f=0.0000 |
| 237 -> 242 | 0.15898 | | | | <S**2>=0.000 | | | | |
| 239 -> 242 | -0.12028 | | | | 228 -> 242 | 0.16061 | | | |
| 241 -> 246 | -0.10514 | | | | 240 -> 244 | 0.36013 | | | |
| Excited State 7: | Singlet-AG | 4.1716 eV | 297.21 nm | f=0.0000 | 240 -> 247 | -0.10339 | | | |
| <S**2>=0.000 | | | | | 241 -> 248 | 0.49761 | | | |
| 241 -> 245 | 0.69945 | | | | 241 -> 249 | -0.12182 | | | |
| Excited State 8: | Singlet-AG | 4.5873 eV | 270.28 nm | f=0.0000 | Excited State 17: | Singlet-AG | 5.1658 eV | 240.01 nm | f=0.0000 |
| <S**2>=0.000 | | | | | <S**2>=0.000 | | | | |
| 236 -> 242 | 0.21117 | | | | 240 -> 244 | 0.57666 | | | |
| 238 -> 242 | 0.66342 | | | | 241 -> 248 | -0.31451 | | | |
| Excited State 9: | Singlet-AU | 4.6594 eV | 266.09 nm | f=0.0164 | Excited State 18: | Singlet-AU | 5.2126 eV | 237.85 nm | f=0.0122 |
| <S**2>=0.000 | | | | | <S**2>=0.000 | | | | |
| 234 -> 242 | -0.30170 | | | | 231 -> 242 | 0.11669 | | | |
| 235 -> 242 | -0.26762 | | | | 240 -> 245 | 0.15999 | | | |
| 237 -> 242 | 0.53884 | | | | 241 -> 250 | -0.25697 | | | |
| 240 -> 243 | -0.12741 | | | | 241 -> 251 | 0.58118 | | | |
| Excited State 10: | Singlet-AG | 4.7251 eV | 262.40 nm | f=0.0000 | Excited State 19: | Singlet-AG | 5.2389 eV | 236.66 nm | f=0.0000 |
| <S**2>=0.000 | | | | | <S**2>=0.000 | | | | |
| 217 -> 242 | 0.24737 | | | | 217 -> 242 | -0.12481 | | | |
| 230 -> 242 | 0.10699 | | | | 218 -> 242 | 0.15327 | | | |
| 233 -> 242 | -0.30194 | | | | 223 -> 242 | 0.12710 | | | |
| 236 -> 242 | 0.48650 | | | | 227 -> 242 | 0.18246 | | | |
| 238 -> 242 | -0.18233 | | | | 228 -> 242 | 0.37490 | | | |
| Excited State 11: | Singlet-AU | 4.7350 eV | 261.84 nm | f=0.0044 | 230 -> 242 | -0.29461 | | | |
| <S**2>=0.000 | | | | | 233 -> 242 | -0.22153 | | | |
| 214 -> 242 | -0.14281 | | | | 241 -> 248 | -0.28931 | | | |
| 215 -> 242 | 0.12641 | | | | Excited State 20: | Singlet-AU | 5.2443 eV | 236.41 nm | f=0.0185 |
| 231 -> 242 | 0.49660 | | | | <S**2>=0.000 | | | | |
| 232 -> 242 | -0.10758 | | | | 215 -> 242 | 0.11509 | | | |
| 237 -> 242 | -0.12469 | | | | 229 -> 242 | 0.19343 | | | |
| 239 -> 242 | 0.10400 | | | | 231 -> 242 | 0.10580 | | | |
| 240 -> 248 | 0.10915 | | | | 232 -> 242 | 0.51726 | | | |
| 241 -> 247 | -0.23882 | | | | 235 -> 242 | 0.18701 | | | |
| Excited State 12: | Singlet-AG | 4.7352 eV | 261.83 nm | f=0.0000 | 239 -> 242 | 0.12706 | | | |
| <S**2>=0.000 | | | | | 240 -> 243 | -0.24190 | | | |
| 217 -> 242 | -0.25453 | | | | 241 -> 246 | -0.10139 | | | |
| | | | | | Excited State 21: | Singlet-AG | 5.3108 eV | 233.46 nm | f=0.0000 |
| | | | | | <S**2>=0.000 | | | | |

| | | | | | | | | | | | |
|-------------------|-----------|-----------|-----------|----------|--|-------------------|-----------|-----------|-----------|----------|--|
| 240 -> 248 | 0.45150 | | | | | 227 -> 244 | -0.12293 | | | | |
| 240 -> 251 | 0.11586 | | | | | 238 -> 244 | 0.10598 | | | | |
| 241 -> 257 | -0.11601 | | | | | 240 -> 248 | 0.19594 | | | | |
| 241 -> 259 | 0.14530 | | | | | 241 -> 253 | 0.38363 | | | | |
| Excited State 33: | Singlet-A | 6.1557 eV | 201.41 nm | f=0.0084 | | 241 -> 254 | -0.20592 | | | | |
| <S**2>=0.000 | | | | | | 241 -> 257 | 0.20031 | | | | |
| 227 -> 244 | 0.10791 | | | | | 241 -> 259 | -0.22364 | | | | |
| 230 -> 242 | 0.19191 | | | | | 241 -> 260 | -0.10166 | | | | |
| 231 -> 244 | -0.12642 | | | | | Excited State 41: | Singlet-A | 6.3930 eV | 193.94 nm | f=0.0028 | |
| 232 -> 244 | 0.16159 | | | | | <S**2>=0.000 | | | | | |
| 236 -> 244 | 0.20397 | | | | | 217 -> 242 | 0.13096 | | | | |
| 238 -> 244 | 0.10803 | | | | | 224 -> 242 | 0.26177 | | | | |
| 239 -> 244 | 0.32308 | | | | | 227 -> 242 | -0.11173 | | | | |
| 240 -> 248 | -0.20623 | | | | | 229 -> 242 | 0.54406 | | | | |
| 241 -> 251 | 0.16082 | | | | | 231 -> 242 | 0.25428 | | | | |
| 241 -> 259 | -0.12785 | | | | | Excited State 42: | Singlet-B | 6.4063 eV | 193.54 nm | f=0.0127 | |
| Excited State 34: | Singlet-A | 6.1894 eV | 200.32 nm | f=0.0057 | | <S**2>=0.000 | | | | | |
| <S**2>=0.000 | | | | | | 236 -> 243 | -0.23238 | | | | |
| 222 -> 242 | -0.25156 | | | | | 238 -> 243 | 0.21292 | | | | |
| 227 -> 242 | 0.25477 | | | | | 241 -> 249 | -0.11983 | | | | |
| 229 -> 242 | -0.20912 | | | | | 241 -> 250 | -0.10328 | | | | |
| 231 -> 242 | 0.50354 | | | | | 241 -> 252 | 0.25476 | | | | |
| 232 -> 242 | 0.11570 | | | | | 241 -> 255 | 0.23456 | | | | |
| Excited State 35: | Singlet-B | 6.2363 eV | 198.81 nm | f=0.4857 | | 241 -> 256 | -0.22711 | | | | |
| <S**2>=0.000 | | | | | | 241 -> 258 | 0.25523 | | | | |
| 235 -> 243 | 0.19539 | | | | | 241 -> 262 | 0.18188 | | | | |
| 236 -> 243 | 0.36067 | | | | | 241 -> 265 | 0.12425 | | | | |
| 238 -> 243 | 0.43114 | | | | | Excited State 43: | Singlet-B | 6.4148 eV | 193.28 nm | f=0.0051 | |
| 239 -> 243 | -0.20915 | | | | | <S**2>=0.000 | | | | | |
| 241 -> 252 | 0.10600 | | | | | 219 -> 242 | -0.22667 | | | | |
| Excited State 36: | Singlet-B | 6.2608 eV | 198.03 nm | f=0.0041 | | 223 -> 242 | 0.13274 | | | | |
| <S**2>=0.000 | | | | | | 225 -> 242 | -0.32942 | | | | |
| 218 -> 244 | -0.20244 | | | | | 226 -> 242 | 0.53334 | | | | |
| 220 -> 242 | 0.15796 | | | | | Excited State 44: | Singlet-A | 6.4503 eV | 192.22 nm | f=0.0012 | |
| 222 -> 248 | 0.12876 | | | | | <S**2>=0.000 | | | | | |
| 225 -> 244 | 0.19314 | | | | | 237 -> 243 | 0.62383 | | | | |
| 227 -> 248 | -0.14076 | | | | | 237 -> 245 | 0.12165 | | | | |
| 228 -> 242 | 0.26209 | | | | | 238 -> 244 | -0.13661 | | | | |
| 228 -> 244 | 0.13556 | | | | | Excited State 45: | Singlet-B | 6.4607 eV | 191.91 nm | f=0.0227 | |
| 231 -> 248 | 0.10146 | | | | | <S**2>=0.000 | | | | | |
| 234 -> 244 | -0.20909 | | | | | 235 -> 243 | -0.11891 | | | | |
| 241 -> 252 | 0.23452 | | | | | 236 -> 243 | -0.35402 | | | | |
| Excited State 37: | Singlet-A | 6.2669 eV | 197.84 nm | f=0.0198 | | 237 -> 244 | -0.13827 | | | | |
| <S**2>=0.000 | | | | | | 238 -> 243 | 0.38769 | | | | |
| 222 -> 244 | 0.15115 | | | | | 239 -> 243 | 0.10901 | | | | |
| 227 -> 244 | -0.15810 | | | | | 241 -> 252 | -0.10980 | | | | |
| 230 -> 242 | -0.12657 | | | | | 241 -> 255 | -0.17753 | | | | |
| 236 -> 244 | 0.12234 | | | | | 241 -> 256 | 0.17873 | | | | |
| 239 -> 244 | 0.31272 | | | | | 241 -> 258 | -0.14410 | | | | |
| 239 -> 246 | -0.11686 | | | | | 241 -> 262 | -0.13429 | | | | |
| 240 -> 248 | -0.17429 | | | | | Excited State 46: | Singlet-B | 6.5334 eV | 189.77 nm | f=0.1185 | |
| 241 -> 253 | 0.18241 | | | | | <S**2>=0.000 | | | | | |
| 241 -> 254 | 0.15612 | | | | | 219 -> 242 | -0.23106 | | | | |
| 241 -> 257 | -0.14961 | | | | | 221 -> 242 | -0.12569 | | | | |
| 241 -> 259 | 0.26609 | | | | | 223 -> 242 | -0.12038 | | | | |
| Excited State 38: | Singlet-A | 6.2963 eV | 196.91 nm | f=0.0001 | | 235 -> 243 | 0.27400 | | | | |
| <S**2>=0.000 | | | | | | 236 -> 243 | -0.13518 | | | | |
| 222 -> 244 | -0.11743 | | | | | 236 -> 245 | 0.10536 | | | | |
| 227 -> 244 | 0.12281 | | | | | 239 -> 245 | 0.38377 | | | | |
| 236 -> 244 | -0.17527 | | | | | 240 -> 249 | -0.12897 | | | | |
| 238 -> 244 | -0.11199 | | | | | 241 -> 262 | -0.12000 | | | | |
| 239 -> 244 | -0.23323 | | | | | Excited State 47: | Singlet-A | 6.5393 eV | 189.60 nm | f=0.0000 | |
| 241 -> 253 | 0.48383 | | | | | <S**2>=0.000 | | | | | |
| 241 -> 254 | 0.10776 | | | | | 217 -> 242 | -0.16295 | | | | |
| 241 -> 259 | 0.13889 | | | | | 224 -> 242 | 0.55972 | | | | |
| 241 -> 260 | -0.10550 | | | | | 227 -> 242 | -0.23868 | | | | |
| Excited State 39: | Singlet-B | 6.3533 eV | 195.15 nm | f=0.0106 | | 229 -> 242 | -0.19214 | | | | |
| <S**2>=0.000 | | | | | | 230 -> 242 | 0.10426 | | | | |
| 218 -> 242 | 0.14107 | | | | | 231 -> 242 | -0.11693 | | | | |
| 219 -> 242 | 0.22938 | | | | | Excited State 48: | Singlet-B | 6.5823 eV | 188.36 nm | f=0.0023 | |
| 220 -> 242 | -0.11711 | | | | | <S**2>=0.000 | | | | | |
| 223 -> 242 | -0.17694 | | | | | 219 -> 242 | 0.25194 | | | | |
| 225 -> 242 | -0.22705 | | | | | 220 -> 242 | -0.10257 | | | | |
| 226 -> 242 | 0.11683 | | | | | 221 -> 242 | 0.27649 | | | | |
| 228 -> 242 | 0.46878 | | | | | 223 -> 242 | 0.31988 | | | | |
| 241 -> 252 | -0.10010 | | | | | 225 -> 242 | 0.17627 | | | | |
| Excited State 40: | Singlet-A | 6.3574 eV | 195.02 nm | f=0.0282 | | 226 -> 242 | 0.17458 | | | | |
| <S**2>=0.000 | | | | | | 235 -> 243 | 0.33012 | | | | |
| 222 -> 244 | 0.11124 | | | | | 238 -> 245 | -0.10267 | | | | |

| | | | | | | | | | |
|-------------------|-----------|-----------|-----------|----------|-------------------|-----------|-----------|-----------|----------|
| Excited State 49: | Singlet-B | 6.5909 eV | 188.12 nm | f=0.0212 | 241 -> 257 | -0.25178 | | | |
| <S**2>=0.000 | | | | | 241 -> 259 | -0.12517 | | | |
| 218 -> 242 | -0.15622 | | | | 241 -> 260 | 0.28491 | | | |
| 221 -> 242 | -0.15798 | | | | 241 -> 268 | 0.11867 | | | |
| 223 -> 242 | -0.13603 | | | | 241 -> 270 | 0.10813 | | | |
| 225 -> 242 | -0.25148 | | | | Excited State 57: | Singlet-A | 6.7222 eV | 184.44 nm | f=0.0068 |
| 226 -> 242 | -0.17396 | | | | <S**2>=0.000 | | | | |
| 235 -> 243 | 0.35801 | | | | 235 -> 246 | 0.10348 | | | |
| 236 -> 245 | -0.15278 | | | | 236 -> 244 | 0.10142 | | | |
| 238 -> 245 | -0.15509 | | | | 239 -> 246 | -0.16442 | | | |
| 239 -> 243 | 0.10976 | | | | 240 -> 251 | -0.12836 | | | |
| 239 -> 245 | -0.14523 | | | | 241 -> 254 | 0.36545 | | | |
| 241 -> 255 | -0.14774 | | | | 241 -> 259 | -0.20559 | | | |
| | | | | | 241 -> 260 | 0.38057 | | | |
| Excited State 50: | Singlet-A | 6.5910 eV | 188.11 nm | f=0.0014 | Excited State 58: | Singlet-A | 6.7284 eV | 184.27 nm | f=0.0332 |
| <S**2>=0.000 | | | | | <S**2>=0.000 | | | | |
| 222 -> 242 | 0.43342 | | | | 236 -> 244 | -0.10515 | | | |
| 224 -> 242 | 0.19480 | | | | 240 -> 247 | -0.23321 | | | |
| 227 -> 242 | 0.35232 | | | | 240 -> 248 | -0.11977 | | | |
| 234 -> 243 | 0.18685 | | | | 240 -> 251 | 0.50425 | | | |
| 239 -> 246 | -0.17672 | | | | 240 -> 259 | 0.10685 | | | |
| Excited State 51: | Singlet-A | 6.6125 eV | 187.50 nm | f=0.0105 | 241 -> 254 | 0.21083 | | | |
| <S**2>=0.000 | | | | | 241 -> 257 | 0.10302 | | | |
| 222 -> 242 | -0.31750 | | | | 241 -> 259 | -0.13986 | | | |
| 227 -> 242 | -0.16636 | | | | Excited State 59: | Singlet-B | 6.7481 eV | 183.73 nm | f=0.0068 |
| 234 -> 243 | 0.41592 | | | | <S**2>=0.000 | | | | |
| 235 -> 244 | -0.15740 | | | | 218 -> 242 | -0.10338 | | | |
| 238 -> 246 | 0.10956 | | | | 219 -> 242 | -0.13533 | | | |
| 239 -> 246 | -0.24134 | | | | 221 -> 242 | 0.49172 | | | |
| 241 -> 254 | -0.10410 | | | | 223 -> 242 | -0.14141 | | | |
| Excited State 52: | Singlet-B | 6.6320 eV | 186.95 nm | f=0.0047 | 225 -> 242 | -0.18242 | | | |
| <S**2>=0.000 | | | | | 226 -> 242 | -0.12894 | | | |
| 218 -> 242 | -0.13852 | | | | 238 -> 245 | -0.12120 | | | |
| 219 -> 242 | 0.36839 | | | | 241 -> 255 | 0.19509 | | | |
| 220 -> 242 | 0.32346 | | | | 241 -> 258 | -0.13185 | | | |
| 223 -> 242 | -0.35970 | | | | 241 -> 261 | 0.15142 | | | |
| 226 -> 242 | 0.19562 | | | | Excited State 60: | Singlet-A | 6.7517 eV | 183.64 nm | f=0.0135 |
| 228 -> 242 | -0.18024 | | | | <S**2>=0.000 | | | | |
| Excited State 53: | Singlet-A | 6.6437 eV | 186.62 nm | f=0.0538 | 235 -> 244 | -0.10334 | | | |
| <S**2>=0.000 | | | | | 236 -> 244 | -0.14352 | | | |
| 234 -> 243 | 0.36164 | | | | 238 -> 244 | -0.28992 | | | |
| 235 -> 246 | -0.11344 | | | | 239 -> 244 | 0.16524 | | | |
| 236 -> 244 | 0.22899 | | | | 239 -> 246 | 0.23284 | | | |
| 236 -> 246 | -0.18629 | | | | 240 -> 251 | -0.18653 | | | |
| 238 -> 244 | 0.11296 | | | | 241 -> 254 | 0.29593 | | | |
| 238 -> 246 | -0.18544 | | | | 241 -> 257 | 0.16300 | | | |
| 239 -> 244 | -0.17592 | | | | 241 -> 259 | -0.13087 | | | |
| 239 -> 246 | 0.26838 | | | | 241 -> 260 | -0.19878 | | | |
| 240 -> 248 | -0.10182 | | | | 241 -> 268 | -0.10479 | | | |
| Excited State 54: | Singlet-B | 6.6667 eV | 185.98 nm | f=0.0171 | Excited State 61: | Singlet-B | 6.7584 eV | 183.45 nm | f=0.0065 |
| <S**2>=0.000 | | | | | <S**2>=0.000 | | | | |
| 218 -> 242 | 0.27524 | | | | 221 -> 242 | -0.23518 | | | |
| 220 -> 242 | 0.13271 | | | | 225 -> 242 | 0.11679 | | | |
| 223 -> 242 | -0.11196 | | | | 239 -> 245 | -0.17798 | | | |
| 225 -> 242 | 0.10982 | | | | 241 -> 255 | 0.35334 | | | |
| 226 -> 242 | 0.11050 | | | | 241 -> 258 | -0.32191 | | | |
| 241 -> 256 | -0.12100 | | | | 241 -> 261 | 0.22636 | | | |
| 241 -> 258 | -0.27015 | | | | 241 -> 265 | -0.13869 | | | |
| 241 -> 261 | -0.19104 | | | | Excited State 62: | Singlet-A | 6.7755 eV | 182.99 nm | f=0.0088 |
| 241 -> 262 | 0.29479 | | | | <S**2>=0.000 | | | | |
| 241 -> 265 | 0.18712 | | | | 216 -> 242 | 0.19051 | | | |
| Excited State 55: | Singlet-B | 6.7094 eV | 184.79 nm | f=0.0452 | 217 -> 242 | -0.20198 | | | |
| <S**2>=0.000 | | | | | 229 -> 242 | 0.11597 | | | |
| 215 -> 242 | 0.10157 | | | | 236 -> 246 | 0.14409 | | | |
| 218 -> 242 | 0.32516 | | | | 241 -> 257 | 0.32138 | | | |
| 219 -> 242 | -0.23725 | | | | 241 -> 259 | 0.21263 | | | |
| 223 -> 242 | -0.20508 | | | | 241 -> 260 | 0.27533 | | | |
| 225 -> 242 | 0.12400 | | | | 241 -> 263 | 0.19231 | | | |
| 239 -> 245 | -0.26847 | | | | 241 -> 264 | -0.12039 | | | |
| 241 -> 258 | 0.21257 | | | | Excited State 63: | Singlet-B | 6.7827 eV | 182.79 nm | f=0.0861 |
| 241 -> 262 | -0.14316 | | | | <S**2>=0.000 | | | | |
| Excited State 56: | Singlet-A | 6.7118 eV | 184.73 nm | f=0.0410 | 240 -> 250 | 0.49767 | | | |
| <S**2>=0.000 | | | | | 240 -> 252 | -0.21626 | | | |
| 235 -> 244 | -0.12118 | | | | 240 -> 255 | 0.10366 | | | |
| 236 -> 244 | -0.11381 | | | | 240 -> 258 | 0.22370 | | | |
| 238 -> 244 | -0.23402 | | | | 241 -> 256 | 0.10299 | | | |
| 239 -> 244 | 0.15138 | | | | Excited State 64: | Singlet-A | 6.7945 eV | 182.48 nm | f=0.0191 |
| 239 -> 246 | 0.15544 | | | | <S**2>=0.000 | | | | |
| 241 -> 253 | 0.11695 | | | | 216 -> 242 | -0.29769 | | | |
| 241 -> 254 | -0.26048 | | | | | | | | |

217 -> 242 0.42491
224 -> 242 0.13779
227 -> 242 0.10817

229 -> 242 -0.15546
238 -> 246 -0.11579
241 -> 257 0.18478
241 -> 260 0.16822

5-5. Reference

- (1) For recent reviews on compounds with unsupported single π -bonds, see: (a) M. Abe, *Chem. Rev.* **2013**, *113*, 7011–7088; (b) M. Abe, R. Akisaka, *Chem. Lett.* **2017**, *46*, 1586–1592; For a study on compounds that contain multiple π -bonds unsupported by an underlying σ -bond, see: (c) E. D. Jemmis, B. Pathak, R. B. King, H. F. Schaefer, *Chem. Commun.* **2006**, 2164–2166.
- (2) (a) W. Adam, W. T. Borden, C. Burda, H. Foster, T. Heidenfelder, M. Heubes, D. A. Hrovat, F. Kita, S. B. Lewis, D. Scheutzow, J. Wirz, *J. Am. Chem. Soc.* **1998**, *120*, 593–594; (b) M. Abe, W. Adam, W. M. Nau, *J. Am. Chem. Soc.* **1998**, *120*, 11304–11310; (c) Y. Harada, Z. Wang, S. Kumashiro, S. Hatano, M. Abe, *Chem. Eur. J.* **2018**, *24*, 14808–14815; (d) R. Akisaka, M. Abe, *Chem. Asian J.* **2019**, *14*, 4223–4228; (e) Z. Wang, R. Akisaka, S. Yabumoto, T. Nakagawa, S. Hatano, M. Abe, *Chem. Sci.* **2021**, *12*, 613–625; (f) Y. Miyazawa, Z. Wang, M. Matsumoto, S. Hatano, I. Antol, E. Kayahara, S. Yamago, M. Abe, *J. Am. Chem. Soc.* **2021**, *143*, 7426–7439. See also, ref. 1.
- (3) (a) D. Scheschkewitz, H. Amii, H. Gornitzka, W. W. Schoeller, D. Bourissou, G. Bertrand, *Science* **2002**, *295*, 1880–1881; (b) M. Seierstad, C. R. Kinsinger, C. J. Cramer, *Angew. Chem., Int. Ed.* **2002**, *41*, 3894–3896; (c) W. W. Schoeller, A. Rozhenko, D. Bourissou, G. Bertrand, *Chem. Eur. J.* **2003**, *9*, 3611–3617; (d) M.-J. Cheng, C.-H. Hu, *Mol. Phys.* **2003**, *101*, 1319–1323; (e) D. Scheschkewitz, H. Amii, H. Gornitzka, W. W. Schoeller, D. Bourissou, G. Bertrand, *Angew. Chem., Int. Ed.* **2004**, *43*, 585–587; (f) A. Rodriguez, F. S. Tham, W. W. Schoeller, G. Bertrand, *Angew. Chem., Int. Ed.* **2004**, *43*, 4876–4880; (g) A. Rodriguez, R. A. Olsen, N. Ghaderi, D. Scheschkewitz, F. S. Tham, L. J. Mueller, G. Bertrand, *Angew. Chem., Int. Ed.* **2004**, *43*, 4880–4883.

- (4) (a) T. Nukazawa, T. Kosai, S. Honda, S. Ishida, T. Iwamoto, *Dalton Trans.* **2019**, 48, 10874–10880; (b) T. Nukazawa, T. Iwamoto, *J. Am. Chem. Soc.* **2020**, 142, 9920–9924; (c) T. Nukazawa, T. Iwamoto, *Dalton Trans.* **2020**, 49, 16728–16735.
- (5) C. B. Yildiz, K. I. Leszczyńska, S. González-Gallardo, M. Zimmer, A. Azizoglu, T. Biskup, C. W. M. Kay, V. Huch, H. S. Rzepa, D. Scheschkewitz, *Angew. Chem., Int. Ed.* **2020**, 59, 15087–15092.
- (6) (a) S. Kyushin, Y. Kurosaki, K. Otsuka, H. Imai, S. Ishida, T. Kyomen, M. Hanaya, H. Matsumoto, *Nat. Commun.* **2020**, 11, 4009; (b) C. Foroutan-Nejad, *Nat. Commun.* **2021**, 12, 4037; (c) S. Kyushin, Y. Kurosaki, K. Otsuka, H. Imai, S. Ishida, T. Kyomen, M. Hanaya, H. Matsumoto, *Nat. Commun.* **2021**, 12, 4036.
- (7) M. Kaftory, M. Kapon, M. Botoshansky, in *The Chemistry of Organic Silicon Compounds*, ed. Z. Rappoport, Y. Apeloig, Wiley, Chichester, **1998**, vol. 2, pp. 181–265.
- (8) (a) S. Masamune, Y. Kabe, S. Collins, D. J. Williams, R. Jones, *J. Am. Chem. Soc.* **1985**, 107, 5552–5553; (b) R. Jones, D. J. Williams, Y. Kabe, S. Masamune, *Angew. Chem., Int. Ed. Engl.* **1986**, 25, 173–174; (c) K. Takanashi, V. Ya Lee, M. Ichinohe, A. Sekiguchi, *Chem. Lett.* **2007**, 36, 1158–1159; (d) K. Ueba-Ohshima, T. Iwamoto, M. Kira, *Organometallics* **2008**, 27, 320–323; (e) T. Iwamoto, N. Akasaka, S. Ishida, *Nat. Commun.* **2014**, 5, 5353.
- (9) K. Uchiyama, S. Nagendran, S. Ishida, T. Iwamoto, M. Kira, *J. Am. Chem. Soc.* **2007**, 129, 10638–10639.
- (10) During the preparation of this manuscript, Scheschkewitz et al. reported the metathesis reaction of 1-chloro germadisilabicyclo[1.1.0]butane with nucleophiles; for details, see: P. K. Majhi, M. Zimmer, B. Morgenstern, D. Scheschkewitz, *J. Am. Chem. Soc.* **2021**, 143, 8981–8986.
- (11) In the crystalline state, apparent π – π interactions were not observed for **4** (the shortest intermolecular CPh \cdots CPh distance: 3.75 Å).

- (12) J. Bruckmann, C. Krüger, *Acta Crystallogr., Sect. C: Cryst. Struct. Commun.* **1997**, *53*, 1845–1846.
- (13) T. Sato, Y. Mizuhata, N. Tokitoh, *Chem. Commun.* **2010**, *46*, 4402–4404.
- (14) For details of the calculations, see the Experimental Section.
- (15) The values of the ^{29}Si NMR resonances were obtained from the ^1H - ^{29}Si HMBC 2D NMR spectra in C_7D_8 .
- (16) In addition to **5c**, some conformers of **5** were located at local minima but at higher Gibbs energies than **5p**; for details, see the Experimental Section.
- (17) G. R. Fulmer, A. J. M. Miller, N. H. Sherden, H. E. Gottlieb, A. Nudelman, B. M. Stoltz, J. E. Bercaw, K. I. Goldberg, *Organometallics* **2010**, *29*, 2176–2179.
- (18) G. M. Sheldrick, *SADABS, Empirical Absorption Correction Program*; Göttingen, Germany, 1996.
- (19) G. M. Sheldrick, *Acta Crystallogr., Sect. C: Struct. Chem.*, **2015**, *71*, 3–8.
- (20) K. Wakita, Yadokari-XG: Software for Crystal Structure Analyses, 2001; Release of Software (Yadokari-XG 2009) for Crystal Structure Analyses; C. Kabuto, S. Akine, T. Nemoto, E. Kwon, *J. Crystallogr. Soc. Jpn.*, **2009**, *51*, 218–224.
- (21) M. J. Frisch, G. W. Trucks, H. B. Schlegel, G. E. Scuseria, M. A. Robb, J. R. Cheeseman, G. Scalmani, V. Barone, B. Mennucci, G. A. Petersson, H. Nakatsuji, M. Caricato, X. Li, H. P. Hratchian, A. F. Izmaylov, J. Bloino, G. Zheng, J. L. Sonnenberg, M. Hada, M. Ehara, K. Toyota, R. Fukuda, J. Hasegawa, M. Ishida, T. Nakajima, Y. Honda, O. Kitao, H. Nakai, T. Vreven, J. A. Montgomery Jr., J. E. Peralta, F. Ogliaro, M. Bearpark, J. J. Heyd, E. Brothers, K. N. Kudin, V. N. Staroverov, R. Kobayashi, J. Normand, K. Raghavachari, A. Rendell, J. C. Burant, S. S. Iyengar, J. Tomasi, M. Cossi, N. Rega, J. M. Millam, M. Klene, J. E. Knox, J. B. Cross, V. Bakken, C. Adamo, J. Jaramillo, R. Gomperts, R. E. Stratmann, O. Yazyev, A. J. Austin, R. Cammi, C. Pomelli, J. W. Ochterski, R. L. Martin, K. Morokuma, V. G. Zakrzewski, G. A. Voth, P. Salvador, J. J. Dannenberg, S. Dapprich, A. D. Daniels, Ö. Farkas, J. B. Foresman, J. V.

Ortiz, J. Cioslowski, D. J. Fox, Gaussian 09, Revision D.01, Gaussian, Inc., Wallingford CT, 2009.

- (22) **GRRM14**; (a) S. Maeda, Y. Harabuchi, Y. Osada, T. Taketsugu, K. Morokuma, K. Ohno, see <https://iqce.jp/GRRM/>, accessed date March 21, 2020; (b) S. Maeda, K. Ohno, K. Morokuma, *Phys. Chem. Chem. Phys.* **2013**, *15*, 3683–3701.
- (23) **NBO 7.0**, E. D. Glendening, J. K. Badenhoop, A. E. Reed, J. E. Carpenter, J. A. Bohmann, C. M. Morales, P. Karafiloglou, C. R. Landis, F. Weinhold, Theoretical Chemistry Institute, University of Wisconsin, Madison (2018).

Chapter 6

Reactions of a Bicyclo[1.1.0]tetrasil-1(3)-ene with Nucleophilic Reagents

The contents of this chapter are published in part in

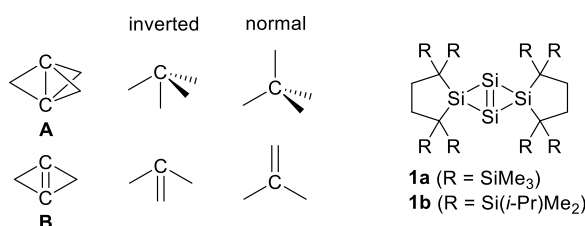
Nukazawa, T.; Iwamoto, T. *Organometallics* **2021**, *40*, 3511–3515.

DOI: 10.1021/acs.organomet.1c00521

6-1. Introduction

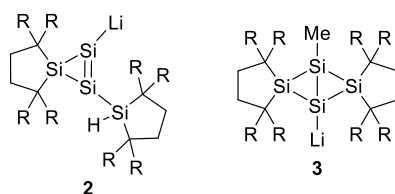
A molecule containing a distorted structure often exhibits unexpected reactivity. For example, [1.1.1]propellane has a nonclassical single bond between bridgehead carbon atoms that adopt an inverted (or hemispheroidal) geometry (Chart 6-1, **A**),^{1,2} which exhibits diradical or ionic characters. Bicyclo[1.1.0]but-1(3)-ene has a strained bridgehead C=C double bond in the bicyclic framework, whereby the orientation of the double bond is diametrically opposite to that of typical double bonds in acyclic alkenes (Chart 6-1, **B**).³ Although **B** and its derivatives have been proposed as reactive intermediates and the formal 1,2-addition of nucleophiles to the bridgehead C=C bond has been reported, the reactivity of such compounds containing an inverted double bond has not been investigated in detail.

Chart 6-1. [1.1.1]Propellane (**A**), Bicyclo[1.1.0]but-1(3)-ene (**B**), and Bicyclo[1.1.0]tetrasil-1(3)-ene **1**



Recently, we synthesized bicyclo[1.1.0]tetrasil-1(3)-enes **1a** and **1b** as the first isolable silicon analogues of bicyclo[1.1.0]but-1(3)-ene (Chart 6-1).⁴ Experimental and theoretical studies disclosed that **1** has a planar Si₄ bicyclic structure with the bridgehead Si=Si bond comprised of a π -bond and an inverted σ -bond as found between bridgehead silicon atoms in pentasila[1.1.1]propellane.⁵ Although halogen abstraction of **1a** from alkyl halides provided 1,3-dihalobicyclo[1.1.0]tetrasilanes that contain an unsupported bridgehead Si-Si π -bond,⁶ the reactivity of **1** for other reagents remains to be elucidated. In this chapter, the author reports the reactions of **1a** with lithium aluminum hydride (LiAlH₄) and methyl lithium (MeLi). The reduction of **1a** with LiAlH₄ provides unexpectedly cyclotrisilenide **2** as the first disilenide with a cyclotrisilene moiety (Chart 6-2),^{7,8} while the reaction of **1a** with MeLi afforded the corresponding 1-methyl-3-lithiobicyclo[1.1.0]tetrasilane **3** (Chart 6-2).

Chart 6-2. Structures of Compound **2** and **3** (R = SiMe₃)

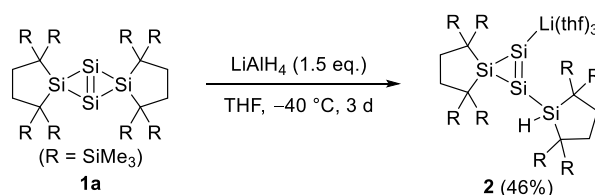


6-2. Results and Discussion

6-2-1. Reaction of **1a** with LiAlH₄

The reaction of **1a** with LiAlH₄ in THF at -40 °C afforded cyclotrisilenide **2** as a reddish-orange solid in 46% yield (Scheme 6-1).^{9,10} The molecular structure of **2** was determined using a combination of multinuclear NMR spectroscopy and single-crystal X-ray diffraction (XRD) analysis. Compound **2** was very air- and moisture-sensitive, but stable in a benzene solution at room temperature for several days.

Scheme 6-1. Reduction of **1a** with LiAlH₄



6-2-2. Molecular Structure and NMR Spectra of Cyclotrisilenide **2**

Recrystallization from pentane at -27 °C provided red crystals of **2** suitable for single-crystal XRD analysis (Figure 6-1a). In the crystalline state, **2** exists as a contact ion pair, and the lithium atom coordinates to three THF molecules. The Si1–Li1 distance [2.655(5) Å] is similar to those of typical sp³-type silyllithiums (2.64–2.70 Å)¹¹ and within those of previously reported sp²-type silyllithiums (2.598(9)–2.853(3) Å).^{12,13} The Si=Si bond distance [Si1–Si2: 2.182(2) Å] is slightly shorter than those in previously reported disilenides (2.192–2.209 Å),¹² and comparable to those of reported cyclotrisilenes (2.118–2.186 Å).¹⁴ The geometry around the unsaturated silicon atoms is almost planar [the angle sums of Si1 and Si2 atoms are 359.64° and 359.81°]. The ²⁹Si NMR resonances in benzene-*d*₆ due to the Si1 and Si2 nuclei [281.0 and

168.1 ppm, respectively, Figure 6-1b] fall in the range for the reported disilenides (100.5–328.4 ppm).¹² The broadening of the signal at 281.0 ppm might arise from the coupling between the ²⁹Si and ⁷Li nuclei.

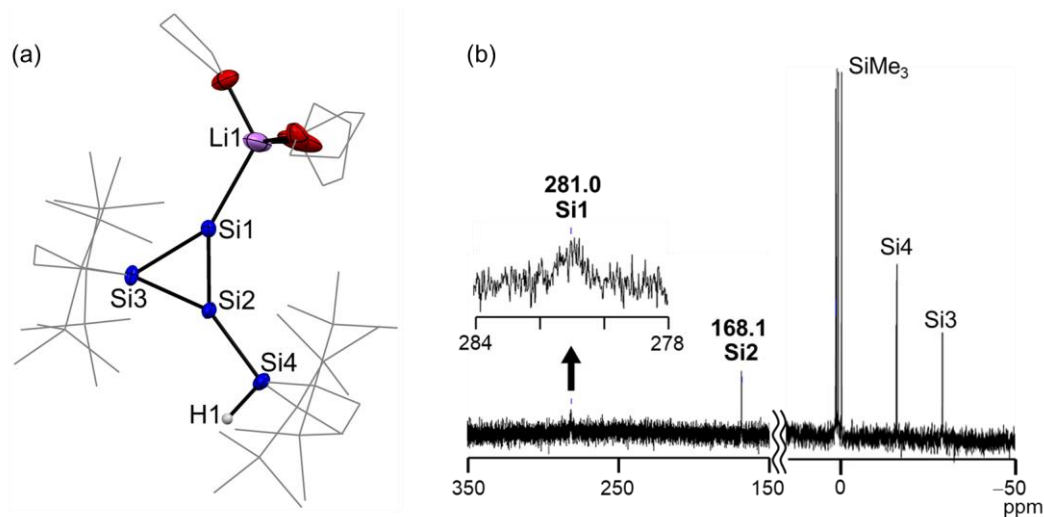


Figure 6-1. (a) ORTEP of **2** with thermal ellipsoids at 50% probability; hydrogen atoms, cocrystallized solvent (pentane), and disordered atoms are omitted for clarity. Selected bond lengths (Å) and angles (deg): Si1–Li1 2.655(5), Si1–Si2 2.182(2), Si1–Si3 2.403(2), Si2–Si3 2.2690(8), Si2–Si4 2.3651(8), Li1–Si1–Si2–Si4 –2.2(4). (b) ²⁹Si NMR spectrum of **2** in benzene-*d*₆ at room temperature.

6-2-3. Theoretical Study

Theoretical calculations provided further insight into the structure of **2**. The optimized structure of **2** (**2**_{opt}) calculated at the B3LYP-D3/6-311G(d) level of theory is in good agreement with the structure of **2** observed in the crystalline state. The ²⁹Si NMR chemical shifts of the unsaturated Si1 and Si2 nuclei in **2**_{opt} calculated at the M06L/6-311+G(2df,p) level of theory (276.9 ppm, 177.5 ppm) is consistent with the observed values of **2** (281.0 ppm, 168.1 ppm) in benzene-*d*₆, suggesting that even in benzene solution, **2** adopts a contact ion pair structure similar to that observed in the solid state.

6-2-4. UV-vis Absorption Spectra of **2**

The author found the remarkable solvatochromism of **2**. When **2** was dissolved in hexane, the color of the solution was orange and the longest-wavelength absorption band was observed at 530 nm ($\epsilon = 200 \text{ cm}^{-1}\text{mol}^{-1}\text{dm}^3$; Figure 6-2a). Conversely, for a yellowish green THF solution of **2**, the longest-wavelength absorption band appeared at 574 nm ($\epsilon = 200 \text{ cm}^{-1}\text{mol}^{-1}\text{dm}^3$; Figure

6-2a). The solvent-dependent color change of **2** is reversible. Similar solvatochromism has been observed in the isolable silenyl lithium reported by Apeloig, in which the color change of the solution arises from the differences in structure between the contact ion pair and the solvent-separated ion pair.¹³ The TD-DFT calculations suggest that the color change of the solution of **2** is also explained by the structure in solution as follows. The predicted longest-wavelength absorption band positions [528 nm (**2**_{opt}) and 569 nm (**2'**_{opt}, free anion of **2**)]¹⁵ at the B3LYP-D3/6-311+G(d)/SCRF(solvent = heptane (**2**_{opt}), THF (**2'**_{opt})) level of theory are consistent with the observed absorption wavelengths (See Figures 6-61 and 6-62). In addition, these absorptions are attributed to a symmetry-forbidden HOMO–LUMO transition: the HOMO is the in-plane anionic lone pair orbital and the LUMO is the $\pi^*(\text{Si}=\text{Si})$ orbitals (Figure 6-2b,c), which is in agreement with the observed small ϵ values.

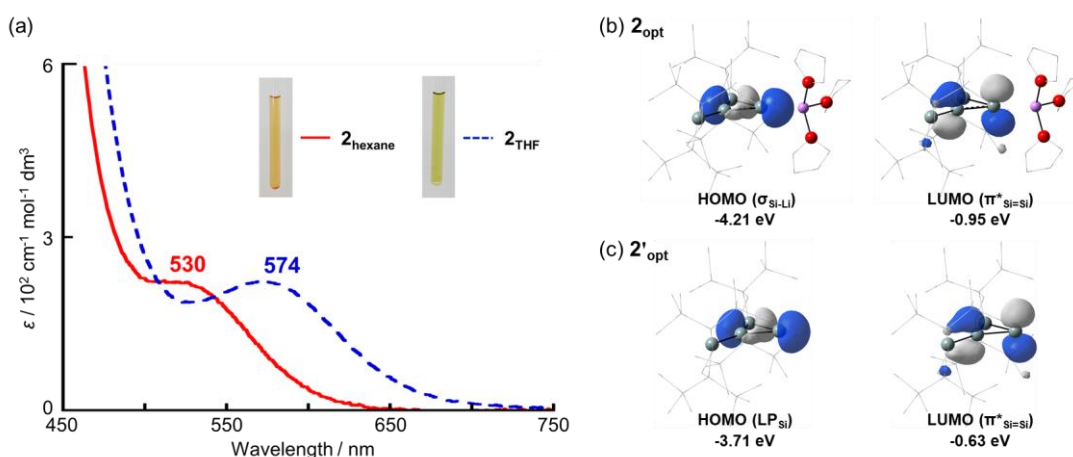


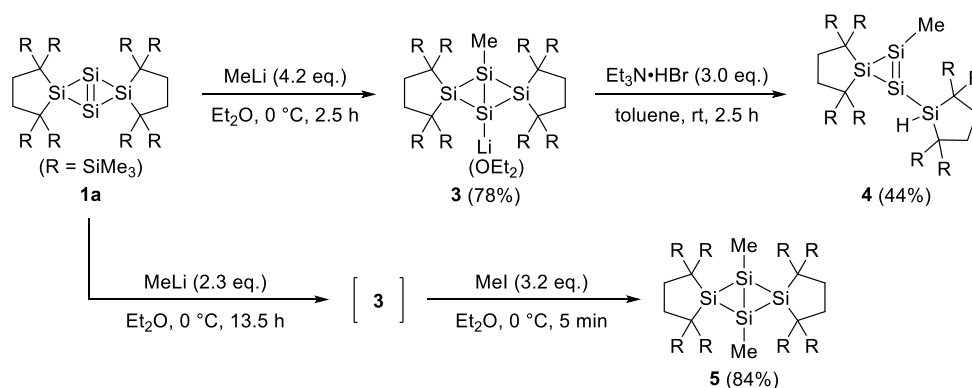
Figure 6-2. (a) UV-vis spectra of **2** at room temperature (red line: in hexane, blue dash line: in THF). (b) Frontier Kohn-Sham orbitals of **2**_{opt} at the B3LYP-D3/6-311+G(d)/SCRF(solvent = heptane)//B3LYP-D3/6-311G(d) level of theory (isosurface level: 0.05 e \cdot au⁻³). (c) Frontier Kohn-Sham orbitals of **2'**_{opt} at the B3LYP-D3/6-311+G(d)/SCRF(solvent = THF)//B3LYP-D3/6-311G(d) level of theory (isosurface level: 0.05 e \cdot au⁻³).

6-2-5. Reaction of **1a** with MeLi

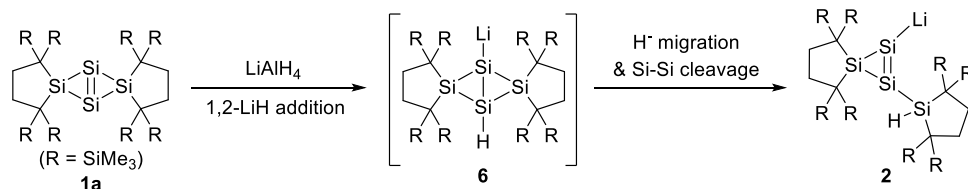
The reaction of **1a** with MeLi provided further insight into the mechanism for the formation of **2**. When **1a** was treated with MeLi in Et₂O solution at 0 °C, 1-methyl-3-lithiobicyclo[1.1.0]tetrasilane **3** was obtained as a pale yellow solid in 78% yield (Scheme 6-2). In this reaction, 1,2-addition of MeLi to the bridgehead Si=Si bond in **1a** occurred similar to the reaction of an acyclic disilene with MeLi.¹⁶ While no isomerization of **3**

was observed in solution, the protonation of **3** with $\text{Et}_3\text{N}\cdot\text{HBr}$ led to full conversion into cyclotrisilene **4** with Me group on the unsaturated silicon atom (NMR yield: 97%, Scheme 6-2), which was isolated as a pale yellow solid in 44% yield. Conversely, when compound **1a** was treated with MeLi followed by MeI, 1,3-dimethylbicyclo[1.1.0]tetrasilane **5** was obtained in 84% yield (2 steps, Scheme 6-2). Compound **5** is stable even at 60 °C. These results indicate that after protonation of **3**, the intramolecular hydride migration from the bridgehead silicon atom to the bridge silicon atom accompanied by the ring-opening affords **4**. These results suggest that the reduction of **1a** with LiAlH_4 afforded the corresponding 1,2-LiH adduct **6** as an initial product and the subsequent hydride migration and ring-opening provided cyclotrisilene **2** (Scheme 6-3). As a 1,3-dichlorobicyclo[1.1.0]tetrasilane undergoes a similar isomerization involving the chlorine migration and the ring opening to afford the corresponding cyclotrisilene,^{6b} relatively high migratory aptitude of hydride¹⁷ and the release of the ring strain may be responsible for the observed transformation to cyclotrisilene derivatives such as **2** and **4**.

Scheme 6-2. Reaction of **1a** with MeLi



Scheme 6-3. Possible Mechanism for Generation of **2**



6-2-6. Molecular Structure of **3**

Recrystallization from toluene at $-27\text{ }^{\circ}\text{C}$ afforded orange crystals of **3** suitable for single-crystal XRD analysis (Figure 6-3).¹⁸ In the single crystals of **3**, two crystallographically independent molecules exhibiting similar structural characteristics were found in the asymmetric unit. Compound **3** exists as a contact ion pair in the crystalline state. Interestingly, the lithium atom was solvated by only one Et_2O molecule, which is consistent with the fact that the ratio of silyl anion moiety: Et_2O is observed to be 1:1 in the ^1H NMR spectrum of **3** (Figure 6-12). The Si1–Si2 distance in **3** [avg. 2.564 \AA] is much longer than those of previously reported bicyclo[1.1.0]tetrasilanes with bent structures ($2.35\text{--}2.47\text{ \AA}$)¹⁹ and those of 1-lithio-1,3-disilabicyclo[1.1.0]butane ($2.3840(16)\text{ \AA}$)^{20a} and potassium pentasilatricyclo[2.1.0.0^{2,5}]pentan-1-ide ($2.3801(6)\text{ \AA}$).^{20b} The Si2–Li1 distance [avg. 2.524 \AA] is shorter than typical Si–Li bond lengths in sp^3 -type silyllithiums ($2.64\text{--}2.70\text{ \AA}$)¹¹ and those of sp^2 -type silyllithiums ($2.598(9)\text{--}2.853(3)\text{ \AA}$).^{12,13}

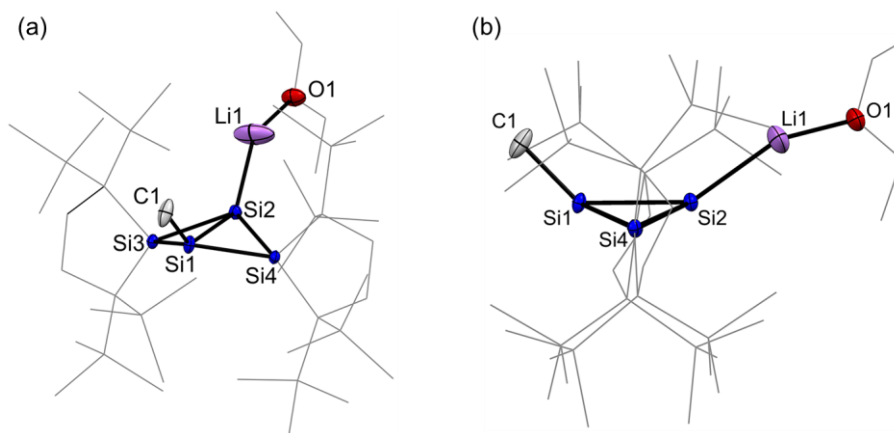


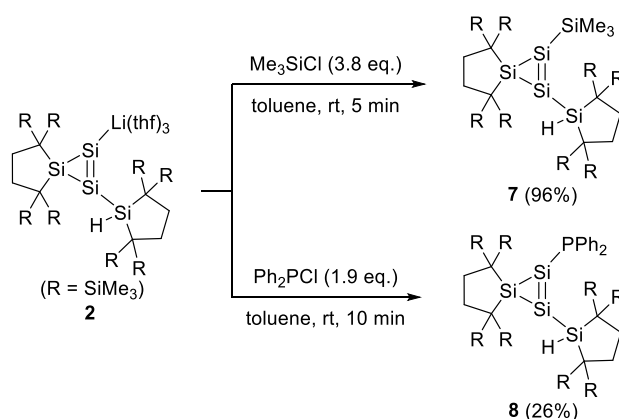
Figure 6-3. ORTEPs of **3** (a: perspective view, b: side view) with thermal ellipsoids at 50% probability; hydrogen atoms are omitted for clarity. One of the two crystallographically independent molecules is shown. Selected bond lengths (\AA) and angles (deg): Si1–C1 $1.912(2)$, Si1–Si2 $2.5577(8)$, Si1–Si3 $2.3205(7)$, Si1–Si4 $2.3054(7)$, Si2–Si3 $2.3148(7)$, Si2–Si4 $2.3189(7)$, Si2–Li1 $2.502(5)$, C1–Si1–Si2 $133.92(9)$, Si1–Si2–Li1 $143.63(14)$, Si2–Li1–O1 $152.3(3)$, Si3–Si1–Si2–Si4 $144.42(3)$.

6-2-7. Reactions of **2** with Electrophiles

Compound **2** readily reacted with Me_3SiCl in toluene to provide Me_3Si -substituted cyclotrisilene **7** in 96% yield (Scheme 6-4). In addition, treatment of **2** with Ph_2PCl afforded phosphanyl-substituted cyclotrisilene **8** in 80% NMR yield, which was isolated as orange

crystals in 26% yield (Scheme 6-4). Compounds **7** and **8** were characterized by a combination of multinuclear NMR spectroscopy, mass spectrometry, elemental analysis, and single-crystal XRD analysis. Compound **8** is the first example of a cyclotrisilene with a phosphanyl substituent on the unsaturated silicon atom.

Scheme 6-4. Reactions of **2** with Electrophiles



6-2-8. Molecular Structure and Electronic Property of Cyclotrisilene 8

Single-crystal XRD analysis of **8** (Figure 6-4a) disclosed that the geometry around the unsaturated Si2 atom is perfectly planar [the angle sums of the Si2 atom is 360.00°], while a slight pyramidalization of Si1 is observed [the angle sums of the Si1 atom is 355.99°]. The Si1–Si2 distance [2.1451(7) Å] falls within the range of the Si=Si double bond in reported cyclotrisilenes (2.118–2.186 Å)¹⁴ and is comparable to those of phosphanyl-substituted acyclic disilenes (2.1542–2.1968 Å).^{21,22} The Si1–P1 distance [2.2746(7) Å] is similar to those of reported phosphanyl disilenes (2.2367(12)–2.3126(10) Å).²¹ In the ²⁹Si NMR spectrum of **8** in benzene-*d*₆, signals assigned to the Si1 and Si2 nuclei were observed at 141.3 and 107.0 ppm, respectively, which were downfield shifted compared with those of reported acyclic phosphanyl disilenes (52.5–111.7 ppm).²¹ The ¹J(Si,P) coupling constant of Si1 nucleus [214.8 Hz] is significantly larger than those of reported phosphanyl disilenes [¹J(Si,P) = 115–133 Hz],²¹ suggesting an increased s-character of the orbital of the silicon atom in the P–Si bond.²³ The UV-vis absorption spectrum of **8** in hexane exhibits a longest-wavelength absorption band at 430 nm, which is bathochromically shifted compared with those of **4** and **7** [373 and 414 nm].

The HOMO of the optimized structure of **8** (**8_{opt}**) calculated at B3LYP-D3/6-311G(d) level of theory represents the interactions between the π -orbital of the Si=Si bond and the lone pair orbital on the phosphorous atom of the PPh₂ moiety (Figure 6-4b). These results suggested the presence of the n - π interaction between the phosphorus lone pair and the Si=Si bond in **8**.

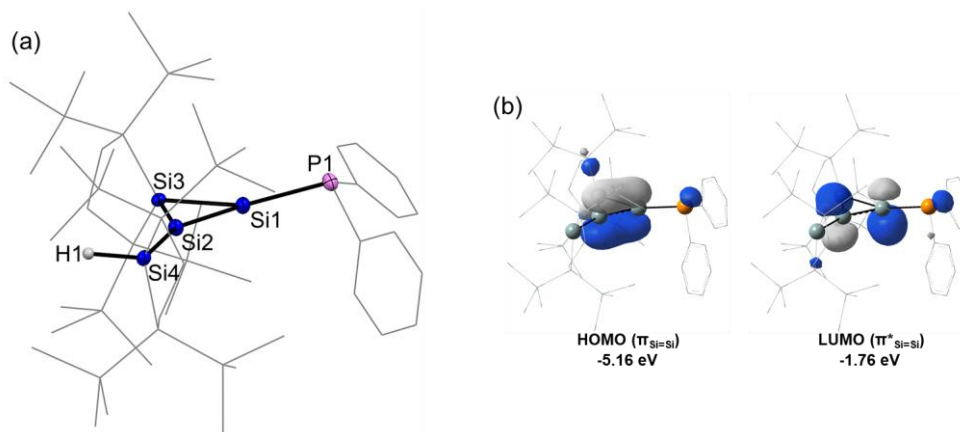


Figure 6-4. (a) ORTEP of **8** with thermal ellipsoids at 50% probability; hydrogen atoms are omitted for clarity. Selected bond lengths (Å) and angles (deg): Si1–Si2 2.1451(7), Si1–Si3 2.3256(7), Si1–P1 2.2746(7), Si2–Si3 2.3500(6), Si2–Si4 2.3871(7), Si4–Si2–Si1–P1 $-17.37(9)$. (b) Frontier Kohn-Sham orbitals of **8_{opt}** at the B3LYP-D3/6-311G(d) level of theory (isosurface level: $0.05 \text{ e}\cdot\text{au}^{-3}$).

6-3. Conclusion

In conclusion, the author investigated the reactions of **1a** with nucleophiles such as LiAlH₄ and MeLi. The reduction of **1a** with LiAlH₄ provided the first isolable cyclotrisilenide **2** as a reddish-orange solid. In the crystalline state, **2** exists as a contact ion pair structure, and the UV-Vis absorption spectra changed depending on the solvent. The reaction of **1a** with MeLi afforded 1,2-adduct **3** and its protonation led to the generation of cyclotrisilene **4**, suggesting that **2** should be formed via the 1,2-addition of LiH to the bridgehead Si=Si bond of **1a** and subsequent intramolecular hydride migration accompanied by ring-opening. Silyl and phosphanyl-substituted cyclotrisilenes **7** and **8** were successfully obtained from the reactions of **2** with the corresponding chlorosilane and chlorophosphine, respectively.

6-4. Experimental Section

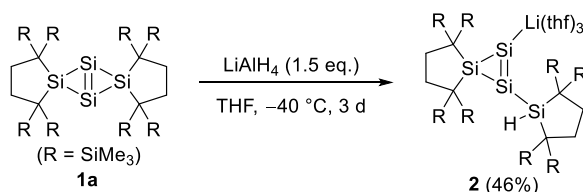
General Procedures

All reactions involving air-sensitive compounds were performed under argon or nitrogen atmosphere using a high-vacuum line and a standard Schlenk techniques, or a glove box, as well as dry and oxygen-free solvents. Reactions at lower temperatures were performed using an EYELA PSL-1400 cryobath. NMR spectra were recorded on a Bruker Avance III 500 FT NMR spectrometer. The ^1H and ^{13}C NMR chemical shifts were referenced to residual ^1H and ^{13}C shifts of the solvents: C_6D_6 (^1H : δ 7.16 and ^{13}C : δ 128.0).²⁴ The ^{29}Si NMR chemical shifts were relative to Me_4Si in ppm (δ 0.00). The sampling of air-sensitive compounds was carried out using a VAC NEXUS 100027 type glove box. Mass spectra were recorded on a Bruker Daltonics Solarix 9.4T spectrometer and a JEOL JMS-T100GCV spectrometer. UV-vis spectra were recorded on a JASCO V-770 spectrometer. X-ray analysis was carried out using a Bruker AXS APEXII CCD diffractometer.

Materials

Dry and degassed hexane, THF, and toluene were prepared using a VAC 103991 solvent purifier. Benzene- d_6 was dried by molecular sieves 4\AA after degassing through three freeze-pump-thaw cycles. Hexamethyldisiloxane and Et_2O were dried by lithium aluminum hydride after degassing through three freeze-pump-thaw cycles. To treat cyclotrisilenide **2** and silyl anion **3**, benzene- d_6 , hexane, and toluene were further dried by potassium graphite (KC_8). Tetrasilabicyclo[1.1.0]but-1(3)-ene^{4b} **1a** and KC_8 ²⁵ were prepared according to published procedure. Lithium aluminum hydride, a diethyl ether solution of methyllithium, triethylamine hydrobromide, iodomethane, chlorotrimethylsilane, and chlorodiphenylphosphine were commercially available and used without further purification.

Reaction of **1a** with Lithium Aluminum Hydride (LiAlH₄) [TN790,808]

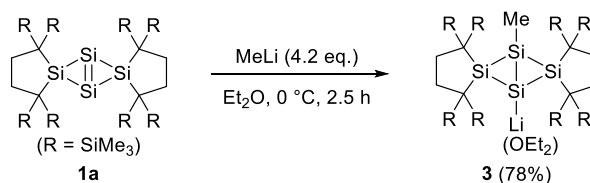


To a Schlenk tube (30 mL) equipped with a magnetic stir bar, compound **1a** (119.9 mg, 150 μmol) and LiAlH₄ (8.6 mg, 227 μmol) were placed. To the mixture dry and degassed THF (10.0 mL) was introduced via a vacuum line under reduced pressure and then the mixture was stirred at $-40\text{ }^\circ\text{C}$ for 3 days. The resulting suspension turned from orange to yellow green. After the volatiles were removed in vacuo at $0\text{ }^\circ\text{C}$, hexane was added to the residue and the resulting insoluble material was filtered off. The volatile was removed under reduced pressure. After hexane was added to the resulting residue, a reddish orange solid was formed and the suspension was left to stand at $-27\text{ }^\circ\text{C}$ for 1 day. Pure **2** (71.1 mg, 69.2 μmol) was obtained in 46% yield after removing the upper layer by pipetting.

2: a reddish orange solid; mp $167\text{-}169\text{ }^\circ\text{C}$ (decomp.); ¹H NMR (500 MHz, C₆D₆, 296 K) 0.46 (s, 18H, SiCH₃), 0.53 (s, 18H, SiCH₃), 0.587 (s, 18H, SiCH₃), 0.593 (s, 18H, SiCH₃), 1.34-1.38 (m, 12H, CH₂ (THF)), 2.11-2.24 (m, 4H, CH₂), 2.28-2.38 (m, 4H, CH₂), 3.43-3.49 (m, 12H, CH₂ (THF)), 5.37 (s, 1H, Si-H); ¹³C NMR (126 MHz, C₆D₆, 296 K); 3.4 (SiCH₃), 5.0 (SiCH₃), 5.1 (SiCH₃), 5.3 (SiCH₃), 9.8 (C), 11.2 (C), 25.5 (CH₂ (THF)), 34.6 (CH₂), 35.1 (CH₂), 68.8 (CH₂ (THF)); ²⁹Si NMR (99 MHz, C₆D₆, 296 K) -27.9 (Si), -14.0 (SiH), 2.7 (SiMe₃), 3.6 (SiMe₃), 4.1 (SiMe₃), 4.4 (SiMe₃), 168.1 (Si=Si-Li), 281.0 (Si=Si-Li); ⁷Li NMR (194 MHz, C₆D₆, 296 K) 0.13; UV-vis (hexane, 293 K) $\lambda_{\text{max}}/\text{nm}$ (ϵ) 530 (sh, 2.0×10^2), 426 (sh, 1.9×10^3), 359 (5.7×10^3), 250 (sh, 2.1×10^4); UV-vis (THF, 293 K) $\lambda_{\text{max}}/\text{nm}$ (ϵ) 574 (2.0×10^2), 441 (sh, 1.6×10^3), 370 (7.2×10^3), 308 (8.7×10^3), 262 (sh, 2.2×10^4).

We have tried to measure the mass spectrum (FD) and elemental analysis of **2**, but sampling of **2** for measurement was unsuccessful due to extremely high sensitivity of **2** toward moisture and oxygen.

Reaction of **1a** with Methyllithium [TN773,780,834]

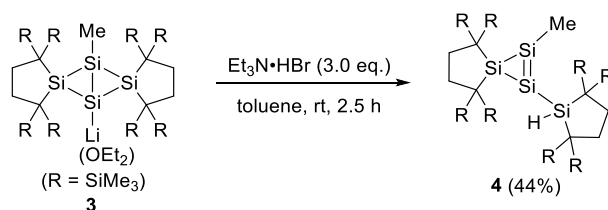


To a Schlenk tube (30 mL) equipped with a magnetic stir bar, tetrasilabicyclo[1.1.0]but-1(3)-ene **1a** (59.9 mg, 74.7 μmol) and dry and degassed Et_2O (5.0 mL) were placed. To the Schlenk tube, a diethyl ether solution of methyllithium (316.1 μmol , (290 μL , 1.09 M)) was added at 0 $^\circ\text{C}$ and the mixture was stirred at 0 $^\circ\text{C}$ for 2.5 hours. After the volatiles were removed in vacuo at 0 $^\circ\text{C}$, toluene was added to the residue and the insoluble material was filtered off. The filtrate was concentrated in vacuo. After hexane was added to the resulting residue, a pale yellow solid was formed and the suspension was left to stand at $-27\text{ }^\circ\text{C}$ for 1 day. Pure **3** (52.3 mg, 58.2 μmol) was obtained in 78% yield after removing the upper layer by pipetting.

3: a pale yellow solid; mp 115-117 $^\circ\text{C}$ (decomp.); ^1H NMR (500 MHz, C_6D_6 , 292 K) 0.47 (s, 36H, SiCH_3), 0.52 (s, 36H, SiCH_3), 0.84 (s, 3H, SiCH_3), 0.88 (t, $J = 7.1$ Hz, 6H, CH_3 (ether)), 2.08-2.23 (m, 8H, CH_2), 2.98 (q, $J = 7.1$ Hz, 4H, CH_2 (ether)); ^{13}C NMR (126 MHz, C_6D_6 , 293 K) 2.0 (SiCH_3), 5.4 (SiCH_3), 6.0 (SiCH_3), 12.0 (C), 14.9 (CH_3 (ether)), 36.2 (CH_2), 66.9 (CH_2 (ether)); ^{29}Si NMR (99 MHz, C_6D_6 , 292 K) -80.6 (Si-Me), 2.9 (SiMe_3), 3.1 (SiMe_3), 16.5 (Si); ^7Li NMR (194 MHz, C_6D_6 , 295 K) 0.53 (broad); UV-vis (hexane, 293 K) $\lambda_{\text{max}}/\text{nm}$ (ϵ) 373 (2.1×10^3), 298 (sh, 1.0×10^4), 236 (2.8×10^4); Anal. Calcd for $\text{C}_{37}\text{H}_{93}\text{LiOSi}_{12}$: C, 49.48; H, 10.44%. Found: C, 49.66; H, 10.25%.

We failed to measure the mass spectrum (APCI, ESI and FD) of **3** because **3** is extremely reactive toward moisture and oxygen and decomposes during sampling for measurement.

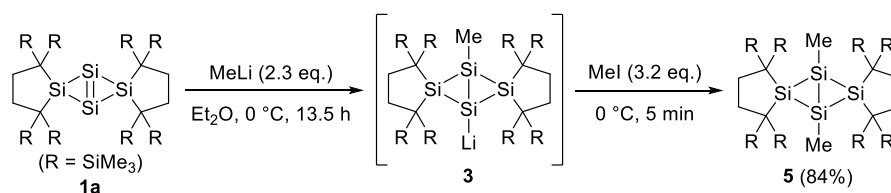
Reaction of **3** with Triethylamine Hydrobromide [TN842,844,845,847]



To a round-bottomed stock bottle (10 mL) equipped with a magnetic stir bar, silyl anion **3** (30.3 mg, 33.7 μmol) and dry and degassed toluene (3.0 mL) were placed. To the stock bottle, triethylamine hydrobromide (18.1 mg, 99.4 μmol) was added at room temperature and the mixture was stirred for 2.5 hours at room temperature. The resulting suspension turned from orange to yellow gradually. After the volatiles were removed in vacuo, hexane was added to the residue and the insoluble material was filtered off. The filtrate was concentrated in vacuo. After hexamethyldisiloxane was added to the resulting residue, a pale yellow solid was formed and the suspension was left to stand at $-27\text{ }^\circ\text{C}$ for 1 day. Pure **4** (12.0 mg, 14.7 μmol) was obtained in 44% yield after removing the upper layer by pipetting.

4: a pale yellow solid; mp 133-136 $^\circ\text{C}$ (decomp.); ^1H NMR (500 MHz, C_6D_6 , 296 K) 0.30 (s, 18H, SiCH_3), 0.33 (s, 18H, SiCH_3), 0.42 (s, 18H, SiCH_3), 0.45 (s, 18H, SiCH_3), 1.21 (s, 3H, CH_3), 1.82-2.05 (m, 8H, CH_2), 4.95 (s, 1H, SiH); ^{13}C NMR (126 MHz, C_6D_6 , 296 K) 3.1 (SiCH_3), 3.5 (SiCH_3), 4.2 (CH_3), 4.5 (SiCH_3), 4.6 (SiCH_3), 10.3 (C), 14.3 (C), 33.8 (CH_2), 34.6 (CH_2); ^{29}Si NMR (99 MHz, C_6D_6 , 295 K) -16.5 (SiH), 2.8 (SiMe_3), 2.9 (SiMe_3), 3.9 (SiMe_3), 5.0 (SiMe_3), 9.4 (Si), 56.0 ($\text{Si}=\text{Si}-\text{Me}$), 154.3 ($\text{Si}=\text{Si}-\text{Me}$); UV-vis (hexane, 293 K) $\lambda_{\text{max}}/\text{nm}$ (ϵ) 373 (2.5×10^3), 293 (sh, 1.1×10^4), 237 (3.1×10^4), 216 (4.0×10^4); HRMS (FD) Calcd for $\text{C}_{33}\text{H}_{84}\text{Si}_{12}$ [M^+], 816.38042; Found, 816.37997; Anal. Calcd for $\text{C}_{33}\text{H}_{84}\text{Si}_{12}$: C, 48.45; H, 10.35%. Found: C, 48.11; H, 10.06%.

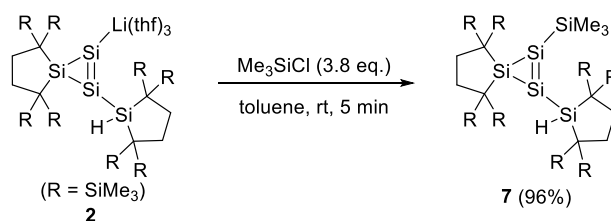
Reaction of 3 with Iodomethane [TN760,762,765]



To a Schlenk tube (30 mL) equipped with a magnetic stir bar, compound **1a** (60.1 mg, 74.9 μmol) and dry and degassed Et_2O (5.0 mL) were placed. To the mixture a diethyl ether solution of methyllithium (174 μmol , (160 μL , 1.09 M)) was added at 0 $^\circ\text{C}$ and then the mixture was stirred for 13.5 hours at 0 $^\circ\text{C}$. The resulting solution turned from orange suspension to orange solution. To the reaction mixture iodomethane (ca. 34 mg, 240 μmol) was added at 0 $^\circ\text{C}$. The resulting solution turned from orange solution to yellow suspension immediately. After the volatiles were removed in vacuo at 0 $^\circ\text{C}$, hot toluene was added to the residue and the insoluble material was filtered off. The filtrate was concentrated in vacuo and the residue was washed with hexane to provide a yellow solid of **5** (52.3 mg, 62.9 μmol) in 84% yield.

5: a yellow solid; mp 196-198 $^\circ\text{C}$ (decomp.); ^1H NMR (500 MHz, C_6D_6 , 333 K) 0.36 (s, 72H, SiCH_3), 1.37 (s, 6H, SiCH_3 (bridgehead)), 1.98 (s, 8H, CH_2); ^{13}C NMR (125 MHz, C_6D_6 , 333 K), 5.2 (SiCH_3), 9.5 (SiCH_3), 13.4 (C), 35.1 (CH_2); ^{29}Si NMR (99 MHz, C_6D_6 , 333 K) -14.6 (Si), 3.6 (SiMe_3), 81.6 (Si-Me); UV-vis (hexane, 293 K) $\lambda_{\text{max}}/\text{nm}$ (ϵ) 422 (sh, 0.8×10^3), 349 (1.5×10^3), 292 (2.4×10^3), 267 (sh, 7.0×10^3), 247 (1.8×10^4); HRMS (APCI_positive) Calcd for $\text{C}_{34}\text{H}_{86}\text{Si}_{12}$ [(M+H) $^+$], 831.40335; Found, 831.40347; Anal. Calcd for $\text{C}_{34}\text{H}_{86}\text{Si}_{12}$: C, 49.08; H, 10.42. Found: C, 48.70; H, 10.15%.

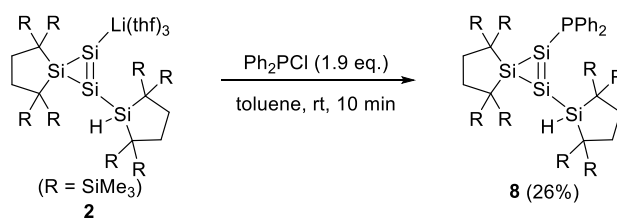
Reaction of 2 with Chlorotrimethylsilane [TN827,828,835]



To a Schlenk tube (10 mL) equipped with a magnetic stir bar, cyclotrisilenide **2** (20.0 mg, 19.5 μmol) and dry and degassed toluene (3.0 mL) were placed. To the Schlenk tube, chlorotrimethylsilane (8.1 mg, 74.6 μmol) was added at room temperature and the mixture was stirred for 5 minutes. The resulting solution turned from red to yellow immediately. After the volatiles were removed in vacuo, hexane was added to the residue and the insoluble material was filtered off. The filtrate was purified by recrystallization from hexane at $-27\text{ }^\circ\text{C}$ to provide orange crystals of **7** (16.4 mg, 18.7 μmol) in 96% yield.

7: orange crystals; mp 225-227 $^\circ\text{C}$ (decomp.); ^1H NMR (500 MHz, C_6D_6 , 296 K) 0.30 (s, 18H, SiCH_3), 0.36 (s, 18H, SiCH_3), 0.42 (s, 18H, SiCH_3), 0.44 (s, 18H, SiCH_3), 0.50 (s, 9H, SiCH_3), 1.88-2.08 (m, 8H, CH_2), 5.24 (s, 1H, SiH); ^{13}C NMR (126 MHz, C_6D_6 , 297 K) 2.5 (SiCH_3), 3.4 (SiCH_3), 3.8 (SiCH_3), 4.8 (SiCH_3), 5.0 (SiCH_3), 10.6 (C), 13.4 (C), 34.0 (CH_2), 34.9 (CH_2); ^{29}Si NMR (99 MHz, C_6D_6 , 296 K) -16.1 (SiH), -10.0 (Si), -4.3 ($\text{Si}=\text{Si}-\text{SiMe}_3$), 3.3 (SiMe_3), 3.6 (SiMe_3), 4.4 (SiMe_3), 5.1 (SiMe_3), 121.6 ($\text{Si}=\text{Si}-\text{SiMe}_3$), 163.4 ($\text{Si}=\text{Si}-\text{SiMe}_3$); UV-vis (hexane, 293 K) $\lambda_{\text{max}}/\text{nm}$ (ϵ) 414 (3.7×10^3), 306 (1.1×10^4), 247 (sh, 2.3×10^4), 221 (3.9×10^4); HRMS (FD) Calcd for $\text{C}_{35}\text{H}_{90}\text{Si}_{13}$ [M^+], 874.40429; Found, 874.40400; Anal. Calcd for $\text{C}_{35}\text{H}_{90}\text{Si}_{13}$: C, 47.98; H, 10.35%. Found: C, 48.01; H, 10.27%.

Reaction of **2** with Chlorodiphenylphosphine [TN817,821,825,829]



To a Schlenk tube (10 mL) equipped with a magnetic stir bar, cyclotrisilenide **2** (19.9 mg, 19.4 μmol) and dry and degassed toluene (3.0 mL) were placed. To the Schlenk tube, chlorodiphenylphosphine (7.9 mg, 35.8 μmol) was added at room temperature and the mixture was stirred for 10 minutes. The resulting solution turned from red to orange immediately. After the volatiles were removed in vacuo, hexane was added to the residue and the insoluble material was filtered off. The filtrate was concentrated in vacuo and the residue was purified by

recrystallization from hexamethyldisiloxane at room temperature to provide orange crystals of **8** (5.0 mg, 5.1 μmol) in 26% yield.

8: orange crystals; mp 155-157 °C (decomp.); ^1H NMR (500 MHz, C_6D_6 , 296 K) 0.30 (s, 36H, SiCH_3), 0.35 (s, 18H, SiCH_3), 0.45 (s, 18H, SiCH_3), 1.82-2.03 (m, 8H, CH_2), 5.17 (s, 1H, SiH), 7.02-7.07 (m, 2H, *p*-CH), 7.10-7.15 (m, 4H, *m*-CH), 7.74-7.80 (m, 4H, *o*-CH); ^{13}C NMR (126 MHz, C_6D_6 , 297 K); 3.4 (SiCH_3), 3.7 (SiCH_3), 4.7 (SiCH_3), 5.0 (SiCH_3), 10.7 (C), 15.9 (C), 34.1 (CH_2), 34.8 (CH_2), 128.8 (*p*-CH), 129.1 (d, $^3J_{\text{CP}} = 7.1$ Hz, *m*-CH), 135.3 (d, $^1J_{\text{CP}} = 22.7$ Hz, *ipso*-C), 136.1 (d, $^2J_{\text{CP}} = 19.0$ Hz, *o*-CH); ^{29}Si NMR (99 MHz, C_6D_6 , 296 K) -15.1 (d, $^3J_{\text{SiP}} = 3.1$ Hz, *SiH*), 3.2 (*SiMe*₃), 3.3 (*SiMe*₃), 4.0 (*SiMe*₃), 5.2 (*SiMe*₃), 18.5 (d, $^2J_{\text{SiP}} = 9.0$ Hz, *Si* in three-membered ring), 107.0 (d, $^2J_{\text{SiP}} = 11.4$ Hz, *Si=Si-P*), 141.3 (d, $^1J_{\text{SiP}} = 214.8$ Hz, *Si=Si-P*); ^{31}P NMR (202 MHz, C_6D_6 , 296 K) -23.2; UV-vis (hexane, 293 K) $\lambda_{\text{max}}/\text{nm}$ (ϵ) 430 (5.2×10^3), 319 (1.7×10^4), 284 (2.3×10^4), 219 (sh, 6.1×10^4); HRMS (FD) Calcd for $\text{C}_{44}\text{H}_{91}\text{Si}_{12}\text{P}$ [M^+], 986.40895; Found, 986.40854; Anal. Calcd for $\text{C}_{44}\text{H}_{91}\text{Si}_{12}\text{P}$: C, 53.48; H, 9.28%. Found: C, 53.61; H, 9.28%.

NMR spectra

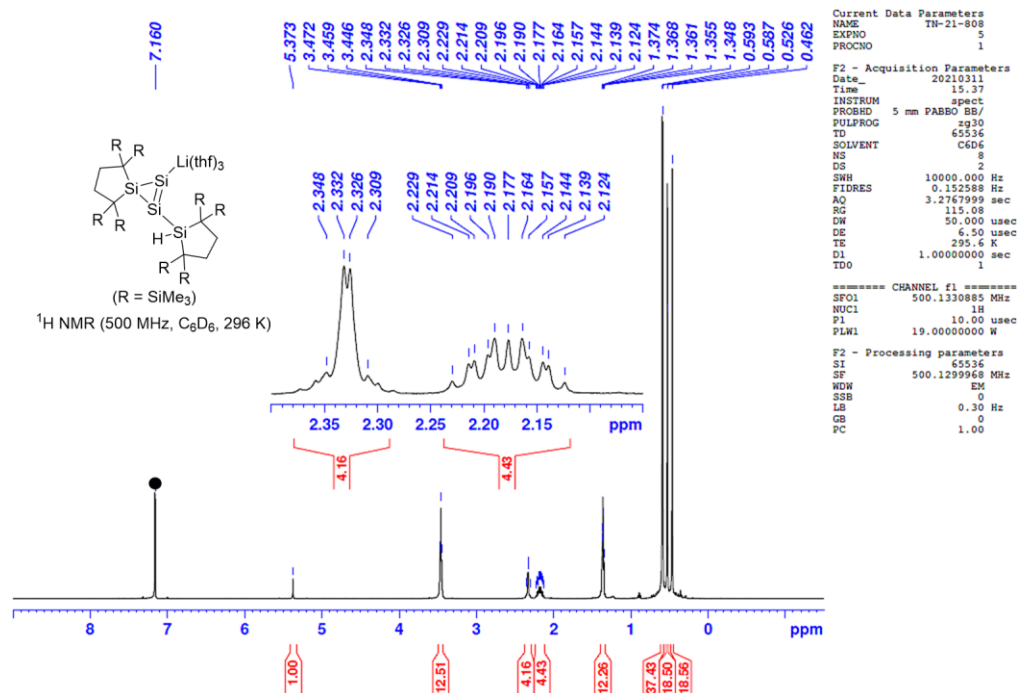


Figure 6-5. ^1H NMR spectrum of **2** in C_6D_6 at 296 K ($\bullet = \text{C}_6\text{HD}_5$).

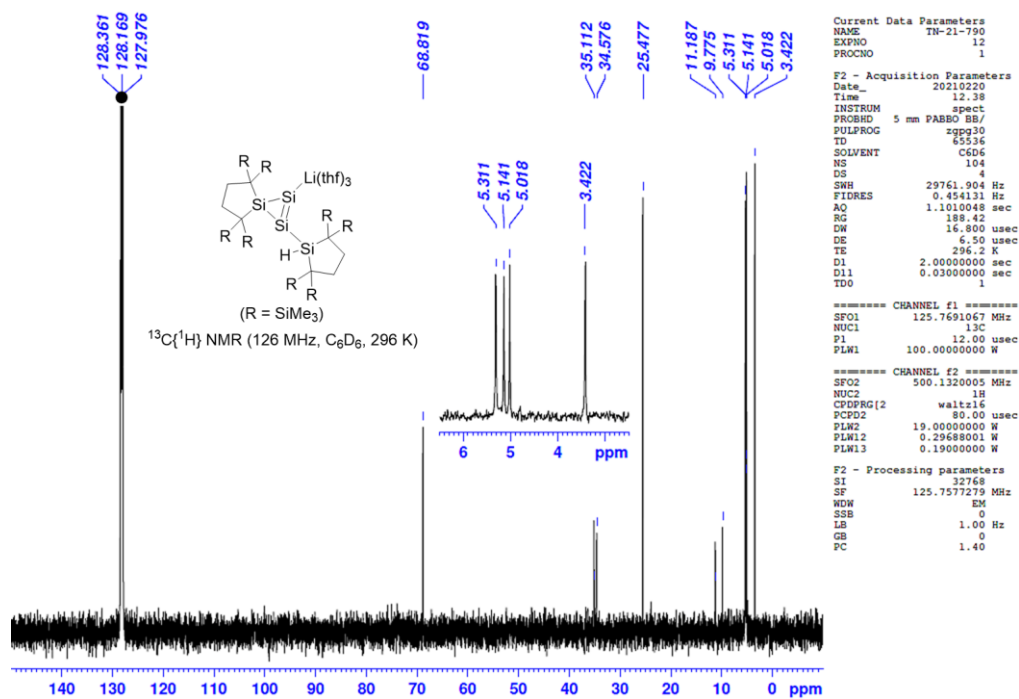


Figure 6-6. $^{13}\text{C}\{^1\text{H}\}$ NMR spectrum of **2** in C_6D_6 in 296 K (● = C_6D_6).

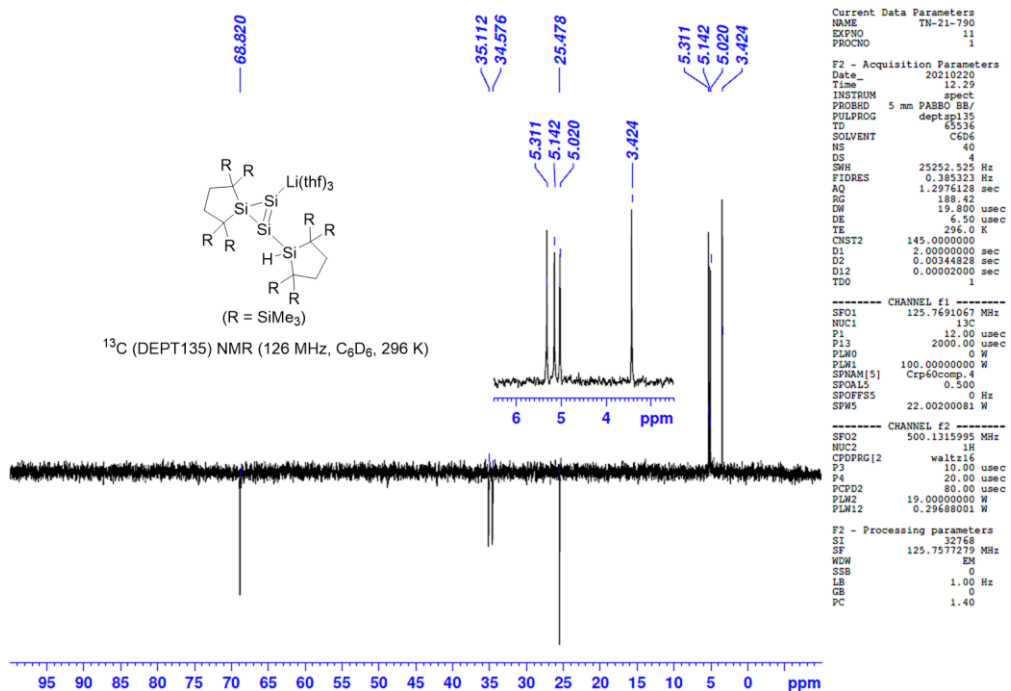


Figure 6-7. ^{13}C (DEPT135) NMR spectrum of **2** in C_6D_6 at 296 K.

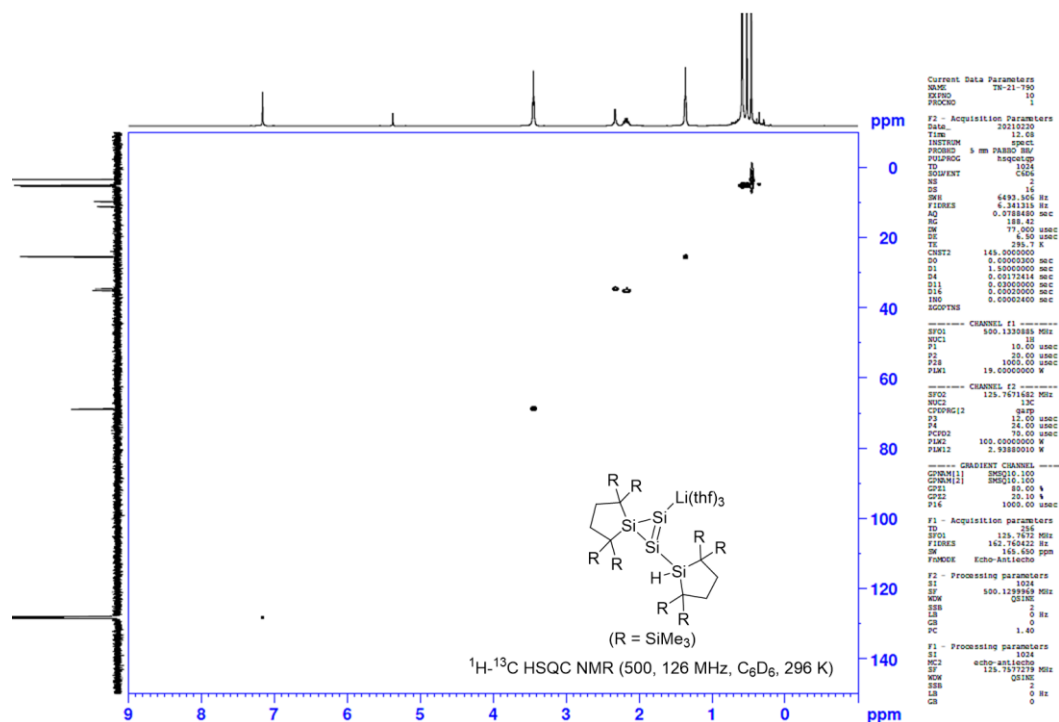


Figure 6-8. ^1H - ^{13}C HSQC NMR spectrum of **2** in C_6D_6 at 296 K.

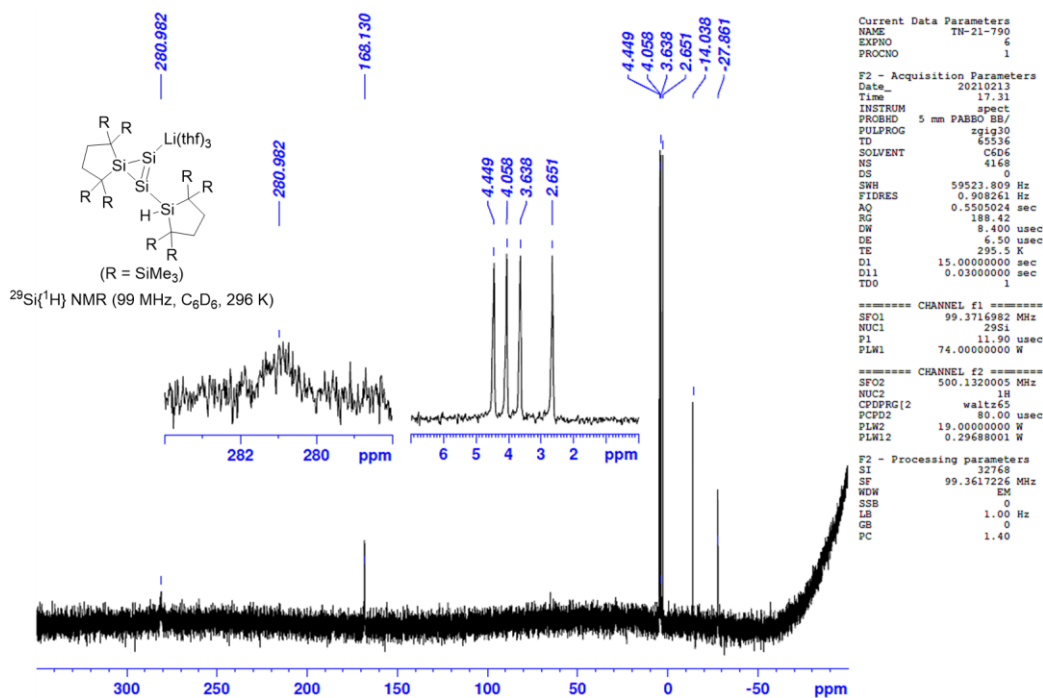


Figure 6-9. $^{29}\text{Si}\{^1\text{H}\}$ NMR spectrum of **2** in C_6D_6 at 296 K.

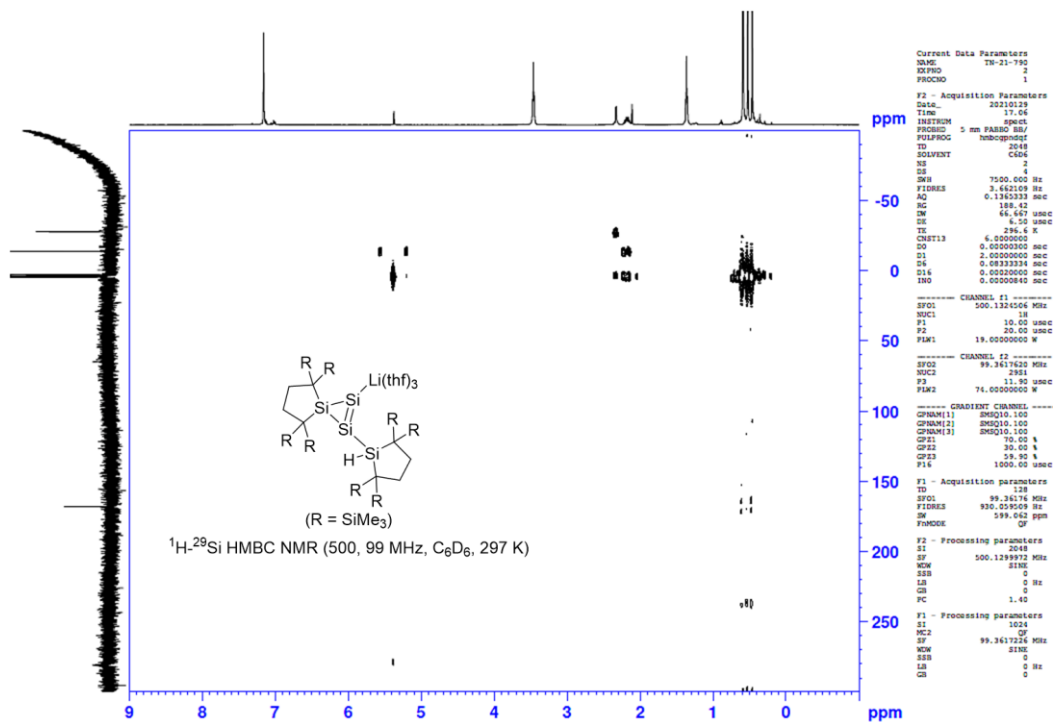


Figure 6-10. ^1H - ^{29}Si HMBC NMR spectrum of **2** in C_6D_6 at 297 K.

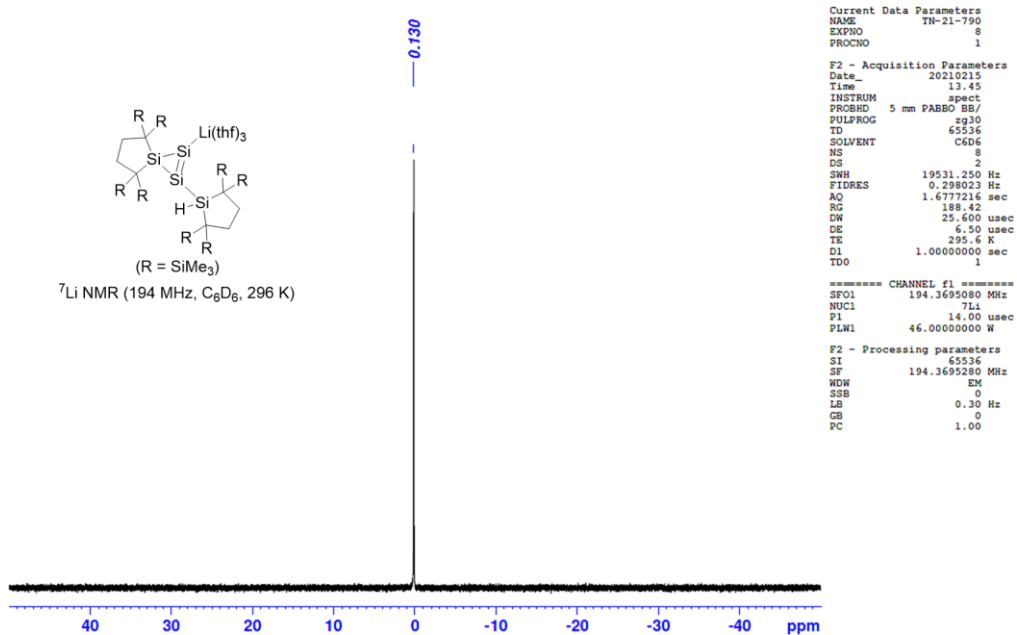


Figure 6-11. ^7Li NMR spectrum of **2** in C_6D_6 at 296 K.

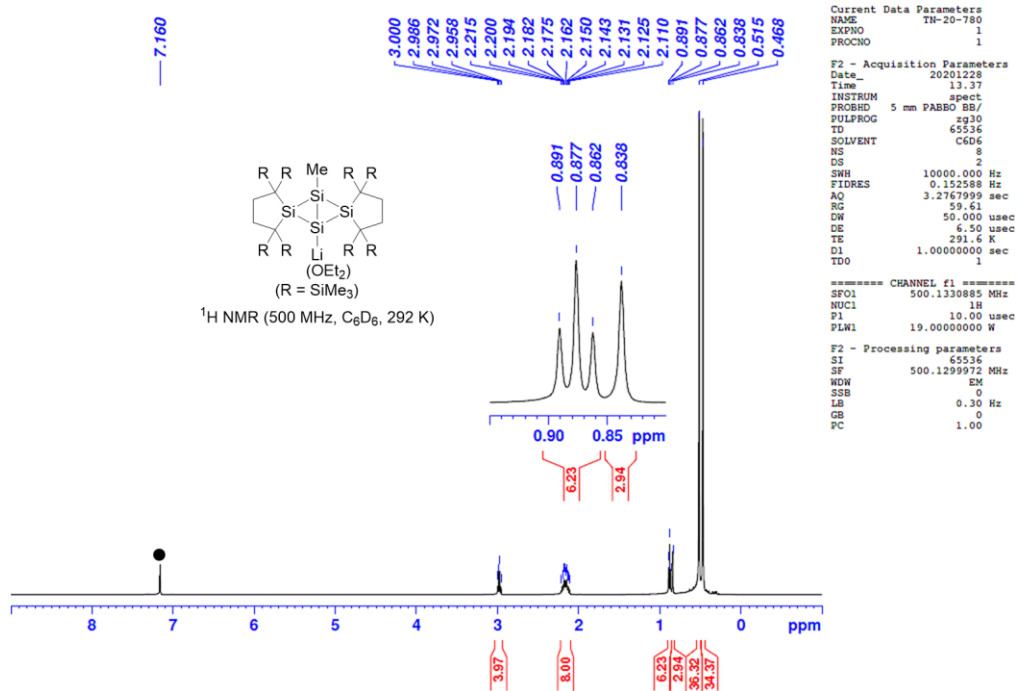


Figure 6-12. ^1H NMR spectrum of **3** in C_6D_6 at 292 K (● = C_6HD_5).

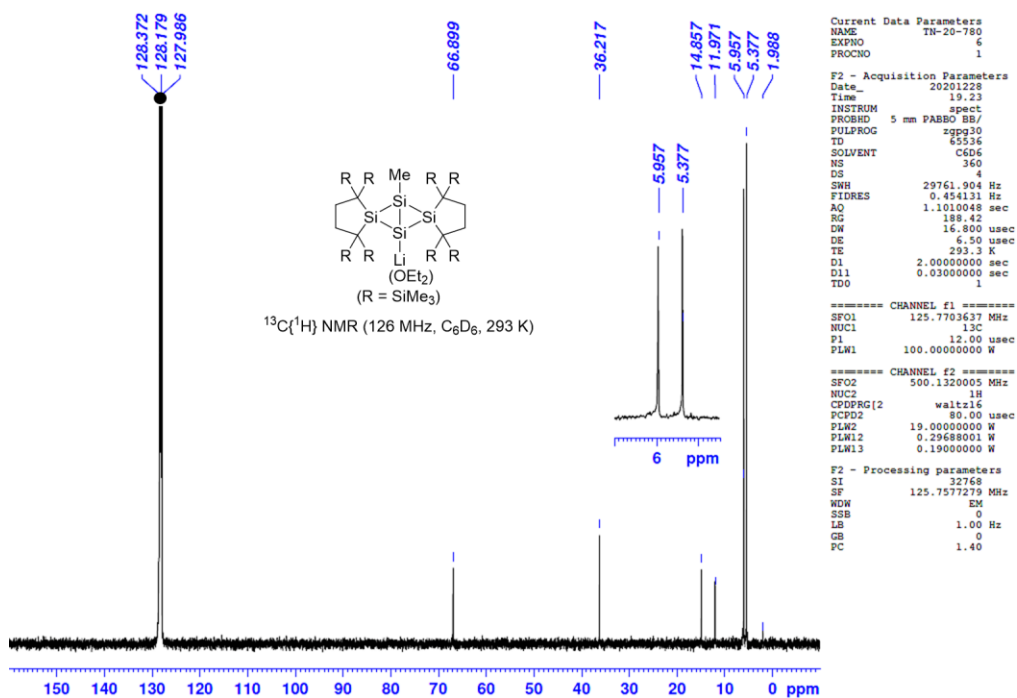


Figure 6-13. $^{13}\text{C}\{^1\text{H}\}$ NMR spectrum of **3** in C_6D_6 in 293 K (● = C_6D_6).

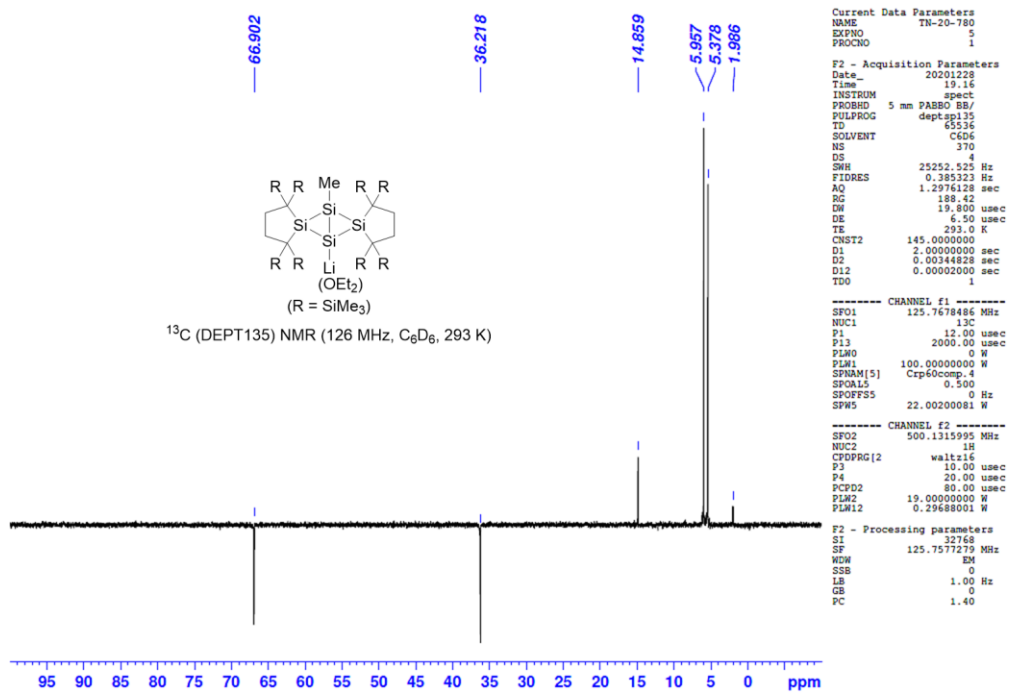


Figure 6-14. ¹³C (DEPT135) NMR spectrum of **3** in C₆D₆ at 293 K.

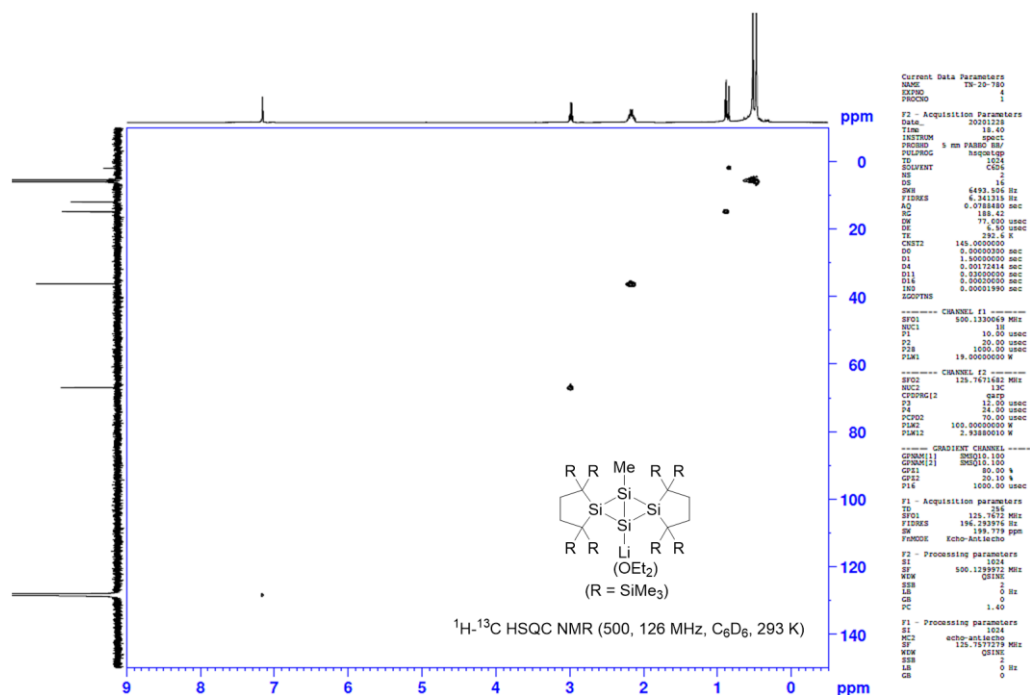


Figure 6-15. ¹H-¹³C HSQC NMR spectrum of **3** in C₆D₆ at 293 K.

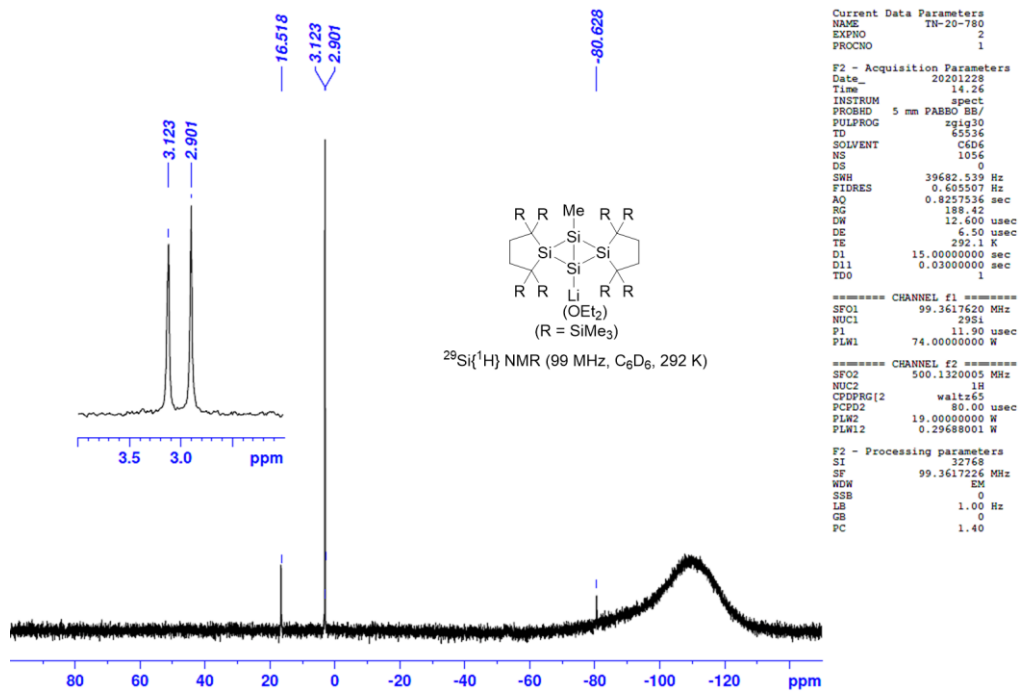


Figure 6-16. $^{29}\text{Si}\{^1\text{H}\}$ NMR spectrum of **3** in C_6D_6 at 292 K.

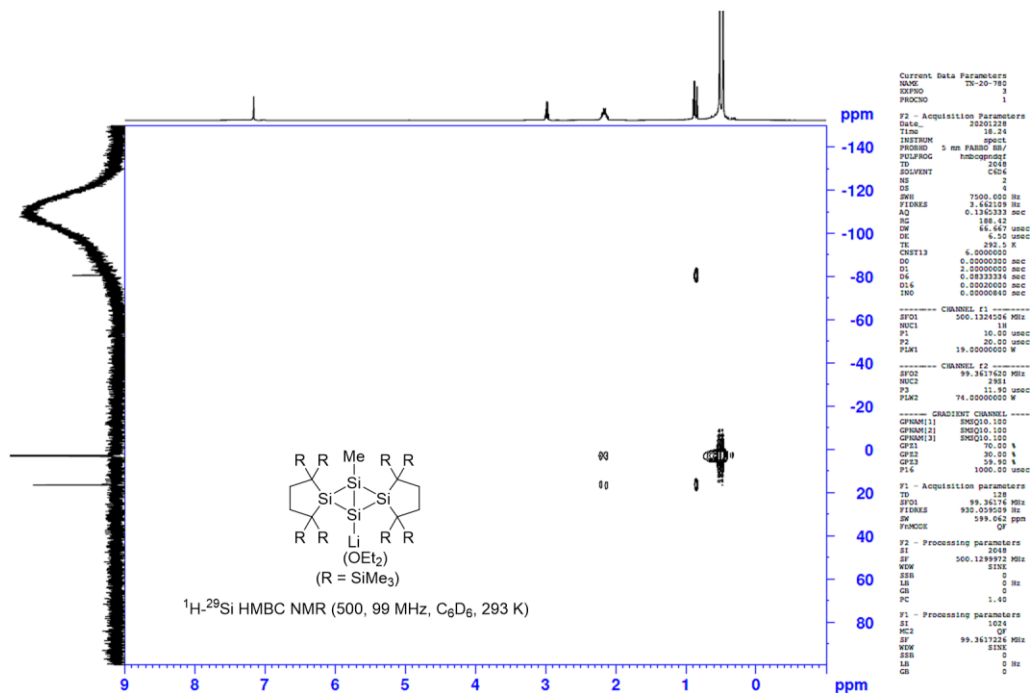


Figure 6-17. ^1H - ^{29}Si HMBC NMR spectrum of **3** in C_6D_6 at 293 K.

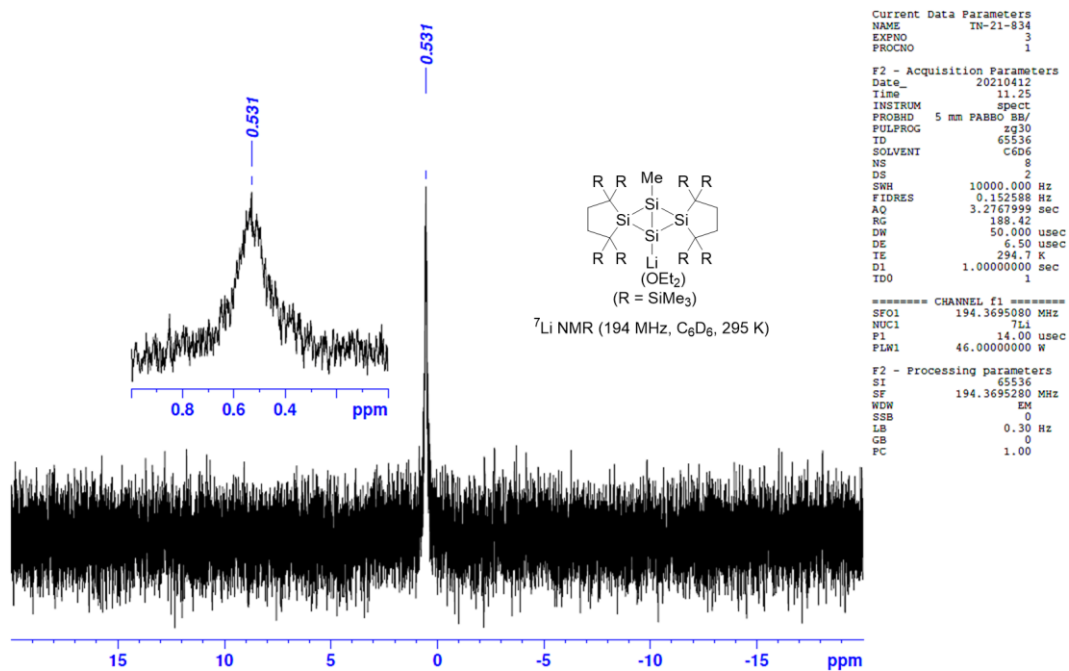


Figure 6-18. ⁷Li NMR spectrum of **3** in C₆D₆ at 295 K.

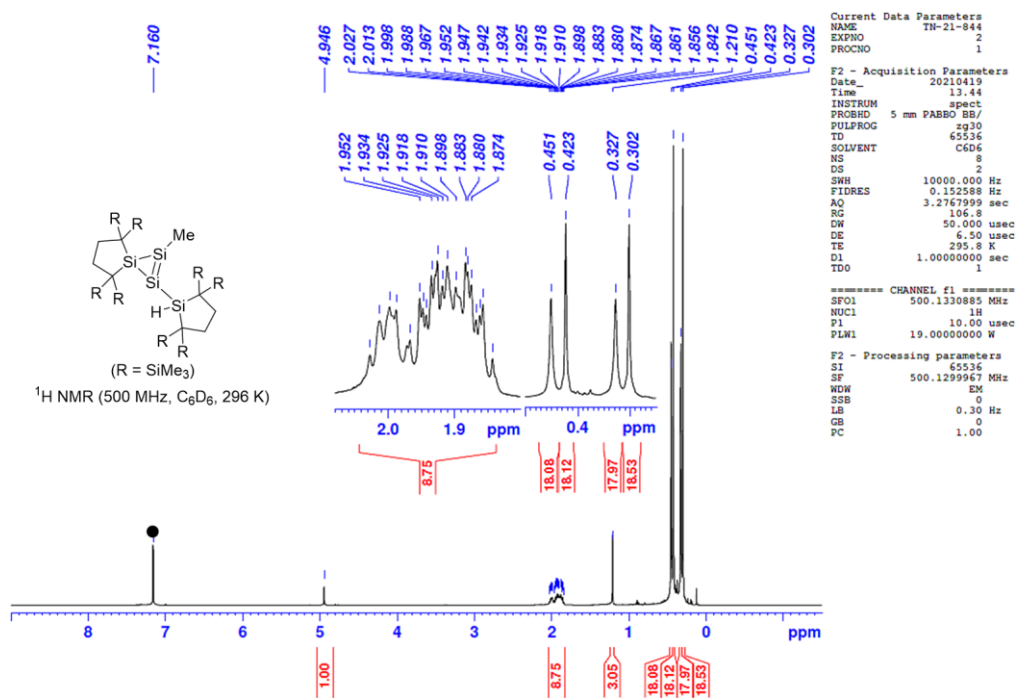


Figure 6-19. ¹H NMR spectrum of **4** in C₆D₆ at 296 K (● = C₆HD₅).

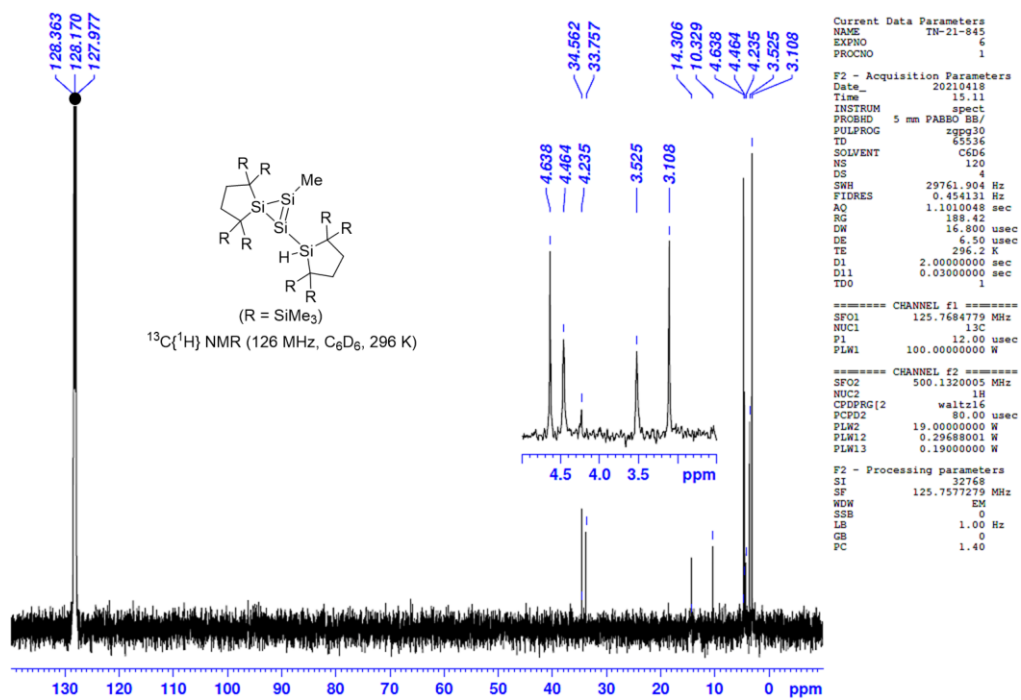


Figure 6-20. ¹³C{¹H} NMR spectrum of **4** in C₆D₆ in 296 K (● = C₆D₆).

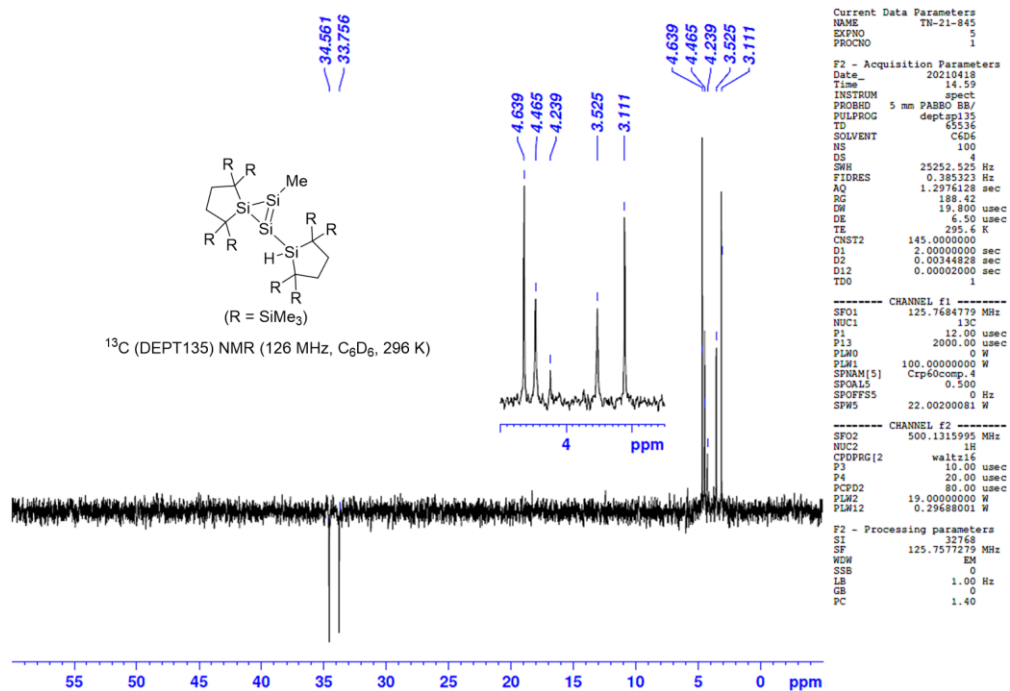


Figure 6-21. ¹³C (DEPT135) NMR spectrum of **4** in C₆D₆ at 296 K.

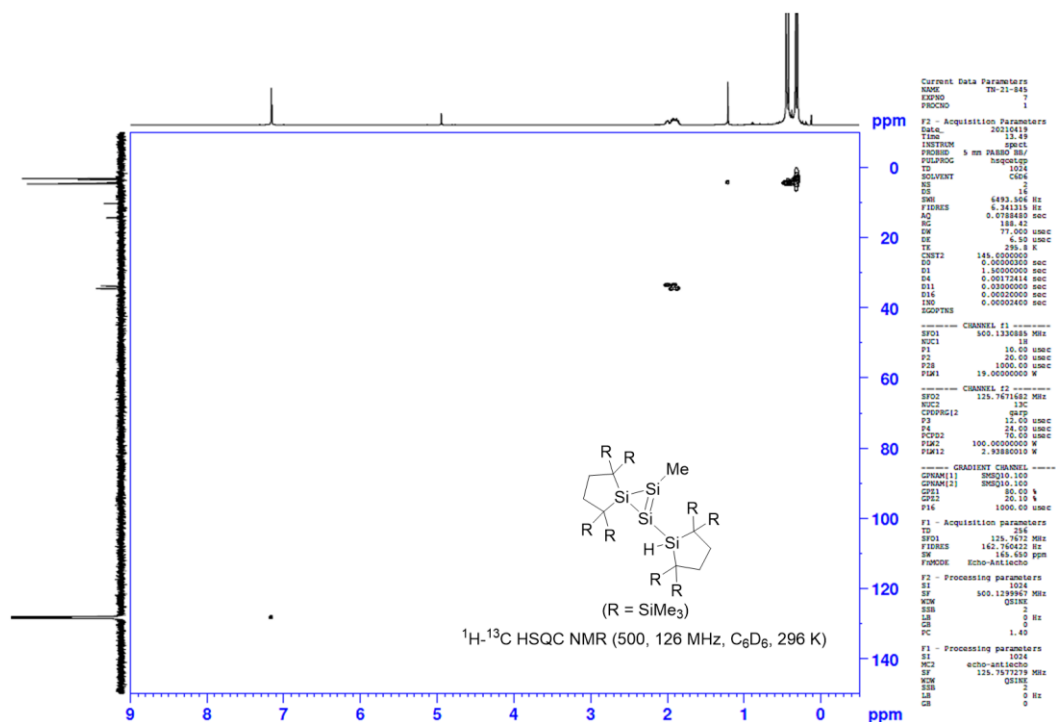


Figure 6-22. ^1H - ^{13}C HSQC NMR spectrum of **4** in C_6D_6 at 296 K.

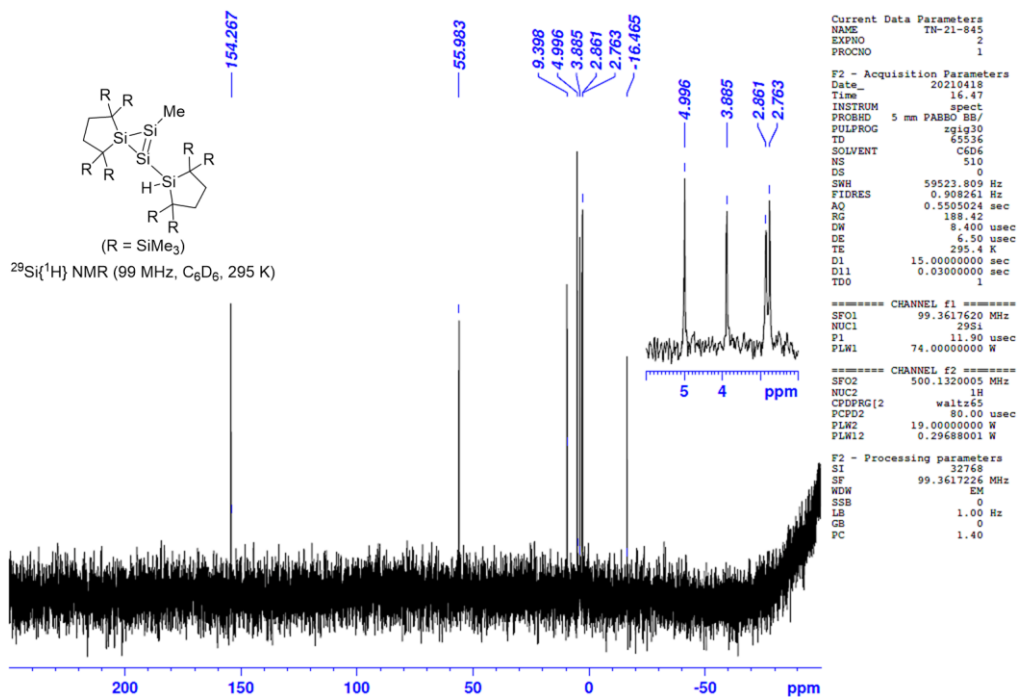


Figure 6-23. $^{29}\text{Si}\{^1\text{H}\}$ NMR spectrum of **4** in C_6D_6 at 295 K.

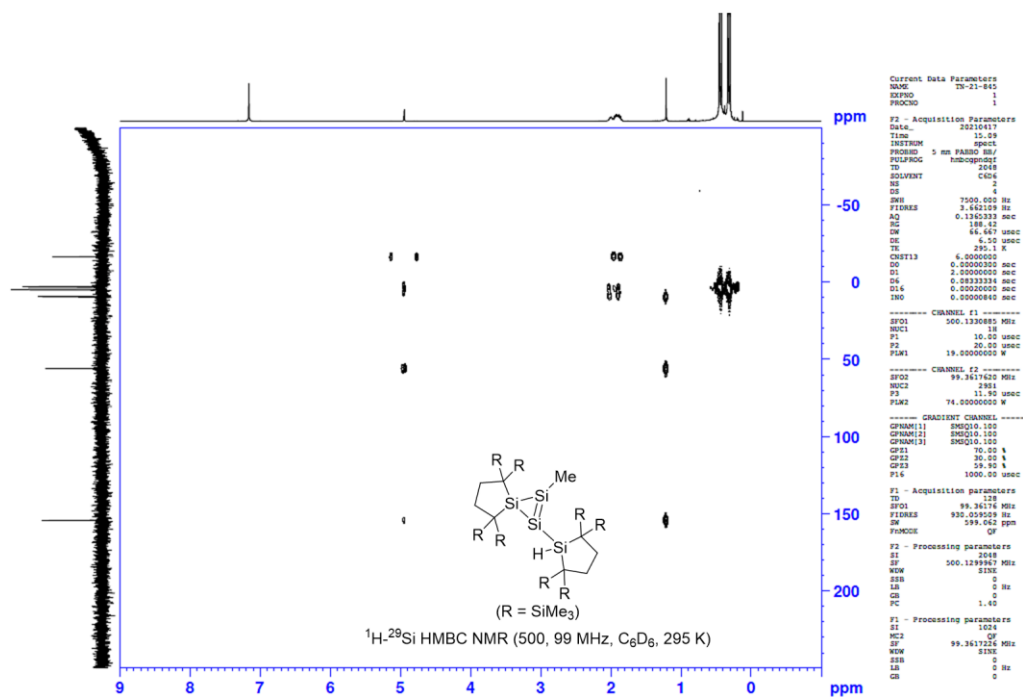


Figure 6-24. ^1H - ^{29}Si HMBC NMR spectrum of **4** in C_6D_6 at 295 K.

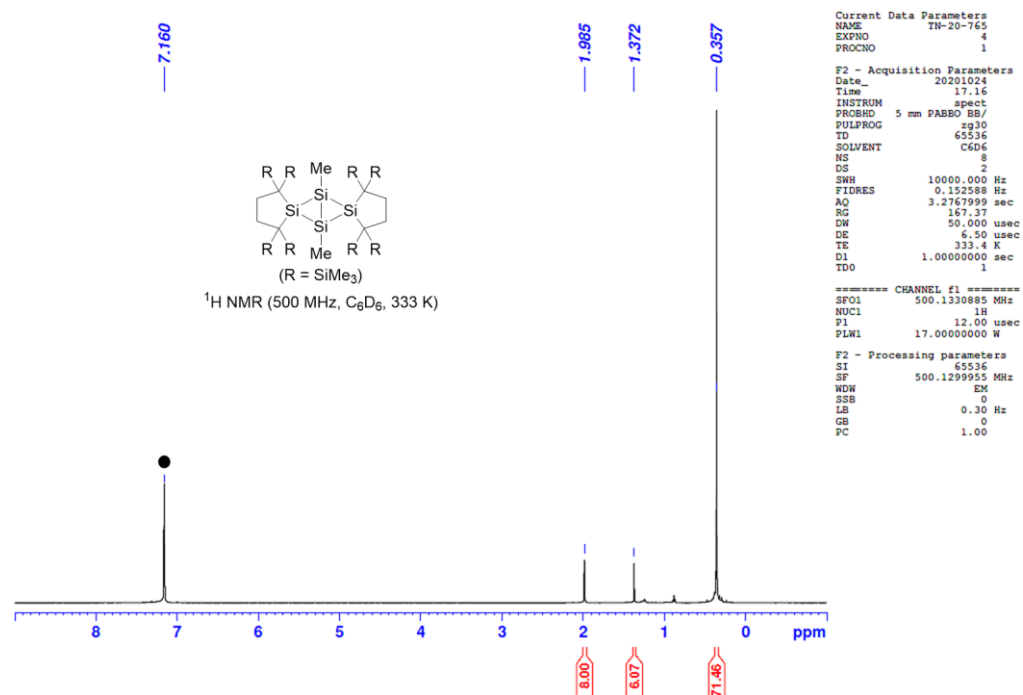


Figure 6-25. ^1H NMR spectrum of **5** in C_6D_6 at 333 K (\bullet = C_6HD_5).

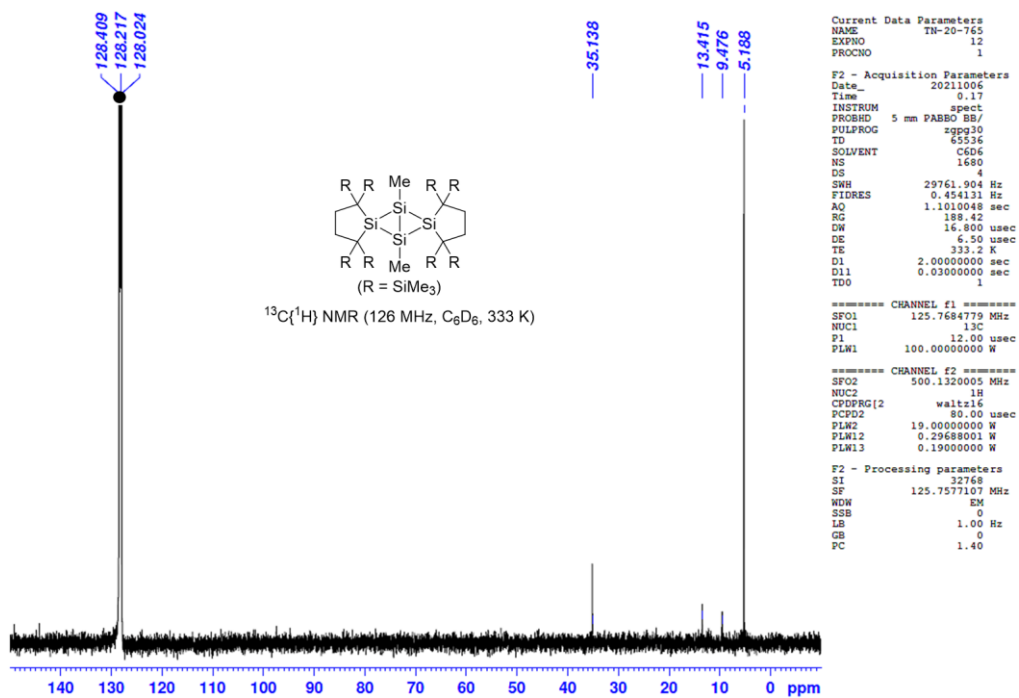


Figure 6-26. $^{13}\text{C}\{^1\text{H}\}$ NMR spectrum of **5** in C_6D_6 in 333 K (● = C_6D_6).

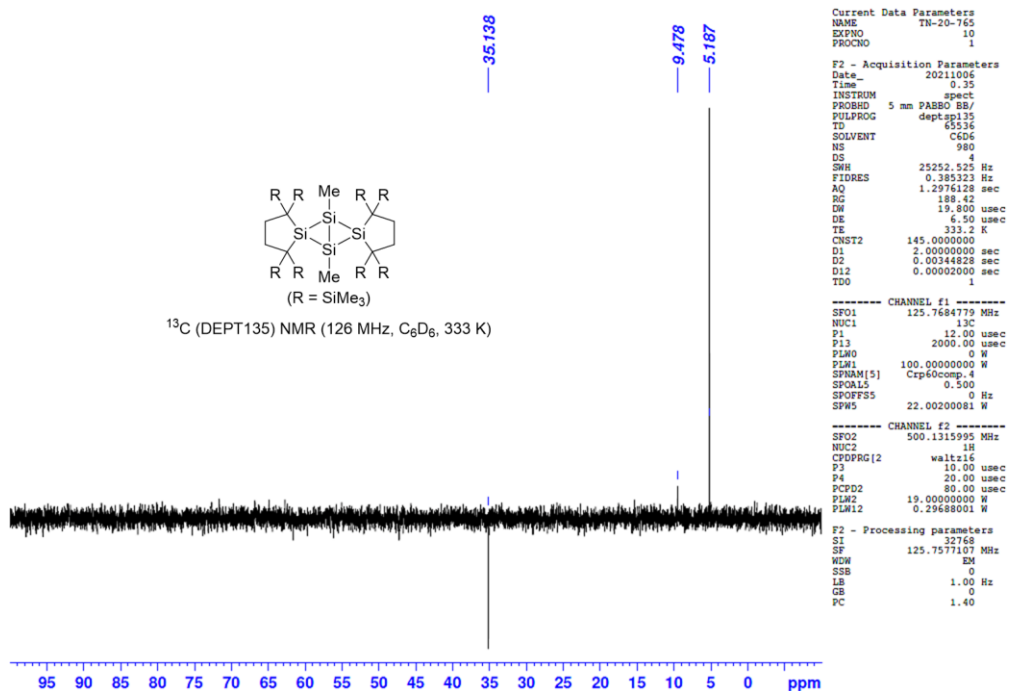


Figure 6-27. ^{13}C (DEPT135) NMR spectrum of **5** in C_6D_6 at 333 K.

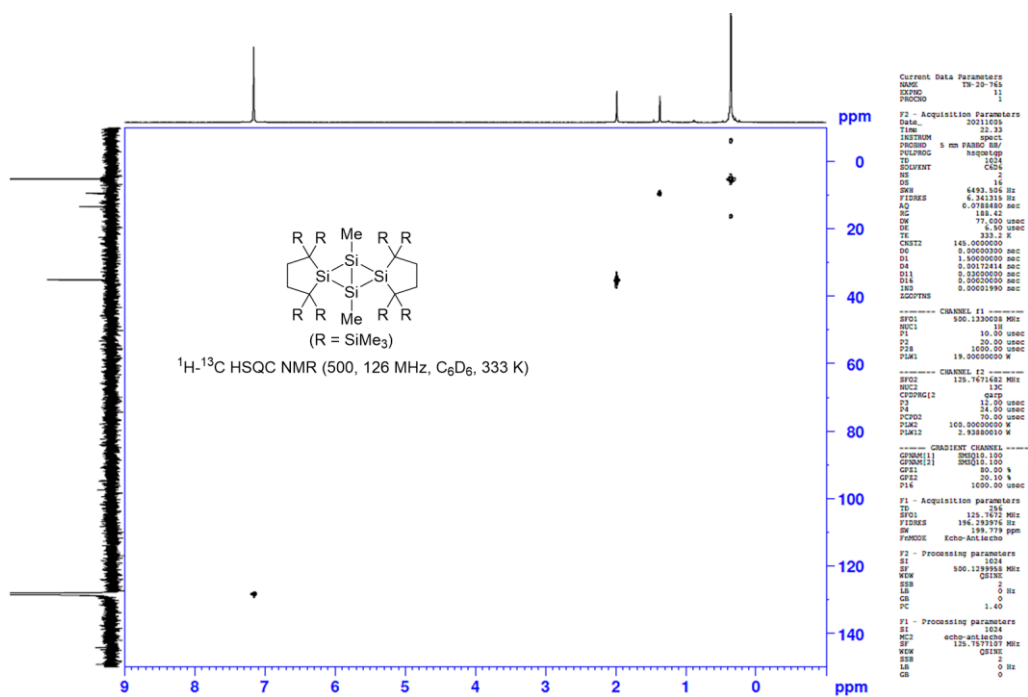


Figure 6-28. ^1H - ^{13}C HSQC NMR spectrum of **5** in C_6D_6 at 333 K.

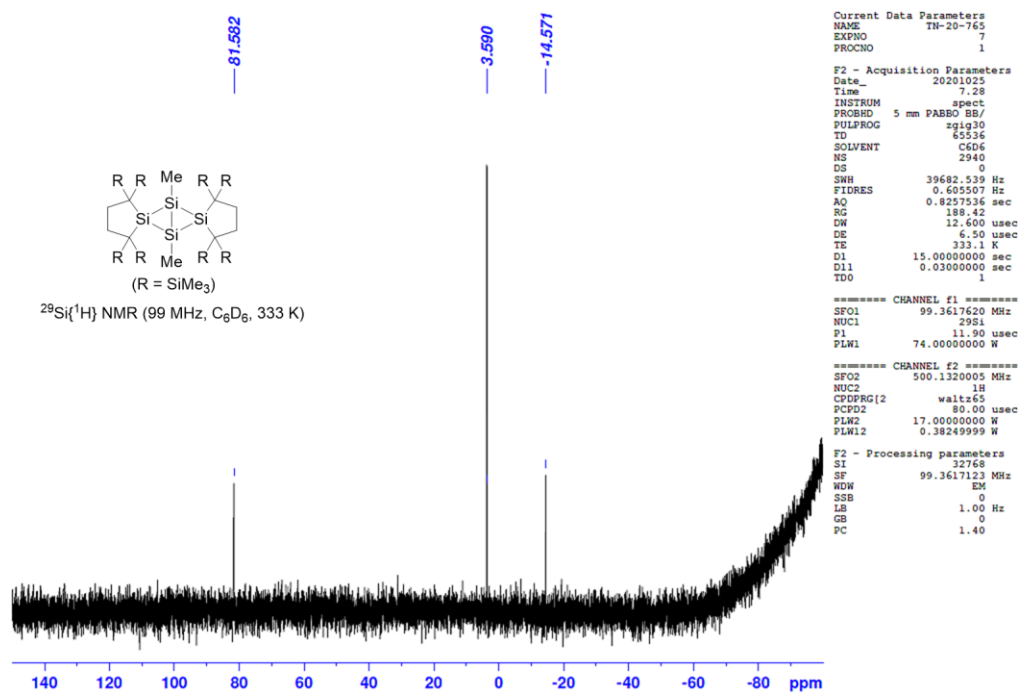


Figure 6-29. $^{29}\text{Si}\{^1\text{H}\}$ NMR spectrum of **5** in C_6D_6 at 333 K.

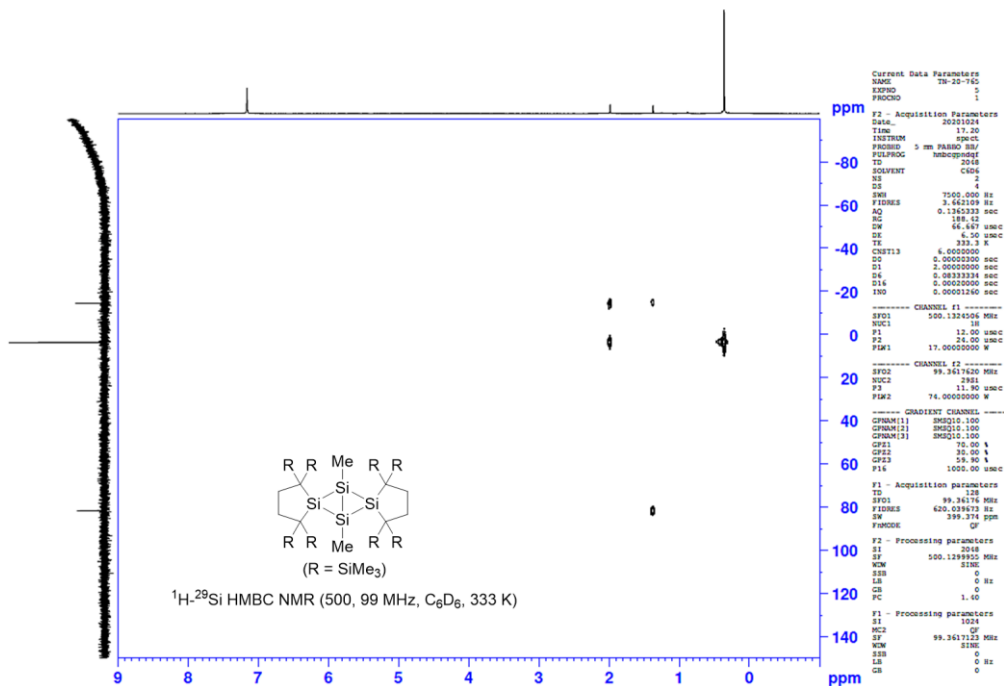


Figure 6-30. ^1H - ^{29}Si HMBC NMR spectrum of **5** in C_6D_6 at 333 K.

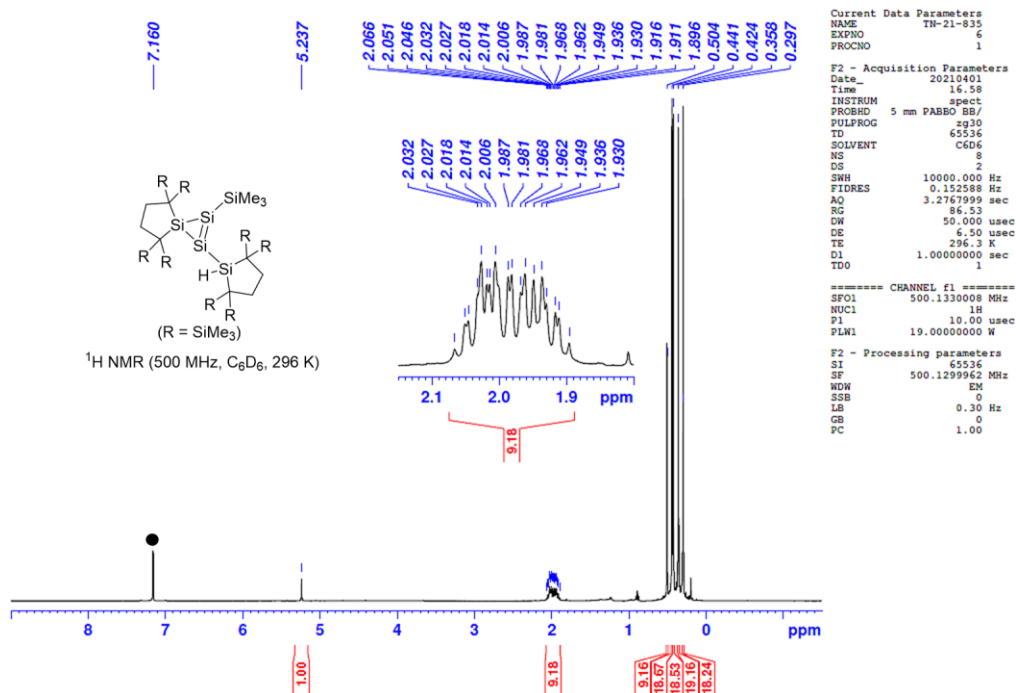


Figure 6-31. ^1H NMR spectrum of **7** in C_6D_6 at 296 K (● = C_6HD_5).

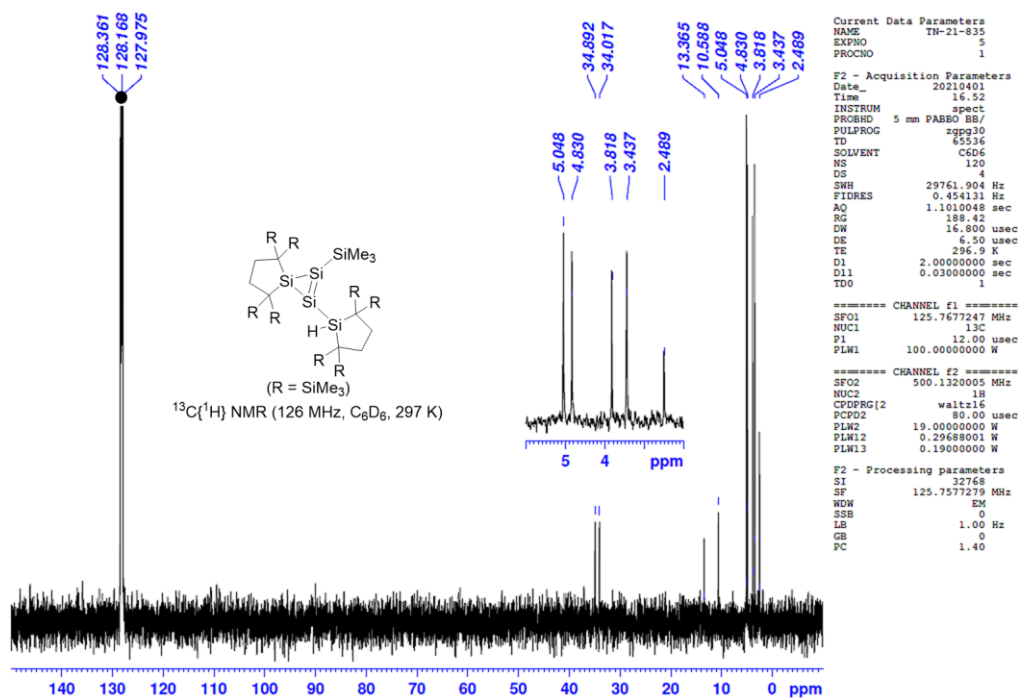


Figure 6-32. $^{13}\text{C}\{^1\text{H}\}$ NMR spectrum of **7** in C_6D_6 in 297 K (● = C_6D_6).

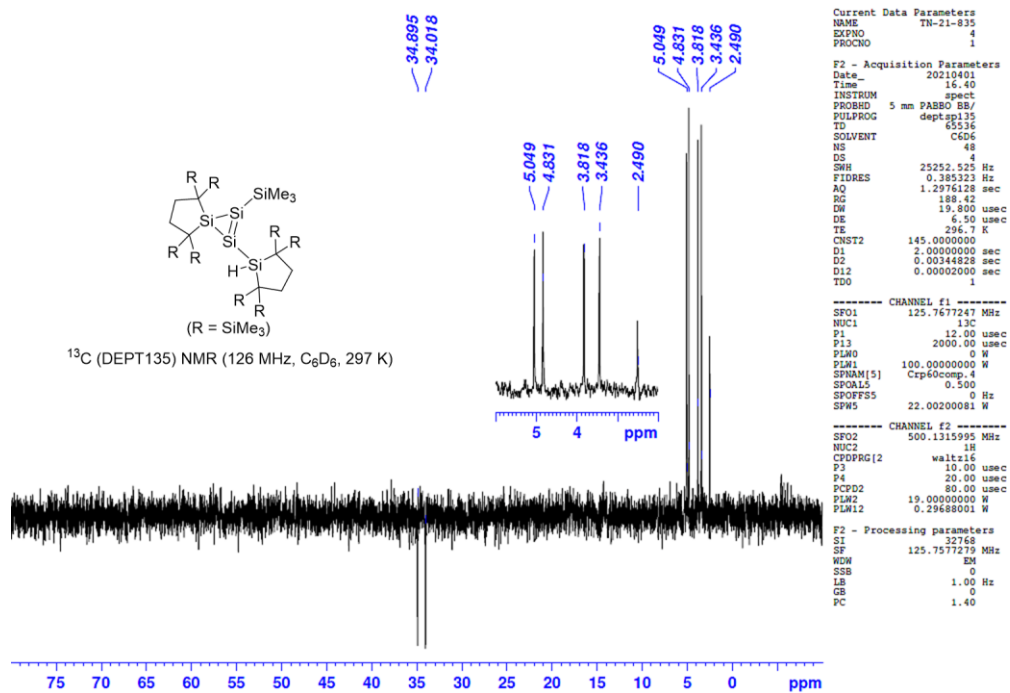


Figure 6-33. ^{13}C (DEPT135) NMR spectrum of **7** in C_6D_6 at 297 K.

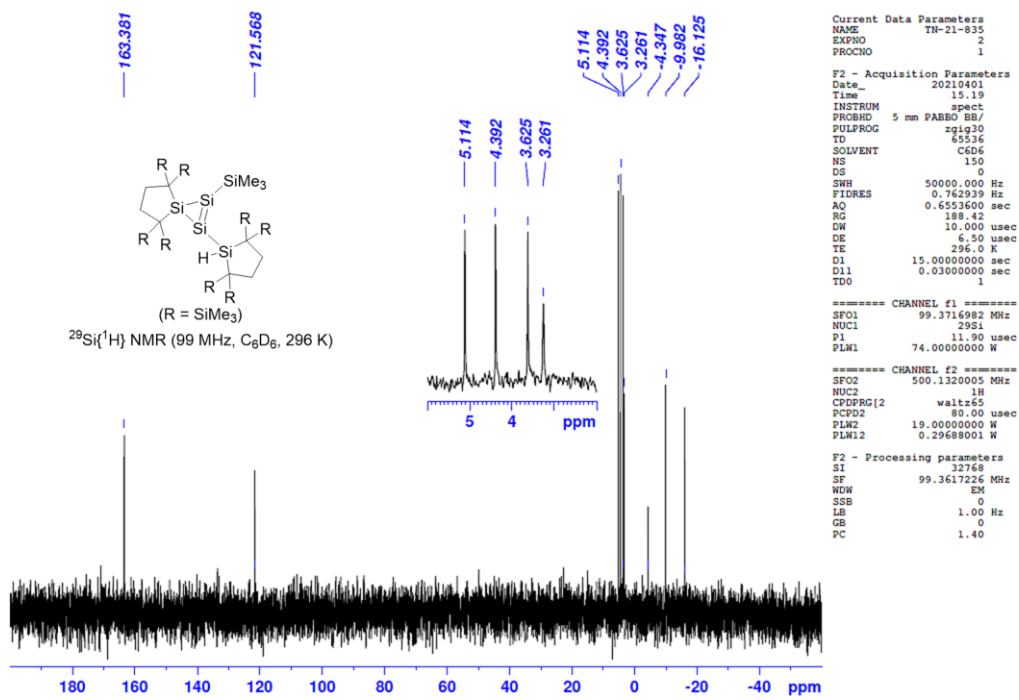


Figure 6-34. $^{29}\text{Si}\{^1\text{H}\}$ NMR spectrum of **7** in C_6D_6 at 296 K.

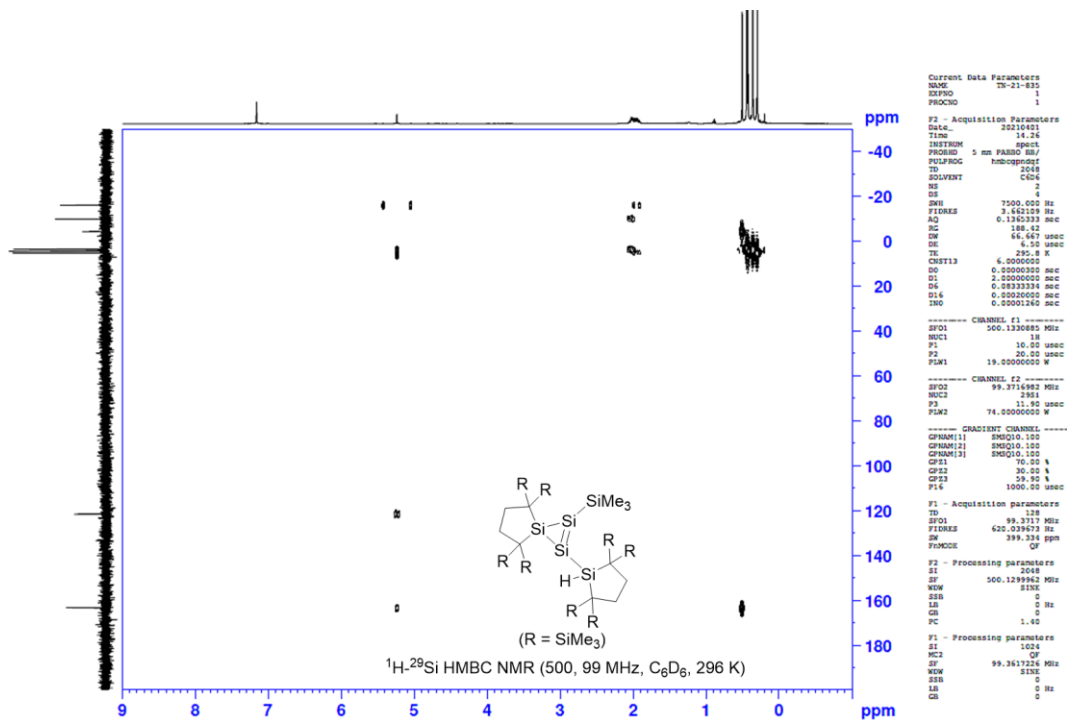


Figure 6-35. ^1H - ^{29}Si HMBC NMR spectrum of **7** in C_6D_6 at 296 K.

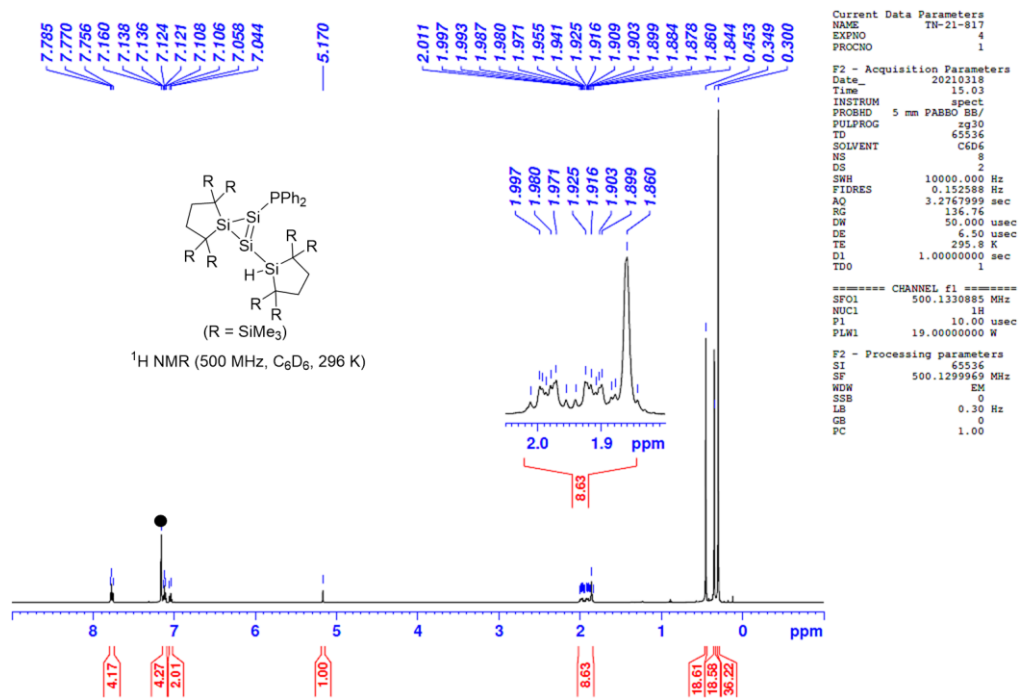


Figure 6-36. ^1H NMR spectrum of **8** in C_6D_6 at 296 K (● = C_6HD_5).

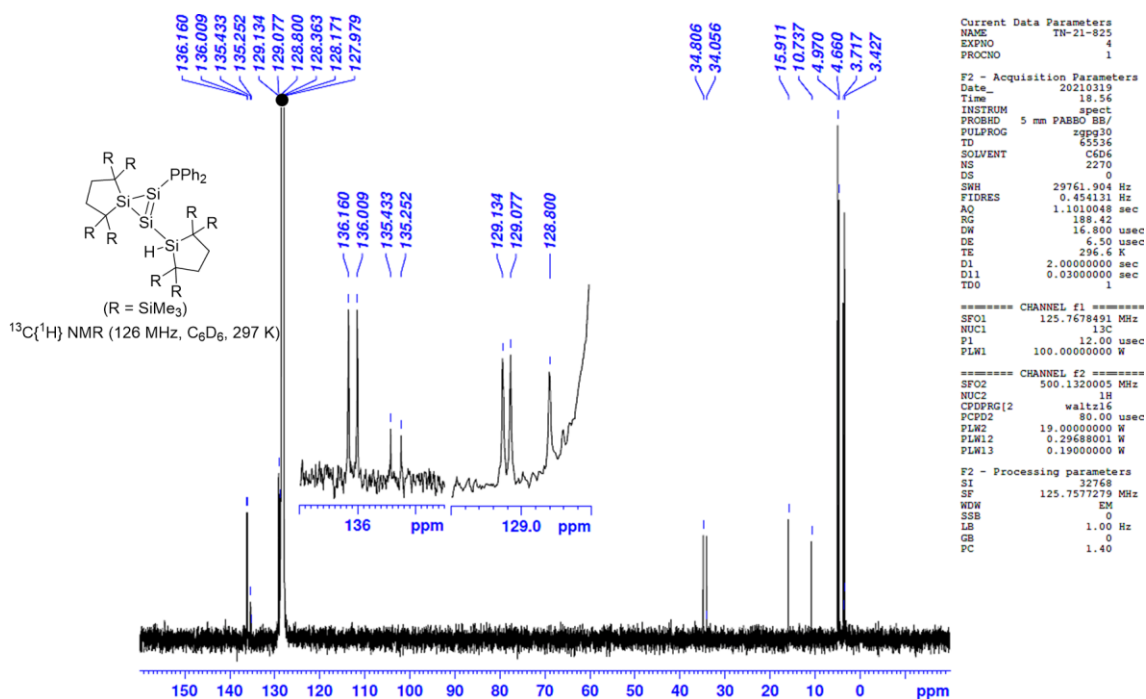


Figure 6-37. $^{13}\text{C}\{^1\text{H}\}$ NMR spectrum of **8** in C_6D_6 in 297 K (● = C_6D_6).

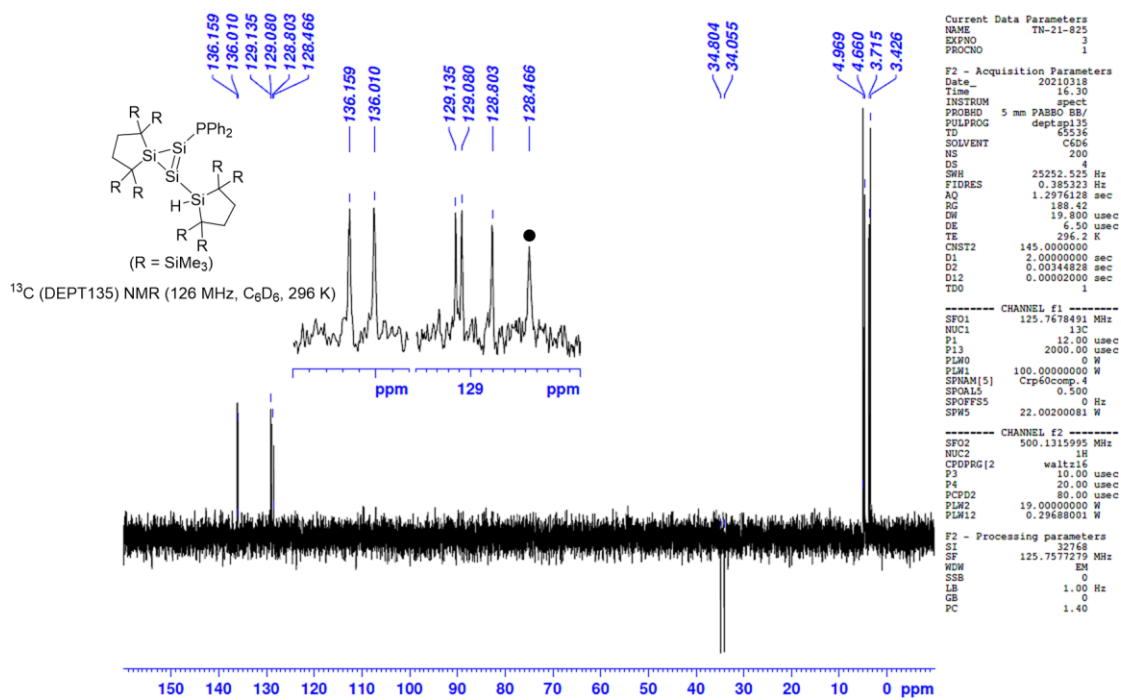


Figure 6-38. ^{13}C (DEPT135) NMR spectrum of **8** in C_6D_6 at 296 K (● = C_6D_6).

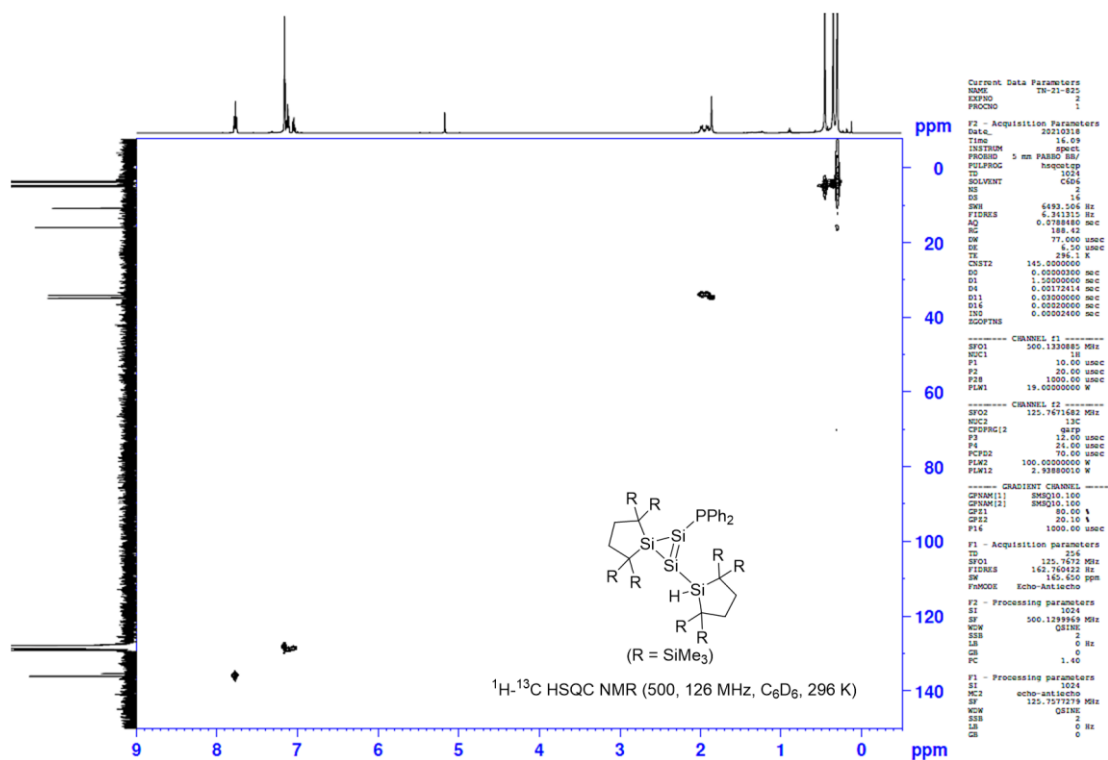


Figure 6-39. ^1H - ^{13}C HSQC NMR spectrum of **8** in C_6D_6 at 296 K.

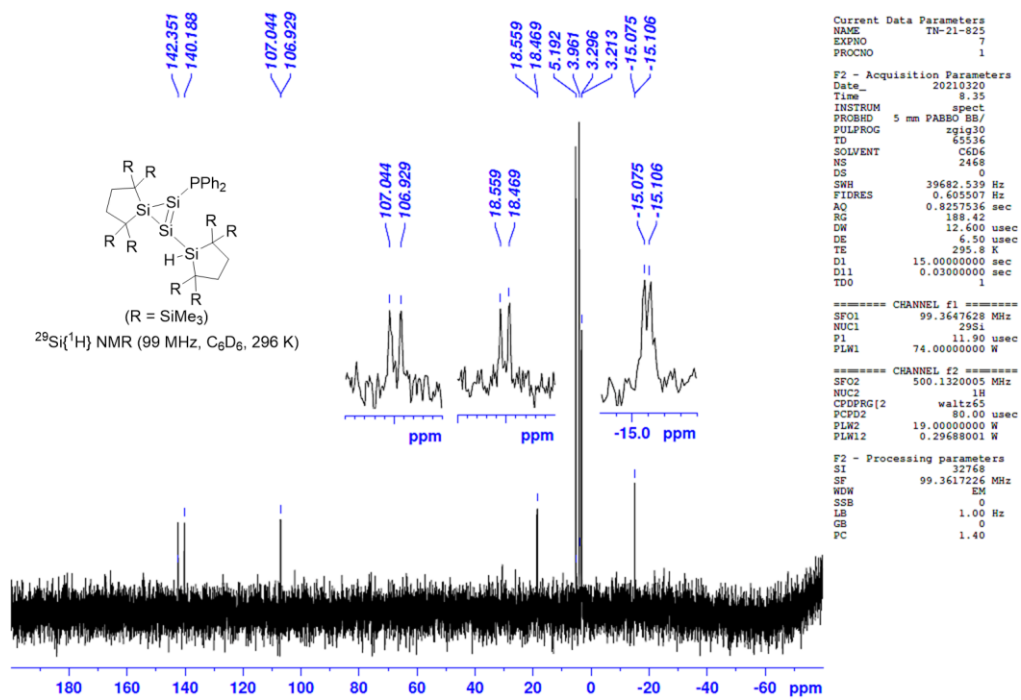


Figure 6-40. ²⁹Si{¹H} NMR spectrum of **8** in C₆D₆ at 296 K.

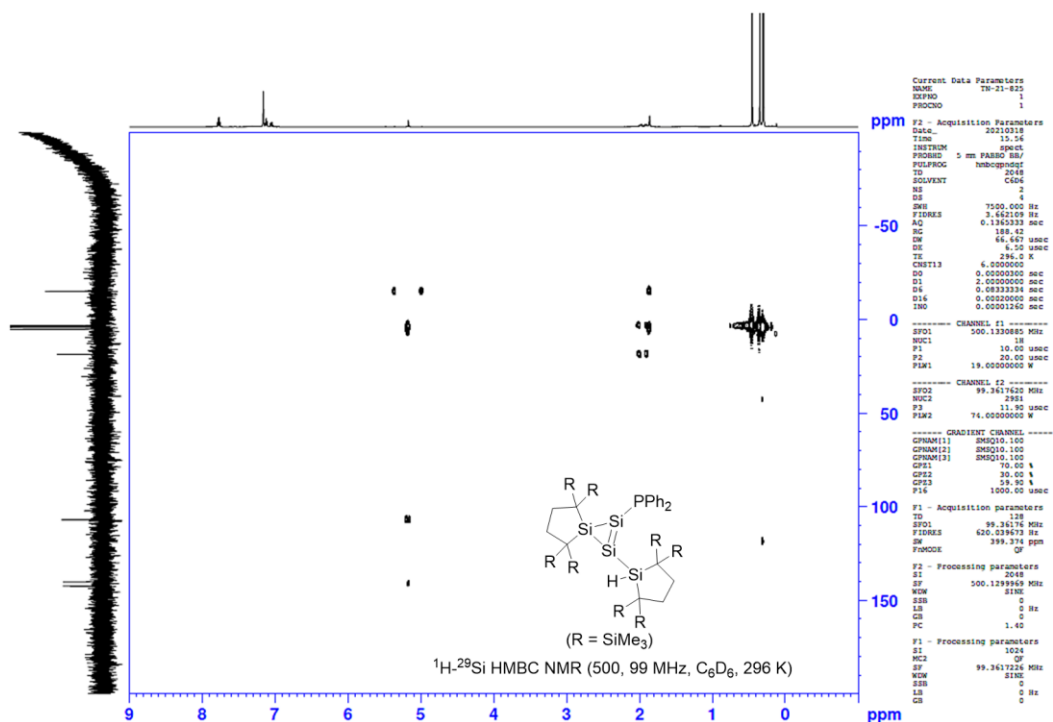


Figure 6-41. ¹H-²⁹Si HMBC NMR spectrum of **8** in C₆D₆ at 296 K.

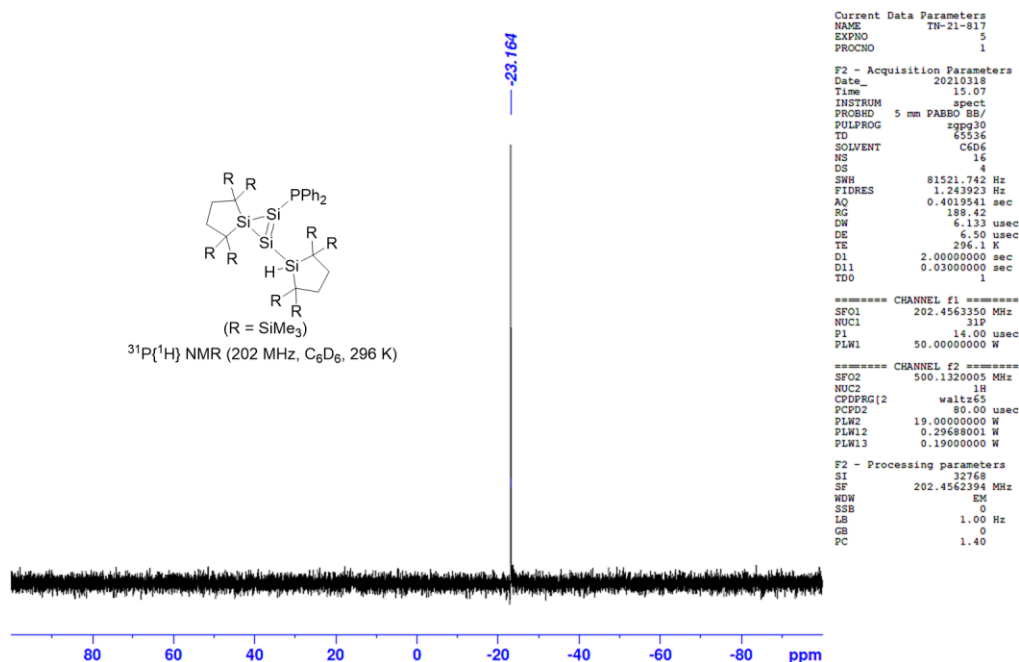


Figure 6-42. ³¹P{¹H} NMR spectrum of **8** in C₆D₆ at 296 K.

X-ray Diffraction Analysis

Single crystals suitable for X-ray diffraction study were obtained by recrystallization in an inert atmosphere using the following conditions; from pentane at $-27\text{ }^{\circ}\text{C}$ for cyclotrisilenide **2**, from toluene at $-27\text{ }^{\circ}\text{C}$ for silyl anion **3**_{CIP} (contact ion pair), from Et₂O at $-27\text{ }^{\circ}\text{C}$ for silyl anion **3**_{SSIP} (solvent-separated ion pair), from toluene at $-27\text{ }^{\circ}\text{C}$ for cyclotrisilene **4**, from benzene at room temperature for bicyclo[1.1.0]tetrasilane **5**, from hexane at $-27\text{ }^{\circ}\text{C}$ for cyclotrisilene **8**. For data collection, the single crystals coated by Apiezon grease were mounted on the glass fiber and then transferred to the cold nitrogen gas stream of the diffractometer. X-ray diffraction data were collected on a Bruker AXS APEX II CCD diffractometer using a graphite monochromated Mo-K α radiation. An empirical absorption correction based on the multiple measurements of equivalent reflections was applied using the program SADABS²⁶ and the structures were solved by direct methods and refined by full-matrix least squares against F^2 using all data (SHELXL-2014).²⁷ Molecular structure was analysed by Yadokari-XG software.²⁸

Crystal data of cyclotrisilenide **2** [tn33f] (100 K) [CCDC-2109131]: $C_{44}H_{105}LiO_3Si_{12}$; Fw 1026.28; Monoclinic, $P2_1/c$, $a = 13.0239(5)$ Å, $b = 26.5332(9)$ Å, $c = 20.0854(7)$ Å, $\beta = 101.5760(10)^\circ$, $V = 6799.6(4)$ Å³, $Z = 4$, $D_{\text{calc}} = 1.073$ Mg/m³, $R1 = 0.0458$ ($I > 2\sigma(I)$), $wR2 = 0.1243$ (all data), GOF = 1.052.

Crystal data of silyl anion **3_{CIP}** [tn66a] (100 K) [CCDC-2109132]: $C_{37}H_{93}LiOSi_{12}$; Fw 898.11; Triclinic; $P-1$, $a = 15.6180(15)$ Å, $b = 18.3260(18)$ Å, $c = 19.5473(19)$ Å, $\alpha = 79.580(2)^\circ$, $\beta = 85.086(2)^\circ$, $\gamma = 81.005(2)^\circ$, $V = 5425.3(9)$ Å³, $Z = 4$, $D_{\text{calc}} = 1.100$ Mg/m³, $R1 = 0.0410$ ($I > 2\sigma(I)$), $wR2 = 0.1113$ (all data), GOF = 1.030.

Crystal data of silyl anion **3_{SSIP}** [tn64b] (100 K) [CCDC-2109133]: $C_{49}H_{123}LiO_4Si_{12}$; Fw 1120.48; Orthorhombic, $Pna2_1$, $a = 28.3355(18)$ Å, $b = 16.0930(10)$ Å, $c = 14.9192(10)$ Å, $V = 6803.2(8)$ Å³, $Z = 4$, $D_{\text{calc}} = 1.094$ Mg/m³, $R1 = 0.0408$ ($I > 2\sigma(I)$), $wR2 = 0.1123$ (all data), GOF = 1.074.

Crystal data of cyclotrisilene **4** [tn50a] (100 K) [CCDC-2109134]: $C_{33}H_{84}Si_{12}$; Fw 818.06; Monoclinic, $P2_1/n$, $a = 16.0494(9)$ Å, $b = 16.6272(9)$ Å, $c = 18.9919(10)$ Å, $\beta = 99.6730(10)^\circ$, $V = 4996.1(5)$ Å³, $Z = 4$, $D_{\text{calc}} = 1.088$ Mg/m³, $R1 = 0.0355$ ($I > 2\sigma(I)$), $wR2 = 0.0940$ (all data), GOF = 1.025.

Crystal data of bicyclo[1.1.0]tetrasilane **5** [tn63ba] (100 K) [CCDC-2114373]: $C_{34}H_{86}Si_{12}$; Fw 832.10; Triclinic, $P-1$, $a = 11.9706(5)$ Å, $b = 12.7911(7)$ Å, $c = 17.8378(7)$ Å, $\alpha = 101.2600(10)^\circ$, $\beta = 100.1120(10)^\circ$, $\gamma = 108.7420(10)^\circ$, $V = 2451.7(2)$ Å³, $Z = 2$, $D_{\text{calc}} = 1.127$ Mg/m³, $R1 = 0.0378$ ($I > 2\sigma(I)$), $wR2 = 0.0922$ (all data), GOF = 1.015.

Crystal data of cyclotrisilene **8** [tn83a] (100 K) [CCDC-2109135]: $C_{44}H_{91}Si_{12}P$; Fw 988.21; Monoclinic, $P2_1/n$, $a = 11.5263(6)$ Å, $b = 29.5998(16)$ Å, $c = 17.3317(10)$ Å, $\beta = 103.9400(10)^\circ$, $V = 5739.0(5)$ Å³, $Z = 4$, $D_{\text{calc}} = 1.144$ Mg/m³, $R1 = 0.0326$ ($I > 2\sigma(I)$), $wR2 = 0.0881$ (all data), GOF = 1.040.

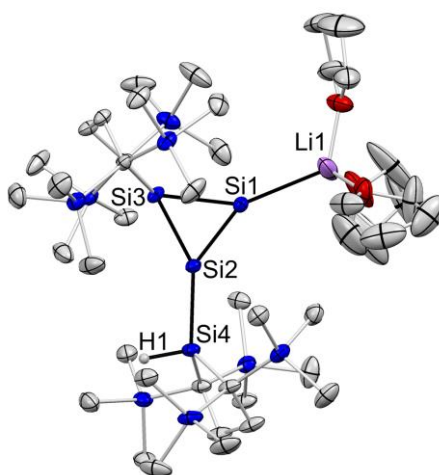


Figure 6-43. ORTEP of **2**. Thermal ellipsoids are shown at the 50% probability level. Hydrogen atoms, co-crystallized solvent, and disordered atoms are omitted for clarity.

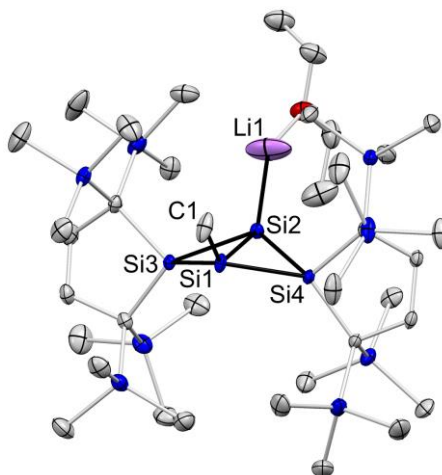


Figure 6-44. ORTEP of **3_{CIP}**. Thermal ellipsoids are shown at the 50% probability level. Hydrogen atoms are omitted for clarity.

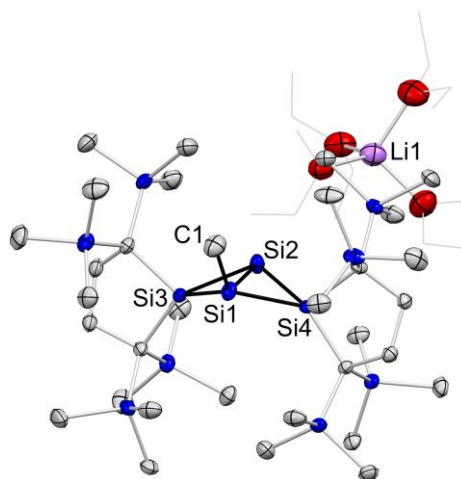


Figure 6-45. ORTEP of **3_{SSIP}**. Thermal ellipsoids are shown at the 50% probability level. Hydrogen atoms are omitted for clarity.

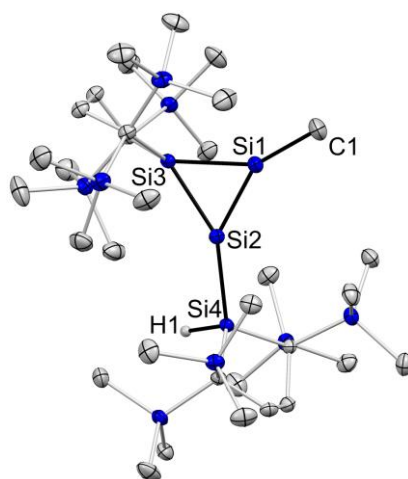


Figure 6-46. ORTEP of **4**. Thermal ellipsoids are shown at the 50% probability level. Hydrogen atoms are omitted for clarity.

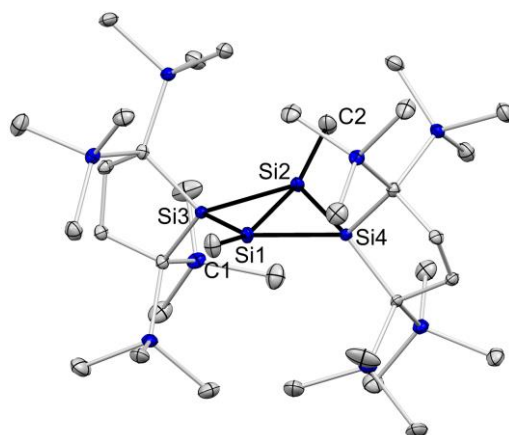


Figure 6-47. ORTEP of **5**. Thermal ellipsoids are shown at the 50% probability level. Hydrogen atoms are omitted for clarity.

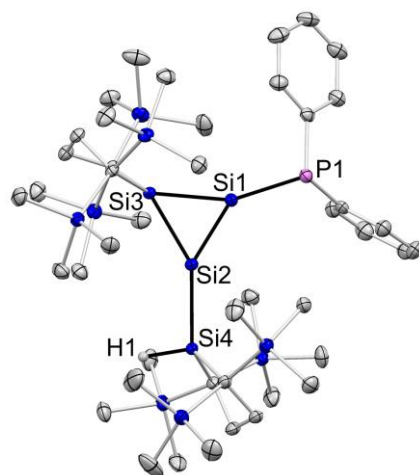


Figure 6-48. ORTEP of **8**. Thermal ellipsoids are shown at the 50% probability level. Hydrogen atoms are omitted for clarity.

UV-vis Absorption Spectrum

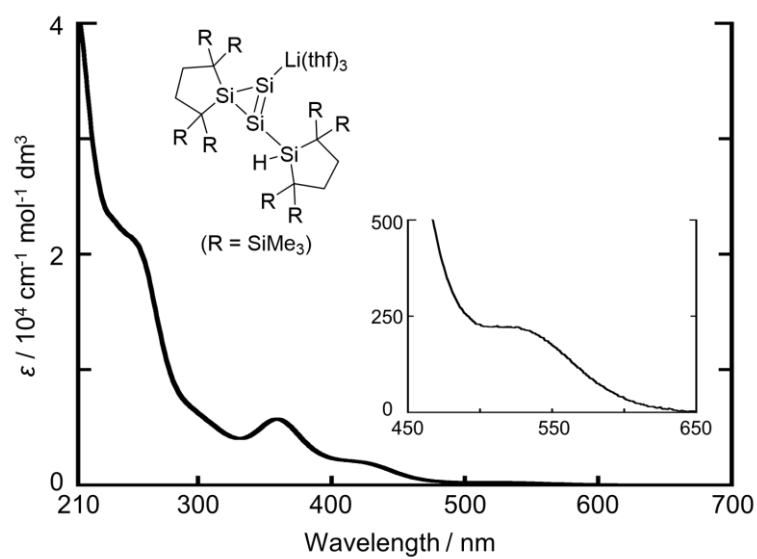


Figure 6-49. UV-vis absorption spectrum of **2** in hexane at room temperature [TN790].

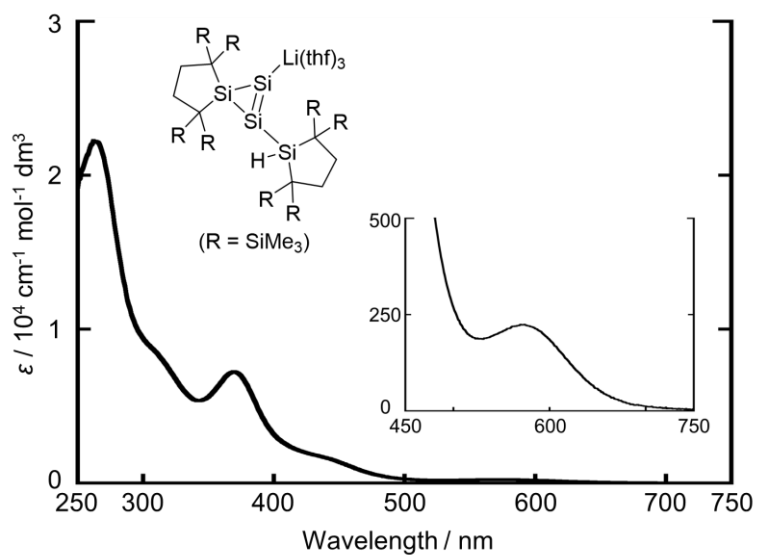


Figure 6-50. UV-vis absorption spectrum of **2** in THF at room temperature [TN790].

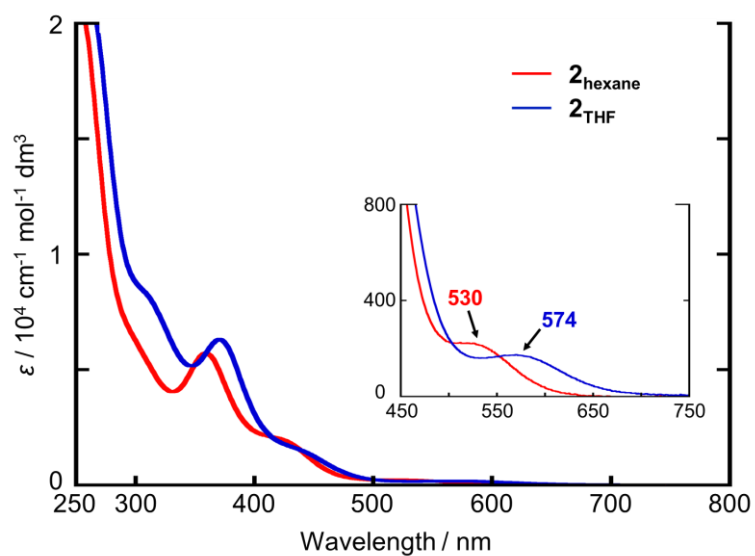


Figure 6-51. UV-vis absorption spectra of **2** at room temperature (red: hexane, blue: THF).

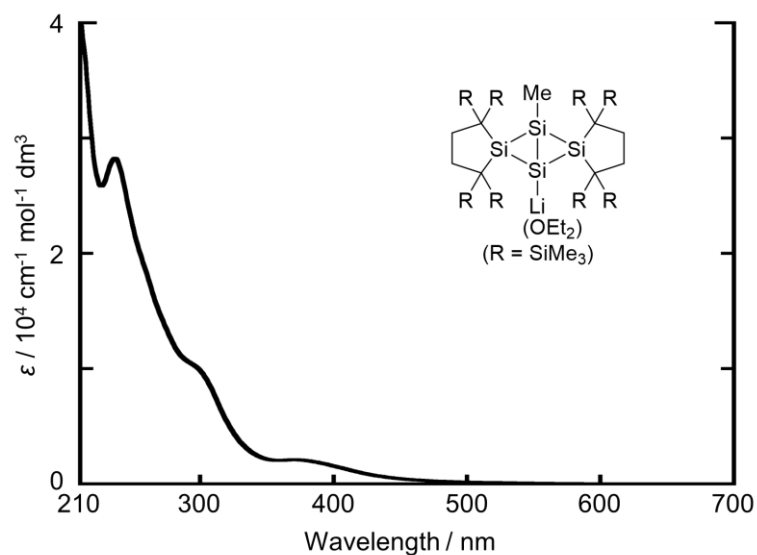


Figure 6-52. UV-vis absorption spectrum of **3** in hexane at room temperature [TN780].

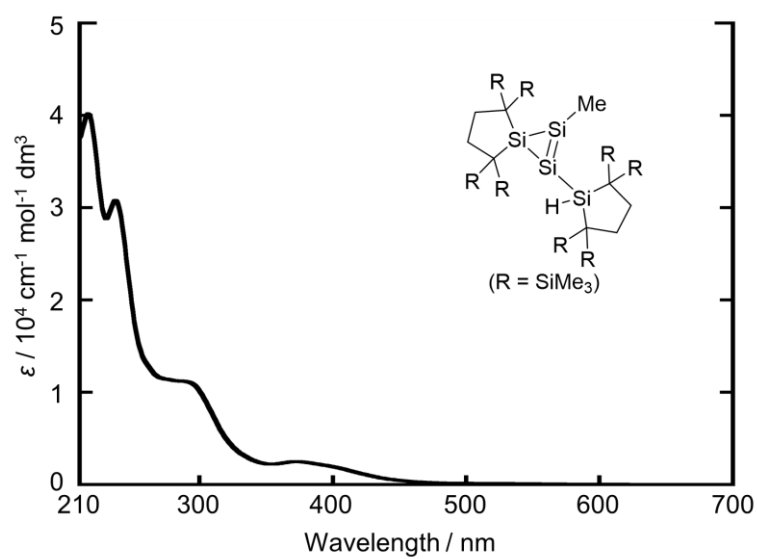


Figure 6-53. UV-vis absorption spectrum of **4** in hexane at room temperature [TN845].

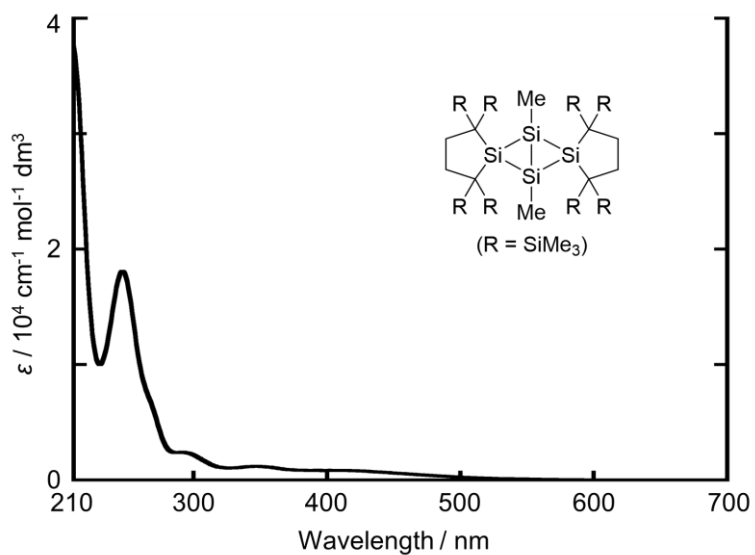


Figure 6-54. UV-vis absorption spectrum of **5** in hexane at room temperature [TN765].

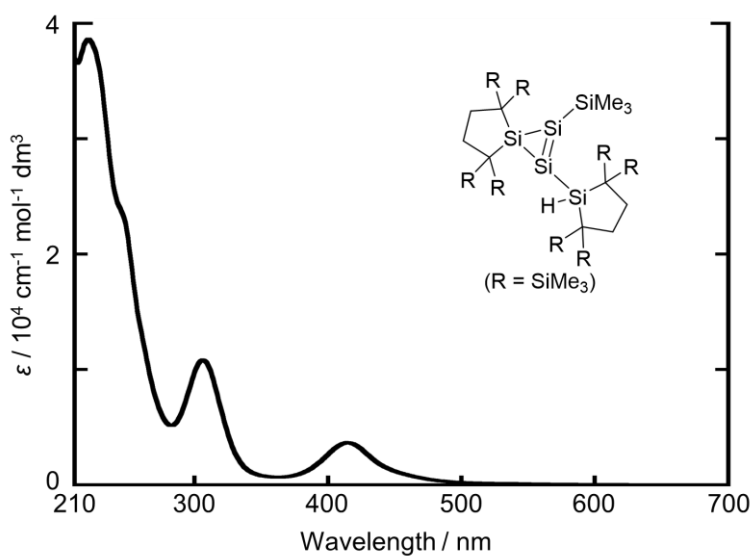


Figure 6-55. UV-vis absorption spectrum of **7** in hexane at room temperature [TN835].

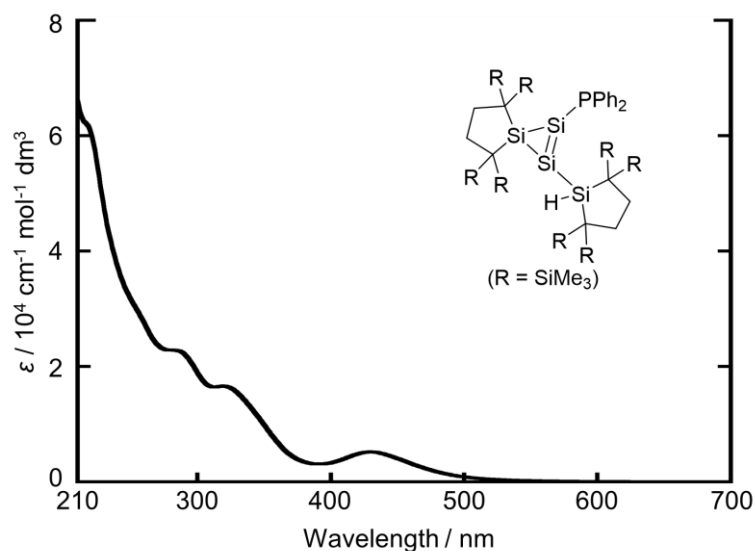
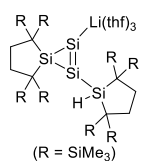


Figure 6-56. UV-vis absorption spectrum of **8** in hexane at room temperature [TN825].

Computational Study

All theoretical calculations were performed using a Gaussian 09²⁹ program or GRRM14 program.³⁰ Geometry optimization was carried out at the B3LYP-D3/6-311G(d) (**2**_{opt}, **2'**_{opt} (free anion of **2**), and **8**_{opt}) and M06-2X/6-311G(d) (**3**_{opt}) level of theory. Frontier Kohn-Sham orbitals and their energy levels of **2**_{opt}, **2'**_{opt}, and **8**_{opt} were shown in Figures 6-57 to 6-59. The optimized structures of model cyclo-trisilene **9** with an SiMe₃ group and a PMe₂ group on the Si=Si double bond and methyl groups on the saturated ring silicon atom at the B3LYP-D3/6-311G(d) level of theory was shown in Figure 6-60. The atomic coordinates and energies of the optimized structures are summarized in Tables 6-1 to 6-6. Isotropic chemical shielding tensors were calculated at the GIAO/M06L/6-311+G(2df,p) level of theory (Tables 6-7 and 6-8). Absolute isotropic shielding tensors of ²⁹Si nucleus in tetramethylsilane were calculated to be 361.4 (GIAO/M06L/6-311+G(2df,p)). Excitation energies and oscillator strengths were calculated at the B3LYP-D3/6-311+G(d)/SCRF(solvent = heptane) (**2**_{opt}) and B3LYP-D3/6-311+G(d)/SCRF(solvent = THF) (**2'**_{opt}) level of theory (Tables 6-9 and 6-10). Natural bond orbital (NBO)³¹ calculation of **8**_{opt} was performed at the B3LYP-D3/6-311G(d) level of theory (Table 6-11).

Table 6-1. Atomic Coordinates of Cyclotrisilene 2_{opt} at the B3LYP-D3/6-311G(d) Level of Theory

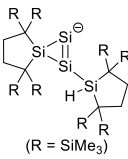


| Atom | X | Y | Z |
|------|-----------------|------------------|-----------------|
| Si | 4.024002480248 | 10.717873381792 | 5.121179003724 |
| Si | 2.092000258213 | 10.150166883217 | 5.974214746097 |
| Si | 2.023584572771 | 11.727859791619 | 4.336664126023 |
| Li | 6.584278763353 | 10.429070719138 | 5.366587736384 |
| Si | 0.969175023987 | 8.859078942263 | 7.625279665549 |
| C | 2.344180623003 | 6.515669243275 | 4.662771044360 |
| H | 2.667762905544 | 7.558500923079 | 4.636451809996 |
| H | 1.497420392878 | 6.411156722021 | 3.986154422360 |
| H | 3.156848870959 | 5.902455818288 | 4.258991181896 |
| C | 1.419421279566 | 4.107103557578 | 6.274729981066 |
| H | 2.232930246634 | 3.538911241015 | 5.810521122340 |
| H | 0.529317807887 | 3.949912976349 | 5.663312904630 |
| H | 1.233625129039 | 3.653680328852 | 7.252578183220 |
| C | 3.634049971592 | 5.794351051833 | 7.291914740933 |
| H | 4.297158033545 | 5.178755938104 | 6.673845573902 |
| H | 3.561394452100 | 5.305377727334 | 8.266655660336 |
| H | 4.119946078444 | 6.756997432884 | 7.431581526821 |
| Si | 1.963622133593 | 5.922794269444 | 6.410097524907 |
| Si | -1.093808336346 | 6.601203092186 | 6.655250366900 |
| C | -1.793485756067 | 5.023982267368 | 7.442806330711 |
| H | -2.720187016297 | 4.745706144577 | 6.929796501239 |
| H | -2.045211524331 | 5.176376889174 | 8.496190085109 |
| H | -1.118288322708 | 4.169163189883 | 7.386732543180 |
| C | -1.119489091796 | 6.385985020612 | 4.775838941356 |
| H | -0.614153403895 | 5.487500908066 | 4.417658794299 |
| H | -0.682614747143 | 7.242863820766 | 4.262338129056 |
| H | -2.164356505407 | 6.320096489690 | 4.454372605351 |
| C | -2.401184682432 | 7.932818667562 | 6.975321816837 |
| H | -2.236621049147 | 8.833445220640 | 6.381365861346 |
| H | -2.486151595921 | 8.237217522114 | 8.019018715135 |
| H | -3.371062281795 | 7.517095841654 | 6.678565613149 |
| C | 0.666210354899 | 6.954874801351 | 7.377342348120 |
| C | 0.691227235488 | 6.467222763862 | 8.879245937122 |
| H | -0.296472672346 | 6.577989960247 | 9.328417205909 |
| C | 0.915628134147 | 5.396165139382 | 8.950557707699 |
| C | 1.699013824913 | 7.263208081510 | 7.732327005597 |
| H | 2.708580157528 | 6.914336760466 | 9.499735241267 |
| H | 1.546205427109 | 7.020490737218 | 10.791545107226 |
| C | 1.589138051497 | 8.809270592619 | 9.471723900694 |
| Si | 0.244604654278 | 9.565991846100 | 10.625496458313 |
| C | -1.273385058279 | 8.448979206002 | 10.813324385950 |
| H | -1.988923202220 | 8.954001909009 | 11.471092218963 |
| H | -1.031200119629 | 7.490324189810 | 11.280442941402 |
| H | -1.787536753621 | 8.247339924230 | 9.873834365388 |
| C | 0.859272749512 | 9.768064978881 | 12.410360782498 |
| H | 1.577325417615 | 10.582111575322 | 12.531706318714 |
| H | 1.315421464493 | 8.878563302851 | 12.808180656586 |
| H | -0.002352778050 | 10.002968937851 | 13.044392254140 |
| C | -0.380158473215 | 11.257802409588 | 10.074624485798 |
| H | -1.011051174202 | 11.6761838845995 | 10.866491166719 |
| H | -0.983956073004 | 11.200866034036 | 9.168655646872 |
| H | 0.419676202802 | 11.973927520074 | 9.883554208753 |
| C | 4.000186273190 | 9.031502656028 | 11.491715523474 |
| H | 5.079353494996 | 9.222179299899 | 11.502357926896 |
| H | 3.868368192528 | 7.954962614720 | 11.637326817025 |
| H | 3.572619288740 | 9.535137791383 | 12.358198840679 |
| C | 3.202661769559 | 11.487881055649 | 9.819631476932 |
| H | 4.202740916683 | 11.923214591414 | 9.903166061788 |
| H | 2.616073261598 | 11.877158642346 | 10.655138753014 |
| H | 2.758783997460 | 11.864091061445 | 8.896061815990 |
| Si | 3.292757700129 | 9.601186883694 | 9.822813111440 |
| C | 4.639713571901 | 9.055718722041 | 8.609918520644 |
| H | 4.352521263563 | 9.143077993180 | 7.562731254397 |
| H | 4.956328223265 | 8.029697012453 | 8.810765432339 |
| H | 5.520664429165 | 9.68858894321 | 8.749803417272 |
| C | 1.338898736979 | 11.536106645526 | 2.510498993912 |
| Si | 2.727218543050 | 11.140412344671 | 1.261859598324 |
| C | 3.977333900372 | 12.560167729767 | 1.147515954189 |
| H | 4.788604049023 | 12.282895603329 | 0.465516201288 |
| H | 4.417851965383 | 12.788038565559 | 2.117252195319 |
| H | 3.528888943491 | 13.478166417890 | 0.758853218673 |
| C | 3.750003716616 | 9.584367956059 | 1.610175402399 |
| H | 3.169430805124 | 8.662758115453 | 1.569297733576 |
| H | 4.222447629555 | 9.628417316999 | 2.594110432635 |
| H | 4.542553997694 | 9.507800057589 | 0.856227678541 |
| C | 2.043468068281 | 10.962253624108 | -0.502235737091 |
| H | 1.453572686389 | 11.831864778789 | -0.806068476195 |
| H | 1.415682686239 | 10.078379229311 | -0.635549714914 |
| H | 2.876854751642 | 10.876755436826 | -1.208287293427 |

| | | | |
|----|-----------------|-----------------|----------------|
| C | 0.467263486684 | 8.524736994685 | 1.943355646422 |
| H | 1.197959731800 | 8.153754222070 | 2.662672466944 |
| H | 0.905040373552 | 8.439110338386 | 0.946364622649 |
| H | -0.395731203939 | 7.852314773994 | 1.973454154807 |
| C | -1.160530725387 | 10.113428012898 | 3.917215935775 |
| H | -2.052305830236 | 9.521823123134 | 3.683934849930 |
| H | -1.496497026069 | 11.067182555409 | 4.324707925657 |
| H | -0.618329950772 | 9.604269508717 | 4.713704937170 |
| Si | -0.099142968224 | 10.280896594296 | 2.359071070051 |
| C | -1.281320526931 | 10.814276678958 | 0.972553120799 |
| H | -0.765675914077 | 11.002914216365 | 0.028316923797 |
| H | -1.841263140488 | 11.718591598102 | 1.226639855986 |
| H | -2.015941396942 | 10.021845189984 | 0.793338876753 |
| C | 0.783928978365 | 12.971788544665 | 2.183692213321 |
| H | 0.875496290200 | 13.213952515075 | 1.117594255533 |
| H | -0.285642522023 | 13.019006411214 | 2.387245291254 |
| H | 1.471874938966 | 14.073047049365 | 3.016921804626 |
| H | 0.909188803049 | 15.008939753171 | 2.908557610635 |
| H | 2.455538603037 | 14.276380554047 | 2.582313954448 |
| C | 1.621688414114 | 13.645057582515 | 4.514808411263 |
| C | -0.259099970759 | 12.839193170517 | 6.945052438229 |
| H | -1.040729809131 | 13.235138789023 | 7.601284949213 |
| H | 0.647307467133 | 12.728243365085 | 7.543550691302 |
| H | -0.557363199924 | 11.837203345213 | 6.633750036912 |
| Si | 0.002800281076 | 14.002687395584 | 5.488195836259 |
| C | -1.555238756241 | 13.968846662974 | 4.403865664392 |
| H | -1.789900138596 | 13.000640015382 | 3.963306030527 |
| H | -1.501807756909 | 14.700342251100 | 3.592100729945 |
| H | -2.407432749024 | 14.251212997768 | 5.031487909777 |
| H | 7.108612651037 | 12.257098328620 | 9.151010251480 |
| H | 6.589088935743 | 11.568305971109 | 9.822610255981 |
| H | 7.070331987192 | 13.251552531779 | 9.598400129169 |
| C | -0.082095587543 | 15.757990850703 | 6.216220397635 |
| H | -1.071537458265 | 15.880217866522 | 6.670292367271 |
| H | 0.022309509935 | 16.536206776413 | 5.456168921893 |
| H | 0.654089221966 | 15.952696744839 | 6.998838965404 |
| C | 3.305865421454 | 14.263897006099 | 7.104158910165 |
| H | 4.172055871223 | 14.802985197295 | 7.502825293780 |
| H | 3.471232591419 | 13.196251352370 | 7.257370614524 |
| H | 2.439271792523 | 14.549705457074 | 7.048486983657 |
| C | 2.903978298524 | 16.495154537455 | 4.994096442379 |
| H | 2.288715170709 | 16.95007114361 | 5.741781799409 |
| H | 2.476619531379 | 16.720911457048 | 4.012236389470 |
| C | 3.895597189320 | 16.959714281903 | 5.024257467440 |
| C | 4.753003217438 | 14.27066832668 | 4.423706008593 |
| H | 4.761474133871 | 14.625929943496 | 3.389872323971 |
| H | 5.037499548416 | 13.218165661414 | 4.432526403985 |
| H | 5.523381846042 | 14.837076713226 | 4.960613653797 |
| C | 8.537669649438 | 11.761590883431 | 8.884497057463 |
| H | 9.030537121525 | 11.361712589127 | 9.772617901094 |
| H | 9.156525747599 | 12.572031870735 | 8.486920030883 |
| C | 8.303506172670 | 10.698007894707 | 8.152376982226 |
| H | 9.150983940886 | 10.546568096966 | 7.143187159738 |
| H | 8.028045124318 | 9.732995789387 | 8.253985832226 |
| O | 7.194938256615 | 11.187314823874 | 7.032950575252 |
| C | 6.481507962007 | 12.224228059231 | 7.757999046051 |
| H | 5.421897215159 | 11.974534550280 | 7.748858752943 |
| H | 6.619876448030 | 13.168101895141 | 7.221980732918 |
| O | 7.614822288440 | 11.421435529628 | 4.033562187296 |
| C | 7.232799076695 | 11.471906456386 | 2.632987272501 |
| H | 6.177723662830 | 11.209146991518 | 2.559448399529 |
| H | 7.825306249337 | 10.724182625752 | 2.095068993503 |
| C | 8.304249501308 | 12.638899402274 | 4.402768564978 |
| H | 9.140170398617 | 12.368484672560 | 5.050313915633 |
| H | 7.613748405173 | 13.277508187998 | 4.961498279332 |
| C | 8.715313858913 | 13.285013048040 | 3.083638442323 |
| H | 8.845437491051 | 14.365150944262 | 3.173066878227 |
| H | 9.655464597843 | 12.856335149093 | 2.722560772478 |
| C | 7.549900953643 | 12.890421415893 | 2.165391694797 |
| H | 7.800737096509 | 12.930032296546 | 1.104115844781 |
| H | 6.693656052874 | 13.544827808757 | 2.336054182308 |
| O | 7.119819896293 | 8.568784842665 | 5.145307966210 |
| C | 6.127121150264 | 7.518824524549 | 5.219291090563 |
| H | 5.235920015870 | 7.947388313132 | 5.670795012011 |
| H | 6.510933398871 | 6.723846584959 | 5.867446437894 |
| C | 5.916648165127 | 7.037384966504 | 3.770404700863 |
| H | 4.965978868939 | 7.392999278805 | 3.375508014318 |
| H | 5.909434387028 | 5.946916514546 | 3.719147191371 |
| C | 7.105747272468 | 7.650483897304 | 2.987599419811 |
| H | 7.614124818622 | 6.928190088020 | 2.345796211409 |
| C | 6.755574100477 | 8.470627387408 | 2.357988607778 |
| H | 8.019165722136 | 8.188499446860 | 4.091306791219 |
| H | 8.703028479583 | 7.414684033650 | 4.464619074319 |
| H | 8.594649559694 | 9.072919848495 | 3.819871314135 |
| Si | 3.083560749287 | 14.620239036106 | 5.262578401794 |
| H | -0.362510953155 | 9.518919214594 | 7.653193248678 |

E+ZPVE = -5446.902126 au, Free E (298.15 K) = -5447.031888 au.
Job name: TN110a

Table 6-2. Atomic Coordinates of Cyclotrisilenide $2'_{opt}$ at the B3LYP-D3/6-311G(d) Level of Theory

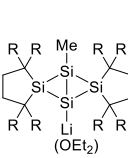


(R = SiMe₃)

| Atom | X | Y | Z |
|------|-----------------|-----------------|-----------------|
| Si | 4.070748781004 | 10.610834035828 | 5.030377952106 |
| Si | 2.119244064366 | 10.172026520648 | 5.983540605594 |
| Si | 2.024142291334 | 11.725197587875 | 4.357453615800 |
| Si | 0.927962658027 | 8.884504405400 | 7.568409407941 |
| C | 2.254050295214 | 6.617552977420 | 4.481954959229 |
| H | 2.309558206359 | 7.703972972211 | 4.393596782499 |
| H | 1.464377222169 | 6.250610307995 | 3.826880736293 |
| H | 3.204030110926 | 6.223750336198 | 4.103619950487 |
| C | 1.723741053719 | 4.197106819626 | 6.237851383320 |
| H | 2.567688142373 | 3.699232017804 | 5.747736915495 |
| H | 0.825327968098 | 3.936703246492 | 5.672827544833 |
| H | 1.626441138953 | 3.757635903942 | 7.234987465366 |
| C | 3.788499096656 | 6.237515905646 | 7.032195974014 |
| H | 4.481214429241 | 5.628046348590 | 6.441285157611 |
| H | 3.855401108699 | 5.894037052320 | 8.067243826957 |
| H | 4.147682435389 | 7.265522534332 | 6.985301376367 |
| Si | 2.065177199884 | 6.071697601142 | 6.276546638392 |
| Si | -1.03459018065 | 6.516982581316 | 6.603277310992 |
| C | -1.631137501069 | 4.886176045332 | 7.380418914135 |
| H | -2.523201073723 | 4.535735470014 | 6.849662396184 |
| H | -1.909223668248 | 5.010205904478 | 8.430992829432 |
| H | -0.883627808082 | 4.092028541180 | 7.330503040273 |
| C | -1.107410425589 | 6.285768193141 | 4.726725881074 |
| H | -0.575467641220 | 5.401812464599 | 4.369408363956 |
| H | -0.717786614701 | 7.150391791103 | 4.189147637083 |
| C | -2.158471802187 | 6.173258458352 | 4.438429655918 |
| H | -2.419203263127 | 7.766309201177 | 6.944449930456 |
| H | -2.319616716606 | 8.661727502251 | 6.328501144638 |
| H | -2.490564967934 | 8.092111404362 | 7.982181148109 |
| H | -3.370940551078 | 7.288319760006 | 6.682884167304 |
| C | 0.703999747870 | 6.960966137930 | 7.301034215682 |
| C | 0.773303543535 | 6.430770920491 | 8.786376491363 |
| H | -0.220762880820 | 6.436290561044 | 9.235300116614 |
| H | 1.095183411018 | 5.383144260004 | 8.828319818380 |
| C | 1.696380836859 | 7.286180787746 | 9.074853145926 |
| H | 2.735437752306 | 7.034352271735 | 9.445271795230 |
| H | 1.553562755335 | 6.996747417093 | 10.724712973260 |
| C | 1.457607187138 | 8.820897748965 | 9.454216697410 |
| Si | 0.017083184136 | 9.436218820846 | 10.562275842721 |
| C | -1.378689027203 | 8.163166627990 | 10.75520621076 |
| H | -2.150893344412 | 8.597185288830 | 11.400262267194 |
| H | -1.031341485052 | 7.2466635377638 | 11.241505319618 |
| H | -1.859199857574 | 7.883806228057 | 9.818506476666 |
| C | 0.532139489502 | 9.732287974934 | 12.370102692867 |
| H | 1.166635003320 | 10.611916268363 | 12.497998855369 |
| H | 1.053440070629 | 8.878129670179 | 12.809688905568 |
| C | -0.376723524498 | 9.900191387255 | 12.958899644938 |
| H | -0.768363124259 | 11.053861352086 | 9.989137036449 |
| H | -1.423410295660 | 11.435319838786 | 10.780617904161 |
| H | -1.370175139505 | 10.930248250493 | 9.088056249517 |
| H | -0.029249354412 | 11.825907868760 | 9.772723209773 |
| C | 3.707166390862 | 9.222508458915 | 11.623928952106 |
| H | 4.786294997797 | 9.404333058881 | 11.671687387405 |
| H | 3.556542165328 | 8.154053888450 | 11.807761614960 |
| H | 3.248451872854 | 9.766729748261 | 12.449588412562 |
| C | 2.863078289730 | 11.611550876921 | 9.865468244872 |
| H | 3.827873218621 | 12.107324297443 | 10.011486178392 |
| H | 2.184955263041 | 11.975564535289 | 10.642095886383 |
| H | 2.479541676208 | 11.940872405534 | 8.898033451702 |
| Si | 3.082467915117 | 9.736858021989 | 9.896514529234 |
| H | 4.540653553015 | 9.280718021654 | 8.791756865862 |
| H | 4.371069951061 | 9.462474136013 | 7.730862513468 |
| H | 4.844901971254 | 8.239899249269 | 8.927066943611 |
| H | 5.391737312470 | 9.903912226421 | 9.089615059241 |
| C | 1.221419331322 | 11.588016484590 | 2.556712668026 |
| Si | 2.533986641982 | 11.143896469150 | 1.245712667243 |
| C | 3.864229462990 | 12.481072519687 | 1.080127233259 |
| H | 4.577118270785 | 12.182019970243 | 0.303307157907 |
| H | 4.4231548880132 | 12.607977622581 | 2.007681970036 |
| H | 3.456197079386 | 13.453505236738 | 0.790471459672 |
| C | 3.469313616990 | 9.523286425702 | 1.509245182761 |
| H | 2.829123251180 | 8.658449782610 | 1.679894938619 |
| H | 4.149149105490 | 9.596343871063 | 2.361356650870 |
| H | 4.074906166300 | 9.317600648876 | 0.618176481125 |
| C | 1.741307625654 | 11.054067234465 | -0.488957518718 |
| H | 1.200386326168 | 11.971106322322 | -0.742412033951 |
| H | 1.043537195386 | 10.221182985155 | -0.604502996028 |
| C | 2.528147271787 | 10.925619528058 | -1.240964296461 |
| H | 0.139886755587 | 8.634078017119 | 1.910599792559 |
| H | 0.847121408476 | 8.147983323208 | 2.582485226029 |
| H | 0.54897935115 | 8.576701589688 | 0.899724392751 |
| H | -0.782082348846 | 8.042882215446 | 1.921904667323 |
| C | -1.234219313860 | 10.179164316173 | 4.075625778937 |
| H | -2.179046948617 | 9.664308675742 | 3.866003078668 |
| H | -1.468238951315 | 11.114136095006 | 4.585129532912 |
| H | -0.666789745524 | 9.574266299659 | 4.782625942051 |
| Si | -0.270032974343 | 10.400312878981 | 2.461082837852 |
| C | -1.529576750277 | 11.043031270951 | 1.183719274076 |
| H | -1.062324865153 | 11.278973848526 | 0.224273211005 |
| H | -2.051035073561 | 11.942053496639 | 1.524619092179 |
| H | -2.291433765745 | 10.276789015384 | 1.001636496173 |
| C | 0.713603482949 | 13.046932884511 | 2.265358307565 |
| H | 0.773321050175 | 13.298498695559 | 1.198321351230 |
| H | -0.343794068853 | 13.138482773512 | 2.511761405643 |
| C | 1.479310826084 | 14.110200358891 | 3.078798433193 |
| H | 0.953197895009 | 15.071416019231 | 2.996081856742 |
| H | 2.453424486479 | 14.272023056599 | 2.607009600662 |
| C | 1.672005108735 | 13.663657769082 | 4.563650315096 |
| H | -0.137408608994 | 12.921024127220 | 7.083279099138 |
| H | -0.909312159238 | 13.333476156458 | 7.741985033582 |
| H | 0.779608542121 | 12.820997504731 | 7.666464879823 |
| H | -0.438354012795 | 11.912677513513 | 6.798426008152 |
| Si | 0.110808405509 | 14.051266776996 | 5.597830379090 |
| C | -1.504121606714 | 14.041645086567 | 4.59041110329 |
| H | -1.768772402544 | 13.075795447268 | 4.161172910371 |
| H | -1.479639353231 | 14.773189087531 | 3.776820658678 |
| H | -2.320962979834 | 14.332791961732 | 5.260520112532 |
| C | 0.080228343987 | 15.816567852249 | 6.319458258976 |
| H | -0.893220893659 | 15.968053123070 | 6.799782542728 |
| H | 0.191459668014 | 16.589754809898 | 5.554833701137 |
| C | 0.844894049926 | 15.987558381064 | 7.080625974730 |
| H | 3.509717470715 | 14.200282398422 | 7.075138805057 |
| H | 4.379652849806 | 14.757716833825 | 7.439351370385 |
| H | 3.712935293657 | 13.135860636211 | 7.210903301227 |
| C | 2.662227719428 | 14.459200507412 | 7.715509995532 |
| H | 3.048776511631 | 16.469298622121 | 5.033744022418 |
| H | 2.502836743828 | 16.966096415374 | 5.836371340865 |
| H | 2.556876036800 | 16.728355357781 | 4.090704528416 |
| H | 4.053045108014 | 16.906266281675 | 5.001222438323 |
| C | 4.800912471460 | 14.202709139332 | 4.305776800177 |
| H | 4.750848144465 | 14.537133302925 | 3.265851101812 |
| H | 5.074245965690 | 13.147045902642 | 4.313806914545 |
| H | 5.614981578946 | 14.761320089029 | 4.782848342866 |
| Si | 3.202464478260 | 14.577276734360 | 5.249796981137 |
| H | -0.436753827708 | 9.480604319862 | 7.550955166330 |

E+ZPVE = -4742.118981 au, Free E (298.15 K) = -4742.222773 au.
Job name: TN112ac

Table 6-3. Atomic Coordinates of Silyl Anion 3_{opt} at the M06-2X/6-311G(d) Level of Theory



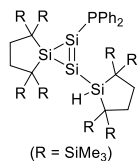
(R = SiMe₃)

| Atom | X | Y | Z |
|------|-----------------|-----------------|-----------------|
| Si | 12.995120510875 | 14.626934134415 | -0.377914250760 |
| Si | 14.010367723791 | 12.990762676301 | 1.269362071146 |
| Si | 15.214121442606 | 14.690299104252 | 0.258392819639 |
| Si | 12.450447475996 | 12.395532288092 | -0.343287818506 |
| C | 11.666613555734 | 16.000747204595 | -0.23387205136 |
| H | 10.909938450331 | 15.856620978448 | -1.009113561085 |
| H | 12.111027221018 | 16.986156359354 | -0.388731648339 |
| H | 11.58583877104 | 16.015999309257 | 0.729930106442 |
| Li | 14.511269197691 | 12.926068258195 | 3.713866142297 |
| C | 12.473469165016 | 10.960531361976 | -1.668087059403 |
| C | 11.147801355771 | 10.181945720722 | -1.340160806909 |
| H | 10.322658560952 | 10.539811042283 | -1.960492292331 |
| H | 11.241256353560 | 9.113361192761 | -1.572778328676 |
| H | 10.739925389141 | 10.367561901468 | 0.123202389927 |
| H | 11.442503664680 | 9.826324550108 | 0.761700037566 |
| H | 9.756514226326 | 9.914984399172 | 0.292223277441 |
| C | 10.758804893517 | 11.884132495213 | 0.483199911066 |
| Si | 12.480148125770 | 11.363541386878 | -3.556992437366 |
| C | 11.061584983120 | 10.423465975999 | -4.394054861839 |
| H | 10.064992584387 | 10.790934133627 | -4.139575903006 |
| H | 11.081601783526 | 9.352184235757 | -4.175185847985 |
| H | 11.174497399303 | 10.536290543531 | -5.476670565193 |
| C | 13.995355727341 | 10.751514243199 | -4.517855113029 |
| H | 13.748160600567 | 10.871204043284 | -5.578312265790 |
| H | 14.237468500188 | 9.698988476744 | -4.365447483685 |
| H | 14.892790559235 | 11.339098346985 | -4.337998359159 |

| | | | | | | | |
|----|-----------------|-----------------|-----------------|----|-----------------|-----------------|-----------------|
| C | 12.27932657166 | 13.175498657109 | -4.066528050274 | H | 20.111162209344 | 15.102908901213 | -1.303329322125 |
| H | 12.818723713724 | 13.330298294779 | -5.005653186608 | H | 20.563908397487 | 13.703487831398 | -0.337677464439 |
| H | 12.673013688432 | 13.887073595979 | -3.338168925617 | Si | 16.286843548541 | 15.190098482977 | -2.748462203318 |
| H | 11.233288701240 | 13.425586258013 | -4.248252969026 | C | 15.015556103638 | 16.540155745895 | -3.095739016405 |
| Si | 13.906632038468 | 9.767457073682 | -1.266825471547 | H | 14.915477873397 | 16.605304431135 | -4.184890222854 |
| C | 13.926315353522 | 9.140095519545 | 0.518898254790 | H | 15.321063329094 | 17.528975496666 | -2.747586666337 |
| H | 14.843230874292 | 8.555894345131 | 0.656408304174 | H | 14.025180837969 | 16.318069659444 | -2.693409970618 |
| H | 13.087709997824 | 8.476941159343 | 0.745460671168 | H | 15.605190131458 | 13.627628140811 | -3.528564301473 |
| H | 13.934595925021 | 9.950100326323 | 1.249294269033 | H | 14.882169440675 | 13.159181249574 | -2.853875330406 |
| C | 13.723682427666 | 8.178768161085 | -2.297111751216 | H | 16.370625826069 | 12.891145607407 | -3.767238797571 |
| H | 13.022539291540 | 8.276963855568 | -3.128812347039 | H | 15.073905367039 | 13.868847858694 | -4.452785251413 |
| H | 13.369885078451 | 7.354602697246 | -1.671939979850 | C | 17.831864998128 | 15.811567329727 | -3.653391294267 |
| H | 14.685535321608 | 7.873110253206 | -2.719222596261 | H | 18.755815623166 | 15.298515052451 | -3.380607892790 |
| C | 15.589800528945 | 10.55466065431 | -1.567973406297 | H | 17.978630587892 | 16.875880387281 | -3.445384771179 |
| H | 15.595787946295 | 11.606379533193 | -1.264845858510 | H | 17.70798999658 | 15.712171007436 | -4.736145903579 |
| H | 15.887633790448 | 10.499878582122 | -2.615597061439 | Si | 16.002886156734 | 15.403315768151 | -3.372223608781 |
| H | 16.357381097979 | 10.045259016819 | -0.977704762920 | C | 14.417831444762 | 15.222158438398 | 4.421561176616 |
| Si | 9.249822600132 | 12.737242372520 | -0.316985963135 | H | 14.629798487195 | 14.604683311961 | 5.305289003052 |
| C | 8.616978121672 | 14.218757260983 | 0.667941029311 | H | 13.536623606053 | 14.837037778660 | 3.897269816471 |
| H | 9.397701796415 | 14.942283994253 | 0.901012545229 | H | 14.118895136461 | 16.195070823420 | 4.816038335218 |
| H | 8.135083785891 | 13.936913302940 | 1.606087802117 | C | 16.894428259081 | 13.732313090447 | 3.527522940773 |
| H | 7.865956973455 | 14.737003845538 | 0.063614100785 | H | 17.960092850333 | 13.873554510219 | 3.329965314037 |
| C | 7.808599632244 | 11.522455952354 | -0.463692945823 | H | 16.564744885623 | 12.93870713227 | 2.854312880609 |
| H | 7.536988809258 | 11.058146806606 | 0.486751797182 | H | 16.829103487715 | 13.379733487980 | 4.565054226961 |
| H | 8.017297136705 | 10.720444295362 | -1.177393620486 | C | 17.130957434502 | 16.524948294713 | 4.388717400354 |
| H | 6.927157690121 | 12.057112183801 | -0.831012895021 | H | 17.363647114756 | 16.034812212669 | 5.339462942667 |
| C | 9.558997161821 | 13.359712562189 | -2.066173094119 | H | 16.698287093575 | 17.497940034457 | 4.619437205742 |
| H | 6.888368252960 | 13.927515246186 | -2.409852882031 | H | 18.081511491981 | 16.700078932710 | 3.877274665801 |
| H | 9.702821715210 | 12.536969921897 | -2.769583673613 | Si | 14.697059814117 | 17.597514460502 | 1.636575242893 |
| H | 10.431642631319 | 14.009348555368 | -2.142765771455 | H | 12.997702616366 | 17.272226626765 | 2.397448219966 |
| Si | 10.613478708355 | 11.987106894783 | 2.366860748110 | H | 12.236095157922 | 17.879344783443 | 1.902765799592 |
| C | 8.917220719475 | 11.362929279795 | 2.937955698424 | H | 12.984490621145 | 17.544216924007 | 3.455053085948 |
| H | 8.728180336012 | 10.344399567907 | 2.586157817381 | H | 12.691226727163 | 16.228891320819 | 2.314442638591 |
| H | 8.076890070775 | 11.983557105214 | 2.622593381596 | C | 14.482334440101 | 18.373672528796 | -0.065164592845 |
| H | 8.901517531089 | 11.330605265811 | 4.032573066075 | H | 14.213205792132 | 17.650750135344 | -0.834325481108 |
| C | 11.781886687555 | 10.780234243347 | 3.246968092692 | H | 15.391317080054 | 18.888662237981 | -0.388891902220 |
| H | 12.818071907418 | 10.860051903601 | 2.918322680319 | H | 13.687548464925 | 19.125161546536 | -0.017675335963 |
| H | 11.458498993394 | 9.743796892906 | 3.113857926892 | C | 15.459983169896 | 18.974962961436 | 2.693457928511 |
| H | 11.746112762865 | 10.994420115154 | 4.321591710706 | H | 14.999459188556 | 19.924471716039 | 2.402327257648 |
| C | 10.841082439860 | 13.720806268526 | 3.091007027418 | H | 16.539266381037 | 19.090799714375 | 2.567519022080 |
| H | 11.378494191804 | 13.668225351041 | 4.044369634692 | H | 15.260079397412 | 18.842996321026 | 3.759129098886 |
| H | 9.880432646153 | 14.202299835461 | 3.288945699431 | O | 14.383498160704 | 11.800463797186 | 5.202934406297 |
| H | 11.417598248674 | 14.366106523241 | 2.426599199900 | C | 14.759080194000 | 10.418156325203 | 5.135003640825 |
| C | 15.782860696003 | 16.030394151418 | 1.605837704199 | H | 13.852565115193 | 9.828187043893 | 4.964524853147 |
| C | 17.220357799781 | 16.388763520843 | 1.104302363409 | H | 15.194889463961 | 10.123036581484 | 6.094220404718 |
| H | 17.547723709496 | 17.374883765896 | 1.453086386166 | H | 15.750980355426 | 10.229747935705 | 4.090925924760 |
| H | 17.954146905262 | 15.672312487326 | 1.501352364170 | H | 15.329336672963 | 10.551945948582 | 3.052318227848 |
| H | 17.279316038510 | 16.317006912838 | -0.423329577577 | H | 16.005159691602 | 9.172880843004 | 3.913829495030 |
| C | 18.297327302942 | 16.509636563420 | -0.773319829433 | H | 16.670441012845 | 10.788164248212 | 4.193743040331 |
| H | 16.664011310067 | 17.128150760791 | -0.825992789290 | C | 13.533890789103 | 12.117668396907 | 6.309752345210 |
| C | 16.739573828014 | 14.937600132016 | -0.921129686507 | H | 12.842674570596 | 11.284372768675 | 6.471243001234 |
| Si | 18.140747559573 | 13.621485308092 | -0.780920491707 | H | 12.940269387800 | 12.982387672362 | 6.003454143520 |
| H | 17.946655644663 | 12.325785241341 | 0.582403760059 | C | 14.337037173367 | 12.428832299577 | 7.558698882484 |
| H | 16.916280418741 | 12.011091538053 | 0.744122317642 | H | 14.931473547723 | 11.572171555099 | 7.880247620560 |
| H | 18.356791820561 | 12.674928090206 | 1.531723588974 | H | 13.667381433016 | 12.698150134732 | 8.377646481081 |
| H | 18.524193008349 | 11.440434084366 | 0.291545382703 | H | 15.012945546088 | 13.267545414832 | 7.380596919785 |
| C | 18.47977715987 | 12.572843841321 | -2.320938741836 | | | | |
| H | 19.435144266015 | 12.069879736599 | -2.135369089864 | | | | |
| H | 18.583591088860 | 13.123364053327 | -3.256067799477 | | | | |
| H | 17.733525089850 | 11.791184075690 | -2.462059653911 | | | | |
| C | 19.800309163059 | 14.477814901950 | -0.461541116220 | | | | |
| H | 19.821195805677 | 15.099482770493 | 0.436398238924 | | | | |

E+ZPVE = -5021.195762 au, Free E (298.15 K) = -5021.305308 au.
Job name: TN107ca

Table 6-4. Atomic Coordinates of Cyclotrisilene δ_{opt} at the B3LYP-D3/6-311G(d) Level of Theory

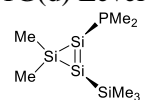


| Atom | X | Y | Z | | | | |
|------|-----------------|-----------------|-----------------|----|-----------------|-----------------|-----------------|
| Si | 0.119169386403 | 16.878955547727 | 10.707247098637 | C | 1.972246318510 | 12.399871069052 | 8.657775078957 |
| Si | 0.142052942680 | 18.865800812973 | 11.498723450820 | H | 2.899206422088 | 12.071031513701 | 8.198324420328 |
| Si | 0.413807379583 | 17.09669404036 | 13.012244676783 | C | 1.270371573278 | 11.543577572044 | 9.503020761067 |
| P | -0.442363307453 | 15.810818073935 | 8.751996381235 | H | 1.648207287933 | 10.547656429074 | 9.709876010947 |
| Si | -0.105513619243 | 21.211965142089 | 11.203324118842 | C | 0.070907683839 | 11.971675548503 | 10.070357142792 |
| C | 0.673836923678 | 16.663583809829 | 7.545187810535 | H | -0.494218315428 | 11.312202348712 | 10.721021649415 |
| C | 0.091693237685 | 17.091264625998 | 6.344052412134 | C | -0.412160130349 | 13.247311955982 | 9.798327640865 |
| H | -0.970005338389 | 16.939264453764 | 6.180863155885 | H | -1.361604401523 | 13.558285125114 | 10.221175201176 |
| C | 0.859639287468 | 17.711177582195 | 5.360436959013 | C | 1.213402990751 | 22.275450500503 | 10.285819170463 |
| H | 0.390991655581 | 18.039781862913 | 4.438491320687 | C | 0.270420251530 | 23.375403575090 | 9.649360870085 |
| C | 2.223354200648 | 17.907329025142 | 5.561074716287 | C | 0.106266763800 | 24.188667271100 | 10.358140466392 |
| H | 2.823949589625 | 18.385667161326 | 4.794049355159 | H | 0.742743351348 | 23.846156911818 | 8.779729988076 |
| C | 2.12326362557 | 17.498277877302 | 6.756407236872 | C | -1.104828033834 | 22.806140363555 | 9.247242777320 |
| C | 3.872253668738 | 17.657913800896 | 6.924641974405 | H | -0.991551913486 | 22.235818705086 | 8.321618846955 |
| C | 2.043772763651 | 16.891782015377 | 7.745376031537 | H | -1.780339671547 | 23.633866261611 | 9.000599320266 |
| H | 2.51393644996 | 16.591694000534 | 8.675323371587 | C | -1.707698985320 | 21.887634765761 | 10.371856615667 |
| C | 3.10673815745 | 14.134945333307 | 9.876195007222 | Si | 2.235339109187 | 21.467952155019 | 8.868627453283 |
| C | 1.501147914179 | 13.686631806663 | 8.402430309457 | H | 1.200223196707 | 20.964977234874 | 7.373449848036 |
| H | 2.068937298316 | 14.337619766130 | 7.749553626361 | H | 1.886928649787 | 20.624878139049 | 6.592591938117 |
| | | | | H | 0.617061906215 | 21.787990041334 | 6.953113341367 |
| | | | | H | 0.527958219821 | 20.133326707161 | 7.573673129193 |
| | | | | H | 3.206867476723 | 19.937570070295 | 9.378404003953 |
| | | | | H | 2.552748534771 | 19.122806393069 | 9.69364959767 |
| | | | | H | 3.926504102128 | 20.122812588325 | 10.173139633239 |
| | | | | H | 3.764890219081 | 19.582115343505 | 8.507420640137 |
| | | | | Si | 2.410816115664 | 23.159732169053 | 11.525551836723 |
| | | | | C | 3.474350568557 | 22.718230774527 | 8.156614507256 |
| | | | | H | 4.260036989856 | 23.020507646221 | 8.850996209448 |
| | | | | H | 2.986966204064 | 23.626711446394 | 7.791393356168 |
| | | | | H | 3.967084714758 | 22.255192194751 | 7.294990611625 |
| | | | | C | 4.034894425544 | 22.235026572327 | 11.819234381916 |

| | | | | | | | |
|----|-----------------|-----------------|------------------|----|-----------------|-----------------|-----------------|
| H | 4.573135706809 | 22.741261675790 | 12.627579996067 | H | -3.624176340146 | 19.451813392462 | 15.144241206903 |
| H | 4.698050710808 | 22.214042241049 | 10.952798559157 | H | -4.110154697101 | 17.807170699445 | 14.748987101648 |
| H | 3.870371287653 | 21.205574682722 | 12.139755365663 | H | -3.244672647880 | 18.779607803325 | 13.564738583557 |
| C | 2.824413694051 | 24.889041953750 | 10.870277265184 | C | -0.620009968076 | 19.556201522219 | 15.490749804909 |
| H | 1.965638869586 | 25.562882383201 | 10.936420684652 | H | -0.319937187828 | 19.982083712387 | 14.533281213470 |
| H | 3.168447117818 | 24.895561866630 | 9.835471179066 | H | 0.279374620919 | 19.395506280550 | 16.087345816804 |
| H | 3.619898893000 | 25.324614978543 | 11.484053250568 | H | -1.217956267177 | 20.313529622952 | 16.008531312676 |
| C | 1.711645325090 | 23.441490007940 | 13.262651005157 | Si | -2.236894043939 | 15.359829679165 | 13.734508603672 |
| H | 1.670868964327 | 22.525472497494 | 13.854388682891 | C | -3.287178616457 | 16.031134572941 | 12.314102794399 |
| H | 0.716816845405 | 23.888465257375 | 13.278272235654 | H | -3.896632599595 | 15.210841752837 | 11.919484877621 |
| H | 2.384746643562 | 24.134619295676 | 13.779877337953 | H | -2.683474637246 | 16.411453223862 | 11.487486196853 |
| Si | -2.846870797125 | 20.593637550518 | 9.527000092921 | H | -3.970458679355 | 16.826714894622 | 12.608661048455 |
| C | -1.905109514730 | 19.432992590828 | 8.368152749514 | C | -1.524324141161 | 13.720715635177 | 13.122242036868 |
| H | -0.973769586192 | 19.042046784243 | 8.773877555871 | H | -2.327214643065 | 13.144532361872 | 12.650182290290 |
| H | -1.682480576239 | 19.911415850783 | 7.411768528776 | H | -1.118449825525 | 13.104508082434 | 13.927459906948 |
| H | -2.542056127590 | 18.567901958462 | 8.155707940249 | H | -0.742069637957 | 13.856676723837 | 12.377457720121 |
| C | -3.766565274884 | 19.531940502844 | 10.784978946937 | C | -3.400448883045 | 14.856446315764 | 15.145149301201 |
| H | -4.421035952928 | 18.824757675560 | 10.265861177896 | H | -4.007073007217 | 15.671817892349 | 15.543090742867 |
| H | -4.388057076575 | 20.107066573644 | 11.475033810771 | H | -2.846973079201 | 14.416561494491 | 15.980175898680 |
| C | -3.065091415243 | 18.938142500868 | 11.374328447352 | H | -4.090587052239 | 14.089072217484 | 14.778347768178 |
| C | -4.094093164632 | 21.435001683684 | 8.372181114995 | Si | 2.943829000095 | 15.095939048541 | 13.217943047813 |
| H | -4.464979682864 | 20.697785900777 | 7.643094774324 | C | 4.632867121679 | 14.808440259789 | 14.037645750721 |
| H | -3.643739438882 | 22.249101264771 | 7.803387627698 | H | 5.026115865880 | 13.857761557232 | 13.661649181502 |
| H | -4.971802253289 | 21.837998664764 | 8.876536333349 | H | 4.551943358686 | 14.711699779193 | 15.123955925382 |
| Si | -2.689695020381 | 22.927308782531 | 11.665413302649 | H | 5.381813088189 | 15.572603041177 | 13.825345203849 |
| C | -1.919706500977 | 24.632340883920 | 11.956294259452 | C | 2.062534079439 | 13.453765284291 | 13.527945840516 |
| H | -2.540031182414 | 25.171422244769 | 12.680292720184 | H | 1.108291139894 | 13.364202281403 | 13.014424575449 |
| H | -1.894048274168 | 25.236794438313 | 11.045182794708 | H | 1.904326456666 | 13.246311526705 | 14.589749494148 |
| H | -0.909526754195 | 24.596484789261 | 12.364419065977 | H | 2.707153311557 | 12.658361474977 | 13.138038484290 |
| H | -0.117451422650 | 21.582876447723 | 12.640582979198 | C | 3.220387351537 | 15.214023225653 | 11.349346227859 |
| C | -4.454531422522 | 23.326440419501 | 11.103084774720 | H | 3.330802262114 | 16.236626092909 | 10.989010110119 |
| H | -5.111398448307 | 22.454492392169 | 11.077861054967 | H | 2.398735889345 | 14.749962210161 | 10.800640662990 |
| H | -4.488374342775 | 23.800291352358 | 10.119025168308 | H | 4.129969710657 | 14.667754461411 | 11.077868794616 |
| H | -4.885888753046 | 24.034093439196 | 11.819202870572 | Si | 3.333200115607 | 18.069527565672 | 14.083630015212 |
| C | -2.825923613035 | 22.051702353971 | 13.334195076399 | C | 4.448052993092 | 18.204049671330 | 12.563871077607 |
| H | -3.69394630197 | 22.432129613241 | 13.883200999569 | H | 3.862876648726 | 18.394995409964 | 11.662880247557 |
| H | -1.944900895285 | 22.211366084126 | 13.958784411025 | H | 5.063967205051 | 17.323251170843 | 12.376457815130 |
| H | -2.956364970040 | 20.974543834449 | 13.231447435867 | H | 5.126513359711 | 19.053072936690 | 12.695846068776 |
| C | -0.847669257761 | 16.528745201226 | 14.371491592176 | H | 4.402935878295 | 17.837714006326 | 15.631757842757 |
| C | 0.093761954968 | 15.699428646364 | 15.319925419404 | H | 5.083090812064 | 18.691808155418 | 15.720432384732 |
| H | -0.322017860095 | 15.599054638581 | 16.326326553652 | H | 5.011338296242 | 16.934279276549 | 15.635106638666 |
| H | 0.199297706416 | 14.681239045640 | 14.942298307459 | H | 3.789928580972 | 17.825586457787 | 16.537817239599 |
| C | 1.498147536541 | 16.326809049415 | 15.393140686991 | C | 2.615246901839 | 19.800290358789 | 14.327300980001 |
| H | 2.172733328080 | 15.667548335523 | 15.952250625648 | H | 3.453263107416 | 20.504017638838 | 14.337536125496 |
| H | 1.434283850439 | 17.247244159007 | 15.987137322381 | H | 2.097672083610 | 19.914421517163 | 15.278559670160 |
| C | 2.046150910324 | 16.640690524710 | 13.9584832524905 | H | 1.933978399922 | 20.114031767545 | 13.537052535330 |
| Si | -1.65533682604 | 17.985465124278 | 15.349055080493 | | | | |
| C | -1.966102850944 | 17.462364087162 | 17.144149611429 | | | | |
| H | -2.566625054380 | 18.233542313393 | 17.638267738736 | | | | |
| H | -1.034490236021 | 17.373950301158 | 17.170868628078 | | | | |
| H | -2.504277017779 | 16.517855353473 | 17.240317948600 | | | | |
| C | -3.311337562116 | 18.540409011416 | 14.625905603433 | | | | |

E+ZPVE = -5546.687948 au, Free E (298.15 K) = -5546.806547 au.
Job name: TN126aa

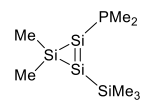
Table 6-5. Atomic Coordinates of Model Cyclotrisilene **9** (*cis*-*bent*) at the B3LYP-D3/6-311G(d) Level of Theory



| Atom | X | Y | Z |
|------|-----------------|-----------------|-----------------|
| Si | -0.485640413711 | 2.147586385438 | -0.770078670931 |
| Si | 0.623818368308 | 0.332738231553 | -0.426200487610 |
| Si | -1.703234273313 | 0.247313940475 | -0.292374098053 |
| P | -0.328155786773 | 4.415298965997 | -0.714944931849 |
| C | -2.710925069144 | -0.518957960615 | 0.273697467031 |
| Si | -2.604683659050 | 0.002700977422 | 1.357113513140 |
| H | -3.614101658615 | 0.425938321303 | 1.316899451018 |
| H | -2.708976726673 | -1.063345589673 | 1.587163365936 |
| H | -2.070034660058 | 0.477794970713 | 2.181733525268 |
| C | -2.731883286889 | -0.611871426886 | -1.630361329965 |
| H | -2.831953145930 | -1.681068766567 | -1.413969567121 |
| H | -3.741854723963 | -0.190603157271 | -1.676554744934 |
| H | -2.271944592391 | -0.505738871098 | -2.614318436355 |
| C | 1.492766004964 | 4.601623089372 | -1.107996477325 |
| H | 1.793623086704 | 4.080777094266 | -2.019906691295 |

E+ZPVE = -1778.675567 au, Free E (298.15 K) = -1778.731279 au.
Job name: t636MINO1G

Table 6-6. Atomic Coordinates of Model Cyclotrisilene **9** (*planar*) at the B3LYP-D3/6-311G(d) Level of Theory



| Atom | X | Y | Z |
|------|-----------------|----------------|-----------------|
| Si | -1.450621449652 | 0.077567005375 | 0.075796322995 |
| Si | 0.681376785434 | 0.247163380647 | 0.275172484848 |
| Si | -0.541948909657 | 2.179856257943 | -0.175737385319 |

| | | | |
|----|-----------------|-----------------|-----------------|
| P | -3.248720810648 | -1.324508692034 | 0.116353471176 |
| Si | 2.727091631844 | -0.858884795591 | 0.676802477615 |
| C | -0.452936545255 | 3.048082942264 | -1.857649393888 |
| H | -1.368205410695 | 3.617261684316 | -2.052676433811 |
| H | 0.382996414971 | 3.755666041562 | -1.884620205987 |
| H | -0.318240399656 | 2.331488950785 | -2.669817740447 |
| C | -0.785016942261 | 3.525935218716 | 1.136761760033 |
| H | 0.047171056270 | 4.238222078320 | 1.119452623967 |
| H | -1.702911351588 | 4.093413038366 | 0.949088668324 |
| H | -0.846340034717 | 3.099739023798 | 2.139753471099 |
| C | -2.457875058428 | -2.775268425652 | 0.998003347443 |

| | | | | | | | |
|---|-----------------|-----------------|-----------------|--|----------------|-----------------|----------------|
| H | -1.972566944238 | -2.497209296966 | 1.936324184554 | C | 3.529260710105 | -0.144943547691 | 2.232427525030 |
| H | -3.231433631248 | -3.518643047666 | 1.208946096252 | H | 2.891618928330 | -0.276750604983 | 3.110470085373 |
| H | -1.716494955238 | -3.240413955748 | 0.345761443473 | H | 4.483745469246 | -0.643549584645 | 2.434320617756 |
| C | -4.204906843023 | -0.574578313504 | 1.544069639638 | H | 3.730347779765 | 0.924633004922 | 2.126784723783 |
| H | -4.582392731075 | 0.409212809069 | 1.258881625680 | C | 2.353736348339 | -2.695144383309 | 0.922653158200 |
| H | -5.066938768566 | -1.213162646833 | 1.755489637562 | H | 1.891332407047 | -3.131575033353 | 0.033283159797 |
| H | -3.612797111625 | -0.472429678529 | 2.456083331330 | H | 3.274823623630 | -3.251850096504 | 1.126806611732 |
| C | 3.887191719425 | -0.623225787573 | -0.796384444971 | H | 1.673312410000 | -2.856572593828 | 1.762972189279 |
| H | 4.842790874503 | -1.128391525358 | -0.617324971723 | E+ZPVE = -1778.675170 au, Free E (298.15 K) = -1778.731764 au. | | | |
| H | 3.459233450220 | -1.034320368950 | -1.714408364618 | Job name: ti636MIN01Gplanar | | | |
| H | 4.099816598442 | 0.434320512360 | -0.975118356175 | | | | |

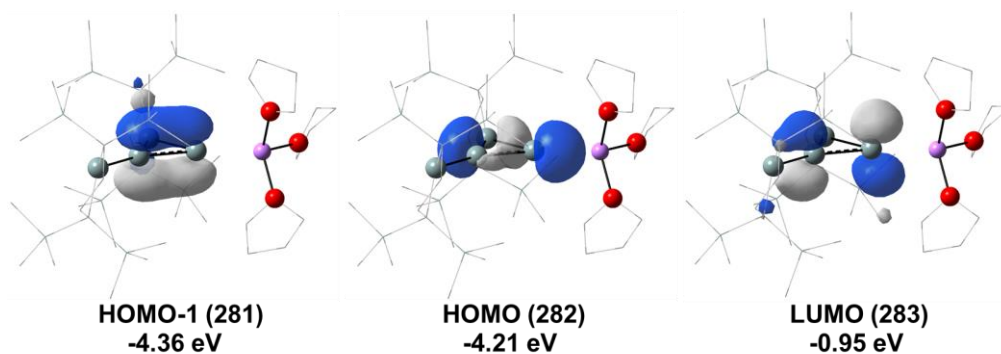


Figure 6-57. Frontier Kohn-Sham orbitals of 2_{opt} at the B3LYP-D3/6-311+G(d)/SCRF(solvent = heptane)//B3LYP-D3/6-311G(d) level of theory (isosurface level: $0.05 \text{ e}\cdot\text{au}^{-3}$). [td_TN110aab3]

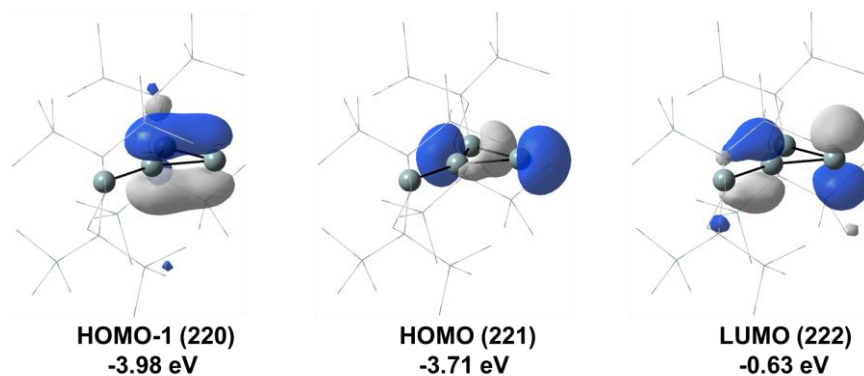


Figure 6-58. Frontier Kohn-Sham orbitals of $2'_{opt}$ at the B3LYP-D3/6-311+G(d)/SCRF(solvent = THF)//B3LYP-D3/6-311G(d) level of theory (isosurface level: $0.05 \text{ e}\cdot\text{au}^{-3}$). [td_b_TN112ac]

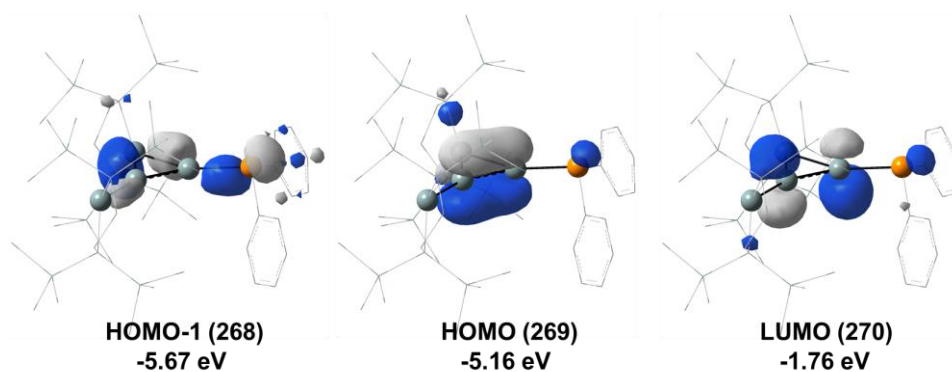


Figure 6-59. Frontier Kohn-Sham orbitals of 8_{opt} at the B3LYP-D3/6-311G(d) level of theory (isosurface level: $0.05 \text{ e}\cdot\text{au}^{-3}$). [TN126aa]

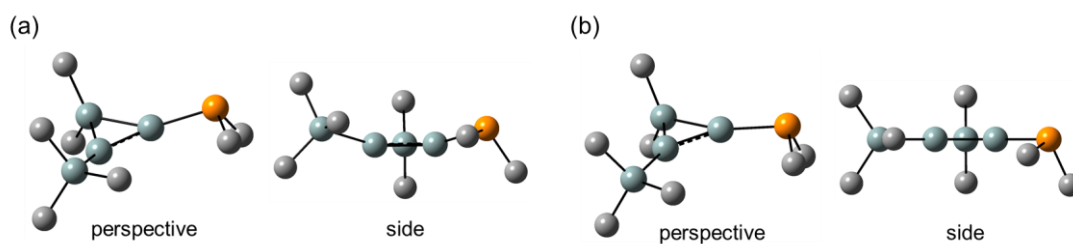
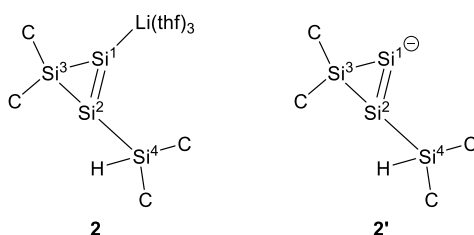


Figure 6-60. Structures of model cyclotrisilene **9**. (a) fully-optimized *cis*-bent structure. (b) partially-optimized planar structure.

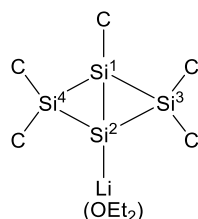
Table 6-7. Experimental and Theoretical Isotropic ^{29}Si Chemical Shifts of **2**, **2_{opt}** and **2'_{opt}**



| Cpd | SiMe ₃ | Si1 | Si2 | Si3 | Si4 | note |
|---------------------------------------|-----------------------------|-----------------|------------------|------------------|------------------|--------------|
| 2^a | 2.7, 3.6, 4.1, 4.4 | 281.0 | 168.1 | -27.9 | -14.0 | TN790_NMR6 |
| 2_{opt}^{b,c} | 3.4 (358.0) ^d | 276.9 (84.5) | 177.5 (183.9) | -39.1 (400.5) | -14.7 (376.1) | nmr_TN110aa |
| 2'_{opt}^{b,c} | 2.9 (358.5) ^d | 325.7 (35.7) | 154.8 (206.6) | -43.1 (404.5) | -14.9 (376.3) | nmr_TN112ac1 |

^aExperimental ^{29}Si chemical shifts of **2** in benzene-*d*₆ at room temperature. ^bGIAO/M06L/6-311+G(2df,p) level of theory. Absolute chemical shift for tetramethylsilane = 361.4. ^cThe absolute chemical shift is shown in the parentheses. ^dAverage values.

Table 6-8. Experimental and Theoretical Isotropic ^{29}Si Chemical Shifts of **3** and **3_{opt}**



| Cpd | SiMe ₃ | Si1 | Si2 | Si3, S4 | note |
|--------------------------------------|-----------------------------|-------------------|------------------|-------------------------------|-------------|
| 3^a | 2.9, 3.1 | -80.6 | - ^e | 16.5 | TN780_NMR2 |
| 3_{opt}^{b,c} | 0.8 (360.6) ^d | -108.4 (469.8) | -98.9 (460.3) | 10.8 (350.6), 17.6 (343.8) | nmr_TN107ca |

^aExperimental ^{29}Si chemical shifts of **2** in benzene-*d*₆ at room temperature. ^bGIAO/M06L/6-311+G(2df,p) level of theory. Absolute chemical shift for tetramethylsilane = 361.4. ^cThe absolute chemical shift is shown in the parentheses. ^dAverage values. ^eNot observed.

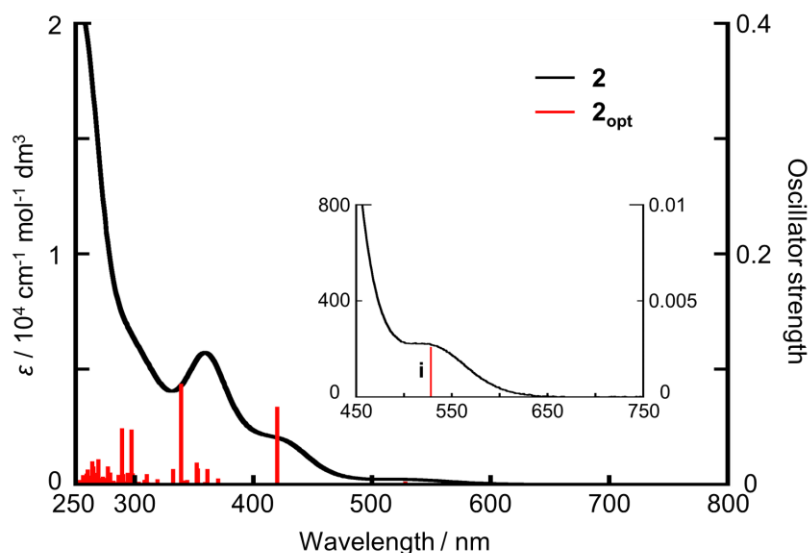


Figure 6-61. Experimental UV-vis absorption spectrum of **2** in hexane at room temperature (black) and calculated band positions of **2_{opt}** at the TD-B3LYP-D3/6-311G+(d)/SCRf(solvent = heptane) level of theory (red bar). i: $\sigma(\text{Si-Li}) \rightarrow \pi^*(\text{Si-Si})$ transition. [td_TN110aab3]

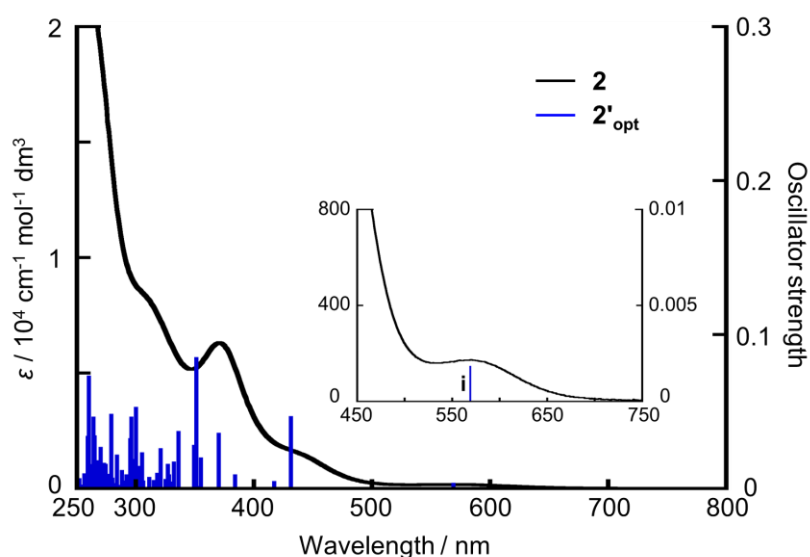


Figure 6-62. Experimental UV-vis absorption spectrum of **2** in THF at room temperature (black) and calculated band positions of **2'_{opt}** at the TD-B3LYP-D3/6-311G+(d)/SCRf(solvent = THF) level of theory (blue bar). i: σ anionic lone pair(Si) $\rightarrow \pi^*(\text{Si-Si})$ transition. [td_b_TN112ac]

Table 6-9. Transition Energy, Wavelength, and Oscillator Strengths of the Electronic Transition of **2_{opt}** (The 282th orbital is highest occupied orbital shown in Figure 6-57) [td_TN110aab3]

| | | | | | | | |
|----------------------------|-----------|-----------|----------|----------------------------|-----------|-----------|----------|
| Excited State 1: Singlet-A | 2.3470 eV | 528.26 nm | f=0.0026 | Excited State 4: Singlet-A | 3.1888 eV | 388.81 nm | f=0.0012 |
| <S**2>=0.000 | | | | <S**2>=0.000 | | | |
| 282 -> 283 | 0.70393 | | | 282 -> 284 | 0.70251 | | |
| Excited State 2: Singlet-A | 2.9489 eV | 420.44 nm | f=0.0673 | Excited State 5: Singlet-A | 3.3485 eV | 370.27 nm | f=0.0052 |
| <S**2>=0.000 | | | | <S**2>=0.000 | | | |
| 281 -> 283 | 0.66352 | | | 281 -> 284 | 0.70116 | | |
| 282 -> 289 | -0.12841 | | | | | | |
| Excited State 3: Singlet-A | 3.0389 eV | 407.99 nm | f=0.0006 | Excited State 6: Singlet-A | 3.4322 eV | 361.23 nm | f=0.0135 |
| <S**2>=0.000 | | | | <S**2>=0.000 | | | |
| 280 -> 283 | 0.70096 | | | 282 -> 285 | 0.63844 | | |

| | | | | | | | | | | | | | | |
|-------------------------------|----------|-----------|-----------|-----------|----------|-------------------------------|----------|-----------|-----------|-----------|----------|--|--|--|
| 282 -> 286 | -0.13106 | | | | | 282 -> 291 | 0.52936 | | | | | | | |
| 282 -> 287 | 0.18413 | | | | | 282 -> 292 | -0.41206 | | | | | | | |
| 282 -> 289 | -0.11504 | | | | | | | | | | | | | |
| Excited State <S**2>=0.000 | 7: | Singlet-A | 3.4574 eV | 358.60 nm | f=0.0021 | Excited State <S**2>=0.000 | 18: | Singlet-A | 3.9815 eV | 311.40 nm | f=0.0018 | | | |
| 282 -> 285 | 0.17878 | | | | | 280 -> 284 | 0.16097 | | | | | | | |
| 282 -> 286 | 0.67262 | | | | | 281 -> 288 | 0.55294 | | | | | | | |
| | | | | | | 281 -> 289 | 0.37395 | | | | | | | |
| Excited State <S**2>=0.000 | 8: | Singlet-A | 3.5142 eV | 352.81 nm | f=0.0138 | Excited State <S**2>=0.000 | 19: | Singlet-A | 3.9859 eV | 311.06 nm | f=0.0088 | | | |
| 281 -> 285 | -0.26026 | | | | | 280 -> 284 | 0.66330 | | | | | | | |
| 281 -> 286 | 0.13708 | | | | | 281 -> 288 | -0.12854 | | | | | | | |
| 281 -> 287 | -0.20528 | | | | | 281 -> 289 | -0.10495 | | | | | | | |
| 281 -> 288 | -0.20023 | | | | | 282 -> 293 | 0.12308 | | | | | | | |
| 281 -> 289 | 0.28026 | | | | | | | | | | | | | |
| 281 -> 292 | -0.12025 | | | | | Excited State <S**2>=0.000 | 20: | Singlet-A | 4.0071 eV | 309.41 nm | f=0.0040 | | | |
| 282 -> 285 | -0.15894 | | | | | 280 -> 284 | -0.14666 | | | | | | | |
| 282 -> 286 | 0.11131 | | | | | 282 -> 293 | 0.67177 | | | | | | | |
| 282 -> 287 | 0.38180 | | | | | | | | | | | | | |
| 282 -> 289 | -0.12344 | | | | | | | | | | | | | |
| Excited State <S**2>=0.000 | 9: | Singlet-A | 3.5216 eV | 352.07 nm | f=0.0188 | Excited State <S**2>=0.000 | 21: | Singlet-A | 4.0218 eV | 308.28 nm | f=0.0038 | | | |
| 281 -> 285 | 0.18911 | | | | | 281 -> 290 | 0.65400 | | | | | | | |
| 281 -> 286 | -0.15952 | | | | | 281 -> 291 | -0.15128 | | | | | | | |
| 281 -> 287 | 0.18516 | | | | | | | | | | | | | |
| 281 -> 288 | 0.17609 | | | | | Excited State <S**2>=0.000 | 22: | Singlet-A | 4.0649 eV | 305.01 nm | f=0.0013 | | | |
| 281 -> 289 | -0.24595 | | | | | 281 -> 288 | -0.11606 | | | | | | | |
| 281 -> 292 | 0.10714 | | | | | 281 -> 289 | 0.26643 | | | | | | | |
| 282 -> 285 | -0.15258 | | | | | 281 -> 291 | 0.33765 | | | | | | | |
| 282 -> 287 | 0.45769 | | | | | 281 -> 292 | 0.53870 | | | | | | | |
| 282 -> 289 | -0.11721 | | | | | | | | | | | | | |
| Excited State <S**2>=0.000 | 10: | Singlet-A | 3.6052 eV | 343.90 nm | f=0.0038 | Excited State <S**2>=0.000 | 23: | Singlet-A | 4.0894 eV | 303.18 nm | f=0.0022 | | | |
| 281 -> 285 | 0.54061 | | | | | 281 -> 290 | 0.18034 | | | | | | | |
| 281 -> 286 | 0.37730 | | | | | 281 -> 291 | 0.55298 | | | | | | | |
| 281 -> 287 | -0.10091 | | | | | 281 -> 292 | -0.37118 | | | | | | | |
| 282 -> 287 | 0.11332 | | | | | | | | | | | | | |
| 282 -> 289 | 0.10155 | | | | | Excited State <S**2>=0.000 | 24: | Singlet-A | 4.1447 eV | 299.14 nm | f=0.0069 | | | |
| Excited State <S**2>=0.000 | 11: | Singlet-A | 3.6270 eV | 341.84 nm | f=0.0033 | 281 -> 293 | 0.48464 | | | | | | | |
| 281 -> 285 | -0.27982 | | | | | 281 -> 302 | -0.12132 | | | | | | | |
| 281 -> 286 | 0.53356 | | | | | 282 -> 294 | 0.27959 | | | | | | | |
| 281 -> 287 | 0.26009 | | | | | 282 -> 297 | 0.13259 | | | | | | | |
| 281 -> 288 | 0.11949 | | | | | 282 -> 302 | -0.22313 | | | | | | | |
| 281 -> 289 | -0.18142 | | | | | | | | | | | | | |
| Excited State <S**2>=0.000 | 12: | Singlet-A | 3.6597 eV | 338.78 nm | f=0.0874 | Excited State <S**2>=0.000 | 25: | Singlet-A | 4.1532 eV | 298.53 nm | f=0.0096 | | | |
| 281 -> 283 | 0.11080 | | | | | 281 -> 292 | -0.10054 | | | | | | | |
| 281 -> 285 | -0.12458 | | | | | 281 -> 293 | 0.43028 | | | | | | | |
| 281 -> 286 | -0.13366 | | | | | 282 -> 294 | -0.35524 | | | | | | | |
| 282 -> 287 | 0.28206 | | | | | 282 -> 297 | -0.15642 | | | | | | | |
| 282 -> 288 | -0.27251 | | | | | 282 -> 302 | 0.22080 | | | | | | | |
| 282 -> 289 | 0.46319 | | | | | | | | | | | | | |
| 282 -> 291 | -0.15277 | | | | | Excited State <S**2>=0.000 | 26: | Singlet-A | 4.1799 eV | 296.62 nm | f=0.0476 | | | |
| 282 -> 292 | -0.15337 | | | | | 280 -> 285 | 0.37517 | | | | | | | |
| Excited State <S**2>=0.000 | 13: | Singlet-A | 3.7313 eV | 332.28 nm | f=0.0135 | 280 -> 286 | -0.21387 | | | | | | | |
| 281 -> 287 | 0.57847 | | | | | 280 -> 287 | 0.24874 | | | | | | | |
| 281 -> 288 | -0.19654 | | | | | 280 -> 288 | 0.24789 | | | | | | | |
| 281 -> 289 | 0.26502 | | | | | 280 -> 289 | -0.31451 | | | | | | | |
| 281 -> 292 | -0.12273 | | | | | 280 -> 291 | 0.10039 | | | | | | | |
| | | | | | | 280 -> 292 | 0.13578 | | | | | | | |
| Excited State <S**2>=0.000 | 14: | Singlet-A | 3.8440 eV | 322.54 nm | f=0.0004 | 282 -> 294 | 0.46476 | | | | | | | |
| 282 -> 288 | 0.60890 | | | | | 282 -> 297 | -0.31803 | | | | | | | |
| 282 -> 289 | 0.32543 | | | | | 282 -> 298 | 0.20536 | | | | | | | |
| | | | | | | 282 -> 299 | -0.13201 | | | | | | | |
| Excited State <S**2>=0.000 | 15: | Singlet-A | 3.8835 eV | 319.26 nm | f=0.0045 | 282 -> 302 | 0.20782 | | | | | | | |
| 282 -> 290 | 0.66210 | | | | | 282 -> 303 | 0.12063 | | | | | | | |
| 282 -> 291 | -0.18254 | | | | | 282 -> 308 | -0.11112 | | | | | | | |
| Excited State <S**2>=0.000 | 16: | Singlet-A | 3.9126 eV | 316.88 nm | f=0.0010 | Excited State <S**2>=0.000 | 28: | Singlet-A | 4.2336 eV | 292.86 nm | f=0.0004 | | | |
| 282 -> 289 | 0.27534 | | | | | 280 -> 285 | -0.18757 | | | | | | | |
| 282 -> 291 | 0.36565 | | | | | 282 -> 295 | 0.60852 | | | | | | | |
| 282 -> 292 | 0.51708 | | | | | 282 -> 296 | -0.22359 | | | | | | | |
| | | | | | | 282 -> 297 | 0.12032 | | | | | | | |
| Excited State <S**2>=0.000 | 17: | Singlet-A | 3.9413 eV | 314.57 nm | f=0.0017 | Excited State <S**2>=0.000 | 29: | Singlet-A | 4.2461 eV | 292.00 nm | f=0.0028 | | | |
| 282 -> 290 | 0.18584 | | | | | 280 -> 285 | 0.44687 | | | | | | | |
| | | | | | | 280 -> 286 | 0.49716 | | | | | | | |

| | | | | | | | | | | | | | | | | | |
|---------------|------------|-----------|--------|----|--------|----|------------|----------|--|---------------|------------|-----------|--------|----|--------|----|----------|
| | 282 -> 295 | 0.12720 | | | | | 280 -> 289 | -0.21102 | | | | | | | | | |
| | | | | | | | 282 -> 300 | 0.44674 | | | | | | | | | |
| Excited State | 30: | Singlet-A | 4.2488 | eV | 291.81 | nm | f=0.0012 | | | | | | | | | | |
| <S**2>=0.000 | | | | | | | | | | Excited State | 39: | Singlet-A | 4.3796 | eV | 283.09 | nm | f=0.0020 |
| | 280 -> 286 | 0.12083 | | | | | | | | <S**2>=0.000 | | | | | | | |
| | 281 -> 291 | -0.11709 | | | | | | | | | 280 -> 287 | 0.34881 | | | | | |
| | 281 -> 293 | 0.23497 | | | | | | | | | 280 -> 288 | -0.11485 | | | | | |
| | 281 -> 294 | -0.27742 | | | | | | | | | 280 -> 289 | 0.16608 | | | | | |
| | 281 -> 297 | -0.15276 | | | | | | | | | 281 -> 294 | 0.12654 | | | | | |
| | 281 -> 302 | 0.39518 | | | | | | | | | 281 -> 295 | 0.20700 | | | | | |
| | 281 -> 303 | 0.16089 | | | | | | | | | 282 -> 300 | 0.45075 | | | | | |
| | 281 -> 304 | 0.11554 | | | | | | | | | 282 -> 302 | -0.10462 | | | | | |
| Excited State | 31: | Singlet-A | 4.2698 | eV | 290.37 | nm | f=0.0075 | | | Excited State | 40: | Singlet-A | 4.3907 | eV | 282.38 | nm | f=0.0031 |
| <S**2>=0.000 | | | | | | | | | | <S**2>=0.000 | | | | | | | |
| | 280 -> 286 | 0.13809 | | | | | | | | | 281 -> 294 | -0.22819 | | | | | |
| | 282 -> 295 | 0.20238 | | | | | | | | | 281 -> 295 | 0.56304 | | | | | |
| | 282 -> 296 | 0.61708 | | | | | | | | | 281 -> 299 | -0.23111 | | | | | |
| | 282 -> 299 | -0.10981 | | | | | | | | | 281 -> 302 | -0.14861 | | | | | |
| Excited State | 32: | Singlet-A | 4.2724 | eV | 290.19 | nm | f=0.0089 | | | | 282 -> 300 | -0.10442 | | | | | |
| <S**2>=0.000 | | | | | | | | | | Excited State | 41: | Singlet-A | 4.4171 | eV | 280.69 | nm | f=0.0004 |
| | 280 -> 285 | -0.27682 | | | | | | | | <S**2>=0.000 | | | | | | | |
| | 280 -> 286 | 0.37025 | | | | | | | | | 281 -> 295 | 0.11620 | | | | | |
| | 280 -> 287 | 0.27700 | | | | | | | | | 281 -> 296 | 0.66632 | | | | | |
| | 280 -> 288 | 0.14564 | | | | | | | | | 281 -> 302 | 0.11016 | | | | | |
| | 280 -> 289 | -0.19848 | | | | | | | | Excited State | 42: | Singlet-A | 4.4436 | eV | 279.02 | nm | f=0.0103 |
| | 282 -> 295 | -0.20654 | | | | | | | | <S**2>=0.000 | | | | | | | |
| | 282 -> 298 | -0.10694 | | | | | | | | | 282 -> 297 | -0.11968 | | | | | |
| | 282 -> 299 | 0.15545 | | | | | | | | | 282 -> 301 | 0.61562 | | | | | |
| | 282 -> 302 | 0.10238 | | | | | | | | | 282 -> 302 | -0.24130 | | | | | |
| Excited State | 33: | Singlet-A | 4.2904 | eV | 288.98 | nm | f=0.0487 | | | Excited State | 43: | Singlet-A | 4.4502 | eV | 278.60 | nm | f=0.0020 |
| <S**2>=0.000 | | | | | | | | | | <S**2>=0.000 | | | | | | | |
| | 280 -> 285 | 0.13515 | | | | | | | | | 281 -> 297 | 0.41034 | | | | | |
| | 280 -> 286 | -0.14797 | | | | | | | | | 281 -> 298 | 0.52708 | | | | | |
| | 282 -> 294 | 0.11441 | | | | | | | | | 281 -> 300 | 0.10947 | | | | | |
| | 282 -> 296 | 0.19071 | | | | | | | | Excited State | 44: | Singlet-A | 4.4620 | eV | 277.87 | nm | f=0.0155 |
| | 282 -> 297 | 0.19120 | | | | | | | | <S**2>=0.000 | | | | | | | |
| | 282 -> 299 | 0.43555 | | | | | | | | | 281 -> 298 | 0.19225 | | | | | |
| | 282 -> 301 | 0.13426 | | | | | | | | | 282 -> 301 | -0.18724 | | | | | |
| | 282 -> 302 | 0.28227 | | | | | | | | | 282 -> 302 | -0.16601 | | | | | |
| Excited State | 34: | Singlet-A | 4.3018 | eV | 288.22 | nm | f=0.0009 | | | | 282 -> 303 | 0.47615 | | | | | |
| <S**2>=0.000 | | | | | | | | | | | 282 -> 304 | 0.13995 | | | | | |
| | 282 -> 297 | 0.40636 | | | | | | | | | 282 -> 308 | -0.19564 | | | | | |
| | 282 -> 298 | 0.55597 | | | | | | | | | 282 -> 310 | -0.11015 | | | | | |
| Excited State | 35: | Singlet-A | 4.3194 | eV | 287.04 | nm | f=0.0031 | | | | 282 -> 312 | 0.11590 | | | | | |
| <S**2>=0.000 | | | | | | | | | | | 282 -> 315 | 0.12475 | | | | | |
| | 281 -> 294 | 0.12760 | | | | | | | | Excited State | 45: | Singlet-A | 4.4699 | eV | 277.38 | nm | f=0.0057 |
| | 281 -> 299 | -0.10360 | | | | | | | | <S**2>=0.000 | | | | | | | |
| | 282 -> 295 | 0.10066 | | | | | | | | | 281 -> 295 | 0.13817 | | | | | |
| | 282 -> 297 | -0.26366 | | | | | | | | | 281 -> 297 | -0.32879 | | | | | |
| | 282 -> 298 | 0.28154 | | | | | | | | | 281 -> 298 | 0.23290 | | | | | |
| | 282 -> 299 | 0.42936 | | | | | | | | | 281 -> 299 | 0.49725 | | | | | |
| | 282 -> 301 | -0.16922 | | | | | | | | | 281 -> 301 | -0.16073 | | | | | |
| | 282 -> 302 | -0.17969 | | | | | | | | | 281 -> 302 | -0.11367 | | | | | |
| Excited State | 36: | Singlet-A | 4.3273 | eV | 286.51 | nm | f=0.0083 | | | Excited State | 46: | Singlet-A | 4.5201 | eV | 274.30 | nm | f=0.0047 |
| <S**2>=0.000 | | | | | | | | | | <S**2>=0.000 | | | | | | | |
| | 281 -> 294 | 0.39338 | | | | | | | | | 281 -> 298 | -0.14188 | | | | | |
| | 281 -> 297 | -0.26662 | | | | | | | | | 281 -> 299 | 0.10316 | | | | | |
| | 281 -> 298 | 0.21090 | | | | | | | | | 281 -> 300 | 0.63987 | | | | | |
| | 281 -> 299 | -0.23615 | | | | | | | | | 281 -> 302 | -0.10304 | | | | | |
| | 281 -> 303 | 0.10657 | | | | | | | | Excited State | 47: | Singlet-A | 4.5295 | eV | 273.72 | nm | f=0.0068 |
| | 281 -> 308 | -0.17264 | | | | | | | | <S**2>=0.000 | | | | | | | |
| | 281 -> 315 | 0.10069 | | | | | | | | | 281 -> 299 | 0.10464 | | | | | |
| | 282 -> 297 | 0.12051 | | | | | | | | | 281 -> 300 | -0.17125 | | | | | |
| | 282 -> 299 | -0.18514 | | | | | | | | | 282 -> 302 | -0.12626 | | | | | |
| Excited State | 37: | Singlet-A | 4.3690 | eV | 283.78 | nm | f=0.0002 | | | | 282 -> 304 | 0.45847 | | | | | |
| <S**2>=0.000 | | | | | | | | | | | 282 -> 305 | 0.21012 | | | | | |
| | 280 -> 287 | -0.16795 | | | | | | | | | 282 -> 306 | -0.20390 | | | | | |
| | 281 -> 294 | 0.37860 | | | | | | | | | 282 -> 310 | 0.15521 | | | | | |
| | 281 -> 295 | 0.28616 | | | | | | | | | 282 -> 314 | 0.13541 | | | | | |
| | 281 -> 296 | -0.14235 | | | | | | | | | 282 -> 322 | 0.11330 | | | | | |
| | 281 -> 297 | 0.14697 | | | | | | | | Excited State | 48: | Singlet-A | 4.5771 | eV | 270.88 | nm | f=0.0055 |
| | 281 -> 298 | -0.10282 | | | | | | | | <S**2>=0.000 | | | | | | | |
| | 281 -> 299 | 0.20057 | | | | | | | | | 281 -> 299 | -0.14539 | | | | | |
| | 281 -> 302 | 0.22229 | | | | | | | | | 281 -> 300 | 0.13661 | | | | | |
| | 282 -> 300 | -0.19808 | | | | | | | | | 281 -> 302 | 0.11446 | | | | | |
| Excited State | 38: | Singlet-A | 4.3771 | eV | 283.26 | nm | f=0.0003 | | | | 281 -> 303 | -0.22821 | | | | | |
| <S**2>=0.000 | | | | | | | | | | | 281 -> 304 | -0.14465 | | | | | |
| | 280 -> 287 | -0.41873 | | | | | | | | | 281 -> 308 | 0.17873 | | | | | |
| | 280 -> 288 | 0.15139 | | | | | | | | | | | | | | | |

| | | | | | | | | | | | |
|---------------|----------|-----------|-----------|-----------|----------|---------------|----------|-----------|-----------|-----------|----------|
| 282 -> 313 | 0.40272 | | | | | 281 -> 311 | -0.16651 | | | | |
| 282 -> 314 | -0.17279 | | | | | | | | | | |
| Excited State | 69: | Singlet-A | 4.8545 eV | 255.40 nm | f=0.0007 | Excited State | 71: | Singlet-A | 4.8924 eV | 253.42 nm | f=0.0039 |
| <S**2>=0.000 | | | | | | <S**2>=0.000 | | | | | |
| 278 -> 283 | 0.11814 | | | | | 278 -> 283 | 0.57419 | | | | |
| 281 -> 307 | 0.65805 | | | | | 281 -> 307 | -0.18346 | | | | |
| 281 -> 309 | -0.10077 | | | | | 281 -> 308 | -0.12949 | | | | |
| | | | | | | 281 -> 309 | -0.16478 | | | | |
| Excited State | 70: | Singlet-A | 4.8597 eV | 255.13 nm | f=0.0029 | 281 -> 310 | 0.12926 | | | | |
| <S**2>=0.000 | | | | | | 281 -> 312 | -0.10879 | | | | |
| 278 -> 283 | -0.17521 | | | | | 281 -> 313 | -0.13578 | | | | |
| 281 -> 302 | -0.13243 | | | | | Excited State | 72: | Singlet-A | 4.8972 eV | 253.17 nm | f=0.0025 |
| 281 -> 304 | -0.11393 | | | | | <S**2>=0.000 | | | | | |
| 281 -> 305 | -0.15995 | | | | | 281 -> 305 | -0.11703 | | | | |
| 281 -> 306 | 0.28154 | | | | | 281 -> 309 | 0.60049 | | | | |
| 281 -> 308 | -0.26768 | | | | | 281 -> 314 | 0.21021 | | | | |
| 281 -> 310 | 0.41216 | | | | | | | | | | |

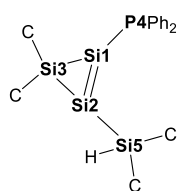
Table 6-10. Transition Energy, Wavelength, and Oscillator Strengths of the Electronic Transition of 2[']_{opt} (The 221th orbital is highest occupied orbital shown in Figure 6-58) [td_b_TN112ac]

| | | | | | | | | | | | |
|---------------|----------|-----------|-----------|-----------|----------|---------------|----------|-----------|-----------|-----------|----------|
| Excited State | 1: | Singlet-A | 2.1775 eV | 569.39 nm | f=0.0037 | 221 -> 228 | 0.36189 | | | | |
| <S**2>=0.000 | | | | | | 221 -> 229 | -0.14324 | | | | |
| 221 -> 222 | 0.70535 | | | | | 221 -> 230 | 0.23290 | | | | |
| Excited State | 2: | Singlet-A | 2.8781 eV | 430.79 nm | f=0.0471 | Excited State | 11: | Singlet-A | 3.6954 eV | 335.51 nm | f=0.0373 |
| <S**2>=0.000 | | | | | | <S**2>=0.000 | | | | | |
| 219 -> 222 | 0.17402 | | | | | 221 -> 227 | 0.47061 | | | | |
| 220 -> 222 | 0.64279 | | | | | 221 -> 228 | 0.36531 | | | | |
| 221 -> 228 | -0.11182 | | | | | 221 -> 229 | 0.33047 | | | | |
| 221 -> 229 | 0.10784 | | | | | Excited State | 12: | Singlet-A | 3.7304 eV | 332.36 nm | f=0.0176 |
| Excited State | 3: | Singlet-A | 2.9738 eV | 416.93 nm | f=0.0048 | <S**2>=0.000 | | | | | |
| <S**2>=0.000 | | | | | | 220 -> 224 | 0.11955 | | | | |
| 219 -> 222 | 0.68051 | | | | | 221 -> 227 | -0.44478 | | | | |
| 220 -> 222 | -0.15401 | | | | | 221 -> 228 | 0.12154 | | | | |
| | | | | | | 221 -> 229 | 0.47062 | | | | |
| Excited State | 4: | Singlet-A | 3.2282 eV | 384.06 nm | f=0.0092 | Excited State | 13: | Singlet-A | 3.7465 eV | 330.94 nm | f=0.0045 |
| <S**2>=0.000 | | | | | | <S**2>=0.000 | | | | | |
| 221 -> 223 | 0.66597 | | | | | 220 -> 224 | 0.46745 | | | | |
| 221 -> 224 | 0.17480 | | | | | 220 -> 225 | -0.11973 | | | | |
| Excited State | 5: | Singlet-A | 3.3541 eV | 369.65 nm | f=0.0362 | 220 -> 227 | 0.15058 | | | | |
| <S**2>=0.000 | | | | | | 220 -> 228 | -0.26141 | | | | |
| 220 -> 222 | 0.13581 | | | | | 220 -> 229 | 0.33512 | | | | |
| 221 -> 223 | -0.18281 | | | | | 220 -> 230 | -0.12638 | | | | |
| 221 -> 224 | 0.60704 | | | | | 221 -> 227 | 0.13399 | | | | |
| 221 -> 228 | 0.22853 | | | | | 221 -> 229 | -0.11041 | | | | |
| Excited State | 6: | Singlet-A | 3.4914 eV | 355.12 nm | f=0.0202 | Excited State | 14: | Singlet-A | 3.7814 eV | 327.88 nm | f=0.0091 |
| <S**2>=0.000 | | | | | | <S**2>=0.000 | | | | | |
| 220 -> 223 | 0.61724 | | | | | 220 -> 225 | 0.59563 | | | | |
| 220 -> 224 | 0.21372 | | | | | 220 -> 226 | 0.11908 | | | | |
| 220 -> 230 | 0.10639 | | | | | 221 -> 230 | 0.24689 | | | | |
| 221 -> 225 | -0.17167 | | | | | 221 -> 232 | -0.13436 | | | | |
| Excited State | 7: | Singlet-A | 3.5084 eV | 353.39 nm | f=0.0016 | Excited State | 15: | Singlet-A | 3.7853 eV | 327.54 nm | f=0.0161 |
| <S**2>=0.000 | | | | | | <S**2>=0.000 | | | | | |
| 220 -> 223 | 0.14904 | | | | | 220 -> 225 | -0.31278 | | | | |
| 221 -> 225 | 0.66725 | | | | | 221 -> 226 | -0.12712 | | | | |
| | | | | | | 221 -> 228 | -0.19057 | | | | |
| Excited State | 8: | Singlet-A | 3.5285 eV | 351.38 nm | f=0.0854 | 221 -> 230 | 0.50873 | | | | |
| <S**2>=0.000 | | | | | | 221 -> 232 | -0.19268 | | | | |
| 221 -> 224 | 0.20719 | | | | | Excited State | 16: | Singlet-A | 3.8106 eV | 325.37 nm | f=0.0062 |
| 221 -> 226 | 0.50191 | | | | | <S**2>=0.000 | | | | | |
| 221 -> 227 | 0.11225 | | | | | 220 -> 223 | -0.10440 | | | | |
| 221 -> 228 | -0.25202 | | | | | 220 -> 225 | -0.13305 | | | | |
| 221 -> 229 | 0.26788 | | | | | 220 -> 226 | 0.64105 | | | | |
| Excited State | 9: | Singlet-A | 3.5323 eV | 351.00 nm | f=0.0130 | 220 -> 230 | 0.11238 | | | | |
| <S**2>=0.000 | | | | | | 220 -> 232 | -0.10794 | | | | |
| 220 -> 223 | -0.27084 | | | | | Excited State | 17: | Singlet-A | 3.8606 eV | 321.15 nm | f=0.0262 |
| 220 -> 224 | 0.43264 | | | | | <S**2>=0.000 | | | | | |
| 220 -> 228 | 0.32354 | | | | | 221 -> 229 | 0.11585 | | | | |
| 220 -> 229 | -0.25454 | | | | | 221 -> 230 | 0.24094 | | | | |
| 220 -> 230 | 0.10772 | | | | | 221 -> 231 | 0.46674 | | | | |
| Excited State | 10: | Singlet-A | 3.5452 eV | 349.72 nm | f=0.0283 | 221 -> 232 | 0.39661 | | | | |
| <S**2>=0.000 | | | | | | Excited State | 18: | Singlet-A | 3.8975 eV | 318.11 nm | f=0.0103 |
| 221 -> 224 | -0.19370 | | | | | <S**2>=0.000 | | | | | |
| 221 -> 226 | 0.42429 | | | | | 221 -> 230 | -0.16254 | | | | |
| 221 -> 227 | -0.14553 | | | | | | | | | | |

| | | | | | | | | | |
|-------------------|-----------|-----------|-----------|----------|-------------------|-----------|-----------|-----------|----------|
| 221 -> 231 | 0.45647 | | | | 221 -> 236 | 0.15092 | | | |
| 221 -> 232 | -0.45469 | | | | | | | | |
| 221 -> 235 | 0.12837 | | | | Excited State 28: | Singlet-A | 4.1690 eV | 297.40 nm | f=0.0026 |
| 221 -> 238 | -0.10475 | | | | <S**2>=0.000 | | | | |
| Excited State 19: | Singlet-A | 3.9336 eV | 315.19 nm | f=0.0056 | 219 -> 223 | -0.23099 | | | |
| <S**2>=0.000 | | | | | 219 -> 224 | 0.44844 | | | |
| 220 -> 227 | 0.23539 | | | | 219 -> 228 | 0.27693 | | | |
| 220 -> 228 | 0.48355 | | | | 219 -> 229 | -0.23364 | | | |
| 220 -> 229 | 0.36538 | | | | 219 -> 230 | 0.10862 | | | |
| 220 -> 236 | -0.12836 | | | | 220 -> 231 | -0.15611 | | | |
| 220 -> 240 | -0.15659 | | | | 221 -> 234 | -0.14417 | | | |
| Excited State 20: | Singlet-A | 3.9900 eV | 310.74 nm | f=0.0075 | Excited State 29: | Singlet-A | 4.1895 eV | 295.94 nm | f=0.0468 |
| <S**2>=0.000 | | | | | <S**2>=0.000 | | | | |
| 220 -> 227 | 0.60517 | | | | 219 -> 223 | -0.23505 | | | |
| 220 -> 229 | -0.30739 | | | | 220 -> 231 | 0.49857 | | | |
| Excited State 21: | Singlet-A | 4.0482 eV | 306.27 nm | f=0.0052 | 220 -> 232 | -0.26938 | | | |
| <S**2>=0.000 | | | | | 221 -> 236 | 0.26158 | | | |
| 220 -> 226 | -0.14455 | | | | Excited State 30: | Singlet-A | 4.2049 eV | 294.86 nm | f=0.0327 |
| 220 -> 227 | 0.12037 | | | | <S**2>=0.000 | | | | |
| 220 -> 228 | -0.15091 | | | | 221 -> 232 | -0.11174 | | | |
| 220 -> 230 | 0.46707 | | | | 221 -> 234 | -0.18709 | | | |
| 220 -> 231 | -0.10103 | | | | 221 -> 235 | 0.16636 | | | |
| 220 -> 232 | -0.29088 | | | | 221 -> 236 | -0.31094 | | | |
| 221 -> 233 | -0.19740 | | | | 221 -> 237 | 0.45398 | | | |
| Excited State 22: | Singlet-A | 4.0676 eV | 304.81 nm | f=0.0235 | 221 -> 238 | 0.21251 | | | |
| <S**2>=0.000 | | | | | 221 -> 240 | 0.15952 | | | |
| 219 -> 223 | 0.13586 | | | | Excited State 31: | Singlet-A | 4.2475 eV | 291.90 nm | f=0.0093 |
| 220 -> 230 | 0.21917 | | | | <S**2>=0.000 | | | | |
| 220 -> 231 | -0.12428 | | | | 221 -> 236 | -0.15715 | | | |
| 221 -> 233 | 0.37575 | | | | 221 -> 237 | -0.41512 | | | |
| 221 -> 235 | -0.15102 | | | | 221 -> 238 | 0.41982 | | | |
| 221 -> 236 | 0.30147 | | | | 221 -> 239 | 0.17732 | | | |
| 221 -> 238 | 0.12375 | | | | 221 -> 240 | 0.12975 | | | |
| 221 -> 239 | 0.12459 | | | | 221 -> 241 | 0.12075 | | | |
| 221 -> 240 | 0.21883 | | | | Excited State 32: | Singlet-A | 4.2642 eV | 290.76 nm | f=0.0053 |
| Excited State 23: | Singlet-A | 4.0890 eV | 303.21 nm | f=0.0122 | <S**2>=0.000 | | | | |
| <S**2>=0.000 | | | | | 220 -> 229 | 0.11245 | | | |
| 219 -> 223 | -0.18996 | | | | 220 -> 231 | 0.12529 | | | |
| 220 -> 230 | 0.13209 | | | | 220 -> 236 | 0.19071 | | | |
| 220 -> 231 | 0.10579 | | | | 220 -> 239 | 0.10263 | | | |
| 221 -> 233 | 0.47310 | | | | 220 -> 240 | 0.17328 | | | |
| 221 -> 234 | 0.16158 | | | | 221 -> 236 | -0.24559 | | | |
| 221 -> 236 | -0.25345 | | | | 221 -> 237 | -0.15695 | | | |
| 221 -> 240 | -0.20619 | | | | 221 -> 238 | -0.17723 | | | |
| 221 -> 241 | 0.10054 | | | | 221 -> 240 | 0.35522 | | | |
| Excited State 24: | Singlet-A | 4.1090 eV | 301.74 nm | f=0.0147 | 221 -> 241 | -0.25169 | | | |
| <S**2>=0.000 | | | | | Excited State 33: | Singlet-A | 4.2877 eV | 289.16 nm | f=0.0049 |
| 219 -> 223 | 0.26394 | | | | <S**2>=0.000 | | | | |
| 220 -> 229 | 0.11615 | | | | 220 -> 228 | 0.11351 | | | |
| 220 -> 230 | 0.34084 | | | | 220 -> 229 | 0.16599 | | | |
| 220 -> 231 | 0.31560 | | | | 220 -> 234 | -0.16062 | | | |
| 220 -> 232 | 0.33620 | | | | 220 -> 236 | 0.32591 | | | |
| 221 -> 233 | -0.11302 | | | | 220 -> 239 | 0.14536 | | | |
| Excited State 25: | Singlet-A | 4.1270 eV | 300.42 nm | f=0.0531 | 220 -> 240 | 0.29887 | | | |
| <S**2>=0.000 | | | | | 220 -> 241 | -0.10473 | | | |
| 219 -> 223 | 0.38836 | | | | 221 -> 237 | 0.10667 | | | |
| 219 -> 224 | 0.21475 | | | | 221 -> 238 | 0.12955 | | | |
| 220 -> 230 | -0.13969 | | | | 221 -> 239 | 0.11748 | | | |
| 220 -> 232 | -0.25430 | | | | 221 -> 240 | -0.20687 | | | |
| 221 -> 234 | 0.36544 | | | | 221 -> 241 | 0.18772 | | | |
| 221 -> 236 | -0.14123 | | | | Excited State 34: | Singlet-A | 4.2992 eV | 288.39 nm | f=0.0120 |
| Excited State 26: | Singlet-A | 4.1329 eV | 299.99 nm | f=0.0192 | <S**2>=0.000 | | | | |
| <S**2>=0.000 | | | | | 221 -> 237 | 0.10241 | | | |
| 219 -> 223 | -0.28733 | | | | 221 -> 238 | -0.25206 | | | |
| 220 -> 231 | -0.15569 | | | | 221 -> 239 | 0.57505 | | | |
| 220 -> 232 | 0.12980 | | | | Excited State 35: | Singlet-A | 4.3516 eV | 284.91 nm | f=0.0024 |
| 221 -> 232 | -0.11675 | | | | <S**2>=0.000 | | | | |
| 221 -> 233 | -0.13693 | | | | 219 -> 224 | 0.11318 | | | |
| 221 -> 234 | 0.46891 | | | | 219 -> 229 | 0.12777 | | | |
| 221 -> 235 | -0.10633 | | | | 220 -> 233 | 0.62387 | | | |
| 221 -> 237 | 0.13664 | | | | 220 -> 235 | -0.15274 | | | |
| 221 -> 238 | 0.14924 | | | | Excited State 36: | Singlet-A | 4.3708 eV | 283.67 nm | f=0.0221 |
| 221 -> 240 | 0.15383 | | | | <S**2>=0.000 | | | | |
| Excited State 27: | Singlet-A | 4.1533 eV | 298.52 nm | f=0.0050 | 219 -> 224 | 0.43494 | | | |
| <S**2>=0.000 | | | | | 219 -> 225 | -0.12375 | | | |
| 221 -> 233 | 0.16717 | | | | 219 -> 227 | 0.15598 | | | |
| 221 -> 234 | 0.13372 | | | | 219 -> 228 | -0.24740 | | | |
| 221 -> 235 | 0.62400 | | | | 219 -> 229 | 0.34985 | | | |
| | | | | | 219 -> 230 | -0.14227 | | | |

| | | | | | | | | | | | |
|-------------------|-----------|-----------|-----------|----------|--|-------------------|-----------|-----------|-----------|----------|--|
| 220 -> 233 | -0.19255 | | | | | 221 -> 242 | 0.21515 | | | | |
| Excited State 37: | Singlet-A | 4.3871 eV | 282.61 nm | f=0.0035 | | 221 -> 243 | 0.31165 | | | | |
| <S**2>=0.000 | | | | | | 221 -> 247 | -0.17284 | | | | |
| 220 -> 232 | -0.17991 | | | | | Excited State 47: | Singlet-A | 4.5545 eV | 272.22 nm | f=0.0084 | |
| 220 -> 234 | 0.53375 | | | | | <S**2>=0.000 | | | | | |
| 220 -> 237 | 0.15067 | | | | | 219 -> 227 | 0.14269 | | | | |
| 220 -> 238 | 0.15054 | | | | | 219 -> 228 | 0.25711 | | | | |
| 220 -> 240 | 0.15511 | | | | | 219 -> 229 | 0.16220 | | | | |
| 221 -> 238 | -0.10953 | | | | | 220 -> 239 | 0.22356 | | | | |
| 221 -> 239 | -0.10063 | | | | | 221 -> 243 | -0.31700 | | | | |
| 221 -> 240 | 0.11170 | | | | | 221 -> 244 | 0.14896 | | | | |
| 221 -> 241 | 0.17323 | | | | | 221 -> 245 | 0.34710 | | | | |
| Excited State 38: | Singlet-A | 4.3986 eV | 281.87 nm | f=0.0006 | | Excited State 48: | Singlet-A | 4.5627 eV | 271.73 nm | f=0.0120 | |
| <S**2>=0.000 | | | | | | <S**2>=0.000 | | | | | |
| 219 -> 225 | 0.67091 | | | | | 220 -> 238 | -0.17015 | | | | |
| 219 -> 226 | 0.11625 | | | | | 220 -> 239 | -0.15710 | | | | |
| Excited State 39: | Singlet-A | 4.4074 eV | 281.31 nm | f=0.0035 | | 220 -> 240 | 0.13066 | | | | |
| <S**2>=0.000 | | | | | | 220 -> 241 | -0.14392 | | | | |
| 220 -> 234 | -0.24815 | | | | | 221 -> 242 | 0.34724 | | | | |
| 221 -> 238 | -0.22410 | | | | | 221 -> 243 | 0.15553 | | | | |
| 221 -> 239 | -0.18472 | | | | | 221 -> 245 | 0.34168 | | | | |
| 221 -> 240 | 0.29128 | | | | | 221 -> 247 | -0.26444 | | | | |
| 221 -> 241 | 0.45681 | | | | | Excited State 49: | Singlet-A | 4.5963 eV | 269.75 nm | f=0.0270 | |
| 221 -> 243 | -0.11008 | | | | | <S**2>=0.000 | | | | | |
| Excited State 40: | Singlet-A | 4.4211 eV | 280.44 nm | f=0.0070 | | 219 -> 227 | 0.42063 | | | | |
| <S**2>=0.000 | | | | | | 219 -> 228 | 0.35038 | | | | |
| 219 -> 225 | -0.11031 | | | | | 220 -> 238 | -0.21358 | | | | |
| 219 -> 226 | 0.29521 | | | | | 220 -> 239 | -0.16091 | | | | |
| 220 -> 233 | 0.17093 | | | | | 221 -> 243 | 0.22201 | | | | |
| 220 -> 235 | 0.55667 | | | | | 221 -> 245 | -0.13271 | | | | |
| 220 -> 236 | 0.12428 | | | | | 221 -> 247 | 0.13663 | | | | |
| Excited State 41: | Singlet-A | 4.4353 eV | 279.54 nm | f=0.0485 | | Excited State 50: | Singlet-A | 4.6119 eV | 268.84 nm | f=0.0119 | |
| <S**2>=0.000 | | | | | | <S**2>=0.000 | | | | | |
| 219 -> 226 | 0.57998 | | | | | 221 -> 243 | 0.22945 | | | | |
| 220 -> 235 | -0.30544 | | | | | 221 -> 244 | 0.60316 | | | | |
| Excited State 42: | Singlet-A | 4.4765 eV | 276.97 nm | f=0.0008 | | 221 -> 247 | 0.21609 | | | | |
| <S**2>=0.000 | | | | | | Excited State 51: | Singlet-A | 4.6182 eV | 268.47 nm | f=0.0105 | |
| 220 -> 234 | -0.19785 | | | | | <S**2>=0.000 | | | | | |
| 220 -> 235 | 0.14181 | | | | | 219 -> 227 | 0.46638 | | | | |
| 220 -> 236 | -0.39362 | | | | | 219 -> 228 | -0.22966 | | | | |
| 220 -> 237 | 0.41380 | | | | | 219 -> 229 | -0.39766 | | | | |
| 220 -> 238 | 0.16935 | | | | | 221 -> 243 | -0.10317 | | | | |
| 220 -> 240 | 0.16874 | | | | | 221 -> 244 | 0.10458 | | | | |
| Excited State 43: | Singlet-A | 4.4885 eV | 276.23 nm | f=0.0096 | | 221 -> 247 | -0.11394 | | | | |
| <S**2>=0.000 | | | | | | Excited State 52: | Singlet-A | 4.6433 eV | 267.02 nm | f=0.0183 | |
| 221 -> 239 | -0.11646 | | | | | <S**2>=0.000 | | | | | |
| 221 -> 241 | -0.12929 | | | | | 219 -> 228 | -0.13188 | | | | |
| 221 -> 242 | 0.52733 | | | | | 220 -> 238 | 0.11722 | | | | |
| 221 -> 243 | -0.19643 | | | | | 221 -> 243 | 0.18143 | | | | |
| 221 -> 245 | -0.18063 | | | | | 221 -> 244 | -0.20911 | | | | |
| 221 -> 247 | 0.24221 | | | | | 221 -> 245 | 0.31097 | | | | |
| Excited State 44: | Singlet-A | 4.5302 eV | 273.68 nm | f=0.0004 | | 221 -> 246 | 0.31073 | | | | |
| <S**2>=0.000 | | | | | | 221 -> 247 | 0.36113 | | | | |
| 220 -> 234 | -0.11850 | | | | | Excited State 53: | Singlet-A | 4.6818 eV | 264.82 nm | f=0.0010 | |
| 220 -> 236 | 0.31220 | | | | | <S**2>=0.000 | | | | | |
| 220 -> 237 | 0.37490 | | | | | 220 -> 241 | 0.11223 | | | | |
| 220 -> 239 | -0.32984 | | | | | 221 -> 243 | -0.12001 | | | | |
| 220 -> 240 | -0.29355 | | | | | 221 -> 244 | 0.14010 | | | | |
| Excited State 45: | Singlet-A | 4.5333 eV | 273.50 nm | f=0.0160 | | 221 -> 245 | -0.14756 | | | | |
| <S**2>=0.000 | | | | | | 221 -> 246 | 0.56476 | | | | |
| 219 -> 228 | 0.12075 | | | | | 221 -> 247 | -0.18684 | | | | |
| 220 -> 234 | -0.14566 | | | | | Excited State 54: | Singlet-A | 4.6879 eV | 264.48 nm | f=0.0345 | |
| 220 -> 237 | -0.24794 | | | | | <S**2>=0.000 | | | | | |
| 220 -> 238 | 0.50027 | | | | | 219 -> 226 | -0.11375 | | | | |
| 220 -> 239 | -0.18058 | | | | | 219 -> 229 | 0.18951 | | | | |
| 220 -> 241 | 0.11802 | | | | | 219 -> 230 | 0.42818 | | | | |
| 220 -> 245 | 0.12152 | | | | | 219 -> 232 | -0.16483 | | | | |
| 221 -> 242 | 0.11343 | | | | | 220 -> 239 | 0.14695 | | | | |
| Excited State 46: | Singlet-A | 4.5414 eV | 273.01 nm | f=0.0168 | | 220 -> 240 | -0.18709 | | | | |
| <S**2>=0.000 | | | | | | 220 -> 241 | -0.25208 | | | | |
| 220 -> 237 | 0.21591 | | | | | 221 -> 245 | -0.14014 | | | | |
| 220 -> 239 | 0.27202 | | | | | 221 -> 247 | -0.13434 | | | | |
| 220 -> 240 | -0.18705 | | | | | Excited State 55: | Singlet-A | 4.6951 eV | 264.07 nm | f=0.0466 | |
| 220 -> 241 | 0.18108 | | | | | <S**2>=0.000 | | | | | |
| 220 -> 243 | -0.11257 | | | | | 219 -> 228 | -0.16462 | | | | |
| 220 -> 247 | 0.11514 | | | | | 219 -> 230 | 0.44882 | | | | |
| 221 -> 241 | 0.17392 | | | | | 220 -> 239 | -0.16111 | | | | |
| | | | | | | 220 -> 240 | 0.19627 | | | | |

| | | | | | | | | | | | |
|-------------------|----------|-----------|-----------|-----------|----------|-------------------|----------|-----------|-----------|-----------|----------|
| 220 -> 241 | 0.34331 | | | | | 218 -> 222 | -0.11579 | | | | |
| 220 -> 243 | -0.12607 | | | | | 221 -> 249 | -0.33533 | | | | |
| Excited State 56: | | Singlet-A | 4.7184 eV | 262.77 nm | f=0.0104 | 221 -> 250 | 0.40993 | | | | |
| <S**2>=0.000 | | | | | | 221 -> 251 | 0.23740 | | | | |
| 220 -> 238 | 0.18636 | | | | | 221 -> 252 | -0.17268 | | | | |
| 220 -> 239 | -0.22058 | | | | | 221 -> 253 | 0.15482 | | | | |
| 220 -> 241 | -0.26636 | | | | | 221 -> 259 | -0.11650 | | | | |
| 220 -> 242 | 0.35734 | | | | | Excited State 65: | | Singlet-A | 4.8673 eV | 254.73 nm | f=0.0025 |
| 220 -> 243 | -0.11117 | | | | | <S**2>=0.000 | | | | | |
| 220 -> 245 | -0.27153 | | | | | 217 -> 222 | 0.46997 | | | | |
| 220 -> 247 | 0.27211 | | | | | 218 -> 222 | -0.33104 | | | | |
| Excited State 57: | | Singlet-A | 4.7490 eV | 261.07 nm | f=0.0158 | 220 -> 242 | 0.10293 | | | | |
| <S**2>=0.000 | | | | | | 221 -> 250 | -0.22714 | | | | |
| 219 -> 230 | 0.11043 | | | | | 221 -> 251 | -0.18631 | | | | |
| 219 -> 231 | 0.27851 | | | | | Excited State 66: | | Singlet-A | 4.8808 eV | 254.02 nm | f=0.0004 |
| 219 -> 232 | 0.23347 | | | | | <S**2>=0.000 | | | | | |
| 221 -> 248 | 0.54524 | | | | | 220 -> 243 | 0.24531 | | | | |
| Excited State 58: | | Singlet-A | 4.7586 eV | 260.55 nm | f=0.0734 | 220 -> 244 | 0.57958 | | | | |
| <S**2>=0.000 | | | | | | 220 -> 247 | 0.22624 | | | | |
| 219 -> 231 | 0.43040 | | | | | Excited State 67: | | Singlet-A | 4.9107 eV | 252.48 nm | f=0.0068 |
| 219 -> 232 | 0.25033 | | | | | <S**2>=0.000 | | | | | |
| 220 -> 241 | -0.18407 | | | | | 220 -> 243 | 0.14466 | | | | |
| 221 -> 248 | -0.39092 | | | | | 220 -> 244 | -0.19466 | | | | |
| Excited State 59: | | Singlet-A | 4.7958 eV | 258.53 nm | f=0.0341 | 220 -> 245 | 0.22713 | | | | |
| <S**2>=0.000 | | | | | | 220 -> 246 | 0.21994 | | | | |
| 219 -> 230 | 0.10522 | | | | | 220 -> 247 | 0.29520 | | | | |
| 219 -> 231 | -0.39641 | | | | | 221 -> 251 | 0.31118 | | | | |
| 219 -> 232 | 0.48834 | | | | | 221 -> 252 | 0.26089 | | | | |
| 220 -> 241 | -0.10211 | | | | | 221 -> 253 | -0.20450 | | | | |
| 220 -> 242 | -0.13742 | | | | | Excited State 68: | | Singlet-A | 4.9131 eV | 252.35 nm | f=0.0056 |
| Excited State 60: | | Singlet-A | 4.8035 eV | 258.11 nm | f=0.0053 | <S**2>=0.000 | | | | | |
| <S**2>=0.000 | | | | | | 220 -> 243 | -0.12361 | | | | |
| 219 -> 232 | 0.11721 | | | | | 220 -> 244 | 0.26601 | | | | |
| 220 -> 242 | 0.48310 | | | | | 220 -> 245 | -0.21567 | | | | |
| 220 -> 243 | -0.12281 | | | | | 220 -> 246 | -0.16306 | | | | |
| 220 -> 245 | 0.37714 | | | | | 220 -> 247 | -0.25933 | | | | |
| 220 -> 247 | -0.17219 | | | | | 221 -> 251 | 0.29246 | | | | |
| 220 -> 250 | 0.10175 | | | | | 221 -> 252 | 0.32037 | | | | |
| Excited State 61: | | Singlet-A | 4.8143 eV | 257.54 nm | f=0.0078 | 221 -> 253 | -0.21332 | | | | |
| <S**2>=0.000 | | | | | | Excited State 69: | | Singlet-A | 4.9500 eV | 250.47 nm | f=0.0013 |
| 220 -> 241 | 0.12712 | | | | | <S**2>=0.000 | | | | | |
| 220 -> 242 | 0.14216 | | | | | 218 -> 222 | 0.11867 | | | | |
| 220 -> 243 | 0.38221 | | | | | 219 -> 233 | 0.35582 | | | | |
| 220 -> 244 | -0.13258 | | | | | 219 -> 235 | -0.13082 | | | | |
| 220 -> 245 | -0.17875 | | | | | 219 -> 236 | 0.17533 | | | | |
| 220 -> 247 | -0.14532 | | | | | 220 -> 246 | -0.21523 | | | | |
| 221 -> 246 | -0.13069 | | | | | 221 -> 252 | 0.24820 | | | | |
| 221 -> 250 | -0.19570 | | | | | 221 -> 253 | 0.26210 | | | | |
| 221 -> 251 | 0.27478 | | | | | 221 -> 254 | -0.10944 | | | | |
| 221 -> 252 | -0.15149 | | | | | 221 -> 255 | -0.11755 | | | | |
| 221 -> 253 | 0.11369 | | | | | Excited State 70: | | Singlet-A | 4.9573 eV | 250.10 nm | f=0.0026 |
| Excited State 62: | | Singlet-A | 4.8233 eV | 257.05 nm | f=0.0043 | <S**2>=0.000 | | | | | |
| <S**2>=0.000 | | | | | | 219 -> 233 | 0.37716 | | | | |
| 220 -> 241 | 0.11031 | | | | | 219 -> 235 | -0.14349 | | | | |
| 220 -> 242 | 0.19327 | | | | | 219 -> 236 | 0.10833 | | | | |
| 220 -> 243 | 0.36128 | | | | | 220 -> 246 | 0.27733 | | | | |
| 220 -> 247 | -0.10459 | | | | | 220 -> 247 | -0.11648 | | | | |
| 221 -> 246 | 0.13572 | | | | | 221 -> 252 | -0.25937 | | | | |
| 221 -> 248 | -0.10387 | | | | | 221 -> 253 | -0.28234 | | | | |
| 221 -> 250 | 0.30452 | | | | | Excited State 71: | | Singlet-A | 4.9651 eV | 249.71 nm | f=0.0045 |
| 221 -> 251 | -0.27259 | | | | | <S**2>=0.000 | | | | | |
| 221 -> 252 | 0.16215 | | | | | 220 -> 245 | -0.11725 | | | | |
| 221 -> 253 | -0.11964 | | | | | 220 -> 246 | 0.48345 | | | | |
| Excited State 63: | | Singlet-A | 4.8372 eV | 256.32 nm | f=0.0098 | 220 -> 247 | -0.16235 | | | | |
| <S**2>=0.000 | | | | | | 221 -> 252 | 0.26504 | | | | |
| 217 -> 222 | 0.20832 | | | | | 221 -> 253 | 0.30383 | | | | |
| 218 -> 222 | -0.12602 | | | | | Excited State 72: | | Singlet-A | 4.9799 eV | 248.97 nm | f=0.0017 |
| 221 -> 249 | 0.55541 | | | | | <S**2>=0.000 | | | | | |
| 221 -> 250 | 0.23497 | | | | | 217 -> 222 | 0.25182 | | | | |
| 221 -> 255 | 0.11120 | | | | | 218 -> 222 | 0.40684 | | | | |
| Excited State 64: | | Singlet-A | 4.8534 eV | 255.46 nm | f=0.0020 | 219 -> 233 | -0.32229 | | | | |
| <S**2>=0.000 | | | | | | 219 -> 234 | -0.23063 | | | | |
| 217 -> 222 | 0.22256 | | | | | 219 -> 236 | 0.21556 | | | | |
| | | | | | | 219 -> 240 | 0.11171 | | | | |

Table 6-11. Natural Bond Orbital (NBO) Analysis for **8_{opt}**

| NBO | NBO ^a analysis | | | |
|---------|---------------------------|--------------|---|------------------|
| | occ., ^a | population | hybrids | WBI ^a |
| Si1-Si2 | 1.938 | 48.84% (Si1) | s 31.24%, p 68.40%, d 0.35% (sp ^{2.19} d ^{0.01}) (Si1) | 1.7338 |
| | | 51.16% (Si2) | s 31.00%, p 68.66%, d 0.34% (sp ^{2.21} d ^{0.01}) (Si2) | |
| Si1-Si2 | 1.791 | 46.41% (Si1) | s 0.08%, p 99.51%, d 0.41% (sp ^{99.99} d ^{5.12}) (Si1) | - |
| | | 53.59% (Si2) | s 0.07%, p 99.65%, d 0.28% (sp ^{99.99} d ^{3.83}) (Si2) | |
| Si1-Si3 | 1.888 | 56.83% (Si1) | s 33.70%, p 66.07%, d 0.23% (sp ^{1.96} d ^{0.01}) (Si1) | 1.0038 |
| | | 43.17% (Si3) | s 19.93%, p 79.54%, d 0.53% (sp ^{3.99} d ^{0.03}) (Si3) | |
| Si1-P4 | 1.934 | 46.16% (Si1) | s 34.80%, p 64.92%, d 0.28% (sp ^{1.87} d ^{0.01}) (Si1) | 0.9010 |
| | | 53.84% (P4) | s 13.78%, p 85.75%, d 0.47% (sp ^{6.22} d ^{0.03}) (P4) | |
| Si2-Si3 | 1.857 | 54.56% (Si2) | s 27.91%, p 71.77%, d 0.32% (sp ^{2.57} d ^{0.01}) (Si2) | 0.9907 |
| | | 45.44% (Si3) | s 24.18%, p 75.34%, d 0.48% (sp ^{3.12} d ^{0.02}) (Si3) | |
| Si2-Si5 | 1.970 | 56.08% (Si2) | s 40.80%, p 59.01%, d 0.19% (sp ^{1.45}) (Si2) | 0.9231 |
| | | 43.92% (Si5) | s 25.11%, p 74.39%, d 0.50% (sp ^{2.96} d ^{0.02}) (P4) | |

^aNBO: natural bond orbital. occ.: occupancy. WBI: Wiberg bond indices. JOB number: nbo1TN126aa

2-5. Reference and Notes

- (1) (a) Wiberg, K. B.; Walker, F. H. *J. Am. Chem. Soc.* **1982**, *104*, 5239–5240. (b) Levin, M. D.; Kaszynski, P.; Michl, J. *Chem. Rev.* **2000**, *100*, 169–234. (c) Nied, D.; Breher, F. *Chem. Soc. Rev.* **2011**, *40*, 3455–3466. (d) Dilmaç, A. M.; Spuling, E.; de Meijere, A.; Bräse, S. *Angew. Chem., Int. Ed.* **2017**, *56*, 5684–5718.
- (2) (a) Wiberg, K. B. *Acc. Chem. Res.* **1984**, *17*, 379–386. (b) Iwamoto, T.; Ishida, S. *Chem. Lett.* **2014**, *43*, 164–170. (c) Heider, Y.; Scheschkewitz, D. *Dalton Trans.* **2018**, *47*, 7104–7112. (d) Heider, Y.; Poitiers, N. E.; Willmes, P.; Leszczyn´ska, K. I.; Huch, V.; Scheschkewitz, D. *Chem. Sci.* **2019**, *10*, 4523–4530. (e) Heider, Y.; Scheschkewitz, D. *Chem. Rev.* **2021**, *121*, 9674–9718.
- (3) (a) Szeimies, G.; Harnisch, J.; Baumgärtel, O. *J. Am. Chem. Soc.* **1977**, *99*, 5183–5184. (b) Szeimies-Seebach, U.; Harnisch, J.; Szeimies, G.; Van Meerssche, M.; Germain, G.; Declerq, J.-P. *Angew. Chem., Int. Ed. Engl.* **1978**, *17*, 848–850. (c) Zoch, H.-G.; Szeimies, G.; Romer, R.; Schmitt, R. *Angew. Chem., Int. Ed. Engl.* **1981**, *20*, 877–878.

- (d) Schlüter, A.-D.; Harnisch, H.; Harnisch, J.; Szeimies-Seebach, U.; Szeimies, G. *Chem. Ber.* **1985**, *118*, 3513–3528.
- (4) (a) Iwamoto, T.; Abe, T.; Sugimoto, K.; Hashizume, D.; Matsui, H.; Kishi, R.; Nakano, M.; Ishida, S. *Angew. Chem., Int. Ed.* **2019**, *58*, 4371–4375. (b) Nukazawa, T.; Kosai, T.; Honda, S.; Ishida, S.; Iwamoto, T. *Dalton Trans.* **2019**, *48*, 10874–10880. (c) Fujinami, M.; Seino, J.; Nukazawa, T.; Ishida, S.; Iwamoto, T.; Nakai, H. *Chem. Lett.* **2019**, *48*, 961–964.
- (5) Nied, D.; Köppe, R.; Klopper, W.; Schnöckel, H.; Breher, F. *J. Am. Chem. Soc.* **2010**, *132*, 10264–10265.
- (6) (a) Nukazawa, T.; Iwamoto, T. *J. Am. Chem. Soc.* **2020**, *142*, 9920–9924. (b) Nukazawa, T.; Iwamoto, T. *Dalton Trans.* **2020**, *49*, 16728–16735. See also ref 4a and 4b.
- (7) As an example of a functionalized cyclotrisilene derivative, the generation of a cyclotrisilyl radical has been suggested as an intermediate in the reaction of a cyclotrisilene with disilenes. See: Leszczyńska, K.; Abersfelder, K.; Majumdar, M.; Neumann, B.; Stammer, H.-G.; Rzepa, H. S.; Jutzi, P.; Scheschke, D. *Chem. Commun.* **2012**, *48*, 7820–7822.
- (8) Very recently, Scheschke et al. have reported cyclotrimetalenes ligated by a nickel. See: (a) Majhi, P. K.; Zimmer, M.; Morgenstern, B.; Scheschke, D. *J. Am. Chem. Soc.* **2021**, *143*, 8981–8986. (b) Majhi, P. K.; Zimmer, M.; Morgenstern, B.; Huch, V.; Scheschke, D. *J. Am. Chem. Soc.* **2021**, *143*, 13350–13357.
- (9) West et al. have reported that the reaction of tetramesityldisilene with LiAlH_4 provided the corresponding 1,2-dihydridodisilane. See: West, R. *Science* **1984**, *225*, 1109–1114.
- (10) When **1a** was treated with 3 equiv of LiAlH_4 in THF, a complex reaction mixture was obtained, suggesting that **2** reacts with LiAlH_4 .
- (11) (a) Teclé, B.; Ilsley, W. H.; Oliver, J. P. *Organometallics* **1982**, *1*, 875–877. (b) Dias, H. V. R.; Olmstead, M. M.; Ruhlandt-Senge, K.; Power, P. P. *J. Organomet. Chem.* **1993**,

- 462, 1–6. (c) Heine, A.; Herbst-Irmer, R.; Sheldrick, G. M.; Stalke, D. *Inorg. Chem.* **1993**, *32*, 2694–2698.
- (12) (a) Scheschkewitz, D. *Angew. Chem., Int. Ed.* **2004**, *43*, 2965–2967. (b) Ichinohe, M.; Sanuki, K.; Inoue, S.; Sekiguchi, A. *Organometallics* **2004**, *23*, 3088–3090. (c) Inoue, S.; Ichinohe, M.; Sekiguchi, A. *Chem. Lett.* **2005**, *34*, 1564–1565. (d) Abersfelder, K.; Güclü, D.; Scheschkewitz, D. *Angew. Chem., Int. Ed.* **2006**, *45*, 1643–1645. (e) Ichinohe, M.; Sanuki, K.; Inoue, S.; Sekiguchi, A. *Silicon Chem.* **2007**, *3*, 111–116. (f) Iwamoto, T.; Kobayashi, M.; Uchiyama, K.; Sasaki, S.; Nagendran, S.; Isobe, H.; Kira, M. *J. Am. Chem. Soc.* **2009**, *131*, 3156–3157. (g) Tian, M.; Zhang, J.; Yang, H.; Cui, C. *J. Am. Chem. Soc.* **2020**, *142*, 4131–4135. (h) Yasuda, H.; Lee, V. Ya.; Sekiguchi, A. *J. Am. Chem. Soc.* **2009**, *131*, 6352–6353.
- (13) Pinchuk, D.; Mathew, J.; Kaushansky, A.; Bravo-Zhivotovskii, D.; Apeloig, Y. *Angew. Chem., Int. Ed.* **2016**, *55*, 10258–10262.
- (14) For studies on cyclotrisilenes, see: (a) Iwamoto, T.; Kabuto, C.; Kira, M. *J. Am. Chem. Soc.* **1999**, *121*, 886–887. (b) Ichinohe, M.; Matsuno, T.; Sekiguchi, A. *Angew. Chem., Int. Ed.* **1999**, *38*, 2194–2196. (c) Iwamoto, T.; Tamura, M.; Kabuto, C.; Kira, M. *Science* **2000**, *290*, 504–506. (d) Iwamoto, T.; Tamura, M.; Kabuto, C.; Kira, M. *Organometallics* **2003**, *22*, 2342–2344. (e) Wiberg, N.; Vasisht, S. K.; Fischer, G.; Mayer, P. *Z. Anorg. Allg. Chem.* **2004**, *630*, 1823–1828. (f) Leszczyńska, K.; Abersfelder, K.; Mix, A.; Neumann, B.; Stammeler, H.-G.; Cowley, M. J.; Jutzi, P.; Scheschkewitz, D. *Angew. Chem., Int. Ed.* **2012**, *51*, 6785–6788. (g) Kosai, T.; Nishimura, S.; Hayakawa, N.; Matsuo, T.; Iwamoto, T. *Chem. Lett.* **2019**, *48*, 1168–1170. (h) Koike, T.; Honda, S.; Ishida, S.; Iwamoto, T. *Organometallics* **2020**, *39*, 4149–4152. (i) Honda, S.; Sugawara, R.; Ishida, S.; Iwamoto, T. *J. Am. Chem. Soc.* **2021**, *143*, 2649–2653.
- (15) Optimized structure of **2'**_{opt} was calculated at B3LYP-D3/6-311G(d) level of theory.
- (16) (a) Iwamoto, T.; Sakurai, H.; Kira, M. *Bull. Chem. Soc. Jpn.* **1998**, *71*, 2741–2747. (b) Ichinohe, M.; Kinjo, R.; Sekiguchi, A. *Organometallics* **2003**, *22*, 4621–4623.

- (17) Higher migratory aptitude of hydride has been reported for some unsaturated silicon compounds. See: (a) Yamaguchi, T.; Sekiguchi, A. *J. Am. Chem. Soc.* **2011**, *133*, 7352–7354. (b) Agou, T.; Sugiyama, Y.; Sasamori, T.; Sakai, H.; Furukawa, Y.; Takagi, N.; Guo, J.-D.; Nagase, S.; Hashizume, D.; Tokitoh, N. *J. Am. Chem. Soc.* **2012**, *134*, 4120–4123. For theoretical studies on hydride migration in unsaturated silicon compounds, see: (c) Nagase, S.; Kudo, T. *J. Chem. Soc., Chem. Commun.* **1984**, 1392–1394. (d) Krogh-Jespersen, K. *Chem. Phys. Lett.* **1982**, *93*, 327–330. (e) Gordon, M. S.; Truong, T. N.; Bonderson, E. K. *J. Am. Chem. Soc.* **1986**, *108*, 1421–1427. (f) Ernst, M. C.; Sax, A. F.; Kalcher, J. *Chem. Phys. Lett.* **1993**, *216*, 189–193. (g) McCarthy, M. C.; Yu, Z.; Sari, L.; Schaefer, H. F., III; Thaddeus, P. *J. Chem. Phys.* **2006**, *124*, 074303. (h) Maier, G.; Reisenauer, H. P.; Glatthaar, J. *Chem. Eur. J.* **2002**, *8*, 4383–4391. (i) Dolgonos, G. *Chem. Phys. Lett.* **2008**, *466*, 11–15.
- (18) Recrystallization from Et₂O at –27 °C also provided orange crystals that exhibit a solvent-separated ion pair structure (see Figure 6-45).
- (19) (a) Masamune, S.; Kabe, Y.; Collins, S.; Williams, D. J.; Jones, R. *J. Am. Chem. Soc.* **1985**, *107*, 5552–5553. (b) Jones, R.; Williams, D. J.; Kabe, Y.; Masamune, S. *Angew. Chem., Int. Ed. Engl.* **1986**, *25*, 173–174. (c) Takanashi, K.; Lee, V. Ya.; Ichinohe, M.; Sekiguchi, A. *Chem. Lett.* **2007**, *36*, 1158–1159. (d) Ueba-Ohshima, K.; Iwamoto, T.; Kira, M. *Organometallics* **2008**, *27*, 320–323. (e) Iwamoto, T.; Akasaka, N.; Ishida, S. *Nat. Commun.* **2014**, *5*, 5353.
- (20) (a) Iwamoto, T.; Yin, D.; Kobayashi, A.; Tamura, M.; Motomatsu, D.; Akasaka, N.; Yokouchi, Y.; Ishida, S.; Kira, M. *Organometallics* **2021**, *40*, 2557–2566. (b) Lee, V. Ya.; Yokoyama, T.; Takanashi, K.; Sekiguchi, *Chem. Eur. J.* **2009**, *15*, 8401–8404. For studies on metalsubstituted cyclotrimetallanes, see: (c) Ichinohe, M.; Toyoshima, M.; Kinjo, R.; Sekiguchi, A. *J. Am. Chem. Soc.* **2003**, *125*, 13328–13329. (d) Abersfelder, K.; Scheschkewitz, D. *J. Am. Chem. Soc.* **2008**, *130*, 4114–4121. (e) Lee, V. Ya.; Horiguchi, S.; Gapurenko, O. A.; Minyaev, R. M.; Minkin, V. I.; Gornitzka, H.; Sekiguchi, A. *Eur. J. Inorg. Chem.* **2019**, 4224–4227. (f) Heider, Y.; Willmes, P.; Huch,

- V.; Zimmer, M.; Scheschkewitz, D. *J. Am. Chem. Soc.* **2019**, *141*, 19498–19504. (g) Guddorf, B. J.; Feldt, M.; Hepp, A.; Daniliuc, C. D.; Lips, F. *Organometallics* **2020**, *39*, 4387–4394. (h) Lee, V. Ya.; Sakai, R.; Takanashi, K.; Gapurenko, O. A.; Minyaev, R. M.; Gornitzka, H.; Sekiguchi, A. *Angew. Chem., Int. Ed.* **2021**, *60*, 3951–3955.
- (21) (a) Hartmann, M.; Haji-Abdi, A.; Abersfelder, K.; Haycock, P. R.; White, A. J. P.; Scheschkewitz, D. *Dalton Trans.* **2010**, *39*, 9288–9295. (b) Willmes, P.; Cowley, M. J.; Hartmann, M.; Zimmer, M.; Huch, V.; Scheschkewitz, D. *Angew. Chem., Int. Ed.* **2014**, *53*, 2216–2220. (c) Izod, K.; Evans, P.; Waddell, P. G. *Angew. Chem., Int. Ed.* **2017**, *56*, 5593–5597.
- (22) Model cyclotrisilene **9**, which has an SiMe₃ group and a PMe₂ group on the Si=Si double bond and methyl groups on the saturated ring silicon atom, adopts a *cis*-bent structure with pyramidalized unsaturated silicon atoms at the B3LYP-D3/6-311G(d) level of theory (see Figure 6-60). However, the energy difference between the optimized bent structure and a planar structure is only 1 kJ/mol, indicating that the geometry around the Si=Si double bond should be sensitive to the steric demand of the substituents. Therefore, it is difficult to discuss the effects of the PR₂ group on the geometry around the Si=Si double bond using the structural characteristics of **8** obtained by XRD analysis.
- (23) A natural bond orbital (NBO) analysis suggested an sp^{1.87} hybridization for the Si orbital in the Si–P bond in **8**_{opt} (Table 6-11).
- (24) Fulmer, G. R.; Miller, A. J. M.; Sherden, N. H.; Gottlieb, H. E.; Nudelman, A.; Stoltz, B. M.; Bercaw, J. E.; Goldberg, K. I. *Organometallics* **2010**, *29*, 2176–2179.
- (25) Weitz, I. S.; Rabinovitz, M. *J. Chem. Soc., Perkin Trans. 1*, **1993**, 117–120.
- (26) Sheldrick, G. M. *SADABS, Empirical Absorption Correction Program*; Göttingen, Germany, 1996.
- (27) Sheldrick, G. M. *Acta Crystallogr., Sect. C: Struct. Chem.*, **2015**, *71*, 3–8.

- (28) Wakita, K. Yadokari-XG: Software for Crystal Structure Analyses, 2001; Release of Software (Yadokari-XG 2009) for Crystal Structure Analyses, Kabuto, C.; Akine, S.; Nemoto, T.; Kwon, E. *J. Crystallogr. Soc. Jpn.*, **2009**, *51*, 218–224.
- (29) Gaussian 09, Revision D.01, Frisch, M. J.; Trucks, G. W.; Schlegel, H. B.; Scuseria, G. E.; Robb, M. A.; Cheeseman, J. R.; Scalmani, G.; Barone, V.; Mennucci, B.; Petersson, G. A.; Nakatsuji, H.; Caricato, M.; Li, X.; Hratchian, H. P.; Izmaylov, A. F.; Bloino, J.; Zheng, G.; Sonnenberg, J. L.; Hada, M.; Ehara, M.; Toyota, K.; Fukuda, R.; Hasegawa, J.; Ishida, M.; Nakajima, T.; Honda, Y.; Kitao, O.; Nakai, H.; Vreven, T.; Montgomery, J. A., Jr.; Peralta, J. E.; Ogliaro, F.; Bearpark, M.; Heyd, J. J.; Brothers, E.; Kudin, K. N.; Staroverov, V. N.; Kobayashi, R.; Normand, J.; Raghavachari, K.; Rendell, A.; Burant, J. C.; Iyengar, S. S.; Tomasi, J.; Cossi, M.; Rega, N.; Millam, J. M.; Klene, M.; Knox, J. E.; Cross, J. B.; Bakken, V.; Adamo, C.; Jaramillo, J.; Gomperts, R.; Stratmann, R. E.; Yazyev, O.; Austin, A. J.; Cammi, R.; Pomelli, C.; Ochterski, J. W.; Martin, R. L.; Morokuma, K.; Zakrzewski, V. G.; Voth, G. A.; Salvador, P.; Dannenberg, J. J.; Dapprich, S.; Daniels, A. D.; Farkas, Ö.; Foresman, J. B.; Ortiz, J. V.; Cioslowski, J.; Fox, D. J. Gaussian, Inc., Wallingford CT, 2009.
- (30) **GRRM14**, Maeda, S.; Harabuchi, Y.; Osada, Y.; Taketsugu, T.; Morokuma, K.; Ohno, K. see <https://iqce.jp/GRRM/> (accessed date March 21, 2020); Maeda, S.; Ohno, K.; Morokuma, K. *Phys. Chem. Chem. Phys.* **2013**, *15*, 3683–3701.
- (31) **NBO 7.0**, Glendening, E. D.; Badenhoop, J. K.; Reed, A. E.; Carpenter, J. E.; Bohmann, J. A.; Morales, C. M.; Karafiloglou, P.; Landis, C. R.; Weinhold, F. Theoretical Chemistry Institute, University of Wisconsin, Madison (2018).